New England Intercollegiate Geological Conference

94th annual meeting

New York State Geological Association

74th annual meeting

Guidebook for Fieldtrips in New York and Vermont

Lake George, New York
September 27, 28, 29, 2002

Organized and Edited by
James McLelland and Paul Karabinos

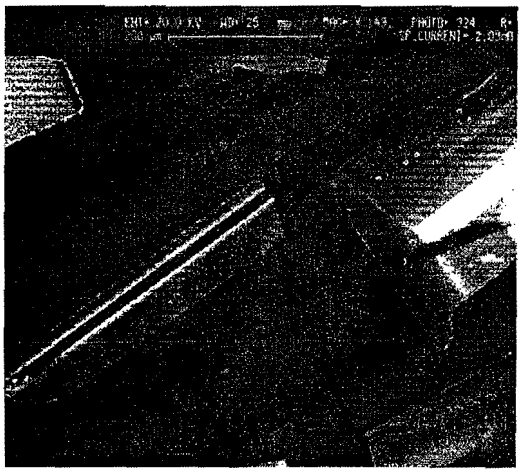

CL image of ca. 1155 Ma igneous zircons from the Marcy Anorthosite

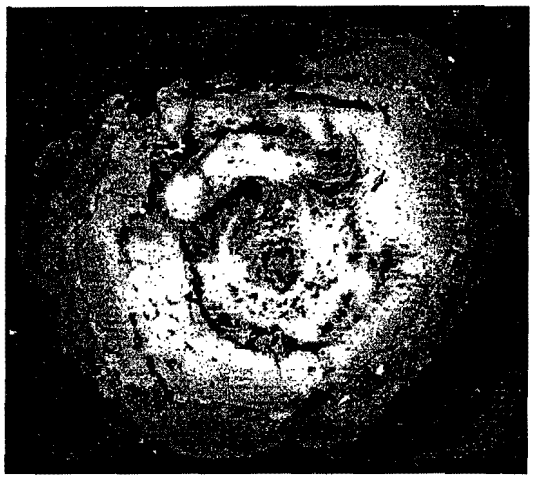

Ca X-ray map of spiral garnet from the Gassetts Schist

Meeting hosted by Colgate University and Williams College

THIS GUIDEBOOK AND MEETING ARE DEDICATED TO

W. YNGVAR ISACHSEN - (1920-2001)
GEOLOGIST, FRIEND, AND TEACHER EXTRORDINAIRRE

For many years, Yngvar served as Senior Scientist at the New York Geological Survey in Albany. During that time, he investigated, and became familiar with, the nature and problems of rocks in his beloved Adirondacks. He also was keenly attuned to the Proterozoic of the Hudson Highlands and the remarkable tectonic history of the Taconic belt of New York. His efforts were crucial in compiling the 1970 edition of the Geological Map of the State of New York that all of us still rely on to this day. At about the same time, he and Jim Olmsted organized an immensely successful and important conference on the "Origin of Anorthosite and Related Rocks". Yngvar served as editor for the volume generated by that conference and bearing the same name Today the "Origin of Anorthosite and Related Rocks" (New York State Museum and Science Service Memoir 18, 1969) continues to serve as a centerpiece for investigators in this very significant field.

Throughout his career Yngvar was deeply interested in brittle fracturing and produced important studies on "zero-displacement crackle zones in the Adirondacks and mylonitization along the Carthage-Colton Zone separating the Highland and Lowland terranes. In his later years he also conducted research on Catskill fracture patterns that may record a meteorite impact. One of his most important pieces of research was that concerning the age of uplift of the Adirondack Dome. He provided compelling evidence for a recent (>20 Ma) date for this event.

Besides his scientific contributions, Yngvar was one of the great teachers of his time. He was blessed with the ability to transmit ideas in remarkably clear terms and to generate interest as he did so. Those of us who now spend our time investigating Adirondack problems are forever grateful to this Teacher of Teachers for showing us the way, pointing out problems, making astute suggestions, and ALWAYS encouraging us. Whatever advances come out of current and future Adirondack research, they will forever carry the stamp of Yngvar's influence.

Finally, we note that Yngvar was a dear and important friend to many of us. Although we might not always agree, we could always exchange ideas in constructive and cooperative ways. A day in the field with Yngvar was a day spent generating both ideas and excitement – and a great deal of warm laughter. When the day was done, it was time to join in good food and good drink, and there was never a better companion in these endeavors – many of them at his lovely Brant Lake home with his gracious wife, Stasia. The times were many; the memories are grand.

We miss him; we think of him; and we honor him. Hail Yngvar!

Table of contents

ISSN 1061-8724

GEOLOGY AND GEOCHRONOLOGY OF THE SOUTHERN ADIRONDACKS

James McLelland, Dept. Geology, Colgate University (Emeritus) and Skidmore College, Saratoga Springs, NY
Lara Storm and Frank Spear, Dept. Earth and Environmental Studies, Rensselaer Polytechnic Institute, Troy, NY

INTRODUCTION

The location of the Adirondacks within the larger Grenville Province is shown in Fig. 1.Topographically, the Adirondacks are divided into Highland (H, Fig 2) and Lowland (L, Fig. 2) sectors. The former is underlain principally by orthogneiss, the latter by paragneiss rich in marble, and the Carthage-Colton Mylonite Zone separates the two regions (Fig 2a,b). The region has experienced multiple metamorphic and intrusive events and large-scale ductile structures are common (McLelland, 1984;McLelland *et al,* 1996). U-Pb zircon geochronology (Table 2) indicates that the oldest igneous rocks exposed are ca 1350-1300 Ma tonalitic, arc-related plutons (Fig.1a) intrusive into older Highland paragneisses of uncertain age (McLelland *et al.*, 1996). The oldest igneous rocks in the Lowlands consist are ca. 1200 Ma granodiorites (Fig.1a) intrusive into older paragneisses of uncertain age (Wasteneys *et al,* 1999). In both the Highlands and Lowlands metapelitic migmatites >1200-1300 Ma contain anatectic material of ~1170 Ma age. Following intrusion ca. 1207 Ma granodiorites in the Lowlands, leucogranitic and tonalitic rocks were emplaced at ca 1172 Ma (Fig.1a,b) and were accompanied by deformation and metamorphism (Wasteneys *et al,* 1999) assigned to the latest, culminating phase (ca. 1220-1160 Ma) of the Elzevirian Orogeny of Moore and Thompson (1980).

From ca 1160-1150 Ma the entire Adirondack-Frontenac region was intruded by anorthosite-charnockite-mangerite-granite (AMCG, 1155 Ma, Fig. 1b) magmas that are associated with four anorthosite massifs (Marcy, Oregon, Snowy, Carthage) recently dated *directly* at 1155 $\pm$ 10 Ma by SHRIMP II zircon techniques. Early age determinations of the anorthosite (McLelland and Chiarenzelli, 1990; Silver, 1969) were based on multigrain dating of MCG granitoids that exhibit mutually crosscutting relationships with the Marcy Anorthosite Massif (MM, Fig. 2b) and are interpreted as coeval with it. The absence of direct dating of the anorthosite was due to the sparse igneous zircon populations in rocks of this composition, a condition that posed a serious obstacle to the study of anorthosites prior to the advent of single grain TIMS and SHRIMP II methods. Current SHRIMP II direct dating of the Adirondack anorthosite massifs demonstrates that both they and their associated ferrodiorites and granitoids were emplaced at 1155 $\pm$ 10 Ma and that the entire complex represents a classic AMCG suite.

The final major events of Adirondack evolution comprise: 1) the emplacement of the Hawkeye granite suite at ca 1095 Ma (Fig 2b) followed almost immediately by 2) high-grade metamorphism (Storm and Spear, Appendix to this article; Spear and Markussen, 1997; Bohlen *et al* 1985; Valley *et al.,* 1990) resulting in vapor-absent, peak granulite facies conditions in the Highlands (T ~ 750°-800° C, P ~ 6-8 kbar) and associated with widespread recumbent, isoclinal folding and the development of intense penetrative fabrics. This granulite facies metamorphism and deformation are assigned to the collisional Ottawan Orogeny of Moore and Thompson (1980), evidence of which occurs throughout the Grenville Province (cf. Rivers, 1997; McLelland *et al.*, 2001b). Toward the end of this major orogenic event much of the Adirondack region was intruded by late- to post-tectonic leucogranites (ca. 1055 Ma, Fig 1a) belonging to the Lyon Mt. Granite (LMG) and thought to be related to delamination and extensional collapse of the orogen (McLelland *et al,* 2001). The Elzevirian and Ottawan Orogenies, taken together, comprise the Grenville Orogenic Cycle (ca. 1350-950 Ma) of Moore and Thompson (1980).

GENERAL GEOLOGY

The southern Adirondacks are underlain by a package of older rocks that is only sparsely represented north of the Piseco anticline. These same lithologies are present in the eastern Adirondacks east of the Northway (Rt 87). The package is characterized by a significant thickness of migmatitic metapelites (Stop 1), some very thick orthoquartzites (Stop 2), tonalitic and granodioritic plutons (Stops 3and 4), and various members of the AMCG suite (Stops 5 and 8). Marbles are present (Stop 7) and deformation is profound (Stops 6 and 9). Taken as a whole, the southern and eastern Adirondacks appear to have been derived from one or more magmatic arcs (Fig. 4) similar to those elsewhere in the Central Metasedimentary Belt (cf., Rivers, 1997; Carr *et al.*, 2000). The growth and amalgamation of these arcs spans the time interval ca 1400-1170 Ma and is referred to as the Elzevirian

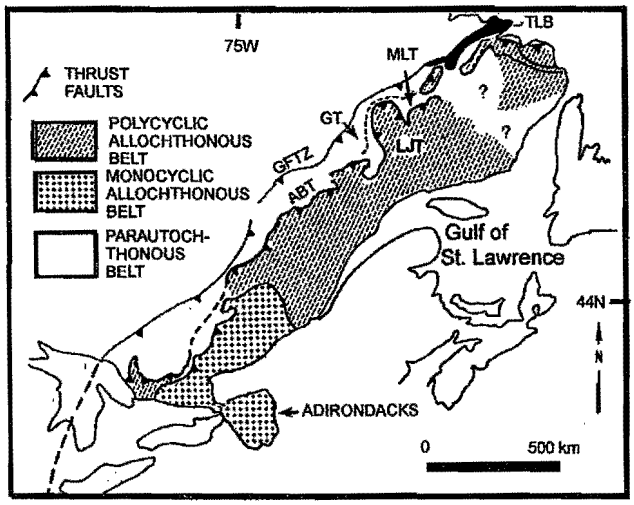

Fig. 1. Location of the Adirondack Mts. within the greater Grenville Province. Tectonic subdivisions after Rivers (1997). GFTZ - Grenville Front Tectonic Zone; ABT- Allochthon Boundary Thrust; GT-Gagnon Terrane; LJT-Lac Jeune Terrane; MLT-Melville Lake Terrane; TLB - Trans-Labrador Batholith

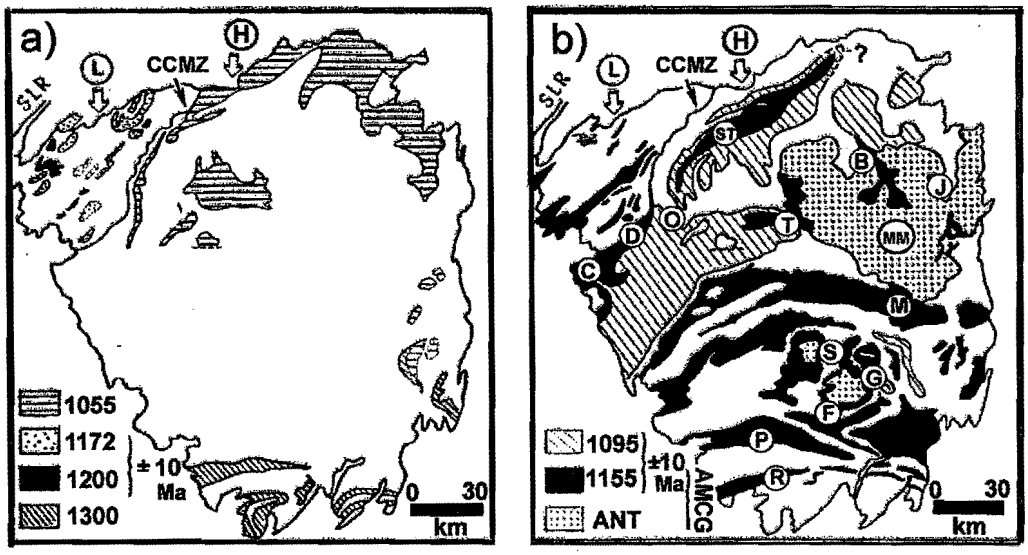

Fig. 2- Generalized geologic-chronologic maps of the Adirondacks broken into two panels for ease of viewing. The major metaigneous units are shown by patterns and their ages are given in the legend. C-Carthage, D-Diana, B-Bloomingdale; J-Jay;F- Oregon Dome Ferrodiorite; G-Gore Mt; O-Oswegatchie; P-Piseco; R-Rooster Hill; T-Tupper Lake; ST-Stark; MM-Marcy Massif, CCMZ- Carthage Colton Mylonite Zone;H-Highlands; L-Lowlands; SLR-St. Lawrence River.

Orogeny. The culminating Elzevirian Orogeny is thought to have occurred during the interval ca 1210-1170 Ma and resulted from the collision of the Adirondack-Green Mt block with the southeastern margin of Laurentia, which at that time was represented by a magmatic arc of northwest polarity developed on the present day Adirondack Lowlands. This culminating collision resulted in deformation and metamorphism that can be recognized in the southern and central Adirondack Highlands. The tonalites and granodiorites manifest the arc(s) and the migmatitic metapelites represent its apron of flysch. The thick orthoquartzites and thin marbles may represent shelf sequences developed on the passive margin of the Adirondack Highlands-Green Mt block prior to the culminating collision. These events are summarized in Fig. 4.

Following the culminating Elzevirian collision, the overthickened orogen began to delaminate and rebound as buoyancy forces dominated those of contraction. As the orogen rebounded, it underwent structural collapse and exhumation, and regional extensional basins formed and accumulated sediments, e.g., the Flinton Basin and Flinton Group (Fig. 4). At the base of the orogen hot new athenosphere moved in to replace delaminated lithosphere $\pm$ lower crust, and depressurization led to the production of gabbroic melts that ponded at the crust-mantle interface in response to density inversion. Due to the dominance of buoyancy forces, the crust-mantle environment was relatively stable, and the gabbroic melts were able to undergo quiescent crystallization. Under these conditions olivine and pyroxene sank to the floor of the chambers while plagioclase crystals floated and accumulated into crystal-rich mushes along the chamber roof. Simultaneously, the latent heat of crystallization from this process provided enough thermal energy to cause significant partial melting of the overlying continental crust. The resultant melts were largely anhydrous and ranged from syenitic, to monzonitic, to granitic and, with the crystallization of orthopyroxene, yielded mangerites and charnockites. Ultimately the crust grew weak enough, and the plagioclase mushes (ie gabbroic anorthosite) of sufficiently low density that they began to ascend and were emplaced at upper crustal levels (<10 km, Valley, 1985; Spear and Markussen, 1997) where they crystallized into AMCG complexes. Continued low-pressure fractionation of the anorthositic magmas led to further growth of plagioclase and the consequent evolution of increasingly mafic interstitial, residual liquid. Many of these were filter-pressed into fractures to form dikes and sheets of ferrodiorite; others pooled into plutonic ferrodioritic masses. We speculate that ultimately the evolving liquids became so mafic that they underwent immiscibility to produce magnetite-ilmenite concentrations such as those at Tahawus (Fig. 2) and comb-textured clinopyroxene-plagioclase dikes similar to those seen at Jay on trip C-1. Representative whole rock compositions of the AMCG suite are given in Table 1. U-Pb dating of all of these rock-types documents that the Adirondack AMCG suite was emplaced at ca 1155 $\pm$ 10 Ma (Table 2). Recent attempts to assign an age of ~1040-1050 Ma to the emplacement of the Marcy Massif are inconsistent with this hard evidence and are quite simply wrong.

Table 1. Representative whole Rock Analyses of AMCG suite Rocks

	1*	2*	3*	4*	5*	6*	7*	8*
SiO_2	42.8	55.88	56.89	53.65	62.12	51.63	54.54	53.54
TiO_2	6.04	1.6	0.47	0.52	0.87	3.1	0.67	0.72
Al_2O_3	10.53	23.18	23.82	24.90	16.48	14.23	25.61	22.50
Fe_2O_3	21.6	2.4	1.21	0.41	1.49	2.1	1.00	1.26
FeO	na	6.57	1.3	0.70	3.96	13.5	1.26	4.14
MnO	0.02	0.09	0.02	0.02	0.09	0.16	0.02	0.07
MgO	5.68	2.08	0.65	1.45	1.06	2.63	1.03	2.21
CaO	8.77	4.87	8.19	12.21	. 3.27	6.5	9.92	10.12
Na_2O	2.17	4.26	5.38	3.92	4.81	2.67	4.53	3.70
K_2O	0.84	2.76	1.13	1.20	5.13	2.41	1.01	1.19
P_2O_5	0.66	0.48	0.09	0.09	0.30	0.57	0.09	0.13
Total	99.34	101.47	99.57	99.9	99.9	99.5	100.1	100.00

1*- Oregon Dome Ferrodiorite; 2*- Gabbroic Anorthosite, Green Mt; 3*- Anorthosite, Green Mt; 4*- Anorthosite, Owl's Head; 5*- Mangerite, Tupper Lake; 6*- Keene Gneiss, Hull's Falls; 7*- Marcy Facies Anorthosite; 8* - Whiteface Facies Anorthosite.

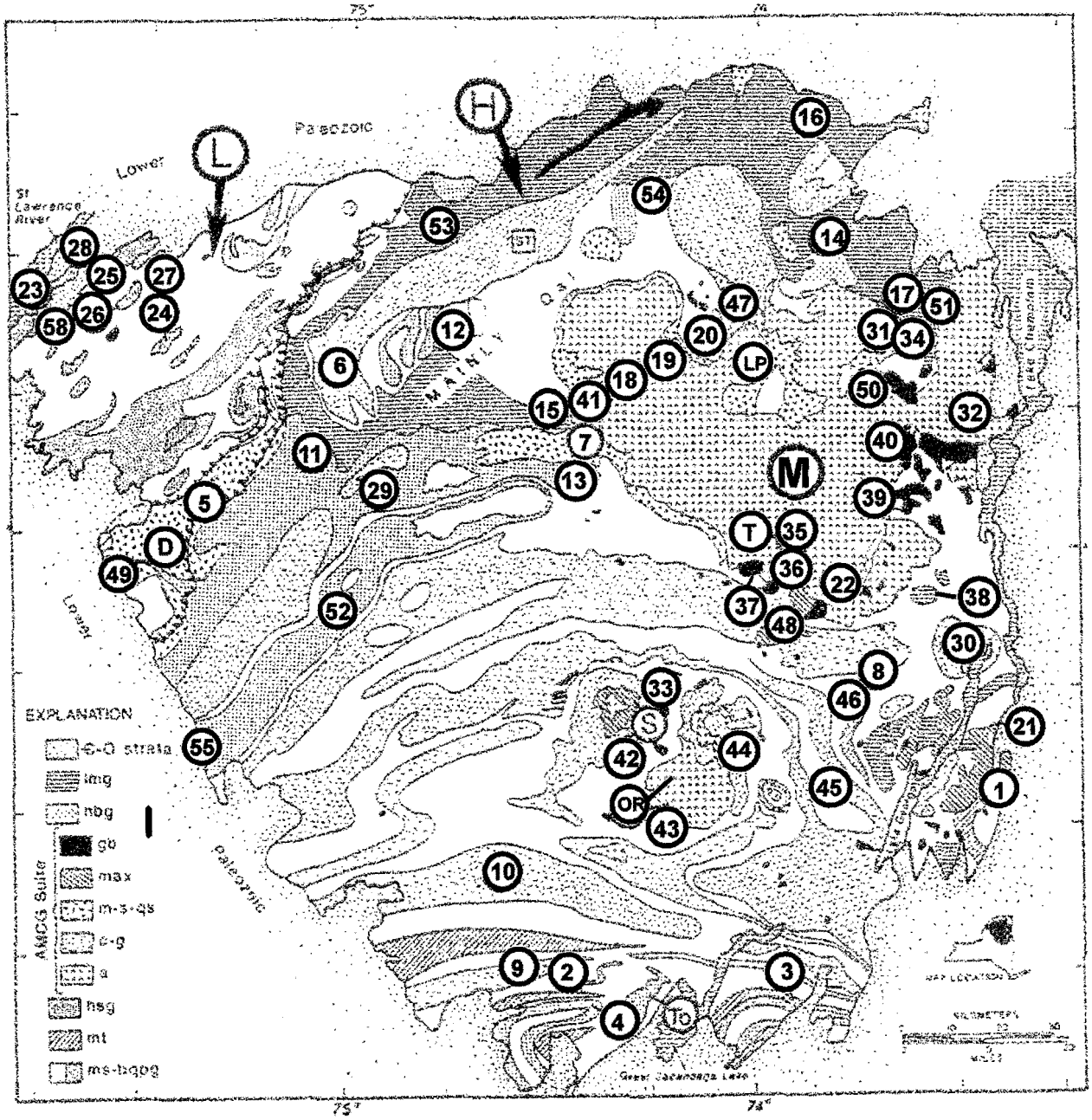

Fig. 3. Generalized geologic map of the Adirondack Mts. showing locations of samples dated by U-Pb techniques and keyed to Table 2. H- Highlands, L- Lowlands, CCMZ- Carthage Colton Mylonite Zone, D- Diana, LP- Lake Placid, OR- Oregon Dome,M- Marcy Massif, T- Tahawus, To- Tomantown pluton, ST- Stark Anticline, lmg- Lyon Mt Granite, hbg- hornblende granite, ga- gabbro, max- mangerite with andesine xenocrysts, m-s-qs- mangerite,syenite,quartz syenite, c-g- charnockite, granite, a- anorthosite, hsg- Hyde School Gneiss, mt- metatonalite, ms-bqpq- metasediments. biotite-quartz-plagioclase

Table 2. Summary of U-Pb Zircon Geochronology For Adirondack Metaigneous Rocks

Map Number	Sample Number	Location	Multigrain TIMS AGE (Ma)	Multigrain TIMS ERR	Singlegrain TIMS AGE (Ma)	Singlegrain TIMS ERR	SHRIMP II Analysis AGE (Ma)	SHRIMP II Analysis ERR	TDM
HIGHLANDS									
Tonalite and Granodiorite									
1	AM87-12	South Bay	1329	37					1403
2	AM86-12	Canada Lake	1302	6					1366
3	LDT	Lake Desolation	>1336						1380
4	AM87-13	Canada Lake	1253	41					
Mangerite and Charnockite									
5	AM86-2	Diana Complex	1155	4			1154	17	1430
6	AM86-15	Stark Complex	1147	10					1495
7	AM85-6	Tupper Lake	1134	4			1169	11	1345
8	9-23-85-7	Schroon Lake	1125	10			ca 1155		
9	AM86-17	Rooster Hill	1156	8					1436
10	AM86-9	Piseco Dome	1150	5					1346
11	AC85-2	Oswegatchie	1146	5					
30	Silver,'69	Ticonderoga	1113	16			ca 1155		
42	AM86-8	Snowy Mt	>1095				1177	22	
44	AM87-3	Gore Mt	>1088				1155	6	
47	AC85-10	Bloomingdale	1133	51			1160	14	
48	AM87-10	Minerva	>1082				1159	12	
49	AM86-1	Croghan	1155	13					
41	Granitedike	Wabeek Quarry					ca 1155		
50	AC85-11	Yard Hill	1143	33					
Anorthosite and Olivine Gabbro									
18	AC85-8	Rt 3, Saranac Lk, ANT	>1113, 1054	22			1149	35	
19	AC857	Rt 3, Saranac Lk, ANT	>1087, 1052	20			1161	12	
20	AC85-9	Forest Home Rd, ILM	996	6					
21	AM87-11	Dresden Station Gab.	1147	7					1331
22	CGAB	North Hudson Gabbro	>1109, 1057	conc			1150	14	
31	BMH01-4	Jay, ANT Pegmatite					1160	15	
34	BMH-01-3	Jay, Cpx-Pgf Dike					1140	18	
35	BMH01-1	Tahawus ANT					ca 1155		
36	BMH01-2	Blue Ridge ANT					1153	11	
37	BMH01-1	Blue Ridge Gabbro					ca 1155		
39	BMH01-19	Exit 29 NWY, ANT					ca 1155		
40a		Woolen Mill Gabbro					1154	9	
40b		Woolen Mill ANT2					1151	6	
43	AM87-8	Oregon Dome Fer'd'r't					1155	6	
Hawkeye Granite Suite									
12	AM86-3	Carry Falls	1100	12					
13	AM86-6	Tupper Lake	1098	4					1314
14	AM86-13	Hawkeye	1093	11					
45	Moon Mt.	Moon Mt	1103	15					
52	NOFO-1	Stillwater Reservoir	1095	5					
53	AM87-6	St. Law/Fran. Co. Line	1090	6					
54	AM87-7	Santa Clara	1080	4					
Lyon Mt Granite									
15	AM86-4	Piercefield	1075	17			1058	18	1576
16	AM86-10	Dannemora	1073	6			1052	11	
17	AM86-14	Ausable Forks, Qt-Ab	1057	10			1041	16	1350
29	CLFG	Wanakena	1113	10	1069	10	1047	10	
38	9-23-85-6	Grasshopper Hill	>1065		1049	3			
51	AM86-11	Ausable Fks., Fay GRT	1089	26	1047	2			
55	PL-3	Port Leyden			1035	4			
LOWLANDS									
Hyde School Gneiss									
23	AM86-16	Wellesley Island	1416		1172	5			1440
24	AC85-4	Gouverneur	1284						1525
25	AC87-4	Fish Creek	1236		1172	5			1210
26	AC85-5	Hyde School	1230		1172	5			1360
27	AC85-1	Reservoir Hill	ca 1172						
Antwerp Granitoid									
58	ANTG	Antwerp-Rossie	1183	7			1207	20	

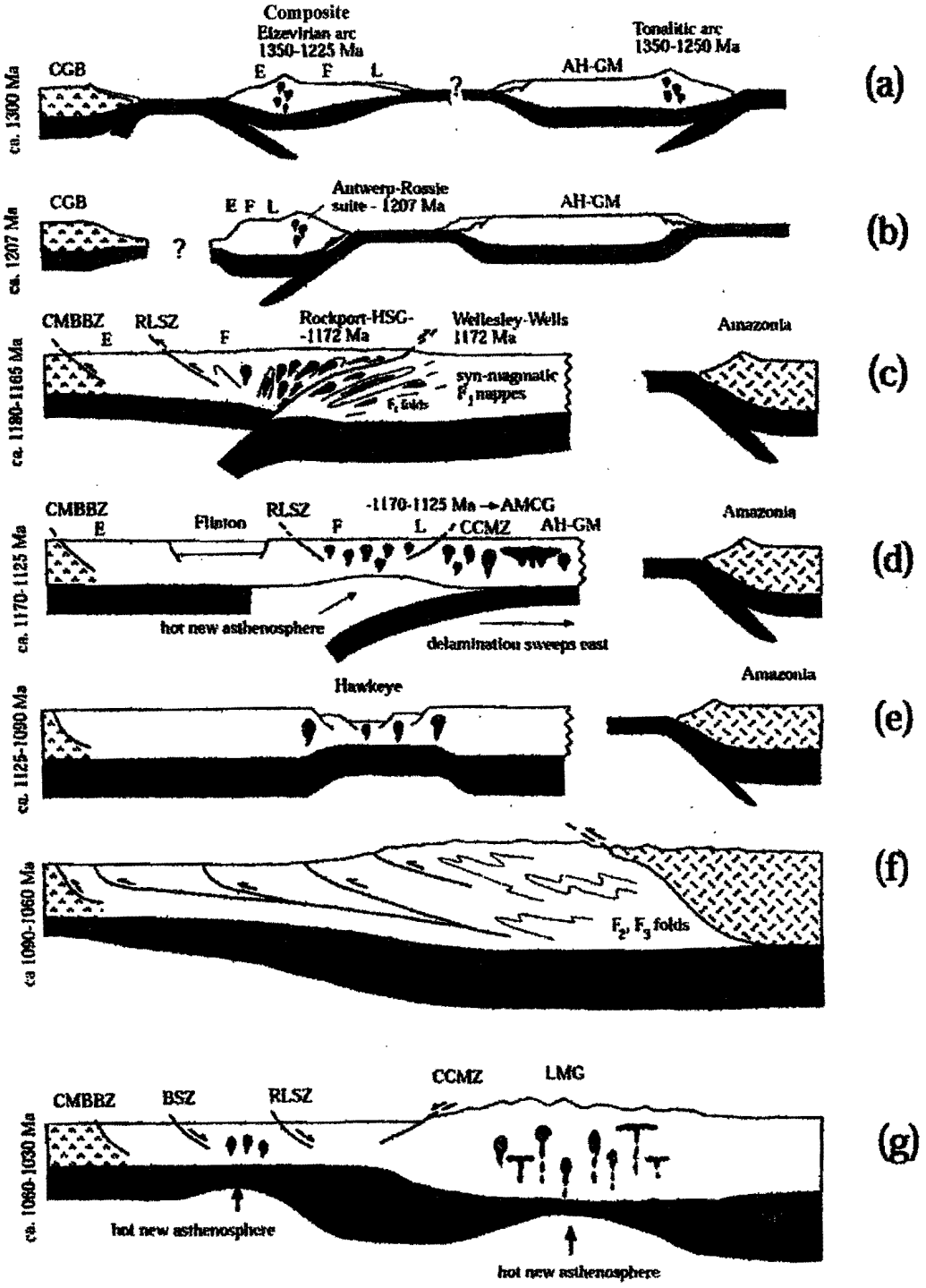

Fig. 4. Tectonic cartoon showing the evolution of the Grenville Province. See text for discussion. Modified after McLelland et al. (1996) and Wasteneys et al. (1999). Abbreviations as follows: AH-GM, Adirondack Highlands–Green Mountains; BSZ, Bancroft shear zone; CGB, Central Granulite Belt; CCMZ, Carthage Colton mylonite zone; CMBBZ- Central Metasedimentary Belt Boundary Zone; RLSZ, Robertson Lake Shear Zone; E, Elzevir terrane, F. Frontenac terrane; HSG, Hyde School gneiss; L, Adirondack Lowlands; LMG, Lyon Mountain granite.

As pointed out by Buddington (1939), there exist several facies and types of anorthosite and related rocks. Examples are given in Table 1. The coarse Marcy facies appears to be a cumulate, and in its purest form is found in rafts of 10-20cm quasi-euhedral grains with ~10% subophitic pyroxene. These are interpreted as rafts formed by plagioclase flotation at the base of the crust and subsequently transported upward by other, less coarse and commonly more mafic facies of anorthosite. The composition of these large plagioclases ranges from An_{45}-AN_{52}. Fram and Longhi (1994) showed that pressure decreases the An content of plagioclase crystallizing from gabbroic magma at the rate of ~ 1%An/kbar. Since the rafts are thought to have crystallized from gabbro at ~10-12 Kbar, this would explain their relatively sodic compositions. The presence of giant (10-25cm) aluminous orthopyroxene in the rafts is also consistent with this model. It is common for rafts to be disrupted by the transporting magma and numerous large, blue-gray andesine crystals in finer grained anorthositic rocks are of this origin. The various plagioclase mushes that were emplaced within the crust are thought to have been broadly similar to the Whiteface facies (Buddington, 1939) and evolved towards more pure anorthosite (generally less coarse than rafts) by low-pressure fractionation of plagioclase. During this process ferrodioritic residual magmas were produced and were commonly filter-pressed into dikes and sheets (McLelland et al, 1990). Ultimately, the residual magmas became so mafic that they split into immiscible silicate and Fe, Ti-oxide phases to yield magnetite-ilmenite deposits such as those at Tahawus.

Emplacement of the AMCG suite was followed by ~50 Ma of relative quiescence terminated by emplacement of the Hawkeye granitic suite at 1103-1095 Ma. This interval corresponds almost exactly with the major magmatism in the plume-related Mid-continent Rift, and we attribute Hawkeye magmatism to far-field echoes from the Mid-continent plume (Cannon, 1994). This far-field effect is interpreted to have thinned the crust and lithosphere and led to significant crustal melting to produce the mildly A-type Hawkeye suite. At the same time, the crust underwent heating that continued to be present when the culminating collision with Amazonia (?) took place thus initiating the Ottawan Orogeny at ca 1090 Ma. Note that magmatism in the Mid-continent Rift was shut off at this time by westward-directed thrust faults. Within the Adirondacks, the already heated crust was loaded by thrusting and contraction along ~NW-SE lines of tectonic vergence. This heating followed by loading led to a counterclockwise P,T,t path (see Fig. 12 as well as Appendix by Storm and Spear). From ~1090-1060 Ma contraction dominated the region and great nappe structures formed (Figs. 5,6). These are represented today by extremely large isoclinal, recumbent folds such as the Canada Lake isocline and the Little Moose Mt syncline, both of which have ~E-W axial trends and plunge gently about the horizontal (Fig. 6). It is uncertain, but possible, that these structures were initiated as thrusts and then toed-over to form a greatly thinned and attenuated lower limb. Associated with the nappes are pervasive penetrative fabrics imposed upon Hawkeye and older rocks and attesting to the extraordinarily high temperature ductile strains imposed on these rocks (McLelland, 1984).

As discussed by Spear and Markussen, garnet coronas in mafic rocks appear to have formed during late-Ottawan isobaric cooling from ~800-600°C. Associated with these coronitic rocks are small, equant zircons interpreted as metamorphic in origin and yielding ages of ~1050 Ma. As discussed in the text for Stop 8, these are thought to date the corona-forming reaction. This is consistent with the Sm-Nd age of ca 1050 Ma for the large Gore Mt garnets (Mezger *et a.l*, 1992). Following isobaric cooling the Ottawan orogen is thought to have undergone delamination and rebound. This was accompanied by emplacement of the distinctive Lyon Mt Granite suite that hosts the great Kiruna-type low-Ti magnetite deposits of the Adirondacks and is exposed across wide tracts of the Highlands. Zircon dating of the Lyon Mt Granite by both single grain TIMS and SHRIMP II methods (McLelland et al, 2002) documents that the thick, and oscillatory zoned, mantles of its zircons grew from melts at 1050 ± 10 Ma. The cores of these zircons are of AMCG and Elzevirian age and whole rock Nd-model ages are consistent with the production of Lyon Mt Granite from melting of these earlier lithologies. An especially interesting member of the Lyon Mt Granite is a quartz-albite (Ab_{98}) that is associated with the iron-oxide deposits and is interpreted to be the result of sodic hydrothermal alteration (McLelland *et al.*, 2002).

Further relevant details accompany the descriptions presented in at individual stops.

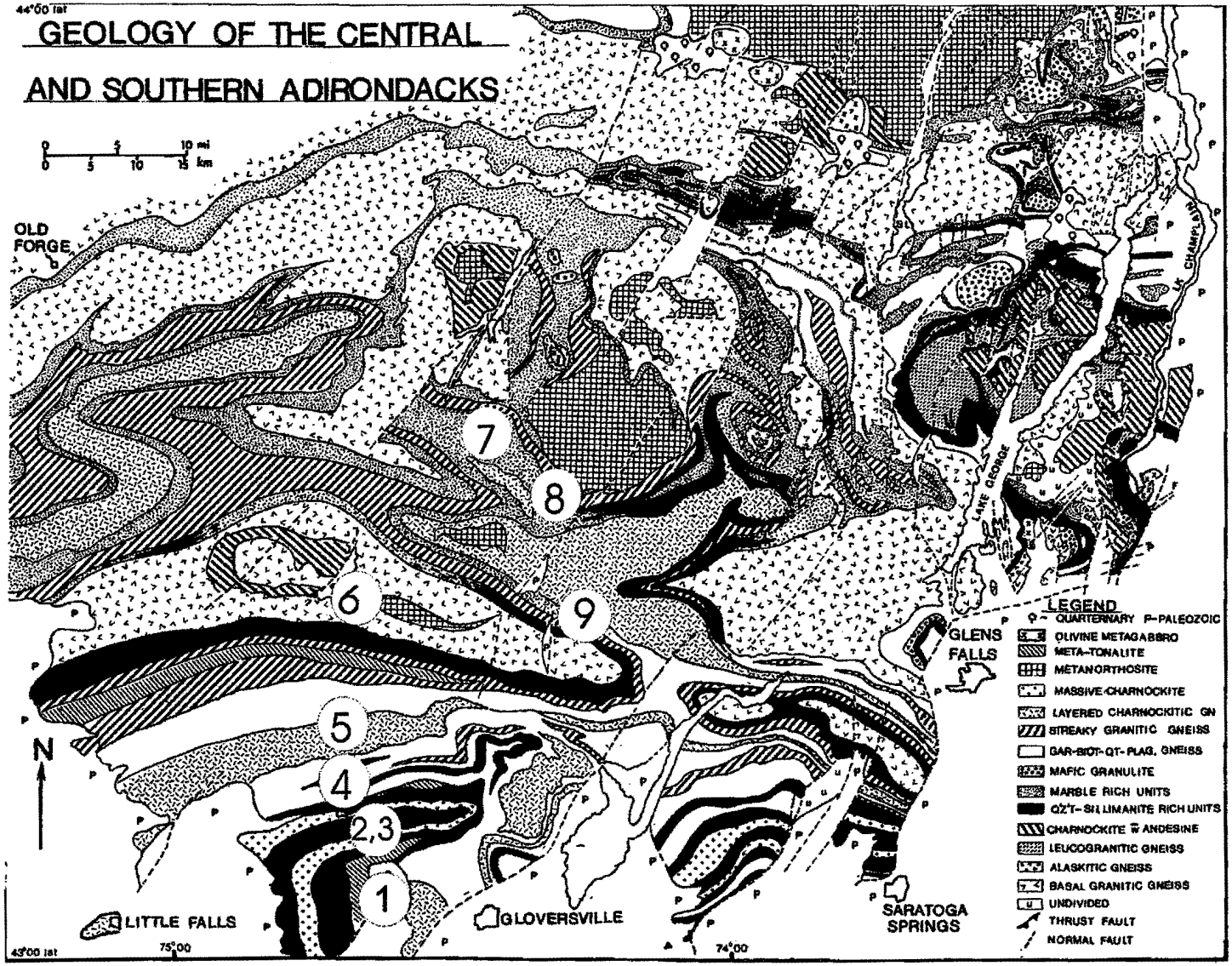

Fig. 5 Generalized geologic map of the southern and central Adirondacks showing field trip stops 1-9.

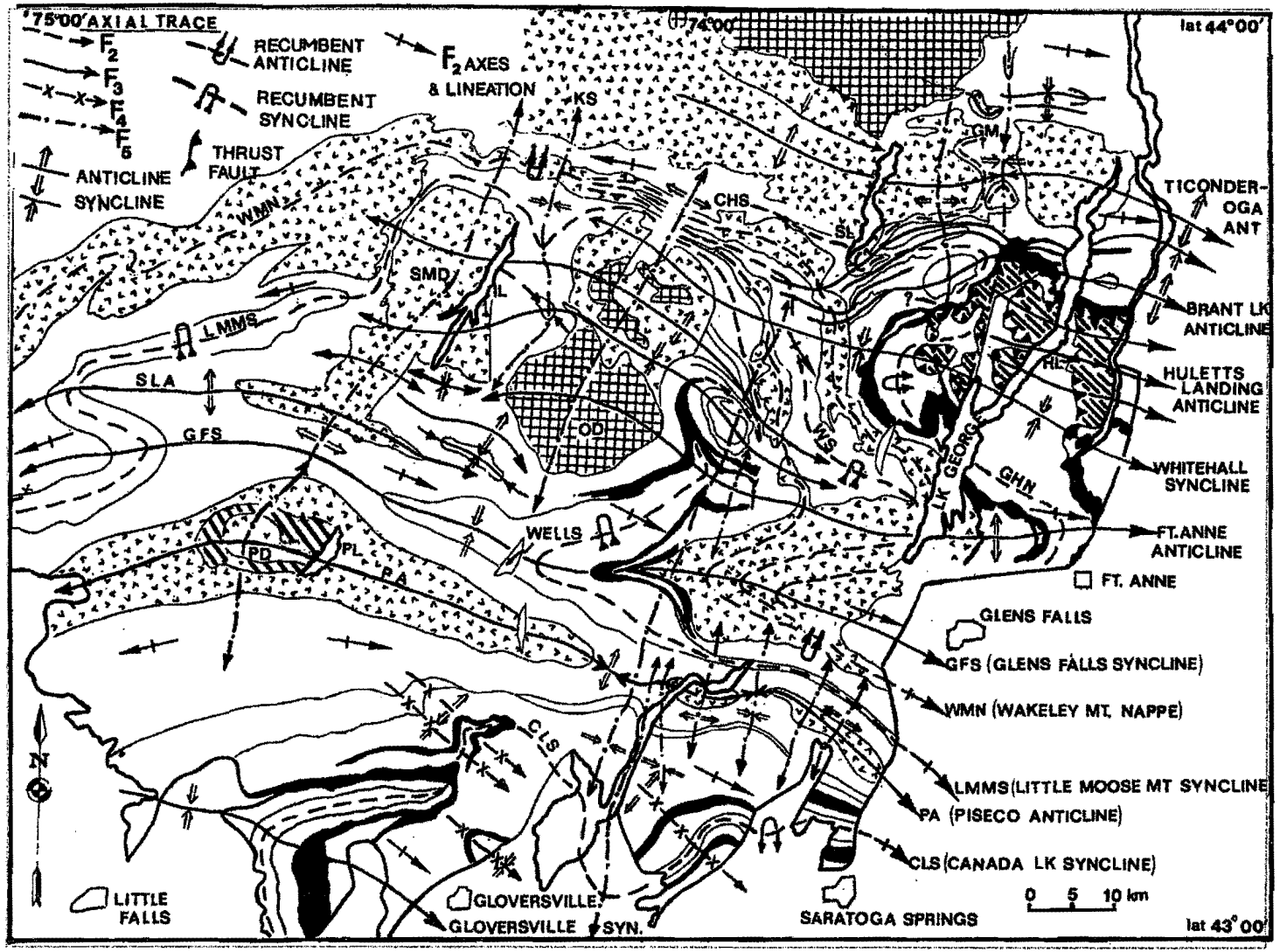

Fig. 6 Fold structures of the southern and central Adirondacks

ROAD LOG

MILEAGE

0.0 Caroga Lake Post Office in Caroga Lake, NY.

2.8 Roadcuts of migmatitic metapelite. Park on right (west) shoulder of Rt 29A.

STOP 1. PECK LAKE MIGMATITIC METAPELITE. (30 MINUTES). This exposure along Rt 29A just north of Peck Lake is the type locality of the Peck Lake migmatitic metapelites that consist of restitic sillimanite-garnet-biotite-quartz-oligoclase melanosome and quartz and two-feldspar leucosome of approximately minimum melt composition (McLelland and Husain 1986). Small red garnets are common in the leucosome and, in most cases, grow across foliation. The leucosomes occur as irregular, elongate bodies generally parallel to foliation but quite commonly exhibiting crosscutting relationships with respect to the restite and to one another. Based upon these compositional and crosscutting relations, the leucosomes are interpreted as anatectites and a reasonable metapelitic source rock can be prescribed by reintegrating their composition with that of the restite (Table 3) to yield a greywacke-slate precursor. The restriction of these partial melts to within the migmatite is thought to be the result of near-solidus, hydrous melting that would cause ascending melts to intersect the solidus as they began to rise. Close inspection of the leucosomes reveals that, in their most pristine configuration, they consist of coarse granite and pegmatite. In low strain zones elsewhere in the Adirondacks it is manifestly clear that the leucosomes originally formed an anastamosing arrays of veins, dikes, sheets, and pods. Subsequent high strain resulted in rotation into psuedoparallelism and commonly produced disruption that caused separate grains of white feldspar some of which show elongate tails – ie, the rock was on its way to becoming a mylonitic "straight gneiss". At the last stop (Stop 9) of this trip we shall see the end result of this process in a series of platy, stretched, and highly grain size reduced and mylonitic equivalents of the rocks seen here. The anatectic origin of these units is further suggested by the uncommon, but not rare, occurrence of plagioclase- and/or garnet-rimmed hercynitic spinel in the restite. Recently, Bickford and McLelland have run a U/Pb zircon pilot study on the age of the anatectites and have found that they contain 1220-1250 Ma cores, 1020-1050 Ma metamorphic rims, and relatively thick, nicely zoned mantles that fall into the interval 1190-1170 Ma. Some of the rims show zoning, but this is minor compared to the mantling zircon. These results demonstrate that majority of the anatectites were produced by partial melting during the culminating Elzevirian Orogeny dated at ca 1210-1170 Ma (Wasteneys and McLelland, 1999) and are not of Ottawan origin. Currently, we are continuing this research by utilizing both zircon and monazite geochronology.

TABLE 3. COMPOSITIONS OF AVERAGE LEUCOSOME, HOST, AND SELECTED CLASTICS

	Average Leucosome (N = 31)	Average Host (N = 12)	Average Host + 15% Average Leucosome	Average Greywacke (N = 23)	Average PC Slate (N = 33)	Average Slate (N = 36)
SiO2	74.39	61.75	63.12	64.70	56.30	60.64
Al203,	13.85	17.83	17.18	14.80	17.24	17.32
TiO2	.05	1.32	1.15	.50	.77	.73
Fc2O3	.89	8.70	7.55	4.10	7.22	4.81
MgO	.27	2.07	1.83	2.20	2.54	2.60
CaO	1.25	2.60	2.40	3.10	1.00	1.20
Na20	2.77	2.44	2.76	3.10	1.23	1.20
K2O	5.83	3.20	3.44	1.90	3.79	3.69
MnO	.02	.07	.06	.10	.10	
P205	.08	.15	.12	.20	.14	
LOI	.30	.42	.40	2.40	3.70	4.10
TOTAL	99.70	100.55	100.00	101.00	98.70	98.00

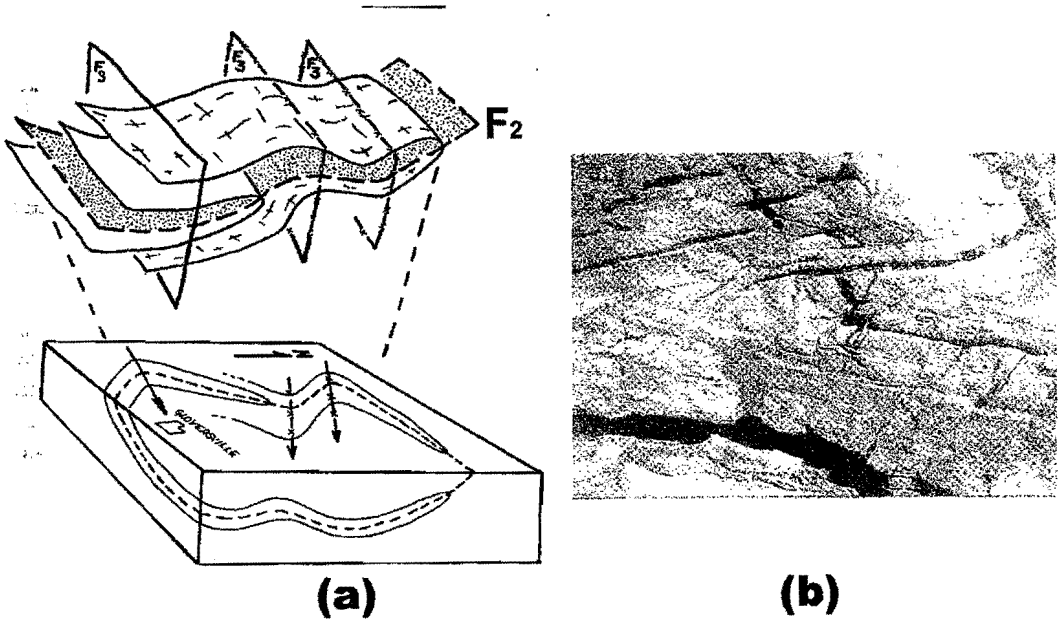

Fig. 7 (a) Three dimensional cartoon showing geometry of interference of isoclinal and upright folds in the Canada Lake Isocline (F_2) and the resultant outcrop pattern. (b) F_2 minor fold recently blasted from roadcuts at stop 2.

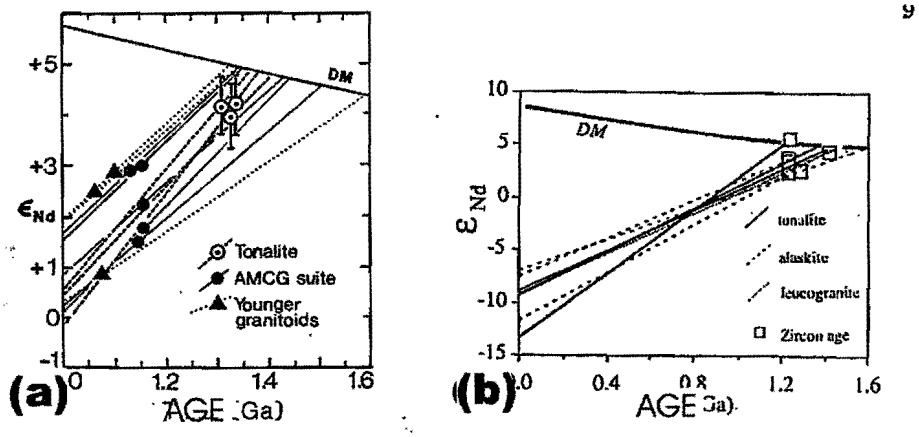

Fig. 8 Epsilon Nd plots for the Adirondack Highlands (a) and Lowlands (b)

This outcrop provides an excellent mesoscale example of Adirondack structure (Fig. 7a). The overall strike of foliation is N60-70W and dips vary from north to south and pass through the vertical demonstrating that the roadcut defines a large minor isoclinal, recumbent fold. Smaller, meter-scale isoclinal folds are also well exposed and are aligned parallel to the roadcut-scale fold. All of these are similar in style, and parallel to, the very large, regional Canada Lake isocline or nappe (F_2, Fig 7a). It is clear that the Canada Lake nappe stage of deformation rotates an earlier foliation (due to F_1) and has a moderately dipping axial planar foliation that intersects the earlier foliation high angles. The time interval between these foliations remains unspecified, but it is clearly post-anatexis and probably all Ottawan (ca 1090-1030 Ma). It appears that the Ottawan has successfully obliterated most Elzevirian fabrics. Note that some of the smaller minor folds contain apparently terminated compositional layers that could very well represent Elzevirian isoclinal noses. If so we are looking at isoclinally refolded isoclines.

Migmatitic metapelites of this sort occur throughout the southern and western Adirondacks as well as in the Adirondack Lowlands. We interpret them as flysch sequences of shale and greywacke that were being shed from the Elzevirian magmatic arcs that dominated the region from ca 1400-1300 Ma. Tonalites and granodiorites of the arcs locally crosscut the metapelites and provide a minimum age for them. In a broad sense, they are thought to be coeval. The metapelites of the Adirondack Lowlands are compositionally similar, but are thought to represent a different, younger, and uncorrelative arc environment.

3.5 Turn around at Peck Lake and head back north on Rt 29A.
5.9 Junction NY Rt. 29A and NY Rt. 10. Continue due north into Caroga Lake.
7.3 Nick Stoner Inn on west side and Nick Stoner Golf Course on east side of Rt 29A-10.
7.8 Town of Caroga sand and gravel depository on east (right) side of Rt 29A-10. Pull in and park.

STOP 2. IRVING POND QUARTZITE. (20 Minutes). The Irving Pond quartzite unit cores the Canada Lake isocline and is folded back on itself. At map scale it is exposed across strike for over 3000m but its "true?" thickness is on the order of 1000m. Notwithstanding, it represents an enormous volume of orthoquartzites with minor pelitic intercalations. Its minimum age is unknown but is being investigated by zircon geochronology. Similar quartzites along the St Lawrence River contain zircons as young as 1300 Ma, and the same may prove to be true for the Irving Pond. It is suggested that these quartzites may have been deposited along the present eastern margin of the Adirondack-Green Mt block between ca 1250 and 1200 Ma (see Fig. 4). During that interval, this margin was passive as the block moved westward towards the Elzevirian subduction zone that dipped westward beneath Laurentia and its leading margin, ie, the Adirondack Lowlands (Fig. 4b,c). Upon collision, (ca 1200-1170 Ma), the accumulated sandstones were deformed and metamorphosed. Although this scheme is speculative, it is consistent with the little that is known about Elzevirian events.

Within the clearing there are three small, but informative outcrops. The first consists of 30-40cm-scale layers of pure quartzite together with 2-3cm-scale metapelitic layers of. These dip gently to the southeast. The bulk of the Irving Pond quartzite consists of layer upon layer of the pure quartzite with little, if any, intervening metapelite. The second exposure is located a few tens of feet to the west where the rocks form a low ledge running uphill. The southern termination of the ledge that faces the clearing shows steeply dipping layers that are discordant with underlying layers. The discordance is due to some sort of ductile shearing in the outcrop but does not affect the following interpretation. Looking back to the first outcrop, it is clear that the gently dipping layers seen there can be projected up above the ground surface so that they must have been situated overhead at this locality; however, they must also have suddenly dipped steeply and rotated through the vertical in order to have their present configuration, ie, they form recumbent isoclinal folds of the F_2 set. The trend of this recumbent, isoclinal fold axis is ~N70W and the plunge is ~15 deg. southwest, ie, it is a minor fold of the Canada Lake isocline family and of Ottawan age. At the base of the southernmost outcropping, and below a small ledge, there is preserved a foot-scale isoclinal nose. Inspection of the geometry makes it clear that the outcrop preserves an isoclinally refolded F_1 isocline-perhaps of Elzevirian age.

Farther down the clearing towards the highway a clean outcrop consists of pure, glassy quartzite dip slopes exposed together with dark layer-like bodies of fine-grained pyroxene-plagioclase granulite. The chemistry of the granulites approximates that of diabase and locally exhibits microscopic diabasic texture (McLelland and Husain,

1986). The igneous nature of the granulites is further manifested by the xenoliths of quartzite present in them. Elsewhere the metadiabases are isoclinally folded and the limbs of these folds clearly truncate 10-15 cm-scale intrafolial isoclinal folds (F_1) that are rotated by the isocline. We interpret this older set of isoclinal minor folds to be of Elzevirian age. A recently blasted F_2 fold in metadiabases is shown in Fig 7b. The metadiabases have not been dated, but they are similar to some mafic AMCG rocks and are tentatively assigned a ca 1150 Ma age.

8.0 Large roadcuts of charnockite on both sides of Rt. 29A-10. Park on right hand (east) side just past guardrails at crest of hill.

STOP 3. CANADA LAKE CHARNOCKITE. (20 MINUTES). Large roadcuts expose the type outcrops of the Canada Lake charnockite (Figs. 8-11). This highly deformed orthogneiss has a granodioritic composition, and consists of 20-30% quartz, 40-50% mesoperthite, 20-30% oligoclase, and 5-10% mafics including small, sporadic grains of orthopyroxene. The exposures exhibit the drab olive color typical of charnockites around the world. In the woods these rocks tend to weather pink and exhibit a maple sugar brown weathering rind. The unit is ~500m thick and consists throughout of relatively homogeneous granitoid with pegmatites and minor amphibolitic layers. A multigrain U-Pb zircon age 0f 1251 $\pm$ 33 Ma (McLelland and Chiarenzelli, 1990) indicating that this unit belongs with other calcalkaline rocks of broadly Elzevirian age. Mapping along its contact for a total distance of ~300 km, has not revealed any crosscutting features, but xenoliths of country rock have been recognized and substantiate an intrusive origin. The apparent conformity is attributed primarily to extreme and ductile tectonism. In addition, an original conformable, sheet-like form is quite possible. Rocks of similar age and composition are found in the Green Mts. of Vermont (Ratcliffe and Aleinikoff, 1991).

9.2 Canada Lake Store on the left (south side) of Rt. 29A-10. Turn in to parking lot and park diagonally.

STOP 4. ROYAL MT. TONALITE (30 MINUTES). Steep roadcuts exposed across from the Canada Lake Store expose typical tonalitic rocks that are relatively common within the southern and eastern Adirondacks, the Green Mts of Vermont, and the Elzevir terrain of the Central Metasedimentary Belt of the Canadian Grenville. In all of these occurrences, the tonalites manifest the presence of magmatic arcs that existed along the southeastern margin of Laurentia during the interval ca 1400-1200 Ma diagnostic of the Elzevirian. Within the Adirondacks, multi- and single-grain TIMS U-Pb zircon geochronology indicate emplacement of the tonalitic magmas at ca 1350-1300 Ma. The present outcrop has been dated by both TIMS methods and the single grain age is constrained at 1307 $\pm$ 2 Ma (Aleinikoff, pers comm., 1991). Well-documented examples of these arc terrains extend to the Llano uplift and Van Horn areas of Texas (Mosher, 1999; Patchett and Ruiz, 1990; Roback, 1996) and attest to a global-scale system that may have been an ancient analogue of the present day East Indies arc. During the Elzevirian, various arcs must have collided and amalgamated, and continental arcs may have come into existence as well. These details remain to be unraveled, but in the meantime we note that the Elzevirian came to a close at ~1210-1170 Ma with the collision of the Adirondack Highlands-Green Mt block with the Andean-style arc then existent along the southeastern edge of Laurentia (Fig 4c). McLelland , in Wasteneys et al (1991), refers to this collisional event as the "culminating Elzevirian Orogeny" that closed out the Elzevirian interval of arc magmatism and amalgamation in the area.

The whole rock chemistry of the Adirondack calcalkaline rocks are shown in Figs (9,10,11) where their calcalkaline affinities are clearly visible. In addition, ε_{Nd} characteristics are presented in Fig. 8 and demonstrate that the tonalites represent juvenile additions to the crust from the mantle, and partial melting of the older rocks can produce younger Adirondack granitoids. Neither the Sm-Nd data, nor any other isotopic data, give any hint of pre-1350 Ma crust in the Adirondacks and suggest that the original arc must have been of ensimatic origin.

Disrupted amphibolitic sheets are present here and within Adirondack tonalites in general. Their origin is enigmatic but they do not appear to have been derived locally. Their elongate, sheet-like character suggests that they may represent coeval mafic dikes of the sort commonly observed in tonalites. It is also possible that they represent enclaves incorporated from an amphibolitic source region. Isotopic studies are needed here.

In a few places the tonalite crosscuts the migmatitic metapelites seen at Stop 1. This fixes a minimum age for the latter at ca 1300 Ma. As indicated in the discussion at Stop 1, the tonalites and metapelitic rocks may represent an original, essentially coeval, magmatic arc-flysch system.

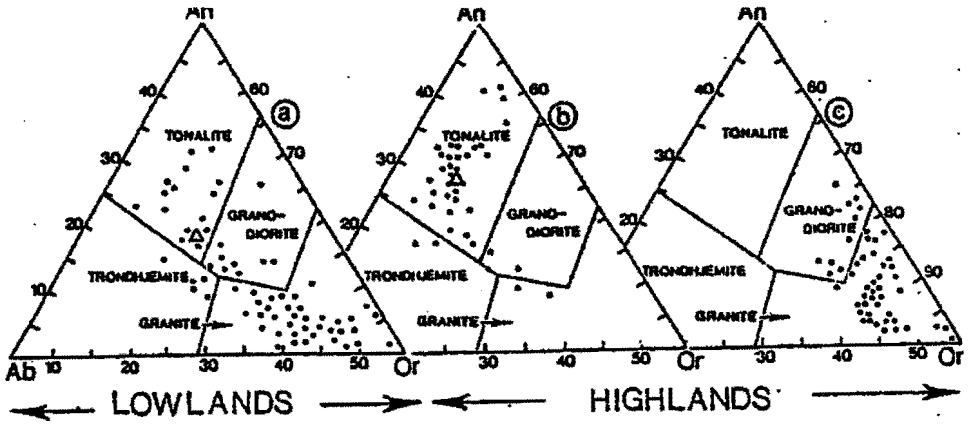

Fig. 9. Plots of normative Ab-An-Or for (a) Hyde School Gneiss, 9b) Highlands tonalites and © Tomantown pluton.Open symbols gives average value for tonalites. Fields after Barker(1979).

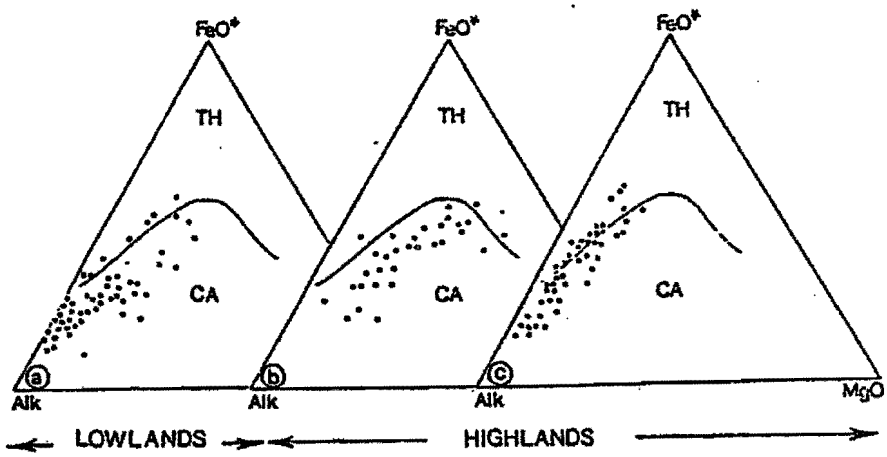

Fig. 10. AFM plots for (a) yde School Gneiss, (b)Highland tonalites, and © Tomantown pluton.

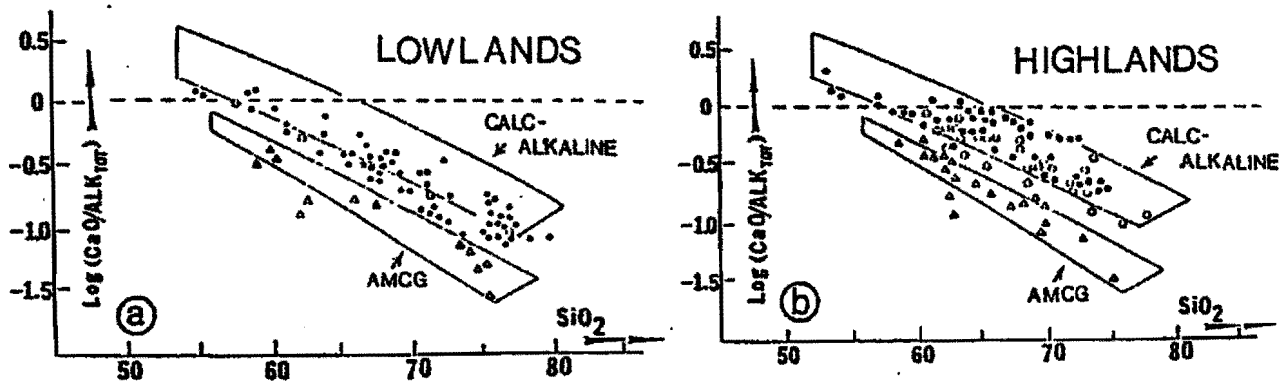

Fig. 11. Calcalkali ratio versus SiO2 for (a) the Adirondack Lowlands and (b) the Adirondack Highlands. In (a) open circles are average values for 1172 Ma Hyde School Gneiss, closed circles for typical Hyde School, and open triangles for ca 1155 Ma AMCG rocks. In (b) open circles are for the ca 1250 Ma Tomantown pluton, closed circles for the older (ca 1300 Ma) calcalkaline rocks, and open triangles for AMCG rocks.

11.0 Pine Lake. Junction of Rts 29A and 10. Turn right (north) on Rt 10 towards Speculator.
16.7 North end of East Stoner Lake. Pull off into parking area just north of Town of Arietta sign.

STOP 5. ROOSTER HILL MEGACRYSTIC CHARNOCKITE. (20 MINUTES). This deformed charnockite is characterized by the presence of 20-40% megacrysts (2-4cm) of alkali feldspar set in a groundmass of quartz, oligoclase, biotite, hornblende, garnet, and sporadic orthopyroxene. In general, these have undergone dynamic recrystallization during high temperature shear strain and have developed asymmetrical tails, although flattening reduces the degree of asymmetry in most cases. In cases where tail asymmetry permits, a southeast side up and to the northwest (N70W, 10-15SE) is clearly the dominant displacement sense. As the degree of shear strain intensifies, both feldspars and quartz become elongated in the direction of tectonic transport and ribbon or pencil gneisses result. The orientation of these fabric-forming elements is parallel to the regional isoclinal fold axes. In Fig. 8 the ε_{Nd} growth curve for Rooster Hill charnockite lies on one of the AMCG suite growth lines that pass through the tonalite region indicating that this suite can be derived by partial melting of the ca 1300 Ma arc rocks.

19.2 Low roadcut in migmatitic metapelites.
20.6 Avery's Hotel on left (west) side of Rt 10.
21.7 Roadcut through granite, gabbro, and tonalite.
23.2 Pink AMCG granitic rocks, gabbro, and small exposure of fine-grained anorthosite. A large inclusion of calcsilicate in pink granite is exposed and interpreted as a xenolith.
23.5 Roadcut of metasedimentary quartzites and pelitic rocks together with anatectites.
29.2 Fault breccias in charnockite.
29.7 Junction of Rt 10 (ends) and Rt 8. Turn right (east) on Rt 8.
30.2 Long roadcut of mylonitic ribbon gneiss in pink granitic rocks of the Piseco anticline. Ribbons trend N70W and plunge 10-15 SE parallel to both recumbent F_1 isoclines and upright $F_{2\,such}$ as the Piseco anticline. A multigrain U-Pb zircon date from this outcrop gives an age of 1155 ± 10 that is interpreted as the age of magmatic emplacement.
32.5 Pull off and park on LEFT (NW) shoulder of Rt 8.

STOP 6. RIBBON GNEISS IN THE CORE OF THE PISECO ANTICLINE. (30 MINUTES).

A long, low roadcut on the left (northwest) side of Rt 8 exposes outstanding examples of ribbon gneiss developed in a megacrystic facies of the Piseco core rocks. The overall composition here is similar to that of the Rooster Hill megacrystic charnockite examined at Stop 5, but here the original feldspars and quartz have been extended into ribbons on the order of 60cmx.25mmx.05mm (McLelland, 1984). Assuming interstitial quartz aggregates of ~1cm diameter, the current dimensions indicate an extension of 6000%, ie, if this strain were to be equally distributed throughout a 1km thick block of crust that block would be 60km long.25 km wide, and .005 km thick. Of course, such high ductile strain cannot be integrated through the entire crust, but the numbers provide some flavor for the strain involved.

The ribbon gneisses exposed here are folded into a minor anticline that rotates the foliation of these L>>S tectonites. The axis of this minor fold trends N70W and plunges 10-15SE. This orientation is parallel to the axis of the F_3 Piseco anticline, to the F_2 recumbent isoclines of the Adirondacks (Figs. 6,7), and to the axis-parallel elongation lineations associated with these isoclines. The fact that all of these structural elements are parallel to one another indicates that they all shared some common kinematic experience during their tectonic evolution. In order to identify the common experience, we first note that all of the deformation in these ca 1150 Ma rocks must be of Ottawan age. Next we note that minor isoclinal folds in the outcrop lie with their axial planes in the foliation and their axes defining rod-like structures parallel to the N70W extension lineation. The low dip of the lineation suggests that the mechanism responsible for it was likely to have been thrust faulting out of the southeast and towards the northwest. This would have resulted in the stretching that elongated the quartz and feldspar. The thrusting could also have rotated earlier fold axes into the thrust plane and parallel to the direction of tectonic vergence. However, rather than rigid rotation of the axes, it is proposed that the early folds became too ductile to buckle and their axes began to "flow" as passive markers in the direction of tectonic transport, i.e., the recumbent fold axes began to undergo increasing curvature in response to the velocity gradients in the ductile flow field. The ultimate result of this process is sheath folds, and it is suggested that the isoclinal folds with axes parallel to the ribbon lineation represent parts of sheath folds. It is further suggested that the Canada Lake isocline may itself be

a large sheath fold whose southern closure is obscured by Paleozoic overburden. The large F_3 folds such as the Piseco anticline and the Gloversville syncline are interpreted as structures formed by NS constrictional forces that arose in response to the EW elongation associated with the large scale, ductile thrusting of the Ottawan Orogeny. Later NNE upright folds of the F_4 set were superimposed on the F_2 sheath folds and the F_3 corrugations by continued, but waning, NW-SE contraction associated with the NNE suture situated somewhere beneath, or beyond, the present day Coastal Plain. Finally, it should be remarked that the ribbon lineations and upright lineation-parallel corrugations described above are similar to those encountered in core complexes. The problem with this alternative is that the late- to post-tectonic Lyon Mt Granite emplaced at ca 1050 Ma is unaffected by these fabrics. Accordingly, we associate the fabrics with ductile Ottawan thrusting. Orogen collapse similar to core complex kinematics is thought to have taken place at ca 1050-1030 Ma.

43.2 Junction of Rt 8 and Rt 30 in Speculator. Turn right (south) on Rt 30.
46.7 Roadcuts of Marble. Park on right (south) shoulder.

STOP 7. MARBLE AND CALCSILICATE. (30 Minutes). Exposed in roadcuts on both sides of the highway are examples of typical Adirondack marbles and their associated lithologies, ie, garnetiferous amphibolite, calcsilicates, and various disrupted blocks of both internal and external members. The disruption and boudinage attests to the extremely ductile behavior of the marbles. Also exposed are vertical, crosscutting, and undeformed veins of tourmaline-quartz symplectite. Besides calcite, the marbles contain diopside, tourmaline, sulfides, and graphite. The graphite has a biogenic carbon signature, and the marbles are thought to have formed inorganically via stromatolite accretion in an evaporitic environment. Some calcsilicate layers consist of almost monomineralic white, Mg-rich diopside crystals up to 10 cm in length. These are probably the result of metasomatism by fluid phases. The presence of the approximately Mg-pure assemblage

tremolite =>enstatite+diopside+quartz+H_2O

allowed Valley *et al* (1983) to calculate a fluid with $X(H_2O)$ = .11-.14 for the reaction. Elsewhere in the outcrop localized occurrences of wollastonite reflect the presence of H_2O as an agent lowering CO_2 activity. In both cases, the metamorphic conditions were T=710°C and P = 7 kbar. These cases provide excellent examples of how the dilution of a fluid phase by a second constituent lowers activities and allows reactions to run to the right at P,T conditions below that for the pure fluid.

In the High Peaks region there exist many well-exposed examples of places where marble and calcsilicate xenoliths occur within anorthosite. This relationship documents that the marbles are older than ca 1150 Ma. It is likely that they formed during the same shelf sequence event that was posited for the Irving Pond quartzite precursor sands, ie, ca 1220-1200 Ma.

47.2 Roadcuts of steeply dipping metasediments.
47.6 Long roadcuts in ping granitic gneiss interlayered with calcsilicates. The layering here is interpreted as tectonic and the granite as intrusive.
48.7 Small, high roadcut on right (southwest) side of Rt 30. Park on right shoulder.

STOP 8. MASSIF ANORTHOSITE AND FERRODIORITE OF THE OREGON DOME. (30 MINUTES). This small, but instructive roadcut has outstanding examples of two important facies of anorthosite as well as a typical ferrodiorite dike associated with massif anorthosite. The best vantage point for examining the anorthosite and ferrodiorite is on top of the roadcut. Whole rock analyses of these rocks are given in Table 1.

On climbing to the top of the outcrop at its south end, one immediately sees a distinctive dark dike of ferrdiorite filled with plagioclase grains (white, ~An_{43}) and andesine xenocrysts (blue-gray, ~An_{52}); note reaction rims on the blue-gray andesine. The dike exhibits somewhat soft contacts and irregular veinlets shoot off in a fashion suggesting that the anorthosite was not yet wholly solidified when the dike intruded. Farther up the outcrop two ~30cm-scale xenoliths occur in a ~5-10m-scale ferrodiorite; one of these is fine grained and the other coarse. The eastern contact of the ferrodiorite is situated just to the highway-side of the coarse xenolith. Calcsilicate xenoliths also occur in the ferrodiorite and are characterized by sulfidic staining near road level.

Farther up the outcrop the exposed rock consists entirely of anorthosite. A fine-grained, leucocratic facies forms a matrix to large (5-20cm long) crystals of blue-gray, iridescent andesine that is typical of massif

anorthosite. In places these crystals appear broken as if disrupted from a larger mass. An example of a still intact mass is found at the far end of the outcrop where a raft of very coarse grained Marcy-type anorthosite with ophitic to sub-ophitic orthopyroxene sits in a matrix of fine-grained leucoanorthosite that clearly disrupts the raft at its edges. Close inspection of the matrix reveals that its small pyroxenes exhibit subophitic texture; hence the finer grained facies must be magmatic. Workers in Adirondack anorthosite have always noted that grain size reduction produces leucanorthosite similar to this this fine-grained facies, and examples of this may be seen at this stop. However, it is possible to distinguish between the grain size reduced and the fine-grained igneous varieties by noting that plagioclase in the former has the same composition as the coarse plagioclase, whereas the igneous variety is invariably 5-10% less anorthitic than the coarse plagioclase; in this case 52% versus 44% (Boone et al, 1969). Genetic interpretations and further details of the anorthositic suite are given in the main text.

The smooth, upper surface of the outcrop affords excellent opportunities to examine the garnet coronas or "necklaces" that are found throughout the Adirondack anorthosites. These are accounted for by the reaction

Orthopyroxene + Plagioclase + Fe,Ti-Oxide => Garnet + Clinopyroxene $\pm$ SiO_2

Spear and Markussen (1997) have studied this, and other garnet-producing reactions, and determined that they took place during isobaric cooling (P~6-7 kbar) from ~700°-~630°C during waning stages of the Ottawan Orogeny (1090-1030 Ma). McLelland et al (2001) have suggested that this reaction took place at ca 1050 Ma, which is the age of small, equant metamorphic zircons associated with the coronites. The zirconium was provided by Fe-Ti oxide, which accepts significant Zr into the Ti lattice site.

Recent SHRIMP II U-Pb dating of zircons from the ferrodiorite documents its age as 1155 $\pm$ 9 Ma, and this sets a minimum age for the anorthosite. Thirty kilometers to the northeast at Gore Mt, charnockite enveloping, and showing mutually crosscutting relationships with the Oregon Dome anorthosite (Lettney, 1969), yields a SHRIMP II age of 1155 + 6 Ma. These results document that the anorthosite series of the Oregon Dome was emplaced at ca 1150 Ma. This age is indistinguishable from emplacement ages of the Marcy massif and marks the time of emplacement of the Adirondack AMCG suite.

50.7 Minor marble, calcsilicate, amphibolite together with meter-scale layers of white quartz-feldspar leucosomes containing sporadic sillimanite and garnet. SHRIMP II ages of zircons from these outcrops indicate that the leucosomes crystallized from melt at 1180-1170 Ma. This interval is interpreted as the time of anatexis associated with the migmatitic metapelites of the region, and falls into the culminating Elzevirian Orogeny.

51.7 Junction of Rt 8 and Rt 30. Continue south on Rt 30.

52.2 Charnockite on the north limb of the Glens Falls syncline.

54.5 Entering the town of Wells that sits on a Paleozoic inlier dropped down at least 700m by a NNE trending graben structure.

55.0 Leaving town of Wells.

58.7 Pumpkin Hollow. As you round the big bend next to the river look for a large parking area on the right (west) side of Rt 30. Pull into it and park.

STOP 9. MYLONITIC STRAIGHT GNEISS OF MIGMATITIC METAPELITE. (30 MINUTES). Large roadcuts on the east side of Rt 30 expose excellent examples of migmatitic metapelite identical to that seen at Stop 1, but now at a high grade of strain that has resulted in extreme ductile grain size reduction that has produced long tails on the feldspars and remarkable long ribbons of quartz now consisting of annealed subgrains in the process of annealing further into smaller grain size. The high strain has produced a platy mylonite that is a "par-excellence" example of straight gneiss. The alternating light and dark layers represent porcellaneous leucosome together with restitic biotite-garnet-quartz-feldspar $\pm$ sillimanite. Numerous intrafolial isoclinal minor folds can be seen, especially in the leucosome. All of these observations make it clear that the "layering" seen in the outcrop has nothing to do with any primary or "stratigraphic" features, although some observers still try to make this assertion. The layering is strictly tectonic in origin and provides a fine learning opportunity with which to make the case with students (and others). Note the strong N70W lineation on foliation surfaces. A strong component of flattening has also affected these rocks making it difficult to interpret kinematic indicators.

At the south end of the outcrop the mylonitic migmatite is in contact with homogeneous, strongly foliated granitoids of the Piseco anticline. These granitoids have been dated at ca 1155 Ma, while the structurally

overlying migmatites must be at least 1300 Ma of age since they are crosscut by the tonalites. The absence of any crosscutting contact emphasizes how ductile high strain can wipe out angular discordances.

The northerly dip of the mylonitic migmatite sequence is due to the fact that we are located on the southern limb of the Glens Falls syncline or the northern limb of the Piseco anticline. These dipping layers are locally broken across by ductile normal faults with brecciated pegmatite fillings. These features have not been dated, but a ca 1050 Ma age is expected.

END OF FIELD TRIP!! ON TO LAKE GEORGE VILLAGE AND THE WELCOMING PARTY!!!!

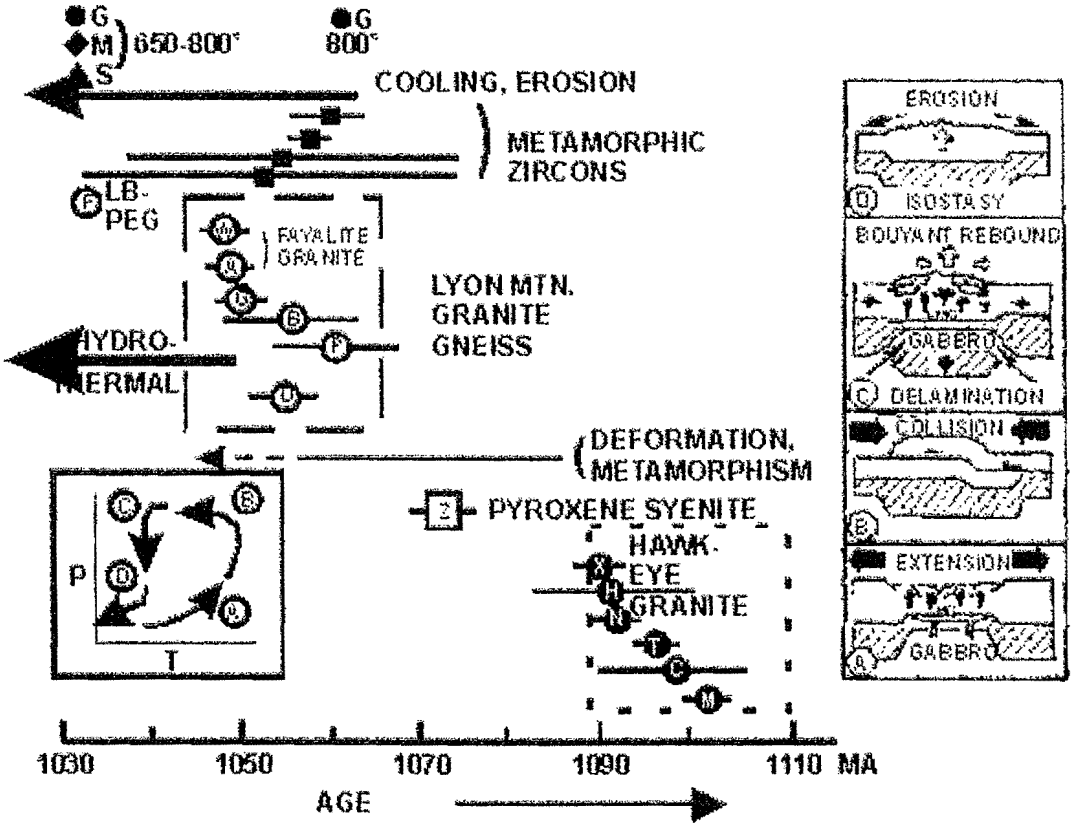

Fig. 12. Geochronological-tectonic history of the Adirondacks during Hawkeye-Ottawan time (ca 1100-1030 Ma). After Mclelland et al (2001). Cartoon on right side depicts dated events on the left. P,T plot shows counterclockwise path suggested by sequence of dated events.

REFERENCES CITED

Barker, F., 1979. Trondhjemite: definition, environment, and hypothesis of origin, in, Barker, F. (ed.), Trondhjemites, dacites, and related rocks: Elsevier, New York, p. 1-12.

Boone, G. M., Romey, W. D., and Thompson, D. S., 1969. Oscillatory zoning in calcic andesine-labradorite relict phenocrysts in anorthosite of Oregon Dome and Giant Mountain, Adirondack Highlands, in, Isachsen, Y. W. (ed), Origin of anorthosite and related rocks: New York State Museum and Science Memoir 18, p. 317-329.

Bohlen, S. R., Valley, J. W., and Essene, E. J., 1985. Metamorphism in the Adirondacks. I. Petrology, pressure, and temperature: Journal Petrology, v. 26, 971-992.

Buddington, A. F., 1939. Adirondack igneous rocks and their metamorphism: Geological Society of America, Memoir 7, 354 p.

Cannon, W. F., 2001. Closing of the Mid-continent rift - a far field effect of Grenvillian compression: Geology, v. 22, p. 155-158.

Carr, S. D., Easton, R. M., Jamieson, R. A., and Culshaw, N. G., 2000. Geologic transect across the Grenville orogen of Ontario and New York.: Canadian Journal Earth Sciences, v. 37, p. 193-216.

Fram M. S. and Longhi, J., 1992. Phase equilibria of dikes associated with Proterozoic anorthosite complexes: American Mineralogist, v. 77, p. 607-616.

Lettney, C., 1969. The anorthosite-norite-charnockite series of the Thirteenth Lake Dome, south central Adirondacks, in, Isachsen, Y. W., ed., Origin of Anorthosite and related rocks: New York State museum and Science Service Memoir 18, p. 329-342.

McLelland, J. M., 1984. Origin of ribbon lineation within the southern Adirondacks, U.S.A.: Journal Structural Geology, v. 6, p. 147-157.

McLelland, J. M. and Husain, J., 1984. Nature and timing of anatexis in the eastern and southern Adirondack Highlands: Journal Geology, v. 94, p. 17-25.

McLelland, J.M. and Chiarenzelli, J., 1990. Isotopic constraints on the emplacement age of anorthositic rocks of the Marcy massif, Adirondack Mts., New York: Journal Geology, v. 98, p. 19-4.

McLelland, J. M. and Chiarenzelli, J., 1991. Geochronological studies in the Adirondack Mountains and the implications of a middle Proterozoic tonalitic suite, in, Gower, C., Rivers, T., and Ryan, B., eds., Mid-Proterozoic geology of the southern margin of Laurentia-Baltica: Geological Association of Canada Special Paper 38, p. 175-194.

McLelland, J. M., Ashwal, L., and Moore, L., 1994. Composition of oxide-, apatite-rich gabbronorites associated with Proterozoic anorthosite massifs: examples from the Adirondack Mountains, New York: Contributions to Mineralogy and Petrology, v. 116, p. 225-238.

McLelland, J. M., Daly, J. S., and McLelland, Jo., 1996. The Grenville Orogenic Cycle (ca. 1350-1000 Ma): an Adirondack perspective: Tectonophysics, v. 265, p. 1-28.

McLelland, J. M., Hamilton, M., Selleck, B., McLelland, Jo., Walker, D., and Orrell, S., 2001. Zircon U-Pb geochronology of the Ottawan Orogeny, Adirondack Highlands, New York: regional and tectonic implications: Precambrian Research, v. 109, p. 39-72.

McLelland, J. M., Morrison, J., Selleck, B., Cunningham, B., Olson, C., and Schmidt, K., 2002. Hydrothermal alteration of late- to post-tectonic Lyon Mountain Granitic Gneiss, Adirondack Mountains, New York: Origin of quartz-sillimanite segregations, quartz-albite lithologies, and associated Kiruna-type low-Ti Fe-oxide deposits: Journal Metamorphic Geology, v. 20, p. 175-190.

Mezger, K., Essene, E. J., and Halliday, A. N., 1992. Closure temperatures of the Sm-Nd system in metamorphic garnets: Earth and Planetary Science Letters, v. 113, p. 397-409.

Moore, J. and Thompson, P., 1980. The Flinton Group: a late Precambrian sedimentary succession in the Grenville Province of eastern Ontario: Canadian Journal of Earth Science, v. 17, 1685-1707.

Mosher, S., 1998. Tectonic evolution of the southern Laurentian Grenville orogenic belt: Bulletin of the Geological Society of America, v. 110, p. 1357-1375.

Patchett, J. and Ruiz, J., 1990. Nd isotopes and the origin of the Grenville-age rocks in Texas: Implications for the Proterozoic evolution of the United States, mid-continent region: Journal of Geology v. 97, p. 685-696.

Ratcliffe, N. M., Aleinikoff, J. N., Burton, J. N., and Karabinos, P., 1991. Trondhjemitic, 1.35-1.31 Ga gneisses of the Mount Holly Complex of Vermont: evidence for an Elzevirian event in the Grenville basement of the U.S. Appalachians: Canadian Journal Earth Sciences.

Silver, L. T., 1969. A geochronologic investigation of the Adirondack Complex, Adirondack Mountains, New York, in, Isachsen, Y. W., ed., New York State Museum and Science Service Memoir 18, p. 233-252.

Spear, F. S. and Markussen, J. C., 1997. Mineral zoning, *P-T-X-M* phase relations, and metamorphic evolution of some Adirondack granulites, New York: Journal Petrology, v. 38, p. 757-783.

Roback, R. C., Characterization and tectonic evolution of a Mesoproterozoic island arc in the southern Grenville Orogen, Llano uplift, central Texas: Tectonophysics, v. 265, p. 29-52.

Rivers, T., 1997. Lithotectonic elements of the Grenville Province: review and tectonic implications: Precambrian Research, v. 86, p. 117-154.

Valley, J. W., 1985. Polymetamorphism in the Adirondacks, in, Tobi, A. and Touret, J., eds., The deep Proterozoic crust of the North Atlantic Provinces, NATO ISI Series V. 158: D.Reidel, p. 217-236.

Valley, J. W., McLelland, J. M., Essene, E. J., and Lamb, W., 1983, Metamorphic fluids in the deep crust: evidence from the Adirondacks: Nature, v. 301, p. 226-228.

Wasteneys, H., McLelland, J. M., and Lumbers, S., 1999. Precise zircon geochronology in the Adirondack Lowlands and implications for revising plate tectonic models of the Central Metasedimentary Belt and Adirondack Mts, Grenville Province, Ontario and New York: Canadian Journal Earth Sciences, V. 36, p. 967-984.

METAMORPHISM, COOLING RATES, AND MONAZITE GEOCHRONOLOGY OF THE SOUTHERN ADIRONDACKS[1]

by
Lara C. Storm and Frank S. Spear
Department of Earth and Environmental Sciences, Rensselaer Polytechnic Institute, Troy, NY 12180

[1]This article accompanies the field trip guide "Geology and Geochronology of the Southern Adirondacks"

INTRODUCTION

Metamorphism in the Adirondacks has been the subject of investigation for over a century, beginning with the early work of Ebenezer Emmons. As summarized by Bohlen et al. (1985) and Valley et al. (1990), the Adirondack highlands have been characterized by a more-or-less concentric ("bull's eye") pattern of peak-metamorphic isotherms, based largely on re-integrated Fe-Ti oxide and feldspar thermometry (Fig. 1a). Published P-T paths for the central Adirondacks are counter-clockwise with cooling from peak conditions inferred to be nearly isobaric (Bohlen et al., 1985; Spear and Markussen, 1997).

The initial motivation for undertaking petrologic investigation of the southern Adirondacks was two-fold. Firstly, significant outcroppings of high-grade pelitic gneisses (migmatites) occur in the southern and eastern Adirondacks, and rocks of these bulk compositions have not been examined in detail using modern petrologic methods. Secondly, the isotherm pattern (Fig. 1a) indicates that the lowest grade metamorphic rocks (<675 °C) occur in the southern Adirondacks, making this an excellent area to test the validity of the metamorphic "bull's eye". Additionally, previous studies (e.g. Whitney, 1978) report the presence of migmatites in the southern Adirondacks, suggesting that the peak temperatures might be significantly higher than suggested by Fe-Ti oxide and feldspar thermometry.

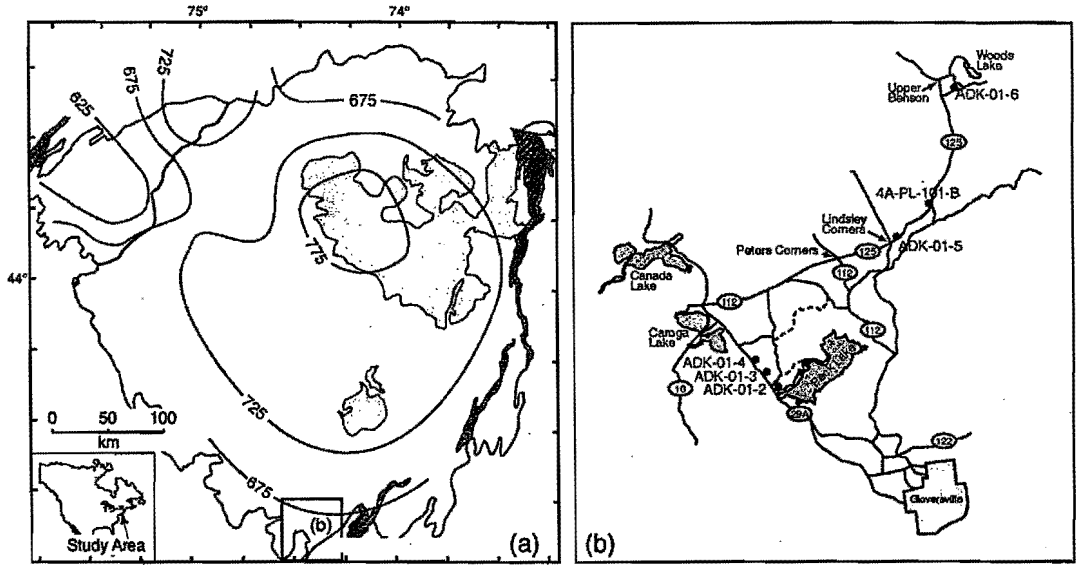

Figure 1. (a) The thermal "bull's eye" of Bohlen et al. (1985) superimposed on a map of the Adirondacks. An enlarged map of area (b) showing roads, locations, and sample numbers.

PETROGRAPHY

Eleven samples from five outcrops in the southern Adirondacks were collected during the winter of 2001 for detailed investigation (see Fig. 1b for localities). An additional sample (4A-PL-101-B) was obtained from J. McLelland. All outcrops examined contain highly foliated aluminous pelitic gneisses and many of the samples are sillimanite-bearing. Migmatites are abundant with the percentage of leucosomes ranging from a few per cent to one-fourth of the outcrop.

The dominant assemblage in the investigated samples includes biotite + quartz + plagioclase + K-feldspar ± garnet ± sillimanite + Fe-Ti oxides ± monazite ± apatite. Melanosomes contain the above assemblage whereas leucosomes are dominated by quartz + plagioclase + K-feldspar. Many leucosomes contain garnet crystals, suggesting leucosome formation by the reaction

$$Bt \pm Sil + Pl + Qtz = Grt + Kfs + L \quad (1)$$

Prograde muscovite (except for retrograde sericite) is not present, indicating that peak P-T conditions were above the muscovite dehydration melting reaction. In addition, late muscovite has been found in only one sample, suggesting that in most samples, all melt that was produced from muscovite dehydration (Rxn. 2) has been expunged from the rock.

$$Ms + Pl + Qtz = Kfs + As + L \quad (2)$$

The single muscovite-bearing sample (ADK-01-5) displays the unusual texture of muscovite pseudomorphs after sillimanite, in association with quartz. Retrograde progress of reaction 2 is inferred to be the origin of this late muscovite.

Cordierite and orthopyroxene were not observed in any samples (and, to our knowledge have not been reported in metapelitic rocks from the southern Adirondacks), restricting P-T conditions to lie below the reactions

$$Bt + Sil + Pl + Qtz = Grt + Crd + Kfs + L \quad (3)$$

and

$$Bt + Grt + Pl + Qtz = Opx + Sil + Kfs + L \quad (4)$$

These petrographic observations are consistent with the migmatites having formed from dehydration melting. During dehydration melting the activity of water (a_{H_2O}) is buffered by the solid + liquid assemblage to values less than $P_{H_2O} = P_{total}$, consistent with the general observation of low a_{H_2O} in Adirondack granulites. Thus, in the absence of large scale fluid infiltration (e.g. Valley et al., 1990), experimental and calculated dehydration melting reactions place broad limits on the peak P-T conditions of the southern Adirondacks (Fig. 2).

GARNET ZONING AND REACTION HISTORY

Garnet crystals are resorbed and display chemical zoning that reflects a multiple-stage growth history (Fig. 3). Garnet cores are relatively unzoned in major elements ($X_{prp} = 0.053$, $X_{alm} = 0.330$, $X_{sps} = 0.0095$, $X_{grs} = 0.017$). Towards the garnet rim, Fe and Fe/(Fe+Mg) increase whereas Mg decreases, consistent with diffusion controlled zoning produced during melt crystallization by the retrograde progress of reaction 1 during cooling.

Grossular content is higher near garnet rims and does not display diffusive zoning as seen in Fe and Mg. The higher grossular content on the rims can be explained by the following reaction sequence. Progress of the muscovite melting reaction (Rxn. 2) exhausted the southern Adirondack rocks of all muscovite and altered the modes and compositions of plagioclase, potassium feldspar, and sillimanite. Reaction 2 (muscovite dehydration melting) proceeds over a relatively small temperature interval until all muscovite is exhausted. Plagioclase involved in this reaction becomes more anorthitic as melting proceeds, as does coexisting melt. Garnet is not involved in Reaction 2, so at the beginning of the reaction, garnet will be in equilibrium with a plagioclase that is more albitic than at the end of the reaction. When garnet growth resumes by Reaction 1, newly grown garnet will be more Ca-rich,

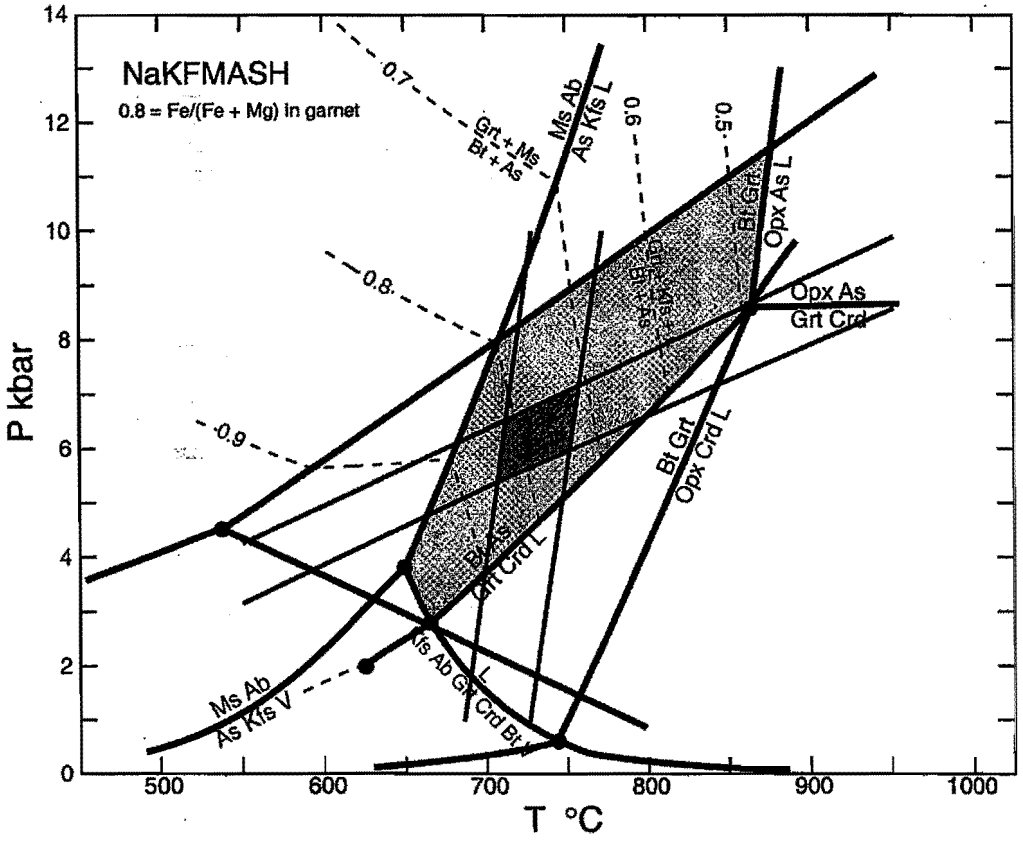

Figure 2. A P-T diagram showing the narrow P-T region to which the peak metamorphic conditions are restricted. The boundaries of the region are determined by the presence of melt and the absence of cordierite or orthopyroxene in metapelitic rocks. The darker parallelogram shows the peak P-T conditions defined by geothermobarometry.

reflecting equilibrium with the more anorthitic plagioclase, producing the observed discontinuous increase in grossular content (e.g. Spear and Kohn, 1996). Therefore, the high-calcium rims are thought to represent the melt-produced garnet, and lower Ca-cores are garnet produced by sub-solidus reactions.

THERMOBAROMETRY

There is clear evidence in the southern Adirondack metapelites for both retrograde Fe-Mg exchange reactions (ReERS) and retrograde net transfer reactions (ReNTRs), making recovery of peak metamorphic compositions for use in thermobarometry difficult (e.g. Kohn and Spear, 2000). ReNTRs and ReERs produce different compositional changes in garnet and biotite. Fe-Mg exchange results in garnet increasing and biotite decreasing their Fe/(Fe+Mg) at the reaction interface as temperature decreases. Reaction 1r results in both garnet and biotite increasing their Fe/(Fe+Mg) as temperature decreases. Temperatures calculated using garnet-biotite pairs that have been affected by ReNTRs and ReERs can be higher, lower, or fortuitously the same as the peak temperature.

Retrograde Fe-Mg exchange has clearly affected biotite inclusions within garnet (Fig. 4). The zoning observed at garnet rims (Fig. 3), in addition to the resorbed shape, suggests retrograde progress of reaction 1:

$$\text{Grt} + \text{Kfs} + \text{L} = \text{Bt} \pm \text{Sil} + \text{Pl} + \text{Qtz} \qquad \text{(1r)}$$

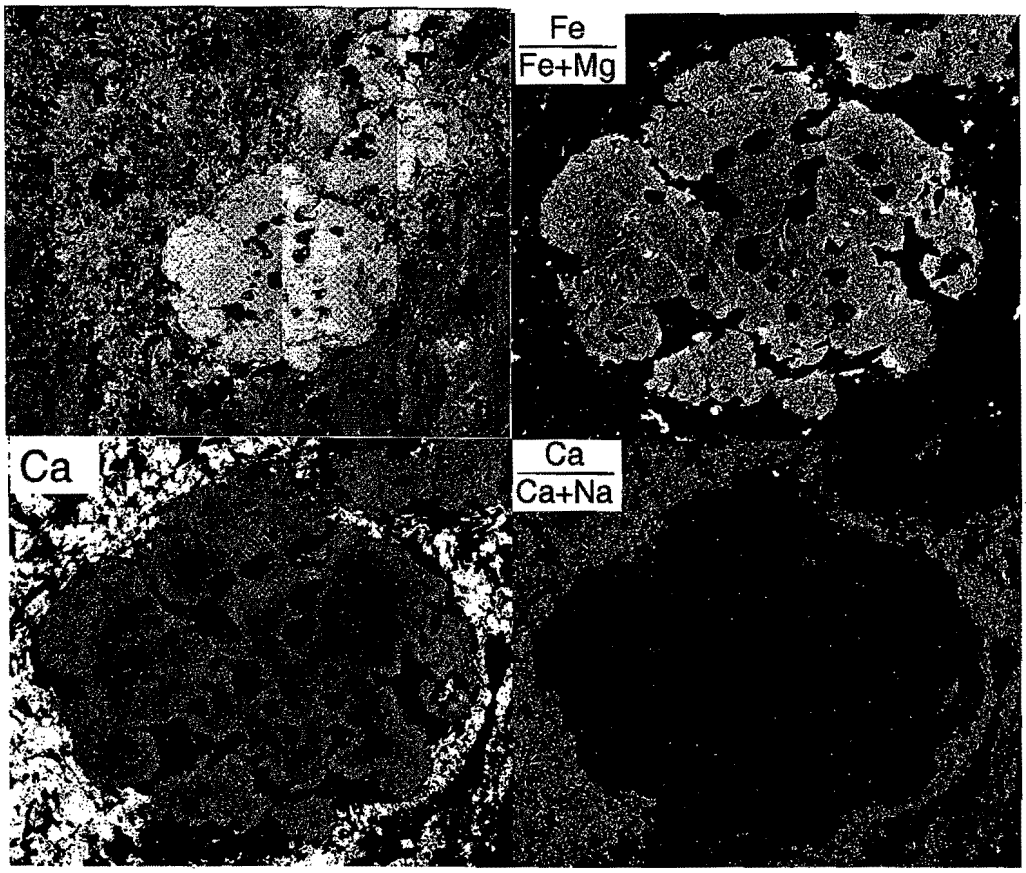

Figure 3. X-ray maps of a garnet from sample 4A-PL-101-B. This garnet displays rims with higher Ca and Fe/(Fe+Mg), which is interpreted to be garnet produced during dehydration melting. The garnet also shows a textural change across the high-Ca rim where inclusions are smaller and more numerous. The matrix plagioclase is slightly zoned in Ca/(Ca+Na).

which occurs as melt crystallizes in leucosomes. ReNTRs such as reaction 1r are ubiquitous in migmatites because the H_2O needed to rehydrate the solid phases (in this case biotite) is dissolved in the liquid and exsolves as the liquid crystallizes. The presence of muscovite pseudomorphs after sillimanite further suggests retrograde progress of reaction 2.

The approach taken here is to use the composition of the garnet core well away from biotite inclusions with the composition of matrix biotite away from the garnet rim. Although the matrix biotites may have been affected by reaction 1r (which would yield a temperature higher than the peak T), the extent of reaction 1r is not large, as evidenced by the absence of Mn zoning on the rim. Peak pressures were calculated using the high-Ca rim with matrix plagioclase.

Results of thermobarometry calculations are summarized in Figure 2. The garnet-biotite thermometer of Patiño Douce et al (1993) was used because it takes into consideration the Ti-content of biotite. The GASP barometer of Hodges and Crowley (1985) was used to determine minimum and maximum pressures (high-Ca garnet with low-Ca plagioclase and vice-versa) which define a narrow pressure range. Only curves representing the range of conditions believed to be representative of the peak conditions are shown. The peak temperature is approximately 710-740 °C

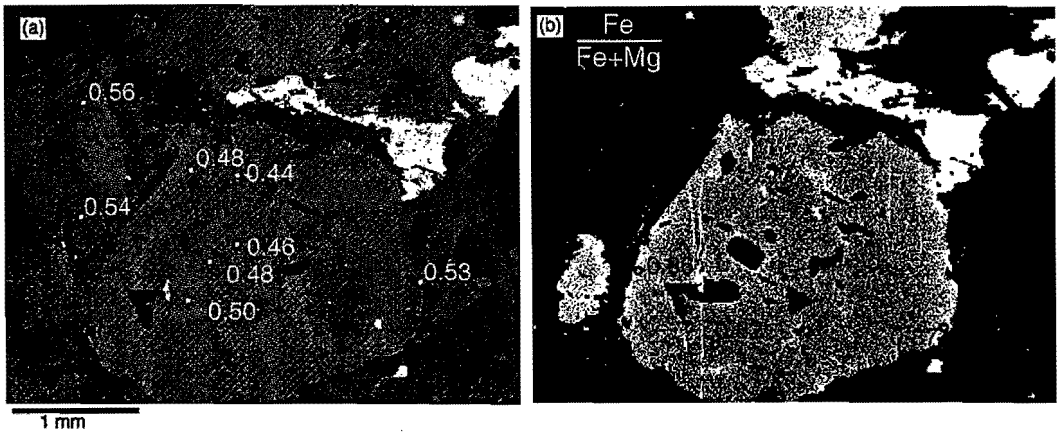

Figure 4. (a) Backscatter image of garnet from sample ADK-01-5, which contains a plethora of variably sized biotite inclusions. Numbers are Fe-Mg ratios for different biotite grains. Note that Fe/(Fe+Mg) of biotite within garnet is a function of the size of the inclusion. (b) X-ray map showing Fe/(Fe+Mg) in garnet. Numbers are measured Fe/(Fe+Mg). Note high-Fe rims on garnet and high halos around biotite inclusions. Cooling rate calculations performed on this garnet yield a cooling rate of around 2 to 5 °C/Ma (see Figure 6).

at 6 kbar, and is consistent with the constraints imposed by mineral assemblages. It should be noted that this temperature is significantly higher than the < 675 °C predicted by the bull's eye pattern (Fig. 1a), and suggests that the peak metamorphic temperatures in the Adirondacks may not be concentric around the anorthosite (see also Whitney, 1978). It may also be significant that the peak pressure of 6 kbar is lower than that recorded in the central highlands (e.g. Spear and Markussen, 1997), suggesting that there may be a gradient in peak pressure from north to south.

COOLING RATES FROM GARNET-BIOTITE FE-MG EXCHANGE

Spear and Parrish (1996) present a method that utilizes the exchange of Fe and Mg between biotite inclusions within garnet and garnet host to estimate post-peak cooling rates. As seen in Figure 4, there is a correlation between the Fe/(Fe+Mg) of biotite inclusions and size of the inclusion. Minor zoning of Fe/(Fe+Mg) is observed in garnet around biotite inclusions, but the magnitude of this zoning prohibits precise constraints on cooling rates. This method circumvents this limitation by using the composition of the biotite as a monitor of the total flux of Fe and

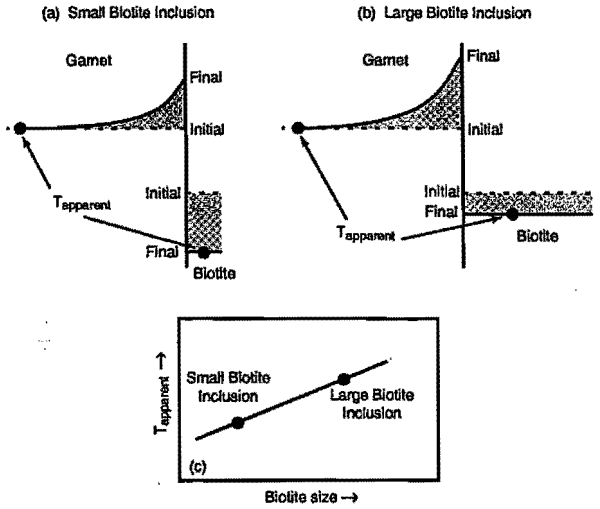

Figure 5. An illustration of the relationship between biotite inclusion size and Fe/Mg. (a) The smaller biotite inclusion experiences a greater increase in Mg than the larger biotite (b) because for a fixed diffusive flux there is a smaller volume over which to distribute the incoming Mg. (c) A plot of the apparent T calculated from garnet-biotite thermometry versus log of biotite size showing the predicted linear relationship.

Mg between biotite and garnet. Because diffusivity of Fe and Mg in biotite is rapid relative to garnet, biotite inclusions are generally homogeneous. Application of this method is simple. An apparent temperature is calculated using the composition of the biotite inclusion and the composition of the garnet core away from the inclusion (so that it has not been affected by diffusion; see Fig. 5). The apparent temperature is plotted against a measure of biotite size, and cooling rate isopleths are estimated from model simulations of the diffusive exchange between garnet and biotite at different cooling rates. A large uncertainty in application of the method stems from the difficulty in obtaining an accurate measure of the volume of the biotite inclusion. Firstly, the shape of the crystals is irregular, and it is not usually apparent what geometry should be assumed. Secondly, there is no certainty that the thin section cut goes through the maximum dimension of the biotite so that the true size can be viewed in thin section. Spear and Parrish (1996) explored a number of ways of measuring the biotite size including the use of area percents and linear measurements coupled with cylindrical and spherical geometries. They concluded that the uncertainties were similar with each method and gave similar cooling rates (provided that the model diffusion calculations were plotted each with the same measure of size). A simple linear measure of biotite diameter along the cleavage trace proved to be the easiest way to apply this approach.

Results of the application of this approach to one sample from the southern Adirondacks are presented in Figure 6. Although there is some scatter in the data, the plot reveals the cooling rate to be between 1 and 10 °C/Ma. This is a relatively slow cooling rate and is consistent with the post-peak cooling rate inferred by Mezger et al. (1989, 1991) of about 5 °C/Ma based on U/Pb geochronology of the minerals garnet, biotite, hornblende, sphene, monazite, and rutile.

A slow cooling rate is also consistent with the inferred P-T path of nearly isobaric cooling. The peak P-T conditions of around 725 °C and 6 kbars reflect an elevated geotherm (i.e. higher than steady state) at the peak of metamorphism. Thermal decay of such an elevated geotherm back to a steady state condition by thermal conduction over the length scale of the entire crust (40-60 km) occurs over a time scale ($t = x^2/K$) of 50-100 Ma, requiring 100-200 million years to cool from the peak temperature of approximately 725 °C to the steady state value of approximately 525 °C at 0.6 GPa. This simple cooling model of 200 °C in 100-200 million years yields an average cooling rate of approximately or 1-2 °C/Ma.

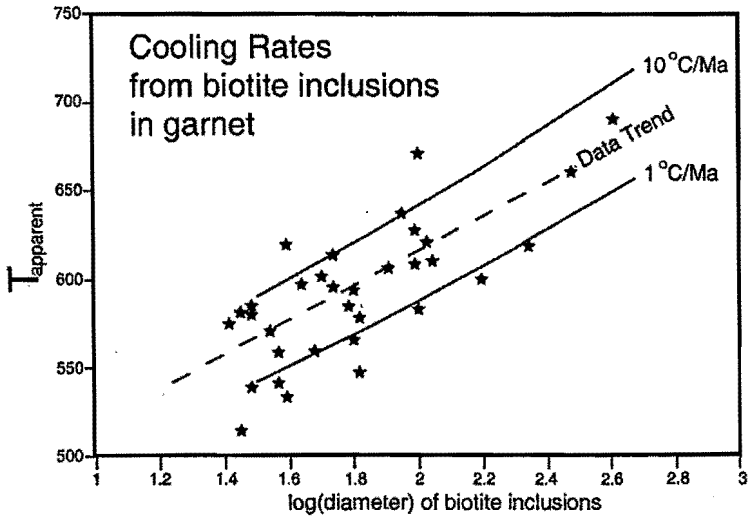

Figure 6. A plot of apparent temperature vs. log of the biotite inclusion diameter for sample ADK-01-5 (Fig. 4). Apparent temperatures are obtained using garnet-biotite thermometry (inclusion + garnet core composition). The cooling rate isopleths were calculated using a finite-difference diffusion program. The plot reveals a cooling rate between 1 and 10 °C/Ma.

GEOCHRONOLOGY

Introduction

Chemical dating using the electron microprobe is a texture-sensitive approach that enables ages of discrete chemical domains within monazite to be determined. Under optimal conditions, Pb can be measured on the electron microprobe to a precision of ±25 ppm (1 σ s.e.). In Proterozoic monazites such as are found in the southern Adirondacks, the Pb content is typically greater than 2000 ppm, enabling ages to be determined to a precision on the order of 1% (i.e. 10 Ma out of 1000). In practice, multiple analyses of the same material yield a precision on the order of ±20-30 Ma (1 σ s.e.), but this age resolution is sufficient to distinguish various phases of Grenville metamorphism.

Monazite petrography, chemical zoning, and ages

Monazite is nearly ubiquitous in the migmatitic gneisses of the southern Adirondacks. It occurs as inclusions in all the major phases and within the matrix. Monazite is complexly zoned, suggesting that it might record several episodes of growth.

Monazite inclusions within other phases. Monazite inclusions are found in garnet in at least one sample from every outcrop (Fig. 1b). Several monazite crystals in this textural setting are rounded with compositional truncations that can be seen in BSE images (Fig. 7). X-ray maps reveal chemical zoning characterized by high Y values separated by a low-Y region, suggesting a multiple-stage growth.

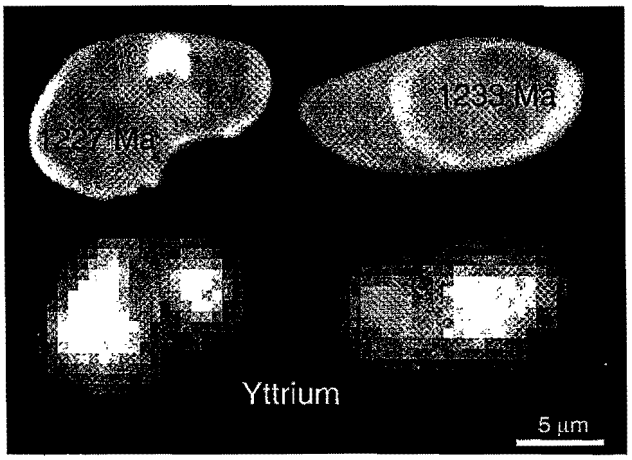

Figure 7. Monazites from sample ADK-01-2 showing what appear to be detrital cores that give ages of around 1230 Ma. These monazites occur as inclusions in garnet and range from about 5 to 10 microns in diameter. The X-ray maps show that the old cores have a higher concentration of Y. The youngest ages given by monazites included within garnet (not shown) are Ottawan.

Ages determined from the CHIME method yield 1227-1233 ± 10 Ma for the high-Y parts. These are some of the oldest ages encountered in the southern Adirondack monazites and represent an Elzevirian event. The age of the sedimentary protolith of the southern Adirondack paragneisses is not known, and it may be that these monazites pre-date sedimentation. We make the tentative suggestion that these are detrital relics.

Partially included and matrix monazites. Several monazites examined in this study are embedded in the outer, melt-produced rims of garnet (Fig. 8 and 9). Others are in the rock matrix. Zoning in all of these monazites is complex (Figs. 8-10) and indicates several growth phases. The similarities in zoning and overlap in ages indicates that the partially included monazites were in equilibrium with the matrix throughout the metamorphic history.

Several groups of ages are recorded in these monazites (Figs. 8-11), including 1165-1185 Ma, 1125 Ma, 1088-1112 Ma, 1028-1048 Ma, 923 Ma, and 386 Ma. In general, the ages are arranged with oldest in the cores and youngest on the rims. Furthermore, the age domains are usually chemically distinct. The oldest group (1165-1185 Ma) occurs only in the cores of monazite crystals. These ages correspond to either the waning stages of the Elzevirian orogeny (1300-1180 Ma), or the earliest stages of the intrusion of the AMCG suite (1160-1120). The 1125 Ma age is found in the chemically distinct core of a partially included monazite (Fig. 8). It is not possible at this time to ascertain whether this monazite formed during the waning stage of the AMCG suite intrusion, or during the initial stage of the Ottawan orogeny (1090-1045 Ma). Near the rims of several

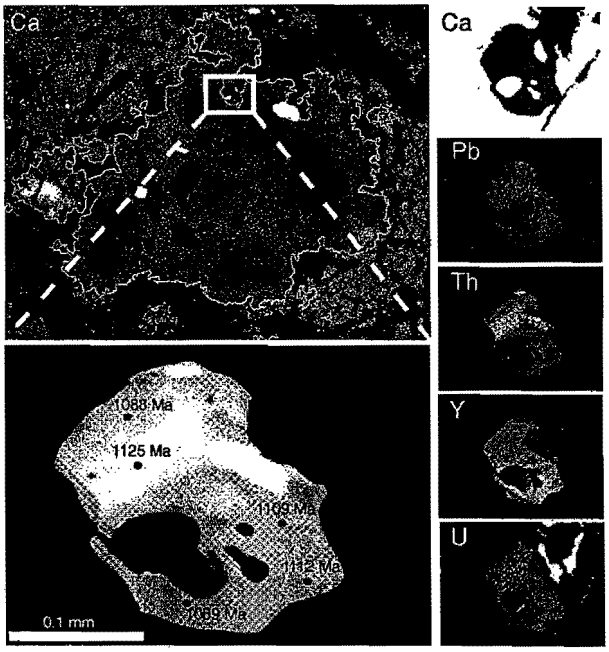

Figure 8. Garnet and monazite from sample ADK-01-4. The garnet has a high-Ca, melt-generated rim. Monazite is embedded (not included) within the garnet. The age distribution (1125-1088 Ma) corresponds to chemical zoning in monazite.

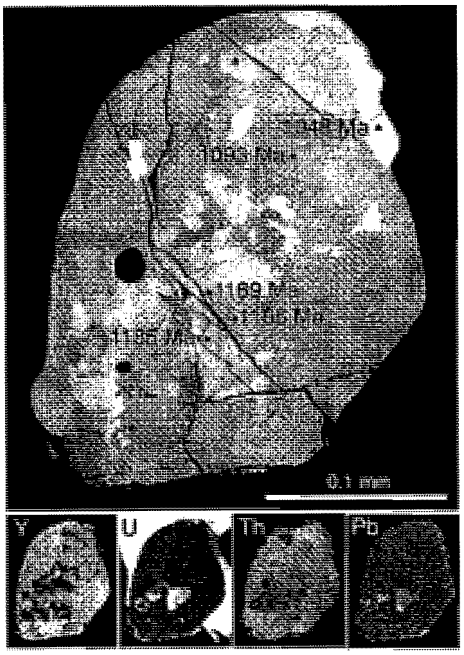

Figure 9. A partially included monazite grain from sample ADK-01-2 displaying complex patchy zoning of Y, U, Th, and Pb. This monazite appears to have three age populations at 1165-1185 Ma, 1093 Ma, and 1048 Ma.

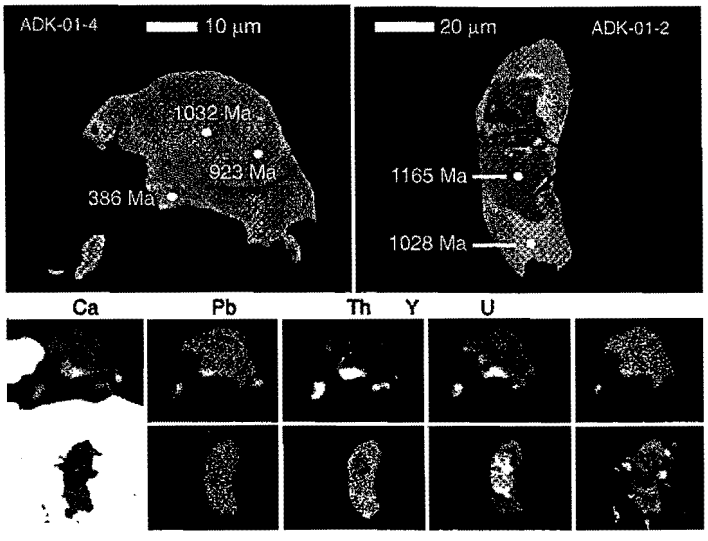

Figure 10. Top panels: BSE images of matrix monazite grains from samples ADK-01-4 and ADK-01-2 showing CHIME ages. Bottom panels: X-ray maps showing chemical zoning in the same grains. Age distribution correlates well with observed zoning patterns. Note the Acadian rim on the monazite from sample ADK-01-4.

monazites are ages of 1112-1088, which correspond to the early stages of the Ottawan orogeny, and possibly represent monazite growth during prograde metamorphism of the pelite. Another suite of ages ranging from 1028-1048 Ma occurs on the monazite rims. The fact that these ages occur on the rims of rocks that had undergone partial melting suggests that they may have formed during melt crystallization. If so, these ages represent the waning stages of the Ottawan orogeny. The 923 Ma age (Fig. 10) may reflect monazite growth associated with the Cathead Mountain dike swarm, which is dated at 935 ± 9 Ma. (McLelland et al., 2001).

A few matrix monazites yielded Paleozoic ages of approximately 400 Ma on their outermost rims (e.g. Fig. 10). The chemistry of these monazite rims is distinct from the rest of the grain and is readily observable with BSE or chemical mapping. The significance of monazite growth at these times is not entirely clear. The inferred thermal history of the Adirondacks predicts that these rocks should not have been hotter than approximately 400 °C, so it is not reasonable that prograde metamorphic reactions were responsible for this growth. The most likely interpretation is that these bits of monazite were deposited from hydrothermal fluids. The correlation of the measured ages with the Acadian metamorphic events to the east may not be coincidental. It is suggested that hydrothermal fluids expunged from rocks to the east by tectonic loading may have been the agent of monazite formation during the Paleozoic.

Allanite geochronology

Monazite crystals from one sample (ADK-01-3) display thin rims of allanite (Fig. 11). This sample exhibits sericite alteration of K-feldspar and minor chloritization of biotite. The allanite is unusually Th-rich, probably because the monazite from which it was formed was Th-rich.

Chemical dating of three allanite rim spots yields ages of 353, 155, and 144 Ma. It is suspected that the 353 Ma age may be a mixed age combining the Proterozoic core and Jurassic rim. Jurassic ages are surprising from the southern Adirondacks, and their significance is not entirely clear. During prograde metamorphism, allanite replaces monazite in the biotite zone (T ~ 300-350 °C; Wing et al., 1999). Apatite fisson tracks from the Adirondacks (closure temperature of 100-120 °C) record ages that are slightly younger (100-125 Ma; Roden-Tice et al., 2000), so it is clear that the rocks could not have been very hot (or deep) when the allanite formed. The cause of the allanite formation is even more perplexing. The continent was undergoing rifting at this time and allanite must be the product of hydrothermal alteration. Its formation is likely to have been caused by the same fluids that caused seritization and chloritization. North-south trending normal faults are prevalent in this area, and it is possible that hydrothermal fluids gained access to moderate crustal levels as a consequence of this faulting.

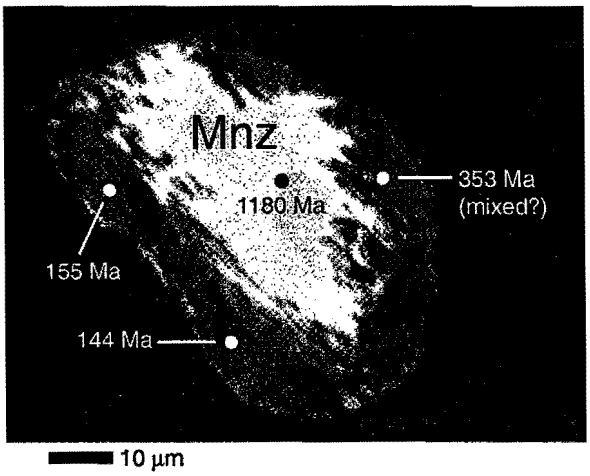

Figure 11. A Proterozoic monazite from sample ADK-01-3 displaying alteration rims of allanite that were formed during the late Jurassic.

Cooling history

Figure 12 shows the inferred thermal history of the southern Adirondacks based on these and published data. The temperature corresponding to the oldest monazite ages (1220-1230 Ma – detrital?) is unconstrained. Ages corresponding to intrusion of the AMCG suite (1160-1120 Ma) may reflect early contact metamorphism or hydrothermal activity associated with plutonism. Ages in the range 1088-1112 Ma likely reflect monazite growth during prograde Ottawan metamorphism and ages in the range 1028-1048 Ma corresponds to monazite

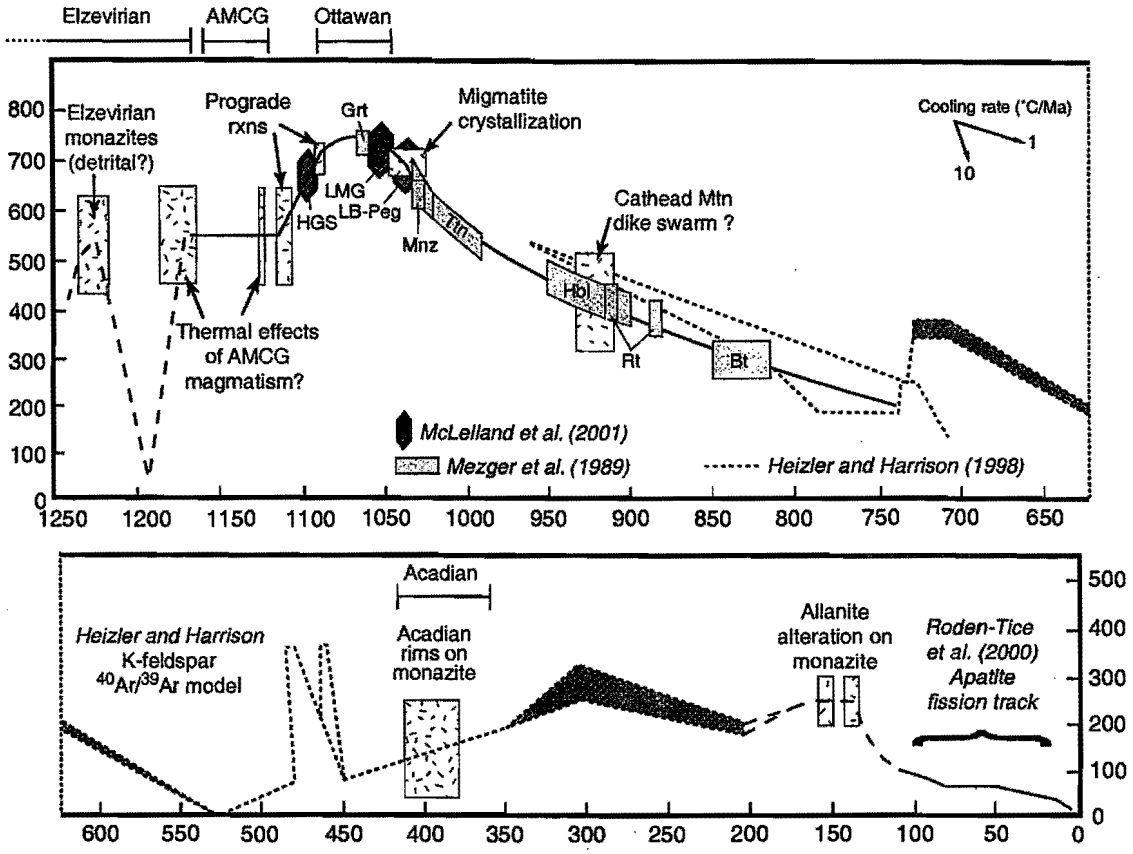

Figure 12. Temperature-time plot summarizing data from Mezger et al. (1989), McLelland et al. (2001; zircon shapes), Heizler and Harrison (1998; $^{40}Ar/^{39}Ar$)), Roden-Tice et al. (2000; apatite fission track), and this study (boxes with the confetti pattern). Abbreviations are: HGS = Hawkeye Granite Suite, LB-Peg = Undeformed pegmatite from Lyonsdale Bridge Falls, LMG = Lyon Mountain Gneiss; mineral abbreviations include Bt = biotite, Grt = garnet, Hbl = hornblende, Mnz = monazite, Rt = rutile, Ttn = titanite (sphene).)

growth during melt crystallization. The still younger age of 923 Ma probably represents monazite growth in association with pegmatite intrusions.

The Adirondacks were overlain unconformably by the Potsdam sandstone in the early Cambrian, so the temperature of the rocks must have been near surface temperatures. $^{40}Ar/^{39}Ar$ thermochronology (Heizler and Harrison, 1998) indicates a complex Paleozoic thermal history, with maximum temperatures reaching 400 °C. The temperature of allanite formation is not known, but it is probably between 200-300 °C. Fission track ages require a temperature of 100-120 °C at 120 Ma, suggesting that there may have been a pulse of rapid uplift in the middle Jurassic.

REFERENCES CITED

Bohlen, S.R., Valley, J., and Essene, E., 1985, Metamorphism in the Adirondacks. I. Petrology, pressure, and temperature: Journal of Petrology, v. 26, p. 971-992.

Heizler, M.T., and Harrison, T.M., 1998, The thermal history of the New York basement determined from $^{40}Ar/^{39}Ar$ K-feldspar studies: Journal of Geophysical Research, v. 103, no. B12, p. 29795-29814.

Hodges, K.V., and Crowley, P.D., 1985, Error estimation and empirical geothermobarometry for pelitic systems: American Mineralogist, v. 70, p. 702-709.

Kohn, M.J., and Spear, F.S., 2000, Retrograde net transfer reaction insurance for pressure-temperature estimates: Geology, v. 28, no. 12, p. 1127-1130.

McLelland, J., Hamilton, M., Selleck, B., McLelland, J., Walker, D., and Orrell, S., 2001, Zircon U-Pb geochronology of the Ottawan Orogeny, Adirondack Highlands, New York: regional and tectonic implications: Precambrian Research, v. 109, p. 39-72.

Mezger, K., Hanson, G.N., and Bohlen, S.R., 1989, High-precision U-Pb ages of metamorphic rutile: application to the cooling history of high-grade terranes: Earth and Planetary Science Letters, v. 96, p. 106-118.

Mezger, K., Rawnsley, C., Bohlen, S., and Hanson, G., 1991, U-Pb garnet, sphene, monazite, and rutile ages: Implications for the duration of high grade metamorphism and cooling histories, Adirondack Mts., New York: Journal of Geology, v. 99, p. 415-428.

Patino Douce, A. E., Johnston, A.D., and Rice, J.M., 1993, Octahedral excess mixing properties in biotite: A working model with applications to geobarometry and geothermometry: American Mineralogist, v. 78, p. 113-131.

Roden-Tice, M.K., Tice, S.J., and Schofield, I.S., 2000, Evidence for differential unroofing in the Adirondack Mountains, New York State, determined by apatite fission-track thermochronology: Journal of Geology, v. 108, p. 155-169.

Spear, F.S., and Kohn, M.J., 1996, Trace element zoning in garnet as a monitor of crustal melting: Geology, v. 24, p. 1099-1102.

Spear, F.S., and Markussen, J.C., 1997, Mineral zoning, P-T-X-M phase relations, and metamorphic evolution of some Adirondack granulites, New York: Journal of Petrology, v. 38, no. 6, p. 757-783.

Spear, F.S., and Parrish, R.R., 1996, Petrology and cooling rates of the Valhalla Complex, British Colombia, Canada: Journal of Petrology, v. 37, no. 4, p. 733-765.

Valley, J., Bohlen, S.R.; Essene, E.J., and Lamb, W., 1990, Metamorphism in the Adirondacks. II. The role of fluids: Journal of Petrology, v. 31, pt. 3, p. 555-596.

Whitney, P.R., 1978, The significance of garnet isograds in the granulite facies rocks of the Adirondacks: in Metamorphism in the Canadian Shield, Geol. Survey of Canada, Paper 78-10, p. 357-366.

Wing, B.A., Ferry, J.M., and Harrison, T.M., 1999, The age of andalusite and kyanite isograds in New England from Th-Pb ion microprobe dating of monazite: Geological Society of America Abstracts with Programs, v. 31, p. A-40.

BEST KEPT GEOLOGIC SECRETS OF THE ADIRONDACKS AND CHAMPLAIN VALLEY

by
Mary K. Roden-Tice, Center for Earth and Environmental Science, Plattsburgh State University of New York, Plattsburgh, NY 12901

INTRODUCTION

Finding clear, well-exposed field locations to help illustrate important aspects of petrology and structural geology to undergraduate students can be a challenge for a professor. In this field trip, we will visit the following four field stops in the Adirondack Mountains and Champlain Valley that are routinely used in my classes: the Cannon Point intrusive south of Essex; the Craig Harbor faultline scarp in Port Henry; the intrusion breccia in Roaring Brook on Giant Mt.; and Split Rock Falls crackle zone south of New Russia. In structural geology, the class works on field exercises that illustrate normal faulting at Craig Harbor and different orientations of joint sets at Split Rock Falls. Petrology students compare Proterozoic anorthosite containing xenoliths of metasedimentary rocks from the Roaring Brook intrusion breccia on Giant Mt. with a Cretaceous laccolith of trachyte porphyry on the shore of Lake Champlain. All of these outcrops are easily accessible and provide excellent opportunities for experiential learning.

REGIONAL GEOLOGY

Summary

The Adirondack Mountains are a regionally elevated exposure of Grenville age (ca. 1.0-1.35 Ga; McLelland et al., 1988; McLelland and Chiarenzelli, 1990; Mezger et al., 1991; McLelland et al., 1996) high-grade metamorphic rocks in northern New York state. This field trip will examine granulite-facies metaplutonic rocks (McLelland and Isachsen, 1986) in the Adirondack Highlands which comprise the central and eastern portions of the massif. An abrupt transition in topography occurs between the Adirondack Highlands and the Lake Champlain Valley between New York and Vermont with local relief along Lake Champlain varying from ~170 to 370 m. The flatter terrain of the Champlain Valley in New York is composed of Paleozoic sedimentary rocks ranging in age from Cambrian Potsdam Sandstone through Ordovician carbonates of the Trenton Group (Fisher, 1968; Isachsen and Fisher, 1970). Both the Proterozoic metamorphic rocks and Paleozoic sediments are intruded by Early Cretaceous (105-146 Ma) alkalic plutons and dikes throughout northeastern New York, northern New England and southern Quebec (McHone and McHone, 1999). In this field trip, outcrops of Precambrian anorthosite, gneiss, metagabbro and marble, Paleozoic carbonates and a Cretaceous trachyte porphyry will be visited (Figure 1).

Proterozoic Metamorphic and Paleozoic Carbonate Rocks

Roaring Brook Intrusion Breccia. Giant Mt. is composed dominantly of Proterozoic anorthosite and gabbroic anorthosite (Jaffee and Jaffee, 1986; Whitney et al., 1989). Apatite fission-track (AFT) ages of 168-83 Ma (standard error of ~± 10 % of AFT age) for Proterozoic crystalline rocks from the Adirondack Mountains indicate unroofing in this region occurred from Late Jurassic to Early Cretaceous. The High Peaks region of the Adirondacks yielded the oldest AFT ages ranging from ~140-170 Ma. This indicates that the High Peaks area was the first part of the Adirondacks to become unroofed in the Late Jurassic. An anorthosite sample from the southeast side of Giant Mt. at 2800 ft. elevation yielded an AFT age of 135 Ma (Roden-Tice et al., 2000).

From Roaring Brook Falls on the southwest side of the Giant Mt., a stop on the trail to the intrusion breccia, a beautiful view of the Great Range in the High Peaks of the Adirondacks can be obtained. Several varieties of anorthosite, anorthositic gabbro, and leuconorite showing mutually cross-cutting relationships suggesting multiple intrusions outcrop within and near the brook (Whitney et al., 1989).

Farther up Roaring Brook trail and after bushwhacking up Roaring Brook to a few hundred feet above the 2260 ft. level, a spectacular intrusion breccia is exposed (Kemp, 1920; deWaard, 1970; Jaffee and Jaffee, 1986; Whitney et al., 1989). The intrusion breccia crops out in large pavement outcrops in the stream bed. Jaffee and Jaffee (1986) describe the exposure as containing numerous blocks of angular, dark gray, fine-grained rocks that are completely embayed and surrounded by coarse-grained pink rock composed of mainly blue plagioclase and abundant garnet.

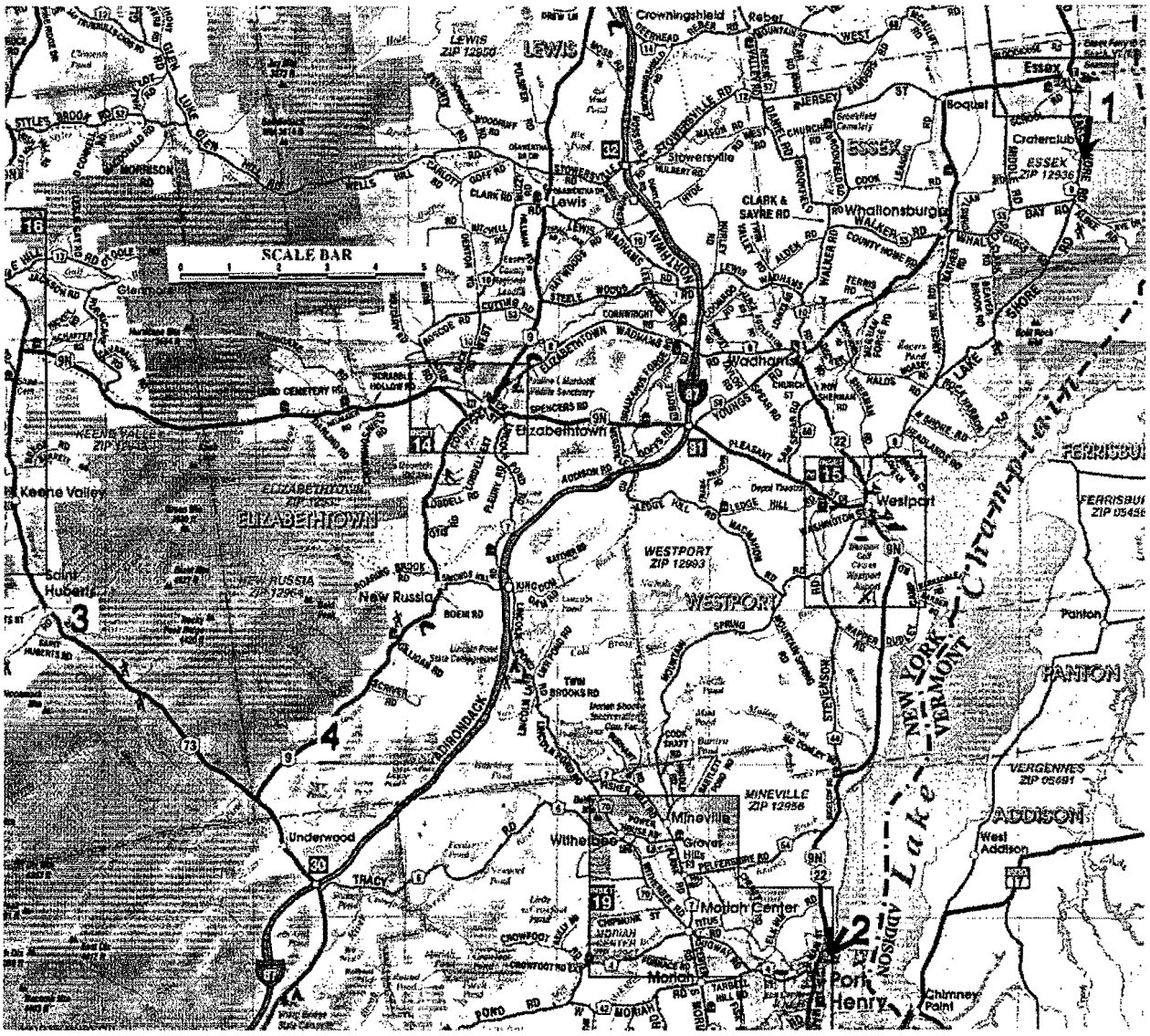

Figure 1. Field trip route map showing the locations of stops 1-4.

The blocks are xenoliths of Grenville rock that has been previously deformed and rotated and is compositionally metasedimentary and mafic granulite (Figure 2; Whitney et al., 1989).

The metasedimentary xenoliths are in general fine-grained, equigranular, diopside-K-feldspar-plagioclase-quartz rocks which show fine-scale (mm) laminations that may represent sedimentary layering or perhaps, foliation (Whitney et al., 1989). The host rock is anorthositic metagabbro ranging in composition to mafic mangerite and jotunite and is stained pink as a result of oxidation of abundant iron-rich pyroxenes (Whitney et al., 1989; Jaffee and Jaffee, 1986). It contains plagioclase, two pyroxenes, Fe-Ti oxides, garnet (as discrete grains and as garnet-plagioclase symplectites around oxides), hornblende, and K-feldspar, with minor quartz and apatite (Whitney et al., 1989). Jaffee and Jaffee (1986) describe clots and veins of black to blue-green pyroxenes and pearly white K-feldspar that occur throughout the anorthositic gabbro. The intrusion breccia is reported to extend intermittently to nearly the summit of Giant Mountain (Kemp, 1920; deWaard, 1970; Jaffee and Jaffee, 1986).

The intrusion breccia is an excellent locality for petrology students to interpret intrusive and cross-cutting relationships. It also underscores the complexity of Adirondack geology and structure. From the vantage point of

Roaring Brook Falls, the Mesozoic unroofing history of the Adirondacks (Roden-Tice et al., 2000) can be discussed and evidence for ongoing Adirondack uplift (Isachsen, 1975; 1981) presented.

Figure 2. Metasedimentary xenolith in gabbroic anorthosite at Roaring Brook intrusion breccia.

Split Rock Falls: Zero-Displacement Crackle Zone. Split Rock Falls is located on the Boquet River lineament which is one of a major set of NNE-trending faults and linear valleys that dominate the topography of the southeastern Adirondacks (Figure 3; Isachsen et al., 1983). The lineaments have been interpreted to be the result of two kinds of brittle deformation: 1) high-angle normal faults and 2) "zero-displacement crackle zones" (ZDCZs) (Isachsen et al., 1983). ZDCZs are defined as intensely fractured rocks that differ from faults because they lack throughgoing shear planes or visible offsets and from joints in having an extremely diverse array of fracture directions (Isachsen et al., 1983; Whitney et al., 1989).

An anorthosite sample from the upper falls yielded an AFT age of 102 Ma (Gaudette et al., 2001) indicating the unroofing in this area occurred significantly later than in the High Peaks region of the Adirondacks. A trend of Early to Late Cretaceous AFT ages (~120-80 Ma) exists for all of the southeastern Adirondacks and across the Lake Champlain Valley into western Vermont (Gaudette et al., 2001; Roden-Tice et al., 2001).

The outcrop on the west side of Rt. 9 across from Split Rock Falls shows strongly foliated gabbroic anorthosite containing inclusions of unfoliated coarse-grained anorthosite and plagioclase megacrysts and is cross-cut by two thin basaltic dikes. A large slickensided surface is exposed at the southwestern end of the outcrop.

Whitney et al. (1989) describe the Boquet River lineament at Split Rock Falls as a NE-trending zone of right-stepping, en echelon segments measuring about 200 m in length. The segments are stepped 20-80 m apart along N30W and N60W connecting segments that are usually unexposed. The crackle zone segments are 5 to 15 m wide and occur in a 45-100 m zone of fracturing. The segments trend N30E and dips vary from 80°NW to 80°SE. Whitney et al. (1989) also state that late faults, striking N50E to N80E, cross the crackle zone but do not show any topographic expression.

Wiener and Isachsen (1987) measured attitudes and spacings of all fractures longer than 10 cm along two-meter wide traverses spaced 200 m apart. When plotted on stereonet diagrams, variations in fracture geometry across the crackle zone from anastomosing, to planar-parallel, and planar-intersecting types can be seen. Closely-spaced, steeply-dipping fractures within the crackle zone increase in diversity of strikes, dips and curvature towards the center of the zone. Whitney et al. (1989) state that because the fractures parallel the regional joint system that the aligned microcracks formed during regional jointing. Isachsen et al. (1983) suggest that these crackle zones are tension features that form at shallow depths resulting from crustal extension over a rising elongate dome. Crackle zones may form at shallow crustal levels while tensional fractures form at the surface.

Split Rock Falls ZDCZ provides an opportunity for structural geology students to collect attitude measurements on the different planar orientations present in the crackle zone (Figure 4) and make a density plot of the data. Each student takes 20 measurements from different parts of the upper and lower falls and shares their data with the rest of the class. From this complied data, each student makes a density plot of all the data on a Schmidt stereonet as poles to planes. This density plot is then used to make a contour diagram of the fracture orientations with a Kalsbeek counting grid. The exercise combines field skills with statistical presentation of data. It also allows the students to interpret the dominant paleostress directions in the crackle zone.

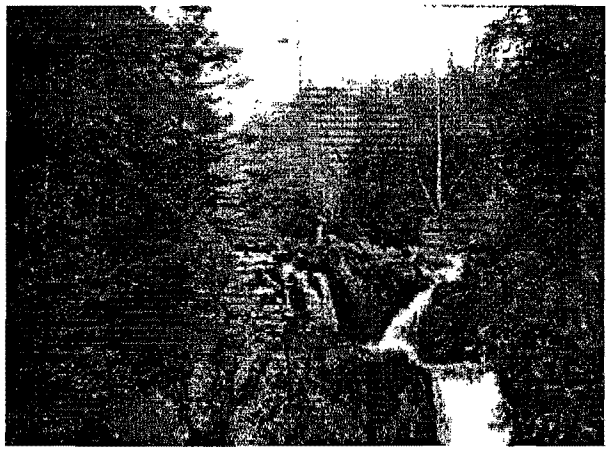

Figure 3. Split Rock Falls: Zero displacement crackle zone.

Figure 4. Measuring fracture attitudes at Split Rock Falls.

Craig Harbor Faultline Scarp. McHone (1987) provides an excellent description of the Craig Harbor locality on Lake Champlain in Port Henry, New York. The exposures include complicated field relations of Proterozoic marbles and calc-silicates, older basement granitic gneisses, lenses of metagabbro, a magnetite ore body, part of the Paleozoic carbonate shelf sequence and a large-scale normal fault that juxtaposes Paleozoic and Precambrian rocks.

The northern wall of Craig Harbor, a small embayment now cut off from Lake Champlain by the Delaware and Hudson Railroad, is a 165-ft.-high fault scarp at the north end of the Port Henry fault block which separates the Proterozoic and Paleozoic sections (McHone, 1987). The upper west cliff face, composed of Proterozoic marble, contains amazingly contorted, folded and disrupted lenses of gneiss and calc-silicate (Figure 5). This marble with its inclusions, and high-temperature minerals was first noticed by Emmons (1842) and suggested to be of igneous origin. The marbles have been suggested to be either part of the Paradox Lake Formation (Walton and deWaard, 1963) or above the biotite-quartz-plagioclase Eagle Lake Gneiss (Wiener et al., 1984; McHone, 1987).

Figure 5. Deformed gneiss lens in Proterozoic marble in Craig Harbor faultline scarp.

Below the marble in the cliff face, an orange-weathering hornblende-rich granite gneiss outcrops showing west dipping layers of foliation and a magnetite horizon (Emmons, 1842; Kemp and Ruedemann, 1910; McHone, 1987). A sample of this gneiss yielded an AFT age of 123 Ma which is slightly higher than but within analytical error of AFT age of the Split Rock Falls sample (102 Ma) but significantly lower than AFT ages from the High Peaks region which range from ~140-170 Ma (Roden-Tice et al., 2000).

North along the railroad tracks, the contact between dark, fine-grained granular metagabbro composed of altered plagioclase, brown hornblende, and augite, and the overlying gneiss containing hypersthene, augite, hornblende, microcline and plagioclase is exposed (McHone, 1987). Farther north, the metagabbro becomes coarser with an ophitic texture and contains coronas of garnet, brown hornblende, biotite, and clear plagioclase surrounding cores of magnetite, augite or hypersthene (Kemp, 1894, 1920; Gillson et al., 1928; McHone, 1987). P-T conditions of 8 kb and 800°C (granulite facies) were estimated for similar corona textures from other Adirondack metagabbros by Whitney and McLelland (1975) and McLelland and Whitney (1980).

A small magnetite prospect is located in the gneiss above the metagabbro. The deposit was known before the 1840s but was not worked because the ore is unusually high in sulfur and especially titanium which made it difficult to work with in the early forges (McHone, 1987).

South of Craig Harbor along the railroad tracks, the Cambrian Ticonderoga Dolostone and Ordovician Whitehall Dolostone are well-exposed and have an estimated thickness of 800 ft. (McHone, 1987). The uniform, "dove-colored", Ordovician Whitehall Dolostone is the first unit exposed in the cliffs south along Lake Champlain. It is a lower unit of the Beekmantown Group and is about 300 ft. thick with dips to the northeast (Welby, 1961). An inferred fault through a swale separates the Whitehall Dolostone outcrops from those of the Cambrian Ticonderoga Dolostone (Kemp and Ruedemann, 1910). The Ticonderoga Dolostone is sandy, characterized by crossbedding, channel depressions and blue-black chert layers and nodules and shows low easterly dips in its layers (McHone, 1987). The swale once contained a crushing mill and a quarry that once produced carbonate flux material for the local iron industry (McHone, 1987).

The timing of faulting is not well established but at Craig Harbor has to postdate the Lower Ordovician Whitehall Dolostone. Comparable high-angle faults occur throughout the southeastern Adirondack Mountains, Lake Champlain Valley of New York and Vermont, and the St. Lawrence River Valley of Quebec (McHone, 1987; Quinn, 1933; Welby, 1961; Stanley, 1980). Reactivation of Adirondack border faults, such as the McGregor fault system located about 80 km south of Craig Harbor near Wilton, New York, has been suggested in the Late Precambrian, Paleozoic and possibly Holocene (McHone, 1987; Willems et al., 1983; Isachsen et al., 1983). Evidence for Late Mesozoic reactivation of faulting in the Champlain Valley has been shown by cross-cutting relationships with Early Cretaceous alkalic intrusions in Vermont (McHone, 1978; Stanley, 1980). Early to Late Cretaceous igneous activity and fault reactivation in the Champlain Valley and perhaps along Adirondack border

faults may help explain the younger (80-120 Ma) AFT ages in the southeastern Adirondacks and Champlain Valley indicating more recent unroofing than those determined for the High Peaks region of the Adirondacks (140-170 Ma; Roden-Tice et al., 2000; Roden-Tice et al., 2001).

Craig Harbor is a superb field location for an undergraduate structural geology exercise. First, the students describe and make attitude measurements on the Paleozoic carbonates along the railroad tracks south of Craig Harbor. They learn to distinguish the two dolomite formations based on their sedimentary characterisitics and infer the normal fault that juxtaposes the formations. Then, the students examine the gneisses and metagabbro north of Craig Harbor and interpret the normal fault that brings these Proterozoic metamorphics in contact with the Paleozoic carbonates. Finally, the students are confronted with the marble containing deformed inclusions of gneiss, metagabbro and calc-silicates in the cliff along the faultline scarp (Figure 6). They are often awestruck by the deformation shown by the inclusions and spend a great deal of time in discussion on how this outcrop could have formed. Craig Harbor provides a great backdrop for a thought-provoking field lab on the P-T conditions and depths necessary in the Precambrian to produce the deformation now seen at the Earth's surface.

Figure 6. Variety of deformed inclusions in Proterozoic marble at Craig Harbor faultline scarp.

Mesozoic Intrusive Rocks

Cannon Point Intrusive. At Cannon Point on Lake Champlain, a laccolith trachyte porphyry sheet with interlayers of shale outcrops along the lake shore for ~.75 mi. and extends ~.5 mi eastward underneath a private camp known as the Crater Club (Figure 7; Buddington and Whitcomb, 1941). The laccolith intrudes upper Middle Ordovician Canajoharie Shale and is conformable with the bedding. The trachytic rocks were classified as bostonite (trachyte having felty clumps of alkali feldspar apparent only in thin section; McHone and Mc Hone, 1999) by Kemp and Marsters (1893) based on occurrence, trachytic texture and leucocratic characteristics.

The Cannon Point trachyte porphyry has a distinctive pinkish-brown color in outcrop and is porphyritic containing large K-feldspar phenocrysts approximately 2-5 mm in length (Buddington and Whitcomb, 1941). In thin section, the euhedral K-feldspar phenocrysts and laths in the groundmass show a crude trachytic flow texture. Plagioclase phenocrysts are present but rare (Buddington and Whitcomb, 1941). Kemp and Marsters (1893) determined the K-feldspar to be primarily anorthoclase which makes the Cannon Point trachyte porphyry similar in composition to Early Cretaceous trachytes in Vermont. They also found approximately 10% interstitial quartz in the groundmass, some of which was in micrographic intergrowth with K-feldspar, trace amounts of zircon, magnetite, and apatite but no other primary mafics.

In outcrop, the Cannon Point laccolith shows conformable relations with the Canajoharie Shale and locally contains thin included layers of shale and injected apophyses up to 2 ft. in length into the shale (Figures 8 and 9). The intrusive weathers with a platy structure that is parallel to the bedding and flow structure (Buddington and Whitcomb, 1941). The laccolith sheet strikes N60W and dips gently to the north (Buddington and Whitcomb, 1941). The lowest section of the intrusive is exposed ~0.4 mi. south of Cannon Point and contains rounded

inclusions of Paleozoic limestone and Potsdam sandstone. To the west beyond the outcrops in the Crater Club, the laccolith is covered by overburden. Buddington and Whitcomb (1941) speculated that a lack of surface float from the laccolith in this vicinity suggested that the intrusive either pinches out or is cut off by faulting. The upper part of the intrusive at ~0.3 mi. north of Cannon Point is 5 ft. thick and weathers to a pale buff color. It has a dense texture and the phenocrysts are small and sparse (Figure 7).

Figure 7. Northern end of the Cannon Point trachyte porphyry laccolith on Lake Champlain.

Figure 8. Cannon Point laccolith with Canajoharie shale layer included.

An estimate of the crystallization age of the Cannon Point laccolith can be obtained from partial Rb-Sr data collected by Fisher (1968) which suggests an age of "less than 140 Ma" (McHone and McHone, 1999). This data fits a whole-rock Rb-Sr isochron of 125 ± 5 Ma detemined for seven trachyte dikes from the Burlington area (McHone and Corneille, 1980). No AFT age was determined for the Cannon Point intrusive. However, an Early Cretaceous camptonite dike located about 10 miles north of Cannon Point on Willsboro Point on Lake Champlain yielded an AFT age of 116 Ma (Roden-Tice et al., 2000). This is consistent with K-Ar ages of 113, 123, 127 Ma for camptonite dikes from the eastern Adirondacks determined by Isachsen and Seiderman (1985). The similarity between the K-Ar crystallization ages and AFT ages suggests that the Early Cretaceous intrusives in the Champlain Valley and eastern Adirondacks were emplaced at shallow levels (~3-4 km depth) and temperatures < 100°C (closure temperature for fission-track retention in apatite). Eby (1984) concluded a similar shallow intrusion depth for the Monteregian Hills in southern Quebec because their AFT ages were comparable to their Rb-Sr crystallization ages (~120 Ma).

The Cannon Point laccolith shows excellent examples of contact relationships between a conformable intrusive and the shale country rock such as baked zones, apophyses, and included layers of shale (Figures 8 and 9). Its large size (~1 square mi in area) is also impressive to petrology students who are used to seeing small dikes that are only a few feet wide at most. Standing on the shore of Lake Champlain, the instructor can point across the lake to the Early Cretaceous Barber Hill syenite stock at Charlotte, Vermont which forms a low hill in the foreground. The Barber Hill stock has been dated by K-Ar as 111 ± 2 Ma on a biotite separate by Armstrong and Stump (1971) and is considered to be cogenetic with trachyte dikes in the Charlotte area (McHone and McHone, 1999). The comparable position of these two large contemporaneous igneous intrusives on opposite sides of the lake plus the abundance of both trachyte and lamprophyre (camptonite and monchiquite) dikes along the lake in both New York and Vermont provides for an interesting discussion on Mesozoic tectonics in this region.

Figure 9. Cannon Point laccolith apophysis in Canajoharie shale country rock.

ROAD LOG

Mileage Total	Mileage by Point	
0	0	Start trip from the parking lot of the Comfort Inn in Plattsburgh. Exit parking lot and turn left (west) on Cornelia St. (Rt. 3)
0.2	0.2	Intersection of Cornelia St. (Rt. 3) and Interstate 87. Turn left onto Interstate 87 south.
18.7	18.5	Take Exit 33 - Willsboro/Essex Ferry. Turn left (east) at end of exit ramp and proceed across overpass and straight through blinking red light on Rt. 22 south to Willsboro.
28.5	10.0	Remain on Rt. 22 through town of Willsboro (cross bridge and turn right).
32.9	4.4	Stop sign/light. Continue straight south through the village of Essex on Essex County Rt. 80.
34.7	1.8	Park along County Rt. 80 where possible. The road is very narrow and winding and has little shoulder. Outcrop is down stairs behind picnic table along Lake Champlain shore opposite large brown house set far back from road (44°15.507, 73°20.924).

STOP 1. CANNON POINT LACCOLITH. (45 Minutes).

This is the north end of the intrusion which is located on private property owned by the Crater Club. We will be walking south along beach at the low water mark. The intrusion is exposed along the shore and beneath private

homes. If visiting this outcrop during May through October, permission to access the intrusion should be obtained from the Crater Club and homeowners. We will walk south along the lakeshore through the exposure of the Cannon Point intrusion and observe its contact relationships with the host Canajoharie Shale.

Return to cars and continue south on County Rt. 80 (Lake Shore Rd.).

44.0	9.3	Lake Shore Rd. intersects with Rt. 22. Turn left onto Rt. 22 south into Westport.
44.05	0.05	Turn left again on Rt. 22 and Rt. 9N.
53.4	9.3	Entering Port Henry. Turn left at Craig Harbor Campground sign and proceed down steep hill to the end of the road at the lakeshore (44°3.482', 73°27.227').

STOP 2. CRAIG HARBOR FAULTLINE SCARP. (1.5 Hours).

This is private property but permission to visit the site is easily obtained. The name and address of the owner are given on the posted sign at the entrance. We will begin by walking south along Lake Champlain and the railroad tracks to examine the Paleozoic carbonates. These tracks are used several times a day by both Amtrack passenger and freight trains. Caution and listening for trains is strongly advised. There is generally room to stand safely on the side of the tracks.

After studying the Paleozoic dolostones, we will proceed north along the tracks across Craig Harbor to see the faultline scarp, Proterozoic marble, gneiss, and metagabbro. The faultline scarp is visible just north of Craig Harbor. From the tracks, one can determine that the marble in the cliff has an unusual structure. We will get to look at the marble up close later. Orange-stained, strongly foliated, Proterozoic gneiss is the first rock type encountered along the railroad tracks north of Craig Harbor. A few feet further north, the fault contact between the gneiss and coarse-grained, iron-oxide stained, metagabbro is visible. Further north across from a small railroad cut on the lakeside of the tracks, a rough path disappears uphill into the woods. We will scramble up it and view the magnetite prospect. Be careful of the poison ivy!

After returning to the cars, we will drive a short distance within the campground to one of the campsites that borders the faultline scarp. At this location, there are fantastic exposures of Proterozoic marble with abundant and diverse deformed inclusions. A contact between the Proterozoic marble and the Ordovician Whitehall Dolostone can be seen along the faultline at the west end of the outcrop.

If permission to visit the campsite cannot be obtained, similar spectacular outcrops of marble with deformed inclusions can be seen along the lakeshore by walking north along the railroad tracks from the magnetite mine for about 0.5 mi. The entire site can be accessed from the south by walking along the railroad tracks from the marina south of the dolostone outcrops. Parking is available at the public boat launch in Port Henry. McHone (1987) gives a good description of this route to Craig Harbor.

Return to Rt. 22, turn left (south) and continue south into the village of Port Henry.

54.2	0.8	Stop at Stewart's on left side of road in Port Henry for lunch, drinks or snacks. Return to cars and retrace route north on Rt. 22 (Main St.) down steep hill to Beach Rd. We will have lunch in a village park near the marina on Lake Champlain. After lunch, take Rt. 22 back up steep hill and turn right on Broad St. (Essex County Rt. 4). Proceed west up hill to Moriah.
56.0	1.8	Intersection of County Rts. 4 and 42. Turn right (northwest) and continue on County Rt. 4.
57.4	1.4	Stop sign in Moriah Center at the intersection of County Rt. 4 and Center Rd. (County Rt. 7). Turn right (north) at Old Mine Saloon, cross bridge and then immediately bear left on Essex County Rt. 70 to Witherbee.

EARLY PALEOZOIC CONTINENTAL SHELF TO BASIN TRANSITION ROCKS: SELECTED CLASSIC LOCALITIES IN THE LAKE CHAMPLAIN VALLEY OF NEW YORK STATE

James C. Dawson
Distinguished Service Professor
Center for Earth and Environmental Science
State University of New York
Plattsburgh, NY, 12901
james.dawson@plattsburgh.edu

TRIP ABSTRACT

Well-exposed classic localities in the Lake Champlain Valley of New York provide opportunities to examine the transition from Early Cambrian to Early and Medial Ordovician continental clastic and carbonate shelf sequences (e.g. Upper Cambrian Potsdam Group, Lower Ordovician Theresa Formation and Beekmantown Group, and Middle Ordovician Chazy Group) to the Medial Ordovician foreland basin carbonates and calcareous shales (Middle Ordovician Trenton Group).

INTRODUCTION

This field trip is designed to begin at the SUNY Plattsburgh campus at 8:00 a.m., and end near Plattsburgh, NY about 4:00 p.m., in time for participants to drive to Lake George, NY to make their lodging arrangements, have dinner, and attend the conference welcoming party. This trip visits many of the localities that are commonly visited in the introductory geology classes at SUNY Plattsburgh. The field trip description is largely based on the work of Fisher (1968) and Isachsen, et. al. (2000) and is not based on any significant research by this author. The trip is included among the package of four trips originating in Plattsburgh, NY, in order to round out the offerings so that they include an opportunity to see a portion of the Lower Paleozoic section. Other faculty at SUNY Plattsburgh are involved in offering opportunities to see Adirondack bedrock geology, glacial geology, and hydrology and geomorphology localities in the area.

TECTONIC SETTING

The Paleozoic rocks of the Lake Champlain Valley of northeastern New York State consist of a sequence that began in the Late Cambrian and continued through the Early Ordovician as a typical, quartz sandstone and carbonate, passive shelf margin sequence, that transitions to the initiation of the Taconic foredeep basin in Medial Ordovician time (Isachsen, et. al, 2000). The shelf sequence was deposited on the passive margin that formed in the Late Proterozoic on, what is today, the eastern edge of Proto North America (called Laurentia by Hoffman, 1988 and others), as the continental landmasses, that were later to form Gondwanaland, rifted eastward to form the Iapetus Ocean (Isachsen, et. al., 2000).

Isachsen, et. al., (2000) suggest that the Iapetus Ocean began to open approximately 640 Ma; however the earliest of the shelf depositional units are not found in northeastern New York until 120 million years or so later, when the Upper Cambrian Potsdam Sandstone, which lies directly on Precambrian metanorthosites and metagabbros, is deposited. Overlying the Potsdam Sandstone (Figure 1), at approximately the Cambro-Ordovician boundary, is the Theresa Dolostone/Sandstone which is followed by the dolostones of the Lower Ordovician Beekmantown Group. The shallow shelf carbonates, and the well known patch reef bioherms, of the Chazy Group overly the Beekmantown Group. The Chazy Group is followed by the relatively thin, eastern representation of the Black River Group that is not well exposed in the area (Fisher, 1968).

Toward the end of the Early Ordovician, approximately 480 Ma, an eastward dipping Taconic subduction zone, with an adjacent Taconic Island Arc lying immediately east of the subduction zone, were rafted westward to close a portion of the western Iapetus Ocean. The collision of this Taconic subduction zone and its

adjacent Taconic Island Arc with Proto North America created the Taconic Orogeny during medial Ordovician time, approximately 460 Ma (Isachsen, et. al., 2000). The beginnings of this Taconic Orogeny are represented in northeastern New York by the lower portion of the Trenton Group.

Figure 1. Rock Section (after Fisher, 1968).

Late Jurassic/ Early Cretaceous	Lamprophyre Dikes			STOPS 1 and 16
'uncertain'	LaColle Melange			STOPS 8 and 9
Ordovician	Trenton Group	Iberville and Stony Point Shales	1000'+	
		Cumberland Head Argillite	200'+	STOPS 2 and 4
		Glens Falls Limestone		
		Montreal Member	150-200'	STOP 1
		Larrabee Member	30'	
	Black River Group	Isle LaMotte Limestone	30'	
		Lowville Limestone	12'	
		Pamelia Dolostone	5-40'	
	Chazy Group	Valcour Limestone		
		upper argillaceous	80-125'	
		lower reefs/calcarentite	40-55'	STOPS 6 and 10
		Crown Point Limestone	50-250'	STOPS 7 and 16
		Day Point Limestone	80-300'	STOP 5
	Beekmantown Group	Providence Island Dolostone	150-200'	STOP 3
		Fort Cassin Limestone/Dolostone	150'+	
		Spellman Limestone	100'+	
		Cutting Dolostone	200'+	
		concealed dolostone 75-275'		
	Saratoga Springs Group	Theresa Dolostone/Sandstone	50'	STOP 12
Cambrian		Potsdam Sandstone		
		Keeseville Sandstone	455'+	STOPS 11, 13 and 14
		Ausable Arkose	250'+	
		'Basal Member'	unknown	STOP 15
Precambrian	Metanorthosite penetrated by Metagabbro both pierced by Diabase Dikes.			

As the Taconic Orogeny collision progressed, the eastern edge of Proto North America was uplifted while the region to the west of the uplift, that is now northeastern New York, was down warped into a foredeep basin that is associated with steep angle strike slip faulting (Stone, 1957). The beginnings of a part of the northern portion of this downwarp are represented by the Cumberland Head Argillite of the Trenton Group with younger portions of the formation being deposited as flysch in progressively deeper water (Hawley, 1957). As the collision progressed, Lower Cambrian quartz sandstone and carbonate shelf deposits were thrust westward, probably as gravity driven slides, as thick allochthonous sheets. These thrust faults over rode the

eastern portions of the Cumberland Head Argillite creating significant folding and shearing within the eastern portions of the Cumberland Head Argillite. Portions of the Middle Ordovician Cumberland Head Argillite also form allochthonous strata that appear to have overridden portions of the Lower Ordovician Beekmantown Group. Allochthonous Chazy Group strata are not found in northeastern New York, although they have been described further south near Granville, NY (Selleck and Bosworth, 1985).

The next portion of the tectonic setting is represented by the many mafic dikes (Kemp and Marsters, 1893; Hudson and Cushing, 1931) that cross cut the Paleozoic sequence. These have been interpreted (Fisher, 1968) as being of Late Jurassic/Early Cretaceous age and may be related to the ultrabasic intrusives of the Monteregian Hills of southern Quebec that have been dated at 110 Ma.

STRATIGRAPHIC SUMMARY

Saratoga Springs Group

The Potsdam Sandstone (Figure 1) was described by Emmons, (1843) as being the base of the 'Transition System' in quarries near Potsdam, NY. Three lithologic facies are generally recognized including a 'Basal' Member, the Ausable Member and the Keeseville Member. The 'Basal' Member consists of a maroon hematitic, feldspathic micaceous quartzose sandstone with some maroon shale interbeds (STOP 15). Portions of this basal unit may be older than Late Cambrian. The Ausable Arkose is a cross laminated, feldspar rich sandstone that occurs irregularly throughout the main Potsdam section. The Keeseville Member (STOPS 11, 13, and 14) is a fine to coarse quartz sandstone. Detailed lithologic descriptions of the three units can be found in Lewis (1971) and Wiesnet (1961). Most authors have interpreted the Potsdam Sandstone as being deposited in a complex arrangement of fluvial to intertidal and barrier beach environments (Fisher, 1968).

This field trip guide follows Fisher (1968) and includes the Theresa Dolostone/Sandstone (STOP 12) in the Saratoga Springs Group although some authors have included it in the overlying Beekmantown Group. The Theresa is a thick bedded, quartz rich dolostone that occupies the stratigraphic position between the quartz sandstones of the Potsdam below and the dolostones of the Beekmantown above.

Beekmantown Group

The Beekmantown Group (Figure 1) was erected (Clarke and Schuchert, 1899) as a new name for the Calciferous Sandrock (Formation) of Emmons (1843) and others and was named for Beekmantown, NY. Unfortunately, the section at Beekmantown, NY is not well exposed and the two main sections described by Brainerd and Seely (1890) as five units (Divisions A through E), north of Shoreham, VT and at West Cornwall, VT, are generally accepted as the type section. Fisher (1968) made a determined effort to carry the Brainerd and Seely (1890) units to northeastern New York and in ascending order he has mapped the Cutting Dolostone, Spellman Formation, Fort Cassin Formation and Providence Island Dolostone. The prevalent unit is the Providence Island Dolostone (STOP 3), a supratidal dolostone.

Chazy Group

The Chazy Group (Figure 1) comprises what is arguably the best known unit of northeastern New York and adjacent Vermont. The Group was originally defined by Emmons (1843); but, many researchers (Brainerd, 1891; Brainerd and Seely, 1888 and 1896; Oxley and Kay, 1959; Pitcher, 1964a and 1964b) have contributed to our understanding of the Group. The Chazy Group consists of three well defined limestone formations. The Day Point Formation (STOP 5) consists of gray, cross bedded, calcarenite in northeastern New York with small bioherms of bryozoans, corals and sponges near the top that we will not see on this trip. Above the Day Point lies the Crown Point Limestone (STOPS 7 and 16) an argillaceous, medium textured, calciciltite to argillicalcilutite (Fisher, 1968). The characteristic, large, planispiral gastropod, *Maclurites magnus* Le Sueur (1818) (STOP 7) is common and small stromatoporoid reefs can be found. The Valcour Limestone is the youngest unit of the Chazy Group. The lower part of the Valcour (STOPS 6 and 10) contains extensive bioherms of bryozoans, sponges,

algae and stromatoporoids and reef flank calcarenites. The upper portion becomes more argillaceous and grades into the Pamelia Dolostone of the Black River Group.

Black River Group

In northeastern New York the exposures of the Black River Group (Figure 1) are limited. Fisher (1968) has mapped, in ascending order, the Pamelia Dolostone, Lowville Limestone and Isle La Motte Limestone as a single Black River group unit with limited success. The Black River group in northeastern New York is relatively thin and consists of thick bedded dolostone, and some argillacous dolostone, of the Pamelia just above the Valcour Formation, and massive, light gray limestones, that are interbedded as the Lowville and Isle La Motte. The best exposures occur in two quarries, one of which has been mined out (International Lime and Stone Quarry southeast of Chazy) and one of which is full of water (a shallow quarry southwest of Rouses Point, NY). We will not attempt to visit the Black River Group on this field trip.

Trenton Group

In northeastern New York the Trenton Group (Figure 1) consists of the lower Glens Falls Limestone and the upper Cumberland Head Argillite (STOPS 2 and 4). The Glens Falls Limestone in turn is subdivided into a lower Larrabee Member (Kay, 1937), a thick bedded medium gray limestone that we will not see on this field trip and an upper Montreal Limestone, the Shoreham Limestone of Kay (1937) (STOP 1). The transition from the continental shelf deposits of the main portion of the Chazy Group to the more argillaceous grayish black limestone of the Montreal represents a transition from pre-Taconic shelf deposits to the incipient formation of the Taconic Orogeny foredeep basin. The Cumberland Head Argillite is a regionally restricted unit that formed as a flysch, turbidity current deposit in a portion of the early foredeep basin of the Taconic Orogeny. Above the Cumberland Head Argillite very limited exposures of the Stony Point Shale, can be found in northeastern New York. The non-calcareous Iberville Shale is only found in Vermont and Quebec (Hawley, 1957).

LaColle Melange

Initially the La Colle (Conglomerate) Melange (Figure1) was described as a sedimentary formation (Clark and McGerrigle, 1936; Kay, 1937); but, Stone (1957) and Fisher (1968) have interpreted the unit as a Taconic Orogeny tectonic rock formed by the Tracy Brook (normal) Fault (STOPS 8 and 9) and by thrust faults where it is found in Vermont.

ROAD LOG

The trip begins in the parking lot at the west end of Hudson Hall on the SUNY Plattsburgh campus. To reach the Hudson Hall parking lot from the Exit 37 (the Plattsburgh-Cornelia Street/Route 3 Exit) of I-87, 'the Adirondack Northway', head east from Exit 37 on Cornelia Street/Route 3. Continue east past a congested series of traffic lights and pass under the Northway bridge. Approximately 0.5 miles east of the bridge under the Northway , at a traffic light, make a slow right on to Broad Street (Plattsburgh Plaza is to your left/north and the WIRY radio station is set back to your right/south at this intersection). Continue east on Broad Street for another 0.3 miles past the traffic light at Prospect Avenue and past the traffic light at Draper Avenue. Turn left/north into the parking lot on the north side of Broad Street, just east of Draper Avenue, and west of Hudson Hall. If you miss the parking lot you will go under a concrete pedestrian bridge over Broad Street.

Hudson Hall is named after Professor George H. Hudson (Hudson, 1905; Hudson, 1907; Hudson, 1931; Hudson and Cushing, 1931) who taught science and music for many years at SUNY Plattsburgh. His portrait hangs in the foyer of the building.

Mileage

0 Leave the parking lot at the west end of Hudson Hall on the SUNY Plattsburgh campus and turn left/east on to Broad Street.

0.5 Continue east on Broad Street under the pedestrian bridge, pass through the traffic lights at Beekman Street and Rugar Street, and turn right/south on to South Catherine Street at the traffic light.

1.0 Continue south on South Catherine Street, pass through the Pine/Steltzer Street traffic light, and cross the Saranac River bridge.

1.1 Immediately after crossing the river turn left/east on to South Platt Street.

1.5 Continue east on South Platt Street to the traffic light at Route 9/United States Avenue and turn right/south. This is a slow right and you should avoid the hard right on to Peru Street, i.e. follow the sign for Clinton Community College.

1.8 Continue south on Route 9 to the traffic light at New York Road and turn left/east.

1.9 Continue east on New York Road and pass through the gate to the 'old base' side of the former Plattsburgh Air Force Base that is now being operated under the auspices of the Plattsburgh Area Redevelopment Corporation (PARC).
Turn right/south on to Ohio Avenue East.

2.2 Note the 'old base' stone buildings constructed in the 19th century of Potsdam Sandstone.
Turn left/east, at the bike route sign, on to a narrow access road.

2.3 Continue on the access road and immediately cross a steep bridge (sound your horn). Continue through the sharp U-turn to the left and continue to the end of the road and park on the apron area near a small boat launch to Lake Champlain (**STOP 1**).

STOP 1. Montreal Member of the Glens Falls Limestone of the Trenton Group and Lamprophyre (Monchiquite Dike).

You are parked on the apron of the former Plattsburgh Air Force Base marina and boat launch. To reach the outcrop hike, approximately 2000' north along the cobble beach shore of Lake Champlain. The Pleistocene sediments forming the bluff between the railroad track and Lake Champlain along the way include a contact between earlier Lake Vermont varved and later Champlain Sea sediments. The Montreal Member and a cross cutting Lampophyre Dike are exposed to varying degrees depending on the water level of Lake Champlain. The Montreal Member is a medium-bedded limestone with some shale partings, that weathers to medium dark gray. Crab Island (the smaller island that can be seen in Lake Champlain two miles southeast of this stop) takes its name from the trilobite, *Isotelus*, that is commonly found in exposures of the the Montreal Member on the island. Fisher (1968) maps the Lamprophyre Dike as a monchiquite dike, containing phenocrysts of titanaugite with some biotite and barkevikite (a monoclinic amphibole), phenocrysts of olivine and titanomagnetite. After visiting the outcrop return to the vehicles.

2.9 After returning to the vehicles, retrace your route back across the narrow railroad bridge (sound your horn again) and through the former Plattsburgh Air Force Base to the 'old base' gate and Route 9. Turn right/north on Route 9.

3.2 Continue north on Route 9/United States Avenue with the 'old base' buildings to your right/east. At the traffic light with South Platt Street bear right and continue north on Route 9.

3.3 Pass the Fort Brown historic site markers on your left/west. Fort Brown was the left/west flank of the American defense during the land portion of the Battle of Plattsburgh on September 6 - 11th, 1814.

4.0 Continue north on Route 9, through the traffic light at the Hamilton Street/Pike Street intersection, to the T-intersection with Bridge Street. Turn left/west on Bridge Street which becomes Route 9.

4.1 Turn right/north on to City Hall Place which becomes Route 9.

4.3 Continue north past the Plattsburgh City Hall on your left and Macdonough (American naval commander during the battle of Plattsburgh) Monument on your right.
Just past the City Hall, turn left/west and then immediately turn right/north again on to

Miller Street which becomes Route 9.

4.8 Continue north on Miller Street, cross the railroad tracks at the Delord Street level crossing. Make a slow right, at the traffic light, on to Margaret Street, which becomes Route 9.

6.3 Continue north on Margaret Street/Route 9 past the Georgia-Pacific paper mill at the Cumberland Head Avenue/Boynton Avenue intersection.
Cross the small Scomotion Creek bridge. Continue north on Route 9 through the traffic light at the Route 314 (Exit 39 entrance to the Northway) intersection.

8.8 Continue north on Route 9 past the North Country Shopping Center on your left/west.
Cross under the transmission lines that carry St. Lawrence Seaway energy across Woodruff Pond and Lake Champlain on your right/east to Vermont and pass the Pioneer Motel on your left/west.

9.3 Pull over to the right/east side of Route 9 and park near a low road cut (**STOP 2**).

STOP 2. Cumberland Head Argillite of the Trenton Group.

The Cumberland Head Argillite is exposed in this road cut on both sides of Route 9, although the exposures are better on the left/west side. The roadcut (Fisher, 1968 - Figure 27) is typical of the Cumberland Head Argillite. The thin bedding (it looks like varves) of fairly distal turbidite deposition can clearly be seen as more calcarous layers alternate with the thinner, pale buff-colored quartz-silt bearing layers being slightly more resistant to erosion. Fresh surfaces of the rock are uniformly black; however, the thin layers can still be distinguished. The rocks in the vicinity are folded; but, the strike is generally N35E with a dip of 23 degrees N. Be sure to look north along Route 9 and see the slight dip that the highway makes north of the road cut. STOP 3 is just beyond the dip.

9.7 Return to the vehicles and continue north on Route 9, cross the slight topographic dip, and pull over to the right/east side at the next low road cut and park (**STOP 3**).

STOP 3. Providence Island Dolostone of the Beekmantown Group.

The Providence Island Dolostone is exposed in this road cut on both sides of Route 9, although the exposures are better on the right/east side (Fisher, 1968 - Figure 17). Before examining the outcrop, be sure to look south along Route 9 and recognize that you can see Stop 2. The Rocks at STOP 3 are nearly horizontal, compared to the steeper dips at STOP 2 and the entire Chazy Group and lower portion of the Trenton Group (some 400' or more of rock section) are missing. Fisher (1968) has mapped the edge of the Cumberland Head Allochthon, a Taconic thrust fault, as passing between these two trip stops on the basis of missing section at both the surface and in a 200' deep water well on Cumberland Head. The Providence Island Dolostone is a thick bedded, massive unit that weathers to the buff color characteristic of dolostones. With careful examination, horizons that display significant soft sediment rip ups and other features characteristic of supratidal enviornments. The dolostone is sometime vuggy and fracture zones that have been filled with secondary crystalline calcite are common.

10.1 Return to the vehicles and continue north on Route 9 and turn right/east on to the Point au Roche Road.

11.7 Continue east on the Point au Roche Road to the entrance to Point au Roche State Park and turn right/south to enter the Park. You will be entering the western entrance to the Park that leads to the beach.

12.3 Follow the Park road south past the entrance gate to the beach parking lot and head to the far right/southwest corner of the parking lot and park (**STOP 4**).

STOP 4. Cumberland Head Argillite at Point au Roche State Park.

Walk the short distance from the parking lot to Lake Champlain and examine the large outcrop of Cumberland Head Argillite along the shore. The folding and jointing associated with the Taconic thrusting is very obvious. The rock is essentially the same as that seen at Stop 2 and again the thinning bedding of the fairly

distal turbidite deposition can be seen as the more calcareous layers alternate with the thinner, pale buff-colored, quartz silt bearing layers being more resistant to erosion.

12.9 Return to the vehicles and retrace your route back to the Point au Rocke State Park entrance.
14.5 Turn left/west on the Point au Roche Road and retrace your route back to Route 9 and turn right/north on to Route 9.
15.8 Continue north on Route 9 past the intersection with Route 456 on the left/west. A hump in the road will indicate that you are crossing the Ingraham Esker (Denny, 1972).

16.6 A series of sand pits can be seen to the right/east after you first cross the Esker. Route 9 crosses the Ingraham Esker again, just before the hamlet of Ingraham on the left/west.
19.2 Continue north on Route 9 past the Giroux Poultry Farm.
19.6 Continue north on Route 9 past Trombley Lane (formerly Slosson Road).

19.7 At a low road cut on the left/west that is located in front of a robin's egg blue home pull over and park (**STOP 5**).

STOP 5. Day Point Limestone of the Chazy Group. (THIS IS NOT A HAMMER STOP.)

This road cut is part of the upper part of The Day Point Limestone, probably the Fleury Member of Oxley and Kay (1959). It is a medium gray calcarenite that is both cross bedded and regular bedded in this small exposure. Fisher (1968) mentions this outcrop as containing pelmatozoan debris.

20.7 Return to the vehicles and continue north on Route 9 and at a point where Route 9 makes a bend to the left/west turn right/east on to Sheldon Lane.
21.2 Continue east on Sheldon Lane and you will see a quarry on the left/north. There is a large new white home at the east end of the quarry. Park on Sheldon Lane opposite the west end of the quarry (**STOP 6**).

STOP 6. Valcour Limestone of the Chazy Group at Sheldon Lane. (THIS IS NOT A HAMMER STOP.)

This is the first of two opportunities that we will have (see also STOP 10) to see the bioherms in the Valcour Limestone.

21.7 Return to the vehicles and turn around. There is a place to do a Y-turn on the left/north side of Sheldon Lane just ahead. Retrace your route back to Route 9. Turn right/north on Route.
22.4 Just past a red barn on your right/east there is an amateurish 'stone henge' and an old road. The road leads to the abandoned International Lime and Stone quarry where the Pamelia Dolostone, the Lowville Limestone and the Isle LaMotte Limestone formations of the Black River Group (Fisher, 1968 - Figure 25) were once exposed. A few years ago the remainder of this outcrop was mined and the quarry floor today consists of Valcour Limestone. None of the Black River Group remains.
23.2 At the Fiske Road (formerly Old Route 348) turn left/southwest.
24.6 Continue southwest on the Fiske Road and follow the road as it bends left/west. As the Fiske Road approaches the bridge over I-87, the Adirondack Northway, pull over on the right/north and park (**STOP 7**).

STOP 7. Crown Point Limestone of the Chazy Group at the Northway in Chazy:
***Maclurites magnus* Le Sueur, Death Assemblage** (THIS IS NOT A HAMMER STOP.)

To reach the outcrop cross the open area and enter the woods on a vague trail behind and to the right of the obvious transmission pole. The vague trail heads north a few yards in a white cedar forest and then bends left/west toward the Northway. The outcrop is close to the Northway, a short distance north of the Fiske Road Bridge and is illustrated in Fisher, 1968 (Figure 20).

26.0 Return to the vehicles and turn around. Retrace your route back /northeast along the Fiske Road to route 9. Turn left/north on Route 9.
26.1 Continue north on Route 9 and cross the Little Chazy River.
26.4 Continue north and pass under the railroad bridge.
26.5 Immediately after passing under the railroad bridge turn/left on to the Miner Farm Road. As you turn left watch for an opportunity to continue with your left turn on to a short dead end street that enters the intersection and park on the apron **(STOP 8).**

STOP 8. Lacolle Melange at the Chazy Railroad Bridge.

The road cut is located along the west side of Route 9 as you walk toward the railroad bridge and is figured in Fisher, 1968 (Figure 30). Fisher, 1968 maps this locality and the STOP 9 locality as part of the Tracy Brook (normal) Fault. The wide range of angular clasts are composed of angular sandstone fragments in a sandstone matrix, presumably a tectonically crushed portion of the Keeseville Sandstone.

27.7 Return to the vehicles and carefully return to Route 9 heading north. Continue north on Route 9 and cross Corbeau Creek. Corbeau Creek was studied, as a monitored watershed, by a succession of students at SUNY Plattsburgh in the 1970s and early 1980s. In recent years SUNY Plattsburgh students have been engaged in watershed studies on the Altona 'Flat Rock' lands owned by the William H. Miner Institute and some of this work is described in Field Trip A. 6 of this field conference.
29.1 Turn right/east on Route 9B.
30.8 Cross the Great Chazy River in Coopersville.
31.1 Cross the bridge over the railroad.
31.4 Just past the Hayford Road pull over in front of a small outcrop and park **(STOP 9).**

STOP 9. Lacolle Melange at Coopersville.

The small outcrop is located adjacent to the south side of Route 9B and is figured in Fisher, 1968 (Figure 29). The breccia clasts include a wide range of sizes and the lithology of the clasts is predominately made of carbonate fragments that appear to of Black River group and Trenton Group origin.

31.9 Return to the vehicles and continue east on Route 9B. Cross the Dumont Road.
32.2 Continue east on Route 9B as it bends left/north and after passing a brown log cottage (#862) on your left/west turn left into a driveway that leads to an agricultural field and park **(STOP 10).**

STOP 10. Valcour Limestone of the Chazy Group at the Bechard Quarry, Near Kings Bay.

To reach the quarry walk across the agricultural field to the higher vegetated are that is visible to the west. Once you reach the top of the vegetated mound the quarry can be seen as illustrated in Fisher, 1968 (Figure 22). The bioherms consist intertidal stromatolites (algae), stromatoporoids, and bryozoans with the various colonies being completely compatible (Pitcher, 1964b) and building their colonies on top of one another.

33.6 Return to the vehicles and turn around. Follow Route 9B back south and then east and re-cross the Great Chazy River in Coopersville.
35.3 Turn right/north on to Route 9.
37.2 At the Clinton Farm Supply enterprise on the left/west turn left into the northern most drive way and park **(STOP 11).**

STOP 11. Keeseville Sandstone of the Potsdam Sandstone at the Clinton Farm Supply, Champlain.

The outcrop is exposed along the north side of the northernmost of the two driveways and in the flat area behind the Farm Supply building. In a series of articles (Erickson, 1993a. Erickson, 1993b. Erickson and Bjerstdt, 1993. Erickson, Connett, and Fetterman, 1993) the stratigraphy and trace fossils of the Keeseville Sandstone and Theresa Dolostone/Sandstone have been described. STOP 11 (Erickson, 1993a, and Erickson,

Connett and Fetterman, 1993) consists of medium bedded, cream colored Keeseville Sandstone. At this locality large scale ripple marks, and an unusual abundance of trace fossils can be seen.

38.5 Return to the vehicles and continue north on Route 9. Cross Route 11 at a traffic light.
39.1 Continue north as Route 9 enters Champlain as Main Street. Follow Main Street north as it descends and begins to bend to the left/west. Turn right on Elm Street and immediately cross the Great Chazy River.
39.2 After crossing the Great Chazy River follow Elm Street to the right/east. Do not make the sharp right turn on to River Street and do not make the left turn on to Oak Street which is marked as a dead end. After a short distance on Elm Street turn left at an antique shop on to Prospect Street (formerly the Bostock Hill Road).
40.9 Follow Prospect Street north and east past the Village of Champlain water supply to a stop sign at Route 276. Turn left/north on to Route 276.
41.2 Follow Route 276 north to a driveway on the left that is paved with thick cement and turn left/west into the driveway. Park on the left when you see the quarry ahead and to your left after a short distance **(STOP 12).**

STOP 12. Theresa Dolostone/Sandstone at Champlain.

The Theresa Dolostone/Sandstone consists of an interlayed, medium and thick bedded, quartz dolostone. Bjerstedt and Erickson (1989) and Erickson and Bjerstedt (1993) have described the trace fossils of the Theresa in detail and *Skolithos* can be located on the south wall of this quarry.

43.3 Return to the vehicles and retrace your route south on Route 276, turn right/west on Prospect Street. Follow Prospect Street west and south to Elm Street and follow Elm Street the short distance across the Great Chazy River to Route 9. Turn left/south on Route 9.
43.9 Turn right/west at the traffic light on to Route 11.
44.5 Follow Route 11 across I-87, the Northway at Exit 41. Anyone needing to leave the trip early can conveniently do so at this point.
47.7 Continue west on Route 11 and cross the Great Chazy River.
51.1 Continue west on Route 11 and enter Mooers. Route 22 enters from the south on the left.
53.8 Continue west and then southwest on Route 11 and turn right/west on to the Davison Road.
59.2 Continue west on the Davison Road to the stop sign in Cannon Corners. Turn left/south on to the Cannon Corners Road and immediately cross the English River.
59.7 Turn right/west at the Adirondack Nature Conservancy 'Gadway Sandstone Pavement Barrens' sign on to the unpaved Gadway Road. The road enters **STOP 13** and the road log continues with two **STOPS** on the way in and a final third **STOP** at a turn around.

STOP 13. Keeseville Sandstone of the Potsdam Sandstone at the Gadway Preserve.

This stop requires driving in to the Gadstone Preserve of the Adirondack Nature Conservancy and consists of three short STOPS within the STOP. Vehicles with low clearance should not attempt this and we will consolidate riders at the entrance.

60.0 Continue west on the Gadway Road and **STOP** and park at a bare rock rock wash. Carefully cross over a barbed wire fence to examine a pavement of large scale ripples in the Keeseville Sandstone.
60.1 Continue west on the Gadway Road and **STOP** and park at the next significant open area on the right/north and stop and park. At the north end of the open area near a red posted sign there is a 4 meter long (10 cm wide) *Climachtichnites* track. Yochelson and Fedonkin (1993) illustrate several similar examples of this trace fossil in the Keeseville Sandstone of northern New York. Additional trace fossils can be seen near the Adirondack Nature Conservancy sign.
60.8 Continue west on the Gadway Road. Follow the arrow to the left track at the Y-intersection.

At this point the road becomes solid rock. Continue to the marked turn around loop and park (**STOP**).

Walk about 100 paces beyond the turn around loop and pass an arrow sign. On the left/south side of the road you can locate additional *Climachtichnites* tracks. One track is 1.4 meters long (11 cm wide) and some partial tracks appear cross over one another. Additional trace fossils may be *Protichnites*, and northern New York examples of these in the Keeseville Sandstone are also illustrated in Yochelson and Fedonkin (1993)

61.9 Return to the vehicles that are parked at the turn around and carefully drive back to the Cannon Corners Road. Turn right/south on the Cannon Corners Road.
63.4 Turn left/east on to Route 11.
65.1 Turn right/south on to the Alder Bend Road (labeled Irona Road).
66.4 At the stop sign turn left/east on to the Irona Road.
69.0 At the stop sign turn right/south on to the Devils Den Road.
69.4 Continue south past the Miner Farm Road on the left/east.
70.2 Continue south on the Devil Den Road as it crosses the Great Chazy River. As the Devils Den road bends to the right/southwest turn left on to the unpaved Rock Road.
70.9 Follow the Rock Road generally south to an obvious outcrop in the road on the left side and park (**STOP 14**).

STOP 14. Trough Cross Stratification in the Keeseville Sandstone of the Potsdam Sandstone on the Rock Road.

The trough cross stratification is located on the east side of the road, within what goes for a right of way. It is a small outcrop of well exposed cross stratification in the Keeseville Sandstone.

72.9 Follow the rock Road south to the intersection with Route 190, the Military Turnpike. Turn left/south.
74.6 Pass the historic Robinson Tavern on the left/east.
76.5 Pass the Blue Chip Farm on the right/west.
76.9 Carefully turn left on to a grassy area by a private driveway and park (**STOP 15**).

STOP 15. Ausable Arkose of the Potsdam Sandstone on the Military Turnpike.

Cross to the ditch on the west side of Route 190.Military Turnpike and walk north. Excellent examples of the 'Basal' Member of the Potsdam Sandstone, a hematitic, feldspathic and micaceous sandstone can be found over much of the distance to the Blue Chip Farm driveway.

77.4 Return to the vehicles and carefully return to Route 190 continuing south. Pass the Murtagh Hill Road on the right/west.
77.5 Pass the Rand Hill dikes on both sides of the road with the best exposure on the left/east side of Route 190. (add more description and reference)
83.8 Turn left/east at the traffic light on to Route 374, the Cadyville Expressway.
86.8 As Route 374 broadens to four lanes pull over on the right/south, 100 yards beyond the 'Lion International' sign, and park (**STOP 16**).

STOP 16. Crown Point Limestone of the Chazy Group with Lamprophyre Dikes on the Route 374/Cadyville Expressway.

This extensive road cut along both sides of Route 374/Cadyville expressway contains two lamprophyre dikes on the south side of the road that intrude the Crown point Limestone with a strike of N70W and a dip 85 degrees N. Only the easternmost of the two dikes appears on the north side of the road. Interesting features, including baked zones, zenoliths and partial zenoliths, can be seen associated with the intrusions. The Crown Point Limestone is mainly a medium to dark gray calcilutite. Some of the large planispiral gastropod, *Maculurites magnus* Le Sueur are present along with trilobite and brachiopod fragments.

87.1 Return to the vehicles and continue east on Route 374, cross the Route 22 intersection and immediately bear right on to Exit 38 to I-87, the Adirondack Northway, southbound.

Those interested in returning to SUNY Plattsburgh may exit I-87 at the next exit, Exit 37, and continue east (it is a right turn at the traffic light off the 'trumpet' exit) on Cornelia Street/Route 3, as described in the first paragraph of this road log, to the Hudson Hall parking lot.

Those wishing to continue to Lake George, NY for the remainder of the field conference should continue south on I-87 to Exit 21. This is the second and more southern exit to Lake George, NY. This trip will take approximately 90 minutes from Exit 38. After leaving I-87 at Exit 21 in Lake George, turn left/east on to Route 9N. Cross under I-87 and turn left/north on to Route 9. As you travel north on Route 9 into Lake George, the Fort William Henry Resort Hotel will be one mile north of the Route 9N intersection on the right/east side of Route 9.

REFERENCES CITED

Bjerstedt, T. W. and J. M. Erickson. Trace Fossils and Bioturbation in Peritdal Facies of the Potsdam-Theresa Formations (Cambrian-Ordovician), Northwest Adirondacks. Palaios, 4: 203-224. 1989.

Brainerd, E. The Chazy Formation in the Champlain Valley. Geological Society of America Bulletin, 2: (3): 293 - 300. 1891.

Brainerd, E. and H.M. Seely. The Original Chazy Rocks. American Geologist, 2: 323 - 330. 1888.

Brainerd, E. and H.M. Seely. The Calciferous Formation in the Champlain Valley. American Museum of Natural History Bulletin 3: 1-23. 1890.

Brainerd, E. and H.M. Seely. The Chazy of Lake Champlain. American Museum of Natural History Bulletin, 8: 305 - 315. 1896.

Clark, T. H. and H. W. McGerrigle. LaColle Conglomerate: A New Ordovician Formation in Southern Quebec. Geological Society of America Bulletin, 47: (5): 665 - 674. 1936.

Clarke, J.M. and C. Schuchert. The Nomenclature of the New York Series of Geological Formations. Science, New Series 10: 874-878. 1899.

Denny, C.S. The Ingraham Esker, Chazy, New York. Pages B35 - B41 *in* Geological Survey Research 1972. United States Geological Survey Professional Paper 800-B. 1972.

Emmons, E. Geology of New-York. Part II. Comprising the Survey of the Second District. Natural History Survey of New York. 437 pages. 1843.

Erickson, J.M. Cambro-Ordovician Stratigraphy, Sedimentation, and Ichnobiology of the St. Lawrence Lowlands-Frontenac Arch to the Champlain Valley of New York. Trip A-3(1). New York Geological Association Field Trip Guidebook, pages 68 - 95. 1993a.

Erickson, J. M. A Preliminary Evaluation of Dubiofossils from the Potsdam Sandstone. New York State Geological Association Field Trip Guidebook. Trip A-3(3), pages 121 - 130. 1993b.

Erickson, J. M. and T. W. Bjerstedt. Traces Fossils and Stratigraphy in the Potsdam and Theresa Formations of the St. Lawrence Lowland, New York. Trip A-3(2). New York State Geological Association Field Trip Guidebook, pages 97 - 119. 1993.

Erickson, J. M., P. Connett, and A. R. Fetterman. Distribution of Trace Fossils Preserved in High Energy Deposits of the Potsdam Sandstone, Champlain, New York. Trip A-3(4). New York State Geological Association Field Trip Guidebook, pages 131 - 143. 1993.

Fisher, D. W. Geology of the Plattsburgh and Rouses Point, New York-Vermont, Quadrangles. New York State Museum and Chart Series Number 10 51 pages. 1968.

Hawley, D. Ordovician Shales and Submarine Slide Breccias of Northern Champlain Valley in Vermont. Geological Society of America Bulletin 68: 55-94. 1957.

Hoffman, P. F. United Plates of America, the birth of a Craton: Early proteroxoic Assembly and Growth of Laurentia. Annual Review of Earth and Planetary Sciences 16: 543-603. 1988.

Hudson, G.H. Contributions to the Fauna of the Chazy Limestone on Valcour Island, Lake Champlain. New York State Museum Bulletin 80: 270-295. 1905.

Hudson, G.H. On Some Pelmatozoa from the Chazy Limestones of New York. New York State Museum Bulletin 107: 97-152. 1907.

Hudson, G. H. The Fault Systems of the Northern Champlain Valley, New York. New York State Museum Bulletin 286: 5 - 80. 1931.

Hudson, G. H. and H. P. Cushing. The Dike Invasions of the Champlain Valley, New York. New York State Museum Bulletin 286: 81 - 112. 1931.

Isachsen, Y. W., E. Landing, J. M. Lauber, L. V. Rickard and W. B. Rogers, Editors. Geology of New York: A Simplified Account. New York State Museum Educational Leaflet Number 28. 294 pages. 2000.

Kay, M. Stratigraphy of the Trenton Group. Geological Society of America Bulletin, 48: 233 - 302. 1937.

Kemp, J.F. and V.F. Marsters. The Trap Dikes of the Lake Champlain Region. United States Geological Survey Bulletin 107. Pages 11-62. 1893.

Le Sueur, C.A. Observations on a New Genus of Fossil Shells. Journal of the Academy of Natural Science, Philadelphia 1: 310-313. 1818.

Lewis, D. W. Qualitative Petrographic Interpretation of Potsdam Sandstone (Cambrian), Southwestern Quebec. Canadian Journal of Earth Sciences, 8: (8): 853 - 882. 1971.

Oxley, P. and M. Kay. Ordovician Chazyan Series of Champlain Valley, New York and Vermont, and Its Reefs. American Association of Petroleum Geologists Bulletin, 43: (4): 817 - 853. 1959.

Pitcher, M. G. Evolution of Chazyan (Ordovician) Reefs of Eastern United States and Canada. Ph.D. Dissertation. Columbia University, New York, NY. University Microfilms, Inc. Ann Arbor, MI. #68-8612. 105 pages. 1964a.

Pitcher, M. G. Evolution of Chazyan (Ordovician) Reefs of Eastern United nStates and Canada. Canadian Petroleum Geology Bulletin, 12: (3): 632 - 691. 1964b.

Selleck, B. and W. Bosworth. Allochthonous Chazy (Early Medial Ordovician) Limestones in Eastern New York: Tectonic and Paleoenvironmental Interpretation. American Journal of Science, 285: (1): 1 - 15. 1985.

Stone, D.S. Origin and Significance of Breccias Along Northwestern Side of Lake Champlain. Journal of Geology 65: 85-96. 1957.

Wieset, D.R. Composition, Grain Size, Roundness, and Sphericity of the Potsdam Sandstone (Cambrian) in Northeastern New York. Journal of Sedimentary Petrology 31: 5-14. 1961.

Yochelson, E. L. and M. A. Fedonkin. Paleobiology of *Climactichnites*, and Enimatic Late Cambrian Fossil. Smithsonian Contributions to Paleobiology Number 74. Smithsonian Institution Press. Washington, D.C. 74 pages. 1993.

LATE GLACIAL WATER BODIES IN THE CHAMPLAIN AND ST. LAWRENCE LOWLANDS AND THEIR PALEOCLIMATIC IMPLICATIONS

By

David A. Franzi, Plattsburgh State University, Plattsburgh, NY 12901
John A. Rayburn, Binghamton University, Binghamton, NY 13902
Catherine H. Yansa, Michigan State University, East Lansing, MI 48824
Peter L.K. Knuepfer, Binghamton University, Binghamton, NY 13902

INTRODUCTION

The late glacial legacy of the Champlain and St. Lawrence Lowlands and northeastern Adirondack Upland region (Figures 1 and 2) is recorded in the deposits and landforms associated with proglacial and marine water bodies that formed during deglaciation. The largest and most persistent proglacial lake in the region was Lake Vermont, which occupied the central Champlain Lowland and was dammed at its northern margin by the receding ice front (Chapman, 1937; Connally and Sirkin, 1969, 1973; Parrott and Stone, 1972; Wagner, 1972; Denny, 1974; DeSimone and LaFleur, 1985, 1986). Lake Vermont expanded northward until ice receded north of the St. Lawrence Lowland and allowed marine water to inundate the isostatically depressed St. Lawrence and Champlain Lowlands, thus forming the Champlain Sea (Chapman, 1937; Occhietti et al., 2001). Deglaciation of the region postdates deglaciation in the upper Hudson Valley (ca. 13.2 ^{14}C ka B.P.; Connally and Sirkin, 1971) and was completed prior to the Champlain Sea marine incursion (ca. 12.0 ^{14}C ka B.P. to 11.5 ^{14}C ka B.P.; Clark and Karrow, 1984; Fulton et al., 1987; Anderson, 1988; Rodriguez, 1988; Occhietti et al., 2001).

The chronology of lake phases in the Lake Champlain basin provides insight into the style and timing of Late Wisconsinan deglaciation, but may also provide information that is relevant to global paleoclimate studies. Broecker et al. (1989) discussed the possibility that freshwater drainage from proglacial lakes within continental North America during the last deglaciation affected North Atlantic ocean circulation and thereby altered global climate. The Champlain Lowland occupied a strategic position during the Late Quaternary deglaciation of the northeastern United States. The north-south trending lowland served both as a source of cold meltwater and as a corridor for the transmission of proglacial lake discharges from the Great Lakes Region to the North Atlantic. The region is also located at the juncture of two freshwater discharge routes. Discharges from Lake Vermont in the Champlain Valley and proglacial lakes in the eastern and central Great Lakes basin were initially routed southward through the Hudson Valley. Ice recession eventually opened the lower St. Lawrence Valley allowing proglacial lakes in the Champlain Valley and Great Lakes basin to drain northeastward to the Gulf of St. Lawrence. The Champlain Valley region is thus a key for recognizing when and where large freshwater discharge events entered the North Atlantic.

On this trip we shall discuss the preliminary results of our on-going investigations of the geomorphic and stratigraphic record of the late glacial water bodies in the Champlain Lowland and the significance of meltwater outflow and throughflow from the lowland to the North Atlantic during deglaciation.

Previous Investigations

Woodworth (1905a, 1905b) was one of the first to study the late glacial freshwater and marine water bodies in the Champlain Lowland. Chapman (1937) later conducted an extensive study of the shoreline deposits and landforms in the region. Chapman recognized that Lake Albany formed in the Hudson Valley when the Champlain Valley was still occupied by ice, and that with retreat of the ice there were two main lake stages that occupied the Champlain Valley before the drop to the marine-phase Champlain Sea. He used hand levelling to determine the elevations of strandline and deltaic features from the first and higher "Coveville" phase, and the later "Fort Ann" phase, as well as lower marine shorelines within the basin.

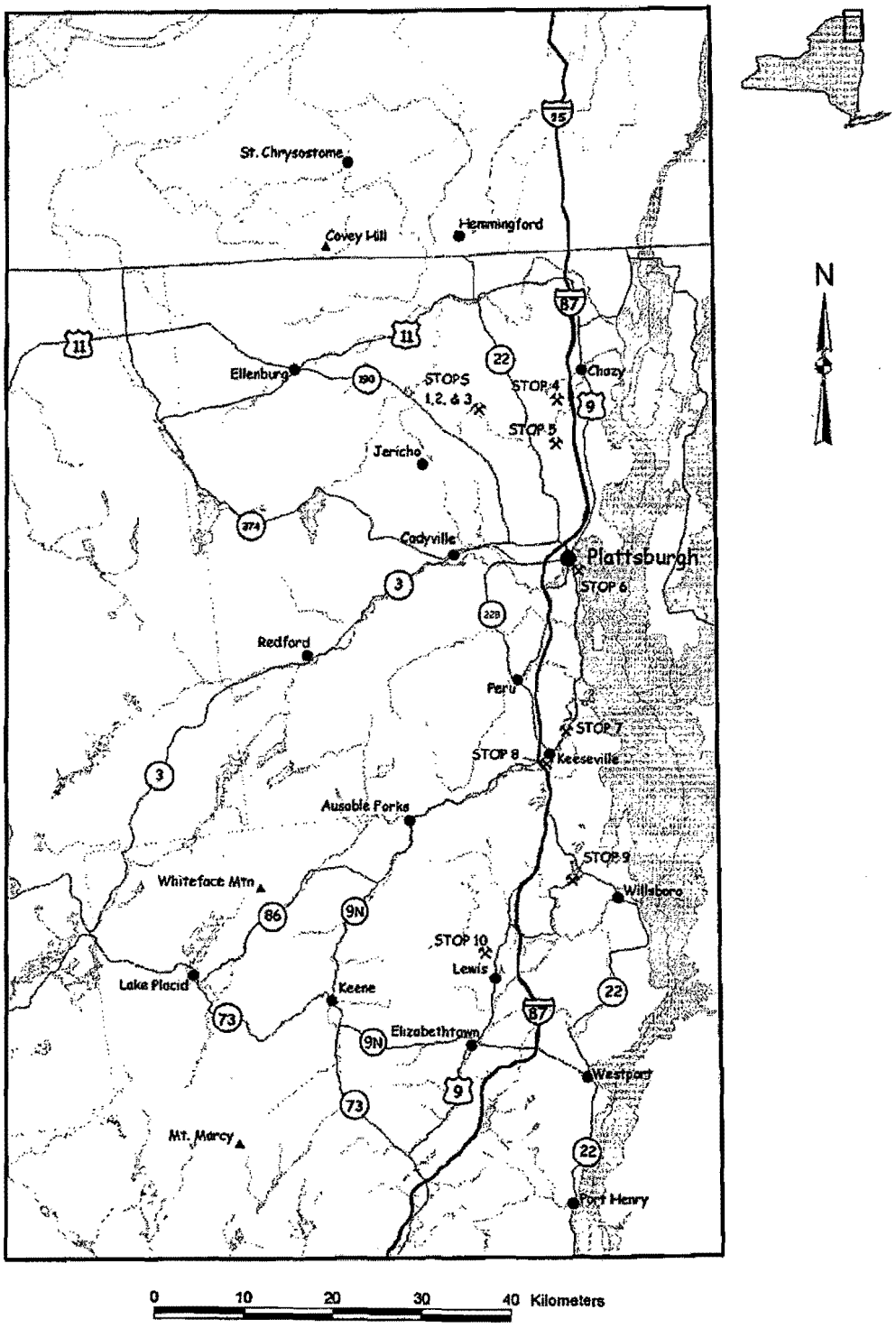

Figure 1. Location map of the northeastern Adirondack Upland and northwestern Champlain Lowland showing the locations of field trip stops.

Chapman (1937) suggested that a rock ledge at Coveville, New York controlled the Coveville lake threshold, and that the lake later dropped to the Fort Ann level when it broke through a barrier at the Hudson Gorge near Schuylerville, New York. He put the Fort Ann threshold at a topographic constriction near Fort Ann, New York, and developed isobases from the Fort Ann shoreline elevations that depict a linear deformation gradient of about 0.95 m/km to the north-northwest.

Connally and Sirkin (1969) suggested that what had, by the late 1960s, been recognized in the upper Hudson Valley as three levels of Lake Albany, and in the Champlain Valley as three separate levels of Lake Vermont, were actually four levels of the same lake. They referred to these (from oldest to youngest) as Lake Albany, Lake Quaker Springs, Lake Coveville, and Lake Vermont. According to Connally and Sirkin (1969), Lake Albany was mostly confined to the Hudson River Valley, and Lake Quaker Springs extended into the Champlain Valley as far north as Ticonderoga, New York and Brandon, Vermont. Their Lake Coveville extended from the Hudson River Valley as far north as Willsboro, New York/Burlington, Vermont, and their Lake Vermont (Chapman's [1937] Fort Ann phase) extended almost to the Canadian border, but was too low to extend into the Hudson River Valley to the south. Connally and Sirkin (1973) describe the relationships of these lakes with the ice margins in detail and speculated about possible outlets. They refer to a "dam" that held back both Lake Albany and Lake Quaker Springs, but which was eventually breached as the water level dropped to Lake Coveville. They put the Fort Ann threshold near Whitehall, New York, with water draining southward to the Hudson River via Wood Creek (now the Hudson-Champlain barge canal), which corresponds to Chapman's (1937) threshold at Fort Ann.

Wagner (1972) and Parrott and Stone (1972) used topographic maps to locate and determine elevations for presumed shoreline features in Vermont. Like Chapman (1937), they emphasized large features such as deltas and kame surfaces. The internal structures of these features, however, are rarely exposed, making it difficult to determine accurate paleo-water level elevations from them. Denny (1967, 1974) traced the Lake Coveville shoreline northward to the Saranac River Valley near Plattsburgh. He also mapped the highest levels for Lake Fort Ann and the Champlain Sea.

DeSimone and LaFleur (1985, 1986) mapped ice margin, lacustrine and fluvial features in the northern Hudson River Valley and the southernmost extent of the Champlain Valley. They identified Lake Albany, Lake Quaker Springs, Lake Coveville, three Lake Fort Ann levels, and suggested that there may have been a "lower Lake Albany" for a short period of time. DeSimone and LaFleur (1985, 1986) did not discuss outlets for Lake Albany or Lake Quaker Springs, as they concentrated on describing meltwater flowing into these lakes and not out of them. They did, however, propose channels at Fort Edward (now Hudson-Champlain barge canal), Durkeetown, and Winchell as Coveville and Fort Ann outlets.

Wall and LaFleur (1995) recognized the lower Lake Albany (which they called "Albany II") and three Fort Ann levels of DeSimone and LaFleur (1985, 1986), and listed elevations of these strandlines at three locations in the Hudson Valley. They examined discharge from the Mohawk River Valley into the Hudson River Valley lakes in detail, but also did not consider ultimate discharge from the Hudson Valley. An important observation from the work of Wall and LaFleur (1995), as well as several of the other earlier investigators, is a suggestion that both Lakes Coveville and Fort Ann were more fluvial in nature south of the Champlain Valley. This change in character between the Champlain Valley and Hudson Valley suggests a constriction between the two.

The breakout of Lake Iroquois through an outlet near Covey Hill, Quebec rerouted Ontario Basin meltwater, which had been draining into the Hudson Valley via the Mohawk River, to the Hudson River through the Champlain Valley. Lake Fort Ann eventually became confluent with the proglacial lakes in the St. Lawrence and Ontario lowlands after ice retreated from the northern slope of Covey Hill (Figures 3A-C; Clark and Karrow, 1984; Pair et al., 1988; Pair and Rodrigues, 1993). The portion of the confluent Lake Fort Ann in the St. Lawrence Lowland has been referred to by the names Lake Belleville, Lake St. Lawrence, and Lake Candona. The reader is referred to Pair and Rodrigues (1993) for a discussion of these names. Finally, ice retreat to the east allowed the proglacial lakes to drain and marine water to invade the isostatically depressed St. Lawrence and Champlain Valleys.

Physiography

The St. Lawrence and Champlain Lowlands form a broad, contiguous lowland region that is underlain by Cambrian and Ordovician sedimentary rocks (Figure 2). The central portions of the lowlands are underlain by relatively thick glacial, lacustrine and marine deposits and are characterized by low to moderate local relief (generally less than 100 meters). Local relief along the northern margin of the St. Lawrence Lowland and northwestern margin of the Champlain Lowland, in the St. Lawrence Hills subdivision of Cressey (1977), ranges up to a few hundred meters. This subdivision is primarily underlain by the Cambrian Potsdam Sandstone and includes the area around Covey Hill, P.Q. and the "Flat Rocks" in Clinton County, New York.

The Adirondack Upland is a dome-shaped upland region primarily underlain by high-grade PreCambrian metamorphic rocks. The highest summit elevations in the Adirondack Mountain Peaks subdivision (Cressey, 1977) are greater than 1500 meters and local relief commonly exceeds 600 meters. Summit elevations in the Adirondack Low Mountains subdivision generally range between 600 and 900 meters but local relief is generally less than 300 meters (Cressey, 1977).

Drainage patterns within the study area are influenced by regional geology. The principal streams in the region, including the Chateaugay, Chazy, Saranac, AuSable and Boquet rivers, represent the northeastern portion of a radial drainage pattern developed in the Adirondack Upland. The St. Lawrence River and Lake Champlain are part of the tangential master stream network that developed in the lowlands surrounding the Adirondack Upland (Ruedemann, 1931; Morisawa, 1985).

GLACIAL DEPOSITS AND LANDFORMS

Ice-Flow Indicators

The direction of Late Wisconsinan ice movement in the Champlain Lowland and northeastern Adirondack Mountain region is inferred from striated bedrock exposures, till-pebble fabrics, roche moutonees, drumlins, moraines, and compositional trends in tills (Ogilvie, 1902; Alling, 1916, 1918, 1919, 1920; Miller, 1926; Kemp and Alling, 1925; MacClintock and Stewart, 1965; Denny, 1974; Craft, 1976; Gurrieri and Musiker, 1990). Two predominant directions of flow are indicated in the published literature, a southerly flow that presumably relates to Late Wisconsinan overriding of the Adirondack Upland by the Laurentide Ice Sheet and a late-glacial flow pattern that was strongly controlled by local physiography. In most instances striation orientation reflects the last ice movement in the region. Kemp and Alling (1925) and Craft (1976) suggested that local alpine glaciers might have contributed to late-glacial ice flow in parts of the Adirondack Uplands.

Meltwater Channels

The morphology and continuity of meltwater channels and channel systems in the region reflect the magnitude and duration of meltwater discharge, the location of meltwater flow relative to the glacier margin, and the composition and structure of the substratum into which the channels are cut.

Small to medium size channels that are sub parallel to the contours of hill slopes often occur as anastomosing channel systems that are cut into surficial deposits or, less commonly, bedrock. Individual channels range from about 0.1 to 1.0 km long, 10 to 150 meters wide, and 1 to 20 meters deep but the channel systems often occur in belts 0.5 to 2 km wide and several kilometers in lateral extent. Good examples of these channel systems occur near Chateaugay (MacClintock and Stewart, 1965; Denny, 1974; Pair and Rodrigues, 1993), along the northwestern margin of the Champlain Lowland between Jericho and Cadyville and between Cadyville and Peru (Denny, 1974), and north and west of Smith Hill near Lewis. The distal ends of many channels or channel systems open onto fluvial or deltaic sandplains that are graded to bedrock thresholds or proglacial impoundments.

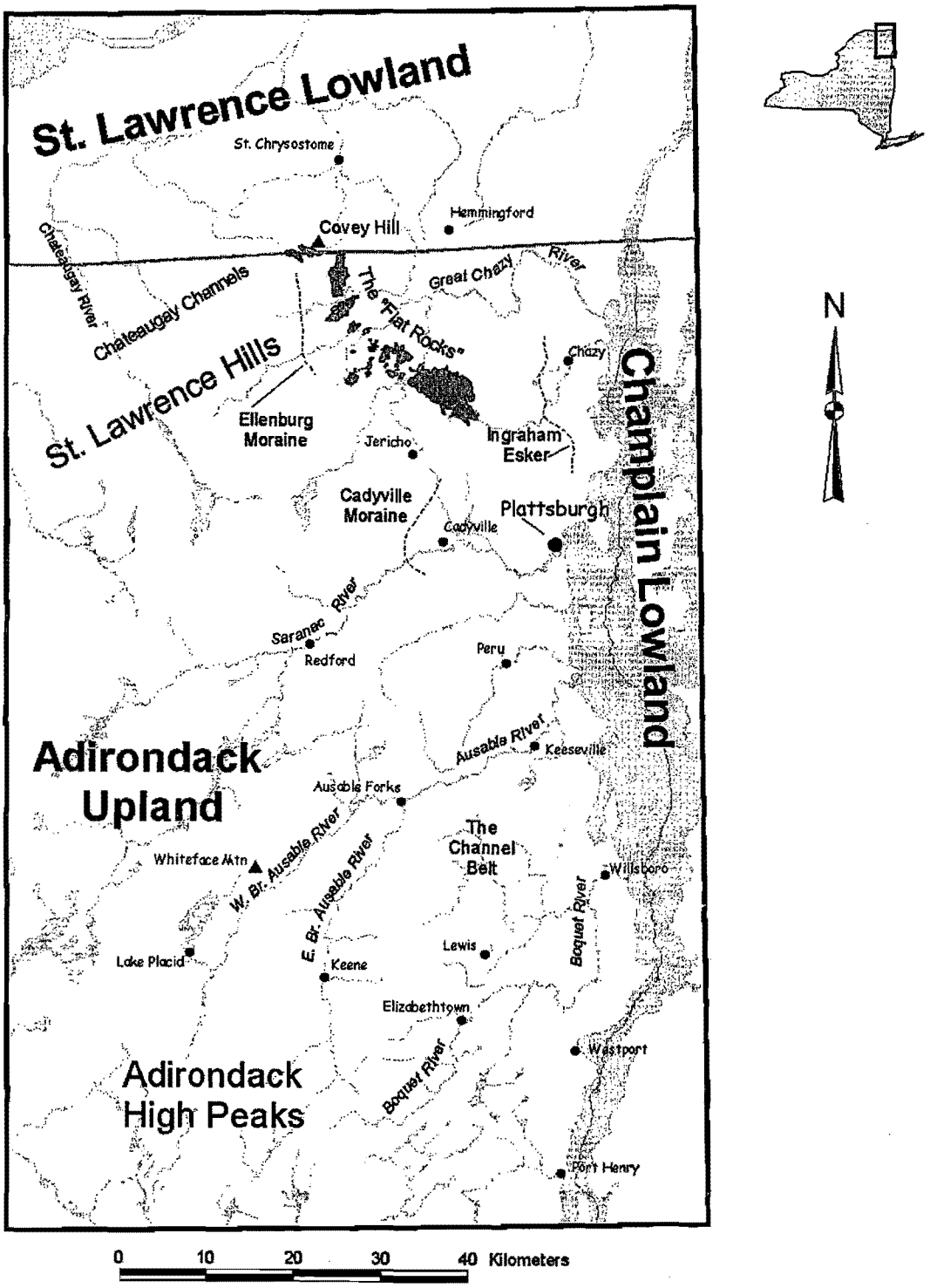

Figure 2. Physiographic regions and geological features of the northeastern Adirondack Upland and northwestern Champlain Lowland region.

Larger and more extensive channels and channel systems cut into bedrock that originate at cols on drainage divides were probably cut by meltwater outflow from proglacial lakes (Alling, 1916, 1918, 1919, 1920; Kemp and Alling, 1925; Miller, 1926; Denny, 1974; Diemer and Franzi, 1988). The outflow channels, presently abandoned or occupied by underfit streams, may attain depths greater than 30 meters and can often be traced more than two kilometers. Bedrock thresholds at the outflow channel heads provided base level control for glaciolacustrine and glaciofluvial sedimentation in the source basin. The elevations of outlet thresholds on drainage divides in Adirondack valleys generally decrease down valley, a distribution that is consistent with the systematic recession of active, valley-bound continental ice lobes (Diemer and Franzi, 1988).

The most extensive outflow channel system is found in the "Channel Belt" (Kemp and Alling, 1925) between Ausable Forks and Lewis (Figure 2). Individual channels may contain deep, circular to ovate plunge basins that are presently occupied by small ponds or swampy depressions. The Channel Belt network heads at the South Gulf and The Gulf outflow channels, on the divide between the Ausable and Boquet drainage basins and was probably cut by the combined erosional effect of outflow and ice-marginal meltwater drainage. Other well-developed bedrock channel systems occur in Wilmington Notch (Diemer and Franzi, 1988), between Redford and AuSable Forks (Miller, 1926; Denny, 1974), and south of The Gulf near Covey Hill (MacClintock and Stewart, 1965; Denny, 1974).

Rock Pavements

Rock pavements, large areas of exposed bedrock, are commonly associated with meltwater channels and channel systems. The largest rock pavements in the region are the sandstone pavements known locally as "Flat Rocks" in Clinton County (Figure 2). The Flat Rocks comprise a discontinuous, 5-kilometer wide belt of sandstone pavements that extend approximately 30 km southeastward into the Champlain Valley from Covey Hill, P.Q. The pavements are believed to have been created by the erosional effects of catastrophic floods from the drainage of glacial Lake Iroquois and younger post-Iroquois proglacial lakes in the St. Lawrence Lowland (Woodworth, 1905a, 1905b; Chapman, 1937; Coleman, 1937; Denny, 1974; Clark and Karrow, 1984; Muller and Prest, 1985; Pair et al., 1988; Pair and Rodrigues, 1993; Franzi and Adams, 1993, 1999). Outflow from the breakout proglacial lakes in the St. Lawrence Lowland was initially directed southeastward along the ice margin where it crossed the English, North Branch and Great Chazy watersheds before eventually emptying into Lake Vermont. The sandstone pavements generally occur on the drainage divides between watersheds where flood scour was greatest and the exposed surfaces were not subsequently covered (Denny, 1974). Smaller sandstone pavements occur south of Cadyville on the divide between the Saranac and Salmon rivers where they are associated with outflow channels from proglacial lakes in the Saranac Valley (Denny, 1974).

Diamictons

Diamictons deposited by glacial (till) and nonglacial processes have been recognized in the Champlain Lowland and northeastern Adirondack Mountain region. Subglacial lodgement or meltout till (Dreimanis, 1976; Lawson, 1979) typically consists of massive to crudely stratified, gray to reddish brown, clast-rich diamicton. The texture and composition of till deposits in the region are variable and reflect local provenance (Denny, 1974; Craft, 1976). Massive, over-consolidated till deposits typically form the basal glacial unit in the Champlain Lowland where they often observed overlying striated bedrock. Till occurs primarily as a discontinuous (1 to 3 meters) veneer over bedrock on hill slopes and upland areas.

Nonglacial diamictons consist primarily of intercalated diamicton and stratified deposits. The diamictons occur as lenticular to planar beds that range from a few centimeters to a few meters thick. Individual beds consist of massive to crudely graded, light gray, clast-rich, sandy diamicton. The lateral continuity of individual diamicton beds ranges from a few decimeters to tens of meters. Stratified interbeds range from thin, discontinuous sand, silt and clay lamina to massive, planar bedded, and cross-stratified sand and gravel beds about a meter thick. The bedded diamicton facies is commonly associated with proglacial lake and ice-marginal deposits and landforms. A greater relative proportion, thickness, and continuity of diamicton to stratified beds are generally associated with ice-proximal or valley-side environments.

Stratified Deposits

Stratified deposits are associated with fluvial, glaciofluvial, subaqueous outwash fan, deltaic, beach, lacustrine, and marine environments. The texture and structure of these deposits is variable and depends on the nature and energy conditions at the site of deposition. Fine-grained sediment, typically associated with low-energy glaciolacustrine and marine environments, include turbidites, pelagic laminites, and varves. Lacustrine deposits of Adirondack provenance are generally less calcareous and coarser grained than those of Champlain Valley provenance (Diemer and Franzi, 1988).

Deltas and beaches provide important evidence for reconstructing the extent of former proglacial lake and marine shorelines. Deltas commonly occur as gently sloping sandplains at the mouths of tributary valleys. The deposits generally grade upward from ripple cross-laminated to planar bedded, fine to medium sand to planar bedded and trough cross-stratified, poorly sorted, coarse sand and gravel (Diemer and Franzi, 1988). The deltas may have been fed by meteoric streams from deglaciated upland areas, ice-marginal or proglacial meltwater streams, or by outflow streams from proglacial lakes in adjacent valleys. Large lacustrine delta plains, deposited primarily by meteoric streams, are commonly found where major rivers entered Lake Vermont. Multiple delta terraces attest to the regrading of inflowing streams as proglacial lake levels dropped.

The Ingraham esker in Clinton County (Figure 2) is a 17 km long, roughly north-south trending, sinuous ridge composed primarily of stratified sand and gravel (Woodworth 1905a, 1905b; Denny, 1972, 1974; Diemer, 1988). The ridge ranges from 100 to 300 meters wide and rises 3 to 10 meters above the surrounding terrain (Diemer, 1988). The esker deposits are interbedded with fine-grained lacustrine deposits, including varved clays, and discordantly overlain by fossiferous gravel, sand, and fine grained marine deposits (Woodworth 1905a, 1905b; Denny, 1972, 1974; Diemer, 1988). Denny (1972, 1974) believed that the ridge formed as an esker in a subglacial tunnel and that its present low relief was due to reworking of the esker deposits by waves and currents in Lake Vermont and the Champlain Sea. Diemer (1988) conducted a detailed sedimentological study of the esker deposits and concluded that the ridge is composed primarily of subaqueous fan deposits. He suggested that the present relief of the esker might be more a primary consequence of subaqueous fan deposition than later resedimentation.

Moraines

Denny (1974) mapped and described several recessional moraine deposits in the northeastern Champlain Lowland. The largest and most extensive moraines in the region are located in the Saranac Valley near Cadyville and in the Great Chazy River Valley near Ellenburg Depot (Figure 2). The Cadyville Moraine consists of a north-trending belt of linear till ridges and knolls and kame sand and gravel bodies that spans the Saranac Valley. The ridges are typically composed of pebbly, sandy till with interbedded sand and gravel (Denny, 1974). Local relief between ridge crest and adjacent swale ranges between a few meters to approximately 20 meters and ridge crests are commonly spaced 60 to 260 meters apart. The length of individual ridges typically ranges from a few hundred meters to about 0.5 km (Denny, 1974). The swales that Denny described in northern part of the moraine are part of a meltwater channel system that extends from Cadyville northward to Jericho (described above). Small sand bodies at the southern end of the channel system may represent small deltas built into proglacial lakes in the Saranac Valley. The southern portion of the Cadyville Moraine terminates against the northeastern flank of Burnt Hill. The rock pavements and channel system south of the moraine were probably formed by outflow from proglacial lakes in the Saranac Valley at the time the moraine was built.

The Ellenburg Moraine consists of a single north-trending ridge that ranges between 300 and 500 meters wide and rises 25 to 30 meters above the surrounding terrain (Denny, 1974). The moraine is composed of sand, gravel and diamicton that are commonly deformed and offset by normal faults, primarily on its eastern flank. Diamicton interbeds are generally massive to crudely stratified and range between a few decimeters to a few meters in thickness (Denny, 1974; Franzi et al., 1993). The moraine rises to the north where it intersects a low-relief, east-trending recessional moraine north of Clinton Mills (Denny, 1974). Denny (1974) considered a small segment of recessional moraine south of Miner Lake to be contemporaneous with the Ellenburg Moraine.

LATE WISCONSINAN STRATIGRAPHY AND GLACIAL, LACUSTRINE, AND MARINE HISTORY IN THE CHAMPLAIN LOWLAND

Proglacial Lake and Marine Water Bodies in the Champlain Lowland

Late glacial ice flow and deglacial sedimentary environments in the Champlain Lowland and northeastern Adirondack Mountain region were influenced by regional physiography. Deglacial drawdown of ice into the Champlain and St. Lawrence Lowlands caused thinning of the ice sheet in upland areas and lobation of the ice front. The Champlain Lobe blocked northward drainage in the lowland and created proglacial Lake Vermont, which drained southward into the Hudson River drainage basin. Lake Vermont expanded with northward recession of the Champlain Lobe.

The names Lake Vermont and Champlain Sea refer to all freshwater and marine phases or levels, respectively, in the Champlain Lowland. The highest phase of glacial Lake Vermont is the Coveville Phase of Chapman (1937), which we shall refer to as Lake Coveville. Denny (1967, 1974) traced the Lake Coveville shoreline northward to the Saranac River near Plattsburgh. Our investigations indicate that Lake Coveville probably extended to Cobblestone Hill and Altona Flat Rock, approximately 12 km farther north than mapped by Denny (1967, 1970). We recognize two lake levels between Lake Coveville and highest marine level, which we refer to as Upper and Lower Lake Fort Ann. The elevations of the lowest two freshwater levels in the St. Lawrence and Ontario lowlands, Belleville and Trenton, (Pair et al., 1988; Pair and Rodrigues, 1993) lie close to the projected elevations of Upper and Lower Lake Fort Ann, which suggests that the Belleville-Upper Lake Fort Ann and Trenton-Lower Lake Fort Ann wader bodies were confluent and controlled by Lake Vermont thresholds.

We have observed that in most cases, the Lower Lake Fort Ann deltas at the mouths of the AuSable and Saranac rivers are notable exceptions, the Lower Fort Ann features are poorly represented in the Champlain Lowland. Because of this, and the fact that both Fort Ann levels occur in the Lake Ontario Basin, we conclude that the Lower Fort Ann level was relatively short lived. Chapman's (1937) Fort Ann shoreline data points are primarily Upper Fort Ann features, however his proposed Fort Ann outlet threshold corresponds to the Lower Fort Ann level. Denny's (1967, 1970) shorelines also correspond to the Upper Lake Fort Ann shoreline.

Stratigraphy

Stratigraphic sections at Plattsburgh Air Force Base Marina, Keeseville Industrial Park and along the Salmon River in South Plattsburgh and Rae Brook in Beekmantown contain complete or nearly records of late glacial, lacustrine, and marine events in the Champlain Lowland. Two of these exposures, the Plattsburgh Air Force Base and Keeseville Industrial Park sections, will be visited as part of this field trip. The stratigraphy of an exposure along Town Line Brook near Burlington (Bierman et al., 1999) is similar to the Plattsburgh Air Force Base and Salmon River sections, however a measured section is not available. Three key stratigraphic marker horizons are observed in these stratigraphic sections; the contacts between bedrock and diamicton (till), diamicton (till) and lacustrine deposits, and lacustrine and marine deposits. The freshwater proglacial lake and marine laminites and rhythmites at these locations have distinctive sedimentology and fossil assemblages that are consistent with similar deposits in other parts of the Champlain Lowland (Hunt and Rathburn, 1988) and the St. Lawrence Lowland (Rodrigues, 1988; Pair et al., 1988; Pair and Rodrigues, 1993). Ostracodes have been recovered from both lacustrine and marine sediment in the basin (Hunt and Rathburn, 1988; Cronin, 1977, 1979, 1981) and provide biostratigraphic information. Terrestrial pollen and plant macro-fossils have also been recovered from lacustrine and marine sediment in one of the study area exposures (Rayburn et al., 2002), which should provide biostratigraphic information, as well as material for ^{14}C dating. We have identified other potentially significant stratigraphic markers in our preliminary investigations including an abrupt change in sediment texture and bedding at the Keeseville section corresponding to a drop in proglacial lake level and a thick (~0.5 meter) sand layer in the lacustrine rhythmites at the Plattsburgh Air Force Base exposure, which may correspond to a large sediment influx into the basin. Finally, a unique bed of red clay has been identified at the same stratigraphic position at the Plattsburgh Air Force Base and Salmon River exposures (Rayburn et

al., 2002), which is similar in nature and stratigraphic position to a red clay bed observed in cores taken north of Montreal, Canada (Jan Aylsworth, pers. comm.).

Glacial lacustrine and marine sediments observed and sampled from exposures at the former Plattsburgh Air Force Base bluff and the bank of the Salmon River have shown that there is good correlation between sites, and that there is sufficient terrestrial pollen and plant macrofossil preservation to produce a paleoecological study during the time of the lacustrine to marine transition, as well as viable AMS ^{14}C ages (Rayburn et al., 2002). The till-lacustrine contact has been observed at Keeseville and Rae Brook, NY. Based on these exposures, we have estimated the ice retreat rate through the study area was about 0.45 km/year. Late marine sands cap the Air Force Base bluff, Salmon River and Rae Brook sites, indicating that they contain a complete post-glacial lacustrine and early marine record. The sediment sequences at the Air Force Base and Rae Brook are about 15 meters and 9 meters thick, respectively. Observed couplet thickness at these locations ranges from about 2mm to 5 cm.

A 4.57 meter-long core was obtained from Long Pond, between Willsboro and Keeseville (Stop 9, Figure 1), in March 2002. Long Pond was flooded by Lake Coveville immediately following ice recession from its valley. Proglacial lake water receded from the Long Pond valley when water level in the Champlain Lowland dropped to the Lake Fort Ann level thus creating an early version of modern Long Pond. The Lake Coveville to Lake Fort Ann drainage event may be recorded in the core by a contact between rhythmically laminated glacial lacustrine silty clay and lacustrine fine sand and silt. A wood sample collected 1 cm above this contact yielded a date of 10.9 ± 76 ^{14}C ka B.P. (Wk -10957).

Cobblestone Hill Ice Margin

Cobblestone Hill forms a conspicuous, elongate ridge on the northern flank of Cold Brook at the southeastern margin of Altona Flat Rock where the ice-marginal breakout flood river from Lake Iroquois entered glacial Lake Vermont. The ridge is more than 15 meters high, 500 m wide, and 2.5 kilometers long and is composed of angular boulders, almost exclusively Potsdam Sandstone, that range from 0.5 to about 3 meters in diameter. The average size of surface boulders decreases to the southeast. The position of the ice-front at the time of the breakout is marked by large kettle holes on the northern flank of Cobblestone Hill. The ice front extended northwestward toward Covey Hill where it corresponds closely to ice-front position No.11 of Denny (1974) (Figure 3).

The Cobblestone Hill deposits occur in crude terraces at elevations of approximately 230 m and 205 m, which lie close to the projected water planes of glacial lakes Coveville and Fort Ann (Chapman, 1937; Denny, 1967, 1970). The highest deposits on Cobblestone Hill correspond to similar deposits at Bear Hollow, approximately 1 km south across the present valley of the Little Chazy River. We believe that these data indicate that the ice front lay along the northern flank of Cobblestone Hill as the Lake Iroquois breakout began. The flood discharge initially deposited large boulders of Potsdam Sandstone, most of which were quarried locally from the sandstone pavements, into Lake Coveville. Glacial Lake Vermont dropped during the later stages of the breakout flood and the lower portions of Cobblestone Hill boulder deposit were graded to the Lake Fort Ann level. It is possible that the large influx of floodwater from the Lake Iroquois breakout overwhelmed whatever dam was impounding Lake Coveville and initiated erosion of the outlet to the Upper Fort Ann threshold. We have also observed that the southern extent of the Ingraham Esker, which extends 27-km northward from Beekmantown to Champlain (Figure), lies close to the reconstructed ice margin at the time when the ice front stood at Cobblestone Hill. We believe that it is also possible that the 30-meter drop in lake level between lakes Coveville and Fort Ann steepened the hydraulic gradients of meltwater within the ice mass and initiated the formation of the Ingraham Esker tunnel system. Cobble and gravel terraces on the northeast flank of Cobblestone Hill represent beach ridges formed in Lake Vermont (Woodworth, 1905a; Chapman, 1937; Denny, 1974) following retreat of the ice from the Cobblestone Hill ice margin.

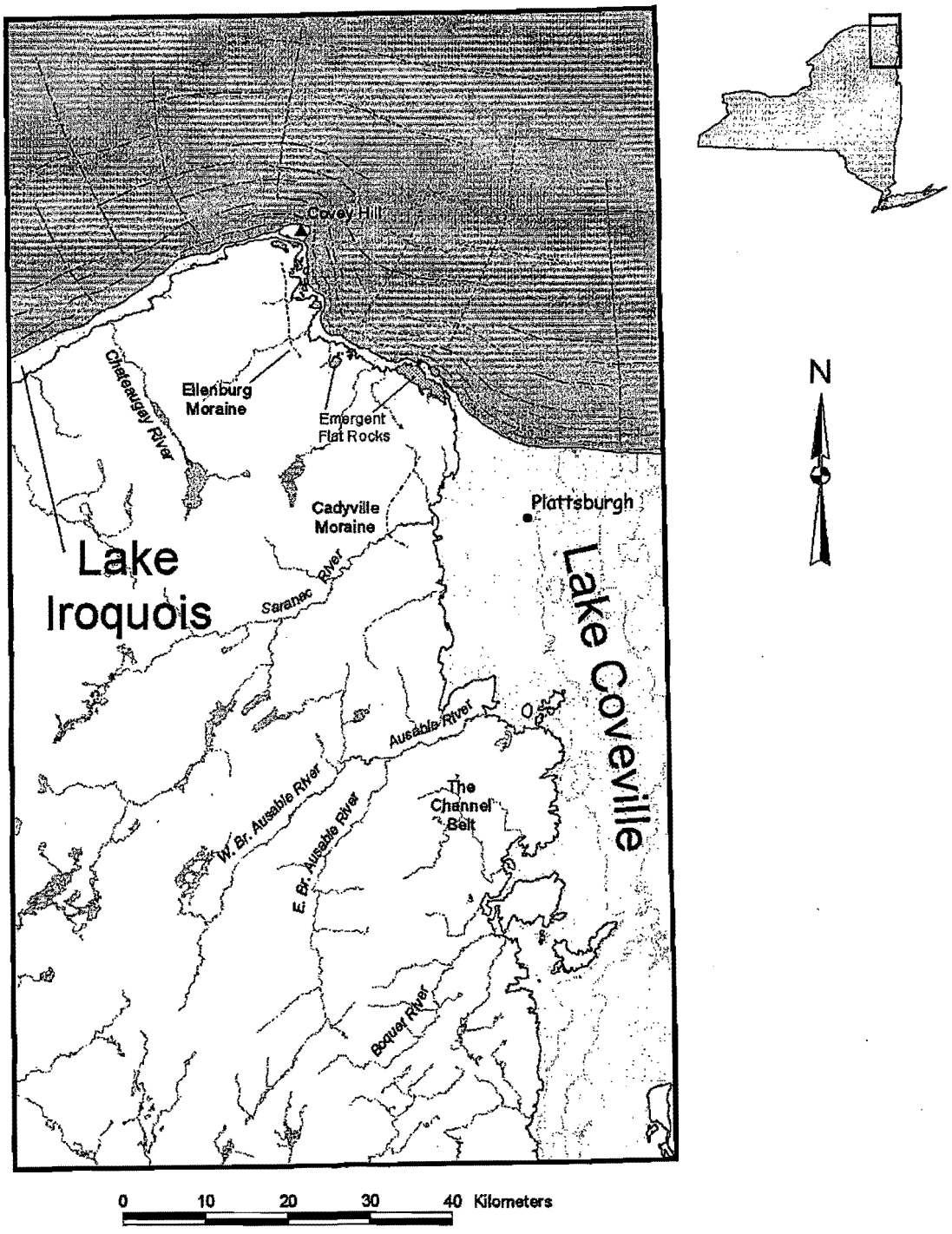

Figure 3. Map of the Champlain Lowland depicting the Cobblestone Hill ice margin and the breakout of glacial Lake Iroquois near Covey Hill.

PALEOCLIMATIC IMPLICATIONS

Ocean/atmosphere general circulation model (GCM) experiments by Rahmstorf (1995, 2000) predict that moderate changes in the flux of freshwater input into the North Atlantic, perhaps less than 0.06 Sv (1 Sv = 10^6 m^3 s^{-1}), can lead to disequilibria in the North Atlantic Deep Water (NADW) circulation, producing substantial changes in regional climate, such as the Younger Dryas event (Broecker et al., 1989). Recent efforts to model freshwater drainage from the North American continent during the last deglaciation by Licciardi et al. (1999) and Marshall and Clarke (1999) estimated that flow changes into the North Atlantic during deglaciation were approximately the same magnitude as those necessary, according to climate models, to affect NADW production. There were three major routes for freshwater discharge into the North Atlantic during the last deglaciation; through the Hudson Strait via Hudson Bay, through the St. Lawrence River, and through the Hudson River. While Licciardi et al. (1999) model recognize all three drainage routes, they acknowledge that the actual duration of southward drainage through the Hudson River is not well constrained. The Marshall and Clarke (1999) model does not have sufficient resolution to distinguish between discharges through the St. Lawrence River and the Hudson River paths (Marshall, pers. comm.).

The northern end of the Lake Champlain Basin is located at the junction of two of these three drainage routes. During the interval between the retreat of the ice margin from the northern slopes of the Adirondack mountains, and deglaciation of the lower St. Lawrence River Valley, all meltwater from the Great Lakes, St. Lawrence Lowland, and Champlain Valley regions that entered the North Atlantic had to pass through the Hudson River Valley via Glacial Lake Vermont in the Champlain Valley (Clark and Karrow, 1984; Pair et al., 1988; Pair and Rodrigues, 1993). When ice margin retreat opened the drainage route through the lower St. Lawrence Valley the southern Lake Vermont outlet was abandoned, and all freshwater drainage from the Great Lakes, St. Lawrence Lowland, and Champlain Valley was re-routed from the Hudson River Valley to the Gulf of St. Lawrence via the Champlain Sea (Clark and Karrow, 1984; Pair et al., 1988; Pair and Rodrigues, 1993).

We estimate that the drop from the Coveville to the Upper Fort Ann level released about 108 km^3 of water (Rayburn et al., 2001). The exposure at Keeseville Industrial Park indicates that this transition occurred within one-half varve year. We have therefore concluded that the discharge from this event was between 0.011 and 0.045 Sv, based on a one to four month event (Rayburn et al., 2001, Rayburn et al., in review). This discharge, about the smallest of the large freshwater discharge events, would have entered the North Atlantic through the Hudson Valley. We estimate the freshwater discharge that entered the North Atlantic through the St. Lawrence Valley during the lacustrine/marine transition was at least four times as large (Rayburn et al., 2002; Rayburn et al., in review). Estimates for water volume change between the Upper and Lower Fort Ann levels, the Main and Frontenac levels of Lake Iroquois, and the Frontenac and Upper Fort Ann levels in the Lake Ontario Basin are currently underway.

Our mapping has indicated that there were three large discharge events associated with transitions within the basin 1) the Coveville to Upper Fort Ann level transition, 2) the Upper Fort Ann to Lower Fort Ann level transition, and 3) the Lower Fort Ann to Champlain Sea level transition. Three other large scale discharge events that passed through the basin have also been recognized 1) the transition from the Main Lake Iroquois to Frontenac level which discharged through an outlet at Covey Hill and entered Lake Vermont at Altona Flat Rock, 2) the confluence of Lake Frontenac and Lake Vermont (the water in Lake Frontenac was roughly 110m higher than the water in the Lake Vermont before the confluence), and 3) at least one large discharge event from Lake Agassiz that was directed to the region through the Great Lakes (Clayton, 1983; Teller, 1987).

ACKNOWLEDGEMENTS

The authors would like to acknowledge the Center for Earth and Environmental Science and the Applied Environmental Science Program at SUNY Plattsburgh and the W.H. Miner Agricultural Research Institute for their unwavering support of our research at Altona Flat Rock. Plattsburgh State University research at the Ecosystem Studies Field Laboratory on Altona Flat Rock is supported by the National Science Foundation under Grant Nos. 9551126, 9912288, and 0139132. John Rayburn's graduate research at Binghamton University is partially supported by a grant from the Geological Society of America and a Graduate Assistantships in Areas of National Need Fellowship from the U.S. Department of Education. The Binghamton University Department of Geological Sciences and Environmental Studies and Dr. William Stein (Binghamton University Department of Biology) provided laboratory space for the pollen and macro-fossil analysis. Special thanks to Jack and Sarah Swan who graciously offered the facilities at the Pok-O-MacCready Outdoor Education Center to support this field trip and our coring efforts on Long Pond in March, 2002.

REFERENCES CITED

Alling, H.L., 1916, Glacial lakes and other glacial features of the central Adirondacks: Geol. Soc. America Bull., V.27, p.645-672.

----------, 1918, Pleistocene geology: in Miller, W.J., The geology of the Lake Placid Quadrangle: New York State Mus. Bull., Nos.211-212, p.71-95

----------, 1919, Pleistocene geology of the Lake Placid Quadrangle: New York State Mus. Bull., Nos.229-230 p.62-84.

----------, 1920, Glacial geology: in Kemp, J.F., Geology of the Mount Marcy Quadrangle: New York State Mus. Bull., Nos.229-230, p.62-86.

Anderson, T.W., 1988, Late Quaternary pollen stratigraphy of the Ottawa Valley-Lake Ontario region and its application in dating the Champlain Sea: in Gadd, N.R., ed., Quaternary evolution of the Champlain Sea basin, Geol. Assoc. of Canada Spec. Paper 35, p.207-224.

Bierman, P.R., Wright, S.F., and Nichols, K., 1999, Slope stability and late Pleistocene/Holocene history, northwestern Vermont: in Wright, S.F., ed., New England Intercollegiate Geologic Conference Guidebook No. 91, p. 17-50.

Broecker, W.S., Kennett, J.P., Flower, B.P., Teller, J.T., Trumbore, S., Banani, G., and Woelfli, W., 1989, Routing of meltwater from the Laurentide Ice Sheet during the Younger Dryas cold episode: Nature, V.341, p.318-321.

Chapman, D.H., 1937, Late-glacial and postglacial history of the Champlain valley: Am. Jour. Sci., 5th Ser. V.34, No.200, p.89-124.

Clark, P.U. and Karrow, P.F., 1984, Late Pleistocene water bodies in the St. Lawrence Valley near Malone, New York, and regional correlations: Geol. Soc. Amer. Bull., V.95, p.805-813.

Clayton, L., 1983, Chronology of Lake Agassiz drainage to Lake Superior: in Teller, J.T., and Clayton, L., eds., Glacial Lake Agassiz, Geological Association of Canada Special Paper 26, p.291-307.

Coleman, A.P., 1937, Lake Iroquois: Ontario Dept. Mines 45th Ann. Report, 1936, V. 45, Part 7, p.1-36.

Connally, G.G., and Sirkin, L.A., 1969, Deglacial history of the Lake Champlain-Lake George Lowland: distributed during field trip, 41st Annual Meeting, New York State Geological Association, 20p.

----------, 1971, The Luzerne readvance near Glens Falls, New York: Geol. Soc. Amer. Bull., V.82, p.989-1008.

----------, 1973, Wisconsinan history of the Hudson-Champlain Lobe: in Black, R.F., Goldthwait, R.P., and Willman, H.B., eds., The Wisconsinan Stage: Geological Society of America Memoir 136, p.47-69.

Craft, J.L., 1976, Pleistocene local glaciation in the Adirondack Mountains, New York: unpublished PhD dissertation, University of Western Ontario, London, 226p.

Cressey, G.B., 1977, Land Forms: in Thompson, J.H., Geography of New York State, Syracuse University Press, p.19-53.

Cronin, T.M., 1977, Late Wisconsin marine environments of the Champlain Valley (New York, Vermont): Quaternary Research, V.7, p.238-253.

----------, 1979, Late Pleistocene benthic foraminifers from the St. Lawrence Lowlands: Jour. Paleo., V.53, p.781-814

----------, 1981, Paleoclimatic implications of Late Pleistocene marine ostracodes from the St. Lawrence Lowlands: Micropaleontology, V.27, p.384-418.

Denny, C.S., 1967, Surficial geologic map of the Dannemora quadrangle and part of the Plattsburgh quadrangle, New York: U.S. Geol. Surv. Misc. Geol. Inv. Map I-630

----------, 1970, Surficial geologic map of the Mooers quadrangle and part of the Rouses Point quadrangle, Clinton County, New York: U.S. Geol. Surv., Geological Quadrangle Map GQ-635.

----------, 1972, The Ingraham Esker, Chazy, New York: U.S. Geological Survey Prof. Paper 800-B, p.B35-B41.

----------, 1974, Pleistocene geology of the northeastern Adirondack region, New York: United States Geological Survey, Professional Paper 786, 50p.

DeSimone, D.J., and LaFleur, R.G., 1985, Glacial geology and history of the northern Hudson basin, New York and Vermont: in Lindemann, R.H., ed., Field Trip Guidebook, 57th Annual Meeting, New York State Geological Association: Skidmore College, Saratoga Springs, New York, p.82-116.

----------, 1986, Glaciolacustrine phases in the northern Hudson Lowland and correlatives in western Vermont: Northeastern Geology, V.9, p.218-229.

Diemer, J.A., 1988, Subaqueous outwash deposits in the Ingraham ridge, Chazy, New York: Canadian Jour. of Earth Sci., V.25, No.9, p.1384-1396.

Diemer, J.A. and Franzi, D.A., 1988, Aspects of the glacial geology of Keene and lower Ausable valleys, northeastern Adirondack Mountains, New York: in Olmsted, J.F., ed., New York State Geological Association Field Trip Guidebook, 60th Annual Meeting, Plattsburgh, N.Y., p.1-27.

Dreimanis, A., 1976, Tills, their origins and properties; in Leggett, R.F., ed., Glacial Till, Royal Soc. Canada, Spec. Pub., No.12, p.11-49.

Franzi, D.A., and Cronin, T.M., 1988, Late Wisconsinan lacustrine and marine environments in the Champlain Lowland, New York and Vermont: New York State Geological Association Field Trip Guidebook, 60th Annual Meeting, Plattsburgh, N.Y., p.175-200

Franzi, D.A., and Adams, K.B., 1993, The Altona Flat Rock jack pine barrens: A legacy of fire and ice: Vermont Geology, V.7, p.43-61.

----------, 1999, Origin and fate of the sandstone pavement pine barrens in northeastern New York: in Wright, S., ed., New England Intercollegiate Geological Conference Guidebook No. 91, p.201-212..

Franzi, D.A., and Adams, K.B., and Pair, D.L., 1993, The late glacial origin of the Clinton County Flat Rocks: New York State Geol. Assoc. Field Trip Guidebook, 65th Annual Meeting, p.

Fulton, R.J., Anderson, T.W., Gadd, N.R., Harrington, C.R., Kettles, I.M., Richard, S.H., Rodrigues, C.G., Rust, B.R., and Shilts, W.W., 1987, Summary of the Quaternary of the Ottawa region: in Fulton, R.J., ed., Quaternary of the Ottawa region and guides for day excursions: XII INQUA International Congress, Ottawa, Canada, p.7-20.

Gooley, L., 1980, A history of Altona Flat Rock, located in Clinton County, New York State: Denton Publications, Inc., Elizabethtown, New York, 103p.

Gurrieri, J.T. and Musiker, L.B., 1990, Ice Margins in the northern Adirondack Mountains, New York: Northeastern Geology., V.12, p.185-197.

Hunt, A.S., and Rathburn, A.E., 1988, Microfaunal assemblages of southern Champlain Sea piston cores: in Gadd, N.R., ed., Quaternary evolution of the Champlain Sea basin, Geol. Assoc. of Canada Spec. Paper 35, p. 145-154.

Kemp, J.F. and Alling, H.L., 1925, Geology of the Ausable Quadrangle: New York State Mus. Bull., No.261, 126p.

Lawson, D.E., 1981, Sedimentological characteristics and classification of depositional processes in the glacial environment: CREEL Report 81-27, 16p.

Liccardi, J.M., Teller, J.T., and Clark, P.U., 1999, Freshwater routing by the Laurentide Ice Sheet during the last deglaciation: in Clark, P.U., Keigwin, L., and Webb, P., eds., Mechanisms of millennial-scale global climate change: American Geophysical Union Monograph 112, p.177-201.

MacClintock, P. and Stewart, D.P., 1965, Pleistocene geology of the St. Lawrence Lowlands: N.Y. State Mus. Bull. 394, 152p.

Marshall, S.J., and Clarke, G.K.C., 1999, Modeling North American freshwater runoff through the last glacial cycle: Quaternary Research, V.52, p. 300-315.

Miller, W.J., 1926, Geology of the Lyon Mountain Quadrangle: New York State Mus. Bull., Nos.271, 101p.

Morisawa, M., 1985, Rivers: Geomorphology Texts, Longman Group Limited, New York, 220p.

Muller, E.H. and Prest, V.K., 1985, Glacial lakes in the Ontario Basin: in Karrow, P.F. and Calkin, P.E., Quaternary Evolution of the Great Lakes, Geological Association of Canada Special Paper 30, p.213-229.

Occhietti, S., Parent, M., Shilts, W.W., Dionne, J., Govare, E., and Harmand, D., 2001, Late Wisconsinan glacial dynamics, deglaciation, and marine invasion in southern Quebec: in Weddle, T.K. and Retelle, M.J., eds., Deglacial history and relative sea-level changes, northern New England and adjacent Canada: Geol. Soc. Amer.,Special Paper 351, p.243-270.

Ogilvie, I.H., 1902, Glacial phenomena in the Adirondacks and Champlain Valley: Jour. Geol., V.10, p.397-412.

Pair, D.L., and Rodrigues, C.G., 1993, Late Quaternary deglaciation of the southwestern St. Lawrence Lowland, New York and Ontario: Geol. Soc. Amer. Bull., v.105, p.1151-1164.

Pair, D., Karrow, P.F., and Clark, P.U., 1988, History of the Champlain Sea in the central St. Lawrence Lowland, New York, and its relationship to water levels in the Lake Ontario basin: in Gadd, N..R., ed., The Late Quaternary development of the Champlain Sea basin: Geological Association of Canada, Special Paper 35, p.107-123.

Parrott, W.R., and Stone, B.D., 1972, Strandline features and Late Pleistocene chronology of northwest Vermont: in Guidebook for Field Trips in Vermont, New England Intercollegiate Geological Conference, 64th Annual Meeting, University of Vermont, Burlington, p.359-376.

Rayburn, J.A., Franzi, D.A., and Knuepfer, P.L.K., 2001, GIS-based volume and discharge calculations for a ctastrophic flood event from glacial Lake Vermont into the Hudson River Valley: Geol. Soc. Amer. Abstracts with Programs, V.33, A-15.

--------, in review, A large late glacial breakout flood through the Champlain and Hudson lowlands: Geol. Soc. Amer. Abstracts with Programs.

Rayburn, J.A., Yansa, C.H., Franzi, D.A., and Knuepfer, P.L.K., 2002., The biology and hydrology of the northern Lake Champlain basin before the Holocene: Geol. Soc. Amer. Abstracts with Programs, V.34, A-15.

Rodriguez, C.G., 1988, Late Quaternary invertebrate faunal associations and chronology of the western Champlain Sea basin: in Gadd, N.R., ed., Quaternary evolution of the Champlain Sea basin, Geol. Assoc. of Canada Spec. Paper 35, p.155-176.

Ruedemann, R., 1931, The tangential master-stream of the Adirondack drainage: Amer. Jour, Sci., V.22, p.431-40.

Teller, J.T., 1987, Proglacial lakes and the southern margin of the Laurentide Ice Sheet: in Ruddiman, W.L., and Wright, H.E., North America and adjacent oceans during the last deglaciation, Geological Society of America, The Geology of North America, V.K-3, p.39-69.

Wagner, W.P., 1972, Ice margins and water levels in northwestern Vermont: in Guidebook for Field Trips in Vermont, New England Intercollegiate Geological Conference, 64th Annual Meeting, University of Vermont, Burlington, p.319-342.

Wall, G.R., and LaFleur, R.G., 1995, The paleofluvial record of glacial Lake Iroquois in the eastern Mohawk Valley, New York: : in Garver, J.I., ed., Field Trip Guidebook, 67th Annual Meeting, New York State Geological Association: Union College, Schenectady, New York, p.173-203.

Woodworth, J.B., 1905a, Pleistocene geology of the Mooers Quadrangle: New York State Mus. Bull. 83, 67p.

----------, 1905b, Ancient water levels of the Champlain and Hudson valleys: New York State Mus. Bull. 84, 265p.

ROAD LOG

Miles Between Points	Cum. Mileage	Description
0.0	0.0	Assemble at the west parking lot of Hudson Hall on the SUNY Plattsburgh campus. Leave the lot and turn right (west) onto Broad Street.
0.2	0.2	Turn right (north) at the second traffic light onto Prospect Street. Continue north on Prospect until it ends at a traffic light on Tom Miller Road.
0.8	1.0	Turn left (west) onto Tom Miller Road and proceed across the I-87 overpass to the traffic light at Quarry Road.
0.2	1.2	Turn right (north) onto Quarry Road and proceed north to the traffic light at the Cadyville Expressway (Rte 374).
0.9	2.1	Quarry Road ends at Cadyville Expressway intersection. Continue straight (north) through the intersection onto Rte 22.
2.7	4.8	The Rae Brook exposure lies on the east side of the small stream valley to your right. The base of the section consists of dark gray, calcareous diamicton (till). The diamicton is overlain by 1.0 to 1.3 meters of thinly laminated rhythmites, which are in turn overlain by marine clays. The faunal assemblages described by Cronin (1977, 1979, 1981) represent the late glacial transition from lacustrine to marine environments in the Champlain and St. Lawrence Lowlands approximately 11.6 to 12.0 ^{14}C ka. B.P. The bottom water temperatures and salinities at this time probably ranged from –2°C to 10°C and 0 to 18 ppt, respectively (Franzi and Cronin, 1988). Continue north on Rte. 22 to the blinking traffic light at Beekmantown Four Corners.
1.5	6.3	Turn left (west) onto O'Neil Road. O'Neil Road bears right at 0.4 miles from the Rte 22 intersection. Continue north on O'Neil Road until it ends at the West Church Street intersection in Chazy.
4.0	10.3	Turn left (west) onto West Church Street.
0.8	11.1	Turn right (north) onto Barnaby Road. Barnaby Road crosses the Little Chazy River 0.1 miles north of the West Church Street intersection.
0.5	11.6	Denny (1970, 1974) mapped low-relief marine beach ridges on the right (east) of Barnaby Road. The hummocky topography for the next 0.5 miles was mapped by Denny (1974) as recessional moraine.
0.4	12.0	Continue straight (north) on Barnaby Road past the Slosson Road intersection.
0.1	12.1	Barnaby Road and the pavement end at this point. Continue straight (north) on Blaine Road. Blaine Road makes a sharp left turn at 0.9 miles. Continue west on Blaine Road.
1.1	13.2	Blaine Road makes a sharp right turn at the gate to the entrance to the Altona Flat Rock property owned by the William H. Miner Agricultural Research Institute. Leave Blaine Road and continue straight (west) through the gate. It is a good idea to open the gate before completing this step. The Altona Flat Rock access road rises onto the northeastern flank of Cobblestone Hill.
0.1	13.3	Park at a clearing near a sharp turn in the access road.

STOP 1. COBBLESTONE HILL BEACHES. (20 minutes) The beaches at this location were first described by Woodworth (1905a) and later by Denny (1974). The deposits consist predominantly of moderately rounded to well rounded, cobble gravel in multiple, low relief ridges or terraces that extend along the northern and eastern flanks of Cobblestone Hill at elevations between 206 and 175 meters above sea level. The highest ridges lie near the projected highest shoreline of the Upper Lake Fort Ann. Individual ridgess are typically 1 to 2 meters high and 10 to 20 meters wide, and often extend laterally for more than 400 meters (Denny, 1974). The gravel is almost exclusively composed of Potsdam Sandstone that was presumably derived from the alluvial cobble to boulder gravel that composes Cobblestone Hill.

The large (0.2 to 1.4 meter diameter), angular boulders that comprise the core of Cobblestone Hill can be seen along the road a short distance above the highest beach ridge. The boulders of Cobblestone Hill represent material washed into Lake Vermont from the sandstone pavements by ice-marginal streams from the breakout of glacial Lake Iroquois (Woodworth, 1905a; Denny, 1974; Clark and Karrow, 1984; Pair et al., 1988). Reworking of these alluvial deposits by wave action with relatively little longshore transport probably formed the beach deposits (Denny, 1974).

Miles Between Points	Cum. Mileage	Description
	13.3	Continue up the access road and turn right at the fork just past the highest beach ridge.
0.1	13.4	Bear right and onto a concrete road (Scarpit Road) at Miner Dam. The Scarpit Road presents many hazards, especially for those driving it for the first time. Please drive slowly and cautiously. The road lies on the southwest flank of Cobblestone Hill following the abandoned shoreline of the former reservoir behind Miner Dam. Miner Dam was part of a failed hydroelectric project initiated by William Miner in 1910 (Gooley, 1980). By the time of its completion in March, 1913, the concrete dam, known locally as the "Million-Dollar Dam", had a maximum height of over 10 meters and stretched more than 700 meters across the Little Chazy River valley. The design capacity of the reservoir was more than 3.5 million cubic meters. The inadequate flow of the Little Chazy River and ground water seepage through Cobblestone Hill, which formed the eastern flank of the reservoir, proved to be major design flaws for the project. A 10 to 15 cm layer of concrete grout was spread over more than 100,000 m^2 along the flank of Cobblestone Hill (the Scarpit) to mitigate the seepage loss. A deep trench was excavated at the base of Cobblestone Hill behind the dam for the purpose of pouring a grout curtain to the underlying sandstone and thereby, presumably, sealing the northeastern flank of the reservoir. The dam and generating station were completed in 1913 but it took almost two years to fill the reservoir to capacity. The grouting effort was partially successful and the power generating plant began operation on January 21, 1915, more than four years from the beginning of the project (Gooley, 1980). The power plant produced electricity intermittently for seven years before mechanical problems forced the abandonment of the project. Construction of a second dam, the Skeleton Dam (Gooley, 1980), approximately 1.5 km upstream was begun in 1920 to provide supplemental flow to the main impoundment. The Skeleton Dam project, however, ended with the failure of the Miner Dam generating station and was never completed.
0.5	13.9	Park near the Scarpit weather station.

STOP 2. COBBLESTONE HILL ICE MARGINAL DEPOSITS. (40 minutes) The Cobblestone Hill boulder deposits occur at two distinct elevations at this location. The upper level lies between 225 and 232 meters above sea level and may correspond to cobble and boulder deposits at a similar elevation near Bear Hollow, on the southwestern side of the Little Chazy River valley. The elevation of these deposits is close to projected elevation of the Coveville Stage if the Coveville shoreline is extended northward from where Chapman (1937) and Denny (1974) mapped the northernmost Coveville shoreline deposits in the Saranac River valley, assuming a northward isobase gradient of approximately1.2 m/km. The lower level lies between 206 and 215 meters above sea level and corresponds to the boulder deposits observed at Stop 1. The lower level boulder deposits lie close to the elevation of the Upper Lake Fort Ann high stand shoreline (Chapman, 1937; Denny, 1970, 1974).

The northeastern flank of Cobblestone Hill contains several large depressions that we interpret to be kettle holes. The northeastern ends of the kettles rise onto a broad terrace composed of beach deposits (Denny, 1970, 1974) at elevations between 201 and 204 meters above sea level. These beach deposits correspond closely to the elevation of Lower Lake Fort Ann.

We believe that these data indicate that the ice margin stood at Cobblestone Hill at the time of the Lake Iroquois breakout and that proglacial water levels in the Champlain Lowland dropped during deposition of the Cobblestone Hill boulder deposits deposition of the Cobblestone Hill boulder deposits.

Miles Between Points	Cum. Mileage	Description
	13.9	Return to the vehicles and continue northwest on the Scarpit Road.
0.3	14.2	Note the outcrop of Potsdam Sandstone on your left. The largest boulders on Cobblestone Hill have long dimensions that exceed 3m.
0.2	14.4	The Scarpit Road makes a sharp right turn and the concrete pavement ends. The road emerges onto Altona Flat Rock within 30 meters of the turn. The transition from the northern hardwood forest on Cobblestone Hill to the jack pine barrens on Altona Flat Rock is abrupt at this location.
0.1	14.5	Park at the USGS observation well.

STOP 3. ALTONA FLAT ROCK SANDSTONE PAVEMENT AND JACK PINE BARRENS. (20 minutes) The large areas of sandstone pavement provide habitat for some of the largest jack pine (*Pinus banksiana*) barrens in the eastern United States (Woehr, 1980; Reschke, 1990). Jack pine is a relatively short-lived (<150 years), shade-intolerant, boreal species that maintains communities on the sandstone pavements because of its adaptations to fire and ability to survive in an area with thin (or absent), nutrient-poor soils.

A large proportion of the pine barrens in northeastern New York are owned by a few public and private sector organizations. The William H. Miner Agricultural Research Institute is the largest landowner of pine barrens with almost 1000 ha (hectares) of jack and pitch pine barrens on Altona Flat Rock. New York State owns an additional 600 ha of the Altona Flat Rock barrens, approximately 100 ha of the Gadway barrens and 200 ha of pine barrens at The Gulf near Covey Hill. The Adirondack Nature Conservancy owns 222 ha of the Gadway jack pine barrens at Blackman Rock.

Plattsburgh State University and the William H. Miner Agricultural Research Institute have collaborated in research and teaching initiatives in the Altona Flat Rock pine barrens for more than 30 years. The hydrogeological equipment and instrumentation at Stops 2 and 3 are part of the Ecosystem Studies Field Laboratory (ESFL), a field station dedicated to undergraduate teaching and research in geology and environmental science. The field site offers an excellent geological, hydrological and

ecological setting for illustrating the interdependence of natural processes and the effects of human activities on natural ecosystems. For the past three years the ESFL site has been the focus of the Plattsburgh Research Experiences for Undergraduates program, which is funded by the National Science Foundation and the William H. Miner Agricultural Research Institute. The reader is referred to Franzi and Adams (1993, 1999) for a more detailed description of the Altona Flat Rock pine barrens and the Ecosystem Studies Field Laboratory Project.

Miles Between Points	Cum. Mileage	Description
	14.5	Turn back onto the Scarpit Road and proceed back toward Miner Dam.
1.1	15.6	Bear left at the end of the Scarpit Road at Miner Dam and continue toward the gate at the entrance to the property.
0.1	15.7	Continue straight through the gate onto Blaine Road and continue to Slosson Road.
1.2	16.9	Turn left (east) onto Slosson Road. Please drive cautiously and watch for children and farm animals as you pass the Parker Farm at 17.1 miles.
0.3	17.2	A marine beach ridge can be seen in the field on the right (south) near the intersection with Vassar Rd. Continue east on Slosson Road to the intersection with Rte. 22.
1.5	18.7	Continue straight (east) on Slosson Road across the Rte. 22 intersection to the Rte. 348 intersection.
1.5	20.2	Continue straight (east) on Slosson Road across the Rte. 348 intersection to the Ashley Road intersection.
0.7	20.9	Turn left (north) onto Ashley Road.
0.5	21.4	Turn right (east) into the Kalvaitis gravel pit.

STOP 4. INGRAHAM ESKER AT THE KALVAITIS GRAVEL PIT. (40 minutes). The Ingraham Esker is one of the most conspicuous glacial landforms in the northern Champlain Lowland. This pit contains esker fan deposits, such as described by Diemer (1988), and deposits resedimented by wave action in the Champlain Sea as described by Denny (1972, 1974). Most of the pit is cut into proximal to medial subaqueous fan gravel and sand. The resedimented deposits consist primarily of fossiliferous gravel that occur as dipping bedsets on the western flank of the esker. Individual beds are several centimeters to a few decimeters thick and are laterally continuous for several meters.

Miles Between Points	Cum. Mileage	Description
	21.4	Leave the gravel pit and turn left (south) onto Ashley Road.
0.5	21.9	Turn left (east) onto Slosson Road.
0.5	22.4	Turn right onto Esker Road. A gravel pit containing esker tunnel and proximal subaqueous fan gravel and sand can be seen on the right (west) side of the road at 22.5 miles.
0.8	23.2	Park beside the road near the head scarp of a gravel pit.

STOP 5. INGRAHAM ESKER AT ESKER ROAD. (10 minutes) This location is the "West Pit" section of Diemer (1988). Most of the sediment consists of coarse-grained channel fill deposits. These deposits generally occur lenticular beds that are meters thick, tens of meters wide and may be traceable for tens of meters in the flow direction (Diemer, 1988). Marine reworking of the esker deposits at this location is restricted to a thin layer (1 to 2 meter) of interbedded sand and gravel near the top of the pit.

Miles Between Points	Cum. Mileage	Description
	23.2	Continue south on Esker Road to the Stratton Hill Road intersection.
1.2	24.4	Turn left (east) onto Stratton Hill Road and cross the I-87 overpass. The esker was removed in the I-87 corridor but the ridge can be seen on the right (south) side of Stratton Hill Road east of I-87.
0.2	24.6	Stratton Hill Road makes a sharp right turn at the stop sign. Turn right (south) and continue on Stratton Hill Road.
0.9	25.5	Turn right (south) onto Rte. 9. The esker ridge parallels Rte. 9 on the right-hand (east) side of the road. The ridge crosses the Rte 9 at 26.2 miles and continues its southward trend on the left-hand (west) side of the road.
6.2	31.7	Enter the City of Plattsburgh on Rte. 9. Continue south.
0.9	32.6	Continue straight through the lights at the intersections of Tom Miller Road and Sailly Avenue near the Georgia-Pacific Paper Mill.
0.2	32.8	Turn left (south) onto Miller Street.
0.5	33.3	Turn left (east) at the end of Miller Street and proceed to the stop sign at City Hall Place near the MacDonough Monument. Turn right (south) onto City Hall Place.
0.2	33.5	Turn right (east) at the stop sign onto Bridge Street and cross over the Saranac River.
0.1	33.6	Turn right (south) at the traffic light onto Peru Street.
0.1	33.7	Continue Straight (south) through the first traffic light and turn left (east) onto Hamilton Street at the second.
0.1	33.8	Continue straight (east) through the MacDonough Street intersection.
0.1	33.9	Turn right (south) onto Club Street and enter the former Plattsburgh Air Force Base. Club Street becomes US Oval West and continues south past the former officers quarters.
0.9	34.8	Continue straight (south) at the stop sign onto Ohio Avenue East.
0.2	35.0	Turn left (east) on the marina access road.
0.1	35.1	Cross the railroad overpass to the parking lot.

STOP 6. PLATTSBURGH AIR FORCE BASE MARINA SECTION AND LUNCH STOP. (80 minutes) The bluffs along the shore of Lake Champlain extend for more than 1 km north from the former Plattsburgh Air Force Base marina. The bluffs probably contain a complete late glacial stratigraphic section, however, no single location contains all of the stratigraphic units. A massive gray diamicton lies at the base of the glacial section. The diamicton is exposed at the north end of the bluffs where it overlies striated bedrock. The upper contact is not exposed.

The base of the section near the marina consists of more than 3 m of dark gray clayey rhythmites, which were probably deposited as varves in glacial Lake Vermont. The rhythmites occur as clay and silty clay couplets that range from a few centimeters thick in the lower part of the section to thin couplets that rarely exceed a few millimeters in thickness near the top of the unit. Soft-sediment deformation structures are common. Rock and sediment clasts are distributed throughout the unit as individual clasts and in discrete layers along bedding planes. A deformed bed of medium sand that is 0 to 0.2 m thick occurs near the base of the exposed section. The lateral extent of this unit is not known. A thick reddish brown clay lamina occurs near the top of the rhythmite unit. This lamina is similar in nature and stratigraphic position to a red clay bed observed in cores taken north of Montreal, Canada (Jan Aylsworth, pers. comm.).

The rhythmites are conformably overlain by 1.5 to 2.0 m of laminated to thinly bedded, fossiliferous marine mud. The mud facies coarsens upward to horizontally bedded silt and fine sand. The silt and sand unit is approximately 7 m thick and the unit coarsens upward. Individual beds range from a few centimeters to a decimeter or two thick and are generally normally graded. These deposits probably record the incursion and gradual regression of the Champlain Sea in the region.

Miles Between Points	Cum. Mileage	Description
	35.1	Turn back across the railroad overpass to Ohio Avenue East.
0.1	35.2	Turn right (north) onto Ohio Avenue East.
0.2	35.4	Turn left (west) onto New York Road and exit the Former Air Force Base.
0.1	35.5	Turn left (south) at the light onto Rte 9. Continue south on Rte. 9 to Keeseville. The road passes Clinton County Community College at 37.6 miles, crosses the Salmon River at 39.2 miles, and crosses the AuSable River at 44.2 miles.
9.1	44.6	The road rises onto a marine delta deposit built by the AuSable River into the Champlain Sea. The upper surface of the delta is at an elevation of about 70 meters above sea level.
1.1	45.7	The road rises onto a higher (elevation = 106 m) marine delta.
1.0	46.7	Cross the AuSable River at AuSable Chasm and turn right into the parking lot on the south end of the bridge.

STOP 7. AUSABLE CHASM DISCUSSION AND PHOTO OP. (15 minutes) AuSable Chasm is one of the most unique scenic spots in the Champlain Lowland. The AuSable River has carved a spectacular gorge that exposes a 135 m thickness of the Keeseville Member of the Potsdam Sandstone. The AuSable River also cuts through the upper marine delta noted in the road log, and thus, the cutting of the chasm postdates the Champlain Sea interval.

Miles Between Points	Cum. Mileage	Description
	46.7	Continue south on Rte. 9.
1.5	48.2	Turn left at the traffic light and follow Rtes. 9 and 22 south. The road crosses the AuSable River and then bears right (south) into the village of Keeseville.
0.4	48.6	Rte. 9 rises out of the AuSable River Valley and onto the surface of a delta that was built into Lower Lake Fort Ann. The delta surface elevation is approximately 156 meters above sea level.
0.9	49.5	Turn right (west) onto Augur Lake Road.

Miles Between Points	Cum. Mileage	Description
0.2	49.7	Turn right (north) onto Industrial Park Road
0.3	50.0	Park beside the road.

STOP 8. KEESEVILLE INDUSTRIAL PARK EXPOSURE. (40 minutes) The Keeseville Industrial Park section is exposed in a landslide scar on the south bank of the AuSable River. The river is deeply incised into a deltaic terrace graded to Lower Lake Fort Ann. The surface elevation of the delta surface is approximately 155 m.

A massive to crudely bedded, dark gray diamicton forms the base of the section. The diamicton is overlain by approximately 2 m of rhythmically laminated silt and clay couplets. Clay laminae are generally 1 cm or less thick and the silt laminae or beds range from about 0.5 to 4 cm thick. The silt beds are commonly internally laminated. The rhythmite section contains about 67 couplets. The rhythmite section is conformably overlain by approximately 7 m of deltaic silt and sand that coarsen upward to sand and gravel.

The sediments at Keeseville Industrial Park record ice recession from the AuSable Valley. The basal diamicton is interpreted to be a till and thus represents ice cover. The rhythmites are probably varves and thus record inundation of the lower AuSable Valley by proglacial Lake Coveville. Assuming that the entire varve sequence represents proglacial Lake Coveville and the overlying silt and sand record the drop of proglacial lake level to Upper Lake Fort Ann, then Coveville occupied the lower AuSable Valley for approximately 67 varve years before proglacial lake levels dropped to the Upper Lake Fort Ann level. The ice front may have receded about 30 km north to the Cobblestone Hill Ice margin over this time interval at an average retreat rate of approximately 0.45 km/yr.

Miles Between Points	Cum. Mileage	Description
	50.0	Follow Industrial Park Road back to Augur Lake Road.
0.3	50.3	Turn left (east) onto Augur Lake Road.
0.2	50.5	Turn left (north) onto Rte. 9 and proceed back toward Keeseville.
0.9	51.4	Turn left (east) at the base of the hill onto Clinton Street.
1.5	52.9	Turn right (south) onto Highlands Road. Highlands Road offers spectacular views of Lake Champlain. Burlington, Vermont lies directly across the lake at this point and is visible on a clear day.
2.1	55.0	A series of marine terraces lie to the left (east) side of the road.
0.3	55.3	A prominent Upper Lake Fort Ann sand and gravel spit parallels the right (west) side of the road. Chapman (1937) identified this feature and measured its surface elevation as 161 meters above sea level.
5.8	61.1	Turn left (south) onto Rte. 22. Long Pond is on the right (west) side of the road at 61.6 miles.
1.6	62.7	Turn right (west) onto Reber Road North.
0.6	63.3	Pull off the side of the road adjacent to Long Pond.

STOP 9. LONG POND CORE. (40 minutes) The Long Pond basin was a deep embayment in Lake Coveville. The drop to the Upper Lake Fort Ann level, however, left proglacial water levels in the Champlain Lowland below the threshold of Long Pond. The bottom sediment of Long Pond was vibra-cored in March, 2002. Wood obtained 1 cm above a horizon that may represent the drainage of Lake Coveville at this site yielded a date of 10.9 ± 76 ^{14}C ka B.P. (Wk - 10957). These discussions will continue at the Pok-O-MacCready Outdoor Education Center 0.5 miles (63.8 miles) west of this location where a portion of the Long Pond Core will be displayed.

Miles Between Points	Cum. Mileage	Description
	63.8	Continue west on Reber Road.
5.1	68.9	Turn right (west) onto Deerhead Road.
1.7	70.6	The Deerhead Road traverses an Upper Lake Fort Ann delta built by the North Branch of the Boquet River.
1.0	71.6	The road rises to the top of a large Lake Coveville delta, known locally as "The Plains". The "The Plains" delta was built by North Branch flow that was augmented in its early stages by outflow from proglacial lakes in the AuSable River basin to the west via the "Channel Belt" (Kemp and Alling, 1925; Diemer and Franzi, 1988).
0.6	72.2	Deerhead Road crosses over I-87. There is a good view of "The Plains" delta to the right (south). Continue west on the Deerhead Road to the Rte 9 intersection.
0.9	73.1	Turn left (south) onto Rte.9 and proceed to the intersection with Pulsifer Road.
2.7	75.8	Turn right (west) onto Pulsifer Road. The road makes a sharp right 0.3 miles from the intersection. Stay on Pulsifer Road.
0.6	76.4	Turn left (west) and proceed through the gate to the NYCO wollastonite quarry at Oak Hill. The road crosses a series of channeled kame terraces and eventually rises to the quarry. Park well off the haul road.

OPTIONAL STOP 10. NYCO WOLLASTONITE QUARRY. (40 minutes) The quarry operators have excavated deeply into ice-marginal stratified drift and diamicton on the flank of Oak Hill. The composition, stratification and texture of these deposits is highly variable. The stratified sediment probably represents sedimentation by ice-marginal streams flowing from the "Channel Belt" (Kemp and Alling, 1925) and local impoundments. The diamicton are probably till or sediment flow deposits.

Miles Between Points	Cum. Mileage	Description
	76.4	Return to the gate at the entrance to the quarry and turn right (south) onto Pulsifer Road.
0.6	77.0	Turn right (south) at stop sign onto Route 9.
1.0	78.0	Turn left (east) onto County Route 12 and proceed to I-87.
1.6	79.6	Turn right (south) onto the I-87 access ramp and proceed to the NEIGC-NYSGA conference center in Lake George.

End of Road Log

THE CHAMPLAIN THRUST SYSTEM IN THE WHITEHALL-SHOREHAM AREA: INFLUENCE OF PRE- AND POST-THRUST NORMAL FAULTS ON THE PRESENT THRUST GEOMETRY AND LITHOFACIES DISTRIBUTION.

Nicholas W. Hayman, Department of Earth and Space Sciences, Box 351310, University of Washington, Seattle, WA 98195, nickh@u.washington.edu
W.S.F. Kidd, Department of Earth and Atmospheric Sciences, University at Albany, SUNY, Albany, NY, 12222

Introduction

The Taconic foreland is an exemplar of collisional tectonics and the Champlain Valley of West-Central Vermont is a pivotal region for mapping and reconstructing this system (**figure 1**). This is because between the latitudes of Middlebury, VT and Whitehall, NY, the shelf sequence gives way to the foredeep and rise sequences along the strike of the eastward dipping range (Stanley, 1987; Kidd et al., 1995) (**figure 2**). Although many significant contacts between the sequences have been recognized as faults, the accrued transport on these faults, and the relationship between them in time and space, is ambiguous. This is partly due to the difficulty in determining the map trace of significant faults across regions of poor outcrop and sharp contrasts in stratigraphic units and sedimentary facies.

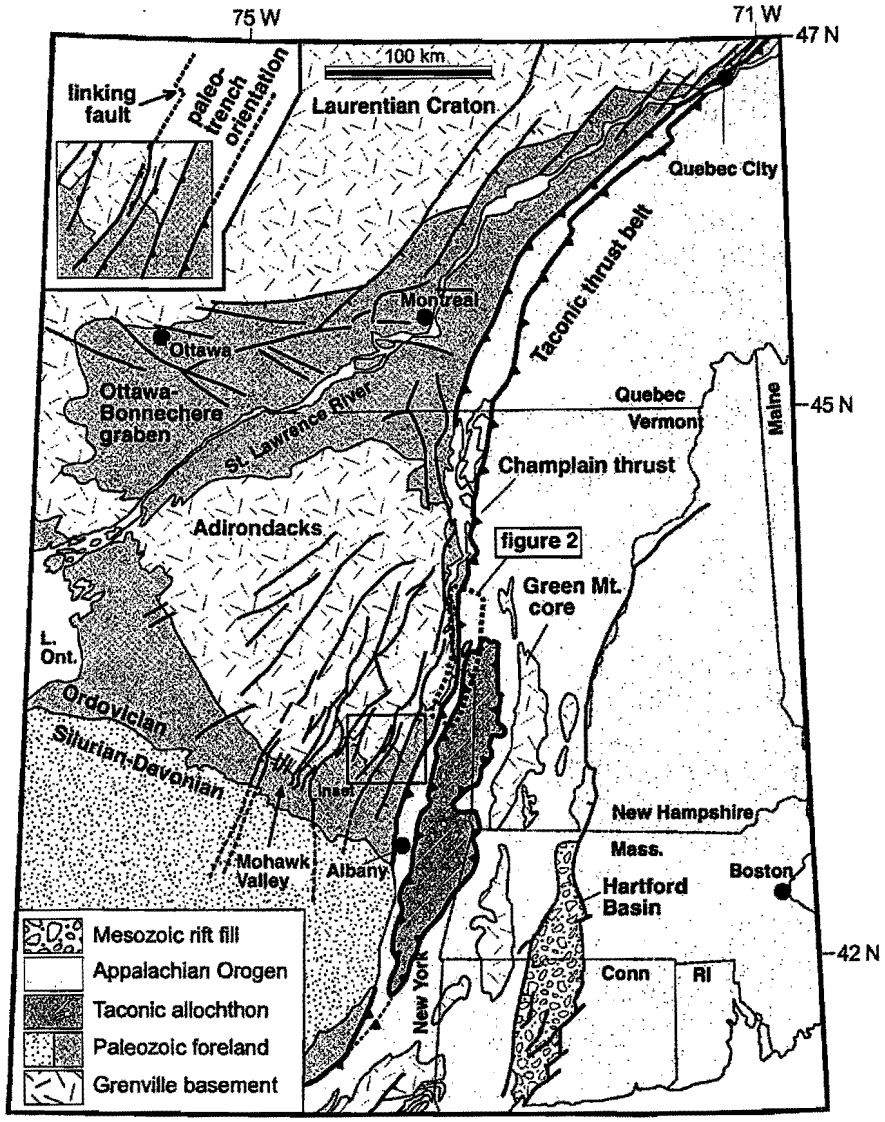

Figure 1. Map of New England illustrating the relationship between geologic provinces. All of the faults depicted are normal faults except for the major thrusts of the Taconic thrust belt. The Hartford and Newark grabens (the latter is not depicted) are Mesozoic structures. Many of the normal faults west of the Taconic thrust belt that cut the southern margin of the Adirondacks, and those in Quebec, are demonstrably medial Ordovician age, without significant earlier or later slip, and in paleotrench parallel, and subordinate paleotrench normal orientations (inset detail from Mohawk Valley; location outline shown by outline box). Dashed lines indicating extensions of normal faults are beneath the Silurian-Devonian cover, and do not cut it.

This field trip visits outcrops along the *Champlain thrust system* (*CTS*), including the *Mettawee* (River) fault, a late normal fault that significantly truncates thrusts of the CTS. These outcrops are from the areas discussed in Hayman and Kidd (2002), a synthesis of our work in the region. Our mapping focused on the CTS, which was responsible for large (>80 km) transport of the shelf section (Rowley, 1982). A cornerstone of our interpretation is that many abrupt changes in map units along-strike, and problems in restoration of cross-sections across the map area, are the consequence of reactivation of preexisting faults. The early (prethrust) faulting occurred in response to extension along the synconvergent flexural forebulge. Other significant lithic changes are the result of late (postthrust) normal faulting associated with one of the several phases of extension that affected the region. The thrust system projects to depth and thus is dynamically related to the overlying Taconic thrusts, and collectively forms a decollement beneath the Green Mountain crystalline core of the Taconic orogen (Rowley, 1982).

The Taconic Sequence

Building on the early work identifying the major faults and unconformities in the Taconic sequence (e.g. Dale, 1899; Keith, 1932; Zen, 1967), several workers refined the allochthonous stratigraphy, related the units to Cambrian-early Ordovician rise and middle Ordovician foredeep sedimentary facies, and recognized that most of the deformational fabric in the rocks post-dated lithification (Delano et al., 1979; Rowley and Kidd, 1983; Bosworth and Rowley, 1984). These observations and inferences provide a restoration of these rocks to their depositional site that requires far-traveled tectonically rooted thrusts such as are found in modern arc-continent collisions (Rowley and Kidd, 1983) (**Figure 3**). The simplest model of such a foreland thrust system predicts a forward-propagating system wherein, for the Taconic foreland, thrusts young to the west. However, many of the fold patterns, deformational fabrics, and cross-cutting relationships of thrusts found in the Taconic foreland require at least some late deformation (Zen, 1972; Rowley and Kidd, 1983; Stanley and Ratcliffe, 1985).

One explanation for late deformation derives from observations of outcrop structures, fabrics, and map patterns in the Taconic foreland requiring at least one out-of-sequence thrust towards the front of the Taconic thrust system. This thrust was awkwardly named *the Taconic frontal thrust* due to its position at the western front of the Taconic Allochthon near Whitehall, NY (Bosworth et al., 1988).

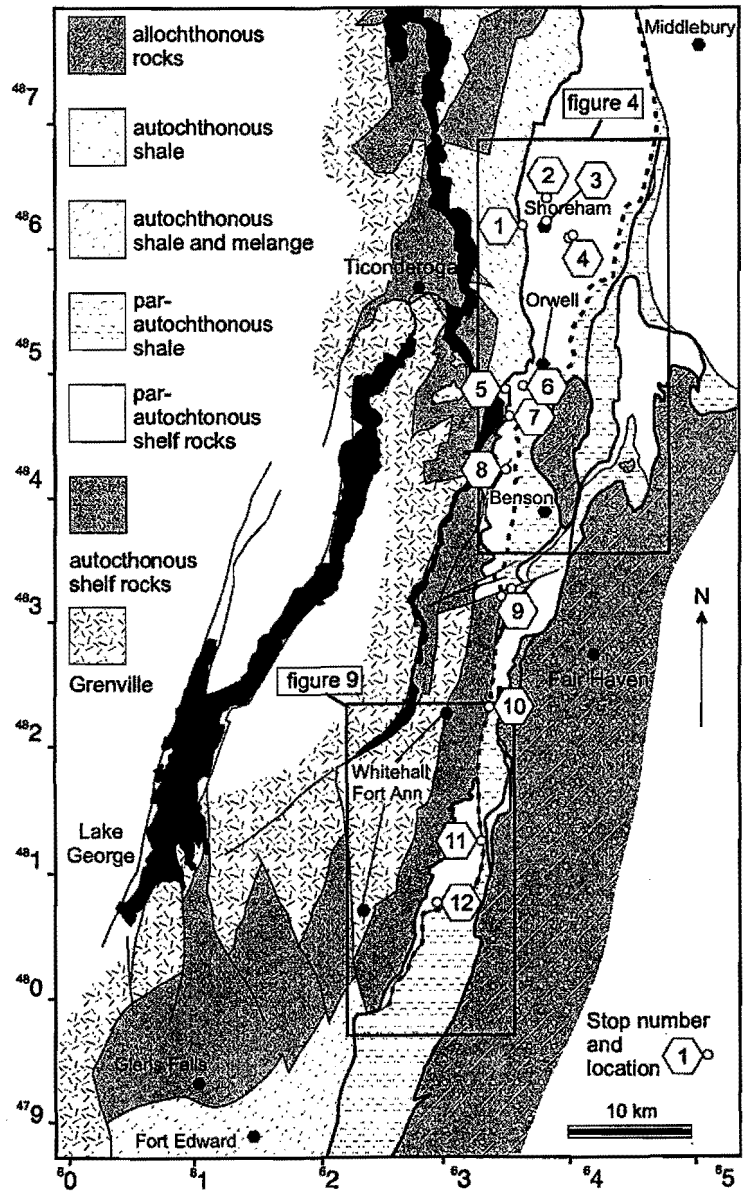

Figure 2. Regional map of west-central Vermont to the upper Hudson River valley of New York illustrating the trace of the Champlain thrust system. The Mettawee fault, in a dashed line, places deformed and low grade metamorphosed shale and flysch, and to the north of Whitehall, imbricated upper shelf carbonates, against the parautochthon. South of the disappearance of the parautochthonous carbonates, it is unclear precisely where the trace of the Mettawee fault or Champlain thrust run.

The Taconic frontal thrust cuts *the Taconic basal thrust*, the thrust responsible for the initial transport of the rise-facies Taconic sequence (Bosworth and Rowley, 1984). Most of the deformational patterns at both the outcrop and map scale can be explained with this model of Middle Ordovician forward propagating thrusting with a component of out-of-sequence thrusting. Two possible, but not preferred, alternative hypotheses for the causes of late foreland deformation are that: (*i*) they resulted from Devonian age tectonics such as the Acadian collision between Laurentia and Avalon (Zen, 1972), or (*ii*) that the system underwent a phase of *retrocharriage* (back- and hinterland-propagating- thrusting) with late Taconic deformation in the internal, eastern portions of the belt (Stanley and Ratcliffe, 1985).

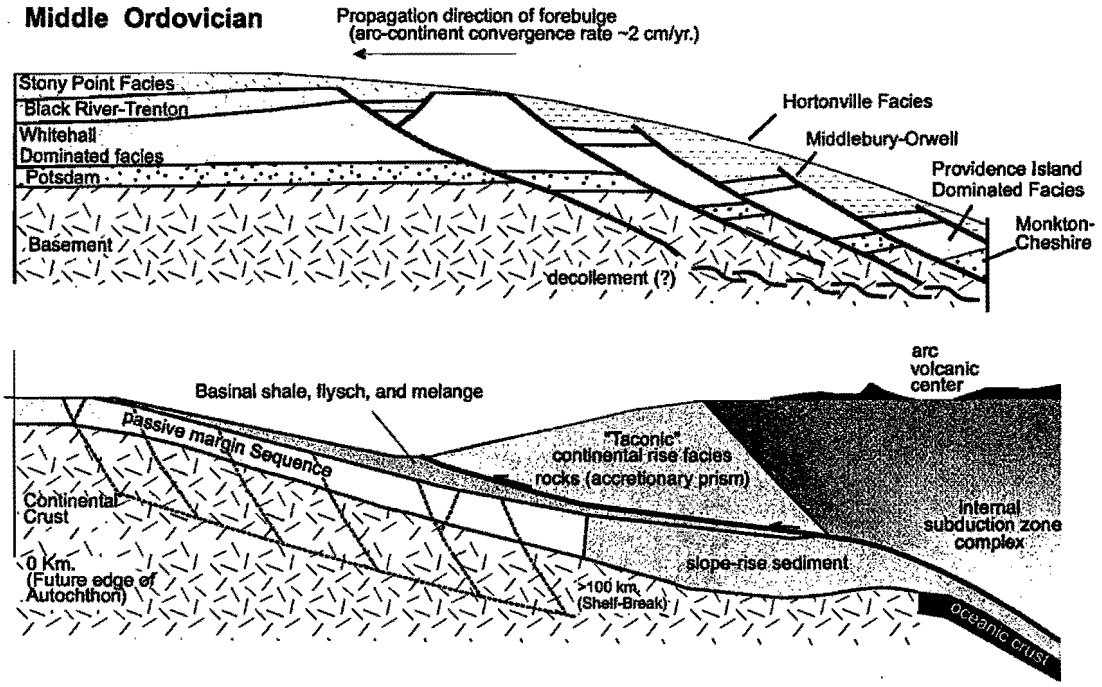

Figure 3. Schematic profiles of the pre- and syn-collisional shelf. The change in sedimentary facies across the shelf is indicated; the Monkton-Cheshire, Providence Island, Middlebury-Orwell, and Hortonville, are distal equivalents to the Potsdam, Whitehall, Black River-Trenton, and Stony Point facies, respectively. Facies transitions between the medial Ordovician units (Black River-Trenton limestones and overlying shales) are partly dependent upon the development of the foredeep, the migration of the forebulge, and syn-depositional normal faulting. Deposition of the younger shales continued after this normal faulting.

The Champlain thrust system

A structure of considerable historic significance, the Champlain thrust is the westernmost thrust in New England with significant transport (Keith, 1932; Rowley, 1982; Stanley, 1987). However, at the latitude of Shoreham, VT, the trace of the Champlain thrust has been uncertain because south of Shoreham there is poor outcrop in the extensive fields separating widely-spaced and densely-forested ridges with better outcrop, and there are several significant along-strike changes in stratigraphic units and sedimentary facies. In this area the Champlain thrust was proposed (Coney et al., 1972) either: (*i*) to splay into a system of several thrusts with a main thrust continuing south as the Taconic frontal thrust or (*ii*) reach a point of zero displacement in the region south of Shoreham. Our mapping determined that thrusts could adequately be traced through the region provided that the stratigraphy was defined on a purely lithologic basis and that some of the along-strike facies changes were localised by reactivation of an earlier generation of faults (Hayman and Kidd, 2002).

Stratigraphy

One of the challenges in mapping the lower Champlain Valley is reconciling outcrop-scale observations of lithologic characteristics with the published stratigraphy. The Centennial map of Doll (1961) and numerous publications (e.g. Cady, 1945; Welby, 1961; Cady and Zen, 1960) define an accepted stratigraphy of the pre-Chazy shelf sequence that includes:

- two massive quartzite/sandstone units (the Cheshire & Monkton/Danby/Potsdam)
- an intermediate dolostone (Winooski)
- a rather complex interfingering of several Beekmantown Group dolostones (Ticonderoga, Whitehall, Cutting, Bascom, & Providence Island, the latter belonging to the Chipman formation)

In contrast, the stratigraphy proposed for the equivalent section in New York (e.g. Fisher, 1985) includes:

- Basal clastics (Potsdam sandstone, Ticonderoga dolomitic sandstone)
- Massive dolostones (Whitehall formation; and which includes a limestone unit, Warner Hill limestone, the cliff forming limestone near Whitehall, NY)
- A second sequence of mixed carbonate and clastic units (Great Meadows formation; which includes Winchell Creek arenite/siltstone, Fort Edward dolostone, & Smiths Basin limestone)
- A second mostly dolostone unit (Fort Ann formation; which includes many impersistent thin limestones)
- A second sequence of mixed carbonates and clastics (Fort Cassin formation; which includes the Ward siltstone, Sciota limestone, & the Providence Island dolostone).

Many of the stratigraphic units in adjacent areas undergo an along-strike facies change when they enter the Champlain lowlands (Cady and Zen, 1960). This complication is compounded by the problem that some of the stratigraphic section does correlate between northern Vermont and New York, but with the unpleasant result that physically similar units have two different names in the literature (Cady, 1945; Welby, 1961; Fisher, 1985). It is our proposal that the stratigraphy of the portion of the Champlain Valley we focus on in this trip is best kept simple – a basal quartzite, an overlying dolomitic section, capped by a Chazy and younger limestone section. Though there may be local exceptions to this simplest passive margin sequence, our mapping of the area between Shoreham and Whitehall has revealed little complication. One notable exception to the simple stratigraphy is that there is a structurally contiguous set of rocks within the Beekmantown Group that contain silty to sandy cross-beds, burrows, and thin limestone members indicative of a proximal shelf facies, and an equivalent section that contains massive dolostones with only *one* thin (less than ten meters) limestone and *one* thin siltstone horizon (**figure 4**). We have named the proximal sequence the *Whitehall facies* after the most prominent autocthonous and parautocthonous carbonate formation in the stratigraphy of Fisher (1984). In contrast, we interpret the massive dolostone with few clastic or limestone horizons to be a distal facies of the Whitehall. We named this the *Providence Island facies* as almost all of it most closely resembles descriptions of the Providence Island formation (Fisher, 1985) and is associated with a thin limestone and thin siltstone that closely resemble Sciota limestone and Ward siltstone. While the Sciota and Ward are defined in the autochthonous shelf near Whitehall, the lithic equivalents in the transported thrust slices near Shoreham appear to transgress stratigraphically (relative to the autochthon) and were probably transitional units forming channels and/or uneven platforms across the shelf.

Our stratigraphy differs from the "official" stratigraphy of Vermont or New York and should best be thought of as a lithologic classification to which we have provided names. This avoids reverting to Brainerd and Seeley's (1890) *divisions a-e*, a difficult terminology to use in field discussions, but rather relates the lithologic traits and the relative stratigraphic position of the rocks to a passive margin sequence of quartzites, dolostones, and limestone. The complicated along-strike facies changes and across-strike repetition of units, such as the basal quartzite, are adequately explained by structural processes of thrust faulting superposed on a phase of prethrust normal faulting.

Reactivation of prethrust normal faults

The middle Ordovician outer trench slope was the site of normal faulting, between the synconvergence flexural forebulge and the trench (Cisne et al, 1982; Bradley and Kusky, 1985; Bradley and Kidd, 1991) (**figure 3**). We propose that these prethrusting faults localised many of the along- and across- strike lithic unit changes within the thrust sheets (Hayman and Kidd, 2002). Reactivation of these faults by thrusts compounds the difficulty in mapping

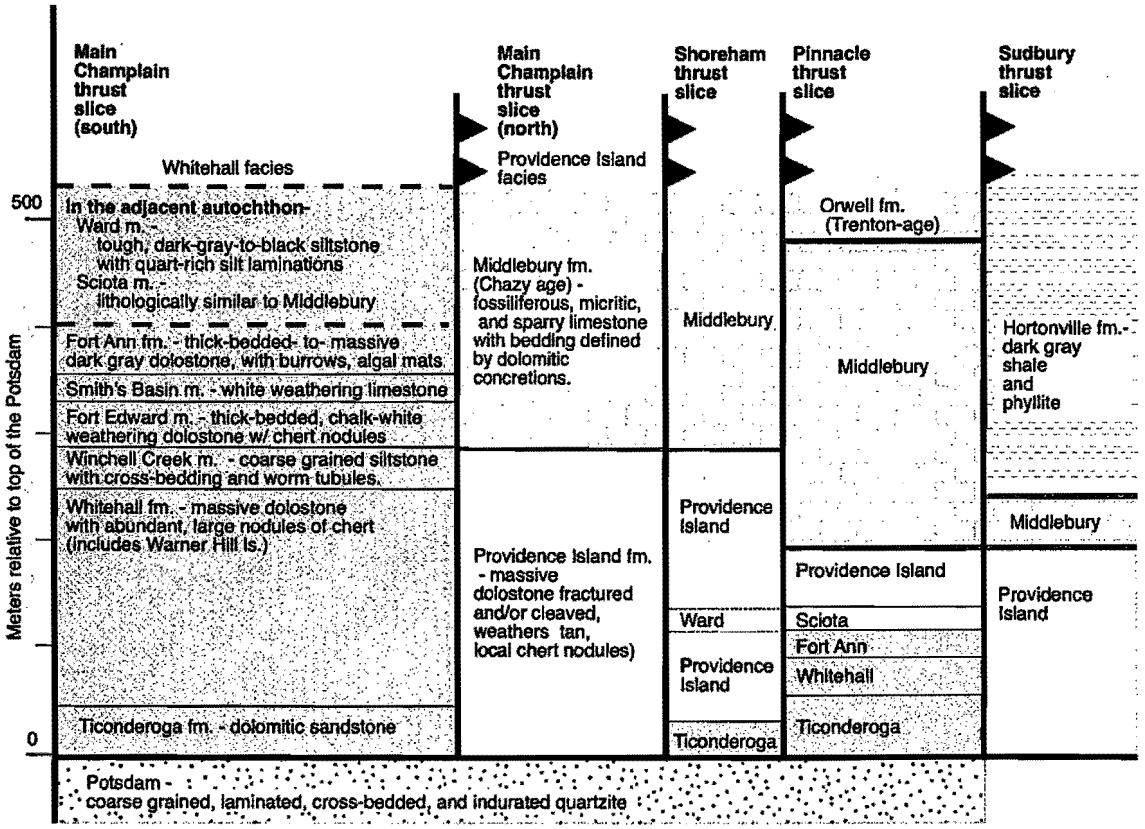

Figure 4. Stratigraphic sections and lithologic criteria for distinguishing map units within the platformal sequence. The solid gray is the Beekmantown Group that is dominantly dolostone but contains many limestone and siltstone horizons. These horizons are assigned formation (fm.) and member (mem.) names (Fisher, 1985). The Whitehall fm. is the characteristic formation of the Whitehall facies and includes the Warner Hill limestone, the cliff-forming limestone in the greater Whitehall region. The Ticonderoga sandstone, Ward siltstone, Whitehall dolostone (within the Pinnacle slice), and Sciota limestone have uneven distribution. The thickness of map units within the different thrust slices is measured from cross-sections; a direct measurement of section is not possible due to inadequate outcrop and limited topographic relief. No age correlation is implied by this diagram.

---

this region because many of the prethrusting stratigraphic contrasts coincide with ramps in the thrusts. Our study is one of a growing number of examples of thrust-reactivation of synconvergence normal faulting (Blisniuk et al., 1998; Scisiani et al., 2001). A clear example of reactivation of early faults by thrusting occurs near Shoreham, VT (**figure 5, 6**) where there are three prominent thrusts, each of which transports a slice of shelf section. The three thrusts are *the Main Champlain* (also known as the *Orwell*), the *Shoreham*, and the *Pinnacle* thrusts (Coney, 1972). Each locally transported Potsdam quartzite, though the thrusts climb from north to south resulting in the disappearance of the quartzite in map-view. Along the Lemon Fair River, the Lemon Fair fault, a northwest-southeast striking cross-fault, cuts all of the thrusts and bounds the southern extent of a densely thrust-imbricated region containing the Shoreham duplex (Washington, 1985, 1987).South of the Lemon Fair, however, the thrust sheets consist of broad,, flat panels of structurally intact shelf sections. Additionally, north of the Lemon Fair there are several thin carbonate map units that are difficult to trace south of the Lemon Fair. An inescapable conclusion is that there is a subtle change in sedimentary facies across the Lemon Fair fault, and a rather striking contrast in structural style of the thrust system. Part of this change in structural style corresponds to an increase in displacement on some of the thrusts from north to south as local thrust-duplexes and zones of thrust-imbrication with hanging-wall anticlines are replaced by broad, flat thrust sheets with no hanging-wall cutoffs — horses and imbricates generally restore to a nearer position than broad, flat thrust sheets. We propose that the dual stratigraphic and structural control of the Lemon Fair is due to its origin as a cross-fault along the prethrusting flexural forebulge.

ROAD LOG

Participants arriving early Friday from MA, CT, RI, Quebec, VT, NH, ME and points farther east should choose their own direct way to the meeting point of the field trip, in Shoreham, VT, at the Mobil station at the intersection of Routes 22A and 73 east. For those staying Thursday night in Lake George, take Route 9 south to the intersection with 149; turn left.

From south: take Exit 20 northbound ramp from Interstate 87; turn left at light at end of exit ramp; go north ~0.4mi to intersection of Route 9 and Route 149 at light turn right onto 149

From north: take I-87 Exit 20 southbound ramp, turn left at end of ramp; go ~0.1mi to intersection with Route 9; turn left at light; go north ~0.5 mi to light at intersection of Route 9 and Route 149; turn right.

	Mileage Increment	Mileage Total
Intersection of Route 9 and Route 149 at light; go east on 149	0.0	0.0
Intersection with Route 4 in Fort Ann; turn left onto Route 4 at light	11.5	11.5
Follow Route 4 across intersection (with light) with Route 22 (east/south) at Comstock	3.8	15.3
Turn half right at light in Whitehall following Route 4 at junction with Route 22 (north)	6.7	22.0
NY-VT border (Poultney River)	6.3	28.3
Take Exit 2 ramp from Route 4	1.5	29.8
End of exit 2 ramp; intersection with Route 22A; turn left onto 22A north	0.2	30.0
Intersection with Route 73 by Orwell; continue north on 22A	14.3	44.3
Intersection with Route 74 (west) in Shoreham; continue north on 22A	6.2	50.5
Intersection with Route 74 (east) in Shoreham; turn right into Mobil station	0.4	50.9
STOP 0 - Meeting Point of Field Trip A-7		
From intersection of Route 74 (east) and Route 22A, turn left and go south on 22A		
Intersection with Route 74 (west); turn right onto 74 (west)	0.4	51.3
Leave Route 74, going straight ahead onto Watch Point Road	0.4	51.7
Park on right at Slateledge Farm.	0.7	52.4
STOP 1 - Orwell/Main Champlain Thrust at Shoreham – ASK PERMISSION AT SLATELEDGE FARM		
Continue west on Watch Point Road to intersection with Basin Harbour Rd; turn right	0.5	52.9
Turn to half right onto N. Cream Hill Road	1.2	54.1
Intersection with Lapham Bay Road; turn right	1.8	55.9
Intersection with Route 22A; turn right	0.8	56.7
Park on right at end of driveway - PARK COMPLETELY OFF THE HIGHWAY	1.1	57.8
STOP 2 - Potsdam/Ticonderoga quartzites/arenites at base of Shoreham Thrust Duplex – ASK PERMISSION AT THE GARAGE, OR AT THE HOUSE ON THE CORNER OF THE 74/22A INTERSECTION		
Continue south on Route 22A into northern part of Shoreham village; turn left into vast parking area 100 yards before Route 74 (east) intersection.	1.2	59.0
STOP 3 - Middlebury Limestone in the Shoreham Duplex		
From the parking area, turn left out onto Route 22A		
Pass intersections with Route 74 (east) [0.1 mi] and Route 74 (west) [0.5 mi]; then turn left at intersection onto Richville Road	0.9	59.9
Junction with N. Orwell Road on the right; parking area on the left, opposite the junction	2.1	62.0
STOP 4A - Potsdam quartzites of the Pinnacle Thrust slice adjacent to the Lemon Fair Fault		
Continue east on Richville Road; across the bridge, turn sharp left onto Buttolph Rd.	0.1	62.1
Park at roadside next to the roadcut	0.1	62.2

STOP 4B - Carbonates adjacent to the Lemon Fair Fault, and just beneath the Pinnacle Thrust

Continue along Buttolph Road; turn right at intersection to follow it		0.2	62.4
Turn right onto Philion Road		0.1	62.5
Take half left returning to Buttolph Road		0.2	62.7
Turn right onto Richville Road		0.05	62.75
Intersection with Route 22A; turn left		2.2	65.0
Intersection with Route 73 by Orwell; turn right onto 73		5.7	70.7
Go straight onto Mt Independence Rd, leaving Route 73		0.4	71.1
Turn left at intersection onto Bascom Road		1.3	72.4
Turn right at intersection with Stevens Orchard Road		0.5	72.9
Park at roadside by house and barn		1.0	73.9

STOP 5 - Champlain/Orwell Thrust at Stevens Orchard

Continue to end of road at orchard buildings,and turn around		0.4	74.3
Continue straight, past Bascom Road junction on left		1.4	75.7
Park on right, before curve to right and roadcut		0.3	76.0

STOP 6 - Shoreham Thrust near Orwell

Continue to intersection with Old Stage Road; turn right		0.2	76.2
Junction with Singing Cedars Road; turn right		1.8	78.0
Park on right near house and barns		1.2	79.2

STOP 7 - Orwell/Main Champlain thrust sheet at Benson Bay/Blue Ledge

Go down to end of road at Benson Bay boat launch; turn around		0.1	79.3
Return to Old Stage Road; turn right		1.3	80.6
Junction with Frazier Hill Road (and N. Cross Road); turn right		0.7	81.3
At bottom of hill, left turn at junction with Turkey Farm Road		1.5	82.8
Junction with N. Lake Road; turn left		0.9	83.7
Park on roadside; enter field on south side through gate	0.2	83.9	

STOP 8 - Shoreham Thrust and end of Orwell/Main Champlain Thrust near Benson Landing – AFTER GETTING PERMISSION AT FARM ON N. LAKE ROAD 0.4 MILES WEST OF FRAZIER HILL ROAD JUNCTION

Continue east/south on N. Lake Road to intersection with Lake Road;	1.8	85.7
Go across and continue south, now on Park Hill Road; this changes name again to Best Road before coming to:		
Junction with Main Road (aka West Haven Turnpike); turn right	3.7	89.4
Junction with Book Road in West Haven; turn left	0.9	90.3
Park on right near entrance to private unpaved road	0.3	90.6

STOP 9A - Shoreham Thrust at West Haven, and

STOP 9B - Mettawee River Fault at West Haven - ASK PERMISSION AT BOOK FARM BEFORE ENTERING - FIND BOOK FARM ALONG BOOK ROAD 1.1 MILES SOUTH OF STOP

Continue south along Book Road; pass Book Farm	1.1	91.7
Poultney River Bridge; NY-VT border; road changes name to Sciota Road	0.6	92.3
Junction with County Route 11; turn right	2.5	94.8
Junction to left with Stalker Road [no sign]; turn left	2.0	96.8
Junction with Fair Haven Turnpike [no sign]; turn left	0.5	97.3
Park just before junction on right with Buckley Road [no sign]	1.0	98.3

STOP 10 - Pinnacle/Comstock Thrust, and Mettawee River Fault, at Fish Hill - OBTAIN PERMISSION FROM HARMONY HILL FARM [0.5 MILE DOWN BUCKLEY ROAD FROM JUNCTION; enter field to north through gateway/over electric fence

Turn right onto Buckley Road, pass Harmony Hill Farm	0.5	98.8
Junction with Route 4; turn right	1.3	100.1
Junction at light with Williams/S. Williams Street; turn left	0.7	100.8
Continue straight onto Upper Turnpike, leaving County Route 12 (turns sharp left)	1.6	102.4
Mettawee River Bridge [slowly!!]	0.3	102.7
Follow paved road - Upper Turnpike - sharp left, blind hill crest, sharp right	0.7	103.4
Follow paved road - sharp left at junction with dirt road	0.7	104.1
Follow paved road - sharp left, blind hill crest, sharp right	2.5	106.6
pavement ends	0.2	106.8
Pull into parking area on left, just beyond low point in road	0.3	107.1

STOP 11 - Mettawee River Fault at the type locality - NO HAMMERS/SAMPLING - NYDEC REGULATIONS

Continue south on Upper Turnpike; pavement resumes	0.6	107.7
Turn half-right at intersection [NOT 3/4 right] onto Sheehan Road Extension	0.3	108.0
Junction with Route 22; Stop, then cross onto Route 40	0.3	108.3
Intersection onto County Route 17 [no name; direction sign to West Granville]; turn right	0.5	108.8
Junction with Dewey's Bridge Road; turn right	1.1	109.9
Park at roadside; Tyler Farm, house on right, barn on left.	1.7	111.6

STOP 12 - Pre-thrust normal fault in Comstock/Pinnacle Thrust slice at Tyler Farm - ASK PERMISSION AT TYLER FARM

Continue west on Dewey's Bridge Road; follow sharp left bend near Champlain Canal	2.1	113.7
Bridge over Champlain Canal	2.6	116.3
Railroad crossing at grade	0.1	116.4
Crossroads junction with Route 4 and Route 149 in Fort Ann; go across onto Route 149	0.1	116.5
Junction of Route 149 with Route 9; turn right for Lake George Village; end of log	11.5	128.0

STOP DESCRIPTIONS

STOP 1 - Orwell/Main Champlain Thrust at Shoreham

ASK PERMISSION AT THE FARMHOUSE to visit this outcrop. Unplanned encounters with an unfriendly bull may result if you ignore this instruction.

From Slateledge Farm house, walk east along the road passing the track to the barn nearest the house, and take the next track which heads toward the low ridge extending north from the second barn. About 100 meters from the road, small exposures of dark grey shales/slates occur at the side of the track. After passing a fence line (and maybe crossing an electric fence across the track, small exposures of steeply east-dipping calcareous dark shale, and more extensive loose material, occur on the western slope of the ridge [43° 53.740'N, 73° 19.723'W]. Based on lithic correlation, these are mid-Ordovician in age, termed Stony Point Formation in this region. They represent the transition to deep-water deposition from the previous shallow passive margin carbonate sedimentation as the Laurentian margin subsided rapidly on entering the Taconic subduction system. On top of the ridge here are outcrops of pale tan-weathering, grey quartzite, gently east-dipping at this position, becoming flat and then moderately west-dipping in a small ramp anticline on going north along the ridge. This quartzite is identified as Potsdam Fm., of mid-Cambrian age. The westernmost major thrust of the Champlain Thrust System at this latitude is located between the quartzite and the dark shale. This fault to the north of the Shoreham area is termed the Champlain Thrust; in the area of Shoreham, where several major splays occur, this one has been called the Orwell Thrust, although we have placed the name "Main Champlain Thrust" on it. The fault surface itself is not exposed here, although the position can be constrained to an interval less than 10 meters wide.

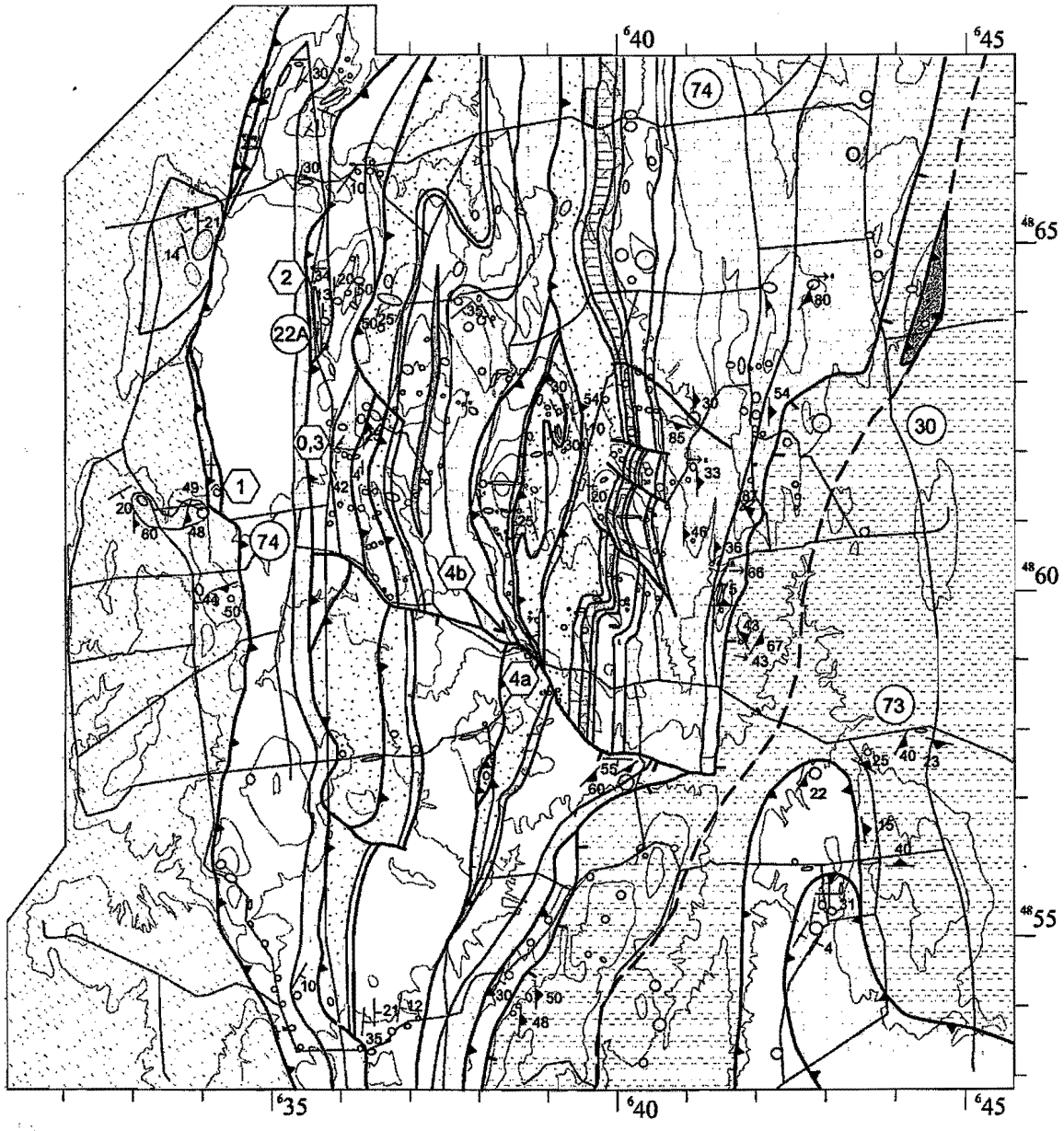
6°40
6°45
48°65
48°60
48°55
6°35
6°40
6°45
74
2
22A
0,3
1
74
4b
4a
30
73
Fort Ann
Smiths Basin
Fort Edward
Winchell Creek
Whitehall
Ticonderoga
Potsdam
Hortonville
Orwell & Middlebury
Providence Island
Ward siltstone
Sciota
Thrust Faults
Normal Faults
Taconic slate (allochthon)
Taconic melange
Iberville shale/flysch
Stony Point (Cumberland Head)
Area of outcrop
144 US Route
Stop number and location 11
1 km.
N

Figure RL-1. Outcrop and geologic maps of the Shoreham and Benson regions with field trip stops 1-8 indicated.

Looking east from the ridge towards Shoreham village, no outcrops occur in the lowlands, but extrapolation from outcrops along strike imply that this belt is underlain by Cambrian-early Ordovician Beekmantown carbonates, largely dolostones, which are stratigraphically above the Potsdam. In Shoreham Village, and farther east, imbricate slices of the Shoreham and Pinnacle Thusts occur, which are examined in subsequent stops. To the west, the Champlain lowlands, under the blanket of Quaternary lake clays, contain a few outcrops of mid-Ordovician shaly strata which are the Taconic trench/foredeep sediments. Walk back to the road, and slates, siltstones and fine-grained greywacke arenites of these mid-Ordovician flysch sediments can be seen in outcrops by the road opposite the farmhouse, and in the small quarry adjacent [43° 53.639'N, 73° 19.832'W]. A well-developed moderately east-dipping slaty cleavage cuts moderately NW-dipping bedding, and excellent slate pencils formed by this oblique intersection weather out. The bedding strikes obliquely towards the N-S trace of the Main Champlain Thrust. We

infer from the strong cleavage and down-plunge lineation that this is probably an imbricate thrust slice attached to and considerably transported by the Main Champlain Thrust; more autochthonous flysch west of the Champlain Thrust in this region tends not to have prominent cleavage.

STOP 2 - Potsdam/Ticonderoga quartzites/arenites at base of Shoreham Thrust Duplex

This stop has DANGEROUS TRAFFIC CONDITIONS (high speeds and limited sight distance) - please park as far off the paved road as possible, be extremely careful crossing the road, and do not stand on or step into the pavement when contemplating the outcrop.

From the parking place specified, cross the road and walk north to the roadcut [43° 55.241'N, 73° 18.743'W]. Pale tan-weathering, grey, well-indurated quartzites and local dolomitic arenites dip gently east. These can be identified as either the upper part of the Potsdam and/or the arenite-rich part of the overlying unit, the Ticonderoga Fm. Small-scale cross-bedding occurs locally. Mapping shows that they form an imbricate slice on the Shoreham Thrust. In this area near Shoreham, the Shoreham Thrust Slice is a complex imbricated stack of slices, forming the Shoreham Duplex.

STOP 3 - Middlebury Limestone in the Shoreham Duplex

ASK PERMISSION to park and view this outcrop AT THE GARAGE, OR AT THE HOUSE ON THE CORNER OF THE 74/22A INTERSECTION.

From the east side of the parking area, walk to the north-east corner, then go east to the nearest outcrop. This is massive limestone, showing a fairly well-developed steep east-dipping cleavage in places. About 50 meters east of the first outcrop, another ridge of limestone [43° 54.144'N, 73° 18.377'W] contains locally prominent large coiled gastropod fossils, probably *Maclurites*, which is common in autochthonous sections of Chazy Group mid-Ordovician limestones. In these transported rocks this limestone is usually termed Middlebury Limestone. These outcrops map as imbricate slices within the Shoreham Duplex. Recent expansion of the parking area has unfortunately resulted in the best outcrop being buried by bulldozed trees, soil and trash. If time is short, or permission is refused, a smaller roadcut outcrop of this limestone can be viewed just east of the Mobil Station parking lot on Route 74 east, but the gastropods are not clearly seen there.

STOP 4A - Potsdam quartzites of the Pinnacle Thrust slice adjacent to the Lemon Fair Fault

From the parking place, cross the road, and view tan-weathering, grey indurated quartzites, locally dolomitic, of the Potsdam Fm. East of the intersection [43° 52.386'N, 73° 16.321'W] they dip steeply southwest; in the outcrop west of the intersection, they dip gently southwest. The monoclinal fold outlined by this dip change, and the oblique strike, we interpret as due to proximity to the Lemon Fair Fault, and the lateral ramp it defines in the thrust geometry. These quartzites are regionally part of the Pinnacle Thrust Slice; this thrust is not exposed here, but its position can be constrained by mapping to the south. The Lemon Fair Fault runs here along the river; looking across from the parking place, limestones on the other side of the fault can be seen at the base of the old bridge abutment. The outcrop of Stop 4B is just beyond this through the trees.

STOP 4B - Carbonates adjacent to the Lemon Fair Fault, and just beneath the Pinnacle Thrust

Roadcut outcrop [43° 52.398'N, 73° 16.280'W] of limestones, dolomitic limestones, and minor dolostones which are adjacent to the Lemon Fair Fault. The generally rather fractured appearance, and the common presence of calcite veins, are indicative of this proximity. The dominant fractures and veins strike NW, dipping steeply north to vertical, subparallel with the Lemon Fair Fault. One vein shows prominent steeply pitching slickensides. These rocks are part of a slice of early-mid Ordovician limestone-dominated carbonates localised immediately under the Pinnacle Thrust in the area north of the Lemon Fair Fault, but not present to the south. This and other substantial changes in structural geometry that occur across the Lemon Fair Fault show that it was used as a major lateral ramp structure by the thrusts of the Champlain System. Because facies and stratigraphic thickness variations only occur in mid-Ordovician units across this structure, we infer that it was generated as a mid-Ordovician cross-strike "flexural" normal fault, and then converted to use as a lateral ramp in the Champlain Thrust System.

STOP 5 - Champlain/Orwell Thrust at Stevens Orchard

Walk up the road from the parking place by the house and barn/garage. On the east side, an outcrop of calcareous dark shale/slate, with a local phacoidally cleaved fault zone, is mid-Ordovician Stony Point Formation. Farther up on the same side just above a driveway there is a smaller outcrop and loose material of the same unit. About 20 feet above this, seen in the roadcut and the ridge going south from it, are dolostones of the Beekmantown Group forming the base of the Main Champlain (or Orwell) Thrust here. A little farther up on the north side of the road [43° 47.077'N, 73° 20.586'W], similar dolostones, showing not very prominent medium to thick-bedding and homogeneous brown-weathering, are exposed. This outcrop also shows the characteristic "fretted" weathering pattern produced by differential removal of abundant narrow calcite veins that are ubiquitously and abundantly developed in these transported dolostones, but are not usually seen in autochthonous dolostone sections in areas to the south. Dolostones like these form all of the body of both the Main Champlain (Orwell) and Shoreham Thrust Slices at this latitude; the Potsdam quartzites are absent because the thrusts have ramped up laterally to within the late Cambrian-early Ordovician carbonate section. Rocks like these are conventionally termed "Providence Island Formation", but we have little confidence that this is stratigraphically meaningful in the sense of strict correlation to the type section on Providence Island. The map pattern of the Main Champlain Thrust in this local area shows that it is very gently east-dipping, or almost flat.

STOP 6 - Shoreham Thrust near Orwell

On the corner with the roadcut outcrop [43° 47.439'N, 73° 19.236'W], east of the parking spot specified, deformed calcareous shales ("Stony Point Fm") make up most of the exposure, although at the western end a contact can be observed with fractured tan-weathering Beekmantown (late Cambrian/early Ordovician) dolostone above the shales. This dolostone forms a low ridge in the woods that parallels the road westwards to beyond the Bascom Road junction and, back along the road in this direction, smaller outcrops of both calcareous and non-calcareous deformed shales can be found locally, with dolostones near or in contact above the shales. The thrust fault defined by this contact is the Shoreham Thrust; the local map pattern demonstrates that this fault also is near flat-lying here. As for the Main Champlain Thrust, the absence here of Potsdam Fm is due to the thrust climbing section southwards, in part across the lateral ramp structure of the Lemon Fair Fault. A much better, even excellent outcrop of this fault exists 20 meters west into the woods near the end of Wilcox Road, about 1.0 mile SW of this outcrop, but the current landowner is most unwelcoming and is quick to display a gun.

STOP 7 - Orwell/Main Champlain thrust sheet at Benson Bay/Blue Ledge

ASK PERMISSION AT THE HOUSE.

The main part of the outcrop visible from the parking area is now only accessible through the pig mud wallow, unfortunately. We recommend viewing it from the road, from where the nearly flat-lying well-defined planar bedding in the dolostones is clearly seen. To see rocks closer up, walk east along the road, to a large oak tree on the corner [43° 45.889'N, 73° 20.399'W], and then go into the bushes a short distance where the same well-bedded sugary-textured dolostones continue to outcrop. Here the existence of common dark chert as nodules and patches in the dolostones can be seen, both in the outcrop and in the talus fragments. This unit is clearly identifiable in the Beekmantown stratigraphy of Fisher (1985) as the Whitehall Formation. Nearby, on White Ledge, the cliff visible to the east of the road, more Whitehall Formation is exposed; above it one can find in the woods good outcrop that shows overlying Beekmantown units matching those of Fisher (1985), including the unmistakeable Winchell Creek cross-bedded arenites. Structurally, we are back down in the Main Champlain Thrust slice (the fault is well-constrained by outcrop on Blue Ledge a few hundred meters to the northwest of this outcrop), yet the whole section carried by the Thrust here is utterly different from the homogeneous, poorly-bedded, veined dolostones at and just south of Stop 5, no more than 1-2 km. away. We identify this change to occur across a NW-trending valley just to the northeast of this stop location, and interpret this to be a lateral ramp in the thrust system inherited from a flexural Ordovician normal fault. The change in the shelf facies that occurs in the "Main Champlain" Thrust sheet here is by far the most pronounced anywhere, and it must represent a very substantial relative distance (we think many tens of kilometers) between the sites of detachment of the stratigraphic sequences north and south of this change. Because the sequence in the MCT slice from here south so closely matches the autochthonous stratigraphic sequence defined by Fisher (1985), we think it is unlikely to have been displaced very far (<10km?). Because it is likely the MCT to the north has significantly larger displacement (at least several tens, and perhaps >80km - Rowley, 1982) we think there must be a large displacement transfer here from the MCT north of this site, along the lateral ramp fault up to

the next thrust, the Shoreham Thrust. Not only is there a substantial change in the MCT hanging wall here, but the footwall also contains a similar (and we think closely related) feature about 1 km. SW of this stop. There is an abrupt change, from mid-Ordovician shales and calcareous shales of the Stony Point Fm as the footwall strata, to an autochthonous shelf carbonate/clastic section of the "Whitehall" sequence. This change takes place across a mapped cross-fault which affects the MCT as a small-offset lateral ramp/tear fault, but which has a much larger stratigraphically-defined offset in the footwall. We think this is also a mid-Ordovician normal fault used soon after to localise a ramp in the lowest part of the thrust system.

STOP 8 - Shoreham Thrust and end of Orwell/Main Champlain Thrust near Benson Landing

GET PERMISSION AT FARM ON N. LAKE ROAD 0.4 MILES WEST OF FRAZIER HILL ROAD JUNCTION
This stop may be omitted if time becomes short.
Enter field on south side of road [43° 43.781'N, 73° 20.562'W] through gate [OPEN AND CLOSE IT BEHIND YOU - PLEASE DON'T CLIMB OVER IT]

About 50 meters from gate [43° 43.751'N, 73° 20.599'W] dark calcareous shales of Stony Point Fm. Follow the track on the east side of the valley for another 50 meters or so; small outcrops of calcareous shales occur at the foot of the ridge to the east, while massive fractured dolostones occur up the slope and at the crest of the ridge. This defines the Shoreham Thrust here (to the south this has been called the Shaw Mountain Thrust). On the hillsides and tableland to the west of this valley, on a longer walk than we have time for, flat-lying shelf strata of "Whitehall facies" that map in the MCT slice are sparingly exposed; there has to be a normal fault bounding these against the Stony Point Fm. shales which continue down this valley in and near the stream. The Main Champlain Thrust terminates against this normal fault, and is not present farther south. We think that this normal fault originated as an Ordovician "flexural" normal fault, and was subsequently reactivated with reverse displacement sense and used by the Champlain Thrust System as a "terminal ramp" including the transfer of the residual displacement on this southernmost part of the MCT up to the Shoreham Thrust.

If desired by those on independent schedules, continue walking down the valley until the stream enters a continuous section exposing dark calcareous shales [43° 43.575'N, 73° 20.934'W]. Outcrops of near flat-lying dolostones (Fort Edward) or cross-bedded arenites (Winchell Creek) are found on the northwestern slope of the valley, e.g. dolostones at [43° 43.636'N, 73° 20.895'W], at an elevation significantly above the shales in the stream bed.

STOP 9A - Shoreham Thrust at West Haven

From the parking place [43° 38.727'N, 73° 20.888'W] walk about 120 meters south along Book Road [43° 38.663'N, 73° 20.929'W] to roadcut on east side. In the center portion of this exposure, black non-calcareous shale (mid-Ordovician) up to 1 meter thick, with a pronounced phacoidal cleavage indicative of large shear strain, occurs below a sharp contact with highly fractured massive dolostones ("Providence Island" lithology). This is the Shoreham Thrust, and mapping of the surrounding area shows unequivocally that it is here the westernmost thrust in the Champlain System - in other words that the "Main Champlain Thrust" farther north has disappeared. To the south across the Vermont-New York border at the Poultney River, the Shoreham Thrust too disappears as a discrete mappable structure, although minor folding and incipient ramps can be detected in shelf rocks at its expected position as far south as the latitude of Whitehall. A major WSW-ENE cross-fault passing north of this outcrop cuts and displaces the autochthonous shelf section and the Champlain Thrust System stack, crossing Book Road at the parking spot. The Shoreham Thrust is offset by this structure with an apparent left lateral displacement of about 2 kilometers. Two other faults like this one pass through the next valley north near West Haven hamlet. These cross faults are discussed in the description of Stop 9B below.

STOP 9B - Mettawee River Fault at West Haven
ASK PERMISSION AT BOOK FARM BEFORE ENTERING - FIND BOOK FARM ALONG BOOK ROAD 1.1 MILES SOUTH OF STOP

From parking place [43° 38.727'N, 73° 20.888'W], enter field on east by walking between the two fences, opening the gate if necessary. Follow the grassed-over track into the edge of the woods (about 100 meters), then along the edge of the woods (about another 200 meters), then angle down the crest of a low ridge in the meadow (about another 100 meters) to the edge of the woods crossing the low ridge [43° 38.850'N, 73° 20.513'W]. Outcrop of fractured tan-weathing dolostone ("Providence Island" lithology) is found just inside the woods at this point. Use

the sketch map below to navigate and understand the geology from this point on. About 200 feet east of the first dolostone outcrop, in the bed of the stream near the south end of the small ravine, dark slates ("Hortonville"), of presumed mid-Ordovician age, are exposed in contact with the dolostones [43° 38.853'N, 73° 20.473'W]. This contact is clearly a steep (60°) east-dipping fault, truncating the moderately east-dipping thick bedding in the dolostones, and the cleavage in the slates. Given the regional context, with no thick dark slates occurring west of this point, but rather the carbonates of the Shoreham Thrust slice, then the underlying autochthonous Cambro-Ordovician "Whitehall facies" sequence, with Potsdam sandstone/quartzite at its base lying unconformably on Grenville Basement, this fault must be a normal fault, and is in fact the Mettawee River Fault first proposed by Fisher (1985) in New York. It is the only complete exposure of this fault, although our mapping demonstrates that it runs continuously from the Mettawee River (to be seen at stop 12) north through this locality at least as far north as the latitude of Shoreham, and all along this length it regionally truncates the thrust stack of the Champlain Thrust System. We suspect that it extends significantly farther north and south than this, but this falls outside our mapping area, and there is a lack of clear truncation of components of the Champlain Thrust System beyond these extents. One reason for suspecting a larger along-strike extent is the minimum displacement, which can be constrained from accurately drawn cross-sections, and which demand at least 1000 meters of throw, and perhaps more than 1500 meters. This fault cuts out very significant parts of the Champlain Thrust stack, and is one of the main reasons why previous attempts to trace the major thrust faults of the System failed. What age is this normal fault? We have no direct younger age limit in the mapped area, other than the observation that it is cut and displaced by the WSW-ENE faults which also cut the Shoreham Thrust. In fact this set of local outcrops (see sketch map) shows that relationship directly, with a smaller splay of the larger WSW-ENE fault displacing in an apparent left-lateral sense the dolostone-slate contact (the Mettawee River Fault). Despite the prominence of the WSW-ENE faults, we have seen no direct evidence in outcrops near the fault valley indicating whether they are really left-lateral strike slip faults or whether the displacements are created by dip slip movement (in this case, it would require north side down) working on consistently east-dipping strata and faults. Thus these ENE-WSW faults, and the Mettawee River Fault, could be Taconic in age, although they might be younger, e.g. Acadian, or even Mesozoic, and they do not necessarily have to belong to the same orogenic episode.

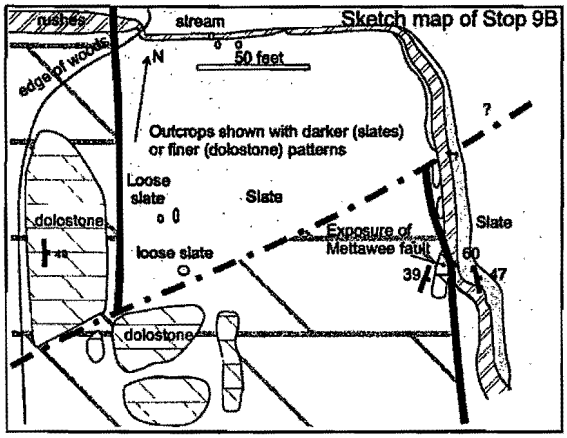

Figure RL-2. Outcrop and geologic map of Stop 9B –the Mettawee fault at West Haven.

STOP 10 - Pinnacle/Comstock Thrust, and Mettawee River Fault, at Fish Hill

OBTAIN PERMISSION FROM HARMONY HILL FARM [0.5 MILE DOWN BUCKLEY ROAD FROM JUNCTION]

Enter field to north of parking point through gateway/over electric fence. Go round pond on western side, loop round north end, crossing dry bouldery bed of stream, and head NE up slope toward outcrops just into the woods. [Cross electric fence at edge of woods]. Find contact between grey indurated quartzites above and tan-weathering crudely bedded dolostones below [43° 33.942'N, 73° 21.398'W], all dipping gently east. About 1 meter below the base of the quartzites, there is a projecting ledge exposing a bedding-parallel surfaceof fractured and veined dolostones, smears of limestone, and loose fragments of dark shale coming from the 10-30 cm unexposed interval between the dolostone above and the ledge with limestone smears below. This is the Comstock Thrust, which we maintain corresponds with the Pinnacle Thrust to the north of Orwell (or more precisely here it is the lowest fault surface in a zone which places imbricated Potsdam and Ticonderoga/Whitehall quartzites and dolostones over Fort Ann and Providence Island dolostones). Walk east along the base of the hillside outcrop; an ~10 meter section mostly of quartzites is conformably overlain by dolostones which extend to near the west end of the barn, where there are some dark cherty patches in the dolostones. Climb up on the outcrop to avoid the manure piles and to find another imbricate fault contact placing the quartzites back on top of the dolostones, with truncation of the dolostone bedding in the footwall as a thrust ramp. Near the east end of the barn [43° 33.920'N, 73° 21.305'W], the quartzite outcrop ends, with locally steep and folded bedding probably reflecting accomodation to the ramp/imbricate geometry underneath. Walk north up into the field over quartzite outcrop, then curve to the east across exposure gap

of about 40 meters to outcrop of dark and strongly deformed, melangy mid-Ordovician shales [43° 33.957'N, 73° 21.281'W]. You have just crossed the Mettawee River Fault, which again must have substantial normal, down to east displacement. You may find the evidence here for the existence of the Comstock/Pinnacle Thrust not wholly compelling, but raise your eyes to the view towards the southwest, where, in the hills south of Whitehall, the map of Fisher (1985) unquestionably demonstrates a) the existence of the Pinnacle/Comstock Thrust duplicating most of the Cambrian-Ordovician shelf stratigraphy from the Potsdam upward, and b) the unquestionable fact that this thrust is truncated on a large scale by the Mettawee River Fault.

To the east of the shale outcrop, up the slope of Fish Hill, limestones and dolostones of early-mid Ordovician age form another of several thrust slices involving only the upper part of the outer Laurentian shelf and the overlying mid-Ordovician dark shales. These slices rest below the westernmost fault bounding the Taconic Allochthon, which outcrops only about a kilometer to the east.

STOP 11 - Mettawee River Fault at the type locality

[NO HAMMERS OR SAMPLING PLEASE - NY DEC REGULATIONS]

From parking area [43° 28.259'N, 73° 22.153'W], walk from northeast corner along path which quickly descends to a bouldery small stream bed. If wet, the path down can be slippery since it passes through well-rounded fluvial pebble gravel and underlying lake clays; the sloping bedding surfaces of the carbonate outcrops can also be treacherous in places. Cross the stream bed near/at the Mettawee River bank and get onto the outcrop along the west bank of the River [43° 28.283'N, 73° 22.103'W]. These carbonates are mapped by Fisher as Providence Island Formation, and dip about 10-20 degrees east. The lowest part of the section here consists of dolostones; the upper 4 meters contains substantial limestones; we think it is possible that the part of the section containing limestones is either basal Chazy or Black River. This shows some bedding surfaces with well-developed ripples, and small mudcracks, and selectively dolomitized burrows. Local meter-scale folding of periclinal type affects these beds near this end of the section. Walk north along the west bank on the outcrop; mostly dolostones are exposed farther north. About 70 meters north, dark highly deformed mid-Ordovician shales extend from the east bank across the river to an almost complete section at the small rapids. Depending on the streamflow, it may or may not not be possible to examine the shale closely. The contact of the deformed shale with the dolostone beds at the west side of the stream is not quite fully exposed (even at the lowest water we have seen, there is a gap of 10 cm or so), but is clearly sharp, and parallel with bedding in the dolostones. This is somewhat surprising, for a contact which maps out a short distance to the north as a sharp fault that unquestionably truncates strata of the carbonate shelf stratigraphy, as well as the major thrust fault which duplicates this sequence (see the map of Fisher, 1985). Also surprising, for a fault that must have substantial normal sense displacement, is the fact that most or all quartz fiber slickensides in the shale here give thrust sense of displacement!

We infer either that the normal fault mapped to the north passes east of this outcrop within the shale belt, or that the motion is confined to a surprisingly narrow zone along the contact; the full exposure at Stop 9B suggests the latter possibility is more likely than one might be inclined to think based on this outcrop at Stop 11 alone.

STOP 12 - Pre-thrust normal fault in Comstock/Pinnacle Thrust slice at Tyler Farm

ASK PERMISSION at Tyler Farm house [43° 26.849'N, 73° 24.432'W] before going into fields to north of road. If visiting the western part of the ridge, also ask at the old stone house about 0.2 mi west of Tyler farmhouse.
This stop may be skipped if time runs short.

Refer to the outcrop map to navigate. Outcrops on the slope above the Tyler farmhouse, and above the old stone house 0.2 miles west of this, begin with mid-Ordovician limestones of Black River and/or Trenton age; the thin-bedded shaly ones are termed Glens Falls Fm, the more massive ones stratigraphically below are Orwell Fm. They strike about E-W and dip steeply south. Units of the upper Beekmantown (Providence Island, Sciota Limestone, and Ward Siltstone) are found on and near the crest of the first ridge, with decreasing dips towards the valley to the north in which a fault is located. The zone of steep dips is interpreted as a bend fold ["drag fold"] against the hanging wall of (inferred from its straight trace, and the limestone maximum dips) a steeply south-dipping normal fault, and perhaps also is partly an accomodation to the lateral ramp this fault has provided to the Comstock Thrust. North of this ~E-W striking fault, various units of the older parts of the Beekmantown are found forming mostly a moderately east-dipping panel truncated at the normal fault. These strata are in the hanging wall of the Comstock Thrust (=Pinnacle Thrust), which here is the last and only thrust fault in the exposed part of the Laurentian shelf sequence between the autochthonous Grenville basement and mid-Ordovician shales of the Taconic foredeep. The Comstock Thrust is included on the map of Fisher (1985), although he shows its continuation by joining it to the E-W fault

referred to above, which we think is geometrically and kinematically unlikely. Our map (based on mapping by Y. Pan and W. Kidd), instead interprets the E-W normal fault to intersect the Comstock thrust and to be truncated by it. In addition, we interpret the Comstock Thrust to continue south across the point of this truncation, and the map pattern requires that it abruptly climb stratigraphic level from the Ticonderoga or Potsdam sandstone to near the base of the mid-Ordovician limestones despite no change in its structural level. This requires the thrust to have truncated an existing normal fault that had a throw of several hundred meters, nearly the full thickness of the shelf sequence. Since there is no indication approaching the E-W fault of any thickness or facies change in the pre-Black River section, we infer that this normal fault too is a mid-Ordovician age structure, generated during flexure of the Laurentian continental margin as it approached the Taconic trench and subduction system. (As a additional note on the structure of the local faults, we find no evidence of the existence of the rootless klippen of Potsdam-Whitehall Fm strata shown not far southwest of this locality on Fisher's 1985 map. We think he confused gently dipping autochthonous Winchell Creek and stratigraphically conformable dolostones with the lower units here; there is in our view no stratigraphic or structural evidence requiring this peculiar object to exist).

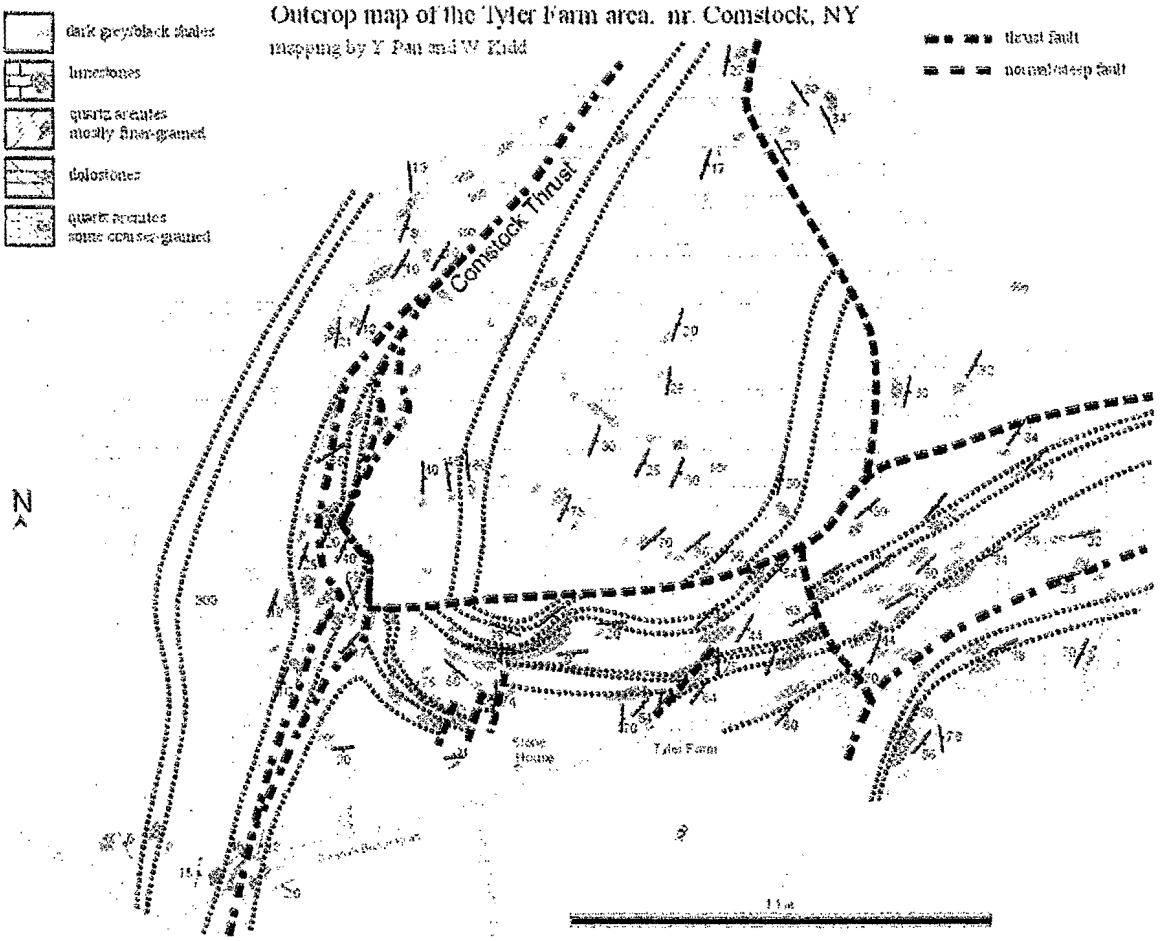

Figure RL-3. Outcrop and geologic map of Tyler farm, stop 12.

GEOLOGY AND GEOCHRONOLOGY OF THE EASTERN ADIRONDACKS

By

James McLelland, Dept. Geology, Colgate Univ. and Skidmore College, Saratoga Springs, New York, 12866
M. E. Bickford, Department Earth Sciences, Syracuse University, Syracuse, New York, 13244-1070
Frank Spear and Lara Storm, Department Earth and Environmental Sciences, RPI, Troy, New York, 12180

INTRODUCTION

Geologic background and detail for the Adirondack region is summarized in the introduction section of trip A-1, "Geology and geochronology of the southern Adirondacks" by McLelland, Storm, and Spear. The reader is referred to that section for relevant background information. Here we summarize broad considerations pertaining to the eastern Adirondacks.

The eastern Adirondacks contain a wide variety of rock types, and this trip aims to visit representatives of the major lithologies. Stops include units recently dated by U-Pb geochronology including multi- and single-grain TIMS and SHRIMP II analyses. Results of these investigations are presented in the text of trip A-1, to which the reader is referred. Broadly, the various lithologies fall into the following groups: 1300-1350 Ma tonalites and granodiorites; 1150-1160 Ma anorthosites, mangerites, charnockites, and granites (AMCG suite); 1090-1100 Hawkeye granite; and 1035-1060 Ma Lyon Mt Granite (LMG). The two major orogenic events associated with these are the Elzevirian and Ottawan Orogenies (Moore and Thompson, 1980). The former falls into the interval ca 1350-1170 Ma and involves protracted arc magmatism and accretion capped by a culminating collisional orogeny from ca 1200-1170 Ma (Wasteneys *et al*, 1999). The latter refers to the Himalayan-type collision of Laurentia with Amazonia during the interval ca 1090-1000 Ma. Most of the metamorphic and structural effects present in the Adirondacks are the result of the Ottawan Orogeny, but Elzevirian features can be recognized locally. Both the AMCG suite and the LMG are thought to be late- to post-tectonic manifestations of delamination of overthickened orogens.

Structurally, the eastern Adirondacks are dominated by the same large, recumbent fold-nappe structures (F_2) as found in the southern Adirondacks, and with fold axes oriented dominantly ~E-W parallel to lineation. As in the southern Adirondacks, the fold-nappes are thought to have sheared-out lower limbs, but this has yet to be demonstrated on a map scale. At least two distinguishable upright fold events are superimposed on the nappes: F_3 with shallow plunging ~E-W axes and F_4 with shallow-plunging NNE axes. All of three fold sets affect Hawkeye and older units, and thus must be of Ottawan age. This also the case with the strongly penetrative rock fabric, including strong ribbon lineations, that are present in these rocks and are associated with the large fold-nappes. Intense fabric of this sort is largely absent from the Lyon Mt Granite and this is interpreted to reflect its intrusion in late, post-nappe stages of the Ottawan. In the northern portion of the eastern Adirondacks the NNE, F4, folds become quite tight and have a strong lineation associated with them. This may be the result of rock sequences being squeezed between large, domical prongs of anorthosite. Finally, we note that there exists abundant local evidence of small isoclinal F_1 folds that pre-date F_2. These, and their associated fabrics, are thought to be Elzevirian in origin, and in a few cases this can be shown to be the case.

A dominant feature of the eastern Adirondacks is the great Marcy anorthosite massif that underlies almost all the High Peaks. Over two-dozen zircon age determinations demonstrate that the anorthosite was emplaced at 1150 $\pm$ 10 Ma (Table 2, Trip A-1) and that associated granitoids and coronitic metagabbros are coeval with it. These relationships make it clear that thermal energy from the anorthosite had nothing, whatever, to do with the granulite facies that characterize the Adirondack Highlands and post-date the AMCG suite by 60-100 million years. The specifics of Adirondack P,T relationships and uplift history are discussed trip A-1 and its appendix AA-1. It is likely that most of the region experienced peak temperatures on the order of ~800° C and pressures of ~8 Kbar. Based upon extensive isotope work by John Valley and his students, it appears most likely that this metamorphism proceeded under fluid-absent conditions (Valley *et al.*, 1983). Note, however, that this does not exclude the presence of late, post peak, fluids associated with the emplacement of Lyon Mt Granite.

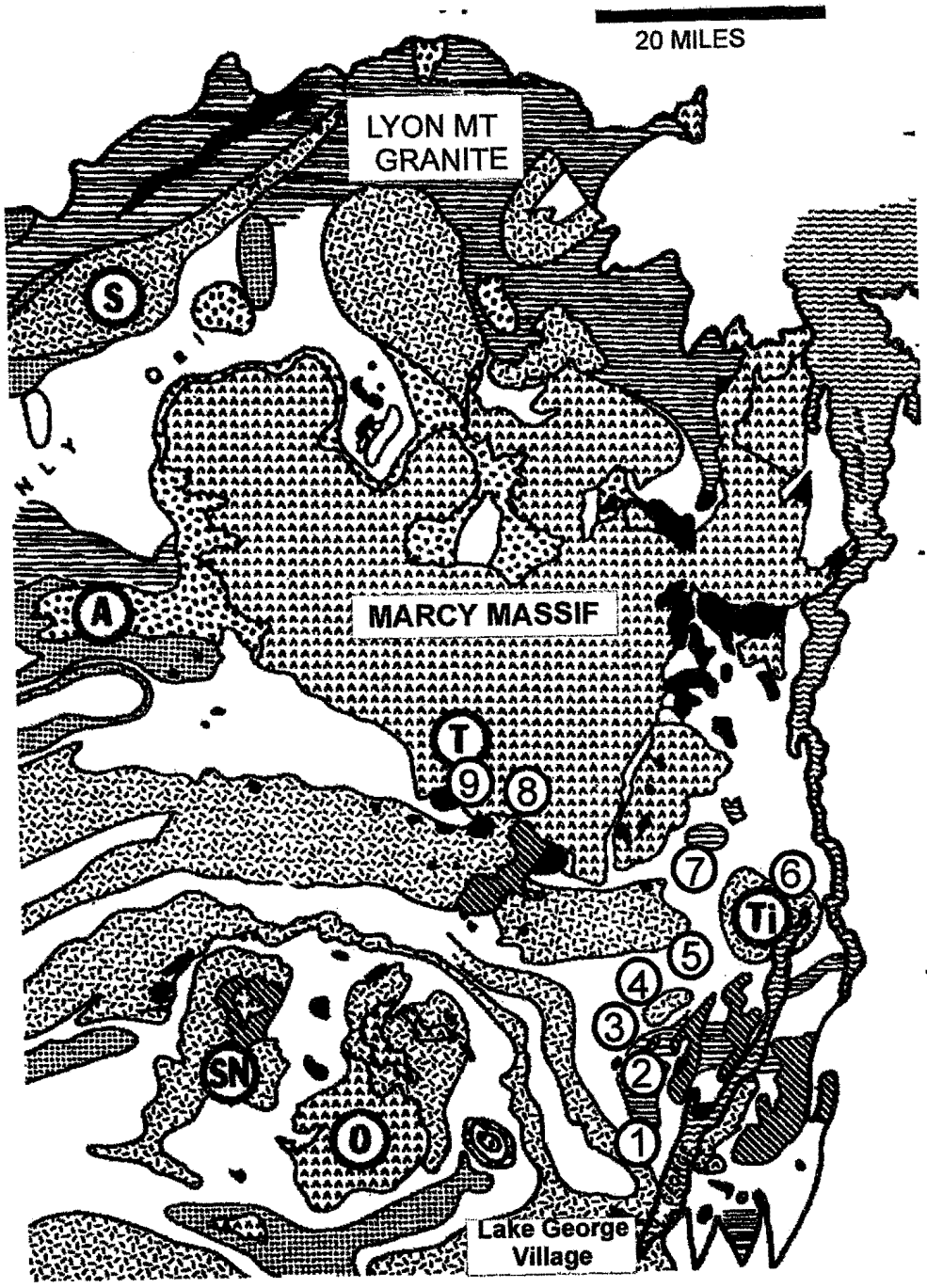

Fig. 1 . Generalized geologic map showing field trip stops. Seetrip A-1 for geologic details. A- Arab Mt anticline, S- Stark anticline, T- Tahawus, Ti- Ticonderoga Dome, O-Oregon Dome, SN- Snowy Mt Dome. See Fig. 3, Trip A-1 for legend .

ROAD LOG

Mileage

0.0 Start in the parking lot of the Fort William Henry Motel and Conference Center, Lake George, NY. T Turn left (south) on Rt. 9.
0.5 Pass Prospect Mt entrance on right.
1.0 Junction with 9N. Turn right at light.
1.2 Turn right (north) on Northway (Rt 87). Note exposures of pink granite along Northway.
4.0 Sulfidic staining on NNE fault in granite.
5.5 Exposure of hornblende granite on left.
5.9 Pegmatite on right.
6.0 Pass metagabbro
6.7 Hornblende granite on both sides.
7.0 Hornblende granite
7.2 Hornblende granite with metagabbro
7.4 Metagabbro, pegmatite, and metasediments on right.
7.5 Take Exit 23 off of Northway
8.0 Turn right at stop sign
8.4 Turn left (north) onto Schroon River Road.
8.8 Junction with Wall St on right. PARK

STOP 1. MEGA-GARNET AMPHIBOLITE. (20 MINUTES). This small roadcut at the intersection of Schroon River Road and Wall Street is an example of what is referred to as a "Poor Man's Gore Mt.". The roadcut contains large (up to 8" across) almandine-rich garnets rimmed by black hornblende and set into an amphibolite matrix that can be shown to have formed from metagabbro. The assemblage is reminiscent of the famous deposits at the Barton Garnet Mine on Gore Mt where garnet growth has been dated at ca 1050 Ma (Mezger *et al*, 1990) using Sm-Nd techniques. The northern contact of the present exposure is characterized by a deformed hornblende-biotite-quartz-oligoclase pegmatite that also crosscuts the interior of the garnetiferous amphibolite. Several other examples of "Poor Man's Gore Mt" occurrences are present in the Adirondacks, and all – including Gore Mt- share in common proximity to high angle faults that host pegmatites, quartz-veins, etc. We propose that the faults served as plumbing systems for hydrous magmas that provided water to the amphibolites at temperatures of ~700°-800° C. This anomalous circumstance resulted in elevated diffusion rates that enhanced garnet growth at a small number of nucleation sites. The hornblende rims represent the excess of hornblende constituents in the area of local garnet growth. Post peak decline in the activity of H_2O, or continued increase of T, caused reactions between garnet and hornblende to produce calcic plagioclase (AN80) and orthopyroxene.

12.6 Bridge across Schroon River
12.7 Stop sign. Turn right (north)
17.7 Park on shoulder of road.

STOP 2. ca 1300 Ma TONALITE. (20 MINUTES). These outcrops consist of tonalitic rocks dated elsewhere as ca 1300-1350 Ma by U/Pb zircon. Their chemistry is calcalkaline, and, together with associated granodiorites, they are interpreted as having formed in one, or more, magmatic arcs during the Elzevirian events of ca 1400-1220 Ma. Locally these units contain xenoliths of, or crosscut, metasedimentary rocks, thus establishing a minimum age for most, if not all, of these units in the Adirondacks. (See Stop 4, Trip A 1-1)

19.7 Junction with Northway (Rt 87). Enter northbound ramp.
31.3 Exit Northway at Pottersville.
31.6 Stop sign. Turn right (north) at junction with Rt 9.
31.7 Continue right on Rt 9.
32.3 Turn right (east) on Glendale Road by Word of Life Bible Camp.

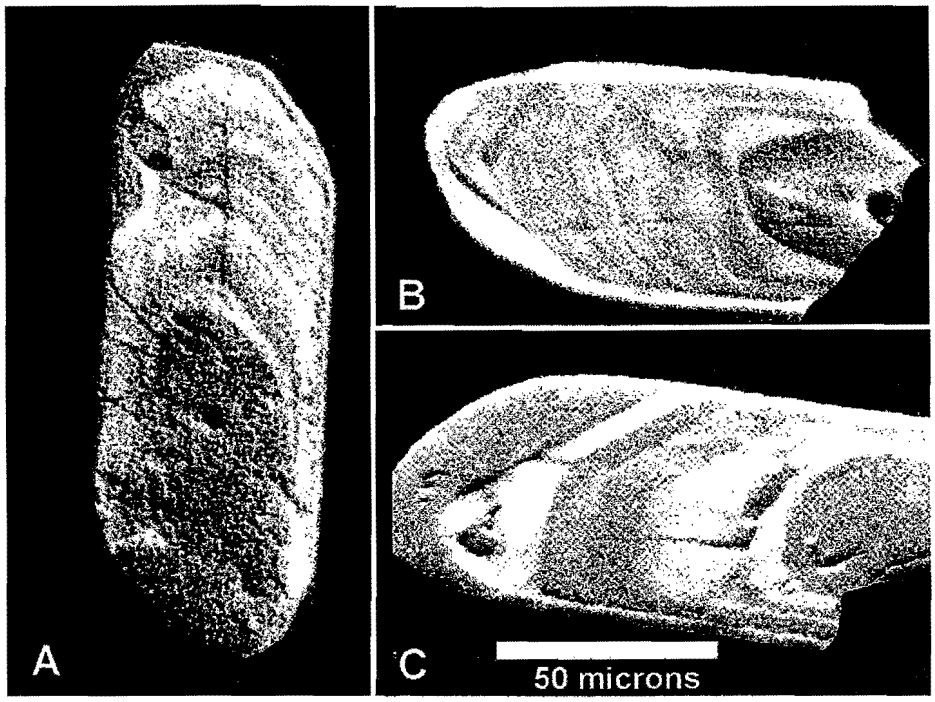

Fig. 2 CL images of zircons from Lyon Mountain Granite at Stop 3. Note the euhedral morphology and sharp terminations as well as the presence of oscillatory zoning in mantling zircon indicative of magmatic growth. Half grains such as B,C yielded 1049 $\pm$ 2 Ma.

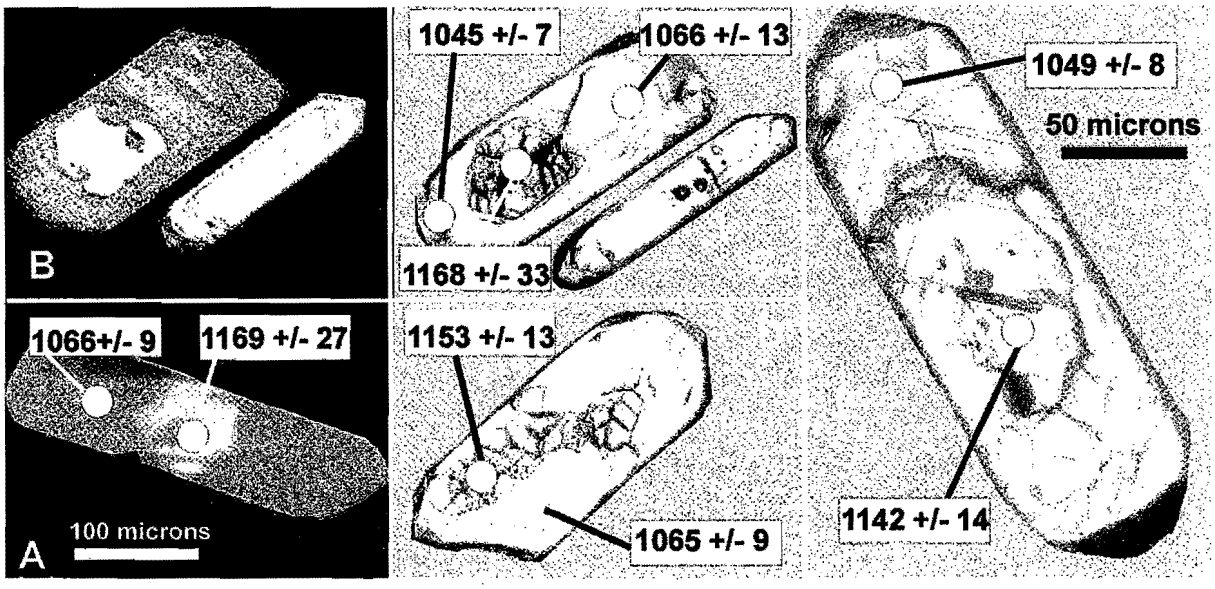

Fig. 3 CL images (A,B) and transmitted light (C,D,E) of typical Lyon Mt Gran2ite. In all cases corroded AMCG cores are surrounded by thick mantles of ~ 1050 Ma zircon that commonly shows excellent oscillatory zoning (E) indicative of magmatic growth.

34.0 Quartz-sillimanite nodules in Lyon Mt Granite.
34.2 Roadcut of Lyon Mt Granite on left (north) side of Road. Park on right next to Smith Pond.

STOP 3. ca 1050 Ma LYON MT LEUCOGRANITE. (30 MINUTES). The medium grained, pink leucogranite is characteristic of the main quartz-microperthite unit of Lyon Mt Granite that occurs in broad tracts across the Adirondack Highlands. The classical low-Ti Kiruna-type magnetite deposits of the Adirondacks are closely associated with the granite, either occurring within it or in rocks (usually metacarbonates) immediately adjacent to it. Magnetite mineralization is commonly accompanied by sodic alteration manifested by checkerboard albite and by quartz-albite (Ab_{98}) replacements of the original quartz-microperthite rocks (McLelland et al., 2002). A total of six occurrences of Lyon Mt Granite from across the Adirondacks have been dated by U/Pb techniques including single and multigrain TIMS and SHRIMP II (Fig. 2). All of these fall into the interval 1050 $\pm$ 10 Ma (McLelland et al., 2001). The present roadcut was dated by single grain TIMS methods and yields an age of 1049 $\pm$ 2 Ma (Fig. 3). Staining of the roadcut reveals that it contains several sheets and layers of quartz-albite one of which is associated with a irregular veinlet of magnetite. Locally, quartz-sillimanite nodules are present in these rocks and are attributed to leaching by high temperature hydrothermal fluids (McLelland et al., 2002). Pegmatites and quartz veins are common.

34.9 Turn left (north) on Short Street
35.4 Turn left (north) on Adirondack Road.
37.3 Turn right (northeast) on Pease Hill Road.
38.2 Stay left at intersection
40.9 Turn left (north) at intersection with Palisades Road.
41.6 Quartz-sillimanite nodules in Lyon Mt Granite included by Walton and deWaard in their "Basement Complex".
43.0 Junction with Rt 8. Turn left (northeast) at stop sign.
43.7 Metapelites assigned by Walton and deWaard to their "Older Paragneiss".
44.3 Marble, calcsilicate of Walton's "Paradox Lake Formation in near continuous outcrop for 2.6 miles.
46.9 Long roadcut of migmatitic metapelite assigned by Walton to the "Treadway Mt Formation". Park.

STOP 4. HIGHLY DEFORMED MIGMATITIC METAPELITES (> 1300 Ma). (30 minutes). The southern and eastern Adirondack Highlands, as well as the Northwest Lowlands, contain a significant thickness of dark garnet-biotite-quartz-oligoclase + sillimanite metapelite accompanied by a garnet-bearing white quartz-feldspar leucosome. McLelland and Husain (1986) interpret the leucosomes as *in situ* anatectic products of the original rock and the dark fraction as restite. Greywacke is a likely precursor. The presence of armored spinel, and rarely corundum, are consistent with this interpretation. In regions of low strain the leucosomes are present as crosscutting, anastamosing, irregular sheets, dikes, and veins of clearly coarse-grained pegmatitic material. As strain increases, the pegmatitic material gets pulled into psuedoconformity, disrupted, and grain size reduced so as to yield porcellaneous layers that are commonly parallel but locally retain their original crosscutting configurations. In short, the apparent layering in these rocks is almost wholly tectonic and has nothing to do with original stratigraphic superposition. They are, in fact, mylonitized migmatites, of the variety referred to as "straight gneiss". As indicated in stop 2, these metapelites are crosscut by the ca 1300 Ma tonalitic suite, and therefore post-date these rocks. Our interpretation is that their current reintegrated compositions are best accounted for by a greywacke-shale precursor, and that these were arc-related, flysch-type sediments approximately coeval with the Elzevirian tonalites. This would also help to explain the relative proximity between these lithologies. The age of anatexis is currently being investigated, but a pilot SHRIMP II study on a leucosome from near Speculator reveals a complicated pattern of zoning and inheritance with cores of age ca 1240 Ma and metamorphic overgrowths of 1010-1040 Ma. Sandwiched between these are mantles with oscillatory zoning and ages of 1170-1180 Ma. We interpret these mantles as zircon grown during anatexis and dating this event as Elzevirian. The absence of further significant anatexis in the granulite facies Ottawan Orogeny (1090-1030 Ma) is thought to be the result of earlier dehydration of the migmatites during the Elzevirian anatexis. Both mafic and granitic sheets can be traced across the roadcut face and reveal the presence of fault offsets. Note that the name "Treadway Mt Formation" assigned to this unit by Walton suggests that it has stratigraphic characteristics and continuity. This assumption is no longer considered to be correct and is, at best, is a lithotectonic assignation.

47.2 Granite and gabbro.

47.9 Large isoclinal fold in quartzites and metapelitic rocks.
48.1 Undeformed gabbro.
48.4 Marble. Park in parking area.

STOP 5. SWEDE MT SEQUENCE. (60 MINUTES INCLUDING LUNCH). The metasediments exposed along the Rt 8 at Swede Mt provide an exceptional opportunity to closely examine both the rocks and structure. At the southwestern end of the sequence (mile 48.9) a well-exposed isoclinal fold can be seen in the large roadcut on the south side of Rt 8. Folded units include marble, quartzite, sillimanite-garnet-quartz-feldspar (khondalite) gneiss, and rusty sulfidic Dixon Schist. The latter is thought to represent a sheared, altered, and graphitic variety of the khondalite. The fold axis trends ~E-W at a low angle of plunge about the horizontal, and its axial plane, which dips from ~50 degrees SW to horizontal, has been folded about upright E-W axial planes. The fold is typical of refolded isoclines in the Adirondacks. Similar rocks at Dresden Station, on the east side of Lake George, are intruded by a metagabbro dated at 1144 $\pm$ 7 Ma. At this locality the metagabbro truncates foliation and even individual garnet grains in the khondalite. These relations indicate that the khondalite was deposited and first metamorphosed in Elzevirian times. Early workers considered the khondalite to be a stratigraphic unit (Hague Gneiss or Spring Hill Pond Formation), but regional mapping suggests that individual units are continuous over distances of miles. Both Dixon schist and the khondalite were mined for flake graphite during the early part of the century. The region around Swede Mt is known as the Dixon National Forest and the former mining hamlet of Graphite is located at mile 49.8.As Rt 8 is followed eastward, an undeformed dolerite dike is encountered. The dike strikes parallel to the highway and has caused brecciation and alteration of the country rock that consists principally of marble at this locality.. At the top of the hill, and across from Swede Pond, a long roadcut exposes typical Adirondack marbles. At the eastern end of these exposures, a thick bed of quartzite is wrapped around the nose of an isoclinal fold. Note the linear features along its axis.
49.7 Elephant rock. Consists of leucocratic sillimanite-garnet-quartz-feldspar gneiss (khondalite).
49.8 Khondalite, Dixon Schist and graphite. Park on right side of road in area leading to old graphite mines.
54.2 Stop sign. Turn left (north) at junction with Rt 9N.
61.2 Charnockite of the Ticonderoga Dome. Park on right side of road.

STOP 6. TYPICAL AMCG CHARNOCKITE OF TICONDEROGA DOME (15 MINUTES). These outcrops were dated at 1113 $\pm$ 10 Ma by Silver (1969) but are certainly ca 1150 Ma member of AMCG suite. Silver's "young" reflects the fact that air abrasion was not yet in use when he did the analyses. Note the strong fabric that is typical of AMCG granitoids.
63.7 Rotary. Bear left (north) on Rt 9N.
64.4 Stop light. Junction with Rt 74. Turn left (west).
65.5 Complex roadcut of marble, calcsilicate, and gabbro.
75.9 Park on right hand (northern) shoulder of Rt 74. DANGEROUS SPOT! USE EXTREME CARE!!

STOP 7. LOW-TI MAGNETITE ORE IN LYON MT GRANITE WITH QUARTZ-ALBITE FACIES. (30 MINUTES). Old magnetite mine workings are located a few hundred feet uphill from the highway and are defined by the excavation of magnetite ore along meter-scale layers dipping ~ 45 degrees north. A meter-thick pillar of magnetite-apatite ore was left in place to support the hanging wall. The area below is strewn with waste rock from the 19th century mining operation. The hanging wall of the mine consists of the quartz-microperthite facies of Lyon Mt Granite (Fig. 2). Thin section study (Fig. 4) reveals that for about 150 ft uphill the perthite is progressively replaced by albite with replacement, and checkerboard albite, increasing in the direction of the mine opening. As the mine opening is approached the amount of K_2O in the rock decreases, and below the mine pillar, the rock consists of quartz-albite rock with magnetite and small quantities of aegerine. McLelland et al (2002) have interpreted both the magnetite and quartz-albite rock to be the result of metasomatic replacement due to the percolation of regional fluids at high temperature. It is thought that the fluids were derived from evolved surface brines rich in Na, Cl, and scavenged iron. Heat from Lyon Mt Granite drove these hydrothermal cells as they penetrated into the outer margins of Lyon Mt Granite plutons shortly after crystallization. This is consistent with oxygen isotope results (McLelland et al, 2002). SHRIMP II geochronology demonstrates that the quartz-albite rock contains cored zircons with mantles showing good oscillatory zoning and ages of ca 1050 Ma. These grains are interpreted as unreplaced zircons remaining from the original quartz-microperthite precursor.

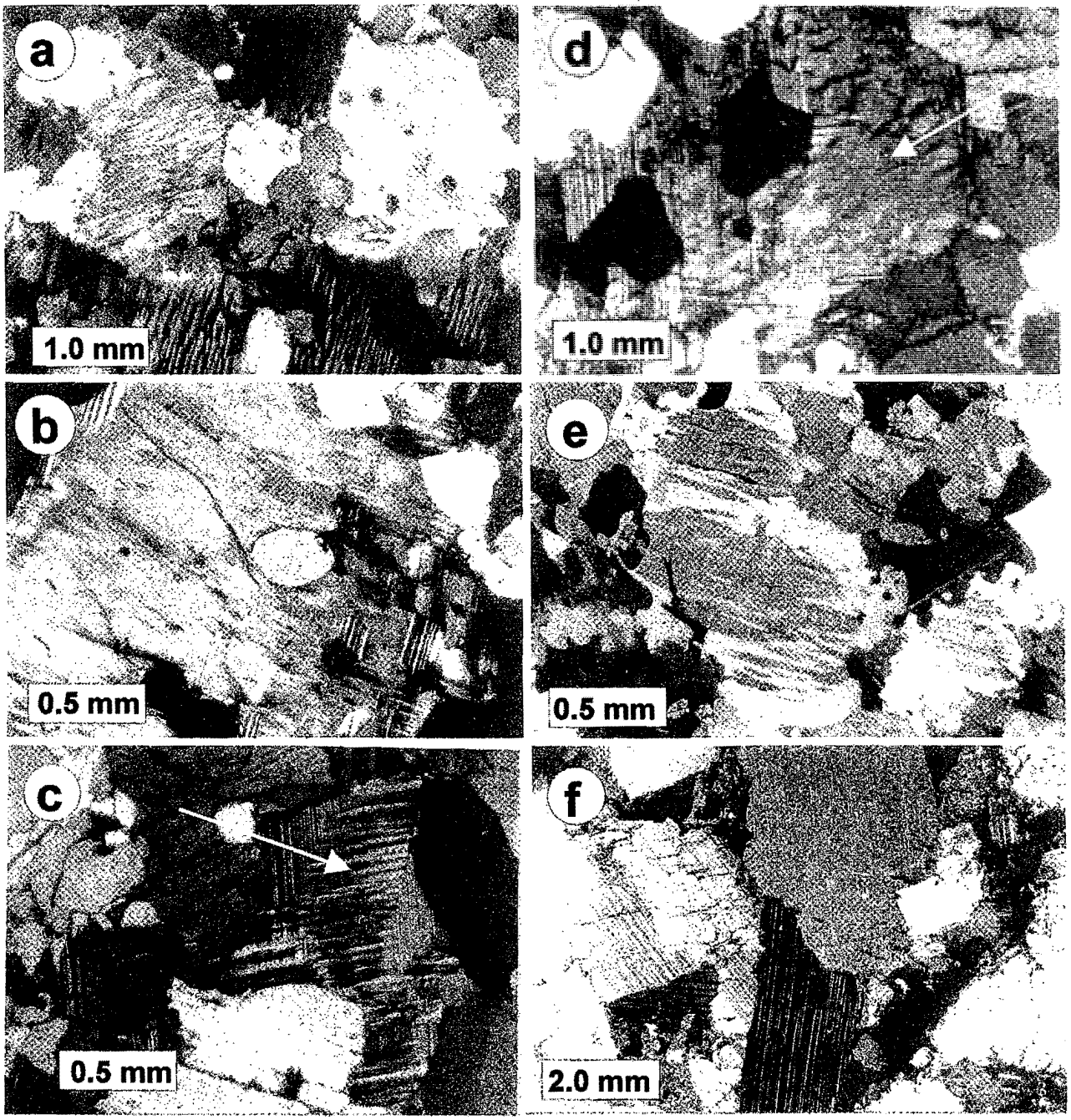

Fig. 4 Photomicrographs (crossed polars) of representative samples of LMG fromSkiff Mt traverse. Photos were chosen to illustrate the progressive replacement of original microperthite (a) by albite leading to checkerboard texture (b). In '(c) most of the dark grain is checkerboard albite and only asmall remnant of microperthite remains (arrow).By (d) only a ghostly remant of microperthite is visible in the checkerboard albite. The grain in (e) thick albite rims have engulfed most of a perthite grain that also shows checkerboard twinning. The end result of this replacemnt is represented by the quartz-albite rock in (f)

76.4 Marble
77.0 Marble then granitic gneiss.
75.5 Marble for next 2.3 miles. Note disrupted amphibolite forming "tectonic fish").
75.6 Junction with Rt 9. Turn right (north) on Rt 9
75.7 Junction with Northway (Rt 87). Turn right on to northbound lane.
83.1 Exit Northway at North Hudson.
83.2 Turn left (west) at stop sign and proceed towards Tahawus and Newcomb on the Blue Ridge Highway.
93.2 Roadcut of anorthosite on right (north) side of highway. Park on shoulder.

STOP 8. MARCY ANORTHOSITE MASSIF DATED AT ca. 1155 Ma. (30 MINUTES). This outcrop has yielded a relatively large volume of remarkably well-formed euhedral zircon grains exhibiting excellent oscillatory zoning. Two of these grains are shown on the guidebook cover. A summary of all Adirondack zircon dating appears in Fig 3 and Table 2 of trip A-1 where it may be seen that that 14 anorthosite suite samples from across the Marcy massif have now been directly dated by SHRIMP II techniques. These cluster tightly about 1155 Ma, which corresponds, almost exactly to the 15 ages for AMCG mangerites and charnockites also shown in Table 2. These results leave little doubt that the Marcy anorthosite and its granitoid envelope were emplaced at ca 1155 Ma. The results also emphasize that the other AMCG complexes in the Adirondacks were emplaced at ca 1155 Ma as well. Attempts to assign a ca 1040 Ma age to the Marcy anorthosite are inconsistent with this geochronology and with field evidence as well. The characteristics of Adirondack massif anorthosite, and a model for its origin and evolution, are presented in Trip A-1 to which the reader is referred for these discussions. The present outcrop is typical of much of the Marcy facies and much of the Marcy massif. Large blue gray andesine grains account for most of the outcrop, but a finer grained matrix is also present. Whether this represents grain size reduction or a distinct magma has not yet been investigated (see Stop 8, Trip A-1). The outcrop contains numerous narrow veinlets of ferrodioritic material that are interpreted as filter-pressed late interstitial magmas from the anorthosite (McLelland *et al*, 1994, see Trip A-1).
96.2 Roadcuts in Whiteface facies of the Marcy massif.
99.2 Large roadcut in coronitic olivine metagabbro. Park on right (north) shoulder.

STOP 9. CORONITIC OLIVINE METAAGABBRO DATED AT 1150 ± 10 Ma. (20 MINUTES). This roadcut is typical of Adirondack coronitic metagabbros that have been described by McLelland and Whitney (1977, see Trip A-1). Under the microscope these rocks display remarkably well-preserved igneous textures most of which are sub-ophitic. Superimposed on these are coronas of garnet and clinopyroxene formed between olivine or pyroxene and plagioclase. During the reaction, the olivine is transformed to orthopyroxene and therefore may be totally exhausted. Excess Fe, Mg, and Na from the reaction site migrates out into surrounding plagioclase to form green hercynitic spinel while, at the same time, Ca displaced from the plagioclase migrates back to the reaction site to form garnet. The effect is to cloud and impart a distinctive pistachio green color to the plagioclase and to reduce its anorthite content. As a consequence, most plagioclase in these rocks has An~32% although normative plagioclase is An~65% (rarely preserved in cores of large grains). The reaction appears to halt at An~28, presumably because plagioclase this sodic no longer participates in the garnet-forming reaction. As of late-August, 2002, this metagabbro had not yet been dated by SHRIMP II. However, an identical metagabbro near the intersection of the Northway and the Blue Ridge Highway yielded abundant zircons many of which were of excellent igneous morphology and showed good zoning. These gave a well-constrained age of 1150 + 14 Ma, and we expect that the same age will be found for the metagabbro at this stop. Coronitic metagabbros of this type occur throughout the Adirondacks but are notably concentrated near the anorthosite massifs. This, coupled with the similarity in age, indicate that these bodies represent batches of the magma that ponded at the core-mantle interface to form plagioclase-rich crystal mushes that ascended to form anorthosite (See trip A-1). The difference is that these gabbroic magmas did not pond but broke through to the upper crust at an early stage. A spectrum of continuous compositions does exist among the metagabbros and suggests that tapping off of these magmas took place at different stages of differentiation.

END OF FIELD TRIP. RETURN TO NORTHWAY AND LAKE GEORGE VILLAGE

GEOLOGY AND MINERAL DEPOSITS OF THE NORTHEASTERN ADIRONDACK HIGHLANDS

by
Philip R. Whitney, New York State Museum, 3140 CEC, Albany NY 12230
James F. Olmsted, 48 Haynes Road, Plattsburgh, NY 12901

INTRODUCTION

On this trip we will examine three of the most notable features of the Adirondack Highlands. The first stop is at the NYCO wollastonite mine at Oak Hill near Lewis, where wollastonite-garnet-pyroxene skarns preserve a record of a giant Proterozoic hydrothermal system that was fed by meteoric waters and driven by heat from the nearby Westport Dome anorthosite intrusion. The following two stops, at Arnold Hill and Palmer Hill near Ausable Forks, are in the granitoids and felsic metavolcanics of the enigmatic Lyon Mountain Gneiss, host to numerous low-titanium magnetite deposits that were the basis of a flourishing iron mining industry in the late nineteenth century. The remaining three stops, one at Jay and two near Elizabethtown, are in metamorphosed anorthosite and its mafic derivatives, and illustrate the structural complexity and lithologic diversity of these rocks which ordinarily appear on maps as undifferentiated blobs.

BRIEF GEOLOGIC HISTORY OF THE ADIRONDACK HIGHLANDS

The oldest known rocks of the Adirondack Highlands are metasedimentary rocks with interlayered metavolcanics. The age of deposition is not well established, but those in the southeastern Adirondacks are intruded by 1330-1307 Ma tonalitic rocks (McLelland and Chiarenzelli 1990) and must therefore be at least 1300 Ma old. Elsewhere in the Highlands they may be as young as approximately 1150 Ma. In the west-central and northeastern regions, the metasediments are dominated by calcsilicates, marbles, and quartzites with minor metapelites. Several features of these rocks indicate hypersaline depositional environments and the former presence of evaporites (Whitney and Olmsted 1993; Whitney et al. 2002). Relative amounts of pelitic and semipelitic gneisses in the metasedimentary section increase toward the southeast. Evidence for an early (pre-1150 Ma, Elzevirian?) tectono-metamorphic event has been found by McLelland et al. (1988) in the southeastern Highlands.

Voluminous igneous rocks of a bimodal anorthosite-mangerite-charnockite- granite (AMCG) suite (McLelland and Whitney 1990; Whitney 1992) intrude the metasedimentary rocks. Multiple episodes of intrusion are likely, with intervening extensional deformation (Fakundiny and Muller, 1993). U/Pb zircon dating indicates that maximum intrusive activity probably took place in the interval 1160-1130 Ma, (McLelland et al. 1996). Similar AMCG complexes are found throughout much of the Grenville Province, and those in the Morin, Lac St. Jean, Lac Allard, and Atikonak River areas have ages close to those of the Adirondack suite (Emslie and Hunt, 1990). Oxygen isotopic evidence from contact-metamorphosed calcsilicate rocks favors a relatively shallow (< 10 km) depth of intrusion for the anorthositic rocks (Valley and O'Neil 1982; Valley 1985). The mafic and felsic portions of the AMCG suite, while approximately coeval, are probably not comagmatic (McLelland and Whitney 1990). Olivine metagabbro bodies scattered throughout the eastern and central Highlands are also approximately coeval with the AMCG magmatism. Slightly younger granitoids, lithologically and geochemically similar to those of the AMCG suite, were emplaced in the interval 1103-1093 Ma (McLelland et al. 2002). Another suite of felsic rocks, the Lyon Mountain Gneiss complex, is discussed in detail below.

Frost and Frost (1997) have proposed that large volumes of reduced, potassium- and iron-enriched type A granitic magmas may be derived from partial melting of underplated tholeiitic basalts and their differentiates in an anorogenic or extensional intraplate setting. They cite the Wolf River Batholith of Wisconsin, the Pikes Peak Batholith of the Colorado Front Range, and the Sherman Batholith of Wyoming as examples of granites that originated in this manner. Each has associated mafic and anorthositic rocks, consistent with the bimodal character of rapakivi and other A-type suites worldwide (Haapala and Ramo, 1999). AMCG granitoids have type A geochemical signatures (McLelland and Whitney 1990) and locally show rapakivi textures (Buddington and Leonard 1962; Whitney et al. 2002); they may be the deformed and metamorphosed equivalent of such intraplate complexes. Subsidence associated with underplating may give rise to intracratonic basins (Stel et al., 1993), which suggests that at least part of the metasedimentary suite in the Adirondack Highlands may be coeval with AMCG magmatism.

Regional granulite facies metamorphism of Ottawan age in the Adirondack Highlands occurred at temperatures of 700-850°C and pressures of 6.5-8.5 kbar (Bohlen and others, 1985; Spear and Markussen, 1997). Early stages of cooling may have been nearly isobaric (Spear and Markussen, 1997), and there is little evidence for

sudden orogenic collapse. These conditions, recorded in rocks of supracrustal and relatively shallow intrusive origin require tectonic thickening of the crust, possibly by SE-over-NW thrusting associated with a collisional event (Whitney, 1983; McLelland and Isachsen 1985). Ottawan deformation is characterized by both large-scale folding and the development of extensive, locally mylonitic, ductile shear zones. Many of the anorthosite bodies have a domical configuration that may reflect either the initial shape of the intrusions or later gravity-driven vertical tectonics following crustal thickening (Whitney 1983). The age of the Ottawan in the Adirondack Highlands is not yet clearly established. McLelland et al. (1996, 2001) place it in the range 1090–1030 Ma, based on extensive U-Pb zircon studies of AMCG suite rocks. Florence et al. (1995) suggest a slightly younger age of 1050-1000 Ma based on U-Pb zircon and monazite ages from nelsonite and metapelites in the western Highlands. The latter interval is in agreement with the 1026–996 ma ages measured by Mezger et al. (1991, 1993) on metamorphic garnet and zircon in the central Highlands. Numerous other concordant or near-concordant zircon U-Pb ages in the 1040–990 Ma range indicate a high-temperature metamorphic event in the Adirondack Highlands after 1050 Ma (Silver 1968; Mclelland et al. 1988; and unpublished N.Y. State Geological Survey data from zircons in anorthosite). A 995 $\pm$ 19 Ma Sm/Nd mineral isochron from a garnetiferous oxide-rich gabbro dike within the Marcy anorthosite massif (Ashwal and Wooden, 1983) also suggests a late date for Ottawan metamorphism. Davidson (1995) reports Ottawan high-grade metamorphism in the ca. 1060-1020 Ma range throughout much of the Grenville Province.

ROCKS OF THE NORTHEASTERN HIGHLANDS

The map of the Ausable Forks Quadrangle (Figure 1) illustrates the mode of occurrence of the major rock units of the the northeastern Adirondack Highlands. Structurally lowermost are the domical metanorthosite bodies, here represented by the Jay and Westport Domes. Smaller amounts of mafic gneisses and granulites ranging in composition from ferrogabbro to monzodiorite are associated with the metanorthosite. Gabbroic metanorthosite also occurs as sheetlike bodies within the overlying metasedimentary section.

Metasedimentary rocks overlying the domical anorthosites consist principally of diopside-rich calcsilicate granulites, impure quartzites, and calcite marbles, with lesser amounts of phlogopite and biotite schists and metapelites, rare dolomite marble, and the economically important wollastonite ore skarns of the Willsboro-Lewis district. The metasedimentary rocks are interlayered with amphibolite and mafic and felsic gneisses of indeterminate ancestry, and contain intrusive bodies of olivine metagabbro and granitoids of the AMCG suite. In the central part of the Ausable Forks quadrangle west of Black Mountain, prominent marble "dikes" crosscut a stratiform body of anorthosite gneiss, illustrating the ductile behavior of the marble relative to that of anorthosite during deformation. These dikes led Emmons (1842) to conclude that marble was the only clearly igneous rock in the Adirondacks!

Several features of these metasedimentary rocks suggest the former presence of evaporites. The preponderance of diopside-rich calcsilicate rocks, the metamorphic equivalent of silicious dolostones, is significant in that dolomite is commonly a product of hypersaline depositional environments (Friedman, 1980). The calcsilicate rocks locally contain major amounts of microcline, possibly the metamorphic equivalent of authigenic or diagenetic adularia. Magnesium-rich metasedimentary rocks, in particular phlogopite schists and enstatite-diopside-tremolite-quartz rocks, are likely granulite facies equivalents of evaporite-related talc-tremolite-quartz schists, such as those found near Balmat in the northwest Adirondacks, in stratigraphic association with diopside-rich rocks and bedded anhydrite (Brown and Engel, 1956). Magnesite-dolomite-chlorite-quartz rocks are a possible sedimentary protolith. Granulite facies metasedimentary rocks similar to those of the Ausable Forks quadrangle occur in the Caraiba mining district of Brazil (Leake and others, 1979), and in the Oaxacan Complex of southern Mexico (Ortega-Gutierrez, 1984); in both localities anhydrite is present in the subsurface.

The metasedimentary complex is overlain in turn by heterogeneous, predominantly felsic gneisses known informally as Lyon Mountain Gneiss, host to local concentrations of low-titanium magnetite ore that were the basis for a flourishing iron mining industry in the late nineteenth century. This trip includes stops in the wollastonite skarn, LMG, and metanorthosite, each described in more detail in the following section.

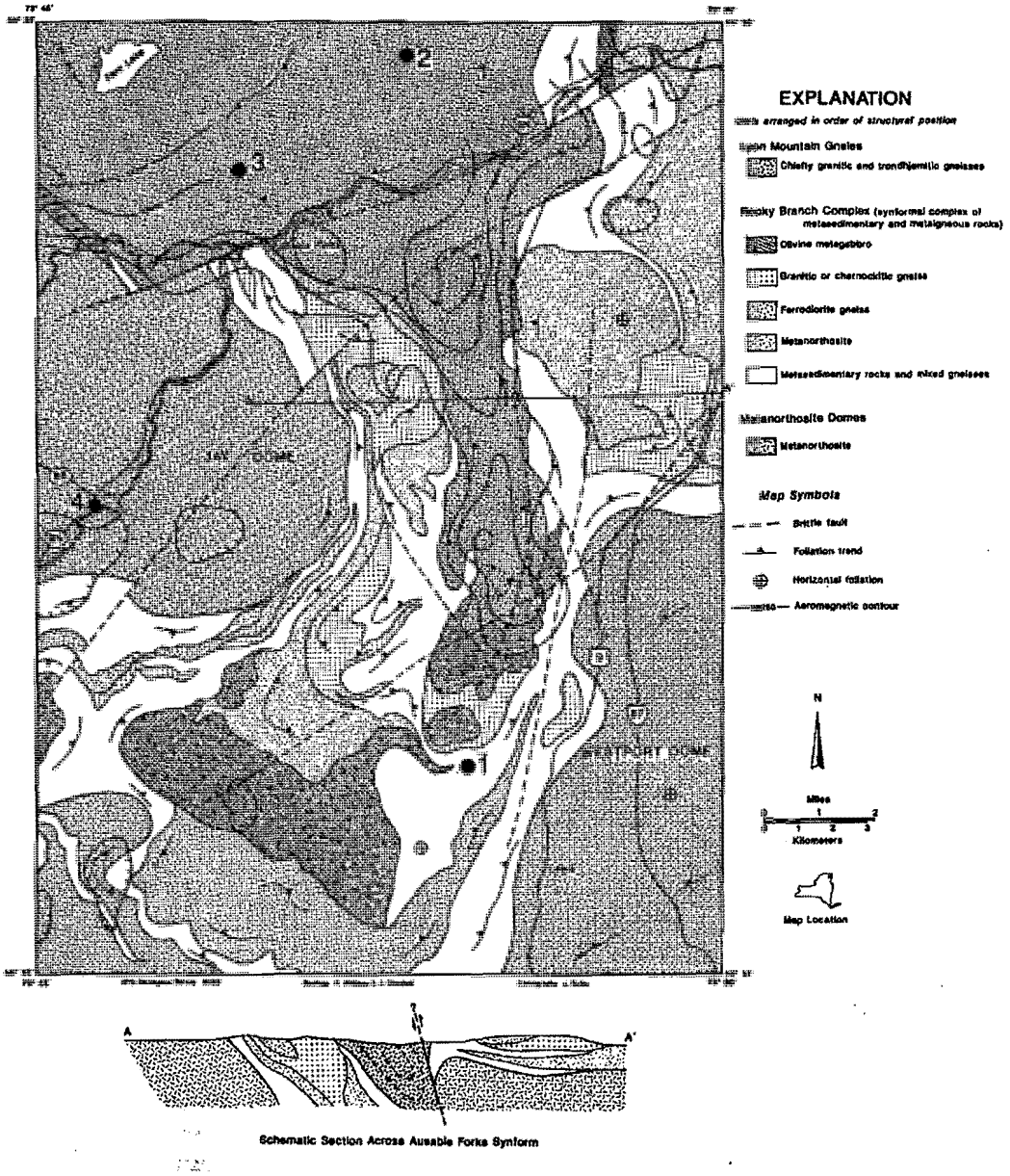

Figure 1. Geologic map of the Ausable Forks 15' Quadrangle, after Whitney and Olmsted (1993)

DESCRIPTIONS OF LITHOLOGIC UNITS

Wollastonite skarns (Stop 1). The presence of wollastonite near Willsboro in the northeastern Adirondacks (Figs. 1, 2) has been known since the early nineteenth century. The earliest reference to it in the geologic literature is by Vanuxem (1821). For over a century, the wollastonite was of little interest except as a mineralogical curiosity. Mining on a small scale began at Fox Knoll near Willsboro in 1938, with the wollastonite being used as a flux for arc welding. In 1951, the Cabot Corporation gained control, and began underground mining in 1960. Interpace Corporation took over and expanded operations in 1969. Product development resulted in uses in ceramic bodies and glazes, as a reinforcing filler in plastics and resins, and as a substitute for short-fiber asbestos. The operation, was purchased in 1979 by a subsidiary of Canadian Pacific (US), Processed Minerals Inc. Open pit mining at the Lewis Mine, ten miles southwest of Willsboro, began in 1980 and in 1982 the underground operation at Willsboro was closed. Development of the Oak Hill

orebody is currently under way. All three properties are now owned by NYCO Minerals, Inc., a subsidiary of Fording Coal Company of Calgary, Alberta.

The Willsboro deposit was mentioned briefly by Buddington (1939, 1950) and Buddington and Whitcomb (1941); the geology is given in more detail by Broughton and Burnham (1944). Putman (1958) described several occurrences of wollastonite in the Au Sable Forks and Willsboro quadrangles, including those at Willsboro, Deerhead, and Lewis (Figure 2). De Rudder (1962) studied the mineralogy and petrology of the Willsboro ores, and attributed them to contact metamorphism with localized alumina metasomatism. Oxygen isotope work by Valley and O'Neil (1982) demonstrated extensive metasomatism involving meteoric water.

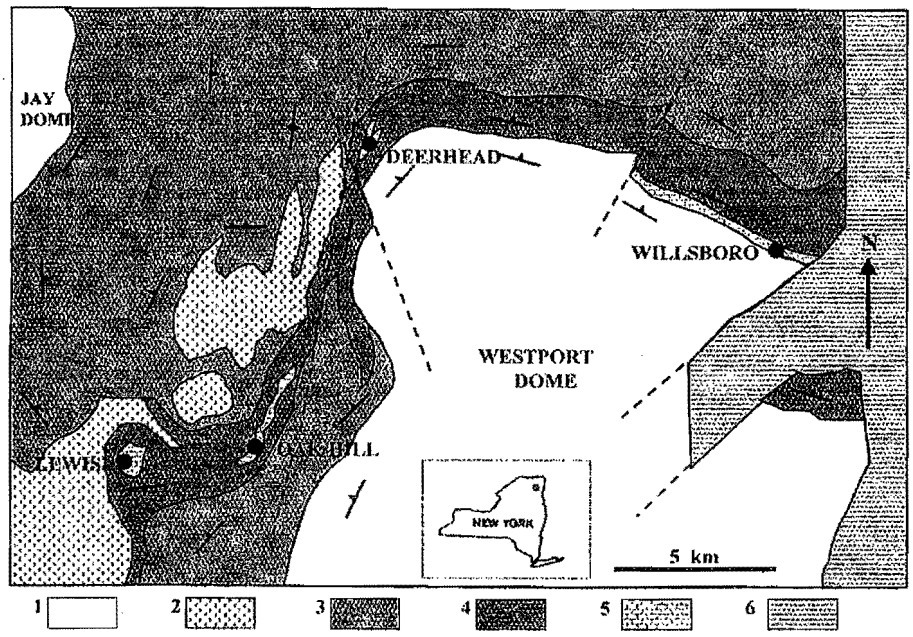

Figure 2. Willsboro-Lewis Wollastonite District. 1. Anorthosite 2. Olivine Metagabbro 3. Mixed gneisses (gabbroic anorthosite, amphibolite, charnockite, granite, metasedimentary rocks) 4. Ore-bearing zone (OBZ) 5. Skarn 6. Paleozoic

Geologic setting: The Westport metanorthosite dome (Figures 1 and 2) is located east and north of the Marcy Massif. It is overlain on its north and west flanks by interlayered granulite facies metaigneous and metasedimentary gneisses, marbles, and calcsilicate rocks. The wollastonite deposits at Willsboro, Oak Hill, and Lewis, as well as the undeveloped prospect at Deerhead, occur within a mappable zone up to 2000 feet thick that extends for at least 14 miles along strike (Figure 2). This ore-bearing zone (OBZ) is characterized throughout by strong to intense foliation and locally prominent lineation. Along the northern flank of the Westport Dome from the Willsboro mine to Deerhead, the OBZ directly overlies the metanorthosite of the dome, foliations dip NNE away from the dome, and lineations plunge NW. Southwestward, near Oak Hill and the Lewis mine, dips flatten and lineations become parallel with the regional NNE trend (Whitney and Olmsted, 1993). Foliation and compositional layering in both skarn and host gneisses is roughly parallel to the contact of the underlying metanorthosite. The skarns are nowhere far from the projected anorthosite contact in the subsurface.

Metaigneous rocks within the OBZ occur as sheets and lenses parallel to foliation, emplaced either as sills or as tectonic slivers. They include gabbroic and anorthositic gneisses, amphibolite, and minor charnockite. Interiors of thick gabbroic layers may display relict igneous textures. In addition to the skarns, metasedimentary rocks consist chiefly of diverse suite of granular-textured garnet-clinopyroxene-plagioclase rocks, calcite marbles, and minor amounts of quartzite and metapelite.

The ore at all four known locations occurs as tabular bodies ranging from a few feet up to as much as 80 feet thick. Multiple wollastonite-bearing horizons, separated by gabbroic or anorthositic gneisses and amphibolite, are present at Willsboro (DeRudder, 1962) and at Oak Hill. The orebodies consist of wollastonite-rich ore with layers and lenses ranging from less than an inch to several feet thick of garnet-pyroxene skarn (GPS). This compositional layering

is ordinarily straight and sharply defined; it is probably not an original sedimentary feature but rather a result of tectonically induced metamorphic differentiation during or subsequent to ore formation. More diffuse compositional layering and foliation within the ore locally exhibits complex folding. Where layering is less prominent, garnet and pyroxene may occur in clusters or lenses up to 2 inches across.

Mineralogy: The ore layers contain the high-variance assemblage wollastonite-grandite garnet-clinopyroxene. Traces of retrograde calcite occur as thin films replacing wollastonite along fractures and grain boundaries. GPS layers within the ore consist chiefly of garnet and clinopyroxene with or without minor wollastonite. Another type of GPS, containing up to several percent of titanite and apatite, occurs at contacts between ore and metaigneous gneisses or amphibolites and, less commonly, as sill- or dike-like bodies within the ore. Minor and trace minerals occurring locally in GPS include scapolite, plagioclase, clinozoisite, vesuvianite, and zircon. Discontinuous layers up to several feet thick of nearly pure garnet, or garnet with minor plagioclase and quartz are present at some ore/gneiss contacts. These "garnetites" pinch and swell along strike or form detached lenses that resemble boudins.

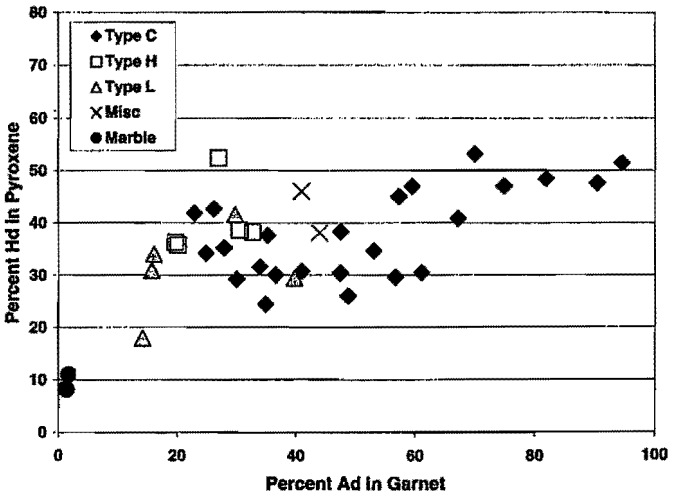

Figure 3. Garnet and pyroxene compositions in wollastonite skarns. Data from Willsboro and Lewis Mines. Hd = Hedenbergite. Ad = Andradite. For explanation of skarn types see text.

The pyroxenes in ore and GPS lie close to the diopside-hedenbergite join, containing >93% (Di + Hd), with acmite (up to 3.2%) as the most common minor component. The garnets are grossular-andradite mixtures, with > 93% (Gr + Ad); almandite (up to 4.9%) and schorlomite (up to 3.1%) are the dominant impurities. Figure 3, after Whitney and Olmsted (1998), shows the range of garnet and pyroxene compositions for the ore and GPS. Compositional variation among grains within a sample can be as great as 20% Ad and 10% Hd for garnet and pyroxene respectively. Individual grains lack detectable internal zoning that may have been initially present but was homogenized by the subsequent granulite facies metamorphism.

Geochemistry: Whitney and Olmsted (1998) describe three distinct types of wollastonite ore and skarn, based on mineralogy and distinctive rare earth element (REE) patterns (Fig. 4a). The most common, type C of Whitney and Olmsted (1998), includes most of the high grade wollastonite ore and consists of wollastonite-garnet- pyroxene and garnet-pyroxene skarns with relatively iron-rich andraditic garnet. Type H, much less abundant, is similar but with generally less wollastonite, more pyroxene, and relatively iron-poor garnet. Both type C and type H appear to be infiltration skarns involving large-scale metasomatic replacement of carbonate protoliths.

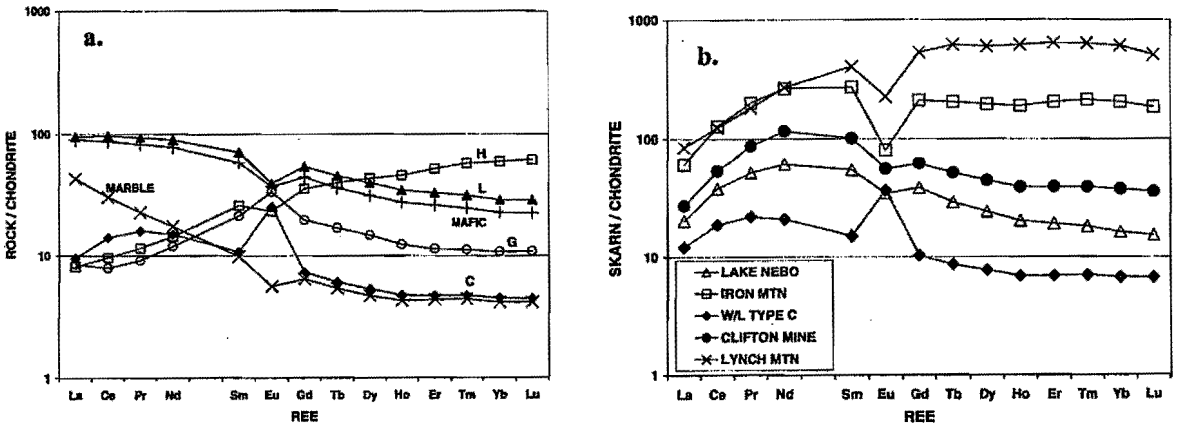

Figure 4. a. Average REE distributions in Willsboro-Lewis wollastonite skarns and in northeastern Adirondack marbles. **b.** REE in garnet-pyroxene layers in type C ores compared to garnet-pyroxene skarns from Adirondack Highlands magnetite ore deposits.

A third variety of skarn (Type L) occurs at contacts of wollastonite ore with intrusive rocks and as thin layers, possibly dikes, within and locally crosscutting wollastonite ore. Type L skarns contain variable amounts of titanite, apatite, and, less commonly, plagioclase or scapolite in addition to garnet and pyroxene; wollastonite is scarce or absent. Their limited extent and localization at igneous contacts suggest localized Ca metasomatism of igneous precursors. All three types lack primary calcite, quartz, and oxide minerals. A fourth distinct skarn type, "garnetite" (G) occurs as layers, lenses or boudins of nearly pure, relatively grossularitic garnet at or near contacts of ore with anorthosite or mafic gneiss; it is especially abundant at the Oak Hill deposit (Stop 1). Note that all skarn REE patterns are substantially different from that of the assumed marble protolith.

The origin of the distinctive REE patterns is discussed by Whitney and Olmsted (1998). Briefly, type C results from uptake of REE from solution by metasomatic garnet, with the maximum in the distribution corresponding to the closest match between the REE^{3+} ionic radius and the size of the dodecahedral (Ca) site in the garnet. The strong positive Eu anomaly may result either from prior interaction of the metasomatic fluid with nearby, Eu-positive anorthosite, preferential uptake of Eu^{2+} on garnet growth surfaces (Whitney and Olmsted 1998), or preferential solubility of Eu relative to other REE during water-rock interaction by complexation (e.g. as $EuCl_4^{-2}$) in chloride-rich solutions (Haas et al. 1995). Note the contrast in Eu anomaly and REE abundance with skarns associated with Adirondack Highlands magnetite deposits (Fig. 4b).

Hydrothermal dissolution of LREE-enriched calcite from marble containing contact-metamorphic garnet and pyroxene previously equilbrated with the calcite may be a significant mechanism in the origin of type H patterns (Whitney and Olmsted 1998). However, pyroxene and garnet in most type H skarns are more iron-rich than those in marbles, and although the shape of the REE patterns are very similar, garnet in most type H samples contains significantly more total REE than does garnet from marble. This suggests metasomatic addition of HREE, in addition to Fe. Fluid composition, pathways, temperature, and oxidation state may have differed substantially from those giving rise to type C.

Type L REE distributions in sphene- and apatite-bearing GPS probably result from localized Ca metasomatism of mafic igneous rocks in contact with ore; compare the L pattern in with that of mafic gneisses from the ore zone ("mafics" in Fig. 4a). In these rocks, LREE are retained in sphene and apatite while the heavy rare earths (HREE) remain in the relatively grossularitic garnet. The middle-REE-enriched pattern (G in Fig. 4 a) found in the garnetites has, as yet, no satisfactory explanation.

Average major and trace element concentrations for the four skarn types are shown in Table 1. Relative to a hypothetical marble protolith, types C and H are enriched in Si, Ti, Al, Fe, Zr, and Ga while Mg, K, Sr, and Ba are strongly depleted. Type H also shows enrichment in Y, Zn, and V relative to both the assumed protolith and to type C. Some of these enrichments may result from concentration of detrital silicates and their metamorphic reaction products; others, such as Fe, Ga, Y, Zn, and the REE are probably largely of metasomatic origin.

TABLE 1
AVERAGE COMPOSITIONS OF SKARNS

type	C	H	L	G
n	23	7	9	3
SiO_2	46.33	44.38	42.84	38.10
TiO_2	0.23	0.45	1.94	0.83
Al_2O_3	3.41	9.69	9.22	16.59
$Fe_2O_3(T)$	8.77	8.39	9.05	8.49
MnO	0.17	0.28	0.21	0.24
MgO	1.53	2.41	3.76	0.52
CaO	38.99	33.94	31.61	33.92
Na_2O	0.16	0.09	0.22	0.17
K_2O	0.00	0.00	0.01	0.04
P_2O_5	0.02	0.05	0.97	0.19
Rb	<1	<1	<1	<1
Sr	34	24	45	30
Ba	2	4	2	<2
Zr	57	73	319	121
Y	8	79	61	56
Nb	2	2	13	11
Ga	11	15	15	27

Metasomatic origin of the ores: Wollastonite commonly occurs as a contact metamorphic mineral formed by reaction of calcite and quartz. However, the Willsboro-Lewis ores show metasomatism on a large scale. The evidence includes:

a. Mineral assemblages and compositions. If the wollastonite ore had been formed by isochemical contact metamorphism, the absence of either quartz or primary calcite would imply a protolith with precisely the right balance of quartz and calcite. This highly improbable requirement, together with the high variance of the ore mineral assemblage, indicates that metasomatism has occurred (Valley and O'Neil, 1982).

b. Oxygen isotopes. Valley and O'Neil (1982) determined oxygen isotopes in both the Willsboro and Lewis deposits. They found $\delta^{18}O_{SMOW}$ in the wollastonite ore from -1.3 to 7.0‰; as much as 25‰ lower than typical Adirondack marbles. Sharp gradients occur between ore and wall rocks. They (Valley and O'Neil, 1982) showed that the $\delta^{18}O$ data could not be explained by isotopic fractionation during devolatilization reactions, but required exchange with large volumes of heated meteoric waters at the time of anorthosite intrusion.

c. Depletion of Na, K, Rb, Ba, and Sr. Only those elements that can be accomodated in the structures of wollastonite, garnet, and pyroxene are present in significant concentrations in the ores and GPS (Table 1). This is particularly clear for the large-ion lithophile elements (LILE) K, Rb, and Ba, which are present in only negligible amounts compared to a hypothetical marble protolith. This is best explained by metasomatic removal. Strontium is also depleted although to a lesser extent.

d. REE distribution. Assuming a carbonate protolith for the ore, comparison of the REE distributions in ore and GPS with those of northeastern Adirondack marbles (Fig. 4a), confirm substantial metasomatic redistribution of REE.

Sequence of ore-forming events. Origin of the ores by hydrothermal metasomatism requires a heat source to provide the minimum temperatures (ca. 450°C) for formation of wollastonite and to drive the hydrothermal circulation. This requirement, and the close spatial association between the ores and the Westport Dome (Fig. 2) strongly indicate that the ore is coeval with emplacement of the anorthosite, in agreement with the conclusions of earlier workers (Buddington 1939, 1950; Broughton and Burnham 1944, DeRudder 1962). Moreover, access of large volumes of dominantly meteoric fluids implies a relatively shallow depth of emplacement (Valley and O'Neil 1982, Valley 1985). Access of fluids would also be facilitated in an extensional tectonic setting. Massif anorthosites are widely believed to be associated with extensional tectonics (Ashwal, 1993). Whitney and Olmsted (1993) have argued that the Adirondack anorthosites were emplaced in an extensional setting that included large listric or detachment faults. We speculate that the present OBZ was the locus of one or more such faults. A similar association of extensional faulting with magmatic doming has been proposed by Lister and Baldwin (1993) for some metamorphic core complexes. Major low-angle

extensional faults can provide channels for circulating hydrothermal fluids (Reynolds and Lister, 1987; Kerrich and Rehrig, 1987). When the Westport Dome was emplaced, hydrothermal circulation driven by heat from the intrusive may have followed the low-angle faults, fed from the surface by meteoric water penetrating along associated high-angle normal faults (Fig. 5; arrows show hypothetical fluid pathways). Where the faults intersected or followed reactive carbonate units, infiltration metasomatism produced wollastonite and andraditic garnet, accompanied by exchange of REE and oxygen isotopes. Ongoing or later deformation produced the foliation in the ore and concentrated garnet and pyroxene into conformable GPS layers and lenses by mechanical metamorphic differentiation. Subsequent granulite facies metamorphism during the Ottawan orogeny had little effect on the mineral assemblage in the skarns but probably resulted in intra-grain homogenization of initially zoned garnet (Whitney and Olmsted 1998).

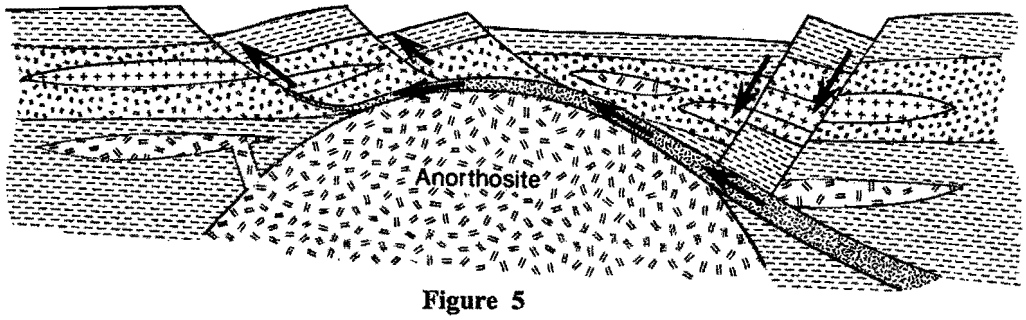

Figure 5

Lyon Mountain Gneiss (Stops 2 and 3)

Description. The Lyon Mountain Gneiss comprises several distinct facies of felsic gneisses, classified by Postel (1952) in terms of the dominant feldspar present (microperthite, microcline, microantiperthite, or plagioclase). Feldspar in the plagioclase facies, i.e. the leucocratic albite gneiss (LAG) of Whitney and Olmsted (1988), is nearly pure albite (Ab_{95}-Ab_{98}). Table 2 shows representative chemical analyses for the several facies. Note the extreme variation of Na and K, far outside the normal igneous range and indicative of extensive alkali metasomatism. Apart from the variation in alkali metals, two geochemically distinct types of LMG are present (Fig. 6). One is enriched in high field stength elements and REE relative to the other, and has significantly higher Ga/Al ratios and more pronounced negative Eu anomalies indicating a more fractionated igneous source. This high-HFS group may be the volcanic equivalent of the fayalite granite exposed at Bailey Hill, within the LMG complex (Whitney and Olmsted 1993; X's in Fig. 6)).

Mineralogy of the gneisses varies widely, not only with respect to the variety of feldspar but also in relative proportions of quartz and feldspar (Fig. 7), and the type and amount of mafic minerals. The latter include nearly ubiquitous magnetite which in some samples is the only dark mineral. The microcline and mesoperthite facies ordinarily also contain accessory to minor amounts of clinopyroxene, biotite, brown hornblende, or, rarely, fayalite. Clinopyroxene in in the antiperthite and plagioclase (LAG) facies commonly contains up to 40% acmite component and is locally accompanied by a blue-gray sodic amphibole (Whitney and Olmsted 1993). In both sodic and potassic facies, titanite occurs as discrete grains and rims on magnetite, and andraditic garnet is present very locally as narrow rims on clinopyroxene or as clusters of small grains. In the vicinity of the Palmer Hill Mine (Stop 3), fluorite is a locally abundant accessory in the gneiss and ore.

Fine- to medium- grained granoblastic textures are the most common, but considerable amounts of coarser-textured gneisses are also present. The latter ordinaily have intermediate alkali metal ratios and may be intrusive rocks that have escaped extensive metasomatic alteration due to lower permeability. In the finer-grained rocks, prominent compositional layering or gneissosity is nearly ubiquitous, although foliation *sensu stricto* is ordinarily subdued due to scarcity of minerals with dimensional anisotropy. Lineation, where present, is defined by streaks of mafic minerals or polycrystalline quartz.

The felsic gneisses are locally interlayered with lesser amounts of metasedimentary rocks and amphibolite. The former include clinopyroxene skarns, rarely with garnet, and a peculiar albite-clinopyroxene gneiss, the mafic albite gneiss (MAG) of Whitney and Olmsted (1988, 1993), with feldspar and pyroxene compositions and accessory minerals similar to those of LAG. MAG is commonly fine-grained, with a sugary granoblastic texture. In some outcrops, it displays a prominent pinstripe layering, with alternating mm-scale pyroxene- and albite-rich layers.

Megacrysts of nearly pure albite, up to 5 cm across, are present locally; quartz content is normally less than 5 percent. MAG probably originated by Na-metasomatism of a calcsilicate protolith.

TABLE 2.
REPRESENTATIVE CHEMICAL ANALYSES
LYON MOUMTAIN GNEISS

	ABS460	AF356	AF470	LMS4B	DAS01	PXS10	PVS01	PVS07	AF664	AF781A	AF658
Facies	**P**	**P**	**P**	**P**	**M**	**M**	**AP**	**AP**	**Ab**	**Ab**	**MAG**
SiO_2	70.72	69.58	74.30	66.70	68.67	70.66	71.12	65.85	71.07	74.56	62.25
TiO_2	0.56	0.50	0.42	0.82	0.54	0.42	0.76	0.58	0.48	0.36	1.01
Al_2O_3	12.24	12.20	11.88	13.25	12.97	12.04	13.37	13.34	13.13	12.00	13.37
Fe_2O_3t	5.71	7.00	5.42	4.39	6.42	6.01	4.93	5.94	5.57	5.48	5.11
MnO	0.01	0.09	0.04	0.09	0.01	0.01	0.03	0.04	0.03	0.01	0.05
MgO	0.17	0.09	0.06	0.75	0.20	0.16	0.64	1.83	0.34	0.15	2.89
CaO	0.49	1.86	1.27	3.06	0.19	0.45	1.39	3.96	2.57	0.47	7.29
Na_2O	2.96	3.88	4.57	4.06	0.97	1.06	5.91	6.64	7.63	6.80	7.89
K_2O	6.49	4.63	2.23	5.18	9.71	8.90	1.70	1.94	0.11	0.31	0.21
P_2O_5	0.11	0.05	0.03	0.21	0.11	0.06	0.21	0.03	0.07	0.03	0.07
Total	99.58	99.70	100.21	98.66	99.86	99.79	100.45	100.30	100.91	100.40	99.83
Rb	192	98	61	167	272	227	45	34	2	4	3
Sr	57	62	28	79	39	21	107	29	25	18	36
Ba	644	526	88	718	1822	905	182	93	27	10	27
Zr	515	1172	1229	635	612	641	582	858	1084	1006	315
Y	82	59	200	94	61	53	72	83	121	111	85
Nb	28	21	53	22	20	20	17	35	38	36	17
Ga	21	25	33	28	17	19	26	27	27	31	18
					MOLECULAR NORMS						
qz	24.09	22.20	32.15	15.96	21.60	25.56	23.24	9.14	18.50	28.14	1.32
or	39.52	28.05	13.43	31.36	59.52	54.65	10.09	11.37	0.64	1.84	1.21
ab	27.39	35.73	41.83	37.36	9.04	9.89	53.34	59.13	67.63	61.36	69.29
an	0.97	2.26	5.42	2.70	0.23	1.88	4.96	0.86	1.24	1.31	0.44
ac	0.00	0.00	0.00	0.00	0.00	0.00	0.00	0.00	0.00	0.00	0.00
hy	5.12	3.94	4.70	0.90	6.31	5.95	5.36	2.65	1.31	4.96	0.00
di	0.63	5.50	0.64	9.16	0.00	0.03	0.48	14.75	8.72	0.67	22.76
wo	0.00	0.00	0.00	0.00	0.00	0.00	0.00	0.00	0.00	0.00	2.42
il	0.80	0.71	0.60	1.17	0.78	0.61	1.06	0.80	0.66	0.50	1.38
mt	1.23	1.50	1.15	0.94	1.39	1.31	1.04	1.23	1.15	1.15	1.04
co	0.00	0.00	0.00	0.00	0.89	0.00	0.00	0.00	0.00	0.00	0.00
ap	0.24	0.11	0.06	0.45	0.24	0.13	0.44	0.06	0.14	0.06	0.14

Facies: P = Perthite AP = Antiperthite MAG = Mafic Albite Gneiss
M = Microcline Ab = Plagioclase

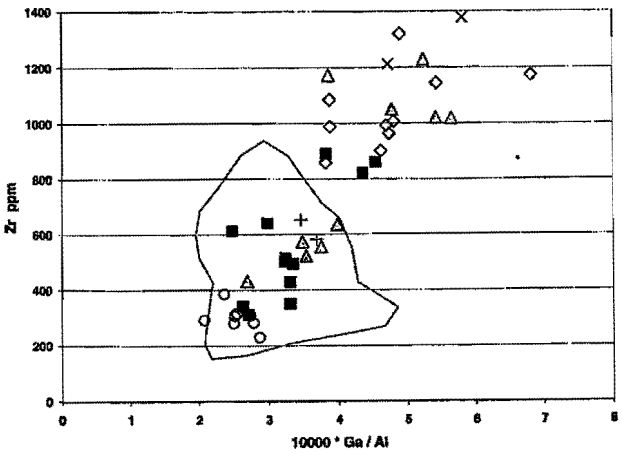

Figure 6. Filled squares: Microcline facies. Triangles: Perthite facies. +'s: Antiperthite facies. Circles: MAG X's: Fayalite granites. Outline: Range of AMCG granitoids.

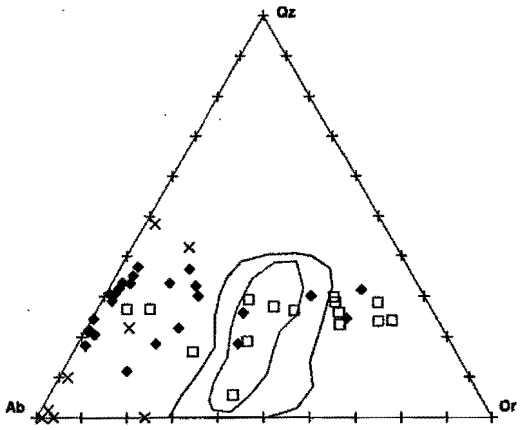

Figure 7. Diamonds: High HFS group. Squares: Low HFS group. X's: Metasedimentary rocks. Outlines: 85% (inner) and 100% (outer) of AMCG granitoids.

Structure and metamorphism: LMG has been interpreted as a late- to post-tectonic plutonic rock (Foose and McLelland 1995; McLelland et al. 2001). However, it exhibits deformation similar in style, intensity, and trend to that in other northeastern Adirondack rocks. Well-developed foliation, lineation, and complex tight to isoclinal minor folds (Stops 2 and 3) are common throughout although locally obscure in the more leucocratic facies. The foliation, lineation, and major structures are concordant with those in the underlying metasedimentary rocks, mafic and granitic gneisses (Postel 1952, 1956; Whitney and Olmsted 1993). Magnetite ore occurs as tabular bodies parallel to foliation and as cigar-shaped "shoots" parallel to lineation and regional fold axes (Postel 1952). Locally LMG contains numerous pegmatites and quartz veins (Postel 1956). Some of these are undeformed and crosscut structure in the gneiss, indicating minor late- or post-tectonic magmatic activity. Fluids associated with the pegmatites may account for localized remobilization of magnetite and secondary albitization of feldspars.

Evidence of metamorphism in the LMG is scarce because the composition of the dominant metaluminous felsic rocks is unsuitable to the development of diagnostic metamorphic assemblages. Nevertheless, pyralspite garnet and sillimanite occur locally, and metamorphic textures are ubiquitous.

Origin: Whitney and Olmsted (1988) postulated that LMG originated as volcanic ash with interlayered metasedimentary rocks deposited in a hypersaline environment and diagenetically altered to yield the wide range of K/Na ratios. This hypothesis, despite good actualistic credentials, fails to provide a plausible explanation for the magnetite concentrations unless they too are of volcanic origin. Alternatively, LMG may have originated as a volcanic-sedimentary complex including substantial volumes of subvolcanic intrusives. Barton and Johnson (1996) have proposed that circulation of fluids, driven by heat from the intusives and enriched in alkali and alkaline earth halides and sulfates mobilized from subjacent evaporites, may account for both alkali metasomatism and deposition of the magnetite ores in geologically similar regions worldwide. This is an attractive explanation for the LMG in view of the evidence for the former presence of evaporites in the underlying metasedimentary rocks. It is likely that metasomatism and ore deposition were largely confined to the more permeable volcanics; most coarse-grained, igneous-looking LMG lacks extreme K/Na ratios.

Age: Zircons in these rocks commonly consist of relatively small cores with robust overgrowths. U/Pb dating using the ion microprobe (McLelland et al. 2001) shows two distinct clusters of ages corresponding to the cores and mantles. The cores yield ages of 1152±11 and 1141±16 Ma for the microcline and plagioclase facies respectively; mantle ages for both facies are 1055±7 Ma. McLelland et al. (2001) conclude that the younger dates represent the age of igneous emplacement, with the older cores attributed to inherited zircons from assimilated AMCG-suite rocks. Other interpretations are possible under the assumption that LMG represents, at least in part, volcanics and

shallow intrusives associated with the ca. 1150 Ma AMCG suite. In that case, the older zircon cores yield the igneous age, with the mantles being metamorphic or metasomatic overgrowths. The later (1055 Ma) age of emplacement has the advantage of providing, at least in the northeastern Highlands, a magmatic heat source for the subsequent Ottawan metamorphism. It requires, however, that Ottawan deformation and metamorphism occurred after 1055 Ma.

Metanorthosite and related mafic rocks (Stops 4, 5, and 6). Metamorphosed anorthositic rocks underlie large areas in the central and northern Adirondacks. These rocks, together with subordinate mafic rocks ranging from monzodiorite to ferrogabbro, comprise the mafic part of the bimodal Anorthosite-Mangerite-Charnockite-Granite (AMCG) intrusive suite (McLelland and Whitney, 1990) in the Adirondack Highlands. In the northeastern Highlands, metanorthosite forms large domical bodies as well as smaller, stratiform intrusions within supracrustal rocks. While Adirondack metanorthosites have in common the presence of intermediate plagioclase (An_{42-60}) as the dominant (70-98%) mineral, they are quite diverse and detailed description presents formidable complexities. Early Adirondack workers distinguished two facies, the "Marcy" facies, which is megacryst-rich, leucocratic, and undeformed to slightly deformed, and the "Whiteface" facies, megacryst-poor, mafic, and more deformed relative to the "Marcy". This classification is difficult to use consistently, because the three variables (abundance of megacrysts, abundance of mafic minerals, and extent of deformation) are at least partially independent. In a single outcrop each of these factors may vary over a wide range; moreover numerous distinct blocks and/or layers may be present.

a. Abundance of plagioclase megacrysts. Gray sodic labradorite to calcic andesine megacrysts are a prominent feature of most Adirondack anorthosites. Size of the megacrysts ranges from one or two cm to giant, 1/2 m "breadloaf" crystals and fragments. Faint to strong parallelism of the megacrysts is locally present, suggesting either cumulus texture or flow foliation. The proportion of megacrysts in the rock ranges from nearly 100% to nil. Where megacrysts are abundant and closely spaced in the rock, varying amounts of fine-grained, clear, recrystallized plagioclase may border the megacrysts and occupy small fractures within them. This is referred to in the older literature as "protoclastic" texture (Miller, 1916; Balk, 1931; Buddington, 1939). Where megacrysts are more widely spaced, interstitial volumes are commonly occupied by a medium-to coarse grained (up to several mm) groundmass of light gray, white or buff plagioclase together with pyroxenes and oxides. This groundmass locally displays igneous textures and may have crystallized from a gabbroic anorthosite magma or crystal mush in which the megacrysts have been entrained.

b. Abundance and type of mafic minerals. Hypersthene, augite, titaniferous magnetite, and ilmenite or hemo-ilmenite are the chief primary mafic minerals in the anorthositic rocks. Metamorphic garnet is common, and forms reaction rims around both hypersthene and oxide minerals, except in strongly deformed anorthosite where it tends to occur as porphyroblasts. Garnet is absent from anorthosites where the MgO/(MgO + FeOt) ratio exceeds roughly 0.4. Metamorphic hornblende and biotite are locally present. The color index varies from one or two percent up to as much as 30% in some anorthositic gabbros.

c. Extent of deformation. Adirondack metanorthosites range from nearly undeformed, igneous-textured varieties to anorthositic gneisses with intense foliation and well-developed lineation. As the degree of deformation increases, megacrysts change from blocky to lenticular in shape, and generally decrease in size and abundance. Rocks near the margins of metanorthosite domes and massifs ordinarily are more deformed than those in the interiors, where deformation is commonly confined to relatively narrow shear zones.

Anorthositic xenoliths in anorthosite are common. This "block structure" suggests multiple intrusions. The blocks may be rounded or angular, and more or less mafic and finer-or coarser-grained relative to the host. Individual xenoliths or megacrysts may be surrounded by a zone enriched in mafic minerals. Xenoliths of metasedimentary rocks, ranging from centimeters to several meters in size, are found in all facies of the anorthosite. Most of these are pyroxene-rich calcsilicate rocks, but rare quartzite and metapelite xenoliths also occur.

Associated mafic rocks: Fractionation of plagioclase during crystallization of anorthositic magmas yields mafic residual liquids enriched in Fe, Ti, and P (Owens et al. 1993, McLelland et al. 1994, Mitchell et al. 1996). These "FTP rocks" have been given a variety of names; Owens et al. (1993) have suggested that the general term jotunite be used these rocks except where extreme concentration of Fe, Ti, and P leads to oxide-apatite gabbronorites (OAGN's). Jotunites in the Adirondack Highlands fall roughly into two groups. One occurs primarily in dikes and sheets external to large anorthosite bodies; it is commonly monzodioritic in composition and gneissic in texture. The other type forms dikes within anorthosite, usually near contacts with surrounding rocks. The latter is ferrodioritic to ferrogabbroic in composition and igneous-textured or granoblastic with little or no foliation; it is known as "Woolen Mill Gabbro" (WMG) after the best-known locality (Stop 6). There is some overlap in composition between the two

types (Fig. 8), which may result from fractionation of a single residual liquid (Mitchell et al. 1996) or possibly from liquid immiscibility. Some WMG approaches OAGN in composition.

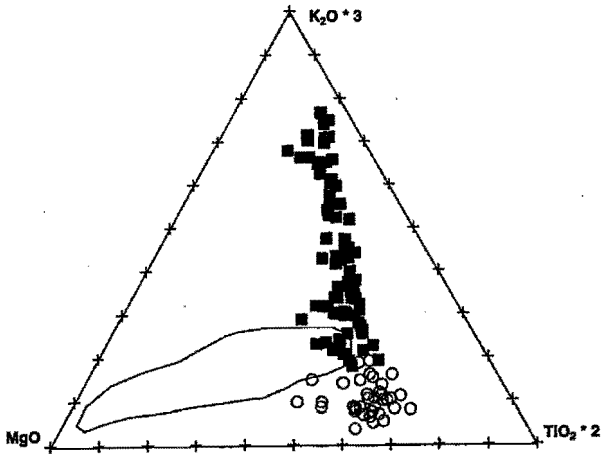

Figure 8. Diagram illustrating the compositional differences between "Woolen Mill Gabbro" (circles), other Highlands jotunites (squares), and olivine metagabbros (outline).

REFERENCES

Ashwal, L. D., 1993, Anorthosites: Springer Verlag, New York, 422 p.

Ashwal, L.D., and J.L. Wooden. 1983. Sr and Nd isotope geochronology, geologic history and origin of the Adirondack anorthosite. Geochimica et Cosmochimica Acta, 47:1975-1986.

Balk, R., 1931, Structural geology of the Adirondack anorthosite: Min. Pet. Mitt., v.41, p. 308-434.

Barton, M.D., and Johnson, D.A., 1996, Evaporitic-source model for igneous-related Fe oxide-(REE-Cu-Au-U) mineralization: Geology, v. 24, p. 259-262.

Bohlen, S. R., Valley, J. W., and Essene, E. J., 1985, Metamorphism in the Adirondacks: I. Petrology, Pressure and Temperature: Journal of Petrology, v. 26, p. 971-992.

Broughton, J. G., and Burnham, K. D., 1944, Occurrence and uses of wollastonite from Willsboro, New York: American Institute Of Mining and Metallurgical Engineers, Technical Publication 1737, 8 p.

Brown, J.S., and Engel, A.E.J., 1956, Revision of Grenville stratigraphy and structure in the Balmat-Edwards district, northwest Adirondacks, New York: Geol. Soc. Amer. Bull., v. 67, p. 1599-1622.

Buddington, A. F., 1939, Adirondack igneous rocks and their metamorphism: Geological Society of America Memoir, no. 15, p. 1-354.

Buddington, A. F., 1950, Composition and genesis of pyroxene and garnet related to Adirondack anorthosite and anorthosite-marble contact zones: American Mineralogist, v. 35, p. 659-670.

Buddington, A.F., and Leonard, B.F., 1962, Regional Geology of the St. Lawrence County magnetite district, Northwest Adirondacks, New York: USGS Professional Paper 376, 145 p.

Buddington, A.F. and Whitcomb, L., 1941, Geology of the Willsboro quadrangle: New York State Museum Bulletin, no. 325, p. 1-137.

Chiarenzelli, J. R., and McLelland, J. M., 1991, Age and regional relationships of granitoid rocks of the Adirondack Highlands: Journal of Geology, v. 99, p. 571-590.

Davidson, A. 1995. A review of the Grenville Orogen in its North American type area. AGSO Journal of Australian Geology and Geophysics, 16:3-24

DeRudder, R. D., 1962, Mineralogy, petrology, and genesis of the Willsboro wollastonite deposit, Willsboro quadrangle, New York: PhD dissertation, Indiana University.

Emmons, E., 1842, Geology of New York. Part II, comprising a survey of the Second Geological district. New York State Geological Survey, Albany. 437 p.

Emslie, R.F., and Hunt, P.A., 1990, Ages and petrogenetic significance of igneous mangerite-charnockite suites associated with massif anorthosites, Grenville Province: Journal of Geology, v. 98, p. 213-231.

Fakundiny, R. H., and Muller, P. D., 1993, Middle Proterozoic emplacement and deformation of metanorthosite and related rocks in the northeastern Marcy Massif, Adirondack Mountains, NY: Geological Society of America Abstracts with Programs, v. 25, p. 14.

Florence, F.P., Darling, R.S., and Orrell, S.E., 1995, Moderate pressure metamorphism and anatexis due to anorthosite intrusion, western Adirondack Highlands, New York. Contributions to Mineralogy and Petrology, v. 121, p. 424-436.

Foose, M.P., and McLelland, J.M., 1995, Proterozoic low-Ti iron oxide deposits in New York and New Jersey: Relation to Fe-oxide (Cu-U-Au-rare earth element) deposits and tectonic implications. Geology, v. 25, p. 665-668.

Friedman, G.M., 1980, Dolomite is an evaporite mineral: evidence from the rock record and sea-marginal ponds of the Red Sea. In Zenger, D.H., Dunham, J.B., and Etherington, R.L., eds., Concepts and models of dolomitization: SEPM Special Publication 28, p. 69-80.

Frost, C.D., and B.R. Frost. 1997. Reduced rapakivi-type granites: The tholeiite connection. Geology, 25: 647-650.

Haapala, I., and O.T. Ramo. 1999. Rapakivi granites and related rocks: an introduction. Precambrian Research, 95:1-7.

Haas, J. R., Shock, E. L., and Sassani, D. C., 1995, Rare earth elements in hydrothermal systems: Estimates of standard partial molal thermodynamic properties of aqueous complexes of the rare earth elements at high temperatures and pressures: Geochimica et Cosmochimica Acta, v. 59, p. 4329-4350.

Kemp, J.F., and Alling, H.L., 1925, Geology of the Ausable Quadrangle: NY State Museum Bull. 261, 126 p.

Kerrich, R., and Rehrig, W., 1987, Fluid motion associated with Tertiary mylonitization and detachment faulting: $^{18}O/^{16}O$ evidence from the Pichaco metamorphic core complex, Arizona: Geology, v. 15, p. 58-62.

Leake, B.E., Farrow, C.M., and Townend, R., 1979, A pre-2000 myr-old granulite facies metamorphic evaporite from Caraiba, Brazil?: Nature v. 277, p. 49-51.

Lister, G. S., and Baldwin, S. L., 1993, Plutonism and the origin of metamorphic core complexes: Geology, v. 21, p. 607-610.

McLelland, J. M., Ashwal, L.D., and Moore, L., 1994, Composition and petrogenesis of oxide-rich, apatite-rich gabbronrites associated with Proterozoic anorthosite massifs - examples from the Adirondack Mountains, New York; Contrib. Mineral. Petrol., v.116, p. 225-238.

McLelland, J. M., and J. Chiarenzelli, 1990, Geochronological studies in the Adirondack Mountains and the implications of a middle Proterozoic tonalitic suite: *in* Gower, C., Ryan, B., and Rivers, T., eds., Proterozoic geology of the southwestern margin of Laurentia and Baltica, Geological Association of Canada Special Paper 38, p. 175-179.

McLelland, J.M.; Chiarenzelli, J.; Whitney, P.R., and Isachsen, Y.W., 1988, U-Pb zircon geochronology of the Adirondack Mountains and implications for their geologic evolution: Geology, v. 16, p. 920-924.

McLelland, J., Daly, J.S., and McLelland, J.M., 1996, The Grenville orogenic cycle (ca. 1350-1000 Ma): an Adirondack perspective: Tectonophysics, v. 256, p. 1-28.

McLelland, J.M., Hamilton, M., Selleck, B., McLelland, J., Walker, D., and Orrell, S., 2001, Zircon U-Pb geochronology of the Ottawan Orogeny, Adirondack Highlands, New York: regional and tectonic implications: Precambrian Research, v. 109, p. 39-72.

McLelland, J. M., and Isachsen, Y. W., 1985, Geological evolution of the Adirondack Mountains: a review: *in* Tobi, A. C., and Touet, J. L. R., eds., The deep Proterozoic crust of the North Altlantic provinces: Reidel, Dordrecht, p. 175-215.

McLelland, J. M., A. Lochhead, and C. Vyhnal. 1988. Evidence for multiple metamorphic events in the Adirondack Mountains, New York. Journal of Geology, 96:279-298.

McLelland, J. M., and Whitney, P. R., 1990, Anorogenic, bimodal emplacement of anorthositic, charnockitic and related rocks in the Adirondack Mountains, New York: p. 301-316 *in* Stein, H.J. and Hannah, J.L., eds., Ore-bearing granite systems: petrogenesis and mineralizing processes: Geol. Soc. Amer. Special Paper 246.

Mezger, K., Rawnsley, C.M., Bohlen, S.R., and Hanson, G.N., 1991, U-Pb garnet, sphene, monazite, and rutile ages: Implications for the duration of high-grade metamorphism and cooling histories, Adirondack Mountains, New York. Journal of Geology, v. 99, p. 415-428.

Mezger, K., Essene, E.J., van der Pluijm, B.A., and Halliday, A.N., 1993, U-Pb geochronology of the Grenville Orogeny of Ontario and New York: Constraints on ancient crustal tectonics. Contributions to Mineralogy and Petrology, v. 114, p. 13-26.

Miller, W. J., 1916, Origin of foliation in the Precambrian rocks of northern New York: Journal of Geology, v. 24, p. 587-619.

Mitchell, J.N., Scoates, J.S., Frost, C.D., and Kolker, A., 1996, The geochemical evolution of anorthosite residual magmas in the Laramie Anorthosite Complex, Wyoming: Journal of Petrology, v. 37, p. 637-660.

Ortega-Gutierrez. F., 1984, Evidence of Precambrian evaporites in the Oaxacan granulite complex of southern Mexico: Precambrian Research, v. 23, p. 377-393.

Owens, B.E., M.W. Rockow, and R.F. Dymek. 1993. Jotunites from the Grenville Province, Quebec: Petrological characteristics and implications for massif anorthosite petrogenesis. Lithos, 30:57-80.

Postel, A.W., 1952, Geology of the Clinton County magnetite district, New York. U.S. Geol. Surv. Prof. Paper 237, 88 p.

Postel, A.W., 1956, Silexite and pegmatite in the Lyon Mountain Quadrangle, Clinton County, New York. New York State Museum Circular 44, 23 p.

Putman, G. W., 1958, The geology of some wollastonite deposits in the eastern Adirondacks, New York: MS thesis, Pennsylvania State University.

Reynolds, S. J., and Lister, G. S., 1987, Structural aspects of fluid-rock interactions in detachment zones: Geology, v. 15, p. 362-366.

Silver, L.T. 1969. A geochronologic investigation of the Adirondack Complex, Adirondack Mountains, New York, p. 233-252. *In* Isachsen, Y.W., ed., Origin of anorthosite and related rocks. New York State Museum Memoir 18.

Spear, F.S., and Markussen, J.C., 1997, Mineral zoning, P-T-X-M phase relations, and metamorphic evolution of some Adirondack granulites, New York. Journal of Petrology, v. 38, p. 757-783.

Stel, H., S. Cloetingh, M. Heeremans, and P. van der Beek. 1993. Anorogenic granites, magmatic underplating, and the origin of intracratonic basins in a non-extensional setting. Tectonophysics, 95:285-299

Valley, J. W., 1985, Polymetamorphism in the Adirondacks: wollastonite at contacts of shallowly intruded anorthosite: *In:* Tobi, A. C., and Touret, J. L. R., (eds.), The deep Proterozoic crust of the North Atlantic Provinces, Riedel, Dordrecht, p. 217-235.

Valley, J. W., and O'Neil, J. R., 1982, Oxygen isotope evidence for shallow emplacement of Adirondack anorthosite: Nature, v. 300, p. 497-500.

Vanuxem, L., 1821, Description and analysis of the table spar from the vicinity of Willsborough, Lake Champlain: Jour. Acad. Nat. Sci. Phil., v. 2, pt. 1, p. 182-185.

Whitney, P.R., 1983, A three-stage model for the tectonic history of the Adirondack region, New York. Northeastern Geology, v. 5, p. 61-72.

Whitney, P.R., 1992, Charnockites and granites of the western Adirondacks, New York, USA: a differentiated A-type suite. Precambrian Research, v. 57, p. 1-19.

Whitney, P.R., and Olmsted, J.F., 1988, Geochemistry and origin of albite gneisses, northeastern Adirondack Mountains, New York: Contrib. Mineral. Petrol., v. 99, p. 476-484.

Whitney,P.R., and Olmsted,J.F., 1993, Bedrock Geology of the Au Sable Forks Quadrangle, northeastern Adirondack Mountains, New York: New York State Museum Map & Chart Series 43, 48 p., with map.

Whitney, P.R., and Olmsted, J.F., 1998, Rare earth element metasomatism in hydrothermal systems: The Willsboro-Lewis wollastonite ores, New York, USA: Geochimica et Cosmochimica Acta, v. 62, p. 2965-2978.

Whitney, P.R., Fakundiny, R.H., and Isachsen, Y.W., 2002 (in press), Bedrock Geology of the Fulton Chain Lakes Area, West-central Adirondack Mountains. New York State Museum Map and Chart Series 44.

ROAD LOG

Begin road log at Exit 32 of Interstate 87

Total Miles	Increment Miles	Route Description
0.0	0.0	**Exit 32, I-87.** If you are coming from the south turn **L.** at Essex Co. 12 and proceed to the southbound exit intersection to zero your odometer. If you have come from the north zero your odometer at the intersection of the exit 32 road and turn **R** on Essex Co. 12
0.45	0.45	Traveling west, "Betty Beaver's" Truck Stop on L.
1.55	1.1	Turn **R.** onto NY Route 9; Proceed north.
2.6	1.05	Turn **L.** onto Pulsifer Road.
2.85	0.25	Sharp **R.** bend; continue on Pulsifer Road.
3.15	0.3	Turn **L.** at blue gates onto Oak Hill Mine Road. This is NYCO property; if following this trip on your own, be sure to get permission at the NYCO office in Willsboro.
4.1	0.95	**Stop 1. OAK HILL WOLLASTONITE MINE.** At the first small quarry on L, park on the R well off the road. From here we will walk through the entire mine complex observing and describing the rock units. As you can see the mine is under development so there may be dangerous situations for which care must be exercised. Please use caution and follow instructions with care.

The Oak Hill Mine was discovered by accident during a logging operation, when a skidder exposed white rock which the logger recognized as wollastonite. It is located at a sharp bend in the OBZ, where the structural trend changes from NNE with a gentle W dip to nearly EW with a gentle to moderate S dip. As of June 2002, mine is being actively developed. Two test pits have been blasted in ore, and work has begun removing overlying rock and glacial deposits in order to begin open-pit mining. Additional exposures may be available at the time of the trip, but others may have been removed or covered. Figure 9, constructed from drill core data, shows the complex nature of the ore body.

The lowermost exposures are knobs of skarn consisting largely of orange-red grossularitic garnet, locally with abundant green, diopsidic clinopyroxene and/or veins and patches of sodic plagioclase and quartz. The garnetite encloses blocks of gabbroic anorthosite gneiss, metagabbro, and pyroxene granulite. Some of these blocks have narrow alteration haloes but otherwise are in sharp contact with the garnetite. They appear to be fragments of disrupted layers in what was probably a marble-hosted tectonic breccia, since metasomatically transformed to garnetite (other interpretations welcome!). Garnetite is much more abundant here than at either Lewis or Willsboro. Drill core data indicate that the the proportion of garnetite to ore increases toward the NE, eventually forming a layer of nearly 200', without ore.

Proceeding upsection, several layers of ore are exposed, separated by septa of mafic gneiss and/or garnetite. Garnetite layers are discontinuous; some appear to be megaboudins.

The hanging wall of the exposed ore consists of strongly foliated and lineated gabbroic anorthosite gneiss. This is overlain in turn by a chaotic marble

melange with detached blocks of intricately folded calcsilicates. The marble also contains masses of crumbly-weathered skarn consisting largely of black (dark orange-brown in transmitted light) garnet and dark green clinopyroxene. This skarn resembles those associated with magnetite deposits elsewhere in the Adirondack Highlands rather than the garnet-pyroxene layers in the ore. The fact that this marble has apparently escaped extensive metasomatism suggests that the metasomatizing fluids that foemed the ore were strongly channelized.

Overlying the marble is mafic gneiss with interlayers af charnockite and coarse, leucocratic augen gneiss, the latter an extreme L-tectonite. Above the gneiss complex, coronitic olivine metagabbro is exposed. The section in the mine is cut by several E-W, nearly vertical faults, one of which exhibits slickensides plunging steeply E. On the N side of the mine road, at the time of writing, bedrock is concealed beneath a thick section of varved glacial lake sediments interlayered with boulder till.

5.05	0.95	Exit NYCO property at the blue gates.
5.6	0.55	Turn L on NY Route 9, going north.
8.3	2.7	Intersection with Deerhead-Reber road; continue on Rt.9.

Section of Oak Hill Mine Development

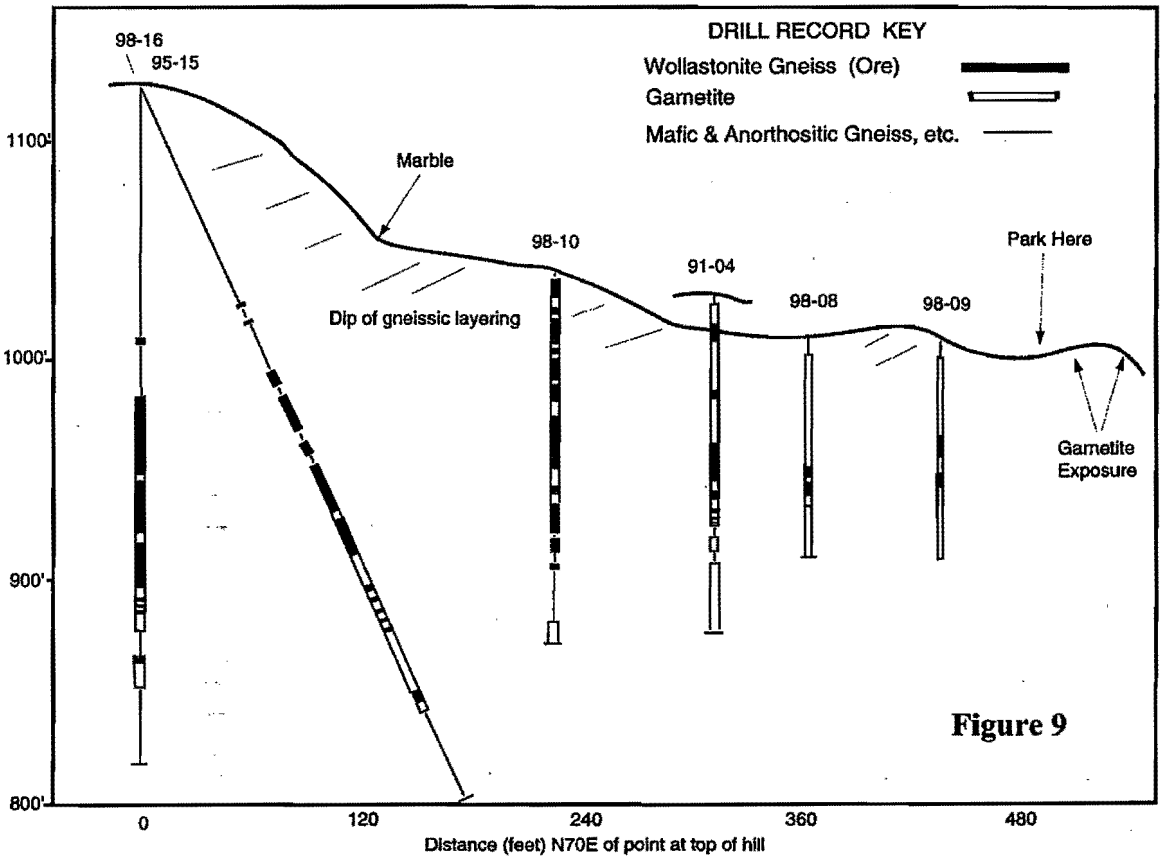

Figure 9

10.0	1.7	Crossing north branch of the Boquet River.
13.8	3.8	Spectacular fault breccia on L. This is one of the numerous NNE- to NE-trending faults that occur throughout much of the eastern and central Adirondack Highlands. Movement on these faults, possibly associated with the opening of the Iapetus Ocean, began in the latest Proterozoic and continued at least into the Ordovician.
14.3	0.5	Pokomoonshine State Park. The prominent cliff is mostly granitic gneiss of the AMCG suite, containing several layers of mafic gneiss that are probably transposed dikes.
16.2	1.9	The prominent white spot in the roadcut on the R is a marble xenolith in jotunite and badly contaminated gabbroic anorthositic gneiss. The marble contains abundant graphite, phlogopite and diopside and lesser amounts of chondrodite, grossular, and sulfides. Wollastonite is absent.
17.1	0.9	Turn **L** at caution light at the intersection with NY 22 adjacent to I-87 Exit 33.
17.2	0.1	Turn **R** at I-87 on ramp.
20.7	3.5	I-87 Exit 34. Turn **R** onto ramp.
20.9	0.2	Turn L onto NY Route 9N Toward AuSable Forks.
24.4	3.5	Cold Spring Road. Continue on 9N
25.5	1.1	Enter hamlet of Clintonville. Reportedly, in the late 19th century this was a town of 10,000 miners, wood cutters, iron forge workers and their families.
26.2	0.7	Bear **R** on Clintonville Rd.
27.4	1.2	Bear **R** on Harkness Road.
28.0	0.6	Turn L on Arnold Hill Road.
28.45	0.45	Cross Allen Hill and Thomasville roads.
28.9	0.45	**Stop 2A. LYON MOUNTAIN GNEISS; Albite gneiss facies.** Park off the road on **R**. The recently blasted low cuts on the L are largely albite gneiss with about 30% quartz, 65% plagioclase (ca. $An_2Ab_{96}Or_2$) with minor magnetite and/or hematite, and traces of biotite, clinopyroxene, titanite, apatite, and zircon. The fine-grained, equigranular texture is typical of this facies of the LMG. Note the small, nearly isoclinal Z-folds, N 10-20° E lineation, and numerous crosscutting quartz-albite pegmatites and quartz veins. The pegmatites locally contain masses of partially martitized magnetite, possibly remobilized from nearby orebodies.
29.2	0.3	**Stop 2B FOLDING IN LYON MOUNTAIN GNEISS.** These flat outcrops at the intersection of Arnold Hill Road and a logging road on the L show complex folding in albite gneiss similar to that at the last stop. Abrupt color changes in the rock crosscut the folding and appear to be contacts of more and less oxidized rock, suggesting a post-deformation oxidation event. This area is not far from the site of the Arnold and Nelson Bush Mines, opened in 1830 and

operated sporadically until 1906 (Kemp and Alling 1925; Postel 1952). The ore at Arnold Hill occurs as three foliation-parallel layers from 3-25' thick in albite gneiss. The layers were known to the miners as the gray, black, and blue "veins". The gray and black veins consist of magnetite, quartz, plagioclase, chlorite, and hornblende; in the blue vein the ore mineral is martite (Postel 1952).
Turn around here and head back down the hill.

29.95	0.75	Turn **R** on Thomasville Road.
30.15	0.2	Small exposure of LMG on R side of road.
32.05	1.9	Bear **L** at fork; then cross over the Little AuSable River.
33.15	1.1	Bear **R** on Harkness Road
33.35	0.2	Continue straight on Palmer Hill road.
34.2	0.85	Coughlin road on R.
35.05	0.85	Turn **R** on Tower Road.
35.95	0.9	Road turns L at intersection with three unpaved roads. Park off road on R. Walk around the iron gate and proceed S along the unpaved road furthest to the R.

Stop 3. PALMER HILL. Follow the road approximately 0.3 miles to the top of Palmer Hill. Along the way are several small pavement outcrops exposing heterogeneous LMG showing complex folding and containing numerous small clots of magnetite ore. Were these formed in place, or are they disrupted fragments of a vein of ore emplaced before deformation? At the top of the hill are several large boulders of Potsdam Sandstone (middle to late Cambrian). The Potsdam unconformably overlies the Proterozoic rocks around much of the perimeter of the Adirondack Dome, and is exposed at the surface less than 6 miles to the NE. An abandoned firetower here has been converted to a cellphone relay. We will then follow a powerline for about 0.1 mile S to the old mine workings. **USE EXTREME CAUTION**, especially in wet weather. Cross a narrow rock bridge over the open cut and turn L to view the mine workings. **Do not go down into the cut; samples of ore will be available.** The ore here occurs in a discontinuous layer up to 20 feet thick, striking NE and dipping NW, roughly parallel to foliation on the SE limb of a NE-plunging synform (Postel 1952). It consists of magnetite with quartz, feldspar, and, locally, apatite, fluorite, and andraditic garnet. The host rock is predominantly the microperthite facies of LMG, although drill cores show almost the entire range of LMG lithologies (Postel 1952). Fluorite is a common accessory in the gneiss, and andraditic garnet occurs locally. Mining at Palmer Hill began in 1825 and continued until 1890 (Newland, 1908).

Return to vehicles, turn around, and head W on Tower Road.

36.85	0.9	Turn **R** on Palmer Hill Road.
37.45	0.6	Turn **L** on Silver Lake Road.
38.15	0.7	Turn **R** on N. Main Street at bottom of hill.
38.35	0.2	Proceed straight through caution light, now on NY 9N.

38.55	0.2	Bear **R** continuing on NY 9N.
40.45	1.9	"Lake Placid Granite" quarries entrance on R. The "granite" here is actually anorthosite.
40.55	0.1	Stickney Bridge road on L.
44.25	3.7	Turn **L** on Mill Hill Road in Hamlet of Jay.
44.55	0.3	Cross one-lane bridge over the East Branch of the Ausable River, turn **R**, and park in sandy area on the R side.

Stop 4. ANORTHOSITE OF THE JAY DOME. Walk back across the bridge **(Beware of traffic!)** and descend the steep bank on the L to outcrops in the river. The river is usually quite low this time of year affording us good looks at several facies of anorthosite and a variety of structural features. Both leucocratic and gabbroic anorthosite are present, as well as a block of coarser gabbroic anorthosite. In one location, a thin layer of pyroxene- and oxide-rich ultramafic rock separates two anorthosite facies, and is offset by parallel small faults. The latter may have formed at relatively high temperatures; foliation in the anorthosite locally shows the effects of drag along the faults. They are subparallel to later, NE-trending brittle faults, some of which are occupied by unmetamorphosed diabase dikes. One such fault-cum-dike offsets a shallow-dipping mylonite zone in the anorthosite. A xenolith of calcsilicate rock in the anorthosite consists largely of diopsidic clinopyroxene. Numerous potholes are present in the outcrop surface.

Walk back across the bridge and, if time permits, up the road beyond the parking area to a glacially polished and striated outcrop showing rouded blocks of coarse gabbroic anorthosite in finer grained, more leuococratic anorthosite.

Return to vehicles and proceed S.

45.05	0.5	Ward Lumber Co. mill and store.
45.15	0.1	Turn **R** on Valley Road.
47.95	2.8	**R** again on Trumbel's Corners Rd.
48.65	0.7	Turn **L** on NY 9N in Upper Jay. Several exposures, of calcsilicates, mafic gneiss and contaminated anorthosites may be seen along Rt. 9N between Upper Jay and Keene.
54.45	5.8	Turn **L** at intersection of NY 9N and NY 73 at the Elm Tree Inn in Keene.
56.25	1.8	**L** on NY 9N going E toward Elizabethtown.
64.65	8.4	**Stop 5. JOTUNITE WITH XENOLITHS.** Park on R beyond the guard rails; cautiously cross the road and walk back to a small outcrop on the N side. The rock here is a jotunite containing numerous metasedimentary xenoliths and one xenolith of anorthosite. The metasedimentary rocks are diopside-rich calcsilcates, some with fine, millimeter to submillimeter-scale layering consisting of alternating pyroxene- and plagioclase-rich layers. The layering is normally straight but locally shows irregular folding or chaotic disruption. The general

appearance of the rocks is similar to that of stromatolite-bearing metasedimentary rocks in the Balmat area on the northwest Adirondack Lowlands. Is it possible that the layering here is of organic origin? What other processes might be responsible?

Carefully observe the foliation in the jotunite near the anorthosite xenolith. If this is, as it appears, a metamorphic foliation then it suggests that penetrative deformation may affect some rocks and not others. Beware of assuming that a rock that crosscuts foliation in another rock is necessarily younger!

Interestingly, jotunites in the Adirondack Highlands commonly form intrusion breccias, whereas granitoids, olivine metagabbro, and ferrogabbro do not. Why?

65.25 0.6 **Stop 6: "WOOLEN MILL" GABBRO, ANORTHOSITE, SYENITE.** Park on the L (north) side. The best exposures are the stream N of the road near the remains of an old dam. This stop provides another opportunity to study the characteristics and complexity of Adirondack metanorthosite and its associated lithologies. Fine-grained mafic granulites consisting of granoblastic plagioclase, clino- and orthopyroxene, garnet, ilmenite, and magnetite are of ferrogabbroic composition. This rock has been informally called the "Woolen Mill Gabbro". Here it intrudes the anorthosite as a network of thin, discontinuous dikes. At the upstream end of the outcrop, one of these terminates in a small bulb. More extensive exposures of this lithology are found in the roadcut on the S side of 9N just across from the parking area. A slightly coarser version of the same rock is exposed upstream on the opposite bank, in sharp contact with the anorthosite.

Also present are small dikes of coarse syenite, some with rows of pyroxene crystals along their contacts with anorthosite. Both these and the ferrogabbro appear to be intruded along fractures in the anorthosite, sometimes in the *same* fractures! (Which came first? Or are these composite dikes formed from two immiscible liquids?).

66.25 1.0 Intersection of routes NY 9 & 9N. The fastest way south is to turn **R** and go south on Rt.9 to Exit 30 of I-87. If you are going north, turn **L** on route 9N, north then east to exit 31 of I-87.

END OF TRIP

GEOLOGY AND MINING HISTORY OF THE BARTON GARNET MINE, GORE MT. AND THE NL ILMENITE MINE, TAHAWUS, NY WITH A TEMPORAL EXCURSION TO THE MACINTYRE IRON PLANTATION OF 1857

William M. Kelly
New York State Museum
3140 Cultural Education Center
Albany, NY 12230

Robert S. Darling
Department of Geology
SUNY, College at Cortland
Cortland, NY 13045

INTRODUCTION

This field trip examines the geology and history of mining at two types of ore deposits, one a metal and one an industrial mineral. Both are strongly identified with the Adirondack Mountains of New York and both have histories that extend for more than a century. While mining activities began at both in the nineteenth century, only the Barton garnet mining venture has remained in continuous operation. Attempts, successful and unsuccessful, to exploit the ore at Tahawus occurred sporadically through the nineteenth and twentieth century. During this time the minerals that were the target and gangue at Tahawus essentially reversed roles.

BARTON GARNET MINE, GORE MT.

The Barton Mines Corporation open pit mine is located at an elevation of about 800 m (2600 ft) on the north side of Gore Mountain. For 105 years, this was the site of the world's oldest continuously operating garnet mine and the country's second oldest continuously operating mine under one management. The community at the mine site is the highest self-sufficient community in New York State. It is 16 km (10 mi) from North Creek and 8 km (5 mi) from NY State Route 28 over a Company-built road that rises 91 m (300 ft) per mile. This road, like others in the vicinity, is surfaced with coarse mine tailings. About eleven families can live on the property. The community has its own water, power, and fire protection systems. On the property are the original mine buildings and Highwinds, built by Mr. C.R. Barton in 1933 as a family residence.

The garnet is used in coated abrasives, glass grinding, metal and glass polishing, and even to remove the red hulls from peanuts. Paint manufacturers add garnet to create non-skid surfaces and television makers use it to prepare the glass on the interior of color picture tubes prior to the application of the phosphors. Barton sells between 10,000 and 12,000 tons of technical-grade garnet abrasive annually. About 40% of the company's shipments are to foreign countries. All current U.S. production of technical-grade garnet is limited to the Barton Mines Corporation. The product is shipped world wide for use in coated abrasives and powder applications (Austin, 1993a,b).

Garnet has been designated as the official New York State gemstone. Barton produces no gem material but collectors are still able to find rough material of gem quality. Stones cut from Gore Mountain rough material generally fall into a one to five carat range. A small number of stones displaying asterism have been found. Garnets from this locality are a dark red color with a slight brownish tint. Special cutting schemes have been devised for this material in order to allow sufficient light into the stone.

HISTORY

The early history of the Barton garnet mine has been compiled by Moran (1956) and is paraphrased below. Mr. Henry Hudson Barton came to Boston from England in 1846 and worked as an apprentice to a Boston jeweler. While working there in the 1850's, Barton learned of a large supply of garnet located in the Adirondack Mountains. Subsequently, he moved to Philadelphia and married the daughter of a sandpaper manufacturer. Combining his knowledge of gem minerals and abrasives, he concluded that garnet would produce better quality sandpaper than that currently available. He was able to locate the source of the Adirondack garnet stones displayed at the Boston jewelry store years before. Barton procured samples of this garnet, which he pulverized and graded. He then produced his first

garnet-coated abrasive by hand. The sandpaper was tested in several woodworking shops near Philadelphia. It proved to be a superior product and Barton soon sold all he could produce.

H.H. Barton began mining at Gore Mountain in 1878 and in 1887, bought the entire mountain from the State of New York. Early mining operations were entirely manual. The garnet was hand cobbed *i.e.* separated from the waste rock by small picking hammers and chisels. Due to the obstacles in moving the ore, the garnet was mined during the summer and stored on the mountain until winter. It was then taken by sleds down to the railroad siding at North Creek whence it was shipped to the Barton Sandpaper plant in Philadelphia for processing. The "modern" plant at Gore Mountain was constructed in 1924. Crushing, milling, and coarse grading was done at the mine site. In 1983, the Gore Mountain operation was closed down and mining was relocated to the Ruby Mountain site, approximately 6 km (4 mi) northeast, were it continues at present.

MINING AND MILLING

The mine at Gore Mountain is approximately one mile in length in an ENE-WSW direction. The ore body varies from 15 m (50 ft) to 122 m (400 ft) and is roughly vertical. Mining was conducted in benches of 9 m (30 ft) using standard drilling and blasting techniques. Oversized material was reduced with a two and one-half ton drop ball. The ore was processed through jaw and gyratory crushers to liberate the garnet and then concentrated in the mill on Gore Mountain. Garnet concentrate was further processed in a separate mill in North River at the base of the mountain. Separation of garnet was and is accomplished by a combination of concentrating methods including heavy media, magnetic, flotation, screening, tabling and air and water separation. Processes are interconnected and continuous or semi-continuous until a concentrate of 98% minimum garnet for all grades is achieved (Hight, 1983). Finished product ranges from 0.6 cm to 0.25 micron in size.

CHARACTERISTICS OF GORE MOUNTAIN GARNET

The garnet mined at Gore Mountain is a very high-quality abrasive. The garnets display a well-developed tectonic parting that, in hand specimen, looks like a very good cleavage. This parting is present at the micron scale. Consequently, the garnets fracture with chisel-like edges yielding superior cutting qualities. The garnet crystals are commonly 30 cm in diameter and rarely up to 1 m with an average diameter of 9 cm (Hight, 1983) The composition of the garnet is roughly 43% pyrope, 40% almandine, 14% grossular, 2% andradite, and 1% spessartine (Levin, 1950; Harben and Bates, 1990). Chemical zoning, where present, is very weak and variable (Luther, 1976). The garnet has been so well analyzed isotopically that it is frequently used as an ^{18}O / ^{16}O standard (Valley et al., 1995). Typical chemical analyses of the garnet are presented in Table 1. Hardness of the garnet is between eight and nine and the average density is 3.95 gm/cm^3.

Table 1. Electron Microprobe analyses of Gore Mt. garnet (almandine-pyrope) normalized to 8 cations and 12 anions. * Calculated by charge balance (Kelly and Petersen, 1993).

Oxide Weight Percent	#29	#41
SiO_2	39.43	39.58
Al_2O_3	21.40	21.20
TiO_2	0.05	0.10
FeO*	22.80	24.45
Fe_2O_3*	1.44	0.72
MgO	10.65	9.60
MnO	0.48	0.74
CaO	3.85	3.97
Na_2O	0.00	0.00
K_2O	0.00	0.00
Total	100.09	100.36

GEOLOGY

The garnet mine is entirely hosted by a hornblende-rich garnet amphibolite unit along the southern margin of an olivine meta-gabbro body (Fig. 1). The garnet amphibolite grades into garnet-bearing gabbroic meta-anorthosite to the east. To the south the garnet amphibolite is in contact with a meta-syenite; a fault occurs parallel to this contact in places.

Figure 1. Geologic maps of Barton garnet mine
(A. modified from Bartholome, 1956, B. Goldblun & Hill, 1992)

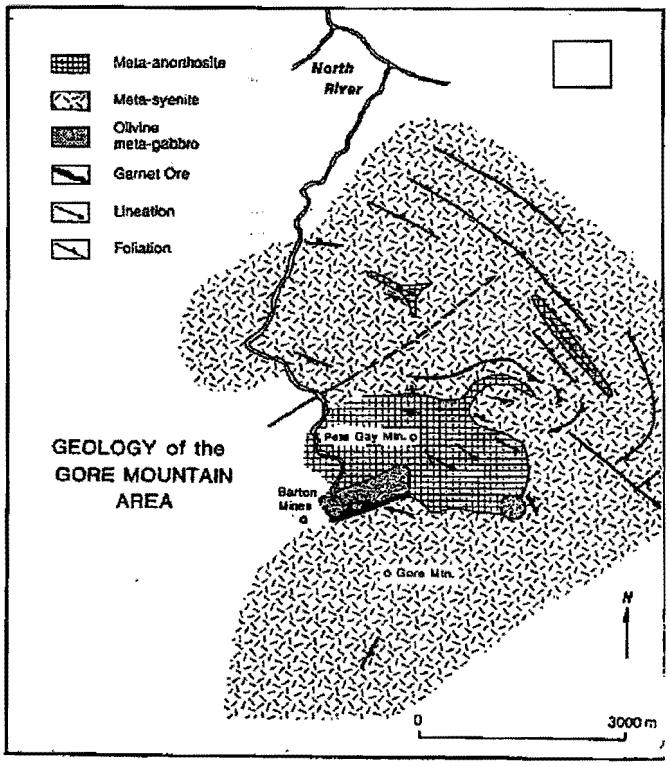

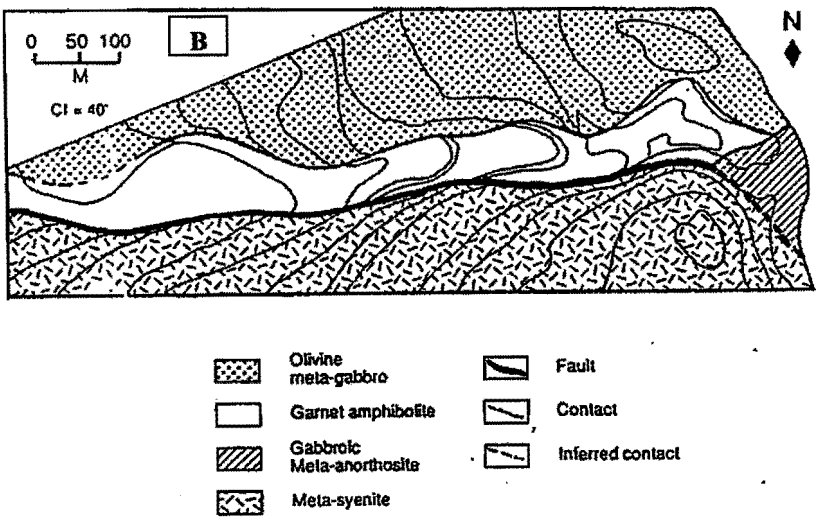

The olivine meta-gabbro bordering the ore zone is a granulite facies lithology with a relict subophitic texture. Preserved igneous features, faint igneous layering, and a xenolith of anorthosite have been reported in the meta-gabbro (Luther, 1976). Prior to metamorphism, the rock was composed of plagioclase, olivine, clinopyroxene and ilmenite. During metamorphism, coronas of orthopyroxene, clinopyroxene and garnet formed between the olivine and the plagioclase and coronas of biotite, hornblende and ilmenite formed between plagioclase and ilmenite (Whitney & McLelland, 1973, 1983). The contact between the olivine meta-gabbro and the garnet amphibolite ore zone is gradational through a narrow (1 to 3 m wide) transition zone. Garnet size increases dramatically across the transition zone from less than 1 mm in the olivine meta-gabbro, to 3 mm in the transition zone, to 50 to 350 mm in the amphibolite (Goldblum and Hill, 1992). This increase in garnet size coincides with a ten-fold increase in the size of hornblende and biotite, the disappearance of olivine, a decrease in modal clinopyroxene as it is replaced by hornblende, and a change from green spinel-included plagioclase to white inclusion-free plagioclase (Goldblum and Hill, 1992). Mineralogy in the garnet amphibolite ore zone is mainly hornblende, plagioclase and garnet with minor biotite, orthopyroxene, and various trace minerals. In both the olivine meta-gabbro and the garnet amphibolite, garnet content averages 13 modal percent, with a range of 5 to 20 modal percent (Luther, 1976; Hight, 1983; Goldblum, 1988). The garnet amphibolite unit is thought to be derived by metamorphism of the southern margin of the granulite facies olivine meta-gabbro. At the west end of the mine, a garnet hornblendite with little or no feldspar is locally present. This rock may represent original ultramafic layers in the gabbro (Whitney et al., 1989). In the more mafic portions of the ore body, the large garnet crystals are rimmed by hornblende up to several inches thick. Elsewhere, in less mafic ore, the rims contain plagioclase and orthopyroxene. Chemical analyses of the olivine meta-gabbro and garnet amphibolite show

Travel to end of Barton Mine Road	5	31.8

Note: the intersection of Barton Mine Road and Rt. 28 is marked by a small cluster of buildings. Among these are a Mom 'n' Pop general store with gas pumps and Jasco's mineral shop. On the east side of Rt. 28 facing south there is a sign opposite Barton Mine Road indicating the Barton Mine (Gore Mt.) mineral shop.

STOP 1. BARTON MINES, GORE MT. (1.5-2 hours) Note: there is a charge of $1.00 per pound of material collected, payable at the mineral shop.

Travel back to Rt. 28	5	36.8
Turn right at stop sign, go to Rt 28N at North Creek	6.6	43.4
Turn left on Rt 28N, go straight at 4-way stop	0.1	43.4
Turn right at Blue Ridge Road	21.5	64.9
Note: Sign for NL Ind., MacIntyre Development and sign for High Peaks Wilderness Area		
Turn left at Tahawus Road	1.1	66
Turn left at Upper Works Road	6.5	72.5
Proceed to dirt road to Cheney Pond	0.6	73.1
Boulders on right, gate on left		

STOP 2. KRONOS, INC., CHENEY POND DEPOSIT (1.5-2 hours)

Proceed north on Upper Works Road	2.0	75.1
Furnace stack is on the right, by the edge of the road, wheel house is close to the river.		

STOP 3. ADIRONDACK IRON AND STEEL CO. "NEW" FURNACE (1 hour)

Please take only photographs at this stop. Do not take artifacts as souvenirs.

NEW VIEWS ON FAULTING, FABRIC DEVELOPMENT, AND VOLUME STRAIN IN THE TACONIC SLATE BELT, WESTERN VERMONT AND EASTERN NEW YORK

by
Jean M. Crespi, Jonathan R. Gourley, and Christine M. Witkowski, Department of Geology and Geophysics, University of Connecticut, Storrs, CT 06269

INTRODUCTION

Slate belts provide an important window into tectonic processes, because they preserve bedding despite the penetrative character of the deformational fabric. The reference frame given by bedding, together with information from strain markers, permits quantitative understanding of the deformation since deposition of the strata. Although the complete deformational history can rarely, if ever, be determined, approaches that involve the integration of different types of data are more likely to advance understanding.

The northernmost part of the Taconic Allochthon (Fig. 1) in western Vermont and eastern New York is one of the best studied slate belts in the world. Geological studies (Dale, 1899) accompanied the development of the quarrying industry, which began in the area in the 19th century, and the Taconic orogenic belt was one of the first ancient orogenic belts to be interpreted in the context of plate tectonics (Chapple, 1973). An arc-continent collision interpretation still stands for the origin of the orogenic belt (Chapple, 1973; Rowley and Kidd, 1981; Stanley and Ratcliffe, 1985); however, debate centers on whether the colliding volcanic arc was the Bronson Hill arc or the more inboard and older Shelburne Falls arc (Karabinos et al., 1998, 1999; Ratcliffe et al., 1998, 1999). Geochronologic and biostratigraphic data (Zen, 1967; Laird et al., 1984; Sutter et al., 1985; Ratcliffe et al., 1998) indicate that collisional orogenesis occurred during Middle to Late Ordovician time. The Taconic Allochthon formed as Cambrian?/Cambrian to Middle Ordovician slope and rise strata were thrust west onto approximately coeval strata of the carbonate platform.

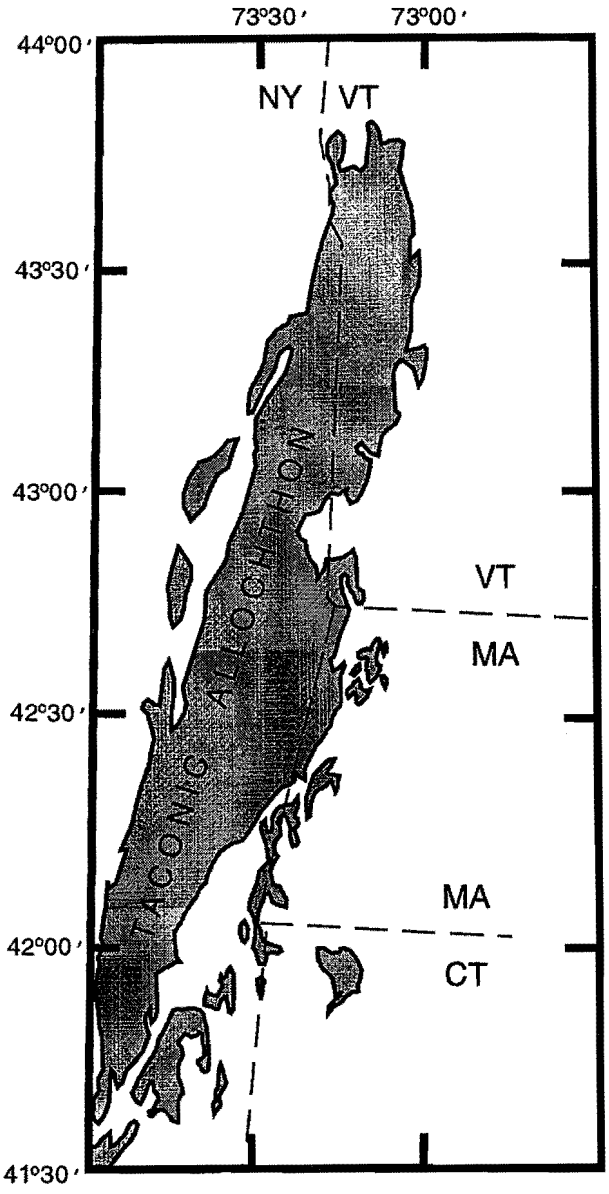

Figure 1. Index map to Taconic Allochthon.

The strata within the slate belt of the northernmost Taconic Allochthon were deformed into a series of west-vergent, tight to isoclinal folds during the main phase (D_2) of deformation. The slaty cleavage (S_2) is parallel or lies at a very low angle to the axial planes of the F_2 folds. Although Zen (1961) proposed that the slate belt is characterized by recumbent and downward-facing folds, implying an earlier D_1 phase of deformation, Bosworth and Rowley (1984) showed that F_1 folds are relatively rare. Locally, S_2 is overprinted by a weakly to moderately developed crenulation cleavage (S_3). Recently obtained $^{40}Ar/^{39}Ar$ ages from closely packed S_3 domains are Devonian and are interpreted as consistent with Acadian rather than Taconian orogenesis (Chan et al., 2001).

This field trip guide builds on a previous NEIGC guide to the area (Goldstein et al., 1997): several outcrops from the 1997 trip are reexamined on this trip in light of

new data from a variety of strain markers. In particular, we compare results from markers that record the total strain with those from markers that record different portions of the total strain. Aspects of the deformation that we focus on include evidence for prelithification tectonic deformation; volume change associated with S_2 development; and variations in S_2 orientation and state of strain with structural level. We also present new observations of meso- and microscale structures within the Bird Mountain slice. Specifically, we focus on the information that these structures provide on the movement history of the Bird Mountain fault with respect to regional deformational events.

STRAIN MARKERS: PREVIOUS AND CURRENT WORK

Strain markers have been analyzed in three stratigraphic units in the Taconic slate belt (Fig. 2). Black slates of the Cambrian Hatch Hill Formation and Ordovician Mount Merino Formation contain strain fringes around pyrite framboids and graptolites. Analyses of strain fringes in the Hatch Hill Formation are presented in Chan (1998); current research focuses on those in the Mount Merino Formation. Because graptolites are not abundant in the Hatch Hill Formation, strain analyses have been conducted only on those in the Mount Merino Formation. Goldstein et al. (1998) used thecal spacing measurements to extract strain values from the graptolites. Two alternative approaches are the subject of current research: reconstruction of the fractured and displaced pyrite blocks forming the graptolites and determination of the surface separating the extension and shortening fields of the instantaneous strain ellipsoid. Finally, maroon slate of the Cambrian Mettawee Formation contains reduction spots. These have been studied by Wood (1974), Hoak (1992), and Goldstein et al. (1995).

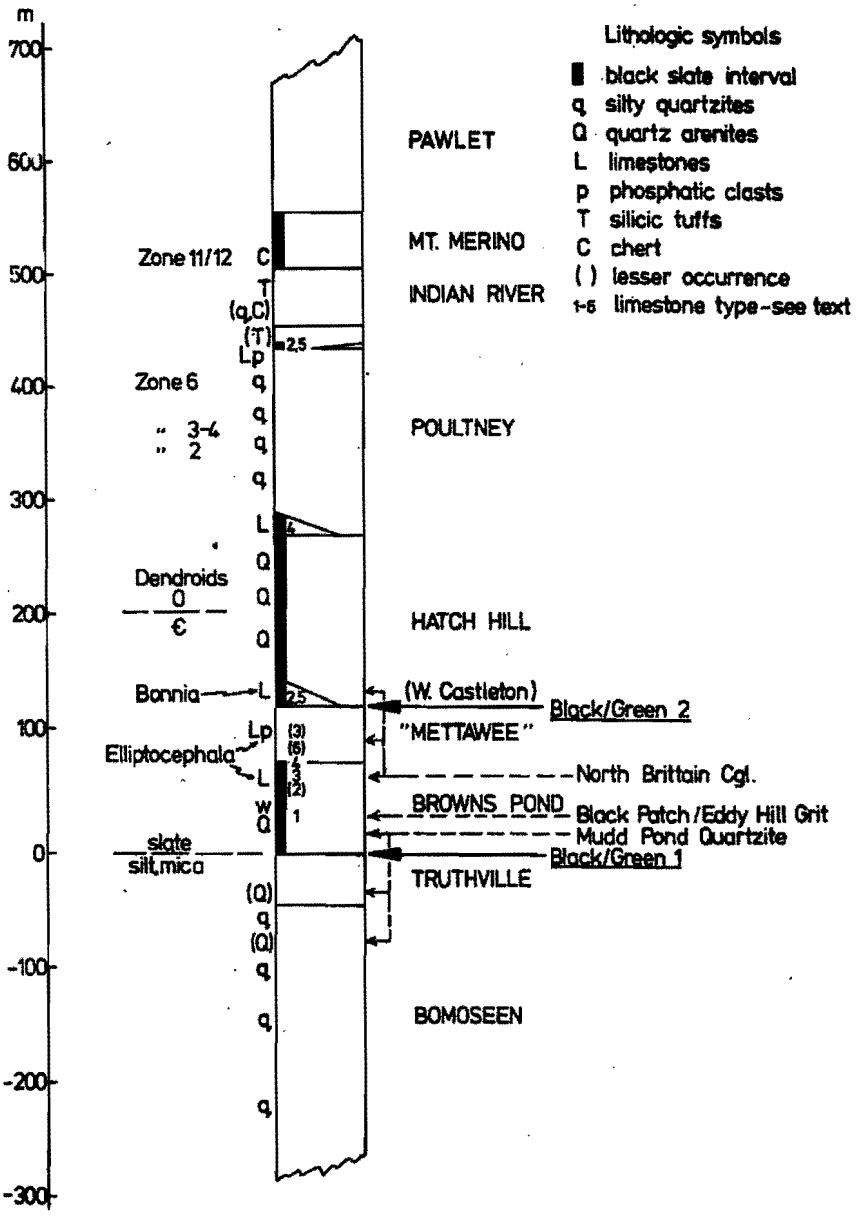

Figure 2. Stratigraphy of Taconic sequence (from Rowley et al. (1979)).

Strain Fringes

Chan (1998) analyzed strain fringes around pyrite framboids in the Hatch Hill Formation along a transect in the vicinity of Route 4 (Fig. 3). The strain fringes are composed of quartz and phyllosilicate fibers, and fiber growth is inferred to be antitaxial on the basis of the marked compositional difference between

the fibers and core object. Along the transect, S_2 dips about 30° to the east, and the mineral lineation (L_2) plunges to the east-southeast. Strain fringes were sampled from four upright and one overturned regional-scale F_2 fold limbs.

In S_2-parallel thin sections (*XY* sections; *X*>=*Y*>=*Z*), the strain fringes indicate plane-strain deformation: the fibers are straight and parallel to L_2, and the strain fringes, which completely bracket the pyrite framboid, do not change width with distance from the framboid. In thin sections cut perpendicular to S_2 and parallel to L_2 (*XZ* sections), the fibers are curved and the sense of curvature is consistent along the transect. Viewed to the north-northeast, individual fibers curve counterclockwise when traced from the portion closest to the framboid to the portion furthest from the framboid, i.e., from youngest to oldest increments of fiber growth. In addition, the youngest increment of fiber growth, which is inferred to lie parallel to the maximum instantaneous stretching axis, is oriented at an angle to S_2. Chan (1998) used these and several other characteristics to infer that fiber growth occurred only during S_2 development and that S_2 development was within a zone of top-to-west-northwest, non-coaxial flow.

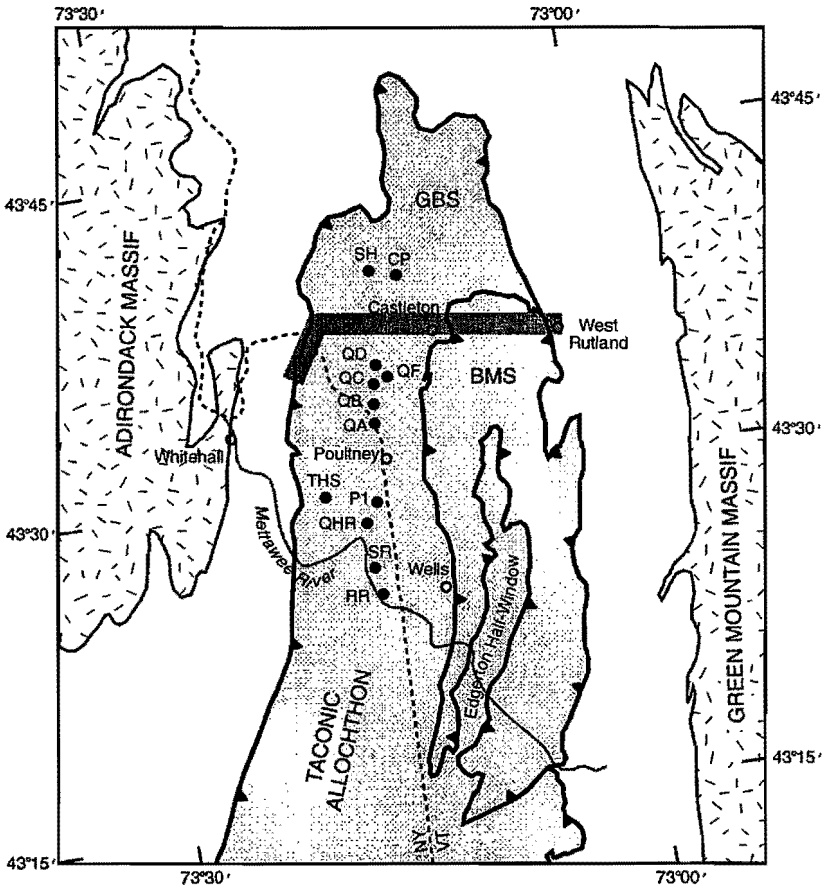

Figure 3. Simplified geological map of northern Taconic Allochthon and surrounding region. GBS--Giddings Brook slice; BMS--Bird Mountain slice; CP, SH, QA, QB, QC, QD, and QF--reduction spot sites from Wood (1974), Hoak (1992), and Goldstein et al. (1995); SR, P1, QHR, RR, and THS--graptolite sites from Goldstein et al. (1998); thick gray line--transect from Chan (1998); unpatterned area--carbonate platform.

Because no strain analysis technique for strain fringes has been designed specifically for fibers that form during non-coaxial flow, Chan (1998) applied the Durney and Ramsay (1973) technique to strain fringes in *XZ* thin sections to make comparisons along the transect of fiber shape and length. Both are relatively uniform. In particular, the mean maximum principal finite stretch ($1 + e_1$) calculated from the fibers using the Durney and Ramsay (1973) technique ranges only between 2.1 and 2.4 for the sites. Chan (1998) used this result as well as the nearly constant orientation of S_2 to infer that the transect lies along the same structural level within a regional-scale shear zone that formed in the pressure-solution regime.

Strain fringes around subspherical core objects in the Mount Merino Formation have been analyzed at three sites around a regional-scale F_2 fold (Fig. 3): on the overturned limb where S_0 and S_2 are essentially parallel (site SR1); on the upright limb where S_0 and S_2 lie at a moderate angle (site SR3); and in the hinge zone where S_0 and S_2 are perpendicular or nearly so (site SR5). Site names are after Goldstein et al. (1998). The sites lie about twenty kilometers south of the transect studied by Chan (1998). S_2 shows little variation in orientation between the three sites and dips about 45°-50° to the east.

difference in degree of fiber curvature between the SR sites and the transect in the vicinity of Route 4 suggests that the degree of non-coaxiality may be less at relatively high structural levels within the shear zone, although this is difficult to quantify. The presence of flattening as opposed to plane strain at the SR sites implies a change in boundary conditions with structural level.

This interpretation of the Taconic slate belt in the context of structural levels is consistent with regional structural and stratigraphic relations. The Taconic Allochthon and underlying autochthonous strata of the carbonate platform are gently folded to form the Middlebury synclinorium. The synclinorium plunges gently to the south (Zen, 1967), as implied by the northern closure of the Taconic Allochthon. This results in the exposure of systematically shallower structural levels from north to south within the Allochthon. In addition, units higher in the Taconic sequence are more common at Earth's surface in the south than they are in the north (see, for example, geological maps of Zen (1961) and Rowley et al. (1979)).

Graptolites

Strain values have been determined for the SR sites using three techniques: thecal spacing of graptolites, strain fringes around subspherical core objects, and reconstruction of pyrite blocks composing the graptolites. Direct comparison of the strain fringe and graptolite results can be made only along directions that S_0 and S_2 have in common, i.e., in the S_0/S_2 plane at site SR1 and along the S_0-S_2 intersection lineation at sites SR3 and SR5. For site SR1, the graptolite thecal spacing analysis yields values for $1 + e_1$ and $1 + e_2$ of 1.24 and 0.57, respectively (Goldstein et al., 1998). The strain fringes, in contrast, yield values for $1 + e_1$ and $1 + e_2$ of 1.65 and 1.3, respectively. The values obtained from the two approaches not only do not agree, but, for the *Y*-axis, the thecal spacing measurements indicate shortening, whereas the strain fringes indicate extension. The value for $1 + e$ along the S_0-S_2 intersection lineation determined from graptolite thecal spacing for sites SR3 and SR5 is 0.97 in both cases (Goldstein et al., 1998). The strain fringes give higher values for $1 + e$ along the S_0-S_2 intersection lineation for sites SR3 and SR5 of 1.15 and 1.30, respectively.

Although the thecal spacing of the graptolites and the strain fringes record different amounts of strain, the microstructure of the graptolites agrees with the strain fringes. At site SR1, the pyrite forming the graptolites has undergone chocolate tablet boudinage. This is consistent with the radial character of the strain fringes. Thus, shortening is indicated for the *Y*-axis by the graptolite thecal spacing, and extension is indicated for the *Y*-axis by the graptolite microstructure and strain fringes.

Comparison of strain values obtained from the strain fringes with those obtained from reconstruction of the pyrite blocks composing the graptolites shows that the strain fringes record more extension than the displaced pyrite blocks. As noted above, average values for $1 + e_1$ and $1 + e_2$ determined from the strain fringes for site SR1 are 1.65 and 1.3, respectively, whereas preliminary values for $1 + e_1$ and $1 + e_2$ determined from pyrite block reconstructions for site SR1 are 1.35 and 1.2, respectively. In addition, as noted above, average values for $1 + e$ along the S_0-S_2 intersection lineation for SR5 determined from the strain fringes and from the pyrite block reconstructions are 1.3 and 1.15, respectively.

The discrepancies in strain values suggest that the various strain markers record different portions of the total strain undergone by the strata. The spacing of the graptolite thecae is affected by any deformational event that occurred after deposition of the graptolite-bearing strata and changed length in the S_0 plane. The displaced pyrite blocks, in contrast, record the deformation that occurred after pyritization of the graptolites. The strain fringes, as noted above, record the strain related to S_2 development. The strain values obtained using graptolite thecal spacing, therefore, imply that the strata underwent shortening parallel to the *Y*-axis prior to the formation of the strain fringes and the pyritization of the graptolites. Subsequent extension was not sufficient to recover the shortening undergone by the strata during this early event, resulting in net shortening of the graptolites along the *Y*-axis. The strain values obtained by reconstruction of the pyrite blocks composing the graptolites, which are consistently lower than those obtained from the strain fringes, imply that pyritization of the graptolites occurred during low-grade metamorphism accompanying S_2 development.

The F_2 folds in the Taconic slate belt are interpreted as flexural folds (Crespi and Byrne, 1987). In theory, flexural folding does not result in changes in length in the S_0 plane, which acts as the shear plane during rotation of the fold limbs. In the absence of direct evidence pointing toward deformation in the S_0 plane during folding, a deformational event other than folding is sought as the cause of early shortening of the strata along the *Y*-axis. Pre-F_2 layer-parallel shortening is a candidate. Unfolding of S_0 at site SR1, which lies on the overturned limb of the fold, rotates the *Y*-axis from north-northeast trending to northwest trending (Fig. 7). This is consistent with the inferred convergence direction during Taconian orogenesis and supports the possibility that the strata underwent layer-parallel shortening during initial incorporation into the Taconic accretionary wedge.

The Mount Merino Formation directly underlies the Pawlet Formation (Fig. 2), which is correlative with the Austin Glen Graywacke and widely accepted to be Taconic flysch. Although many workers (Zen, 1961, 1964, 1967; Shumaker, 1967; Steuer and Platt, 1981; Platt and Steuer, 1982) have inferred an angular unconformity at the base of the Pawlet Formation, Rowley et al. (1979) and Bosworth et al. (1982) concluded that the Pawlet Formation conformably overlies the Mount Merino Formation and that stratigraphic omission between the Pawlet Formation and underlying units in the Taconic sequence, in most cases, is structural. Regardless, the Mount Merino and Pawlet formations contain graptolite fauna belonging to the same zone (Berry, 1962), implying that deposition of the Mount Merino Formation occurred shortly before the formation of synorogenic deposits.

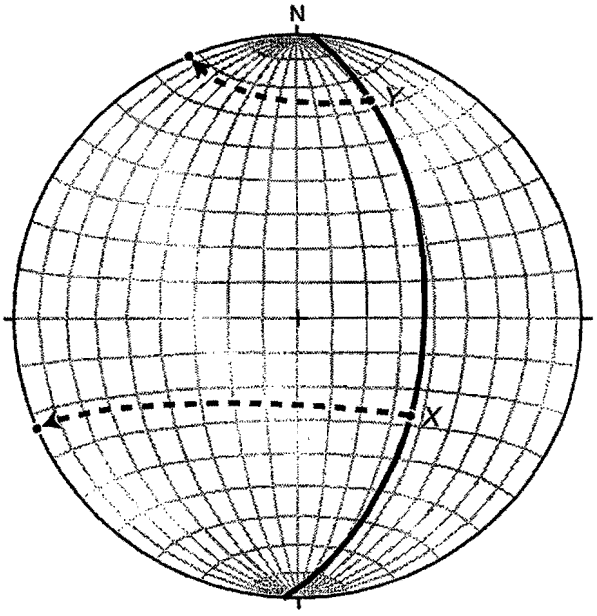

Figure 7. Stereoplot showing rotation of S0/S2 and *X*- and *Y*-axes to horizontal for site SR1. Equal-area, lower-hemisphere projection.

The preceding suggests that the Mount Merino Formation was only partially lithified when it was incorporated into the Taconic accretionary wedge. The proposed early layer-parallel shortening, therefore, may have resulted in tectonic consolidation of the strata such that the volume loss calculated from graptolite thecal spacing reflects, at least in part, loss of porosity rather than rock mass. A minimum value for the amount of shortening related to early layer-parallel shortening can be obtained using data from site SR1 by removing the strain recorded by the strain fringes from that recorded by the graptolite thecal spacing along the *Y*-axis. This results in approximately 55% shortening.

Strain values determined from reconstruction of the pyrite blocks composing the graptolites can be used to estimate the volume change during S_2 development, because pyritization of the graptolites is inferred to have occurred during S_2 development. Minimum and maximum values for the volume change are calculated as a result of cut-effect problems in strain estimation, as discussed above. Minimum and maximum estimates using the preliminary values for $1 + e_1$, $1 + e_2$, and $1 + e_3$ are 0% volume change and 30% volume gain. Because the cut-effect problems result in overestimation of the stretch, we suspect that the minimum volume change estimate is closer to the actual volume change undergone by the strata during S_2 development. These data, therefore, point to approximately constant-volume deformation during S_2 development. Note that the results do not depend on $1 + e_3$ values calculated from the hinge zone of the fold and that the results support the possibility of minor volume gain in fold limbs (see interpretation of reduction spots below).

Geometric relations at site SR3 permit an alternative approach to the understanding of volume change during S_2 development. Graptolites at this site show evidence of imbrication and boudinage, indicating that they have rotated from the instantaneous shortening field into the instantaneous extension field. The following analysis (Fig. 8) describes geometries viewing to the northeast. In the *XZ* plane, the graptolites lie 39° counterclockwise from S_2.

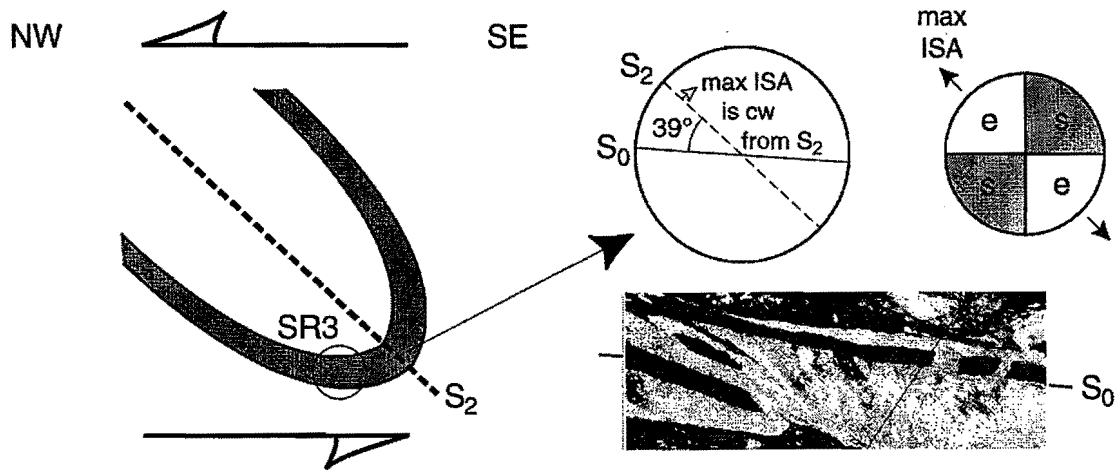

Figure 8. Schematic diagram of S0-S2 relations at site SR3 drawn for *XZ* plane. Graptolites in S0 show evidence of imbrication and boudinage, indicating that they have rotated from instantaneous shortening field into instantaneous extension field. Geometry implies angle between maximum instantaneous stretching axis (max ISA) and line separating extension and shortening fields is at least 39°. Instantaneous strain ellipse on far right shows extension (e) and shortening (s) fields for plane-strain, constant-volume deformation. Instantaneous strain ellipse is not oriented with respect to geographic reference frame. Note geometry, i.e., presence of graptolites that have undergone shortening and extension at an acute angle counterclockwise from S2, is inconsistent with simple shearing (see, for example, Ramsay (1967) and Passchier and Trouw (1996)). Photomicrograph is approximately 350 microns long. Plane polarized light. See text for discussion.

Because the sense of shear is top-to-northwest, S_2 rotated counterclockwise with respect to the shear plane as S_2-related strain accumulated. For plane-strain, constant-volume deformation, the lines of no infinitesimal strain lie at 45° to the maximum instantaneous stretching axis. The maximum instantaneous stretching axis lies clockwise from S_2, because of the counterclockwise rotation of S_2 during strain accumulation, i.e., S_2 initiated parallel to the maximum instantaneous stretching axis. Therefore, the angle between the graptolites and the maximum instantaneous stretching axis in the *XZ* plane is at least 39°. Given that S_2 has rotated to some extent and that the graptolites have rotated past the line of no infinitesimal strain, these geometric relations are consistent with constant-volume deformation. They are also consistent with volume-gain deformation (see, for example, Fig. 7 of Passchier (1990)). We are currently extending the analysis to include flattening strain in order to determine the extent to which the geometric relations preclude volume-loss deformation.

Reduction Spots

In using the reduction spot data to infer a deformation path, Goldstein et al. (1995) noted that there is no clear difference between the shape of the strain ellipsoid for limb sites and hinge sites. This is the case only if the sites are viewed as a whole. Because the strain fringe and S_2 data imply relatively low structural levels to the north and relatively high structural levels to the south, the reduction spot data (Fig. 6) can be divided into two domains. Sites SH and CP, which are located north of the transect studied by Chan (1998), are inferred to lie at a relatively low structural level, and sites QA through QF, which are located south of the transect studied by Chan (1998) and north of the SR sites, are inferred to lie at an intermediate structural level. When grouped by domain, there is a distinction between limb sites and hinge sites such that *YZ* axial ratios are greater for hinge as opposed to limb sites. In addition, *YZ* axial ratios, overall, are higher for the SH/CP domain than for the QA-QF domain, which is consistent with the structural level interpretation. These observations suggest that inference of a deformation path requires separation of the data by domain.

If the reduction spot data are grouped by domain and weighted means are used, then approximately 15% volume loss is required to derive the strain ellipsoid for the hinge site CP from that for the limb site SH and approximately 35% volume loss is required to derive the strain ellipsoid for the hinge site QD from that for the limb sites QA-QC/QF (50% from QA and 30% from the mean of the other three). These values are lower than the 55% volume loss calculated by Goldstein et al. (1995). Unlike Goldstein et al. (1995), who proposed that the 55% volume loss is a minimum estimate for the volume loss undergone by the strata during S_2 development, we propose that the calculated 15% to 35% volume loss is the total amount of volume loss undergone during S_2 development and applies only to hinge zone strata. This interpretation is based on absolute changes in length recorded by strain fringes around pyrite framboids in black slate of the Taconic sequence. The strain fringes show that the strata were undergoing extension along the *X*-axis during S_2 development and that the amount of extension along the *X*-axis was relatively uniform at a given structural level. Thus, if the strata are, for example, undergoing plane-strain deformation, then the *XY* axial ratio of the reduction spots will increase during S_2 development and the increase will be the same across a fold. The greater *YZ* axial ratio for hinge as opposed to limb sites results from greater shortening along the *Z*-axis at the hinge sites. We note that calculaton of the volume loss values given above assumes constant-volume deformation for the limb sites. The data are also consistent with regional-scale, constant-volume deformation, if fold limbs underwent volume gain, in which case less volume loss is required for fold hinges.

On the basis of geochemical data, Erslev (1998) concluded that the Mettawee Formation did not undergo large nonvolatile volume loss during S_2 development. He used two lines of evidence. First, compositional data for the Taconic slate belt, most of which is from samples of the Mettawee Formation, show that the SiO_2/Al_2O_3 and SiO_2/TiO_2 ratios of the slates, on average, are higher than those of Paleozoic shales (see Fig. 10 of Erslev (1998)). This pattern does not indicate large volume loss during S_2 development, unless the protolith of the Mettawee Formation was anomalously high in silica. And second, samples of Mettawee Formation from the Cedar Point quarry have low Zr (see Fig. 12 of Erslev (1998)), which is not consistent with enrichment in this relatively immobile element during S_2 development.

Our interpretation of the reduction spot data is broadly consistent with Erslev's (1998) inference of minimal nonvolatile volume loss during S_2 development. Although we suggest volume loss during S_2 development for the Mettawee Formation, the amount of volume loss is relatively low and occurs only in the hinge zones of the F_2 folds. Hinge zones in the Taconic slate belt are tight, and so most of the strata occupy limb positions. We also note that geochemical data suggest that large element fluxes can occur between the hinge and limbs of a fold or between the inner and outer arcs of a fold, in some cases the hinge or inner arc undergoing volume gain and in other cases volume loss (Gratier, 1983; Erslev, 1998). These data, however, are for mesoscale folds rather than regional-scale folds. Erslev (1998) analyzed samples from the same stratigraphic horizon around the fold hinge exposed in the Cedar Point quarry and noted uniform SiO_2/TiO_2 and Al_2O_3/TiO_2 ratios for samples described as being from the hinge and from the limb. He inferred no significant flux of silicate components. Because the Cedar Mountain syncline is a regional-scale fold, the samples from the quarry are all effectively in the hinge zone of the fold and so large fluxes would not be expected. Although it may not be statistically significant, the quarry samples show a slight overall decrease in SiO_2/TiO_2 in the hinge compared to the limb (see Fig. 11 of Erslev (1998)), which is consistent with the proposal of localization of volume loss in fold hinge zones.

THE BIRD MOUNTAIN FAULT: PREVIOUS AND CURRENT WORK

The Bird Mountain fault is a west-directed, low-angle thrust that bounds the Bird Mountain slice (Fig. 3). The fault is well exposed along and near the eastern shore of Lake St. Catherine in Wells, Vermont, and along Route 30 south of Wells. Excellent exposures within the fault zone provide evidence for its movement history in the context of the tectonic evolution of the Taconic Allochthon. Previous structural interpretations have addressed the Bird Mountain slice in a regional context, focusing in particular on the stacking order of the various Taconic slices and the relative timing of their emplacement. We review past research related to the Bird Mountain slice and present a detailed description of structural features observed within the Bird Mountain slice and Bird Mountain fault zone. The

meso- and microscale structural features support a synkinematic relation between thrusting along the Bird Mountain fault and the development of S_2.

Zen (1961) mapped the Bird Mountain slice as a recumbently folded, west-directed klippe. The slice lies structurally above the Giddings Brook slice, a slice of similar stratigraphy and structural style. Since Zen (1961), opposing interpretations of slice stacking order, timing of S_2 development relative to slice emplacements, and general tectonic interpretations of the Taconic Allochthon have been proposed by subsequent researchers.

Zen (1967) was the first to propose a west-to-east stacking order such that higher slices to the east were emplaced after an initial gravity-slide emplacement of the Giddings Brook and Sunset Lake slices. In addition, Zen (1967) described the nature of the contact between the Bird Mountain and Giddings Brook slices as a sharp, low-angle fault. The Edgerton half-window within the Bird Mountain slice exposes the Giddings Brook slice and controls the topographic expression of the Bird Mountain fault. Shumaker (1967) mapped the southern Bird Mountain slice within the Pawlet quadrangle and described a slice emplacement history similar to Zen (1967).

Further developing his slice theory, Zen (1972) modified his previous implicit interpretation that S_2 formed during the emplacement of the Giddings Brook slice. Evidence from mapping in the higher slices (Zen and Ratcliffe, 1971) indicated that F_2 folding accompanied or immediately followed emplacement of the highest slice. Development of S_2, therefore, was inferred to postdate emplacement of the Giddings Brook slice on the basis of the west-to-east stacking order and axial planar character of S_2 to the F_2 folds. Implicit in this interpretation is the assumption that S_2 developed simultaneously throughout the Taconic Allochthon. Zen (1972) speculated that S_2 developed as the higher slices were emplaced above the Giddings Brook slice but concluded that S_2 probably postdated emplacement of the Allochthon.

In contrast to Zen's interpretations, Rowley et al. (1979) and Rowley and Kidd (1981) proposed an east-to-west stacking order on the basis of the stratigraphic position of the flysch within individual thrust slices and modern subduction/accretionary wedge analogs. They described faults in the Giddings Brook slice as syn to late D_2/S_2, noting that the cleavage within the fault zones is parallel to subparallel to the regional S_2 cleavage (Rowley et al., 1979) (Rowley et al. (1979) define S_1 to be the regional slaty cleavage here defined as S_2). Bosworth and Rowley (1984) maintained the east-to-west stacking order but reinterpreted the D_2 faults of Rowley et al. (1979) as D_3 faults.

Stanley and Ratcliffe (1985) supported Zen's interpretation. They argued that the emplacement of the Bird Mountain slice predated S_2 and associated metamorphism on the basis of the observation that S_2 cuts across the Bird Mountain slice. Goldstein et al. (1995) also supported the view that thrusting predated S_2, noting that S_2 cuts across the Bird Mountain fault without changing orientation. Because the fault truncates F_2 folds, they inferred a sequence of events described by F_2 folding, followed by thrusting, followed by S_2 development. Most recently, Ratcliffe (1999) correlated the Bird Mountain slice with the Chatham slice to the south and maintained the view that the emplacement of younger slices was eastward toward the hinterland.

Metamorphism of the Taconic Allochthon may have been time transgressive (Karabinos, 1988). This has implications for interpretations that consider the formation of S_2 across different slices of the Allochthon to be a single event. S_2 may have formed at different times spatially and so is potentially not a reliable time marker. Another approach to understanding the structural relations within the Taconic Allochthon is to examine meso- and microscale structural features within the slice-boundary faults and the relations of these features to the different cleavages.

New observations suggest that movement along the Bird Mountain fault was coeval with the S_2 cleavage event. Abundant boudined quartz veins form a network, parallel and subparallel to S_2, and are concentrated along the thrust. The veins have been observed at the outcrop, hand-sample, and thin-section scales (Fig. 9). Locally, fibrous quartz within the veins is parallel to S_2. Fragments of slate with a well-developed S_2 are rotated within the fibrous quartz matrix. In addition, chlorite inclusion bands fringe the fragments of slate. The chlorite forms bands parallel to the fragment walls and interfingers with the fibrous quartz. The veins are interpreted to be associated with thrusting along the Bird Mountain fault, because they are spatially associated with the fault. The boudins imply that the veins

formed before or at the same time as S_2. The fragmented and rotated slate suggests that the veins postdated S_2. The chlorite inclusion bands suggest a crack-seal mechanism (Ramsay, 1980; Cox and Etheridge, 1983) that operated during or post S_2. These observations indicate an intimate relation between S_2 and vein formation: the veining is not exclusively pre-S_2 and not exclusively post-S_2, and so is interpreted as syn-S_2.

D_3 structures are also present within the Bird Mountain slice. S_3, which is typically a crenulation cleavage but may also be a disjunctive cleavage, is observed within the slice. These structures strike north-northeast and dip steeply to the east, and are parallel to the regional D_3 structures mapped by Chan (1998) to the north along Route 4. Parallel to the crenulations are asymmetric chevron folds of meter to centimeter scale that intensify close to the fault zone. These chevron folds are observed in outcrops along the topographic expression of the fault and within the interior of the slice. Similar D_3 structures were observed by Rowley et al. (1979) to the west of the Bird Mountain fault. Figure 10 shows the D_2 and D_3 structures recorded within the Bird Mountain slice.

The outcrops along the Bird Mountain fault near and south of Wells, Vermont, are interpreted to be within a pressure-solution shear zone, in which S_2 cleavage formation and large-scale thrust faulting occurred simultaneously. The fault zone is at least several hundred meters thick and contains both ductile and brittle deformational structures at a variety of scales. Preliminary observations at outcrop, hand-sample, and thin-section scales indicate that the Bird Mountain fault was active during S_2 development. Reactivation of the fault may have occurred during the D_3 event considering the spatial pattern of chevron folds within and near the fault zone, but this relation is not clear.

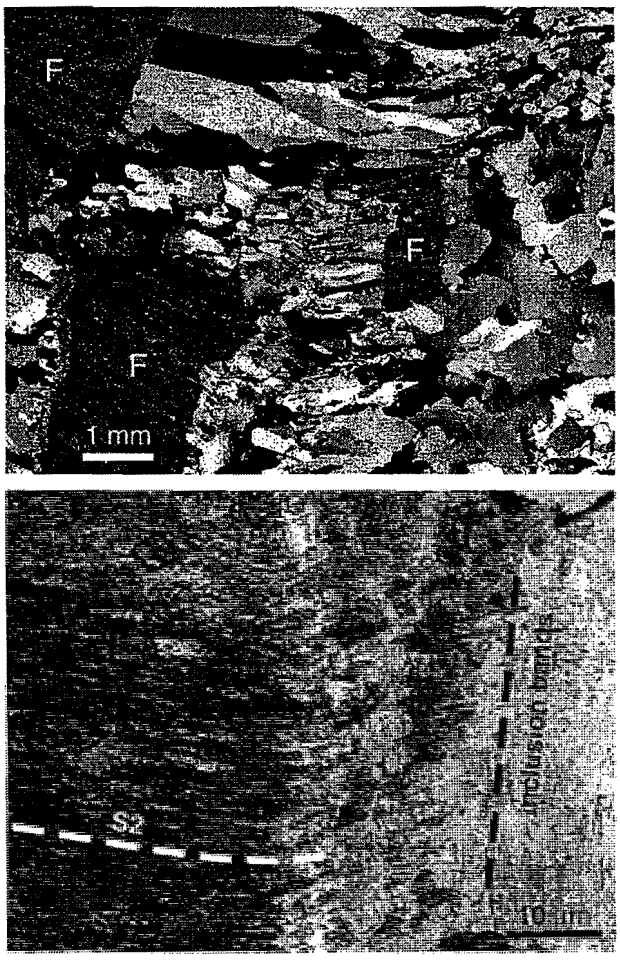

Figure 9. Photomicrographs of (top) rotated slate fragments (F) in a matrix of fibrous quartz that grew parallel to S2 (crossed polarized light) and (bottom) chlorite inclusion bands within S2-parallel fibrous quartz (plane polarized light).

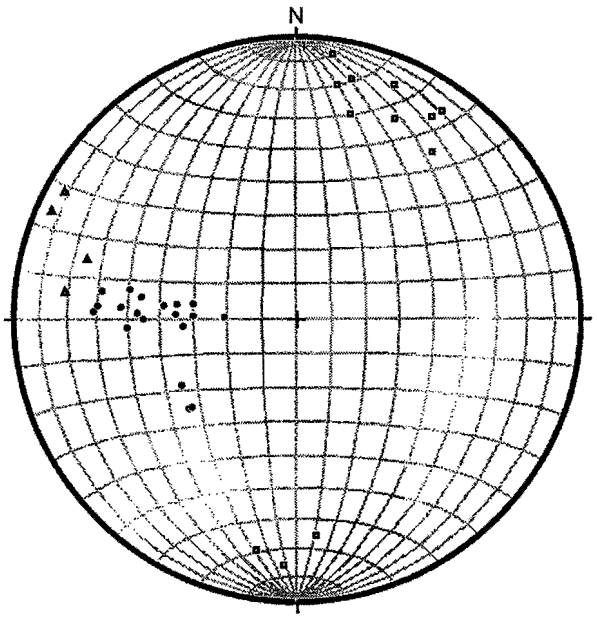

Figure 10. Stereoplot of structural elements associated with Bird Mountain fault. Solid circles represent poles to S2. Triangles represent poles to S3. Boxes represent F3 fold axes. Equal-area, lower-hemisphere projection.

ACKNOWLEDGEMENTS

JMC thanks her GEOL 217 students, who, over the years, have helped guide her understanding of the structural development of the Taconic orogenic belt. JMC and JRG thank Art Goldstein for helpful discussions on the Bird Mountain fault and Taconic geology in general.

REFERENCES CITED

Ando, C.J., Czuchra, B.L., Klemperer, S.L., Brown, L.D., Cheadle, M.J., Cook, F.A., Oliver, J.E., Kaufman, S., Walsh, T., Thompson, J.B., Jr., Lyons, J.B., and Rosenfeld, J.L., 1984, Crustal profile of mountain belt: COCORP deep seismic-reflection profiling in New England Appalachians and implications for architecture of convergent mountain chains: American Association of Petroleum Geologists Bulletin, v. 68, p. 819-837.

Berry, W.B.N., 1962, Stratigraphy, zonation, and age of Schaghticoke. Deepkill, and Normanskill shales, eastern New York: Geological Society of America Bulletin, v. 73, p. 695-718.

Bosworth, W., and Rowley, D.B., 1984, Early obduction-related deformation features of the Taconic Allochthon: Analogy with structures observed in modern trench environments: Geological Society of America Bulletin, v. 95, p. 559-567.

Bosworth, W., Rowley, D.B., and Kidd, W.S.F., 1982, A structure section in eastern New York showing variation in style of deformation across the Taconic Allochthon: Discussion: Northeastern Geology, v. 4, p. 111-116.

Chan, Y.C., 1998, Kinematic and geochronologic constraints on the structural development of the northern Taconic Allochthon in western New England, USA [Ph.D. thesis]: Storrs, University of Connecticut, 117 p.

Chan, Y.C., Crespi, J.M., and Hodges, K.V., 2001, Dating cleavage formation in slates and phyllites with the $^{40}Ar/^{39}Ar$ laser microprobe: An example from the western New England Appalachians, USA: Terra Nova, v. 12, p. 264-271.

Chapple, W.M., 1973, Taconic orogeny: Abortive subduction of the North American continental plate?: Geological Society of America Abstracts with Programs, v. 5, p. 573.

Cox, S.F., and Etheridge, M.A., 1983, Crack-seal fiber growth mechanisms and their significance in the development of oriented layer silicate microstructures: Tectonophysics, v. 92, p. 147-170.

Crespi, J.M., and Byrne, T., 1987, Strain partitioning and fold kinematics in the Giddings Brook slice, Taconic Allochthon, west-central Vermont: Geological Society of America Abstracts with Programs, v. 19, p. 9.

Crespi, J.M., and Chan, Y.C., 1996, Vein reactivation and complex vein intersection geometries in the Taconic slate belt: Journal of Structural Geology, v. 18, p. 933-939.

Dale, T.N., 1899, The slate belt of eastern New York and western Vermont: U. S. Geological Survey, 19th Annual Report, pt. 3, p. 153-300.

Durney, D.W., and Ramsay, J.G., 1973, Incremental strains measured by syntectonic crystal growths, *in* De Jong, K.A., and Scholten, R., eds., Gravity and Tectonics: New York, Wiley, p. 67-96.

Erslev, E.A., 1998, Limited, localized nonvolatile element flux and volume change in Appalachian slates: Geological Society of America Bulletin, v. 110, p. 900-915.

Goldstein, A., Knight, J., and Kimball, K., 1998, Deformed graptolites, finite strain and volume loss during cleavage formation in rocks of the Taconic slate belt, New York and Vermont, USA: Journal of Structural Geology, v. 20, p. 1769-1782.

Goldstein, A., Chan, Y.C., Pickens, J., and Crespi, J.M., 1997, Deformation of the Taconic sequence, western Vermont and eastern New York, *in* Grover, T.W., Mango, H.N., and Hasenohr, E.J., eds., New England Intercollegiate Geological Conference Guidebook: Castleton, Vermont, Castleton State College, p. A1-1:31.

Goldstein, A., Pickens, J., Klepeis, K., and Linn, F., 1995, Finite strain heterogeneity and volume loss in slates of the Taconic Allochthon, Vermont, USA: Journal of Structural Geology, v. 17, p. 1207-1216.

Gratier, J.P., 1983, Estimation of volume changes by comparative chemical analyses in heterogeneously deformed rocks (folds with mass transfer): Journal of Structural Geology, v. 5, p. 329-339.

Hoak, T.E., 1992, Strain analysis, slaty cleavage and thrusting in the Taconic slate belt, west-central Vermont: Northeastern Geology, v. 14, p. 7-14.

Karabinos, P., 1988, Heat transfer and fault geometry in the Taconian thrust belt, western New England, *in* Mitra, G., and Wojtal, S., eds., Geometries and Mechanisms of Thrusting, With Special Reference to the Appalachians: Geological Society of America Special Paper 222, p. 35-45.

Karabinos, P., Samson, S.D., Hepburn, J.C., and Stoll, H.M., 1998, Taconian orogeny in the New England Appalachians: Collision between Laurentia and the Shelburne Falls arc: Geology, v. 26, p. 215-218.

Karabinos, P., Samson, S.D., Hepburn, J.C., and Stoll, H.M., 1999, Taconian orogeny in the New England Appalachians: Collision between Laurentia and the Shelburne Falls arc: Reply: Geology, v. 27, p. 382.

Laird, J., Lanphere, M.A., and Albee, A.L., 1984, Distribution of Ordovician and Devonian metamorphism in mafic and pelitic schists from northern Vermont: American Journal of Science, v. 284, p. 376-413.

Passchier, C.W., 1990, Reconstruction of deformation and flow parameters from deformed vein sets: Tectonophysics, v. 180, p. 185-199.

Passchier, C.W., and Trouw, R.A.J., 1996, Microtectonics: Berlin, Springer-Verlag, 289 p.

Passchier, C.W., and Urai, J.L., 1988, Vorticity and strain analysis using Mohr diagrams: Journal of Structural Geology, v. 10, p. 755-763.

Platt, L.B., and Steuer, M.R., 1982, A structure section in eastern New York showing variation in style of deformation across the Taconic Allochthon: Reply: Northeastern Geology, v. 4, p. 117-119.

Ramsay, J.G., 1967, Folding and fracturing of rocks: New York, McGraw-Hill, 568 p.

Ramsay, J.G., 1980, The crack-seal mechanism of rock deformation: Nature, v. 284, p. 135-139.

Ramsay, J.G., and Graham, R.H., 1970, Strain variation in shear belts: Canadian Journal of Earth Sciences, v. 7, p. 786-813.

Ratcliffe, N.M., 1999, Examination of the slice concept and evidence for primary emplacement structures in the Taconic Allochthons of western New England: Geological Society of America Abstracts with Programs, v. 31, p. 62.

Ratcliffe, N.M., Hames, W.E., and Stanley, R.S., 1998, Interpretation of ages of arc magmatism, metamorphism, and collisional tectonics in the Taconian orogen of western New England: American Journal of Science, v. 298, p. 791-797.

Ratcliffe, N., Hames, W.E., and Stanley, R.S., 1999, Taconian orogeny in the New England Appalachians: Collision between Laurentia and the Shelburne Falls arc: Comment: Geology, v. 27, p. 381.

Rowley, D.B., and Kidd, W.S.F., 1981, Stratigraphic relationships and detrital composition of the medial Ordovician flysch of western New England: Implications for the tectonic evolution of the Taconic orogeny: Journal of Geology, v. 89, p. 199-218.

Rowley, D.B., Kidd, W.S.F., and Delano, L.L., 1979, Detailed stratigraphic and structural features of the Giddings Brook slice of the Taconic Allochthon in the Granville area, *in* Friedman, G.M., ed., New York State Geological Association and New England Intercollegiate Geological Conference Guidebook: Troy, New York, Rensselaer Polytechnic Institute, p. 186-242.

Sanderson, D.J., 1982, Models of strain variation in nappes and thrust sheets: A review: Tectonophysics, v. 88, p. 201-233.

Shumaker, R.C., 1967, Bedrock geology of the Pawlet quadrangle, Vermont: Part 1, central and western portions: Vermont Geological Survey Bulletin, no. 30, p. 1-59.

Stanley, R.S., and Ratcliffe, N.M., 1985, Tectonic synthesis of the Taconian orogeny in western New England: Geological Society of America Bulletin, v. 96, p. 1227-1250.

Steuer, M.R., and Platt, L.B., 1981, A structure section in eastern New York showing variation in style of deformation across the Taconic Allochthon: Northeastern Geology, v. 3, p. 134-137.

Sutter, J.F., Ratcliffe, N.M., and Mukasa, S.H., 1985, $^{40}Ar/^{39}Ar$ and K-Ar data bearing on the metamorphic and tectonic history of western New England: Geological Society of America Bulletin, v. 96, p. 123-136.

Weijermars, R., 1991, The role of stress in ductile deformation: Journal of Structural Geology, v. 13, p. 1061-1078.

Wood, D.S., 1974, Current views of the development of slaty cleavage: Annual Review of Earth and Planetary Sciences, v. 2, p. 369-401.

Zen, E-an, 1961, Stratigraphy and structure at the north end of the Taconic Range in west-central Vermont: Geological Society of America Bulletin, v. 72, p. 293-338.

Zen, E-an, 1964, Stratigraphy and structure of a portion of the Castleton quadrangle, Vermont: Vermont Geological Survey Bulletin, no. 25, 70 p.

Zen, E-an, 1967, Time and space relationships of the Taconic Allochthon and Autochthon: Geological Society of America Special Paper 97, 107 p.

Zen, E-an, 1972, Some revisions in the interpretation of the Taconic Allochthon in west-central Vermont: Geological Society of America Bulletin, v. 83, p. 2573-2587.

Zen, E-an, and Ratcliffe, N.M., 1971, Bedrock geologic map of the Egremont quadrangle and adjacent areas, Berkshire County, Massachusetts and Columbia County, New York: U.S. Geol. Survey Misc. Invest. Map, I-628, 4 p.

ROAD LOG

Mileage

0.0 Trip will begin in Fort William Henry Conference Center parking lot.
3.5 Turn left onto Route 149 east.
15.1 Turn left at light in Fort Anne onto Route 4 north.
25.5 At Whitehall turn right, continuing on Route 4 north (see Fig. 11 for trip route).
30.0 STOP 1. Turn left into driveway just before billboards on hill to left and park in overgrown lot.

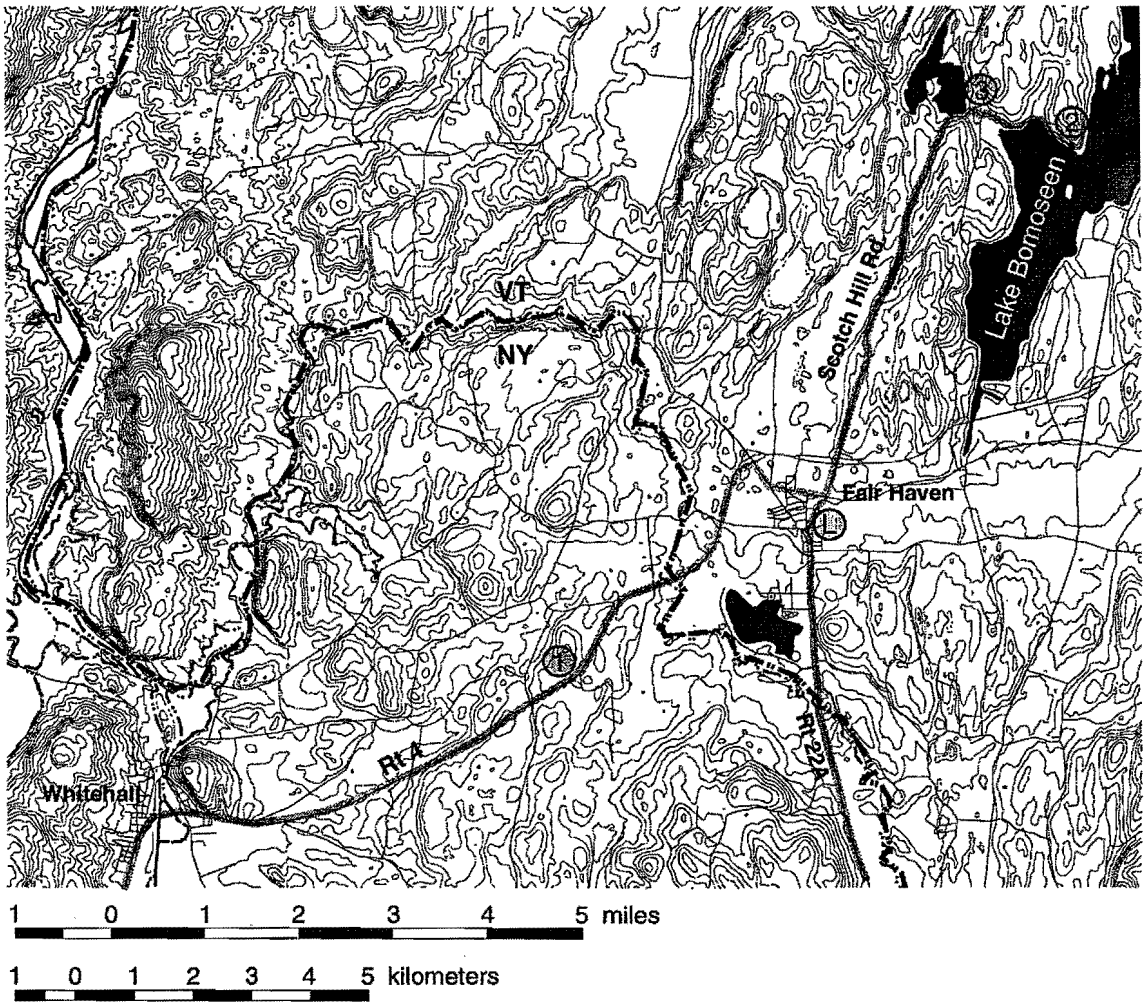

Figure 11. Location map for northern part of field trip. Highlighted roads indicate trip route. Numbered circles indicate stop localities; circled L is lunch stop.

STOP 1. ABANDONED QUARRY. (45 MINUTES) This quarry, which exposes the Cambrian Hatch Hill Formation, lies on the upright limb of the Mount Hamilton syncline, a regional-scale, west-vergent F_2 fold. S_0 lies at a low angle to S_2, which dips about 30°-35° to the east. Fibrous calcite veins are abundant in the strata and lie in a variety of orientations.

The outcrop was included by Chan (1998) in his transect of the Taconic slate belt in the vicinity of Route 4. Strain fringes around pyrite framboids in the strata record top-to-west-northwest, non-coaxial flow. Passchier and Urai (1988) used veins in the exposure to estimate the kinematic vorticity number of the flow. They inferred that the dominant vein set formed at some point during S_2 development; however, these veins and others display characteristics that suggest that they are early pre-folding veins, which were reactivated during S_2 development (Crespi and Chan, 1996). Determination of the flow type required estimation of volume change, which Passchier and Urai (1988) accomplished through geochemical analysis of a sample with a variably developed S_2. They determined a volume loss of 50%. Erslev (1998), in contrast, analyzed samples from the quarry with a penetrative S_2 and concluded, on the basis of geochemical data, that large volume loss occurred only at the scale of individual cleavage domains.

30.0 Turn left back onto Route 4 north.
31.9 Cross Vermont State line (Poultney River) and begin four-lane highway.
33.3 Take exit 2 off Route 4 (Fair Haven/Vergennes).
33.5 Take right off ramp onto Route 22A south.
33.8 Turn left onto Fourth Street.
34.4 Turn left at blinking red light onto Dutton Road (becomes Scotch Hill Road after crossing Route 4).
38.8 Scotch Hill syncline (Stop 3) on left. Bear right, staying on main paved road.
39.0 At Bomoseen State Park entrance take hard left onto Cedar Mountain Road (dirt road).
40.3 STOP 2. Cedar Point quarry. Road ends here. Park in pullout or on north side of road. Do not block driveway opposite quarry entrance. Refer to Fig. 12 for trail map of quarry.

STOP 2. CEDAR POINT QUARRY. (1 HOUR 15 MINUTES) The hinge zone of the Cedar Mountain syncline, a regional-scale, overturned, west-vergent, isoclinal F_2 fold, is exposed at this stop. The folded strata consist of the Cambrian Mettawee Formation. The dominant cleavage in the exposure is S_2, which dips about 25° to the east and is parallel to the axial plane of the fold. A moderately developed S_3 is also present.

Green ellipsoidal reduction spots are common in the maroon slate and can readily be seen in the abandoned blocks on the quarry floor. Irregularly shaped areas of reduction and bands of reduction subparallel to S_0 are also common. Measurements of the ellipsoidal reduction spots have been made by Wood (1974), Hoak (1992), and Goldstein et al. (1995). Minimum volume losses during S_2 development of 55% determined from the reduction spot data (Goldstein et al., 1995) are in conflict with geochemical data from the quarry, which are consistent with minimal nonvolatile volume loss (Erslev, 1998).

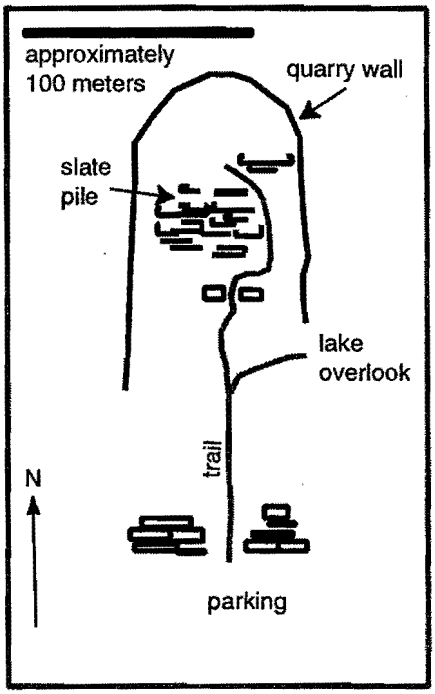

Figure 12. Trail map of Cedar Point quarry. Climb to top of slate pile from east side.

40.3 Return back along Cedar Mountain Road.
41.6 At Bomoseen State Park entrance take right onto Scotch Hill Road.
41.7 Bear left, staying on main paved road.
41.8 STOP 3. Scotch Hill syncline. Turn left into driveway of white house opposite syncline and park on grass to right of driveway. Additional parking on grass on either side of road.

STOP 3. SCOTCH HILL SYNCLINE. (45 MINUTES) This is a well known exposure in New England. The property owner asks that hammers not be used on the outcrop, so please leave your hammer in your vehicle. Also, poison ivy may be dense at the base of the exposure.

This exposure of the Ordovician Poultney Formation lies in the hinge zone of the Scotch Hill syncline, a regional-scale, west-vergent F_2 fold. S_2 dips about 30° to the east and is axial planar to the fold. En echelon, sigmoidal quartz veins provide evidence for flexural folding of the strata with pinning at the hinge. The veins are present on both limbs of the fold but are more systematic on the vertical limb and, thus, provide a better example of vein development within shear zones. (In this context, S_0 acts as the shear plane.) The veins are easily found on the vertical limb of the fold. To observe the veins on the gently dipping, upright limb, go around the small shed and climb to the base of the exposure behind the shed. Veins on both limbs of the fold are folded and/or boudined. On the vertical limb, the veins have a Z-shaped asymmetry (viewed to the north), indicating east-side-down sense of shear along S_0. On the gently dipping, upright limb of the fold, the veins have an S-shaped asymmetry (viewed to the north), indicating top-to-west sense of shear along S_0. Prefolding veins, which are not coaxial with the fold, can also be observed in the exposure. These appear approximately parallel to S_2 on the fold profile plane on both limbs of the fold, but three-dimensional exposures show that the veins lie at an angle to S_2. The prefolding veins lie in

approximately the same orientation on both limbs of the fold. This results because shearing within layering effectively cancelled the change in orientation from rigid rotation of the fold limbs.

41.8 Return back along Scotch Hill Road toward Fair Haven.
46.2 After crossing Route 4 go straight at blinking light to center of Fair Haven.
46.6 LUNCH STOP. Fair Haven green. Trip continues from here on Route 22A south to Middle Granville (see Fig. 13 for trip route).
58.5 Turn left off Route 22A and immediately cross bridge onto Washington County 24.
58.6 Turn left onto Depot Street (opposite Chapman's General Store).
59.3 Turn left onto Stoddard Road.
59.8 STOP 4. Stoddard Road graptolites. Park on right, opposite drained beaver pond under conversion to pasture.

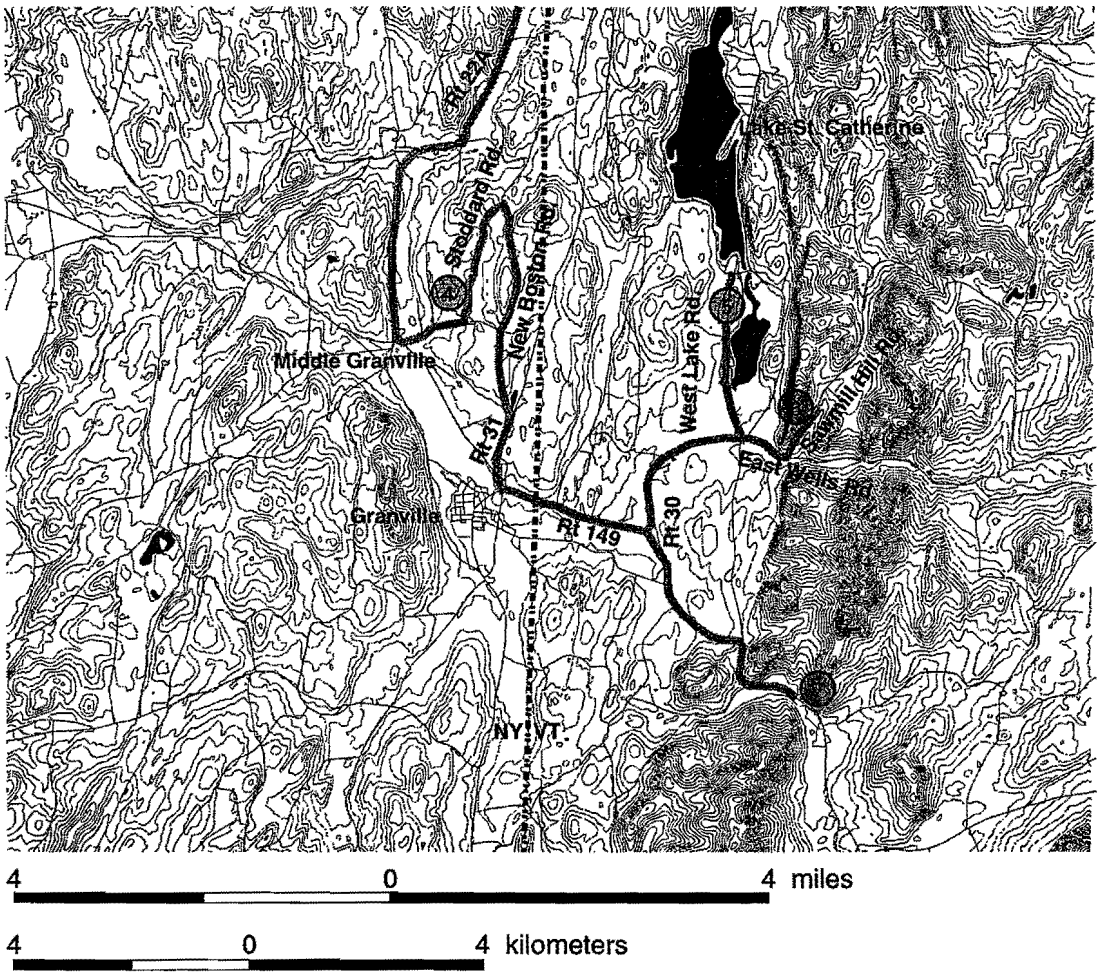

Figure 13. Location map for southern part of field trip. Highlighted roads indicate trip route. Numbered circles indicate stop localities.

STOP 4. STODDARD ROAD GRAPTOLITES. (1 HOUR) The first exposure (SR1) that we will visit at this stop is located immediately east of the road. The second exposure (SR2) is located on the small hill in the middle of the drained beaver pond and, if the area is marshy, can be reached by crossing the small stream at the south end of the drained pond. Both exposures are rather small. Please be kind to them with your hammers so that geologists on trips in the future can also enjoy the graptolites and structural features.

The two exposures are of the graptolite-bearing Stoddard Road Member of the Ordovician Mount Merino Formation. Exposures of the Mount Merino Formation in the vicinity of Stoddard Road are in the core of a regional-scale F_2 syncline. SR1 is located on the overturned limb of the syncline, and S_0 and S_2 are essentially parallel. S_0/S_2 dips about 45°-50° to the east. Graptolites are readily observed in place on the underside of the overhanging S_0/S_2 surfaces and in numerous pieces of float. The hinge zone of a mesoscale fold is exposed at the north end of the outcrop where graptolites can be observed on an S_0 surface at a very high angle to S_2. Mesoscale folds, which cannot be recognized using stratigraphic relations, may be common in the generally poorly exposed slates of the region. SR2 is located in the hinge zone of the regional-scale F_2 syncline. Well-preserved graptolites are present but more difficult to find at the exposure. S_0 lies at very high angles to S_2, which dips about 45°-50° to the east, and the exposure provides good examples of using S_0-S_2 relations to determine whether strata are on the upright or overturned limb of a fold. The axial-planar character of S_2 can be observed in the hinge of the fold, which is exposed on the north side of the hill in a small block that is probably slightly out of place.

59.8 Continue north on Stoddard Road.
60.8 Turn right onto New Boston Road.
62.3 Go straight at intersection with stop sign.
63.3 Turn right onto Route 25 south. Continue to center of Granville.
64.2 At Granville center turn left onto Route 149 east.
65.9 Turn left onto Route 30 north and continue to Wells.
66.7 Turn left onto North Street (Lakeside Realty) just before center green of Wells.
68.1 STOP 5. At top of grassy hill park on right.

STOP 5. BIRD MOUNTAIN FAULT OVERLOOK. (20 MINUTES) From this vantage point, the Bird Mountain fault is clearly expressed as the abrupt topographic transition between the valley containing Little Pond and Lake St. Catherine and the hills to the east. Good exposures of the fault can be viewed in a large roadcut along the east shore of Lake St. Catherine on Route 30, but access is limited and the orientation of the exposure is parallel to strike. To the east of the fault in this region, the Mettawee (St. Catharine Formation of Shumaker (1967)) and West Castleton/Hatch Hill formations underlie the hills of the Bird Mountain slice. Slate quarries are absent from the Bird Mountain slice despite the abundance of the Mettawee Formation. Zen (1967) noted that the Mettawee within the Bird Mountain slice is siltier than Mettawee to the west and, therefore, is unfit for roofing material.

68.1 Continue north on North Road.
68.4 At intersection with West Lake Road drive around traffic island and return past overlook.
70.1 Turn left onto Route 30 north.
70.2 At Wells green go straight onto East Wells Road as Route 30 turns to left.
70.4 Bear left up hill onto Sawmill Hill Road.
71.2 Stop 6. Park on right, opposite small roadcut.

STOP 6. BIRD MOUNTAIN SLICE. (45 MINUTES) This small outcrop records several deformational events to affect the Taconic Allochthon. The rocks are within the Mettawee Formation. S_0 is folded and the fold axes trend northwest. A variably spaced, axial planar S_2 cleavage cuts S_0. S_2 is well defined along limbs of folds but nearly absent in the hinges. A weak spaced cleavage, steeper than the pervasive S_2 cleavage, is interpreted to be S_3. Refer to Fig. 10 to see the local relation between S_2 and S_3. S_2-parallel veins are present at the south end of the outcrop.

71.2 Continue up Sawmill Hill Road to first driveway on left.
71.3 Turn around in driveway on left. Drive down Sawmill Hill Road.
72.1 Turn right onto East Wells Road.
72.3 At intersection go straight onto Route 30 south.
77.4 STOP 7. Turn into driveway of white house (3723 on mailbox). Park in driveway. Outcrop in backyard, northwest of house.

STOP 7. BIRD MOUNTAIN FAULT. (45 MINUTES) Outcrops in the yard behind the house, in the woods above, and along Route 30 (beware poison ivy!) contain abundant veins that are parallel and subparallel to S_2. This is the prominent S_2 cleavage that dominates the Allochthon from here west, but is folded in this manner only near the Bird Mountain fault. In addition, the S_2 surface and veins are deformed into asymmetric chevron folds. The green and purple rocks exposed here are the Mettawee Formation. The orientation of S_2 is highly variable due to the intense chevron folding.

MIDDLE ORDOVICIAN SECTION AT CROWN POINT PENINSULA

by

Charlotte Mehrtens, Department of Geology, University of Vermont, Burlington, VT 05405
Bruce Selleck, Department of Geology, Colgate University, Hamilton, NY 13346

INTRODUCTION

The Chazy, Black River and Trenton Groups are a well known sequence of fossiliferous limestones and sandstones in the Champlain Valley of New York, Vermont and southern Quebec. These rocks record cyclic sedimentation in shallow water environments on the flanks of the Iapetus Ocean during the Middle Ordovician transgression. This field trip reviews the stratigraphy of these units and the evidence for their depositional environments.

CHAZY GROUP

The internal stratigraphy of the Chazy Group in the Lake Champlain Valley was defined by Oxley and Kay (1959). Welby (1962) provides a comprehensive synopsis of stratigraphic relationships between exposures in New York and Vermont. Hoffman (1963) presented a regional lithostratigraphic framework for the Montreal-Ottawa area. Fisher (1968) presents descriptions of Chazy Group strata in the northern Lake Champlain Valley. Biostratigraphic correlations of the Chazy Group have been attempted using brachiopods (Cooper, 1956), trilobites (Shaw 1968) and conodonts (Raring, 1973). Speyer and Selleck (1986) summarize major lithostratigraphic trends in the Chazy Group and the appropriateness of biostratigraphic correlation.

The Chazy Group is nearly 250 meters thick in the northern Champlain Valley (Oxley and Kay, 1959) but thins to the south (approximately 90 meters at Crown Point peninsula; less than 15 meters at Ticonderoga, absent at Whitehall). In the type area in the northern Champlain Valley, a three-part subdivision into Crown Point, Day Point and Valcour Formations is applied. The classic biostromes largely occur within the Day Point Formation. Significant biostromal buildups are absent in the southern exposures. In the vicinity of Crown Point, the entire Chazy Group is placed within the Crown Point Formation (Oxley and Kay, 1959), although there is considerable lithologic variation.

The Chazy Group marks the resumption of shallow marine sedimentation following partial emergence and subaerial erosion of the underlying Beekmantown Group during early Medial Ordovician time. In the southern Lake Champlain Valley, the basal Chazy units are clearly in unconformable contact with tilted, eroded upper Beekmantown Group strata. In the northern Champlain Valley, basal Chazy Group beds are in apparently conformable contact with the Providence Island Dolostone of the Beekmantown Group (Speyer, 1982).

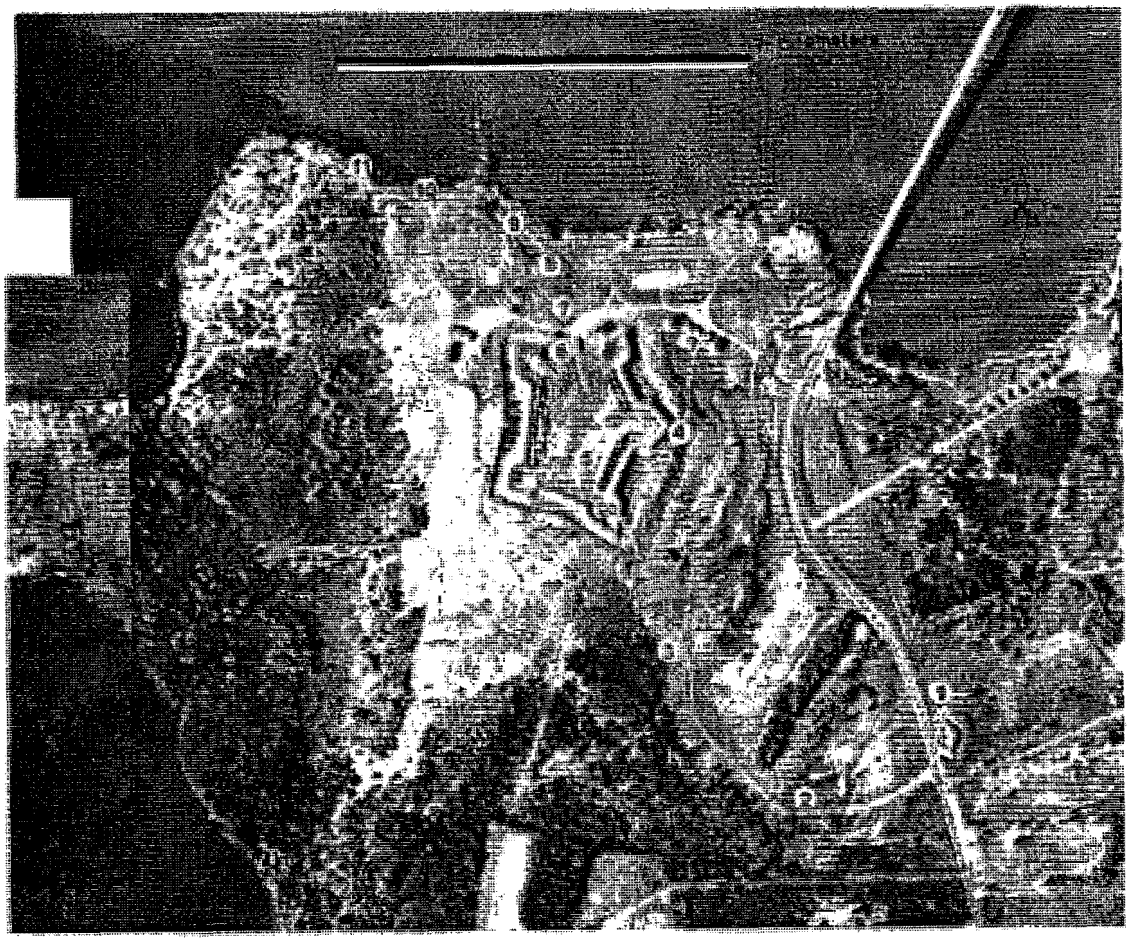

Figure 1 – Location map. See text for location descriptions

Rapid north-to-south thickness and facies changes, and variations in the nature of the basal contact suggest that the Chazy was deposited during or just after a period of block faulting which disrupted earlier Beekmantown and older rocks in some areas. The presence of coarse, angular quartz and feldspar grains within the Chazy Group suggests that Proterozoic basement may have been exposed close to the areas of Chazy deposition (Selleck, et al, 1985). In the Ottawa area, basal Chazy consists of coarse sandstones and pebble conglomerates of braided stream origin, indicating uplifted source terrains in that area (Hoffman, 1963).

The Chazy Group contact with the overlying Black River Group is abrupt, but evidence for significant erosion is generally absent. At Chazy, New York, the contact is apparently conformable (Fisher, 1968; Raring, 1973). The contact is well-exposed on the Crown Point Peninsula and is marked by a coarse quartz sandstone with scattered large, angular feldspar grains.

The Chazy Group at Crown Point consists largely of fossiliferous bioclastic wackestones, packstones and grainstones, with varying degrees of post-depositional dolomitization. Shaley, nodular limestones are present in the sequence, but are rarely exposed at the surface. Environments of deposition varied from subtidal, storm-dominated shelf settings to inshore sand shoals and lower tidal flats. Muddy peritidal facies are generally absent, but intervals of penecontemporaneous cementation and karstic erosion may mark intervals of subaerial exposure (Selleck, 1983).

Cements within the Chazy Group at Crown Point typically consist of an early equant to prismatic lo-Mg calcite followed by later coarse calcite spar. Dissolution and chert replacement of aragonitic bioclasts is common. Dolomitization of Crown Point carbonates is widespread, and is highly selective in some facies. Variations in primary mineralogy (lo-Mg calcite vs. aragonite) appear to have controlled the dolomitization of some bioclastic materials; grain size, sorting, porosity, intensity of burrowing and distribution of early cements (and thus permeability of materials during burial diagenesis) seem to best explain the highly variable patterns of dolomitization (Selleck, 1988).

Stop 1- Redoubt

Approximately 6 m of variously burrowed, slightly dolomitic, thin to medium bedded bioclastic packstone and grainstone is exposed in this section. Some beds are relatively well-sorted grainstones with sharp bases and are interpreted as storm deposits. Note the large intraclasts in the base of one unit in the low ledge at the southeast corner of the ditch. These indicate rip-up of cemented grainstone, apparently by a storm. Abundant "*Girvanella*" algal oncolites are present in beds approximately three meters from the base of the section. Rounded, dark calcite grains (abraded gastropod fragments?) form the cores of the oncolites, and are scattered in other beds. Fossils are relatively abundant, and are best seen on slightly weathered bedding surfaces. Trilobite fragments, brachiopods, bryozoans, pelmatozoan plates, nautiloids and large *Maclurites magnus* are present. Dolomite occurs in shaley weathering laminae and in burrow fills.

The relatively high faunal diversity, general bioturbation, and storm-related sedimentation point to a 'low energy', shallow subtidal environment at depths slightly below normal wave base. The abundant algal oncolites and discrete calcareous algal fossils (e.g. *Hedstromia*) suggest depths well within the photic zone. A possible modern analogue is found in the mixed mud and sand shelf to the west of the emergent tidal flats of Andros Island, Bahamas, as described by Bathurst (1971) and Purdy (1963).

The wavy, irregular dolomite laminae result from dolomitization of lime mud, followed by compaction and pressure solution of calcite that produced irregular, clay- and dolomite-rich stylocumulate seams. Preferential dolomitization of burrows is due to contrasts in permeability of burrow-fill versus burrow-matrix sediment. The burrow-fill material retained permeability longer during diagenesis and allowed more pervasive dolomitization. In similar facies exposed on Bullwagga Bay (west shore of peninsula), nodular limestone with shaley dolostone seams and stringers are present (Fig. 2). The limestone nodules appear to have been cemented prior to significant burial compaction, whereas the shaley dolostone material was compacted around the cemented limestone. The early-cemented limestones were resistant to dolomitization. This sort of fabric selective dolomitization is common in the Chazy and Black River Groups throughout the Champlain Valley. Can you find other evidence of early cementation in this outcrop. Are there hardgrounds?

Stop 2 – Ridge outcrop extending NE from near entrance Gate

Cross-stratified coarse bioclastic grainstones are well-exposed near the main gate along the entrance road and adjacent ridge. Nearly three meters of section form a prominent belt parallel to strike extending from the entrance road to the main highway. Foreset cross-strata show bipolar dip directions. Angular quartz and feldspar grains are concentrated in some laminae. The carbonate particles are dominately sub-rounded, abraded pelmatozoan plates with gastropod and brachiopod fragments. Large *Maclurites* fragments and grainstone intraclasts are present on the upper bedding surfaces of the ledges northeast east of the entrance road.

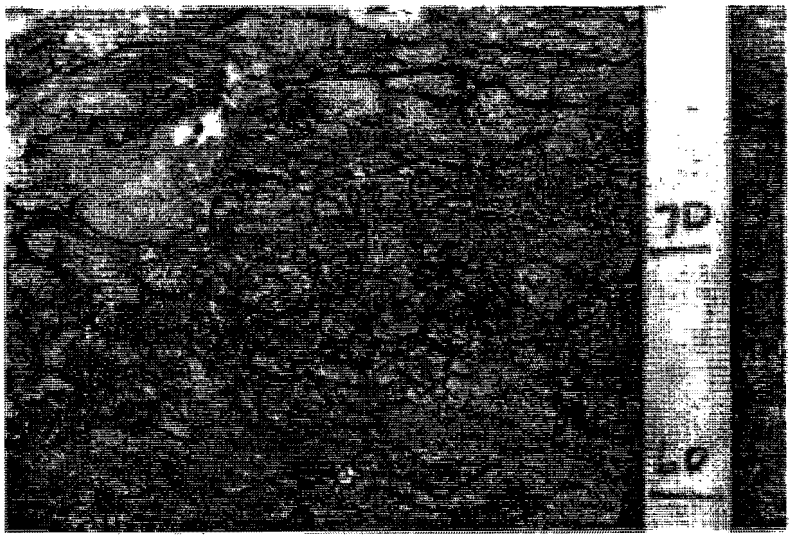

Figure 2: (previous page). Nodular limestone in shaley dolostone matrix. Note apparent truncation of some nodules by stylolites. Dark fragments are *Maclurites* bioclasts. This fabric suggests early cementation of portions of the sediment by calcite, followed by burial, compaction and dolomitization. The disrupted appearance may be due to burrowing and rotation of cemented nodules, plus later soft-sediment deformation of the cemented nodules while the matrix was still uncemented. Scale is centimeters.

Stop 2 – continued from previous page

We envision the environment of deposition of this facies as a shallow subtidal wave and current reworked sand shoal. Active transport of abraded grains may have been accomplished by tidal currents (as suggested by bipolar cross-strata), or by storm-generated currents that produced complex, anastomosing patterns of cross-strata and intervening reactivation surfaces. The lack of burrowing and well-preserved whole-shell body fossils may be due to the inhospitable shifting sand substrate. This environment likely resembled the unstable sand shoal environment of the Bahamas Platform (Bathurst, 1971; Ball, 1967). The scale and style of cross-stratification here are similar to that predicted by Ball (1967) from study of the bedforms present on Bahamian Platform sand bodies. Similar Chazy Group facies in the northern Lake Champlain Valley are oolitic (Oxley and Kay, 1959).

Note that these grainstones are essentially undolomitized. Does this indicate early cementation or diagenetic stabilization prior to deeper burial?

Stop 3 - Low ledges adjacent to entrance road (Picnic Pavilion Ridge) approximately 50 meters north of Stop 2.

Brown-weathering, slightly shaley dolostone exposed here contains lenses and stringers of fossiliferous lime packstone and wackestone. As at Stop 1, trilobites, small brachiopods and *Maclurites* are common.

The environment of deposition is assumed to be subtidal shelf, with less storm activity than at Stop 1.

Note that some of the fossils are almost entirely encased in dolomite, which is assumed to be of replacement origin here. Why are some of the fossils so well-preserved, and not dolomitized?

Stop 4 - SE moat of Fort Crown Point:

Approximately 3 meters of thickly laminated limestone and dolostone are exposed in the southeast 'moat' of the British Fort. The dominant facies here is alternating 0.5-2.0 cm thick laminae of limestone and dolostone – commonly termed 'ribbon rock'. The limestone ribbons are very fine peloid grainstones or 'calcisiltites' and appear blue-grey on slightly weathered surfaces, and are indentations on more deeply weathered surfaces. The dolostone ribbons weather tan-brown, and consist of an interlocking mosaic of 20-300 micron dolomite crystals of replacement origin. Quartz silt grains are present in the dolostone ribbons, versus medium to fine quartz sand in the limestone, suggesting that the limestone ribbons were slightly coarser than the dolostone when originally deposited.

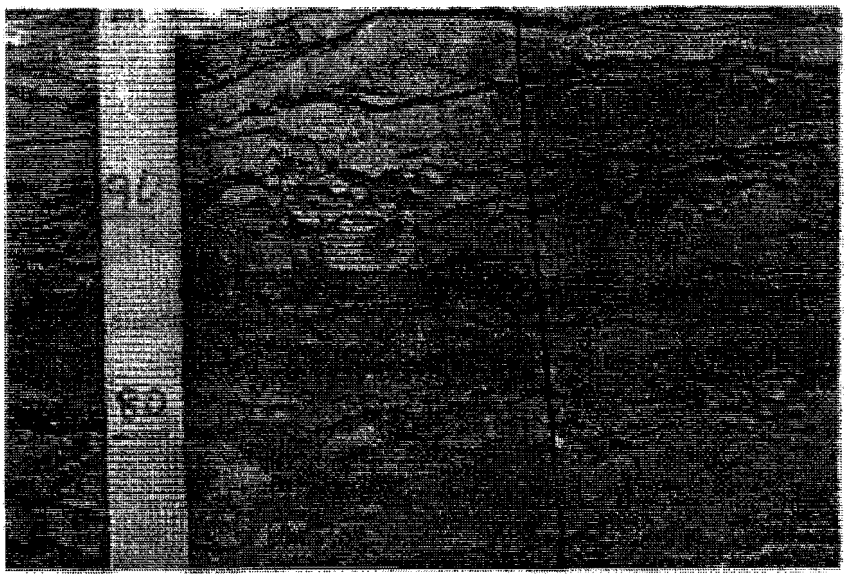

Figure 3: Typical ribbon rock facies with limestone (calcite) layers more resistant and dolomite layers weathering in. This surface is exposed to wind abrasion, and the granular, sugary-textured dolomite is less resistant than the well-cemented limestone. Note the scalloped surface of some limestone layers, perhaps due to burrowing or corrosion of cemented layers. Irregular wisps and knots of limestone in dolostone matrix are probably due to deformation of cemented limestone within soft matrix material that is now dolomitized. Scale in centimeters.

An erosional surface with 10-20 cm relief is exposed near the base of the south wall. Similar erosional surfaces occur within this facies in other exposures, and appear to represent micro-karstic solution surfaces on a tidal rock platform that developed during subaerial exposure of cemented limestone (Fig. 5). Typically, the rock below the surface is mostly calcite limestone, suggesting that cementation and diagenetic stabilization of the limestone occurred prior to development of the erosional surfaces. Overlying rock contains more dolomite. *Maclurites* shell hash can be found in pockets on the erosional surface, suggesting wave transport

of shells onto the rocky platform of the erosional surface. Dolomitized burrows cut across the limestone ribbons in some parts of the outcrop, and trough cross-strata that appear to fill low scours are also visible.

Figure 4: Burrowed ribbon rock on weathered surface shows preferential dolomitzation of burrow-fill material and section through *Maclurites*. On this surface, dolomitized material weathers out in relief because dolomite is more resistant to chemical dissolution.

On the less weathered prominence on the SE corner of the moat, shallow scours containing brachiopods and gastropod debris are seen. Intraclasts or pseudoclasts of limestone in dolostone are also present. Some 'clasts' appear to be cored by dolomitized burrows.

We interpret this sequence as a tidal flat to shallow subtidal facies. The alternating limestone/dolostone 'ribbon rock' may represent rhythms of slightly coarser (limestone) and slightly finer (dolostone) sediment deposited on the lower reaches of a tidal flat, similar to the bedding described by Reineck and Singh (1980) from the mud/sand tidal flats of the North Sea. These coarse-fine alternations might also reflect storm-related, ebb-surge deposition. Early cementation of the slightly coarser limestone ribbons made this lithology less susceptible to later dolomitization, which affected the finer, muddy ribbons that are now dolostone. Variations in intensity of burrowing reflect subtle differences in duration of subaerial exposures of the flat and/or extent of reworking by tidal currents. Limited *in situ* faunal diversity is expected in a stressed tidal flat setting. The absence of mudcracks and evaporite minerals may indicate that only the lower portion of a humid climate tidal flat system is preserved here.

Stop 5 - Parade Grounds near Barracks:

As we enter the parade ground from the southwest corner of the moat, note the array of carbonate rocks used in construction of the barracks. Chazy, Black River, and rare Trenton lithologies can be identified

Restoration of the barracks began in 1916. More recently, starting in 1976, the New York State Division for Historic Preservation undertook protection and stabilization of the ruins.

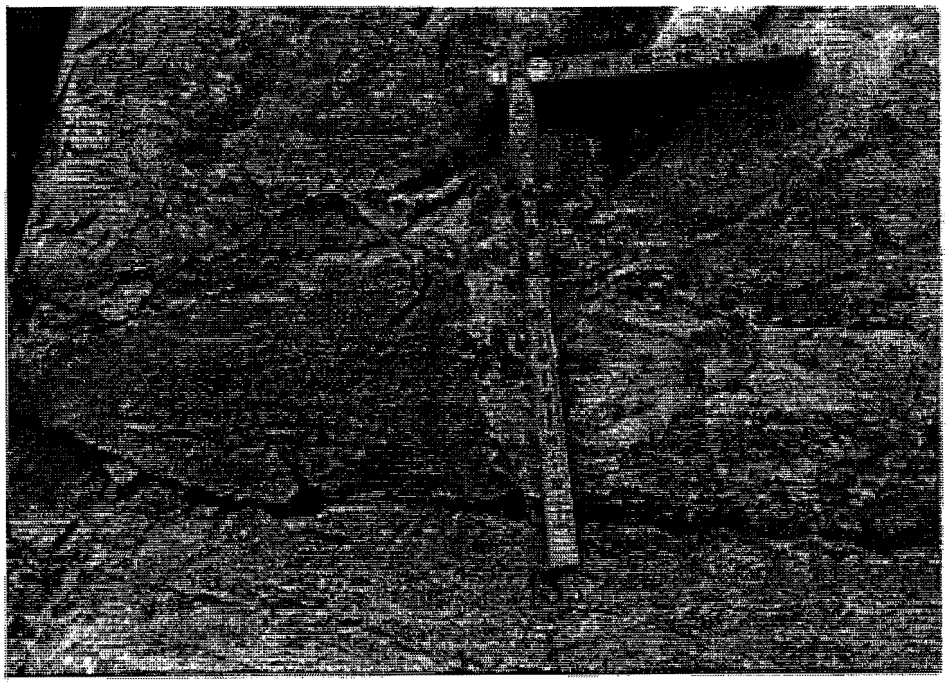

Figure 5: Limestone (dark) forming sharp, scalloped erosional surface beneath dolostone above. The limestone was cemented prior to deposition of overlying sediment. Later dolomitization altered only burrow-fill material in dark limestone, whereas sediment above was thoroughly dolomitized. Scale in inches.

Stop 5 - continued

The low rock pavement just north of the barracks is within the upper part of the 'ribbon rock' unit seen at stop 4. Immediately up-section, cross-stratified grainstone beds are visible. Coarse quartz and feldspar sand is easily seen on weathered surfaces. Trough cross-strata and 'herringbone' co-sets of planar-tabular cross-strata are visible on the low vertical faces. Large, angular clasts of slightly dolomitic grainstone and *Maclurites* are present on bedding surfaces. We interpret this facies as a current-dominated sand shoal environment similar to that seen at stop 2.

Note the polygonal pattern on some outcrop surfaces. Are these mudcracks?

BLACK RIVER GROUP

The Black River Group in the Champlain Valley is a relatively thin unit (85-90 feet thick) consisting of massively-bedded wackestones to packstones representing deposition in lagoonal to shallow subtidal environments. The gradual deepening characterizing this unit and continuing into the Trenton Group and overlying shales is interpreted to represent foreland basin subsidence during the Taconic Orogeny. This gradual deepening was punctuated by both shallowing and deepening events on macroscopic (meter) as well as microscopic (centimeter) scales, the latter visible only in thin section. The Black River Group is so lithologically variable in New York/Ontario/Vermont that stratigraphic names have proliferated, however the Pamelia, Lowville (House Creek and Sawyer Bay Members) and Chaumont Formations can be recognized in the Champlain Valley. Bechtel (1993) summarizes the evolution of nomenclature applied to this unit.

Stop 6 - West parade grounds

Bechtel and Mehrtens (1993) suggested that the sandstone unit in the westernmost parade ground is the basal sandstone of the Black River Group, an interpretation which differs from that of Speyer and Selleck (1988) who suggested that this unit was part of the underlying Chazy Group. In thin section this sandstone is a quartz arenite in composition, very poorly sorted, containing fewer lithic fragments and phosphatic fragments than Chazy sandstones. Visible at the very easternmost portion of this ridge an overlying buff-colored dolomite bed containing pockets of quartz sand (burrow infills?) is exposed. The sandstone and dolomite lithologies are very similar to those described by Walker (1972) for the Pamelia Formation at the type locality in New York. Alternatively, placement of the sandstone within the Chazy Group is consistent with the common presence of coarse quartz and feldspar sand within the Chazy here, whereas siliciclastic material in the Black River Group at Crown Point is mainly fine silt and clay. Whatever the stratigraphic placement of this unit, it marks an interval when sands were transported from a nearby (Adirondack?) source area. This period of subaerial exposure of the shelf was followed by marine reworking of the sand, and deposition of the muddy carbonates of the basal Black River Group.

Stop 7 - Northeastern moat

There is approximately 4 feet of covered interval between the parade grounds and moat exposures. The wall of the northeasternmost moat exposes several feet of the lower Black River Group (Lowville Formation, House Creek Member). At the base of this exposure a series of stylolitized gastropod-bearing (*Liospira*) wackestone beds are overlain by thick beds of Phytopsis-burrowed aphanitic mudstones. This sequence can be interpreted as an example of a "classic" shallowing-up cycle consisting of subtidal to peritidal lagoonal muds. Examine the sharp contact of the aphanitic mudstone with the overlying wackestones, a contact which in thin section appears to be a firmground (Bechtel, 1993).

Examination of *Phytopsis* burrows in thin section (Fig. 6) reveals that many are filled with graded (fining-up) geopedal silt, evidence of cementation in the meteoric vadose zone as shown below.

Continuing upsection, several thick packstone beds are exposed. More detailed examination of these beds reveals that they consist of alternating one to three inch thick intraclast and oncolite-rich packstone horizons interpreted as tempestites, interbedded with fossiliferous wackestone/packstone horizons. The tempestites, or storm-generated deposits, consist of graded and crudely imbricated intraclasts and skeletal fragments. Note the nature of the upper and lower contacts of these horizons. Horizons of tempestite beds within *in situ* fossiliferous muds is a second motif which occurs throughout much of the Black River Group.

Figure 6. At other localities in the Champlain Valley, several of these cycles comprise the base of the Black River. Of the three motifs of repetitious bedding in the Black River Group, these cycles occur at the largest, macroscopic scale and are interpreted to represent 4th order (10,000 to 100,000 years) or smaller cycles.

It is instructive to spend several moments sketching (following page) the basal six feet of the moat exposure. Your sketch could illustrate the basal SUC's as well as the upper and lower contacts and internal fabric of the tempestite-rich beds.

SKETCH HERE

The uppermost third of the outcrop appears to be a massive bed of limestone, however closer examination also reveals small scale "cycles" of alternating wackestone/packstone and grainstone, the third motif of bedding in the Black River. These are characterized by a base of thinly laminated or cross laminated grainstone horizons 1 to 2 inches thick, overlain by fossiliferous wackestones and packstones. In thin section the bases of the grainstones can be identified as firmgrounds, recognizable by the truncations of allochems and cements in the underlying mud.

Figure 7 illustrates the nature of the contact between a peloid-rich grainstone of the base of a cycle and the top of the underlying packstone. The scalloped surface and truncated grains and allochems are characteristic of these contacts.

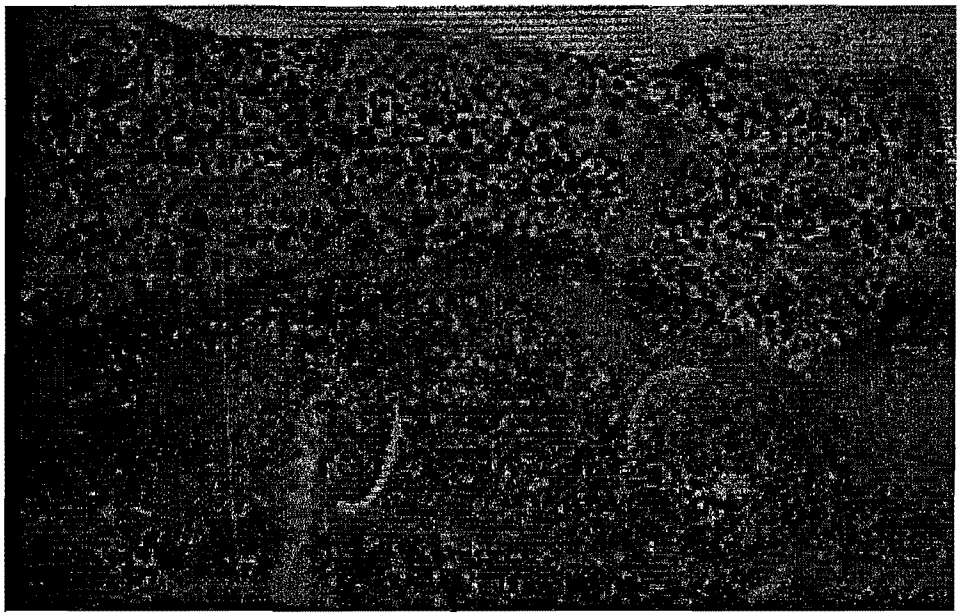

Figure 7. The very top of this exposure (best seen at the next outcrop) exhibits a burrow mottled fabric with selected dolomitization of many burrows. *Tetradium* occurs in life position in these horizons.

Stop 8 - East-west ridge

A black chert layer near the top of Stop 7 provides the correlation to Stop 8, the outcrop across the service road.

The limestone beds on this ridge commonly consist of alternating wackestone/packstone and planar to cross laminated grainstone beds as seen at Stop 7, however bedding plane exposures permit identification of many fossils in these, the most faunally diverse beds in the Black River. Specimens of gastropods (*Liospira, Lophospira, Hormotoma*), *Lambeophyllum, Tetradium*, stromatoporoids, the bivalve *Cyrtodonta, Strophomena* sp. and cephalopods are recognizable. This ridge is most notable for its bedding plane exposures of *Tetradium* and *Lambeophyllum* and is interpreted as recording a wave baffle margin lithofacies described by Walker (1972) at the type section.

A sketch of the third type of cycle, laminated grainstone overlain by bioturbated wackestone, with special attention paid to the nature of the contacts between cycles, would be appropriate. These sequences are

interpreted to represent smaller scale 4th order 'micro-cycles' that could be the result of facies mosaicing and/or small scale base level changes.

SKETCH HERE

There are at least two distinct types of chert occurrences in the Black River. One appears to be fabric selective: infilling horizontal burrows, for example (many other burrows are dolomitized). The other chert occurrence is less frequent and consists of broad, bedding parallel sheets. The uppermost chert horizon on this ridge, traceable down to the shoreline, is of this latter variety. Clearly, there was a significant source of silica available for chert formation, perhaps a combination of silica derived from sponges (*Tetradium*?) and bentonite alteration (the Ordovician sequence in the Champlain Valley is notorious for the paucity of bentonites compared to equivalent strata in central New York and Quebec). In thin section the chert cross cuts all previous cements, including late fracture-filling calcite, and is therefore the youngest, latest example of diagenesis in these rocks.

Stop 9 - Quarry

Be extremely careful around the quarry - the thick algal scum in the quarry water obscures where the grass begins and the quarry wall drops off.

The older, weathered south walls of the quarry show, by color differentiation, two cycles. Closer examination of the more accessible north wall reveals more occurrences of the third motif of Black River bedding: 8 to 10 inch thick beds of planar laminated skeletal and peloidal hash overlain by burrowed wackestones overlain by an intraclast-rich horizon. Interbedded with these cycles are also tempestite couplets of mudstone/wackestone and fossil hash layers in which brachiopod-rich layers are abundant (look for 'nested' pockets of shells).

Sketch the interbedding of the two cycles below:

Before leaving the quarry area, note the numerous quarried blocks stacked between the quarry and the shoreline. See if you can recognize cycles, and from these, topping directions.

Stop 10 - Shoreline

Uppermost horizons in the quarry can be traced down to the shoreline to the north where the Black River section continues (Chaumont Formation of the Black River Group) with small covered intervals up to the Trenton Group limestones. Shoreline bedding planes exhibit horizontal burrows of *Chondrites*, opercula of *Maclurites*, and polished surfaces also reveal large intraclasts, in other words the same internal stratigraphy that could be viewed in cross section on the quarry walls. Note: exposures may only be visible at low water levels.

Cement Stratigraphy of the Black River Group

There are multiple types of cements present within the Black River limestones which record a complex diagenetic history. The general cement stratigraphy pattern records early nonluminescent cement associated with precipitation in oxidizing waters of the shallow meteoric phreatic zone. With increasing reducing conditions, bright and dull luminescent cements represent precipitation in shallow burial conditions. Ferroan calcite with dull to nonluminescence represents precipitation in a late burial situation from high temperature burial fluids. Early marine Black River Group micritic cement is ferroan and very dull luminescence representing deposition in a reducing, lagoonal environment. Subsequent cementation took place in the shallow meteoric phreatic zone, with nonluminescent cements with bright rims representing oxidizing conditions becoming slightly more reducing with burial. These observations are consistent with those of Mussman, et al. (1988) who interpreted such patterns to be related to a cratonward-dipping meteoric water lens beneath tidal flats. Tectonic uplift would lead to stagnation of the aquifer and increasingly reducing conditions. Within this general pattern, however, there are many variations in the Black River limestones which record frequent base level changes associated with sea level fluctuations and block fault movements in the Taconic foreland basin. These base level changes have produced numerous firmgrounds (at all Black River localities) as well as beachrock (at Arnold Bay) and paleo-karst (at Arnold Bay, Chippen Point and Sawyer Bay localities) horizons.

Fractures are common throughout the Black River and their cements record evolving burial conditions. Figures 8 and 9 illustrate some of the observed patterns. The cement stratigraphy of the fractures indicates that their formation occurred throughout the diagenetic history of the Black River, from early syndepositional events associated with karst and beachrock formation, through to deep burial.

TRENTON GROUP

The contact between the Trenton and Black River Groups is covered at most localities in the Champlain Valley, probably because the thinner-bedded and finer-grained Trenton is easily weathered. At Arnold Bay, to the northeast of Crown Point, the contact is exposed and is interpreted to be a disconformity. The dark gray colored, massive homogenous beds of the Black River are in sharp contact with the rubbly, laterally discontinuous beds of the Trenton. Here at Crown Point the Trenton is thinner than elsewhere in the Valley (28 feet), which MacLean (1987) suggested might reflect deposition on a down thrown block in the Taconic foreland basin. MacLean measured 50 feet of Glens Falls in the section at Button Bay (a few miles to the north of Crown Point) which, because it includes both the upper and lower contacts with the Black River Group and Cumberland Head Formation, respectively, represents the only complete exposure of this unit in

the Champlain Valley. Bechtel (1993) summarized the variable nature of the Black River/Trenton contact around the Champlain Valley, New York and Ontario and noted that the regional variation seen would be expected in a foreland basin actively undergoing syndepositional block faulting.

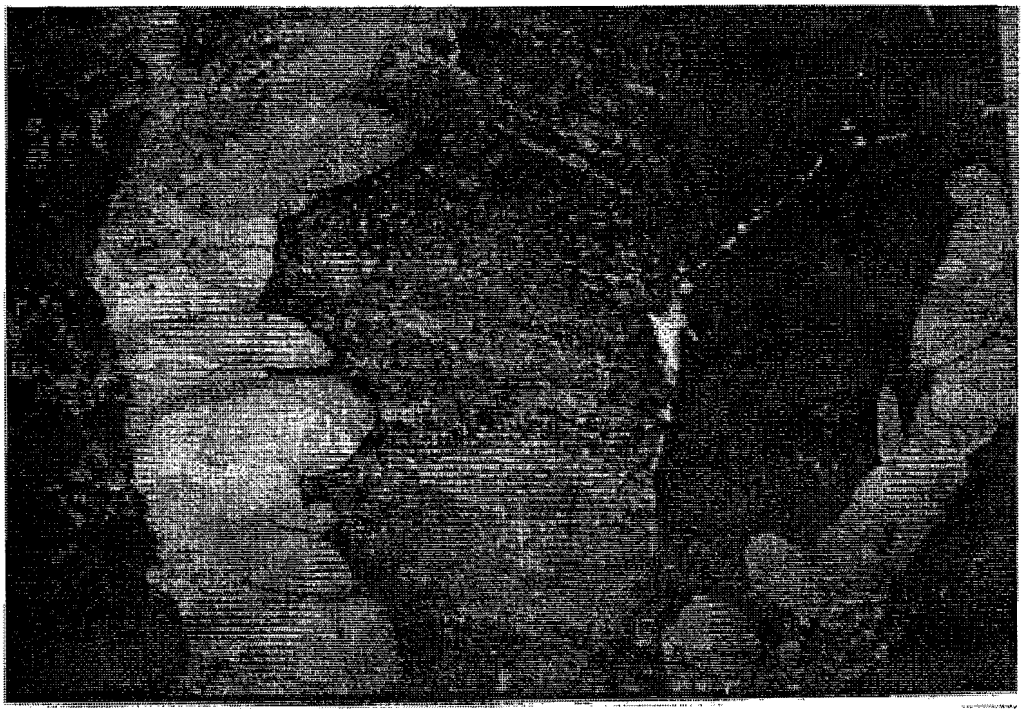

Figure 8 (field of view 1.8cm): Two cement events are visible in the fracture. The first consists of nonferroan scalenohedral crystals extending outward from the fracture wall. These are interpreted to have been precipitated in the meteoric phreatic zone. The later large ferroan equant blocky crystals in the center of the fracture represent a late burial cement precipitated under reducing conditions.

Stop 11 - Shoreline of eastern Bulwaga Bay

Continuing up the shoreline from the uppermost outcrops of Black River a thin covered interval (4') occurs before the basal beds of the Glens Falls Formation. The Glens Falls is characterized by thin, nodular to wavy bedded wackestones, mudstones and rare grainstones, a very different type of bedding style and faunal assemblage from the underlying Black River. Bedding planes along the shoreline contain mostly *Chondites* and *Helmenthopsis* burrows, however as one moves up section recognizable pieces of *Cryptolithus*, *Isotelus*, orthid brachiopods, *Stictopora*, and *Prasopora simulatrix* can be found, the latter is important because it permits the correlation of the lower Glens Falls here in the Champlain Valley to the lower Denley Limestone at the Trenton type section in central New York.

MacLean (1987) interpreted the lithofacies of the basal Glens Falls to represent sedimentation in a shallow subtidal environment periodically influenced by storm activity. In thin section the nodular and wavy bedded wackestones appear thoroughly bioturbated, a process which would influence and enhance subsequent differential compaction. Grainstone beds exhibit more planar bases with basal skeletal fragment lags or finely crushed debris of brachiopod, trilobite and crinoidal material capped by mud (see Fig. 10). MacLean interpreted these as tempestite deposits.

Figure 9. (field of view 0.5 mm) Photographed under cathodoluminescence so the zoning of rhombohedral crystals infilling a fracture can be seen. The very symmetrical zoned patterns starts (from the interior outward) with a nonluminescent nonferroan core, a dull rim, a bright orange rim, another dull rim, to another bright rim and fading to nonluminescent outer rims. The nonferroan to ferroan zonation is indicative of increasing reducing conditions during cementation.

Based on lithologies, fossil assemblages and sedimentary structures, or the lack thereof, the Glens Falls Formation is interpreted to represent sedimentation in a deeper water, subtidal setting relative to the Black River deposits. For those familiar with lower Trenton localities in central New York the paucity of fossiliferous bedding planes here at Crown Point is noteworthy. The overall fine grain size and ichnofauna suggest that bathymetry increased significantly and rapidy from the Black River into the Glens Falls, a transition which might reflect not only rising sea level but base level changes as well. The sedimentologic and faunal transitions from the Glens Falls to the overlying Cumberland Head Argillite and Stony Point Shale are much more gradational that that of the Black River/Glens Falls contact.

LOCATION

All the stops for this trip are within the Crown Point Reservation State Historic Site. From the west, take NY Route 22 north from Ticonderoga, continuing north through the Village of Crown Point. Turn east approximately five miles north of the Village of Crown Point, following signs to the 'Bridge to Vermont'. From the east, take VT Route 22A north from Fairhaven, or south from Burlington area, and follow signs to 'Bridge to New York'. Stop locations are keyed to the aerial photo. Stop 1 is in the ditch and wall of a small outpost fort (the Redoubt) on the east side of Route 8, immediately across the highway from the historic site entrance road. We will enter the historic site and park near the main entrance, then walk back to stop 1. No collecting is permitted in the historic area. Note that groups should register at the main gate upon entry to the site.

Figure 10. A large (3x5 inch) thin section illustrating the lithologic change within a single bed of the Glens Falls Limestone.

BIBLIOGRAPHY

Ball, M. M.(1967) Carbonate Sand Bodies of Florida and the Bahamas; Jour. Sed. Pet. 37; pages 556-591

Bathurst, R. (1971) Carbonate Sediments and Their Diagenesis; Elsevier, 658 pages

Bechtel, S.and Mehrtens, C. (1993) Taconic Foreland Basin Evolution; Sedimentology and Cement Stratigraphy of the Black River Group Limestones in the Champlain Basin; Geol. Soc. America Abstracts B5-16 with Programs, 25; 2, pages 4-5

Cooper, G. (1956) Chazyan and Related Brachiopods; Smith. Misc. Coll. 127; pages 1025-1245

Fisher, D. (1968) Geology of the Plattsburgh and Rouses Point, New York-Vermont Quadrangles; New York State Mus. and Sci. Serv. Map and Chart Series #10; 51 pages

Hoffman, H. (1963) Ordovician Chazy Group in Southern Quebec; AAPG Bulletin 47; pages 270-301

MacLean, D. (1987) Facies relationships within the Glens Falls Limestone of Vermont and New York; Guidebook for Fieldrips in Vermont, Norwich University Dept. Earth Sci., pages 53-79

Mussman, W., Montanez, I., and Read, J. (1988) Ordovician Knox Paleokarst Unconformity, Appalachians; In: Paleokarst, James, N. editor; Springer-Verlag, NY; pages 211-228

Oxley, P. and Kay, G. (1959) Ordovician Chazyan Series of the Champlain Valley, New York and Vermont; AAPG Bulletin 43; pages 817-853

Purdy, E.(1963) Recent Calcium Carbonate Facies of the Great Bahamas Bank. II – Sedimentary Facies; Journal of Geology 71; pages 472-497

Raring, (1973) Condont Biostratigraphy of the Chazy Group (Lower Middle Ordovician), Champlain Valley, New York and Vermont; Dissertation Abstracts Intemation, Section B; 33, 8, page 3831B

Reineck, H. and Singh, I. (1980) Depositional Sedimentary Environments; Springer-Verlag; 561 pages

Selleck, B. (1983) Early Ordovician arid climate vs. medial Ordovician humid climate peritidal carbonates in the north-central Appalachians; Geol. Soc. America Abstracts with Programs 15; 3, page 184

Selleck, B. (1988) Limestone/dolostone fabrics in the Chazy Group (early medial Ordovician) of New York and Vermont; Geol. Soc. America Abstracts with Programs 20; 1, page 69

Shaw, F. (1968) Early Middle Ordovician Chazy Trilobites of New York; Memoir, New York State Museum and Science Service; 163 pages

Speyer, S. (1982) Paleoenvironmental history of the Lower Ordovician-Middle Ordovician boundary in the Lake Champlain Basin, Vermont and New York; Geol. Soc. America Abstracts with Programs 14; 1, page 54

Speyer, S. and Selleck, B. (1986) Stratigraphy and Sedimentology of the Chazy Group (Middle Ordovician), Lake Champlain Valley; New York State Museum Bulletin 462; pages 135-147

Walker, K. (1972) Community Ecology of the Middle Ordovician Black River Group of New York State; Geol. Soc. America Bulletin, 83; 8, pages 2499-2524

Welby (1962) Paleontology of the Champlain Basin in Vermont; Special Publication, Vermont Geological Survey; 88 pages

EARLY PALEOZOIC SEA LEVELS AND CLIMATES: NEW EVIDENCE FROM THE EAST LAURENTIAN SHELF AND SLOPE

by
Ed Landing
New York State Museum, The State Education Department, Albany, NY 12230

INTRODUCTION

Purpose

Field studies undertaken in eastern New York in the early 1800s by Amos Eaton and others led to the birth of American geology (see review by Friedman, 1979). With this early work, geology continued as an important applied discipline, but it developed into an important intellectual and cultural activity that provided the first empirical explanations of physical and biotic change through earth's "deep time." Although almost two centuries have passed since Eaton's first work, "everything isn't known and decided" either about the geology of eastern New York or its significance in opening a window into "deep time."

This field trip (Figure 1) will illustrate recent published syntheses of eastern New York geology that help reconstruct Early Paleozoic sea-level and climate changes. The salient features of these recent syntheses are the following:

A new sequence stratigraphy. A sequence stratigraphy has been developed for the eastern New York–western Vermont shelf (Landing et al., 2003) that shows sequence boundaries at the Cambrian–Ordovician boundary (Stops 6, 7), the Tremadocian–Arenigian boundary (Stop7), and in the middle and terminal Arenigian (Figure 2). As all evidence indicates that this part of Laurentia was a passive margin until within the Late Ordovician (see Mitchell et al., 1997, for the new international convention that mandates that the Chazy, Black River, and Trenton Groups and "Knox unconformity" be assigned to the Late Ordovician), these sequence boundaries correspond to eustatic changes (e.g., Ross and Ross, 1995).

Ending "New England stratigraphy." Our work in this part of the east Laurentian shelf (Landing et al., 2003) has integrated standard lithostratigraphic descriptions from well exposed sections with new macro- and microfossil (primarily conodont) biostratigraphic data to evaluate the areal extent of shelf depositional sequences and formation- and member-level units. This has led to the recognition of regionally extensive stratigraphic units and the abandoning of many formation-level names as junior synonyms following the North American Stratigraphic Commission (1983) rules for nomenclatural priority. Work in Cambrian–Ordovician slope facies of the Taconic allochthon also shows that multiple names have long been used for the same lithologic units along the length of the allochthon. The demonstration of close lithologic similarity in "units" of the same age allowed a reduction of Taconic stratigraphic names to about one third by synonymy (Landing, 1988b; Landing and Bartowski, 1996). Ending "New England stratigraphy," in which each county seems to have its own stratigraphic nomenclature (see Appendix), helps in the reconstruction of geologic history by more accurately and simply recording the areal extent of lithofacies and their depositional environments.

Reconstructing Early Paleozoic paleoclimates and eustasy and correlating enhanced deep-water fossilization potential with greenhouse intervals. Slate colors in the Taconic allochthon are a proxy for Early Paleozoic changes in sea level, in climate, and in relative oxygenation of the mid-water mass on the continental slope. Macroscale alternations of black and green-dominated siliceous mudstones in the external slices of the Taconian

allochthons of New York and Québec (Stops 8–11) reflect paleo-oceanographic changes. Black, organic-rich mud was deposited under a more intense and thicker dysaerobic slope water mass with sea-level rise, resultant climate amelioration (greenhouse intervals), and reduced oceanic circulation. Green (and purple and red) mud deposition reflected improved mid-water oxygenation, climate minimum (icehouse intervals), and increased deep-water circulation (Landing et al., 1992, 2002). The bedded limestones characteristic of black mudstones reflect off-shelf transport of active and prograding carbonate platforms with sea-level rise, while the abundant trace fossils in green slates reflect higher bottom-water oxygen levels. The linkage of green and black mudstone deposition to sea-level fall and rise, and thus to shelf sequence stratigraphy, will be discussed on this trip. The black mudstone and limestone alternations have supplied the majority of biostratigraphic information through the Taconic succession because the limestones yield Cambrian macro- and microfaunas transported from the shelf margin (Landing and Bartowski, 1996; Landing et al., 2002). Similarly, latest Cambrian–Ordovician black shales and limestones yield the majority of the graptolites (e.g., Ruedemann, 1902, 1903; Berry, 1960, 1962) and conodonts (Landing, 1976, 1977, 1994) known from the Taconic allochthon. Taconic black shale intervals are equated with improved deep-ocean taphonomic conditions during greenhouse intervals—with improved preservation of biologic materials transported into a deep-water environment largely devoid of larger organisms.

While macroscale black–green alternations appear to reflect sea-level and climate changes with a periodicity of 3–5 m.y. (Landing et al., 1992), shorter duration climate cycles in the Milankovich band seem to be recorded by asymmetrical, mesoscale Logan cycles in the green-dominated mudstones (Stop 12). Logan cycles, up to 5 m-thick cycles that show an upward decrease in organic content and a corresponding upward increase in carbonate content, are redox cycles known through the Phanerozoic. The significant feature of the macro- and mesoscale color alternations in Taconic slates is that continental slope facies appear to be more sensitive to recording climate changes than adjacent carbonate platform facies.

Route

The route of this field trip (Figure 1) helps emphasize the wealth of geologic history and geologic provinces that are displayed by eastern New York bedrock. The trip originates in Proterozoic basement of the southern Adirondacks (deformed and metamorphosed ca. 1.1 Ga in the Grenvillian orogeny) and ends in the overthrust belt of the Taconic allochthon. This ca. 40 km W–E transect is comparable in geologic content to an excursion beginning in the Proterozoic of the Black Hills massif of South Dakota and ending in the Roberts Mountain allochthon in central Nevada. By this analogy, the route (see geologic map in Fisher, 1984) passes out of the Proterozoic Adirondack basement south of Lake George; crosses the

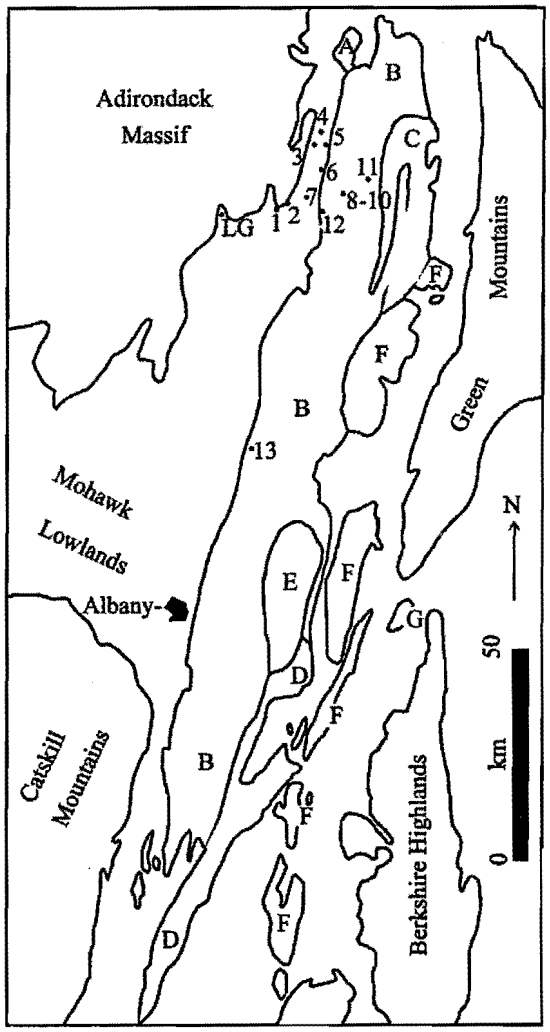

Figure 1. Generalized locality map showing locations of field trip stops (1–13)."LG" is Lake George village; major slices of the Taconic allochthon include A, Sunset Lake; B, Giddings Brook; C, Bird Mountain; D, Chatham, E, Rensselaer Plateau; F, Dorset Mountain–Everett; G, Greylock. Map modified from Zen (1967).

essentially flat-lying (albeit block-faulted) Laurentian Cambrian–Ordovician shelf of southern Warren and western Washington Counties; and then crosses N- and NE-trending block faults that uplift the Proterozoic–Lower Paleozoic in the Whitehall area into a ridge comparable to the Rocky Mountain front range. The narrow belt of deformed autochthonous Cambrian–Ordovician shelf sedimentary rocks east of Whitehall and the Champlain Canal is comparable in geologic position to the Paleozoic succession of the Great Basin. Thrusting of these Cambrian–Ordovician shelf rocks upon themselves on a thrust comparable to the Champlain thrust in the Whitehall area (see mile 31.9 discussion) has an analog in the Sevier belt of central Utah. Finally, the transport of slope and rise facies of the Taconic allochthon onto Laurentia is analogous to the history and facies of the Devonian–Carboniferous Antler orogen of central Nevada–Idaho.

ACKNOWLEDGMENTS

The field and laboratory work that led to this synthesis was first supported by National Science Foundation grant EAR76-10601 and then by the N.Y.S. Museum. The section in the Appendix titled "Revisions in stratigraphic nomenclature—Cambrian–Ordovician platform" is adapted from Landing et al. (2003).

ROAD LOG

A useful map for the route of this trip is the Washington County map published by JIMAPCO (Round Lake, NY), which is available in local gas stations and convenience stores. Fisher's (1984) geologic map is particularly useful. However, some of the stratigraphic names used for Cambrian–Ordovician platform and Taconic units in Fisher (1984) have been subsequently abandoned in favor of older synonyms which help emphasize the regional extent of formation- and member-level units in the Hudson, Mohawk, and Lake Champlain valleys and in the Taconic allochthon (Landing, 1988b; Landing et al., 2003; see also field trip stop discussions and Appendix).

Mileage

0.0 Depart Fort William Henry Resort parking lot. Turn right (South) onto Rte 9. Travel south on Rte. 9 through village of Lake George kitsch. Small road cuts in Grenvillian Proterozoic at south end of village.

3.8 Intersection with Rte 149 at traffic light. Turn left (East).

5.3 At crest of low rise at south end of Proterozoic of French Mountain, note first view of high ridges in Taconic allochthon directly in front of vehicles.

6.5 Road sign shows that vehicles are re-entering Adirondack Park.

8.0 Pass Queenbury Country Club on left. Underlying less resistant Cambrian–Lower Ordovician explains lack of relief.

8.9 Enter Washington County.

9.5 Low road cuts on left (North) in Grenvillian at south end Sugar Loaf Proterozoic inlier.

10.5 Low road cuts in Grenvillian inlier east of Hadlock Pond fault.

13.1 Clear crest of hill and see spectacular view (if weather is clear) of N–S-trending ridges in Taconic allochthon across pastures developed on glacial outwash.

14.5 View to left (NE) of last ridge of Adirondacks east of Welch Hollow fault. East slope is nonconformity surface with lower Upper Cambrian Potsdam Formation eroded off.

14.8 Cross bridge over small creek with medium–massively bedded dolomitic limestone and replacement dolostone. The locally oolitic, thrombolitic, intraclast pebble facies exposed here are more suggestive of the Upper Cambrian Little Falls Formation, rather than the Lower Ordovician Tribes Hill Formation (e.g., "Fort Edward Dolostone" as mapped by Fisher, 1984).

16.4 Enter village of Fort Ann.

16.5 Turn left (North) onto Catharine Street.
16.6 T-junction with Charles Street; turn left (NW) and follow west bank of Halfway Creek.
17.7 Stop and park in unimproved parking lot ca. 75 m south of bridge over Halfway Creek. Walk ca. 90 m to NNE on dirt track to Kane Falls on Halfway Creek.

STOP 1. LOWER ORDOVICIAN AT KANE FALLS: AGE AND LITHOSTRATIGRAPHIC REINTERPRETATIONS. (30 MINUTES). A stratigraphic section for Kane Falls will be distributed on this field trip; this section is available in Landing et al. (2003, fig. 5).

Mazzullo (1974) and Fisher and Mazzullo (1976), respectively, termed the upper part of the Kane Falls sequence a "reference section" for the lower part of the lowest Ordovician "Cutting Formation" and "Great Meadows Formation" (abandoned designations). A planar-laminated silty dolostone 9.55–10.75 m above the base of this 23 m-thick section (Landing et al., 2003, fig. 5) at the top of the falls was regarded as a thin or condensed "Winchell Creek Siltstone" (abandoned term, now Sprakers Member of Tribes Hill Formation; Landing et al., 2002; see Appendix). This interpretation meant that Kane Falls is near the western feather-edge of this lowest "member" of the "Great Meadows" and that a disconformity separated the silty dolostone from the underlying "Whitehall Formation" (abandoned designation, now Little Falls Formation; Landing et al., 2003, see Appendix).

Re-investigation of the Kane Falls section (Landing et al., 2003) led to its re-interpretation. 1) There is no physical evidence for disconformity at the base of the silty dolostone. 2) The medium-gray thrombolitic dolostones and dolomitic limestones of the lower 9.55 m of the section do not resemble the light gray or white thrombolites of the upper Little Falls Formation ("Whitehall") at Steves Farm (Stop 6) or elsewhere in the Lake Champlain Lowlands. These medium-gray thrombolitic facies resemble those in the middle "Fort Ann Formation." 3) Diverse conodonts in the thrombolitic facies and rarer conodont elements in the higher laminated dolostones at Kane Falls are significantly younger than those from the Tribes Hill Formation (="Cutting"/Great Meadows," designations abandoned by Landing et al., 2003). The conodonts from Kane Falls are all referable to middle Lower Ordovician conodont Fauna D of Ethington and Clark (1971), and are comparable to those of the "Fort Ann Formation" elsewhere in the Lake Champlain lowlands.

The "moral" of this stop is the following: Mapping and stratigraphic syntheses on Lower Paleozoic carbonates on the New York Promontory require a combination of a detailed familiarity of lithofacies with adequate micro- and macrofossil investigations to allow age discrimination of broadly similar carbonate platform units.

17.6 At end of stop, return to Fort Ann on Charles Street, pass intersection with Catharine Street.
18.6 T-junction with Rte. 4; turn left (N) and continue on to Whitehall.
19.3 Cross onto uplifted (Proterozoic) block of Welch Hollow Fault and pass by ca. 1 mile of Grenvillian road cuts.
20.3 Stop along road side just south of north exit of Flat Rock Road.

STOP 2. PROTEROZOIC–TERMINAL MIDDLE CAMBRIAN NONCONFORMITY AND THIN LOWER PALEOZOIC SHELF SUCCESSION. (10 MINUTES). Approximately 4 m of east-dipping, medium–coarse grained, slightly dolomitic quartz arenite of the Potsdam Formation nonconformably overlie Grenvillian gneiss with east-dipping exfoliation surfaces. This photogenic locality records the absence of ca. 600 million years of earth history at this planar nonconformity. Flower (1964, p. 156) reported a trilobite fauna (presently unillustrated) approximately 5–6 m above the base of the Potsdam in this area, which he said includes a possible *Crepicephalus* with *Komaspidella,* and *Lonchocephalus*. Following the recent decision (January 2002) of

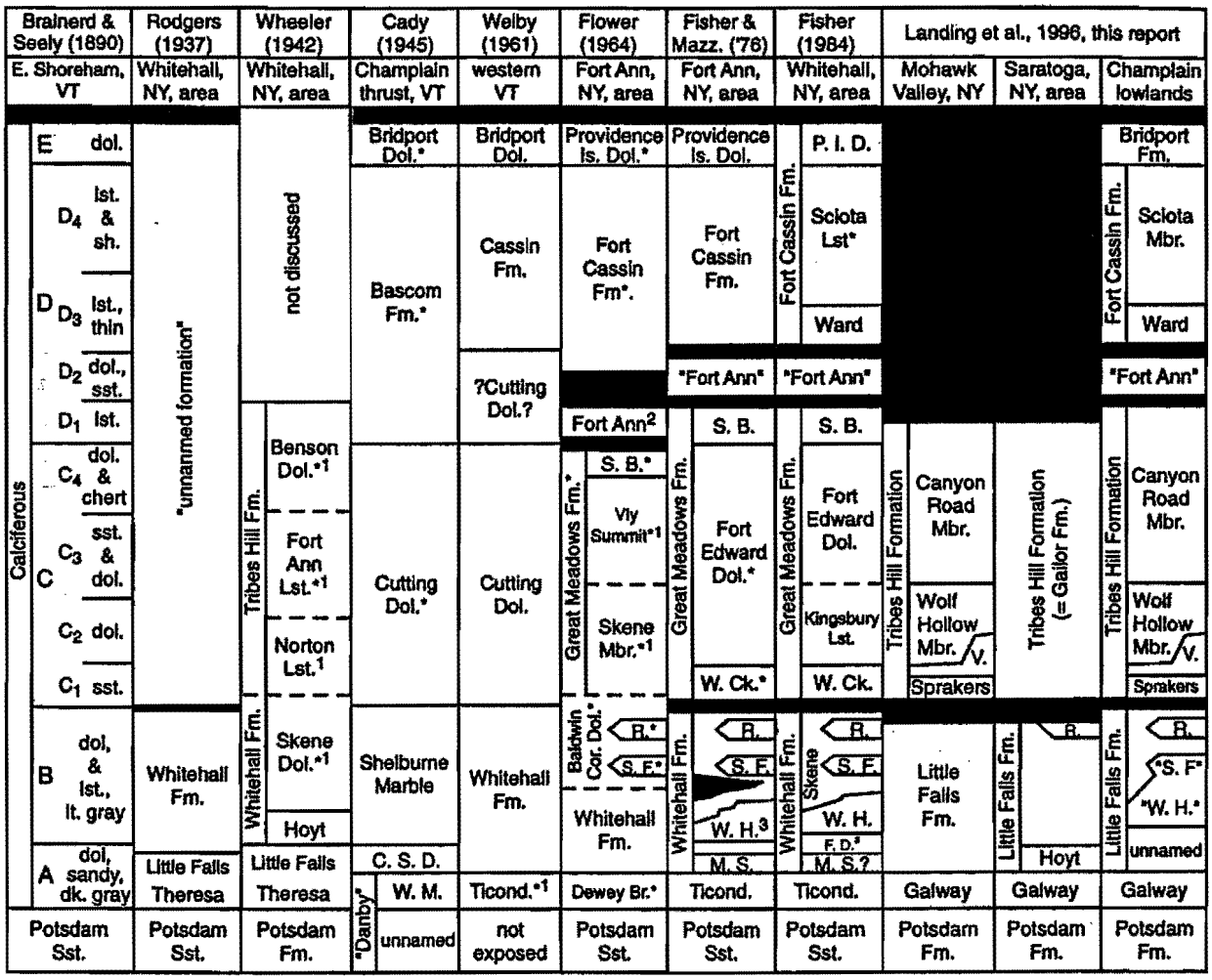

Figure 2. Uppermost Cambrian–Middle Ordovician stratigraphic nomenclature of the Laurentian platform in eastern New York and western Vermont. Cambrian–Ordovician boundary is in hiatus between the Little Falls and overlying Tribes Hill Formations. Presence of *Paraprioniodus costatus-Chosonodina rigbyi-Histiodella holodentata* Interval conodonts (Ethington and Clark, 1981, = conodont Fauna 4 of Sweet et al., 1971) in upper Bridport Formation (E. Landing, unpub. data) indicates that the traditional Beekmantown includes Middle Ordovician. International agreement means that he overlying strata of the Chazy, Black River, and Trenton Groups are now referred to the Upper Ordovician, and the "Knox unconformity" is the lower bracket of the Upper Ordovician. Symbols: asterisk (*) is first proposal of stratigraphic name; superscript 1, inadequate location of type section or description of lithology or contacts; superscript 2, no type section, lithologic description, or contacts provided; superscript 3, unit is junior synonym of earlier named unit, quotation marks, unit not formally recognized in this report. Abbreviations: C. S. D., Clarendon Springs Dolostone; Dewey Br., Dewey Bridge Dolostone; F. D., Finch Dolostone; M. S., Mosherville Sandstone; P. I. D., "Providence Island Dolostone;" R., "Rathbunville School Limestone," Ri., Ritchie Limestone; S.B., Smith Basin Limestone; S.F., "Steves Farm Limestone;" Ticond., Ticonderoga; V, Van Wie Member; W. Ck., Winchell Creek; W. H., Warner Hill Limestone; W. M., Wallingford Member. Figure modified from Landing et al. (2003, fig. 2).

limestone (Canyon Road Member; = "Fort Edward" + "Smith Basin" Members of Fisher [1977] and Flower [1968b]) extend to the top of the Tribes Hill. The top of the Tribes Hill Formation forms the crest of the 132 m (440 foot) hill, and has a paleokarst surface with 30 cm of relief overlain infilled by arenaceous dolostone of the "Fort Ann Formation."

Conodonts from the Tribes Hill Formation comprise a low diversity, restricted marine assemblage that persists unchanged through the formation. This *Rossodus manitouensis* Zone assemblage is referable to the lowest Ordovician (middle–upper Tremadocian-equivalent), and shares no taxa either with the underlying Little Falls Formation or the overlying "Fort Ann Formation." The total replacement of the Upper Cambrian, upper *Cordylodus proavus* Zone fauna of the top Little Falls Dolostone (Stop 6) at the base of the Tribes Hill reflects the duration of the trans-Laurentian Cambrian–Ordovician boundary hiatus on the east Laurentian shelf. Similarly, the total replacement of the Tribes Hill Formation conodonts by Fauna D conodonts at the base of the "Fort Ann Formation" reflects the duration of the trans-Laurentian, intra-Lower Ordovician hiatus that occurs in the Tremadocian–Arenigian boundary interval.

46.0 At end of stop, turn back (East) on Rte 22.
48.3 Intersection with Rte 17A on right (South).
48.5 Enter Town of Granville.
48.8 Intersection with Rte 40.
49.5 Enter village of North Granville and cross into Taconic allochthon.
50.7 Intersection with west exit of Washington Co. Rte 12A, rocks immediately ahead are probably Lower Cambrian Bomoseen Member (argillaceous lithic arenites).

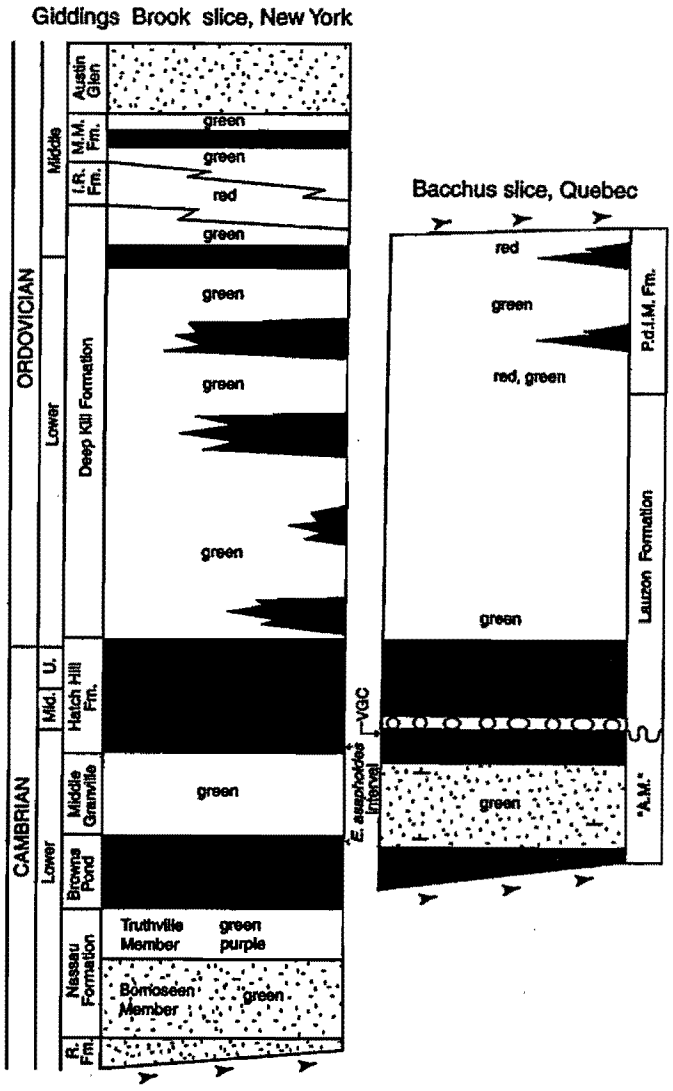

Figure 3. Correlation of proximal (Bacchus slice) and distal (Giddings Brook slice) slope facies in Taconian Quebec and New York, respectively. Figure shows regional extent of dysaerobic black shale-limestone intervals (in black) and more oxygenated, green, purple, and red shale and sand-dominated (dot pattern) facies. Abbreviations: "A.M.", "Anse Maranda Formation;" I.R. Fm., Indian River Formation; M.M. Fm., Mount Merino Formation; P.d.l.M. Fm., Point de la Martiniere Formation; R. Fm., Rensselaer Formation; VGC, *Bicella bicensis* interval at Ville Guay. Black shale-limestone intervals in Point de la Martiniere Formation with middle and upper Arenigian faunas (Rasetti, 1946, p. 698; Landing and Ludvigsen, 1984; Landing et al., 1992). Figure modified from Landing et al. (2002, fig. 3).

51.3 Intersection with east exit of Rte 12A, turn hard left (North).
51.5 Turn right onto Rte 12 in hamlet of Truthville.
51.7 Cross bridge over Mettawee River.
51.8 Turn right (East) onto Middletown Road (dirt).
53.0 Y-intersection with Loomis Road (right), bear left and continue on Middletown Road.
53.3 Intersection with DeKalb Road (paved), turn left (NW) onto DeKalb.
53.4 Intersection with Holcombville Road, turn right (North) onto Holcombville.
54.1 Drive past slate scrap heap and quarry (on left, West) in North Granville Slate.
54.8 Pass Tanner Hill Road on left (West) and continue North.
55.5 Stop just south of Browns Pond at low road cuts on both sides of road.

STOP 8. BROWNS POND: PALEO-OCEANOGRAPHIC CHANGES IN THE LATE EARLY CAMBRIAN. (15 MINUTES). This section may be regarded as the "type locality" for the late Early Cambrian Browns Pond dysaerobic interval on the east Laurentian slope (Landing et al., 2002). The Browns Pond dysaerobic interval is recognized throughout the external thrusts of the Taconic allochthon in New York–Vermont and in Taconian Québec (Figure 3).

This overturned section in the upper Browns Pond Formation shows several meters of dark gray, fine-grained sandstones and slates with thin (decimeter-thick), lensing, sandstone pebble debris flows on the east side of the cut. Small-scale current cross-bedding in the orange-weathering, dolomitic quartz aenites shows that the section is overturned. Although centimeter-wide grazing trails can be found on the top of some of the sandstone beds, burrows are rare, and fine lamination and other primary structures are not disturbed in these rocks. Rare burrows, absence of a shelly fauna, and dark gray (carbonaceous) sediments are all consistent with deposition under dysaerobic conditions (e.g., Sagemann et al., 1991).

The west side of the road cut is dominated by a thick limestone pebble to (rare) boulder clast debris flow with local dark argillaceous matrix. Trilobites, archaeocyathan, mollusk, and calcareous and phosphatic problematica of the lower *Elliptocephala asaphoides* assemblage (see Landing and Bartowski, 1996) appear in the limestone clasts at this locality (Theokritoff, 1964). None of these clasts show derivation from the carbonate platform, and they include nodular lime mudstones and bedded fossil packstones that are interpreted as allodapic clasts that accumulated as limestone on the upper slope. Pyrite-infilled and phosphate-replaced, calcareous conoidal fossils in these clasts (E. Landing, unublished data) is consistent with the deposition/lithification of these limestones in a strongly dysaerobic environment that developed on the upper slope (see Landing and Bartowski, 1996; Landing et al., 2002).

Debris-flow conglomerate lenses are common as the cap unit of the Browns Pond Formation, and some have received local stratigraphic names (e.g., Ashley Hill Conglomerate in Landing, 1984). Locally, allodapic fossil hash packstones and decimeter-thick debris lenses are the cap unit of the Browns Pond (e.g., Landing and Bartowski, 1996). In either case, the conglomerates or bedded limestones are directly overlain by a green/green gray or locally purple or red siliciclastic mudstone unit in the Taconic allochthon. This black–green transition in the late Early Cambrian is seen here at Stop 8 immediately above the conglomerate with the abrupt transition into the lower green slates of the Middle Granville Slate. These green slates form low outcrops in the pasture to the west. Stop 10 further

illustrates this interval of improved oxygenation on the east Laurentian slope and relates the improved oxygenation to the latest Early Cambrian Hawke Bay regression of Palmer and James (1979). Sea-level still-stand and progradation of the shelf margin or sea-level fall at the onset of the Hawke Bay regression are mechanisms to explain the carbonate clast debris flows and allodapic limestones at the top of Browns Pond dysaerobic facies.

55.5 At end of Stop 8, turn south on Holcombville Road.
56.2 Intersection with Tanner Hill Road, turn right (west).
56.4 Park at foot of hill at lowest outcrop of brown-weathering sandstones.

STOP 9. TANNER HILL SYNCLINE:PALEO-OCEANOGRAPHIC CHANGES IN THE LATEST EARLY CAMBRIAN–MIDDLE ORDOVICIAN. (40 MINUTES). The superb Tanner Hill section was first described by Rowley et al. (1979). The walk up hill crosses the overturned east limb of a large syncline.

Dolomitic quartz arenites and interbedded, minor dark gray and black siltstones and shales form the lowest part of the section. The coarse, lensing (apparently channelized), conglomeratic sandstones become thinner bedded and finer grained higher in the section, and black shales become dominant. This entire interval up to an abrupt transition into green-gray mudstones of the overlying Deep Kill Formation is the Hatch Hill Formation. The Hatch Hill records a long interval of persistent dysaerobic deposition on the east Laurentian continental slope (terminal Early Cambrian–lowest Ordovician [early Tremadocian] Hatch Hill dysaerobic interval) (see Landing, 1993; Landing et al., 2002). However, the changes in relative oxygenation of slope waters through this long interval are admittedly poorly known at present. Indeed, the development of three important Upper Cambrian "Grand Cycles" on the northeastern Laurentian shelf (Chow and James, 1987) should have been accompanied by sea-level and climate fluctuations recorded by changes in relative oxygenation on the continental slope. One explanation for the lack of any apparent record for changes in relative oxygenation through this interval may be that the transport and deposition of the thick sandstones that characterize the lower Hatch Hill served to erode and obscure much of the record of relative oxygenation that is recorded elsewhere in the Taconic succession by mudstones of various colors. Even with a maximum estimated thickness of 200 m (Rowley et al., 1979), the 20 m.y. interval bracketed by the Hatch Hill Formation indicates that it is a condensed unit that may have a number of unconformities produced during the transport and deposition of thick sand sheets. These sand sheets may have been emplaced primarily during eustatic lows.

Sandstones disappear in the upper Hatch Hill in the Tanner Hill section. The upper Hatch Hill corresponds to the interval of earliest Ordovician dysarobic mudstone deposition that has been termed "Poultney A" (abandoned designation, Landing, 1988b) by Theokritoff (1959; Zen 1964; see Appendix). A sharp transition from the Hatch Hill Formation into the lowest green-gray mudstones of the Deep Kill can be observed in the drainage ditch on the north side of Tanner Hill Road. Limited outcrop of the Deep Kill Formation likely explains the apparent absence of the black mudstone-limestone mesoscale intervals characteristic elsewhere of the formation (Stops 11, 13; Figure 3).

The transtion into the lowest synorogenic sediments of the Taconic allochthon is observable just west of the crest of the hill with the appearance of low outcrops of the red, thin (ca. 50 m) Indian River Slate. Fisher (1961) attributed the red color of the Indian River to off-slope transport of lateritic sediments produced on the platform during development of the Knox unconformity. However, the rapid development of bacterial films on sediment grains with their transport into marine regimes regularly leads to grayish sediment color, and an alternative explanation for the color of the Indian River must be found. Landing (1988b) noted the multiple lines of evidence (e.g., occurrence of radiolarian cherts and thin volcanic ashes undiluted by background argillaceous sediment; thorough burrow-homogenization of much of the unit; presence of large, up to 3 cm-wide burrowers) in proposing

that the Indian River reflects very slow deposition on an oxygenated sea-floor and long sediment residence time at the sediment-water interface. Cherty red slates are widespread in a number of orogens (e.g., in the Taconian allochthons from New York to western Newfoundland, southern Uplands of Scotland, Hercynian Rheinisches Schiefergebirge and Hart Mountains, and Jurassic of Japan), where they always underlie green mudstones and higher flysch. These data suggest that red, cherty, oxygenated shales in overthrust belts reflect the following history: passage of a peripheral bulge through passive margin successions; consequent flexural uplift and restriction of sedimentation on the peripheral bulge to slowly deposited pelagic muds, radiolarian cherts, and thin volcanic ashes; and final flexural down-warping and increased rates of deposition as sediment provenance changes to the emergent accretionary prism. The transition into the green-dominated, synorogenic mudstones of the overling Mount Merino and then into Austin Glen Formation flysch are present in the core of the Tanner Hill syncline.

56.4 At end of Stop 9, return to Holcombville Road.
56.6 Intersection with Holcombville Road, turn right (South).
57.3 Park at road side opposite slate pile (on East) and next to quarry on right (West).

STOP 10. OXYGENATED MIDDLE GRANVILLE SLATE AND THE HAWKE BAY REGRESSION. (15 MINUTES). This stop serves to fill in the stratigraphic interval between the rocks of Stops 8 and 9.

The large pile of brownish red and minor green slate of Middle Granville Slate on the east side of the road apparently came from the small flooded quarry on the west side of the road. If the light is good, dense *Planolites* traces can be seen on many of the bedding plane-parallel cleavage surfaces of the reddish slate, where they accompany large grazing traces up to 2 cm in width. The abundance of burrows, which led to the general absence of primary depositional structures in the slate, and its reddish color (produced by traces of ferric iron) are consistent with deposition of the Middle Granville Slate under a more oxygenated slope water mass than the underlying Browns Pond Formation.

Landing et al. (2002) noted that the uppermost Lower Cambrian (upper but not uppermost *Olenellus* Zone) on the New York and Québec portions of the eastern Laurentian slope is composed of red and green siliciclastic mudstones. This interval of improved oxygenation of slope waters is equated with the presumed lowered sea-levels, cooler climates, and deeper circulation of oxygenated surface waters during Palmer and James' (1971) Hawke Bay regression. Subsequent sea-level rise and the re-establishment of dysaerobic slope facies (e.g., Hatch Hill Formation and Hatch Hill dysaerobic interval) took place in the terminal Early Cambrian. This Lower–Middle Cambrian boundary interval eustatic rise and climate amelioration led the actual movement of poorly oxygenated slope water onto the continental shelf in such widely separated areas as northern Vermont (Parker Slate) and eastern California (Mule Springs Formation) (Landing and Bartowski, 1996).

57.3 At end of stop, continue south on Holcombville Road.
57.9 Intersection of Holcombville Road with DeKalb Road, turn left (SE) on DeKalb.
58.0 Pass intersection with Middletown Road, continue on DeKalb.
59.5 T-intersection with Steeles Bridge Road, turn right (South) over Mettawee River bridge.
59.7 Intersection with Rte 22A, turn hard left (North) onto Rte 22A.
57.9 Cross Mettawee River again.
58.8 Pass cut in slates and limestone at Raceville.
59.0 Park on right side of Rte 22A just north of road cut. Walk back to cut.

Potter, D.B., 1972, Stratigraphy and structure of the Hosick Falls area, New York–Vermont, east-central Taconics: New York State Museum, Map and Chart Series, 19, 71 p.

Rasetti, F., 1946, Cambrian and Early Ordovician stratigraphy of the Lower St. Lawrence Valley: Geological Society of America Bulletin, v. 57, p. 687–706.

Rodgers, J., 1937, Stratigraphy and structure in the upper Champlain Valley: Geological Society of America Bulletin, v. 48, p. 1573–1586.

Ross, C.A., and Ross, J.R.P., 1995, North American Ordovician depositional sequences and correlations, *in* Cooper, J.D., Droser, M.L., and Finney, S.C., eds., Ordovician Odessey: Short Papers for the Seventh International Symposium on the Ordovician System: Society for Economic Paleontology and Mineralogy, Pacific Section, Fullerton, CA, p. 309–313.

Rowley, D.B., Kidd, W.S.F., and Delano, L.L., 1979, Detailed stratigraphic and structural features of the Giddings Brook slice of the Taconic allochthon in the Granville area, *in* Friedman, G.F., ed., Guidebook for field trips: New York State Geological Association 51st Annual Meeting and New England Intercollegiate Geologic Conference 71st Annual Meeting, Troy, NY, p. 186–242.

Ruedemann, R., 1902, The graptolite (Levis) facies of the Beekmantown Formation in Rensselaer County, New York: New York State Museum Bulletin, v. 52, p. 546–575.

Ruedemann, 1903, The Cambric *Dictyonema* fauna in the slate belt of eastern New York: New York State Museum Bulletin, v. 69, p. 934–958.

Ruedemann, R., 1919, The graptolite zones of the Ordovician shales of New York: New York State Museum Bulletin, v. 227–228, p. 116–130

Ruedemann, R., and Cook, J.H., 1930, Geology of the Capital District (Albany, Cohoes, Troy, and Schenectady quadrangles): New York State Museum Bulletin, v. 285, 218 p.

Ruedemann, R., Cook, J.H., and Newland, D.H., 1942, Geology of the Catskill and Kaaterskill quadrangles: Part 1. Cambrian and Ordovician geology of the Catskill quadrangle: New York State Museum Bulletin, v. 331, 251 p.

Sageman, B.B., Wignall, P.B., and Kauffman, E.G., 1991, Biofacies models for oxygen-deficient facies in epicontinental seas: Tool for paleoenvironmental analysis, *in* Einsele, G., Ricken, W., and Seilacher, A., eds., Cycles and Environments in Stratigraphy: Springer-Verlag, New York.

Taylor, M.E., and Halley, R.B., 1974, Systematics, environment, and biogeography of some Late Cambrian and Early Ordovician trilobites from eastern New York state: U.S. Geological Survey, Professional paper 834, 38 p.

Theokritoff, G., 1959, Stratigraphy and structure of the Taconic sequence in the Thorn Hill and Granville quadrangles, *in* New England Intercollegiate Geologic Conference, 51st Annual Meeting, Rutland, VT, p. 53–58.

Theokritoff, G., 1964, Taconic stratigraphy in northern Washington County, New York: Geological Society of America Bulletin, v. 75, p. 171–190.

Thomas, W.A., 1977, Evolution of the Appalachian–Ouachita salients and recesses from reentrants and promontories in the continental margin: American Journal of Science, v. 277, p. 1233–1278.

Ulrich, E.O., and Cushing, H.P., 1910, Age and relationships of the Little Falls Dolostone (Calciferous) of the Mohawk Valley. New York State Museum, Bulletin 140, p. 97–140.

Webby, B.B., 1998, Steps toward a global standard for Ordovician stratigraphy: Newsletters in Stratigraphy, v. 36, p. 1–33.

Welby, 1961, Bedrock geology of the central Champlain Valley of Vermont: Vermont Geological Survey, Bulletin 14.

Westrop, S.R., Knox, L.A., and Landing, E., 1993, Lower Ordovician (Ibexian) trilobites from the Tribes Hill Formation, central Mohawk Valley, New York state: Canadian Journal of Earth Sciences, v. 30, p. 1618–1633.

Westrop, S.R., Trembley, J.V., and Landing, E., 1995, Declining importance of trilobites in Ordovician nearshore communities: Dilution or displacement?: Palaios, v. 10, p. 75–79.

Wheeler, R.R., 1942, Cambrian–Ordovician boundary in the Adirondack-border region: American Journal of Science, v. 240, p. 518–524.

Williams, H., 1978, Tectonic lithofacies map of the Appalachian orogen: Map 1, Memorial University of Newfoundland, St. John's.

Wilmarth, M.G., 1938, Lexicon of geologic names of the United States (including Alaska): U.S. Geological Survey, Bulletin 896, 2396 p.

Xu G-H. and Lai C.-G., 1983, Cephalopods from the Sanyuodong Group of Yichang, Hubei Province: Bulletin of the Yichang Institute of Geology and Mineral Resources, v. 6, p. 183–206.

Zen, E., 1964, Taconic stratigraphic names: Definitions and synonymies: U.S. Geological Survey, Bulletin 1174, 95 p.

Zen, E., 1967, Time and space relationships of the Taconic allocthon and autochthon: Geological Society of America, Special paper 97, 107 p.

Zenger, D.H., 1981, Stratigraphy and petrology of the Little Falls Dolostone (Upper Cambrian), east-central New York: New York State Museum, Map and Chart 34, 138 p.

APPENDIX

Revisions in Stratigraphic Nomenclature—Cambrian–Ordovician Platform

Tectonic setting and stratigraphic nomenclature. An apparently uniform Upper Cambrian–Lower Ordovician lithostratigraphy occurs in authochthonous sequences on the west side and south end of the Lake Champlain lowlands and in the parautochthonous Champlain slice in west-central Vermont (e.g., Fisher, 1984; Fig. 1). However, a confusing stratigraphic nomenclature obscures the regional extent of lithic units and the simple Early Paleozoic evolution of this stretch of the New York Promontory. This complexity reflects the proposal of synonymous units in New York and Vermont, usually without designation or description of type sections, detailed lithic characteristics, or upper or lower contacts. These contacts were often changed arbitrarily, and lateral correlations were commonly established by assertion rather than by biostratigraphic or lithostratigraphic analyses (Fig. 2).

Tribes Hill, "Cutting" (abandoned), and "Great Meadows" (abandoned) Formation. Ulrich and Cushing's (1910) and Wheeler's (1942) attempts to apply a unified stratigraphic nomenclature to the Upper Cambrian–Lower Ordovician of the Mohawk valley and southern Lake Champlain lowlands showed a great appreciation for the lateral continuity of stratigraphic units in this part of the New York Promontory. Although dismissed without adequate discussion by Fisher and Mazzullo (1976, p. 1443), Ulrich and Cushing's and Wheeler's recognition of the "Tribes Hill Formation" (Ulrich and Cushing, 1910) as a unit that extends from its Mohawk River valley type area into the Lake Champlain lowlands is appropriate. The "Cutting/Great Meadows Formation" of the Lake Champlain lowlands rests unconformably on latest Cambrian carbonates and forms a deepening–shoaling sequence in the *Rossodus manitouensis* Zone. These stratigraphic relationships are identical to those of the coeval Tribes Hill Formation in theMohawk River valley (see Landing et al., 1996). The vertical succession of facies in the Cutting/Great Meadows" in the Lake Champlain lowlands is also so similar to those of the Tribes Hill in the Mohawk valley that the same member-level nomenclature is appropriate (discussed below). These lithologic correspondences mean that "Cutting Formation" and "Great Meadows Formation" must be abandoned for the older synonymous term "Tribes Hill Formation."

Members of the Tribes Hill Formation. Landing et al. (1996) proposed the Sprakers Member for lower Tribes Hill strata that extend upward from the unconformity with the Little Falls Formation to a shale-dominated reentrant

(Van Wie Member of Landing et al., 1996) under the cliff-forming Wolf Hollow Member of Fisher (1954). The Sprakers changes laterally from intertidal carbonates and overlying wave-deposited fossil grainstones and calcisiltites in the western Mohawk valley into micro-cross-laminated silty dolostones and fine-grained dolomitic sandstones in the east (Landing et al., 1996, fig. 2, Hoffmans section). The Sprakers Member at Hoffmans is lithologically similar to Fisher and Mazzullo's (1976) "Winchell Creek Siltstone."

Dark shales with lenticular intraclast and calcisiltite beds of the thin (ca. 1.5 m) Van Wie Member mark the maximum highstand of Tribes Hill deposition in the Mohawk valley (Landing et al., 1996; Landing, 1998). Similar, dark, pyritiferous silt shale and lenticular dolomitic sandstones with bidirectional (wave-generated) cross beds in the upper "Winchell Creek Siltstone" at Tristates Quarry and Comstock (Stops 5, 7) are referred herein to the Van Wie Member (Figure 2). The Tribes Hill is thicker in the Lake Champlain lowlands (e.g., 69 m at Comstock vs. 30 m in the Mohawk valley), and the stratigraphic distance from the top of the Van Wie to the lowest thrombolites is also somewhat more [4.5 m and 10 m at Tristates Quarry and Comstock (Fig. 3) vs. 1.0–4 m in the Mohawk valley; Landing et al., figs. 2, 3]. Interestingly, a lenticular quartz arenite dune in the middle Van Wie at Comstock and Tristates Quarry seems to correspond to the intraclast pebble storm bed in the middle Van Wie in the Mohawk valley (Landing et al., 1996, figs. 2, 3).

Recognition of the Sprakers and Van Wie members as divisions of the lower–middle "Winchell Creek Siltstone" (Fisher and Mazzullo, 1976; abandoned herein) means that a Winchell Creek-type facies reappears above the Van Wie and is transitional into the cliff-forming, thrombolitic facies in the middle Tribes Hill. Fisher (1962b; Fisher and Mazzullo, 1976) referred the carbonate-rich interval of the middle–upper "Great Meadows" to a "Fort Edward Dolostone" member without designating a type section in the Middle Ordovician flysch terrane of the Fort Edward, NY, area. Fisher (1984) later "undesirably restricted" (see North American Stratigraphic Commission, 1983) the "Fort Edward" by separating out the lower thrombolitic interval as a "Kingsbury Limestone" and retaining "Fort Edward" for the remainder. This restriction created an objective homonym of "Fort Edward" in Fisher's (1977, 1984) own publications.

Thrombolites appear only in the upper Wolf Hollow Member in the Mohawk valley (Landing et al., 1996). This highstand facies is now recognized above the Van Wie Member in the Lake Champlain lowlands (Figure 2). The Wolf Hollow Member is recognized as the senior synonym of the upper "Winchell Creek", "Kingsbury," and "Fort Edward" Members (all units abandoned) in the Lake Champlain lowlands, where it extends from the top of the Van Wie to the top of the thrombolite build-ups, as in the Mohawk valley.

The Canyon Road Member (Landing et al., 1996), which is the upper member of the Tribes Hill Formation in the Mohawk valley, includes lower intraclast-fossil hash beds and higher evaporitic dolostones above the highest Wolf Hollow thrombolites (Landing et al., 1996). A similar, carbonate-dominated, aggradational or progradational highstand facies is marked in the Lake Champlain lowlands by replacement of Wolf Hollow thrombolite build-ups by overlying ooid wackestones and higher, mollusk-rich lime mudstone. This lime mudstone is Flower's (1968a) "Smith Basin Limestone" (see Stop 7 discussion). The most appropriate stratigraphic designation for the entire supra-thrombolite, carbonate-dominated interval of the upper Tribes Hill Formation in the Mohawk valley and Lake Champlain lowlands is "Canyon Road Member." "Smith Basin Limestone" is regarded as an informal submember for the massive lime mudstone unit of the uppermost Canyon Road Member in the Lake Champlain lowlands.

Little Falls, Galway, "Ticonderoga" (abandoned), and "Whitehall" (abandoned) Formations. Rodgers (1937) proposed "Whitehall Formation" for a temporally-defined, carbonate-dominated, lowest Ordovician unit in the Lake Champlain Lowlands (Fig. 2). His "Whitehall" overlay an unfossiliferous, but presumably, Upper

Cambrian interval referred to the Little Falls Formation of Clarke (1903) in the Lake Champlain Lowlands. However, the "Whitehall" and Little Falls Formations unconformably underlie the Tribes Hill Formation in the Lake Champlain Lowlands and Mohawk Valley, respectively, and both "units" are now known to range only into the uppermost Cambrian. The "Whitehall" ranges into the uppermost *Cordylodus proavus* Zone (Landing et al., 2003), and the Little Falls in the Mohawk valley ranges into the middle *C. proavus* Zone (Landing et al., 1996). The Little Falls Formation has always been regarded as a carbonate-dominated (now largely dolomitized) unit that overlies a mixed dolostone and quartz arenite "transitional facies" (i.e., the Galway Formation of Fisher and Hansen, 1951) above Potsdam Formation quartz arenites in the Mohawk valley (e.g., Wilmarth, 1938, p. 1194–1196; Zenger, 1981). Similarly, the "Whitehall" overlies the mixed dolostone and quartz arenite facies of the "Ticonderoga Formation" (J. Rodgers *in* Welby, 1961; abandoned by Landing et al., 2003; a junior synonym of Galway Formation in Figure 2), and the latter overlies the Potsdam in the Lake Champlain lowlands. These data on lithologic composition, upper and lower contacts, and age support Ulrich and Cushing's (1910) recognition of the Little Falls Formation (="Whitehall Formation," abandoned) and the replacement of "Ticonderoga" by Galway Formation in the Lake Champlain lowlands.

"Fort Ann Formation." "Fort Ann Formation" is used provisionally for a carbonate-dominated, middle Lower Ordovician unit in the Lake Champlain lowlands that unconformably overlies the Tribes Hill Formation and (probably) unconformably underlies the Ward Siltstone member of the upper Lower Ordovician Fort Cassin Formation (see Fisher, 1984; Brett and Westrop, 1996). The checkered history of "Fort Ann" (Fig. 2) includes its proposal as an undescribed middle member of the Tribes Hill Formation (Wheeler, 1942), and its redefinition (Flower, 1968b) as a formation above the Tribes Hill (i.e., "Great Meadows") Formation in the Lake Champlain lowlands. Thus, the designation "Fort Ann" is an objective homonym in several important early publications that sought to establish a uniform stratigraphic momenclature in the Lake Champlain Lowlands. No type section has been designated for the "Fort Ann," and Fort Ann village itself is surrounded by Middle Ordovician flysch. "Fort Ann" is a depositional sequence that corresponds to the conodont Fauna D interval of the Lake Champlain lowlands and requires a new stratigraphic name (Fisher and Mazzullo, 1976, fig. 5; Fisher, 1977; EL, unpubl. data).

Revisions in Stratigraphic Nomenclature—Taconic Allochthon

A dismaying number of stratigraphic names has been generated for Cambrian–Ordovician units along the ca. 200 km length of the Taconic allochthon from Sudbury, Vermont, to Beacon, near Poughkeepsie, New York (see Zen, 1964). In part, this practice has been a natural consequence of problems involving correlation into the more highly metamorphosed higher (and eastern) thrust slices. However, it is unfortunate, in particular, that separate nomenclatural schemes exist for the northern, central, and southern parts of the Giddings Brook slice (see Zen, 1964; Fisher, 1977) because adequate outcrops and biostratigraphic controls allow reconstruction of the stratigraphic succession and detailed correlations along the length of the slice.

The tectonic history of the Giddings Brook succession (i.e., rift margin feldspathic quartz and lithic arenites [latest Precambrian?–Early Cambrian Rensselaer Formation], Early Cambrian–Middle Ordovician passive margin slope deposits that record sea-level and paleo-oceanographic changes correlateable for long distances along along the slope [Stops 8–13], and progressive evidence for convergence beginning in the Middle–Upper Ordovician [Indian River–Austin Glen formations, Stop 9] led to a uniform stratigraphy that can be recognized in the Sunset Lake, Giddings Brook, and Bird Mountain slices (Landing 1988b). In general, the lithostratigraphic scheme outlined by Rowley et al. (1979) in the northern part of the Giddings Brook slice is appropriate for the external slices. Two exceptions to this scheme were noted by Landing (1988b):

Deep Kill Formation and its synonyms. "Deep Kill Formation" (Ruedemann, 1902) is the senior synonym for the "Schaghticoke Shale" (Ruedemann, 1903; Stop 13); "Poultney Slate" (Keith 1932), particularly "Poultney B and C" of Theokritoff (1959; Zen, 1967); and "Stuyvesant Falls Formation" (Craddock, 1957; Fisher, 1961, 1962). Although Fisher (1961) incorrectly argued that Ruedemann (1902) defined the Deep Kill as a biostratigraphic unit from what is now known to be two slices at the sole of the Taconic master thrust, Ruedemann (1919), Ruedemann and Cook (1930) and Ruedemann et al. (1942) emphasized the "Deep Kill Shale" as a greenish-gray mudstone-dominated, lithologic and map unit of Early Ordovician age (now known to range into the early Middle Ordovician; Landing, 1976) in the central and southern Taconics.

As noted in this field trip and in Landing et al. (1992), the Lower Ordovician, macroscale black shale-limestone–green shale alternations at the type section of the Deep Kill Formation, are recognizeable in "Poultney B and C" and the "Stuyvesant Falls." Considerable confusion has always attended mapping of the black mudstone-dominated interval termed "Poultney A" by Theokritoff (1959; see Zen, 1964, p. 65; Stop 8). Its definition was primarily biostratigraphic, with the assignment of this black shale-limestone interval as a lowest "Poultney Shale" "member" solely on the basis of its Early Ordovician age. "Poultney A" is not distinguishable from the upper "Germantown Formation" and "West Castleton Formation" (Zen, 1964, p. 65), and the latter three units have been abandoned and synonymized with the Hatch Hill Formation (Landing 1988b).

Austin Glen and "Pawlet" Formations. A second problem is posed by names applied to the Upper Ordovician synorogenic flysch because interpreted tectonic setting has influenced nomenclature. "Pawlet Formation" has been used in the northern Taconics (e.g., Rowley et al., 1979) to refer to flysch in stratigraphic continuity with the allochthonous Taconic sequence, and "Austin Glen" has been preferred for coeval "parauthchthonous"? or allochthonous flysch at the leading edge of the allochthon (Potter, 1972; Fisher, 1977). Lithologic similarity of this medium- to massively-bedded arenite-dominated unit within and along the leading edge of the allochthon and the onset of its deposition late in the early Late Ordovician (upper *Nemagraptus gracilis* Chron) lead to the conclusion that Austin Glen Formation is a senior synonym of "Pawlet Formation" (abandoned designation; Landing, 1988a).

DACRYOCONARID BIOEVENTS OF THE ONONDAGA FORMATION AND THE MARCELLUS SUBGROUP, CHERRY VALLEY, NEW YORK

RICHARD H. LINDEMANN

Department of Geosciences
Skidmore College
Saratoga Springs, New York 12866

INTRODUCTION

The Order Dacryoconarida Fisher 1962 is a taxon of extinct and enigmatic conical microfossils that occur in marine strata of the Devonian System. Although the taxonomic status of the group and its phylogenetic affinities are not universally agreed upon, unequivocal dacryoconarids (dacs) range from upper Lochovian strata to the Frasnian-Famennian mass extinction boundary. Regardless of their biologic affinities, the organisms themselves are understood to have been marine animals, which were predominantly planktic in habit and pelagic in habitat.

Within the region of the Old Word Realm, the dacs are represented by more than thirty genera and scores of species from which sets of biozones have been developed rivaling those of the conodonts in their detail and temporal resolution (see Lutke, 1979, 1985; Alberti, 1993; Oliver and Chlupac, 1991; Weddige, 1998). Old World dacs are also diagnostic of several Devonian bioevents, most notably for present purposes the lower Eifelian Chotec Event and the upper Eifelian Kacak-*otmari* Event(s). Such is not the case in the Devonian of eastern North America where the dacs have been afforded little attention, and the stratigraphic ranges of the few known species are themselves incompletely documented. It is the purpose of this field trip to introduce participants to dacryoconarid genera and bioevents as they are currently understood to be recorded in the Onondaga Formation and the Marcellus Subgroup at Cherry Valley, New York (CVNY).

STRATIGRAPHIC SETTING

The focus to this field trip is the occurrence of dacryoconarids within the interval of the Onondaga Formation and the Marcellus Subgroup as they are known from a nearly complete composite section of exposures (Fig. 1) on and adjacent to U.S. Route 20 at Cherry Valley, New York (Sprout Brook, NY. 7.5' quad.). Descriptions of the subjacent Esopus and Carlisle Center (= Schoharie) Formations are provided to broaden the biostratigraphic picture and to facilitate the reporting of dacs, which have recently been discovered in these units at other localities. The lithostratigraphic terminology used herein is an amalgam of that used by Rickard (1975, 1981) and a set of revisions proposed by Ver Straeten and Brett (1995). See Oliver and Klapper (1981), Anderson et al. (1986), or Griffing and Ver Straeten (1991) for additional information on these units and outcrop locality.

Esopus Formation

This is a 7 m thick unit of dark gray shale and medium bedded, gray to black chert (Fig. 1). Whereas the chert contains a sparse and poorly preserved set of gastropods and brachiopods, the ichnofossil *Zoophycos* abounds in the shale (Rickard and Zenger, 1964). *Chondrites*, tsamanitids and rare specimens of *Tentaculites* are also present in the shale at CVNY, and siliceous sponge spicules have been observed in thin sections of the chert. Dacryoconarids are currently unknown from the Esopus at this locality, as well as from all units beneath it.

Carlisle Center Formation

This is a 14 m thick unit of buff-weathering, medium-gray, calcareous, glauconitic, fine-grained quartz arenite (Fig. 1). The strata were pervasively bioturbated by *Zoophycos* in conjunction with a diversity of vertical burrowers. Both the lower and the upper contacts of the unit are abrupt and disconformable.

The Carlisle Center of Rickard (1975) is deemed to be a member-rank condensed equivalent of the Schoharie Formation (Ver Straeten and Brett, 1995). Although Johnson et al. (1985) regarded both the

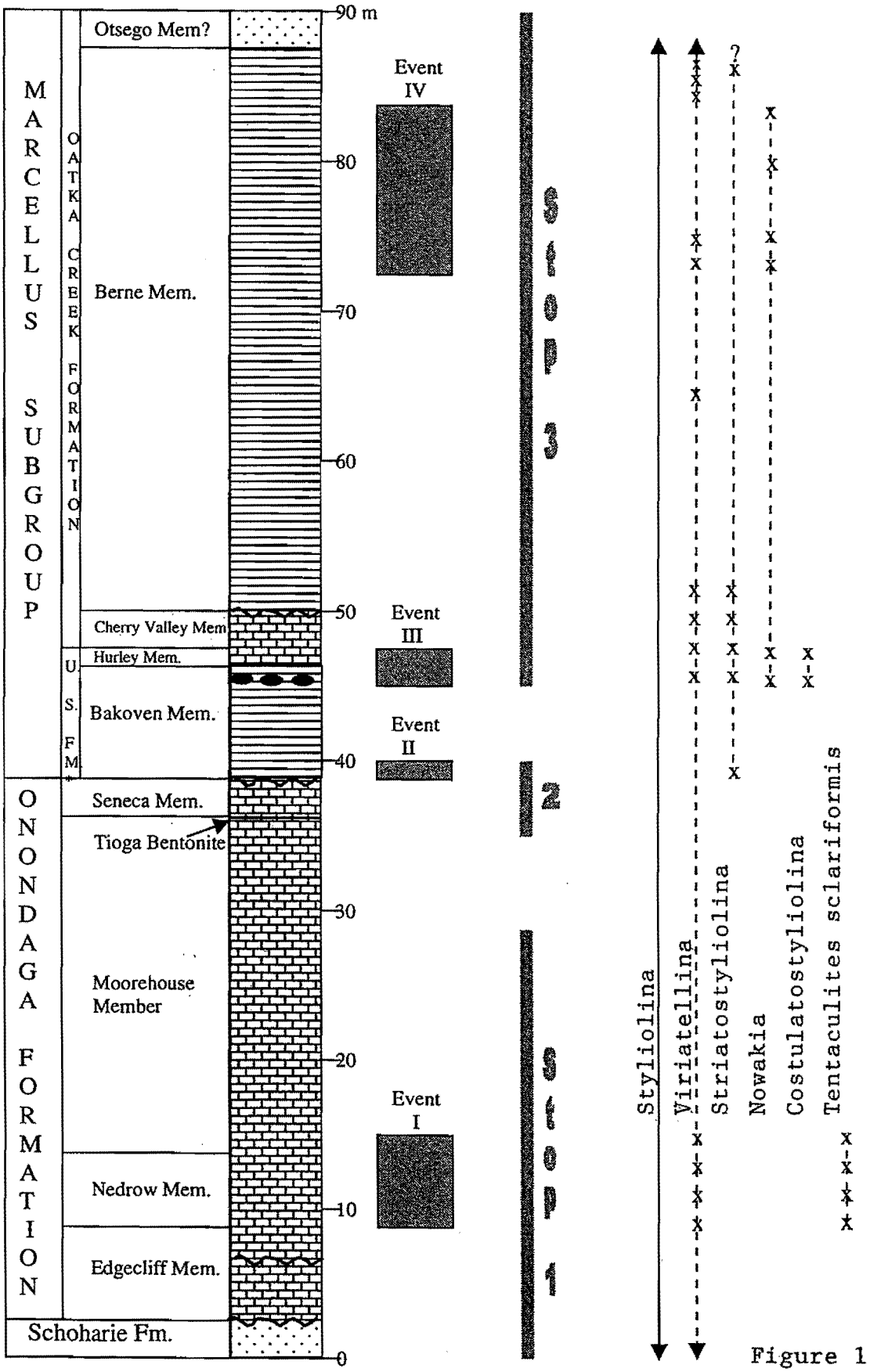
MARCELLUS SUBGROUP
ONONDAGA FORMATION
OATKA CREEK FORMATION
U. S. FM.
Otsego Mem?
Berne Mem.
Cherry Valley Mem
Hurley Mem.
Bakoven Mem.
Seneca Mem.
Tioga Bentonite
Moorehouse Member
Nedrow Mem.
Edgecliff Mem.
Schoharie Fm.
90 m
80
70
60
50
40
30
20
10
0
Event IV
Event III
Event II
Event I
Stop 3
Stop 2
Stop 1
Styliolina
Viriatellina
Striatostyliolina
Nowakia
Costulatostyliolina
Tentaculites sclariformis
?

Figure 1

Esopus and the Carlisle Center to be correlative with Transgressive-Regressive (T-R) Cycle Ib, they regarded the Schoharie and its western New York/Ontario equivalent, the Bois Blanc Limestone, to represent the transgressive phase of T-R Cycle Ic. Acknowledging that there are uncertainties in precise correlation between the Carlisle Center and its Schoharie-Bois Blanc equivalents, particularly in its upper contact, the entire interval is regarded to lie within the *Polygnathus serotinus* conodont zone (Klapper, 1981). Thus, according to the criteria of Ziegler and Klapper (1985) and Oliver and Chlupac (1991), the Carlisle Center is referred to the upper Emsian Stage of the Lower Devonian Series.

Onondaga Formation

This unit is a 37m interval of limestones and chert (Fig. 1), which is divided into four members (Oliver, 1954, 1956) described here in ascending order. The Onondaga is correlative with T-R Ic (Johnson et al., 1985).

The Edgecliff Member typically consists of thick- to massive-bedded, light-gray, coarse-grained grainstones and packstones. The basal bed of the Edgecliff contains well-rounded quartz sand, glauconite, and phosphate nodules. These nodules range in size from granules to cobbles and usually bear numerous borings. Some sectioned specimens show concentric generations of phosphitization and boring, suggesting a polycyclic history of deposition and exhumation prior to final burial. These observations have bearing upon the magnitude and history of the unconformity at the Carlisle Center-Edgecliff contact, which have yet to be satisfactorily worked out. The uppermost bed of the Edgecliff is a packstone (poorly washed biosparite), which contains large (0.5-1.5 cm) nodules of iron pyrite. This appears to be a hardground surface and to represent a minor unconformity at the top of the member (Wolosz et al., 1991).

The lowermost bed of the Nedrow Member is a laminated, argillaceous wackestone (fossiliferous micrite), which abruptly overlies the uppermost Edgecliff. This lowermost argillaceous Nedrow bed is a meter-scale interval, which grades upward into a cleaner wackestone (sparse biomicrite). This coarsening-upward cycle is repeated twice at this locality and five or more times at localities in central and western New York. Based on observations of the member in central New York, Oliver (1954, p. 633) referred to the more argillaceous Nedrow facies as "Zone D" and the coarser-grained facies as "Zone E" and reported a particularly diverse and abundant ostracode fauna in the former. For present purposes it is noteworthy that Oliver (1954, 1956) did not report the occurrence of *Tentaculites scalariformis* within the Nedrow from any locality in the state. Rickard (in Oliver and Klapper, 1981) reported the co-occurrence of the conodonts *Polygnathus costatus patulus* and *P. costatus costatus* 2.3-2.6 m above the base of the Nedrow at CVNY. The stratigraphic overlap of these two taxa occurs only in the lower part of the *costatus* Zone and above the first occurrence of *P. costatus partitus* (Ziegler and Klapper, 1985), an index taxon that is not know to occur in New York (Klapper, 1981).

The Moorehouse Member is an interval of medium-bedded, medium- to dark-gray wackestones and mudstones that contain nodules and thin beds of dark-gray to black chert. At CVNY, the lower Moorehouse includes two sub meter-scale coarsening upward intervals, which are reminiscent of the Nedrow cycles below, though the Moorehouse cycles are thinner and less argillaceous than their Nedrow counterparts. This theme is repeated again higher in the member. Working in the formation's type area of central New York, Oliver (1954, p. 628) referred to the fine-grained intervals of the Moorehouse as "Zone G," and noted that this facies marked a return to a Nedrow-like "Zone D" environment. In the "Zone G" faunal list Oliver (1954, p. 634) reported an abundance of ostracodes, the inarticulate brachiopod *"Discina" minuta*, and very rare specimens of *Tentaculites scalariformis*. The upper beds of the Moorehouse at CVNY are thickly-bedded, light- to medium-gray packstones. The Moorehouse is separated from the atypical massive, medium-gray packstones and grainstones of the Seneca Member by the Tioga Bentonite (= Tioga B of Way et al., 1986). The Seneca is disconformibly overlain by the Bakoven Shale. Although this contact is not exposed at Cherry Valley, NY, it is (sometimes) observable nearby at Optional Stop A and in proximity to Optional Stop B.

Figure 1. Stratigraphic section of interest at Cherry Valley, New York showing lithostratigraphic units, Dacryoconarid Event intervals, field trip stop intervals, and the local range zones of selected dacryoconaids plus *Ttentaculites scalariformis*. Note: The ~~~~ symbol shown in the Edgecliff Limestone should be at be at the Edgecliff-Nedrow contact.

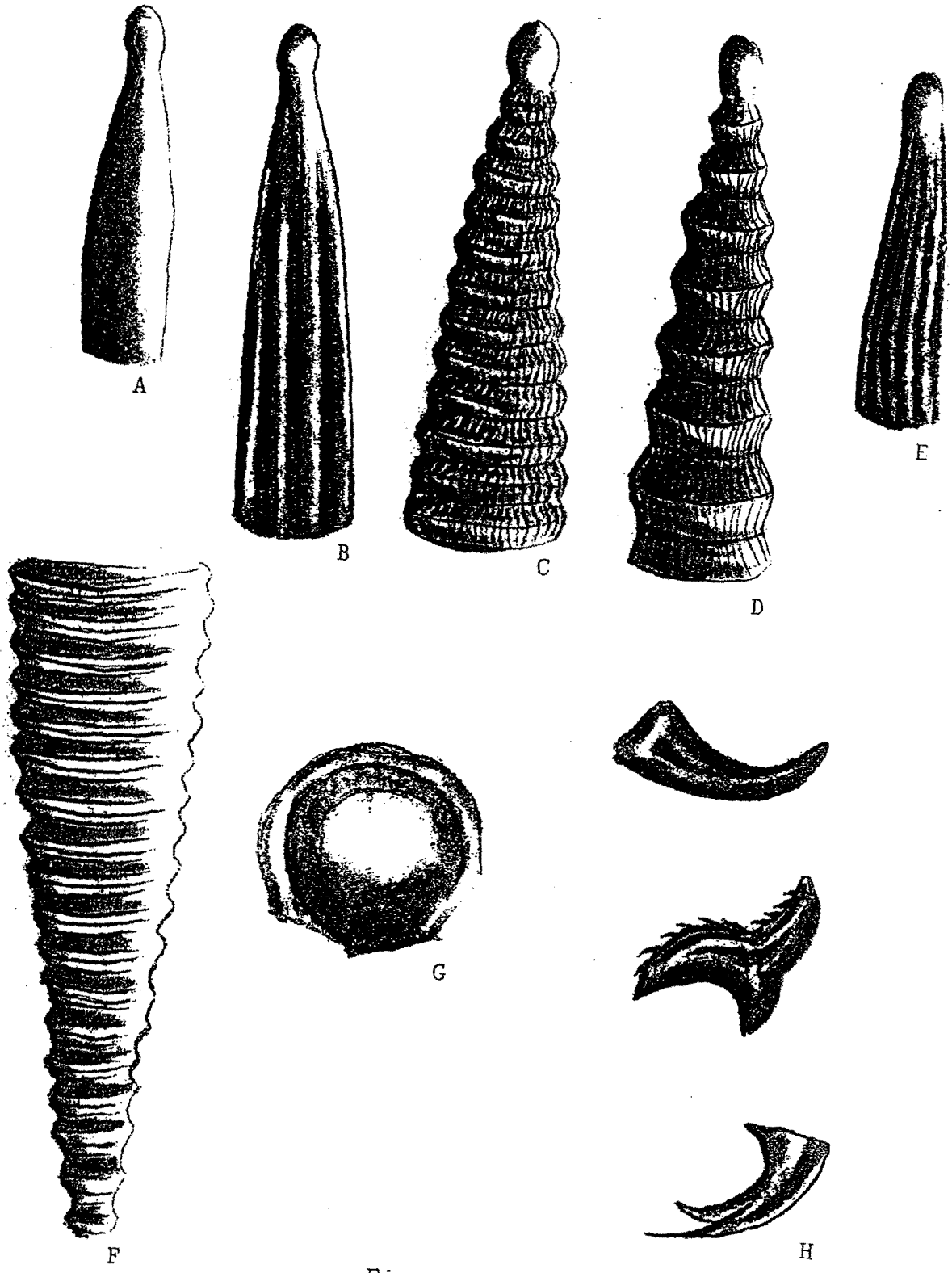

Figure 2

Marcellus Subgroup

In the traditional lithostratigraphic terminology of New York, the Onondaga Formation is overlain by the Marcellus Formation, the basal unit of the Hamilton Group (Rickard, 1975, 1981). Within this classification, the Union Springs Member is the lowermost shale unit of the Marcellus Formation throughout much of the state. The upper Marcellus shale unit is referred to as either the Oatka Creek, Chittenango, or Mount Marion depending on whether one is working in the western, central, or eastern parts of the state. Sandwiched between the two shale units is the Cherry Valley Limestone of Rickard (1952), which was originally referred to as the "Goniatite limestone" by Vanuxem (1842).

Ver Straeten et al. (1994) proposed a revision to this traditional hagiography in which the Marcellus is elevated in rank to "subgroup" status and both Union Springs and Oatka Creek (= Mount Marion) are elevated to the rank of "formation" (Fig. 1). Accordingly, at CVNY, the Union Springs Formation includes the Bakoven and Hurley Members (Fig. 1). The Bakoven Member is a carbonaceous black shale with calcareous concretions in its upper 1.5 m. At this location, the Hurley Member includes a lower 10-25 cm interval of packstone and an upper 3-8 cm interval of gray to black shale, which Ver Straeten and Brett (1995) refer to respectively as the Chestnut Street and Lincoln Park submembers. The Bakoven Member is assigned to the *Tortodus kockelinaus australis* conodont zone and, the Hurley Member lies within the lower part of the *T. kockelinaus kockelianus* zone (Klapper, 1981). The Union Springs Formation, as a whole, was deposited during T-R Cycle Id (Johnson et al., 1985). Both conodonts and stratigraphic sequences place the Union Springs within the Eifelian Stage of the Middle Devonian Series (Woodrow et al., 1988).

The Oatka Creek Formation is the upper shale unit of the Marcellus subgroup in western and central New York. Its eastern New York equivalent is the Mount Marion Formation. Throughout much of the state, the base of both units is the Cherry Valley Member (= Cherry Valley Limestone of Rickard, 1952). The superseding Berne Member is a carbonaceous black shale, which is overlain by the coral-rich Halihan Hill Bed, which marks the base of the arenitic Otsego Member. Although the Halihan Hill Bed has not been observed at this locality, specimens of *Nowakia*, which are comparable to those known from this bed at other localities, have been collected here. Although conodonts are poorly known from the Oatka Creek, the formation has been inferred to lie within the *T. kochelianus kochelinaus* zone (Klapper, 1981). Johnson et al. (1985) refer the Oatka Creek to T-R Cycle Ie and the overlying Skaneateles Formation to T-R Cycle If.

STAGE BOUNDARIES AND GLOBAL BIOEVENTS

The Lower Eifelian Chotec Event

The Global Stratotype Section and Point (GSSP) for the base of the Eifelian Stage is in the Eifel Hills of Germany at the first occurrence of the conodont *Polygnathus costatus partitus* (Ziegler and Klapper, 1985). *P. costatus partitus* is the second in a lineage of *P. costatus* subspecies with *patulus* occurring first and *costatus* third. The basal Eifelian GSSP lies within strata deposited during T-R Cycle Ic only a little below a eustatic deepening known as the Chotec Event (Chulpac and Kukal, 1988; Walliser, 1995; Weddige, 1998). The strata of Europe and north Africa, which were deposited during the Chotec Event, record a facies shift from light-colored, coarse-grained sediments to darker colored shales or dark, argillaceous limestones that contain an abundance of the dacryoconarids *Styliolina* and *Nowakia*.

The base of the Eifelian Stage in the strata of eastern North America is indeterminant due to the absence of the index conondont *P. costatus partitus*. The association of *P. c. patulus* and *P. c. costatus* in the upper beds of the Nedrow Limestone provides an uppermost constraint on the potential horizon for the Emsian-Eifelian boundary. Local tradition combined with this constraint have led to the tentative placement of the boundary either at the base of the Edgecliff Limestone or as high as the base of the Nedrow (Woodrow et al., 1988; Kirchgasser and Oliver, 1993).

Brett and Ver Straeten (1994) reported the occurrence of two laterally continuous beds of black shale at the contact of the Nedrow and Moorehouse Limetones in central New York and discussed the

Figure 2. Paleobiogeographic occurrences of selected dacryoconarid index species during the Emsian (Fig. 2A) and the Eifelian-Givetian (Fig. 2B) intervals. Modified from Johnson and Boucot (1973) by Lutke (1979).

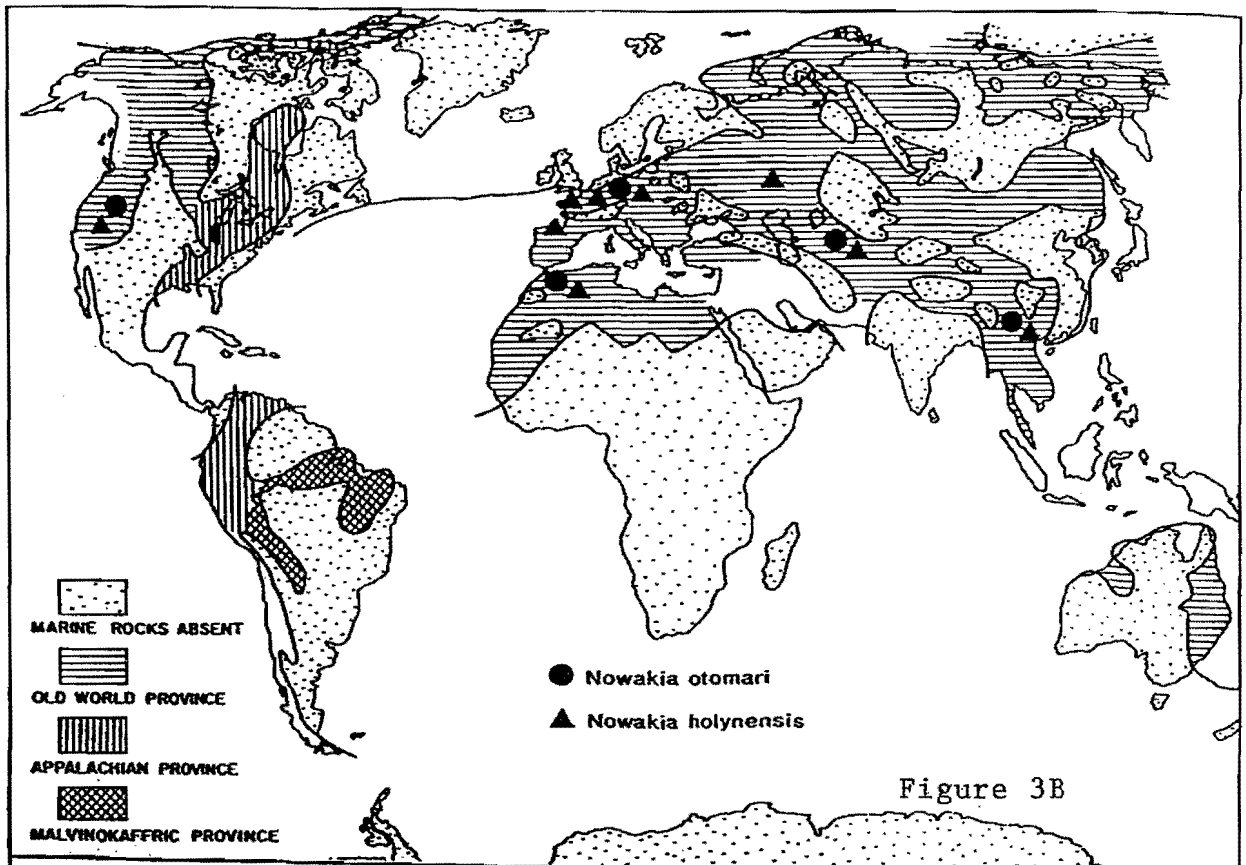

Figure 3B

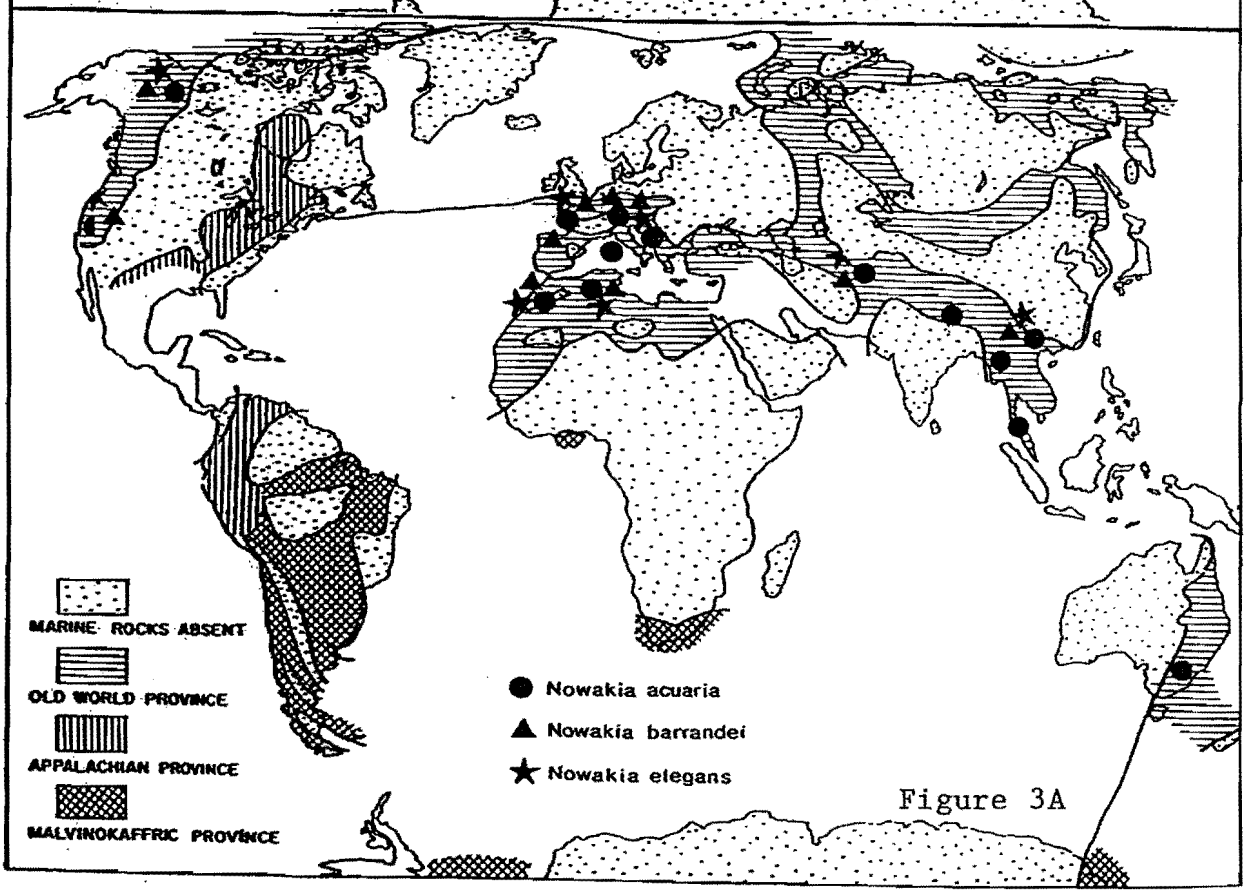

Figure 3A

advantages of using these beds as member-contact diagnostics in place of the traditional lowermost occurrence of dark colored chert. They subsequently reported that these "black beds" are continuous into the Selensgrove Limestone of central Pennsylvania and into the Onondaga Limestone of the central Hudson Valley of eastern New York (Ver Straeten and Brett, 1995). Based upon direct field observations in Europe and North Africa, these "black beds" are now regarded to represent the Chotec Event in the northern Appalachian Basin (C. Ver Straeten and E. Schindler, pers. com. 2002). This lends further support to the placement of the base of the Eifelian Stage at the contact of the Edgecliff and Nedrow Members of the Onondaga Formation.

The Upper Eifelian Kacak Event(s)

The GSSP for the base of the Givetian Stage is in Morocco at the first occurrence of *Polygnathus heminasatus*, a conodont which is unknown in eastern North America (Walliser et al., 1995) and which Sparling (1999) regards to be of dubious taxonomic integrity. Within the stratotype interval, the GSSP lies less than one half of a meter above a bed of black shale, which records the acme of the *otomari* Event (Walliser et al., 1995). Although this bioevent has been know by several names, most commonly Kacak-*otomari,* and variously diagnosed (see Truyols-Massoni et al., 1985), it is generally characterized as an interval of black shale that was deposited during a short term eustatic sea level highstand (House, 1985) and is recognized by the occurrence of the dacryoconarid *Nowakia otomari*. Walliser (1995) divided the "event" into two phases, which he referred to as the Lower Kacak Event and Upper Kacak Event. Referring to the T-R cycles of Johnson et al. (1985), Walliser (1995) placed the Upper Kacak Event (= acme of the *otomari* Event) immediately below the base of the Givetian and regarded both the Lower and the Upper Kacak Events to be correlative with the initial deepening phase of the T-R Cycle If. Differing in this opinion, Weddige (1998) regarded both of the Kacak events to lie within the T-R Cycle Ie and placed the base of the Givetian at the Ie-If boundary. If this proves to be an accurate determination, the base of the Gevetian Stage approximates the contact between the Oatka Creek Formation and the succeeding Skaneateles Formation.

DACRYOCONARID CLASSIFICATION AND SUCCESSION

Eaton (1832) described *Echinus gyracanthus*, a presumed sea urchin spine, from the "Corniferous Limerock" of eastern New York. Vanuxem (1842), Mather (1843), and Hall (1843) illustrated *Tentaculites ornatus* Sowerby from what is now known as the Lower Devonian Manlius Limestone of eastern and central New York. Rejecting the identification of this species by Vanuxem and Mather, and neglecting to mention his own previous illustration of the taxon, Hall (1859) described *T. irregularis* n. sp. and referred all tentaculids from the Manlius to this species. In couched and physically hidden language (see Lindemann and Melycher, 1997), Hall (1861) subsequently transferred his new species to *T. gyracanthus* (Eaton). Lindemann and Melycher (1997) redescribed *T. gyracanthus* (Eaton) and described *T. simmondsi* n. sp., the first new tentaculitid to come from the Devonian of New York since the days of James Hall.

Hall (1843, p. 173, text fig. 68.2) described *Tentaculites scalaris* Schlotheim and figured a specimen collected at Le Roy, NY. Hall (1877, Pl. 26, figs. 3-4) transferred *T. scalaris* to a new species *T. scalariformis* and illustrated a specimen from the "Upper Helderberg group" (= Onondaga Limestone) at Le Roy, NY. He also illustrated a new species *T. sicula* the syntypes of which were collected from "the Upper Helderberg (= Delaware) limestone at Delaware, Ohio (Hall, 1877, pl. 26, figs. 5-11). Hall (1877) is a quintessential James Hall publication, the origin of which is discussed by Oliver (1987). Hall (1879) placed *T. sicula* in synonymy with the earlier described *T. scalariformis,* refigured the species with one specimen from the "cherty (= Onondaga) limestone" at Le Roy, NY (pl. 31., figs 3-4) and, citing both superior abundance and quality of preservation, also refigured the species with specimens from Delaware, Ohio (Pl. 31, figs. 5-11). Hall (1888, pl. 64, fig. 20) again refigured specimens of *T. scalariformis* on a slab of "Corniferous (= Delaware) limestone" from Delaware, Ohio. In Ohio this species is now known to be abundant and widely distributed within both the Columbus and Delaware Limestones (Stauffer, 1909; Westgate, 1926). There have been few reports of this species from the Devonian of New York (Grabau, 1906; Oliver, 1954, 1956) where its range has not been extended since the days of James Hall.

Figure 3. Selected faunal elements of the four dacryoconarid events. A. *Styliolina*; B, *Striatostyliolina*; C, *Viriatellina*; D, *Nowakia*; E, *Costulatostyliolina*; F, *Tentaculites scalariformis*; G, inarticulate brachiopod; H, scolecodonts. Not to scale.

Hall (1843) also described *Tentaculites fissurella* n. sp. from the "Marcellus shale" and the Genesee slate" of central and western New York. Hall (1876, Pl. 31A, figs. 12-14) illustrated three specimens of this species and then refigured these same three as the types of a new species, *T. gracilistriatus*. Referring specimens with transverse sculpture to this new species, Hall (1879, Pl. 31A, figs. 1-34) transferred the more-or-less smooth forms to *Styliola fissurella*. At that time both *Tentaculites* and *Styliola* were regarded to be pteropods. Karpinsky (1884) proposed the new genus *Styliolina* in order to distinguish small conical fossils of the Paleozoic from the pteropod gastropods and transferred Hall's species to *Styliolina fissurella* (Hall). Lindemann and Yochelson (1994) redescribed this species, as well as the genus' type *S. nucleata* (Karpinsky), in order to dispel erroneous interpretations of the genus that had persisted throughout the second half of the 20th Century. Lindemann and Yochelson (1992) also redescribed *Tentaculites gyracanthus*, transferred the species to *Viriatellina gyracanthus* (Hall), and described *V. porteri* n. sp., the first new dacryoconarid to be described from the Devonian of New York since the days of James Hall.

What then is a dacryoconarid? The examples cited above are given, in part, to point out that here has been, and continues to be, a good deal of activity in the areas of classification and taxonomy of the tentaculitids their morphologic allies. Because this group has been virtually ignored in North America since the time of James Hall, most of this work has been undertaken by European paleontologists. The majority of these good people regard the dacs to be a monophyletic group with phylogenetic affinities to the tentaculitids and ally them with the Phylum Mollusca. However, this is not a universally held opinion (see Yochelson and Lindemann, 1986), and its further consideration lies beyond the biostratigraphic purposes of this report.

Paleozoic fossils that share the common characteristics of being small and conical have been in the literature since the early 1800s. They have been variously regarded to be echinoderm spines, brachiopod spines, small cephalopods, pteropod gastropods, or worms (see Yochelson and Lindemann, 1986). Detailed systematic attempts to develop a classification of the tentaculitids and to separate morphologially divergent forms date to the work of the Russian micropaleontologist Lyashenko during the 1950s. See Fisher (1962) or Boucek (1964) for citations to Lyasheko's plethora of publications. Fisher (1962) proposed a classification that further distanced the tentaculitids from divergent forms such as the hyoliths, cornulitids, and coleolids. Fisher (1962, p. W102) proposed the Class Cricoconarida to include the "small, narrow, straight, ringed true cones." He divided the class on the criterion of the morphology of the cone's embryonic chamber. Thus, the proposed Order Tentaculitida includes cricoconarids with a pointed conical embryonic chamber, and the Order Dacryoconarida includes those with a rounder or bulb-like embryonic chamber. The apical terminus of the dacryoconarid embryonic part may possess a small node or spine. The original description of the Order Dacryoconarida (Fisher, 1962, p. W114) is - "Small cricoconarids with pronounced teardrop-like embryonic bulb, which may have tiny apical spine emanating from it. Growth angle relatively greater in Tentaculitida. Exterior smooth or covered by broad ripple-like rings with rounded crest and troughs. Longitudinal ornamentation usually present. Juvenile portion smooth or with weakly developed rings. Shell wall thick or thin: no radial canals observed. Interior wall surface smooth or ringed. No evidence of septa though Novak reported a septum between the embryonic chamber and the rest of the interior. *M.Sil.(Wenlock.)-U.Dev.(L.Famenn.)*." The essence of Fisher's classification that pertains to this report appears below.

Class Cricoconarida Fisher, 1962
- **Order Tentaculitidae** Lyashenko, 1955
  - **Family Tentaculitidae** Walcott, 1886
  - **Family Homoctenidae** Lyashenko 1955
  - **Family Uniconidae** Lyashenko 1955
- **Order Dacryoconarida** Fisher, 1962
  - **Family Styliolinidae** "Grabau 1912"
  - **Family Nowakiidae** Boucek and Prantl, 1960

Boucek (1964) proposed a classification of the tentaculitids and their allies that preserved some aspects of Lyasheko and Fisher's (1962) work and added some of his own. Lardeux (1969) described several new taxa including the genus *Costulatostyliolina*. Since that time both "super" and 'sub" prefixes have abounded throughout the taxonomic hierarchy of the tentaculitids, producing a truly impressive set of categories. Fairly recent examples of this work may be found in Alberti (1993) and Farsan (1994). The outline, which appears below, retains the overall framework of Boucek (1964) with the addition of selected new taxa that have been assigned to the Order Dacryoconarida. It is not intended to even come close to

being comprehensive, but rather is presented only to show the taxonomic locations of the dac genera that are discussed in this report. Descriptions of dacryoconarid genera, which follow, are not formal but are sufficiently diagnostic to facilitate their identification.

Class Tentaculitida Boucek, 1964
- **Order Tentaculitida** Lyashenko, 1955
  - **Family Tentaculitidae** Walcott, 1886
    - *Tentaculites* Schlotheim, 1820
  - **Family Uniconidae** Lyashenko, 1955
- **Order Homoctenida** Boucek, 1964
  - **Family Homoctenidae** Lyashenko, 1955
    - *Homoctenus* Lyashenko, 1955
- **Order Dacryoconarida** Fisher, 1962
  - **Family Nowakiidae** Boucek and Prantl, 1960
    - *Nowakia* Guerich, 1896
    - *Viraitellina* Boucek, 1964
  - **Family Styliolinidae** Grabau and Shimer, 1910
    - *Styliolina* Karpinsky, 1884
  - **Family Striatostylioinidae** Boucek, 1964
    - *Striatostyliolina* Boucek and Prantl, 1961
    - *Costulatostyliolina* Lardeux, 1969

The genus *Styliolina* (Fig. 2A) stands apart from other dacs in that the shell consists of a single, 10 micron thick, layer of homogenous calcite and lacks exterior sculpture with the exception of weak, longitudinal striae. Previous reports of the absence of striae on the surface of *Styliolina* Karpinsky are erroneous (Lindemann and Yochelson, 1994). *Styliolina fissurella* (Hall) is the only representative of the genus that is currently known from eastern North America. An undescribed species of the genus appears to be present in the argillaceous beds of the Nedrow Limestone as well as the Chestnut Street submember of the Bakoven Formation at CVNY., but it is not yet certain. The reported range zone of the *Styliolina* in New York extends from the upper Frasnian Angola Member of the West Falls Formation (Yochelson and Kirchgasser, 1986) down to the base of the Onondaga Formation (Lindemann and Yochelson, 1984). However, I can now report that *Styliolina* occurs in the Emsian the Bois Blanc Limestone of western New York, the lower Schoharie Formation at Kingston, New York, and in the Esopus Formation of central Pennsylvania. At this time, neither *Styliolina* nor *S. fissurella* (Hall) are of any practical use in biostratigraphic work.

Striatostyliolina (Fig. 2B) appears to differ from *Styliolina* primarily in the strength of the longitudinal striae in the surface of the shell. Specimens of *Striatostyliolina* are somewhat longer and more robust than most specimens of *Styliolina*, though this is hardly a diagnostic criterion. *Striatostyliolina* has not been reported formally from eastern North America and is currently know with certainty only from the indicated horizons of the Bakoven and Oatka Creek Formations (Fig. 1) in the vicinity of CVNY. This situation will soon change.

Nowakia (Fig. 2D) is recognized by the presence of sharp-crested transverse rings and longitudinal costae. Although the possible presence of *Nowakia* in Frasnian strata of western New York was mentioned by Yochelson and Kirchgasser (1986), the genus has not been formally reported from eastern North America. It is now know with certainty to be present in the Halihan Hill Bed of the Oatka Creek Formation throughout New York, as well as in the Bakoven Shale and upper Berne Member of the Oatka Creek Formation (Fig. 1) at CVNYwhere it appears that three or more species are present. With the possible exception of the Yochelson and Kirchgasser (1986) report, *Nowakia* is not curretly known to occur in any other New York strata .

Viriatellina (Fig. 2C) differs from *Nowakia* only in the shape of the transverse rings. Those of *Viriatellina* are more rounded and often more subtle than those of *Nowakia.* Comparison of illustrated type specimens of species, variously referred to these two genera, shows that there is a disconcertingly large overlap of ring morphologies. Furthermore, mechanical compaction of specimens often obscures the presence of weak rings and corrasion of the shell surface may obliterate longitudinal costae, taphonomically transforming a *Viriatellina* into a *Styliolina* or a *Costulatostyliolina* mimic.

Tentaculites gracilistratus appears in the faunal lists for many Hamilton Group formations throughout eastern North America. Although many of these are accurate reports of *Viriatellina*

gracilitstriata (Hall), it is now certain that several undescribed species are currently referred to this taxon. The base of the *V. gracilistriata* (Hall) range zone is understood to be in the Union Springs Shale. The*Viriatellina* that occurs in the Nedrow Limestone (Fig. 1) is an undescribed species, which was first reported, though misidentified as *Nowakia*, by Lindemann and Yochelson (1984). Although the known first occurrence of *Viriatellina* in New York is at the base of the Nedrow, specimens that may be referred to the genus have been observed in acetate peels from a sample of Esopus Shale that was collected by C. Ver Straeten in central Pennsylvania.

Boucek's (1964) description of *Metastyliolina* specifies a long, slender dacryoconarid with weak transverse sculpture, numerous longitudinal costae, and a very small, pointy embryonic chamber. Larduex (1979) described the new genus *Costulatosytliolina* (Fig. 2E) to accommodate dacryoconarids that are similar to *Metastyliolina* but possess relatively few, strong costae and a well-developed, rounded embryonic chamber, with or without an small apical node. Hall (1879 p. 180) described several varieties of *Styliolina fissurella* including *S. fissurella strigata*, which he reported from "the Marcellus shale and in limestone concretions in the shale...at Cherry Valley," New York. He figured two specimens, one of which is a *Viriatellina* and the other a *Costulatostyliolina*. The latter is to be the type specimen of *Costulatostyliolina strigata* (Hall), the first species of this genus to be reported from the Devonian of New York (Lindemann, 200?, in prep.). At present, the *Costulatostyliolina* range zone in New York extends only from the concretionary interval of the Bakoven Shale to the Chestnut Street submember of the Hurley Member of the Union Springs Formation (Fig. 1).

DACRYOCONARID BIOEVENTS

Not all bioevents are created equal in that they result from environmental perturbations of many kinds and magnitudes. Daily and annual solar cycles are recorded in the tree rings and the growth lines of brachiopod shells and coral epithecae. The occasional hurricane or tsunami may be recorded as coquinite layer. The first and last occurrences of a given species record a biotic response to some sort of environmental forcing mechanism. Bioevents become more interesting when they are recorded in relatively thin stratal intervals that are lithologically distince and paleontologically unique. These event strata have disconformible bases and are laterally continuous on the regional to global scales. Many such strata are now understood to result from eustatic sea level high stands of geologically brief duration. These flooding events often weakened or totally breached land barriers that had previously existed between ocean basins thereby enabling the geologically instantaneous mixing of formerly isolated marine faunas. Migrants into an ocean basin could potentially colonize their new habitats at about the same rate that the zebra mussel has recently spread throughout he fresh water ecosystems of North America. Migratory, extinctive, and evolutionary faunas preserved in strata that were deposited during these times of profound global change are among the most interesting and biostratigraphically useful of all bioevents. Whereas the K/T asteroid impact captures the imagination, comparable events appear to have been too few and far between to be of much use in chronostratigraphic work.

Prior to presenting the four dacryoconarid bioevents that are currently known at CVNY, it is instructive to establish the biogeographic context of Early and Middle Devonian Earth. Throughout that time interval the global marine environment consisted of three major biogeographic units known as the Old World Realm (OWR), the Eastern Americas (= Appalachian) Realm (EAR), and the Malvinokafferic Realm (MR) as shown in Figure 3. For present purposes it is unproductive to quibble over the terms "province" and "realm." Lutke (1985) and McGhee (1997) respectively discuss the distribution of dacryoconarid and brachiopod taxa in Lower and Middle Devonian strata. They, and the authors cited by them, make clear the case that Early Devonian faunas were initially extremely endemic and became increasingly cosmopolitan over time (Fig. 3A, 3B). Decreased endemism was predominately result of the migration of OWR taxa into the EAR. Lutke (1985) regarded the endemic OWR dacryoconarids to have been tropical organisms, barred from the EAR by water temperature. Lindemann (1996) reported that the first occurrences of genera in the Middle Devonian of New York invariably involve OWR genera, but not species, that migrated into the Appalachian Basin during marine transgressions. The migrations were intermittent, temporally corresponding to eustatic high stands that facilitated both physical accessibility and the occasional warming of the EAR waters. Speciation may have occurred during migration as an adaptation to the indigenous faunas and cooler environments of the EAR. Although it is entirely arm waving speculation at this time, I would suggest that the enigmatic appearances, disappearances, and reappearances of dacs in the Hamilton Group may have been thermally driven.

Dacryoconarid Event I

This bioevent is characterized by the association of *Tentaculites scalariformis* (Fig 2F), *Styliolina, Viriatellina,* tasmanitids, scolecodonts (Fig. 2H), the inarticulate brachiopod *Craniops*? (Fig. 2G), and a diversity of ostracodes. Berdan (1981) lists eighteen ostracode genera as being in the Nedrow and Moorehouse Limestones, many of which became extinct during deposition of the Onondaga Formation. The ichnogenera *Chondrites*, and *Thallasinoides* are also frequently present. The Event I assemblage first occurs at the base of the Nedrow Limestone throughout much of the state. It is recorded in to two argillaceous intervals of the Nedrow at CVNY (Fig. 1) and in at least five argillaceous intervals within the Nedrow of central and western New York. In all known occurrences, the Event I fauna is restricted to the stratigraphic interval between the base of the Nedrow and the two "black beds" at the top of the member (Ver Straeten and Brett, 1995). Although the "black beds" have not been positively identified at CVNY, they may be represented by two argillaceous beds in the lowermost Moorehouse Limestone. In east-central and eastern New York, the lithologies of the upper Nedrow and lower Moorehouse differ from those of the central New York type sections, and the Nedrow-Moorehouse contact is arbitrarily placed at the first occurrence of dark colored chert.

The base of the Nedrow is regarded to be a synchronous event horizon (Oliver, 1954, 1956; Rickard, 1975, 1981) deposited during a eustatic deepening event (Brett and Ver Straeten, 1994). The argillaceous intervals of Dacryoconarid Event I represent the transgressive pulses of parasequence-scale stragigraphic sequences. They culminate in the "black beds," which are regarded by C. Ver Straeten and E. Schindler (pers. com., 2002) to be correlative with the lower Eifelian Chotec Event. The first occurrence of *Polygnathus costatus costatus* 2.3 m above the base of the Nedrow at CVNY constrains the base of the Eifelian to a position somewhat lower than this horizon. Thus, Dacryoconarid Event I is in the lowermost Eifelian, and the base of the interval within which this event fauna is preserved, the base of the Nedrow Limestone, may well be correlative with the base of the Eifelian Stage and the Middle Devonian Series. Currently undescribed species of *Styliolina* and *Viriatellina,* which first occur at the base the Nedrow, have the potential to serve as proxy indexes of the Emsian-Eifelian boundary within the Appalachian Basin. Although it is tempting to suggest that the first occurrence of *Tentaculites scalariformis* may also serve as an index to the base of the Eifelian, it has been reported from the Emsian Springvale Sandstone (= basal Bois Blanc Limestone) of Ontario (Stauffer, 1915). The accuracy of that report must be assessed before further statements regarding the chronostratigraphic utility of the first occurrence of *T. scalariformis* can be made with certainty.

Dacryoconarid Event II

This bioevent is simply the first (lowermost) occurrence of *Striatostyliolina* (Fig. 1). It is coincident with the base of the Bakoven Member of the Union Springs Formation. This is the first report of *Striatostyliolina* from the Devonian of the Appalachian Basin, other than passing references to the taxon (Lindemann, 1996; Robinson and Lindemann, 1997). The Onondaga-Union Springs contact is an unconformible horizon that represents the marine deepening event of T-R Cycle Id (Johnson et al., 1985) and Depositional Sequence 4 of Ver Straeten and Brett (1995).

Dacryoconarid Event III

This bioevent is a dacryoconarid epibole characterized by the association of *Styliolina, Viriatellina, Striatostyliolina, Costulatostyliolina,* and *Nowakia.* It is restricted to the concretionary interval of the Bakoven Shale and to the Chestnut Street submember of the Hurley Member (Fig. 1). Within the Bakoven, the dac fauna is preserved only in the concretions, which are of early diagenetic origin (Dix and Mullins, 1987; Lindemann and Schuele, 1996), and not in the shale proper. Preservation is excellent in the Chestnut Street bed(s). As is the case with *Striatostylioina,* this is the first report of *Costulatostyliolina* from the Devonian of the Appalachian Basin. *Costualtostyliolina* is restricted to the Event III interval. The first (= lowermost) occurrence of *Nowakia* is also at the base of this interval. This genus appears to have emigrated from the region following Event III only to return during Event IV. *Costulatostyliolina,* on the other hand, appears to have emigrated from the region following Event III, never to return.

Dacryoconarid Event IV

This event is characterized by the presence of *Styliolina* and *Nowakia*. *Viriatellina* is present only in the lower beds of the interval (Fig. 1). At CVNY this interval occupies a section of the Berne Mmeber of the Oatka Creek Formtion that extends from 23-34 m above the top of the Cherry Valley Limestone. One of the undescribed species of *Nowakia* within this interval has also been observed in the Halihan Hill Bed that marks the base of the Chittenango and Otsego Members of the Oatka Creek and Mount Marion Formations throughout the state (Baird et al., 1999). *Nowakia* is not known from the Hamilton Group above the Event IV interval.

The Kacak-*otomari* Event has long been regarded to be correlative with some part of the Chittenango Shale (Truylos-Massoni et al., 1990). The location of the precise stratigraphic interval of the event is of biostragraphic interest because the acme of the event (= Upper Kacak Event of Walliser, 1995) lies in very close proximity to the base of the Givetian Stage (Ziegler and Klapper, 1985). Ver Straeten and Brett (1996) reported that the Union Springs and Oatka Creek Formations lie within the Kacak-*otomari* interval and implied that the latter may correspond to the acme of the event. Robinson and Lindemann (1997) concurred in part, but regarded the Chittenango (= Oatka Creek) Shale to be correlative with the Lower Kacak Event. This was based on an ignorance of the presence of *Nowakia* in the Bakoven Shale and the understanding that the Upper Kacak Event was correlative with the eustatic high stand of T-R Cycle If. Now that *Nowakia* is known to occur in the Bakoven the Upper Kacak Event, which has been correlated to the uppermost part to the T-R Cycle Ie high stand, the determination of Robinson and Lindemann (1997) requires modification. Accordingly, I now regard Dacryoconarid Event III to be correlative with the Lower Kacak Event and Dacryoconarid Event IV to be correlative with the Upper Kacak Event. That said, it must be noted that *Nowakia otomari* itself remains unknown in the New York section despite a diligent search for it. At present, I can only assume that this species was ecologically barred from migration into the Eastern Americas Realm but the genus was not. With the exception of *Styliolina fissurella,* it does not appear that Old World species were adapted to the Eastern Americas environment.

ACKNOWLEDGMENTS

This report represents several works-in-progress, not a finished product. Whereas several good people have contributed something to the report, each is innocent of any errors or misrepresentations contained herein. Ellis Yochelson convinced me that dacs are worthy of study more than two decades ago and has been kindly patient with my snail's pace ever since. Dale Robinson (Skidmore, Class of 1996) collaborated with me on the first attempt to locate the Kacak-*otomari* Event. Chuck Ver Straeten has given freely of his time, specimens, and expertise in addition to encouraging my punctuational tendencies. Eberhard Schindler (Honorary Life Member of Friends of Dacryoconarids) has given encouragement and provided access to some of the European literature which I had not previously seen. Margaret Bailey (Skidmore, Class of 2004) executed Figure 2. Kathy Cartwright, fellow laborer in the salt mines of the Skidmore College Department of Geosciences, executed Figure 1. This report would not have come to be had Jim McLelland, now also a fellow laborer at Skidmore, not asked me to run a field trip and then possessed the good grace to not laugh when I suggested the topic.

ROAD LOG

This road log begins at Exit 15 of US I87, the Adirondack Northway. Readers will not fail to note that the road log is in whole-mile increments. The odometer on my 1993 Toyota pickup does not record tenths of miles. That option came only with a touring package, which was excessively costly.

Mileage

0 Take the Saratoga Springs Exit 15 of US I87 west on to NY Rt. 50. Locally, this road has been named the C.V. Whitney Memorial Highway. US Rt. 9 enters from the right (north) at the second traffic light. Continue straight in the right hand lane on the combined Rts. 50 and 9 to Broadway in Saratoga Springs.

1 Cross Broadway continuing straight ahead (west) on to Van Dam Street. Rts. 50 and 9 turn left at Broadway, we do not. NY Rt. 9N enters from a diagonal left. Continue straight on what is now Rt. 9N north past the Saratoga Hospital and the Stewart's ice cream plant into the Town of Greenfield. The ice cream plant is the type locality of Stewart's Shops everywhere.

4 Turn left on to Saratoga County Rt. 21, Middle Grove Road. The upcoming turn is indicated by a blue Kilmer's Lumber sign and a roadcut in the Upper Cambrian Galway Formation on the right side of 9N. If you cross under the railroad overpass, you have missed the turn. FYI: The first left from Middle Grove Road leads to Lester Park, the type locality of the Upper Cambrina Hoyt Limestone and its world famous *Cryptozoon* stromatolite reefs. Continue stratight on Middle Grove Road until it terminates at the intersection with NY Rt. 29.

12 Turn right (west) on to Rt. 29 and continue to Rt. 30A at Johnstown. DO NOT turn on to Rt. 30 toward Amsterdam at Broadalbin.

32 Turn left (south) on to Rt. 30A at Johnstown and descend into the Mohawk Valley.

37 Turn right (west) on to Rt. 5 at Fonda.

48 At the traffic light intersection with Rt. 10 in Palatine Bridge, turn right uphill for a brief rest stop at a popular purveyor of fast food. There will not be another "official" rest stop for some time to come. Follow Rt. 10 through Canajoharie to Sharon Springs.

59 Turn right (west) on to Rt. 20, the Cherry Valley Turnpike, at Sharon Springs.

64 Pull off of Rt. 20 to the right into a state parking area. Here we will regroup and review the overall stratigraphic setting of Cherry Valley. Exit the parking area and continue west on to Rt. 20. Descend into Cherry Valley through a long road cut and ascend the west side through a road cut in the Onondaga Limestone.

76 Pull on to and right shoulder of the road just beyond a large road sign above the top of the road cut. Walk down hill to the baseof the roadcut.

STOP 1. DACRYOCONARID EVENT I. The base of this outcrop is in the upper Carlisle Center, which is characterized by the ichnofossil *Zoophycos*. The sub-Onondaga disconformtiy is marked by abundant phosphate nodules at the Edgecliff-Carlisle Center contact. Much of the Onondaga Formation's Edgecliff Member is a massive to thick-bedded, coraliferous limestone. The upper Edgecliff contains nodules of light-gray chert and the top of the member is easliy recognized the red staining of oxidized pyrite nodules. The base of the Dacryoconarid Event I interval is coincident with the Edgecliff-Nedrow disconformity, which is at the contact of this pyriteiferous Edgecliff bed and base of the lowermost argillaceous Nedrow bed. The base of the Nedrow is also the base of the *Viriatellina* and *Tentaculites scalariformis* local range zones. At this locality, the fauna of Dacryoconarid Event I appears to be restricted to the two argillaceous intervals of the Nedrow. The top of this interval corresponds to the top of the *T. scalariformis* local range zone, and to the uppermost known occurrence of *Viriatellina* in the Onondaga Formation.

The arbitrarily chosen Nedrow-Moorehouse contact is the bed of limestone that contains the lowermost occurrence of dark-gray chert nodules. Immediately above this horizon, there are two argillaceous intervals, which may be correlative with the two uppermost Nedrow "black beds" of central New York. If this correlation proves to be correct, strata referred to the lower Moorehouse at this locality are correlative with the upper Nedrow of central New York and with the Chotec Event. In any case, the base of the Dacryoconarid Event I interval is either at, or in proximity to, the base of the Eifelian Stage.

Drive uphill a short distance and park in the highway department staging area. The Cherry Valley Member and the lower beds of the Berne Member of the Oatka Creek Formation are exposed in the road cut immediately above the staging area. As it is more convenient to examine and collect from this interval here than it is at Stop 3, we will do so.

At end of stop, turn back (east) on Route 20. Drive in the right hand lane and decelerate immediately after passing beneath the old railroad overpass. If the fates have been kind, there will be large talus blocks of the of the Carlisle Center, which may afford excellent bedding plane exposures of *Zoophycos*. If this is the case, we will stop briefly for photographs. Please do not damage, or collect from, these large blocks. There are plenty of small blocks to be had that do not require the use of a hammer.

Continue east on Rt. 20.

77 Park on the shoulder of Rt. 20 adjacent to a 2+ m thick outcrop of massive limestone.

STOP 2. DACRYOCONARID EVENT II

The 2 m exposure of massive grainstone and packstone on the south side of Rt 20 is the easternmost exposure of the Seneca Limestone. The Tioga B Bentonite occurs in the reentrant at the base of the exposure. The low exposure of packstone on the north side of Rt. 20 is in the uppermost Moorehouse. At this locality, both members were deposited toward the culmination of a regressive phase, the beginning

of which is recorded in the Moorehouse at Stop 1. The top of the Seneca is an erosional truncation surface. At other localities in central and eastern New York, this surface is a classic Devonian bone bed.

The base of the Bakoven Shale is not exposed here, though it has been excavated in a stream gully within sight of this outcrop and is (sometimes) exposed nearby at Optional Stop A. The Bakoven was deposited during a eustatic flooding phase which appears to have breached the transcontinental arch, permitting the immigration of dacs from the equatorial Old World Realm, of what is now Arctic Canada, into the Eastern Americas Realm. *Striatostyliolina* was the first new dac to access the northern Appalachian Basin during this highstand. Its first occurrence is coincident with the base of the Bakoven Shale and is the diagnostic of Dacryoconarid Event II

At the end of stop, continue east on Rt. 20 and take the first right hand turn onto Chestnut Street. Park on the wide shoulder, well off of the pavement.

STOP 3. DACRYOCONARID EVENTS III AND IV.

The base of the Chestnut Street road cut is in the upper concretionary part of the Bakoven Shale. The upper part of the outcrop, which is visible from the road, is in the Berne Member of Oatka Creek Formation. The massive limestone bed between them is the Cherry Valley (Fig. 1). The Cherry Valley immediately overlies a centimeter-scale bed of shale, which overlies a 10-25 cm bed of limestone. These are the Lincoln Park and Chestnut Street submembers of the Union Springs' Hurley Member. Dacryoconarid Event III, which is not regarded to be correlative with the Lower Kacak Event of Walliser (1995), occupies the concretionary interval of the Bakoven and the Chestnut Street bed. This is the total know range zone of *Costulatostyliolina* (Fig. 1) in the northern Appalachian Basin. Similarly, *Nowakia* also first occurs in the Bakoven and is present in the Chestnut Street bed. *Nowakia* is absent from the section above this bed until it reappears in the Berne Member of the Oatka Creek Formation 23-34 m above the top of the Cherry Valley. This 11 m thick section of the Berne is interval of Dacryoconarid Event IV. It is now regarded to be correlative with the Upper Kacak Event of Walliser (1995). This part of the section can be accessed either by scrambing up through the very sooty lower Berne above the Cherry Valley or by following a path up hill beneath the power line that intersects the road just above where we turned off of Rt. 20. Intermittant outcrops are present along the south side to this path and the hill side immediately above it. The crest of the section along the powerline is in a fine-grained arenite that lies above the highest occurrence of *Nowakia*, which marks the top of the Dacryoconarid Event IV interval.

This is the final stop of the more formal part of this field trip. Depending on contingencies, we may quit at this point or continue on to Optional Stop A.
If you are returning directly to Lake George, follow the trip log in reverse from Sharon Springs, on to Rt. 10, to Canajoharie. Access the NYS Thurway, US Rt. I90, east at Canajoharie. Remain on the Thruway to Albany and exit on to the Adirondack Northway, US Rt. 87, north to Lake George.

To reach Optional Stop A, continue east on Rt. 20 about 5 miles beyond Sharon Springs to Sharon and turn right (south) toward Cobleskill on Rt. 145. The upper Onondaga Formation and lower Bakoven Shale are exposed in a ditch/ephemeral stream on the west side of the road. If the weather has been dry, it is possible to walk up through the uppermost limestone beds and locate the Onondaga-Bakoven contact. the lowermost shale bed is Daryoconarid Event I, the first occurrence of *Striatostyliolina*. Watch your trip leader carefully for the optimal place to pull on to the right shoulder of the road and park.

At the end of stop, continue south on Rt. 10 thorough Lawyersville and on to Cobleskill. Turn left (east) on to the combined Rts. 145 and 7. A brief visit to a purveyor of fast food is in order here to access the facilities and discuss options. If you are returning to Lake George, continue east on Rts. 145 and 7, and take US Rt. I88 east toward Schenectady. I88 ends at the New York State Thruway, Rt. I90, at Rotterdam. Take the Thruway east to Albany (this is a toll free section) to Albany and exit on to the Adirondack Northway, US I 87, north to Lake George.

Highlighted road maps will be distributed if we are to continue on to Optional Stop B. This stop is a road cut in the Union Springs Formation on Camp Pinnacle Road south of John Boyd Thatcher State Park and above the Helderberg escarpment. The top of the Onondaga Formation is exposed on the flats below the intersection of Beaverdam and Camp Pinnacle Roads. The Cherry Valley Limestone is present in the ditch uphill from the shale exposure. Only *Styliolina* and *Viriatellina* are present in the upper section of the Union Springs at this location. Although *Costulatostylioina* is not present, *Nowakia* is abundant in the lower, darker part of the section. The form of *Nowakia* tthat occurrs in this interval is very similar to N. otomari, though it does not appear to be that species. None the less, this part of the outcrop is referred to

the Dacryoconarid Event III interval and is regarded to be correlative with the Lower Kacak Event of Walliser (1995).

REFERENCES CITED

Alberti, G.K.B., 1983, Dacryoconaride und Homoctenide Tentaculiten des Unter- und Mittel-Devons I: Courier Forschungsinstitut Senckenberg, 158; Frankfurt am Main, 228 p.

Anderson, E.J., Brett, C.E., Fisher, D.W., Goodwin, P.W., Kloc, G.J., Landing, E., and Lindemann, R.H., 1988, Upper Silurian to Middle Devonian stratigraphy and depositional controls, east-central New Museum Bulletin 433, p. 111-134.

Baird, G.C., Brett, C.E., and Ver Straeten, C.A., 1999, The first great Devonian flooding episodes in western New York: Reexamination of Union Springs, Oatka Creek, and Skaneateles Formation successions (latest Eifelian - Lower Geivtian) in the Buffalo-Seneca Lake Region: *in* Baird, G.C., and Lash, G.G., eds., New York State Geological Association, 71st Annual Meeting Guidebook, p. A1-A44.

Berdan, J.M., 1981, Ostracode biostratigraphy of the Lower and Middle Devonian of New York: *in* Oliver, W.A., Jr., and Klapper, G.K., eds., Devonian Biostratigraphy of New York, Part 1. International Union Of Geological Sciences, Subcommission On Devonain Stratigraphy, p.83-96.

Boucek, B., 1964, The Tentaculites of Bohemia. Publishing House of the Czechoslovak Academy of Science, Prague, 215 p.

Brett, C.E., and Ver Straeten, C.A., 1994, Stratigraphy and facies relationships of the Eifelian Onondaga Limestone (Middle Devonian) in western and west central New York State: *in* Brett, C.E., and Scatterday, J., eds., New York State Geological Association, 66 th Annual Meeting Guidebook, p. 221-270.

Chlupac, I., and Kukal, Z., 1986, Reflection of possible global Devonian events in the Barrandian area, C.S.S.R.: *in* Walliser, O.H., ed., Global Bio-Events, Springer-Verlag, Lecture Notes In Earth Sciences, v. 8, p. 169-179.

Dix, G.R., and Mullins, H.T., 1987, Shallow, subsurface growth and burial alteration of Middle Devonian Calcite concretions: Journal of Sedimentary Petrology, v. 57, p. 140-152.

Eaton, A., 1832, Geological text-book. Webster and Skinners, Albany, 134 p.

Farsan, N.M., 1994, Tentaculiten: Ontogenese, Systematik, Phylogenese, Biostratinomie und Morphologie: Abhandlungen der Senckenbergischen Naturforschenden Gesellschaft, 547, Frankfurt am Main, 124 p.

Fisher, D.W., 1962, Small conoidal shells of uncertain affinities: *in* Moore, R.C., ed., Treatise on Invertebrate Paleontology, Part W, Miscellanea. Geological Survey of America and University of Kansas Press, Lawrence, p. W98-W143.

Grabau, A.W., 1906, Guide to the Geology and Paleontology of the Schoharie Valley in Eastern New York: New York State Museum Bulletin 92, 386 p.

Griffing, D.H., and Ver Straeten, C.A., 1991, Stratigraphy and depositional environments of the lower part of the Marcellus Formation (Middle Devonian) of New York State: *in* Ebert, J.R., ed., New York State Geological Association, 63rd Annual Meeting Guidebook, p. 205-249.

Hall, J., 1843, Natural History of New York: Geology, Pt. 4. The Geological Survey of the State of NewYork, 425 p.

Hall, J., 1877, Illustrations of Devonian Fossils: Gastreropoda, Pteropoda, Cephalopods, Crustacea and Corals of the Upper Helderberg, Hamilton and Chemung Groups. Albany, 7 p., 133 plates and explanations.

Hall, J., 1879, Palaeontology: Vol. V, Part II, Containing Descriptions of the Gasteropoda, Pteropoda, and Cephalopoda of the Upper Helderberg, Hamilton, Portage, and Chemung Groups. Geological Survey of New York, Albany, 492 p.

Hall, J., 1888, Palaeontology: Vol. V, Part II. Supplement, Containing Descriptions and Illustrations of Pteropoda, Cephalopoda, and Annelida, p. 1042. *Appended to* Palaeontology: Vol. VII. Geological Survey of New York, Albany, 236 p.

House, M.R., 1985, Correlation of mid-Palaeozoic ammonoid evolutionary events with global sedimentary perturbations: Nature, v. 313, p. 17-22.

Johnson, J.G., and Boucot, A.J., 1973, Devonian Brachiopods, *in* Hallam, ed., Atlas of Paleobiogeography: Elsevier, Amsterdam, p. 89-96.

Johnson, J.G., Klapper, G., and Sandberg, C.A., 1985, Devonian eustatic fluctuations in Euramerica: Geological Society of America Bulletin, v. 96, p. 567-587.

Karpinsky, A.P., 1884, Die fossilen Pteropoden am Ostabhange des Urals: St. Petersbourg Imperial Academy of Science, Memoir series 7, v. 32, no. 1, p. 1-21.

Kirchgasser, W.T., and Oliver, W.A., Jr., 1993, Correlation of stage boundaries in the Appalachian Devonian, eastern United States: Subcommission On Devonian Stratigraphy, Newsletter No. 10, p. 5-8.

Klapper, G., 1981, Review of New York Devonian conodont biostratigraphy: *in* Oliver, W.A., Jr., and Klapper, G., eds., Devonian Biostratigraphy of New York, Part 1: International Union Of Geological Sciences, Subcommission On Devonian Stratigraphy, p. 57-66.

Lardeux, H., 1969, Les Tentaculites d'Europe Occidentale et d'Afrique du Nord: Editions du Centre National ed la Recherche Scientifique, Paris, 238 p.

Lindemann, R.H., 1996, Observations on the coordination of Devonian (Emsian, Eifelian) sea level rise events and dacryoconarid migrations into the Northern Appalachian Basin: Geological Society of America, Abstracts with Programs, v. 28, no. 3, p. 76.

Lindemann, R.H., and Melycher, D.A., 1997, *Tentaculites* (Tentaculitoidea) from the Manlius Limestone (Lower Devonian) at Schoharie, New York: Journal of Paleontology, v. 71, no. 3, p. 360-368.

Lindemann, R.H., and Schuele, F.R., 1996, Mechanical compaction in Middle Devonian Limestones of the Onondaga and Marcellus Formations at Cherry Valley, New York: Northeastern Geology and Environmental Sciences, v. 18, no. 3, p. 219-229.

Lindemann, R.H., and Yochelson, E.L., 1984, Styliolines from the Onondaga Limestone (Middle Devonian) of New York: Journal of Paleontology, v. 58, no. 5, p. 1251-1259.

Lindemann, R.H., and Yochelson, E.L., 1992, *Viriatellina* (Dacryoconarida) from the Middle Devonian Ludlowville Formation at Alden, New York: Journal of Paleontology, v. 66, no. 2, p. 193-199.

Lindemann, R.H., and Yochelson, E.L., 1994, Redescription of *Styliolina* [INCERTAE SEDIS] -- *Styliolina fissurella* (Hall) and the type species *S. nucleata* (Karpinsky): *in* Landing, E., ed., Studies in Stratigraphy and Paleontology in Honor of Donald W. Fisher, New York State Museum Bulletin 481, p. 149-160.

Lutke, F., 1979, Biostratigraphical significance of the Devonian Dacryoconarida: The Devonian System, Special Papers in Palaeontology 23, The Palaeontological Association, London, p. 281-289.

Lutke, F., 1985, Devonian Tentaculites from Nevada (USA): Courier Forschungsinstitut Senckenberg 75, Frankfurt am Main, p. 179-226.

Mather, W.W., 1843, Natural History of New York: Geology, Pt.1. The Geological Survey of the State of New York. 653 p.

McGhee, G.H.., Jr., 1997, Late Devonian bioevents in the Appalachian Sea: Immigration, extinction, and species replacements: *in* Brett, C.E., and Baird, G.C., Paleontological Events: Stratigraphic, Ecological, and Evolutionary Implications, Columbia University Press, New York, p. 493-508.

Oliver, W.A., Jr., 1954, Stratigraphy of the Onondaga Limestone (Devonian) in central New York: Geological Society of America Bulletin, V. 65, p. 621-652.

Oliver, W.A., Jr., 1956, Stratigraphy of the Onondaga Limestone in eastern New York: Geological Society of America Bulletin, v. 67, p. 1141-1147.

Oliver, W.A., Jr., 1987, James Hall and fossil corals: Earth Sciences History, v. 6, no. 1, p. 99-105.

Oliver, W.A., Jr., and Chulpac, I., 1991, Defining the Devonian: 1979-89: Lethaia, v. 24, p. 119-122.

Oliver, W.A., and Klapper, G., 1981, eds., Devonian Biostratigraphy of New York: International Union Of Geological Sciences, Subcommission On Devonian Stratigraphy, Parts 1 and 2, 105 p. and 69 p.

Rickard, L.V., 1952, The Middle Devonian Cherry Valley Limestone of eastern New York: American Journal of Science, v. 250, p. 511-522.

Rickard, L.V., 1975, Correlation of the Silurian and Devonian rocks in New York State: New York State Museum and Science Service, Map and Chart Series No. 4.

Rickard, L.V., 1981, The Devonian System of New York State: *in,* Oliver, W.A.,Jr., and Klapper, G., Devonian Biostratigraphy of New York: International Union Of Geological Sciences, Subcommission On Devonian Stratigraphy, Pt. 1, p. 5-22.

Rickard, L.V., and Zenger, D.Z., 1964, Stratigraphy and Paleontology of the Richfield Springs and Cooperstown Quadrangles, New York: New York State Museum and Science Service, Bulletin 396, 101 p.

Robinson, D., and Lindemann, R.H., 1997, Dacryoconarids of the Kacak-*otomari* Event at Cherry Valley, New York: Geological Society of America, Abstracts with Programs, v. 28, no. 7, p. 75-76.

Sparling, D.R., 1999, Conodonts from the Prout Dolomite of north-central Ohio and Givetian (Upper Middle Devonian) correlation problems: Journal of Paleontology, v. 73, p. 892-907.

Stauffer, C.R., 1909, The Middle Devonian of Ohio: Geological Survey of Ohio, Fourth Series, Bulletin 10, 204 p.

Stauffer, C.R., 1915, The Devonian of Southwestern Ontario: Canada, Department of Mines, Geological Survey, Memoir 34. No. 63, Geological Series, 341 p.

Truylos-Massoni, M., Montesinos, R., Garcia-Alcalde, J.L., and Leyva, F., 1990, Kacak-*otomari* event and its characterization in the Palentine domain (Cantabrian Zone), NW Spain: *in* Kauffman, E.G., and Walliser, O.H., eds., Extinction Events in Earth History, Lecture Notes in Earth Science, v. 30, Springer-Verlag, New York, p. 133-143.

Vanuxem, L., 1842, Natural History of New York: Geology Pt.2. The Geological Survey of the State of New York, 306 p.

Ver Straeten, C.A., Griffing, D.H., and Brett, C.E., 1994, The lower part of the Marcellus "Shale," central to western New York: Stratigraphy and depostional history: *in* Brett, C.E, and Scatterday, J., eds., New York State Geological Association, 66th. Annual Meeting Guidebook, p. 271-321.

Ver Straeten, C.A., and Brett, C.E., 1995, Lower and Middle Devonian foreland basin fill in the Catskill Front: Stratigraphic synthesis, sequence stratigraphy, and the Acadian Orogeny: *in* Garver, J.I., and Smith, J.A., New York State Geological Association, 67th. Annual Meeting Guidebook, p. 313-356.

Ver Straeten, C.A., and Brett, C.E., 1996, The Kacak-*otomari* and associated bioevents (Late Eifelian-early Givetian(?), Middle Devonian) in the Appalachian Basin: Relationship to sequence and tectonic patterns: Geological Society of America, Abstracts with Program, v. 28, no. 3, p. 107.

Walliser, O.H., 1995, Global events in the Devonian and Carboniferous: *in* Walliser, O.H., ed., Global Events and Event Stratigraphy in the Phanerozoic. Springer-Verlag, New York, p. 225-250.

Walliser, O.H., Bultynck, P., Weddige, K., Becker, R.T., and House, M.R., 1995, Definition of the Eifelian-Givetian stage boundary: Episodes, v. 18, no. 3., p. 107-115.

Way, J.H., Smith, R.C., and Roden, M., 1986, Detailed correlations across 175 miles of the Valley and Ridge of Pennsylvania using 7 ash beds in the Tioga Zone: *in* Sevon, W.D., ed., Selected Geology of Bedford and Huntington Counties, 51st Annual Field Conference of Pennsylvania Geologists Guidebook, p. 55-72.

Weddige, K., 1996, Devon-Korrelationstablle: Senckenbergiana lethaea, v. 76(1/2), p. 267-286.

Westgate, L.G., 1926, Geology of Delaware County: Geological Survey of Ohio, Fourth Series, Bulletin 30, 147 p.

Wolosz, T.H., Feldman, H.R., Lindemann, R.H., and Paquette, D.E., 1991, Understanding the east central Onondaga Formation (Middle Devonian) - an examination of the facies and brachiopod communities of the Cherry Valley section, and Mt. Tom, a small pinnacle reef: *in* Ebert, J.R., ed., New York State Geological Association Guidebook, 63rd Annual Meeting, p. 373-412.

Yochelson, E.L., and Kirchgasser, W.T., 1986, The youngest styliolines and nowakiids (Late Devonian) currently known from New York: Journal of Paleontology, v. 60, no. 3, p. 689-700.

Yochelson, E.L., and Lindemann, R.H., 1986, Considerations on the systematic placement of the styliolines (Incertae sedis: Devonian): *in* Hoffman, A., and Nitecki, M.H., eds., Problematic Fossil Taxa. Oxford University Press, New York, p. 45-58.

Ziegler, W., and Klapper, 1985, Stages of the Devonian System: Episodes, v. 8, no. 2, p. 104-109.

GLACIAL LAKE ALBANY IN THE CHAMPLAIN VALLEY

by
G. Gordon Connally, New York State Museum, Research Associate, Albany, NY 12230
Donald H. Cadwell, New York State Museum, Research and Collections, Albany, NY 12230

The purpose of this article is to document and discuss the expansion of Glacial Lake Albany from the northern Hudson Valley into the southern Champlain Valley. The area under consideration extends ±115 km from Crown Point to the Hoosic River. Crown Point (A on Fig. 1) is on Lake Champlain at 44° 02' N. The Hoosic River (B in Fig.1) is an eastern tributary to the Hudson River at about 42° 55' N.

DEGLACIAL HISTORY

The Woodfordian glacier reached its maximum position across Long Island, Staten Island, and northern New Jersey between 21.75 ka (Sirkin and Stuckenrath, 1980) and 20.18 ka (Stone and Reimer, 1989). Recession was underway by 21.20 at the earliest, or 18.57 ka, at the very latest (Connally, in prep). Glacial Lake Hudson of Reeds (1927) was impounded between the Harbor Hill Moraine, at the Staten Island Narrows, and the receding ice. The outlet probably was eastward, over a bedrock threshold at Hell Gate in the East River (Stanford, 1989). When the ice margin reached the Pellets Island/Shenandoah Moraine, north of the Hudson Highlands, the lake expanded north into the mid-Hudson Valley. From then on the lake is referred to as Glacial Lake Albany. Glacial Lake Albany is defined as the proglacial lake that expanded northward in the Hudson-Champlain trough in direct contact with the retreating Woodfordian glacier margin. As the ice margin retreated north, Glacial Lake Albany continued to expand in contact with the ice front.

Figure 1. The field trip region from Crown Point to the Hoosic River. The map is a portion of Landforms of New York, by James A. Bier copyright 1964. Used by permission.

The glacier continued to retreat north, up the Hudson Valley, interrupted by two, or perhaps as many as four, readvances. The Rosendale Readvance (Connally, 1968a) dammed Glacial Lake Tillson in the lower Wallkill Valley and deposited the Red Hook Moraines (Connally and Sirkin 1986) east of the Hudson River, damming Glacial Lake Jansen. That event occurred sometime between 18.57 and 13.67 ka. Next, events described by Dineen et al (1983) and Dineen (1986) as the Delmar and Middleburg readvances occurred in the Capital District. Then the Luzerne Readvance (Connally and Sirkin, 1971) occurred in the northern Hudson Valley just prior to 13.15 ka. After that, the ice began to recede northward into the Champlain Valley, where the recession was interrupted for the final time by the Bridport Readvance (Connally, 1970) at 11.90 ka (Larsen, 2001; Connally, in prep). Final recession into the St. Lawrence Lowland occurred at about 11.50 ka (Pair and Rodriquez, 1993).

As the ice margin retreated north, Glacial Lake Albany continued to expand in contact with the ice front. In the northern Hudson Valley, Lake Albany was about 24 km wide. The lake divided into a west branch ±4 km wide, in the Lake George trough, and an east branch 7 to 12 km wide, in the valley of Wood Creek and the South Bay of Lake Champlain. In the Champlain Valley it widened to ±35 km, The Luzerne (A in Fig. 2) and Bridport (B in Fig. 2) Readvances are illustrated below, as they relate to Lake Albany.

The Luzerne Readvance

By perhaps 13.20 ka, the ice margin had receded to a position somewhere north of Glens Falls. Presumably Lake Albany deltas had been deposited all the way north to that position. Then the ice margin readvanced at least 50 km. Apparently, this was a major readvance on the order of magnitude of the earlier Rosendale Readvance, farther south. The eastern edge of the readvance reached the north-south valley of the Batten Kill, obliterating pre-readvance Lake Albany features for 42 km, from Fair Haven, Vermont to Greenwich, New York. The western edge intruded into the Adirondacks south of Warrensburg. The southern margin may well have reached the vicinity of Cambridge, New York, just north of the Hoosic River.

The Luzerne Readvance deposited a pitted outwash valley train 8 km long, from Lake Vanare to Lake Luzerne in the eastern Adirondacks, and a kame terrace against the edge of the Luzerne Mountains on the west side of the Hudson Valley. The eastern edge of the readvance forced drainage eastward into the Batten Kill drainage system. However, the Batten kill delta has only sparse evidence of the Rebounded Lake Albany level, though perhaps more than recognized by DeSimone (1983). Between the east-west Batten Kill valley there is a plethora of stagnant ice features probably left by wasting ice from the Luzerne Readvance. Thus, the southern margin probably reached the north edge of the Hoosic River, south of the Batten Kill.

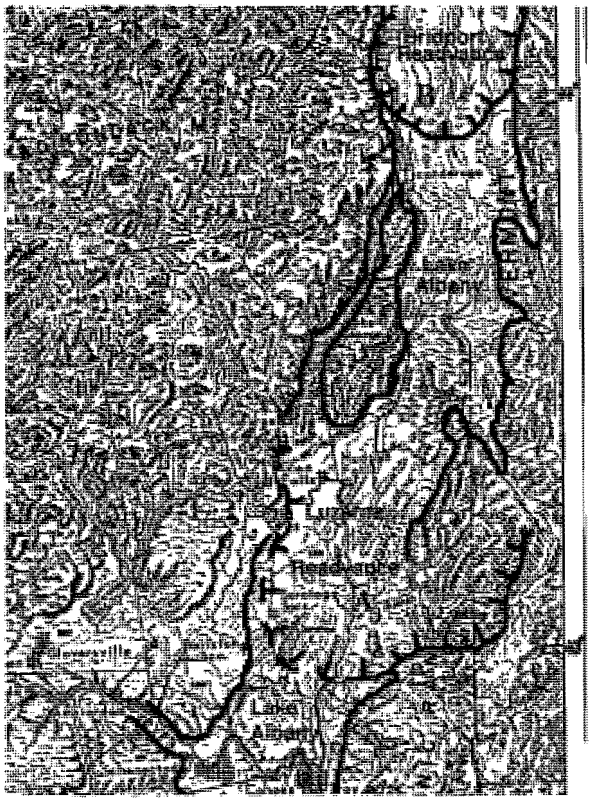

Figure 2. The Luzerne and Bridport Readvances. The borders of Lake Albany are Illustrated south of each readvance

In the Hudson River gorge, east of Corinth, there is a multiple-till section (Figure 3), that is the type section for the readvance. At the base of the section is the main Woodfordian till; a grayish-black (N 2) till with limestone and shale clasts in a silty-clay matrix. At the top is the readvance till; a moderate olive-gray (5 Y 4/2) till, very bouldery, with a sandy-loam matrix.

The small Hidden Valley Moraine marks the terminus of the readvance west of Glens Falls (Connally and Sirkin, 1971, Figs. 2 and 3). Pine Log Camp bog developed in one of the kettles in the pitted outwash on the distal side of the Hidden Valley moraine. Two pollen cores were retrieved two years apart, from this bog. Core #1 was 7.85 m long and Core #2 was 8.10 m long. A ^{14}C date of 12.40±0.20 ka (I-3199) was obtained at -7.85 m for the lowest spruce pollen (A_1, A_2) zone, in Core #1. Two years later, a ^{14}C date of 13.15±0.20 ka (I-4986) was obtained at -8.10 m from the tundra pollen (T) zone, in Core #2.. Sediment accumulation had begun as soon as the kettle ice melted so the actual readvance must slightly pre-date the bog-bottom age of 13.15 ka (Connally and Sirkin, 1971, p. 1002).

The Glens Falls delta on the west, at ±460 ft, and the Fair Haven delta at ±480 ft, on the east, mark the northern extent of Lake Albany in the Hudson Valley. These deltas formed after recession from the Luzerne Readvance maximum, 45 km to the south. However, as the ice margin retreated northward through the Wood Creek valley to the South Bay of Lake Champlain, and through the parallel Lake George trough on the west, Lake Albany continued to expand northward with the ice margin. It would be too much of a coincidence to think that Lake Albany's history ended in the Hudson valley and a new lake replaced it at essentially the same elevation, with the same outlet. There was nowhere for the water to go.

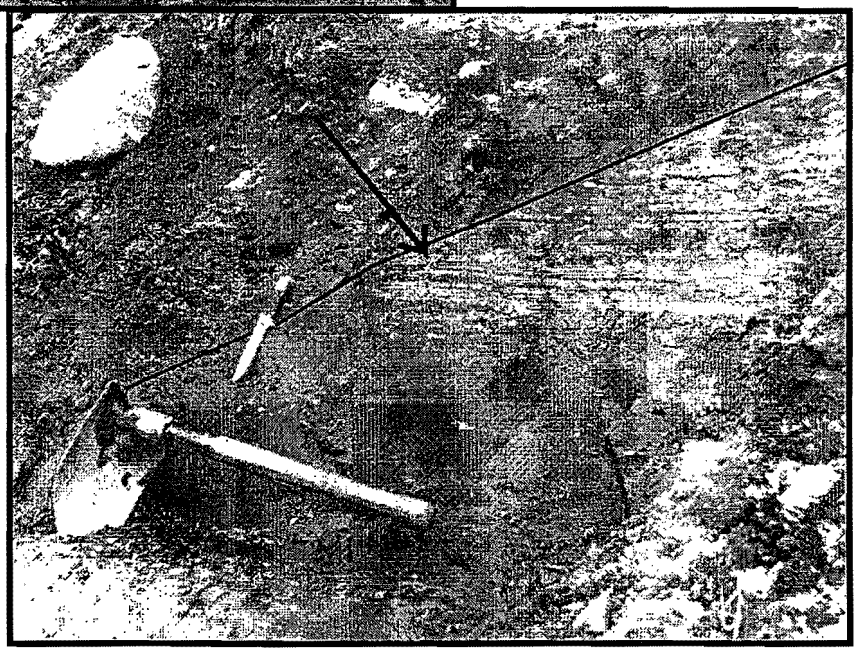

Figure 3. The Luzerne Readvance at the type locality. In 3a, at left, the arrow points to the contact between the olive gray-readvance till above and the grayish-black Hudson Valley till beneath. The late Nancy Austin Wright, former geologist with the NYSGS, appears for scale. In 3b, below at right, the arrow points to the contact between the grayish-black till and a clast of pre-existing lacustrine clay. The Figures are reproduced, with permission, from Connally and Sirkin (1971).

There are several small deltaic (?) deposits bordering Lake George that probably relate to the Lake Albany and lower water planes (see Figure 5). The Lake George trough is connected to the Hudson Valley by two cols. The west col, between French Mountain and the Adirondacks, was filled to ±550 ft with sediment. The east col, between French Mountain and Putnam Mountain, is at ±400 ft. When the ice blocked both cols, drainage from the east left a huge boulder esker (Connally, 1973) that wrapped around the southern end of Putnam and French Mountains. The esker was subsequently buried by Lake Albany sand. The ice remained in the eastern col somewhat longer than the west because there is an outwash delta that prograded southward from the western col. Once the ice had cleared the eastern col, Lake Albany waters invaded the Lake George trough.

Varved lacustrine clays fill the bottom of Wood Creek valley– now the New York State Barge Canal – to an elevation of ±300 ft. To the east, near Fair Haven, the clay cover rises to more than 400 ft. Because the delta at Fair Haven displays a secondary Lake Albany surface that is slightly low, at ±440 ft, it is possible that ice lingered nearby longer than it did in the Lake George trough. However, to the north, both the Brandon delta and the East Middlebury deltas are graded to the Lake Albany water plane. And farther east, in the Otter Creek valley, as far south as Proctor, Vermont there is a plethora of Lake Albany features. In the Neshobe River drainage net, there are several minor deltaic and ice-contact features at the same elevation as the Neshobe River delta at Brandon. The Neshobe River delta displays the features of most lower lake levels.

The Bridport Readvance

The northward expansion of Lake Albany in the Champlain Valley, was interrupted by the Bridport Readvance at 11.90 ka. This readvance does not appear to be as extensive as the Luzerne Readvance. Thus far, the evidence is limited to the type locality and the two great deltas on either side of the Champlain Valley. However, Connally (1970) suggested that the Bridport Readvance was responsible for the many dropstones present in the lacustrine clays in the Champlain Valley, from Shelburne to East Middlebury, Vermont and almost to Ticonderoga adjacent to Lake Champlain. The total extent may be equivalent to the "bouldery clay" unit of the Surficial Geologic Map of Vermont (Stewart and MacClintock, 1970). For additional evidence see the final section on Core Interpretations.

The type locality for the Bridport Readvance was in a gravel pit 8 km west of Bridport, Vermont. The entire pit was removed and reclaimed circa 1972, but photographs from Connally (1970, Plates 5 and 6) are reproduced here as Figure 4. The photographs show lenses of gravel that were being sheared up into the readvance till.

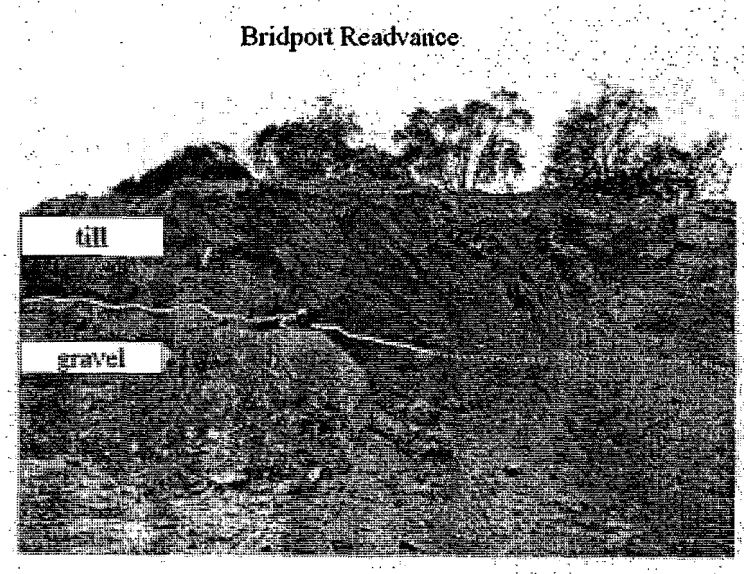

The Bridport Readvance has long been thought to correlate with the Littleton-Bethlehem Moraine in western New Hampshire and eastern Vermont (Ridge, et al., 1999, Fig. 11). Recently, Larson (2001) has recognized the Middlesex Readvance, south of Montpelier, Vermont, that is dated at 11.90±0.05 ka (GX-26457-AMS). The Middlesex Readvance is correlated with both the Bridport Readvance and the Littleton-Bethlehem Moraine, renamed the Littleton-Bethlehem Readvance by Thompson, et al., (1999).

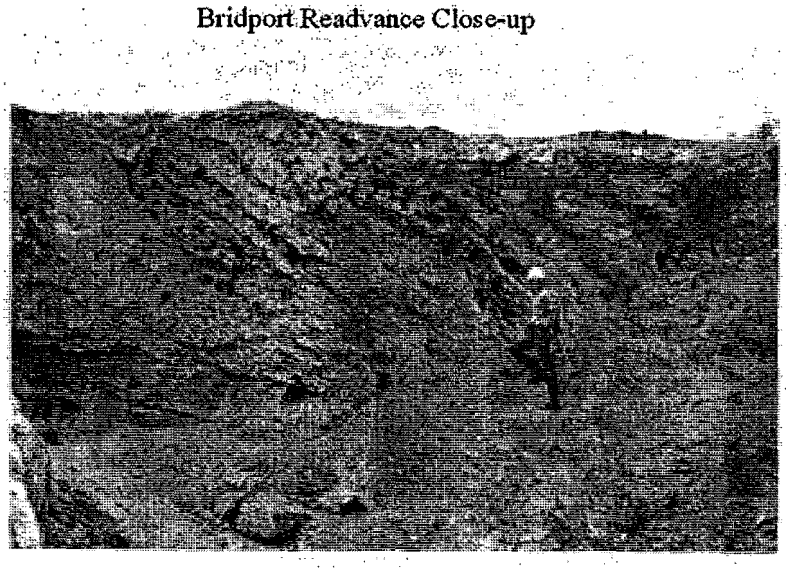

Figure 4. The Bridport Readvance at the type locality. Figure 4a, above, shows the contact between readvance till over gravel. Former Vermont State Geologist Charles Doll is shown behind the large clast. In Figure 4b, at right, the arrow shows a shear plane with gravel dragged into the till. The person in the foreground is Geologist Franklyn Paris. The figure is reproduced from Connally (1970), with permission.

The Bridport Readvance is anchored on the west by the Streetroad delta, a large ice-contact delta adjacent to the Adirondack Mountains and on the east by the East Middlebury delta, a large ice-contact delta adjacent to the Green Mountains. The Streetroad delta was nourished by glacial Putnam Creek. The East Middlebury delta was nourished by the glacial Middlebury River When the ice margin retreated north of Putnam Creek, the Streetroad delta was abandoned and Putnam Creek built the Crown Point delta at the same elevation. This documents the continued existence of Lake Albany even after the recession from the readvance. On the east, the Bristol, South Hinesburg, and Fairfax Falls deltas were deposited successively following retreat from East Middlebury, as discussed by Connally (1982, p.188). Thus, Lake Albany continued to exist as the ice margin retreated into the northern Champlain Valley.

THE DELTAS

There are six great deltas from which the above interpretations have been drawn. These are, from south to north, the Glens Falls, Fair Haven, Brandon, East Middlebury, Streetroad, and Crown Point deltas. This region may have the least complicated set of lacustrine and marine features in the entire Hudson-Champlain trough. Each is discussed below in detail. The spatial relationships are illustrated in Figure 5, extending south to the Hoosic delta and north to the Bristol delta in Vermont.

Throughout this paper, horizontal distances are given in kilometers. However, delta elevations are recorded in feet because they are estimates from the flat upper surfaces observed on topographic maps. Most maps of the Hudson and Champlain Valleys have map scales in English and metric units, while vertical scales remain in English units only. Besides, converting 500 ft to 152.4 m masks the nature of the estimate with an implied precision that does not exist.

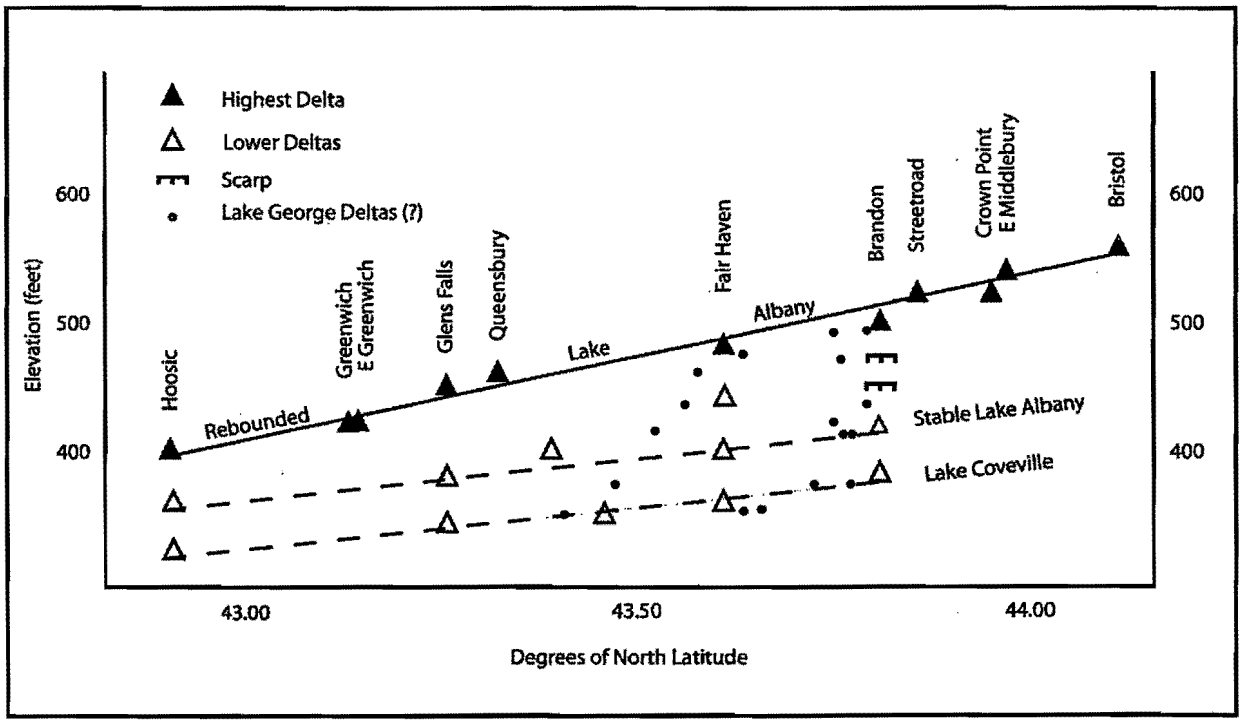

Figure 5. The spatial relations among the Glens Falls, Fairhaven, Brandon, East Middlebury, Streetroad, and Crown Point Deltas. The diagram is extended south to the Hoosic Delta and north to the Bristol Delta. Also shown are seventeen deltaic (?) deposits adjacent to Lake George. Lower "water planes" are included to bracket all the Lake George deposits.

The Glens Falls Delta

When the Luzerne Readvance ice blocked the Hudson River gorge, the water drained southward at the edge of the ice, forming the kame terrace at Wilton. When the ice receded, the Glens Falls delta was deposited by the Hudson River as it debauched from the Luzerne Mountains., southwest of Glens Falls. The upper, sandy surface of the delta is at ±460 ft at Queensbury and ±450 ft adjacent to the gorge. This is the level of Rebounded Lake Albany. There are secondary surfaces at ±380 ft and ±340 ft, with a sandy-clay surface at ±260 ft at Fort Edward. Presumably, these represent Stable Lake Albany, Lake Coveville, and Lake Fort Ann., respectively. There is a 520 to 540 ft ice-contact surface west of Glen Lake that heads at the French Mountain-Adirondack col. That outwash is assigned to a local lake confined to the lower Lake George trough prior to deglaciating the eastern col. All features are displayed on the Surficial Geology of the Glens Falls Region (Connally, 1973)

The Fair Haven Delta

The Fair Haven delta was deposited by the Poultney River, and by its tributary, the Castleton River. It was deposited at the geological contact between the Bomoseen slate belt and the lowland limestones, where the Castleton River debauches from the slate hills. The sandy, pebbly upper surface of the delta appears to be at ±440 ft east of Fair Haven, near Castleton Corners, Vermont. However, outwash adjacent to Lake Bomoseen, and ice-contact deposits in tributary Breton Brook, are graded to ±480 ft. There is a prominent sandy surface at ±400 ft at the village of Fair Haven, while an extensive sand plain to the west is graded to ±360 ft.

The 480 ft surface, clearly associated with active ice withdrawal, is assigned to Rebounded Lake Albany. The 440 ft surface is problematic, between the Rebounded and Stable Lake Albany surfaces. Perhaps the ice lingered there over long, or perhaps the point loading was much less than elsewhere and caused significantly less local rebound. Or, the surface may be erosional. The 400 ft surface is assigned to Stable Lake Albany and the 360 ft surface is assigned to Lake Coveville. Lake Fort Ann features are farther west. However, the Hubbardton River deposited a sandy delta at ±280 ft about 6 km northeast of Fair Haven that is assigned to Lake Fort Ann.

The Brandon Delta

The Brandon delta was deposited by the Neshobe River, where it entered the Otter Creek valley. The upper surface, at Forestdale, is at ±500 ft and represents Rebounded Lake Albany. A flat-topped surface at ±420 ft is assigned to Stable Lake Albany. Hanging deltas at ±380 ft at West Cornwall are ascribed to Lake Coveville, but Lake Fort Ann did not reach as far east as Brandon. These features are displayed on the Surficial Geology of the Brandon-Ticonderoga 15-minute Quadrangles, Vermont (Connally, 1970).

The East Middlebury Delta

The East Middlebury delta was deposited by the Middlebury River where it debauched from the Green Mountains. Ice from the Bridport Readvance blocked westward flow into the valley and diverted the river southward. Initial drainage followed the Halnon Brook channel, thence to a kame terrace at ±600 ft, west of a bedrock ledge. The flat, sandy delta top at ±540 ft is assigned to Rebounded Lake Albany. The foreset slope is south of the river, adjacent to Route 7. In the 1960's and 1970's there were several gravel pits that exposed the smoothly sloping foreset beds. Now, they are occupied by houses and guard dogs. Ice-contact structures were observed in 1965. This delta also is displayed on the Surficial Geology of the Brandon-Ticonderoga 15-minute Quadrangles.

When the Bridport Readvance ice margin retreated northward, the Middlebury River resumed its westward course, depositing a ±420 ft level to the north that is assigned to Lake Coveville. No Stable Lake Albany features have been recognized. Perhaps ice lingered here, blocking westward drainage until Lake Coveville developed. Or, perhaps there

had been a 460 ft surface, and it was a casualty of erosion. However, no evidence has been observed to support either hypothesis. The Lake Fort Ann shoreline is farther west.

The Streetroad Delta

The Streetroad delta has a foreset slope adjacent to Route 22 in the hamlet of Streetroad, New York, 4 km north of Ticonderoga. The gravelly delta top is at ±520 ft, sloping down to 340 ft. The 520 ft surface represents Rebounded Lake Albany. There are no secondary levels developed. Until the 1990's, a large gravel pit exposed the entire foreset slope (Connally and Sirkin, 1969, Stop #3). Meltwater and diverted drainage from glacial Putnam Creek deposited the delta. There is an inversion ridge that crests at ±600 ft, representing the outflow channel from the Adirondack headwaters of Putnam Creek. The discharge was diverted southward, between Buck Mountain on the west and Miller Mountain on the east. Several huge kettles, 80 to 100 ft deep, mark the center of the intermontane channel. Since the 1969 field trip, Van Diver (1980, p. 322, Fig. 9.8) has featured the Streetroad delta in his field guide of Upstate New York.

The presence of this delta, and the diverted flow of Putnam Creek, are undoubted evidence of the presence of Bridport Readvance ice north of Miller Mountain. The type locality for the readvance is 5 km east. When the ice receded, Putnam Creek was free to resume its normal eastward path to Lake Champlain and to deposit the Crown Point delta.

The Crown Point Delta

The Crown Point delta is contiguous with the Streetroad delta. It also has an upper surface at ±520 ft, representing the water plane for Rebounded Lake Albany. Deposition of the Crown Point delta marks the termination of the Bridport Readvance. It captured the drainage that had nourished the Streetroad delta.

The Crown Point delta exhibits inset deltaic deposits and/or levels for Stable Lake Albany at ±440 ft, Lake Coveville at ±340 ft, Lake Fort Ann at ±300 ft, Lake Greens Corners (Wagner, 1972, p. 325) at ±200 ft(?), and the Champlain Sea at ±120 ft. When the Bridport Readvance pulled back from the Adirondacks, Putnam Creek re-occupied its preglacial valley. Importantly, the presence of the 520 ft level is evidence that Rebounded Lake Albany still existed as the ice margin receded north. The surficial map of the Crown Point delta is illustrated by Kantrowitz (1968, Fig. 2). The map was created by Connally during a six-week cooperative study between the New York State Geological Survey and the Groundwater Branch of the U. S. Geological Survey in the autumn of 1966, but was published by Kantrowicz without citation or acknowledgment of authorship.

WHY *REBOUNDED* LAKE ALBANY

Why do we assign all of these positions to Rebounded Lake Albany? Earlier Connally, (1970, 1972); and Connally and Sirkin, (1971, 1973) assigned these deltas to three different lake levels. They assigned the Glens Falls delta to Lake Albany, the Streetroad delta to "Lake Quaker Springs", and the Bridport Readvance to Lake Coveville. However, the interpretation changed beginning in 1978.

The 1972 Model

Connally's initial involvement with Lake Albany began in 1965. As a party chief for the Vermont Geological Survey, he mapped the Lamoille Valley deltas in the Mt. Mansfield Quadrangle (Connally (1968b). He also

mapped the Middlebury River, Neshobe River, and Otter Creek deltas in the Brandon and Ticonderoga Quadrangles (Connally, 1970, Connally and Calkin, 1972). Prior to Connally's involvement, LaFleur (1965a) had completed mapping in the Capital District of New York. LaFleur, (1965a, Fig. 11) suggested that the lake levels he observed probably intersected levels recorded by Chapman (1937, 1942) for Lake Vermont in the Champlain Valley. He adopted Chapman's terminology, referring to four levels, in descending order, as Lake Albany, the Quaker Springs stage, the Coveville stage, and the Fort Ann stage.

In 1966 and 1967, Connally mapped the surficial geology of Clinton, Essex, Washington, and Warren Counties under a contract with the New York Geological Survey (Connally, 1968c). At that time, he recognized the deltas at Glens Falls, Streetroad, and Crown Point on the west side of Lake Albany and the Fair Haven delta on the east. He agreed with LaFleur's prediction of intersection of Hudson Valley and Champlain Valley water planes.

In an oral presentation in the spring of 1972 Connally naïvely proposed the first modern model for proglacial lakes throughout the entire Hudson-Champlain trough. Because lakes were continuous in both the Hudson and Champlain Valleys, he re-designated the lower levels as Lake Quaker Springs, Lake Coveville, and Lake Fort Ann. Unfortunately, after proposing "Lake Quaker Springs" in the Wisconsinan Stage volume (Connally and Sirkin, 1973) the term became entrenched in the literature. The name Lake Quaker Springs never should have been used, as discussed by Connally (1982, p.188). In this model The Connally (1972) model is sketched below as Figure 7a.

Instead of the expected hosannahs, the model was met with catcalls. Well, almost. Actually, a group of friendly geophysicists pointed out that the model depended on geophysical impossibilities combined with highly improbable coincidence. Each lake experienced instantaneous regional isostatic rebound at its termination – even though the glacier had not yet receded.

After the 1972 presentation, Connally revisited all deltas and inferred shoreline features, from The Terminal Moraine north to the Lamoille Valley. This led to minor adjustments, mainly to Lakes Coveville and Quaker Springs, resulting in almost parallel lake levels, sketched as Figure 7b. Even after the adjustments, the model still demanded instantaneous uplift for "Lake Albany". The adjusted model was almost identical to the one more recently re-proposed by DeSimone and LaFleur (1986), and most recently by DiSimone (1992).

The Problem

One problem just would not go away. When the two parallel levels of Glacial Lake Hudson are projected into the mid-Hudson Valley, they coincide with the *lower two levels* clearly recognizable there. The upper level, that has been recognized as Lake Albany since the time of Woodworth (1905), rises more steeply than the lower two from the Hudson Highlands, northward. But, Lake Albany shares the delta of Moodna Creek, at Cornwall, New York, with Lake Hudson. It diverges from that point to Glens Falls as shown in Figure 6.

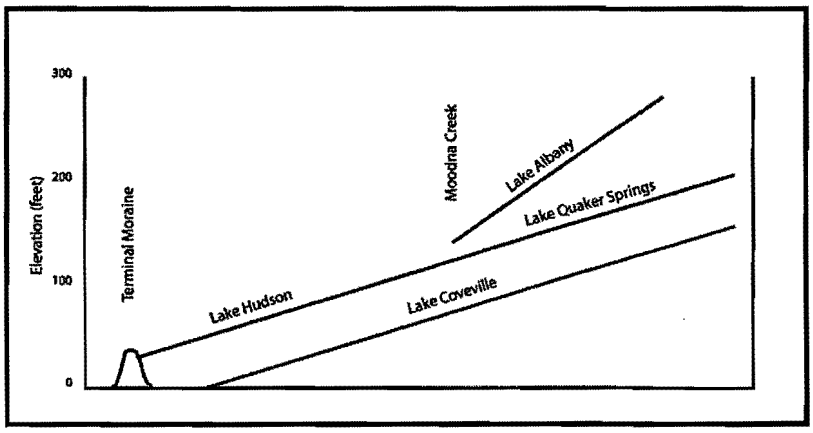

Figure 6. A cartoon illustration of the relationship between lake levels in the lower Hudson Valley during development of the 1972 and 1980 models.

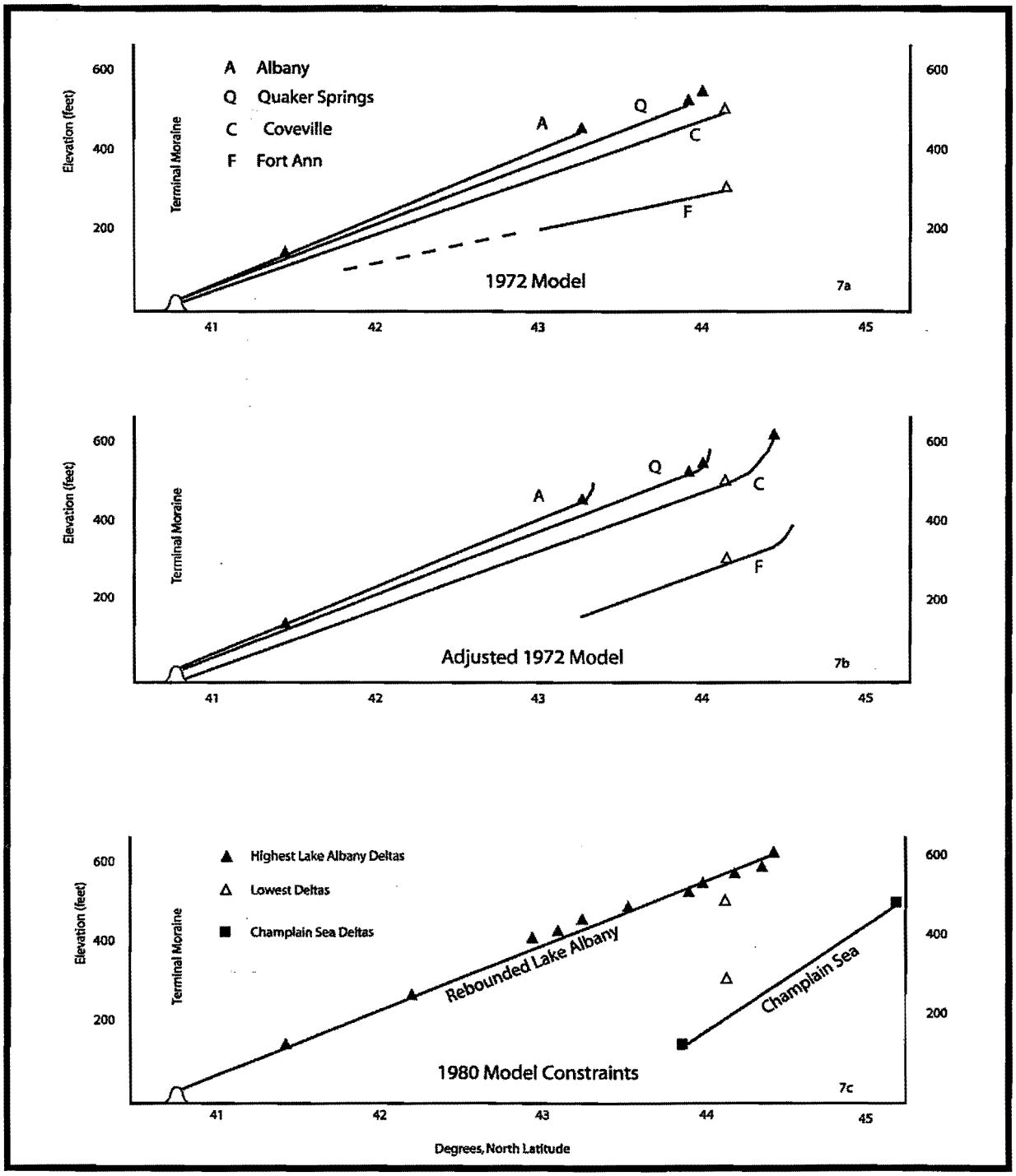

Figure 7. A comparison of the upper constraint on the 1980 model (7c) with the 1972 model (7a) and the adjusted 1972 model (7b) using similar data sets. The lower constraint on the 1980 model is the water plane for the Champlain Sea (7c).

What event could cause a regional isostatic rebound between the two levels? Did Lake Albany exist, and rebound, *before Lake Hudson*? Could ice have remained south of the Hudson Highlands while Lake Albany existed, and rebounded to the north, prior to Lake Hudson? If there was a hinge line at the Hudson Highlands, why didn't it affect lower lake levels? If Lake Hudson projects up the Hudson Valley as the middle level, then isn't that Lake Albany?

The 1980 Model

In the late 1970's, during several consulting projects, Connally re-mapped all the major deltas in the mid-Hudson and lower Hudson Valley. Mapping extended to the Lamoille Valley on the Vermont side and to the Plattsburg vicinity in New York. On the basis of the new mapping, Connally abandoned even the adjusted 1972 model, in its entirety, and re-examined the raw data, disregarding pre-existing models. This led to the development of a new model that was first proposed by Connally (1978) in an oral presentation and illustrated in a consulting report (Connally, 1980) two years later. There were few surprises, and no change in the mid-Hudson Valley. Two differences were obvious, and became constraints for the 1980 model.

The first constraint is that all of the uppermost deltas are related to recession of the ice margin of a single deglaciation. Readvances are considered to be part of that deglaciation. Most of those deltas had been, or could be, demonstrated to relate to an active ice margin. When all of the upper, ice-related deltas were connected by straight-line segments, the lines rose consistently in elevation from the Hudson Highlands to the north end of the Champlain Valley. They all are related to the same "water plane". This eliminated the most serious objection to the 1972 model; it obviates the necessity of proposing isolated rebound events to terminate each lake level. This then is the upper constraint on the model, illustrated in Figure 7c.

The second constraint is that sea level must equal sea level. This is much more than a trite tautology. Sea level, as determined by the Champlain Sea in the Champlain Valley, must equal the sea level at the New York bight, 20 km south of the Harbor Hill Moraine. Chapman (1937, p. 117) reports the Champlain Sea level at 525 ft. at Covey Hill, on the New York side, near the Canadian border. At the Crown Point delta, 120 km to the south, the marine limit is ±120 ft. This is a drop of 405 ft in 120 km or 3.38 ft/km (5.40 ft/mi). If this gradient is projected another 390 km south to the New York bight, it yields a sea level of -1,200 ft. Obviously a sea level 1,200 ft below present sea level is a ridiculous projection. Wagner (1969) reports a Champlain Sea delta top at ±480 ft at Enosburg Falls, on the Vermont side, only 108 km north of Crown Point. Wagner's projection results in a drop of 360 ft in 108 km, or an almost identical 3.33 ft/km (5.33 ft/mi), yielding a sea level of -1,189 ft. This gradient is only slightly more than the 4.7 ft/mi reported by Koteff and Larsen (1985) for the full Connecticut Valley.

How do we find the true marine level in the south? We could go to the various curves for sea level rise. However, as the model developed it became clear that the marine limit bore a consistent relationship to the higher Lake Fort Ann and Lake Coveville levels in the Champlain Valley. In the early 1980's Connally completed mapping all the quadrangles in the mid-Hudson Valley as early preparation for the New York State Surfacial Map (Cadwell and Dineen, 1987 and Cadwell and Pair, 1991), confirming that part of the model presented by Connally and Sirkin, (1986). When Connally and Sirkin recognized that the two projected levels of Lake Hudson projected to "Lake Quaker Springs" and Lake Coveville in the mid-Hudson Valley, it was a simple matter to project a hypothetical sea level there, assuming the same relationship present to the north. In the Champlain Valley, the "Quaker Springs level" is 40 ft above Coveville, 120 ft above Fort Ann, and 260 ft above the marine limit. When the southern level was projected northward, 260 ft below "Quaker Springs" and 220 ft below Coveville, it intersected with the Champlain Valley sea level projection near Ticonderoga, New York. This lower marine limit, that hinges near Ticonderoga, became the lower constraint on the 1980 model, illustrated in Figure 8a.

As implied above, the shorelines immediately above the marine limit in the Champlain Valley are essentially parallel to that limit, as realized by Wagner (1969). In ascending order there is the 1) Champlain Sea, 2) Lake

As implied above, the shorelines immediately above the marine limit in the Champlain Valley are essentially parallel to that limit, as realized by Wagner (1969). In ascending order there is the 1) Champlain Sea, 2) Lake Greens Corners (Lake St. Lawrence[?] of Pair and Rodriguez 1993), 3) Lake Fort Ann (the Fort Ann stage of Chapman, 1937 as modified by Wagner, 1969), 4) Lake Coveville (the Coveville stage of Chapman, 1937, as modified by Connally, 1980), and 5) the highest parallel level, part of which was recognized as Lake Quaker Springs until the term was abandoned, as discussed below. Above the set of parallel water planes, is the Lake Albany water plane that is decidedly not parallel in the 1980 model.

Lakes Coveville and Fort Ann

Before unbending the model to examine Lake Albany, we can make constructive observations about subsequent Lakes Coveville and Fort Ann. Quoting Chapman (1937, p. 95) on Lake Coveville:

> *"... when projected southward, it leads directly to an abandoned channel of the Hudson River... At Coveville, where the southern end of this channel overhang the Hudson River by more than a hundred feet, is a rock ledge which acted as the controlling threshold for the waters during the Coveville stage..."*

In the 1980 model, Lake Coveville projects more than 130 ft above the 200 ft threshold for which it was named. Even Lake Fort Ann projects to 50 ft above the Coveville outlet. It appears that the "Coveville outlet" had no significance, unless it was occupied temporarily as Lake Fort Ann drained. And there is some evidence for such an event. Lake Fort Ann projects 100 ft (Connally, 1978) above it's defined outlet south of Fort Ann, New York. However, lower level, Lake Greens Corners, evidently had its threshold in the Wood Creek valley between Fort Edward and Fort Ann, New York. Yet, three quarters of a century of usage has clearly established nominal priority for the Lake Coveville and Lake Fort Ann features. We suggest that we merely recognize a change in the outlets. But where then was the outlet for Lake Fort Ann?

The *Lakes* Albany

In Figure 8b, we remove the local component of post-Champlain Sea rebound, by straightening the hinge line. Present interpretation moves the hinge line northward from Ticonderoga to the Crown Point vicinity. In this projection, the two levels of Lake Hudson project all the way to the Champlain Valley. The lower level projects as Lake Coveville. In 1978 and 1980, the upper level was unwittingly designated "Lake Quaker Springs". Obviously this water plane represents northward expanding Lake Albany, north of the Hudson Highlands, while the upper divergent level represents traditional Lake Albany. Since 1982 Connally (1982, 1983) and Connally and Sirkin (1986) have recognized *both* upper levels as Lake Albany. The parallel water plane was named Stable Lake Albany.

To complete restoration to Champlain Sea time, the entire model is rotated into the horizontal plane (Figure 8c). This represents the attitude of the water bodies during, and shortly after, the Champlain Sea. From the rotated projection, very similar to that illustrated by Connally (1982, Fig. 4), it becomes obvious why the upper level was named *Rebounded Lake Albany.* This "water plane" diverges from Stable Lake Albany at the Hudson Highlands and does not rejoin it until the Lamoille Valley.

The first question is how did that happen? There are two choices. The first choice - the Big Burp! – is that at the close of Lake Albany time, there was a local rebound event that warped the plane upward. But that also should have involved Stable Lake Albany, and it does not offer any solution to the objections to the 1972 model. Thus, Connally (1982 Fig. 5) and Connally and Sirkin (1986, Fig. 8) invoked the second choice, illustrating a hypothetical "rolling rebound" to explain Rebounded Lake Albany. This was not a regional post-glacial rebound, but rather an adjustment to local unloading of the crust beneath the Hudson-Champlain trough which was comparatively overloaded during glaciation, relative to bounding mountain ranges on either side.

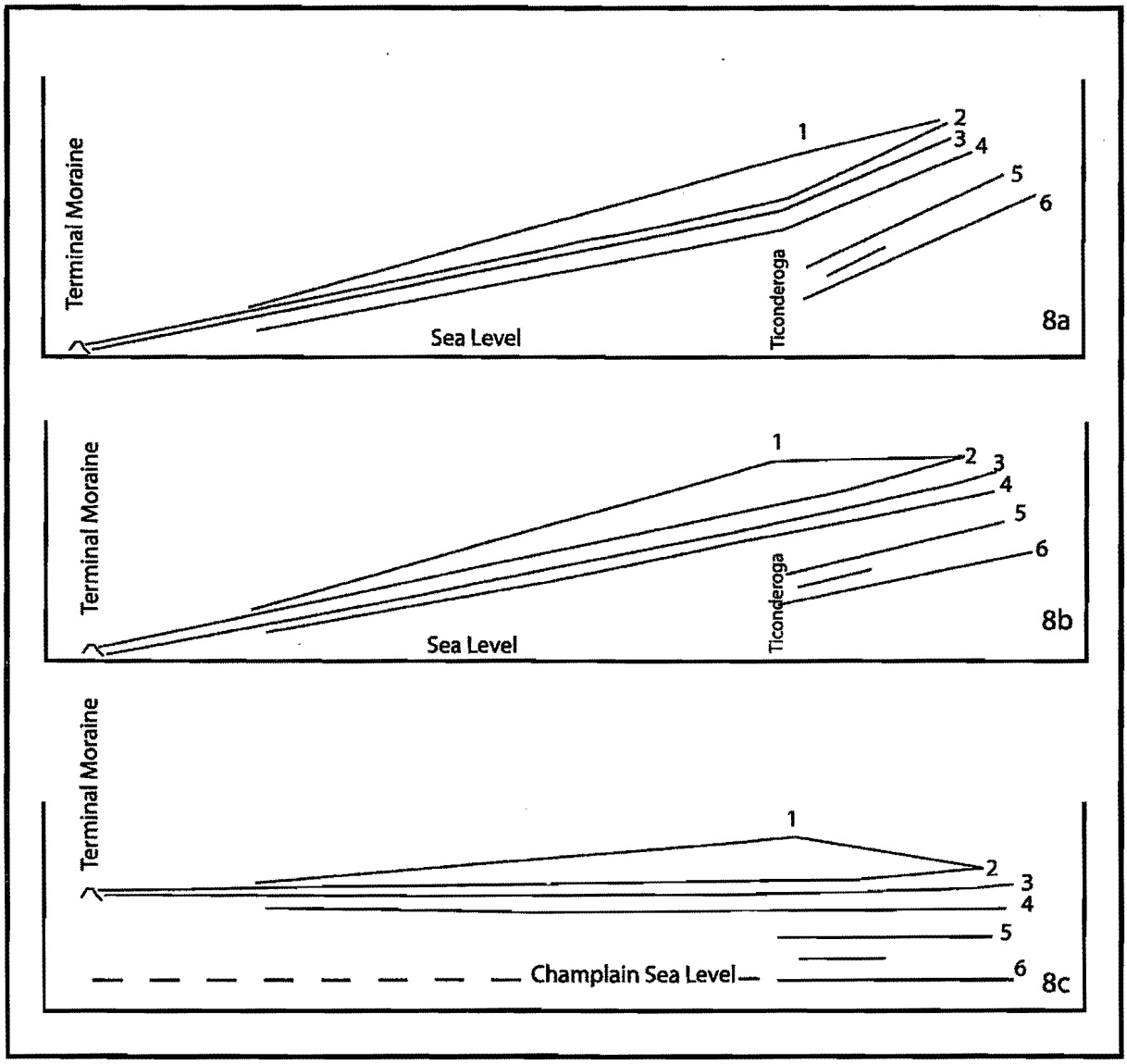

Figure 8: The 2002 model for Rebounded Lake Albany (1), Stable Lake Albany (2), Lake Coveville (3), Lake Fort Ann (4), Lake Greens Corners (5), and the Champlain Sea (6). Connally's data was supplemented with data from Reeds (1927) for the lower Hudson region, LaFleur (1965b) for the Capitol District, and Wagner (1969) for the Champlain Valley. Figure 8a is the actual 1980 model. Figure 8b is the 1980 model with the Ticonderoga hinge line removed. Figure 8c is the 1980 model with the Champlain Sea rotated to a horizontal plane, that should approximate the inferred sea level during that time.

The second question is, why didn't the same thing happen to the other lake levels. The answer almost certainly is time. Time! Glacial Lake Albany existed for 9,000 to 10,000 ^{14}C years. Lakes Coveville and Fort Ann lasted ±2 percent of that time. There is a 400 year period between the Bridport Readvance, at 11.90 ka, and recession into the St. Lawrence Lowland at 11.50 ka. If one half of that is allotted to recession to the Lamoille Valley and the other half to Lakes Coveville and Fort Ann, it only leaves 100 ^{14}C years for each. It does no good to quibble about 11.50 ka. The orders of magnitude remain the same. The time between Lake Albany and the Champlain Sea was comparatively quite short.

Now, to return to the original question, why *rebounded* Lake Albany? Rebounded Lake Albany is marked by a series off large deltas, both east and west in the Hudson and Champlain Valleys. Most, if not all, originated as ice-contact deposits. However, most continued to grow after the ice margin had retreated from each successive position. These deltas have two things in common. They almost all originated in contact with active or stagnant ice and they all are aligned vertically (Figure 9), from south to north. They form what had been called the Lake Albany "water plane". Connally's 1978 title was "Lake Albany: its untimely demise", referring to the probability that it never ever existed as a continuous, horizontal lake body. Whether the water plane marks an actual shoreline, or is an artifact of local rebound, is here immaterial. The important point is that it is a feature that ties all of these deltas to a common origin.

A Proposed Lake History

Lake Albany came into existence shortly after 20.18 ka, a date cited by Reimer (1984) for varves in the southern basin of Glacial Lake Passaic in northern New Jersey. The Terminal Moraine was deposited into Southern Lake Passaic (Stone et al., 1989), so this date probably pre-dates Lake Hudson/Lake Albany inception. Lake Albany continued to exist until about 11.80 ka, as inferred mainly from evidence from the field trip area, summarized in Figure 9.

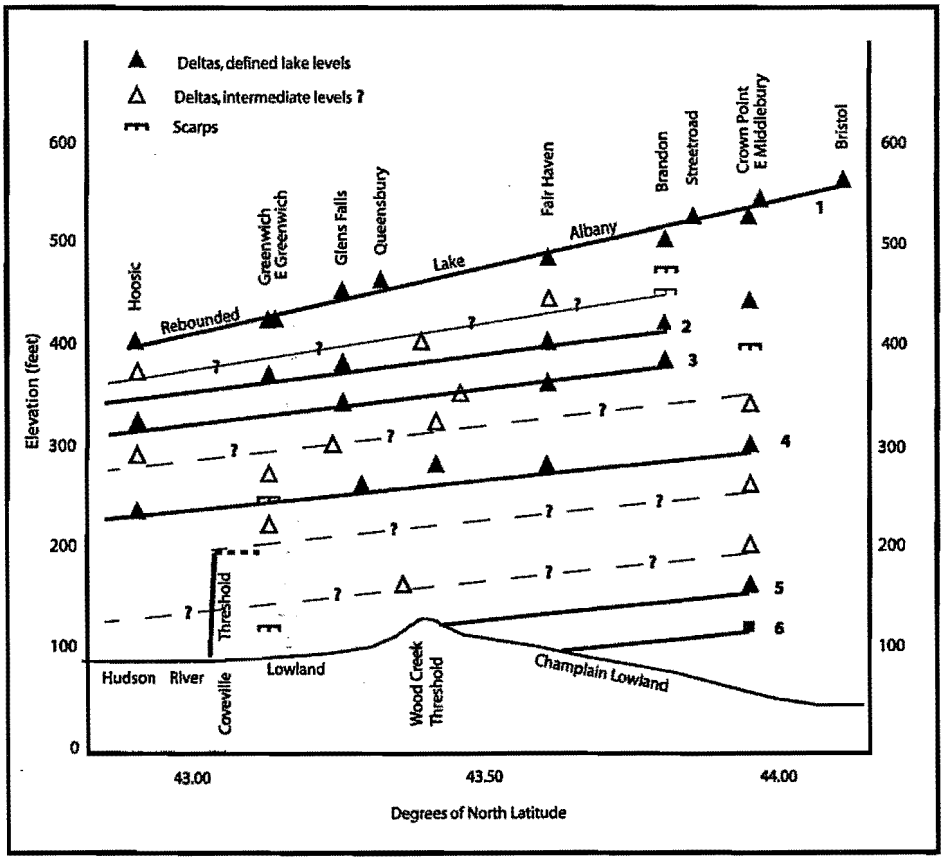

Figure 9. A diagrammatic representation of the inferred "water plane" for Rebounded Lake Albany (1). Also illustrated are the inferred water planes for Stable Lake Albany (2), Lake Coveville (3), Lake Fort Ann (4), Lake Greens Corners (5), and the Champlain Sea (6). The Coveville and Wood Creek Thresholds appear at the base of the diagram. Dashed lines indicate other possible intermediate lake levels.

As the ice margin retreated from the Bridport Readvance, but before it reached the Saranac River (Stevens and Gowan, 1988), the southern threshold for Lake Albany dropped ±40 ft, either due to downcutting at Hell Gate, or to development of a new, slightly lower, outlet. The new threshold controlled Lake Coveville, which became the new stable level, until perhaps 11.80 ka. Then the drift damn at the Staten Island Narrows was breached and Lake Coveville drained. Features in the study area suggest that there may have been a secondary level for Lake Coveville, 40 ft lower than the defined level.

With the draining of Lake Coveville, northern waters were dammed either by the Coveville delta(?) at the Hoosic River, blocking the Hudson River valley, or by the Schenectady delta in the Capitol District. Perhaps Lake Fort Ann waters briefly found an outlet at the Coveville threshold. The 260 ft delta level at Crown Point supports such an interpretation. The 200 ft level at Crown Point suggests a third "Fort Ann" level, perhaps blocked by the Batten Kill delta. We suggest that Lake Fort Ann existed until; ca 11.70 ka. DeSimone (1992, p.4) asked "Can multiple Fort Ann levels be recognized ...?" The answer is that they always have been. A more important question is, could the draining of Lakes Coveville and Fort Ann be the cause of the R6 and R5 freshwater fluxes cited by Clark, et al (2001)?

About 11.60 ka the impediments to the south, whatever they were, were finally breached in the Hudson River channel. Then the Wood Creek channel, north of Fort Ann, served as threshold for Glacial Lake Greens Corners. At 11.50 ka the ice margin cleared the Champlain Valley, creating Glacial Lake St. Lawrence.

CORE INTERPRETATIONS

In August of 2001, we obtained two cores from varved lake deposits east and west of Lake Champlain. An experienced geological consultant extracted the cores using his *geoprobe*. Cores were retrieved in 123 cm segments, in clear plastic tubes. In the lab, each segment was cut in half. Each half was heat sealed in plastic, labeled , and stored. One set of core halves was archived, while the other was transferred to Dr. Jack Ridge's core lab at Tufts University.

Core #3

Core #3 was spudded in Champlain Sea sediment on the St. Pierre Farm, at the southern end of the Crown Point peninsula. The site is 6 km northwest of the type locality for the Bridport Readvance and 7 km northeast of the Crown Point delta. Thus, the varve record was expected to include subsurface evidence for the readvance. The surface elevation is ±13 m above the level of Lake Champlain and 480 m west of the lake shore, where glacially polished and striated limestones are overlain by varved lacustrine clay. The varved clay is capped by shell-bearing marine clay. Marine clam shells were collected by Connally in 1967 from nearby drainage ditches, and by Connally and Sirkin in 1970 from the lake bluffs. The 1970 shells were dated at 14.35 ±0.60 ka (I-4988). Because it was not a reliable date it was never published. The lab description as "... the smallest sample we can measure. We were not able to remove any surface carbonate ... before the analysis." Probably explains the relative antiquity of the date. Wagner (1969, p. 337) obtained a date of 9.62 ±3.5 ka (I-4695) in the Crown Point vicinity.

A 15 m core was retrieved in 20 segments. There was little, if any, stratification evident in the upper 4 m of this core. Below 4.5 m the lacustrine clays are contorted and faulted. As noted during drilling, the top 30 cm of each of the ten lower tubes contained oxidized (5 Y), partly homogenized, lacustrine sediment. We speculated, in the field, that the hole might have partly collapsed after each core segment was withdrawn. During lab inspection, we speculated that the core barrel was pushing a column of compressed air, homogenizing the collapsed(?) sediment as it pushed. If so, then those sediments would be the first cored and would fill the top of each coring tube.

The only usable data from Core #3 came from the upper 4.5 m and is recorded below.

000 – 010 cm	A_p horizon	-- truncated, puddled, organic clay
010 – 012 cm	A_1 horizon	-- crumb structure, no organics
012 – 023 cm	B_1 horizon	-- transitional to B_2, below
023 – 045 cm	B_2 horiizon	-- root casts, some red/yellow patches
045 – 105 cm	C_1 horizon	-- some frost(?) cracks, prominent faulting
105 – 130 cm	C_2 horizon	-- some deep dessication cracks
130 – 380 cm	C_3 horizon	-- parent material; unaltered Champlain Sea sediments including concretions and ghosts
380 – 450 cm		transitional zone
450 cm to base		contorted lacustrine clays as reported above

Ridge (2002, oral communication) encountered similar conditions in marine clay near Plattsburgh, New York. Marine clay evidently flocculates, precluding varve formation. We have no way of knowing whether the contorted lacustrine clays are natural or were disturbed during coring. Thus, we are left with a tantalizing 15 m core that is useless for varve interpretation.

Core #2

Core # 2 was spudded in lacustrine sediment on the Champlainside Farm, 200 m east of the Lake Champlain shore, where glacially polished and striated Ordovician limestones are overlain by varved lacustrine clays. This site is almost exactly opposite Core #3. The surface elevation is ±48 m, 19 m above Lake Champlain and at least 6 m above the highest marine sediments. The elevation and location are critical. This core section never was inundated by the Champlain Sea. It lies 2.8 km north of the type locality for the Bridport Readvance and 1 km from the West Bridport multiple till section (Connally, 1970, p. 22) described below and illustrated in Figure 13.

00 – 02 ft	laminated clay with pebbles and boulders
02 – 18 ft	yellow brown lacustrine silt
18 – 22 ft	dark gray (N 3) clay-loam till
22 – 23 ft	oxidized (5 Y) till (?)
23 – 25 ft	gray-black (N 4) till
25 – 29 ft	light-gray (N 2) till

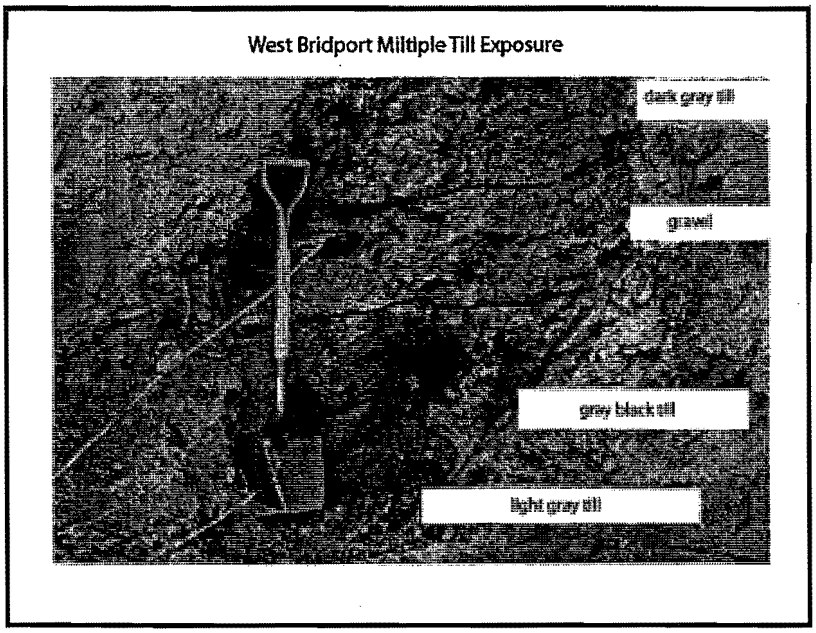

Figure 10. The West Bridport multiple till section, described above, as it was exposed in 1965. Figure reproduced from Connally (1970), with permission.

The basal light-gray till was interpreted as Shelburne till. The gray-black and dark-gray till, including the gravel lens, were interpreted as Burlington till. As in Core #3, the subsurface record should include evidence for the readvance and both preceding and succeeding lacustrine sedimentation. The entire record should be pre-Champlain Sea.

Core #2 is much more coherent than Core #3. It bottoms in 30 cm of dark-gray (N 3) Burlington till, identical to that in the West Bridport section, described above. Immediately on top of the till is a 38.67 cm sequence of 9 varves. Overlying the varves is a 40 cm, oxidized (5 Y) interval consisting of very contorted, mostly homogenized, lacustrine sediment. During drilling, this was interpreted as Bridport Readvance till, consistent with nearby exposures. However, because it is at the top of a core segment, and is so similar to the presumed "collapse" material on Core #3, its identification is problematic. In the overlying core segment, is a 6.1 cm interval of pebbly lacustrine material, overlain in turn by 101 cm yielding 13 distinct varves. There are four additional varves in the next 14 cm that are very disturbed; they were recognized on the basis of fragments of summer layers. The uppermost 246 cm is too disturbed to permit varve identification, even below the solum. A brief description of the core appears below.

000-015 cm	A_p horizon – dark, with organics
015-032 cm	B_2 horizon – red/yellow color patches
032-052 cm	B_{2t} horizon – massive clay, no peds
052-109 cm	B_3 horizon – frost riven with cryoturbation(?)
109-167 cm	C_1 horizon – obvious open dessication cracks
167-246 cm	C_3 horizon – lacustrine parent material
246-260 cm	5 indistinct varves
260-361 cm	13 distinct varves
361-367 cm	pebbly lacustrine sediment
367-407 cm	Bridport Readvance till (or "collapse")
407-446 cm	9 distinct varves
446-476 cm	dark gray (N 3) Burlington till

The varves in Core #2 were counted and calibrated at Tufts University, with the cooperation and guidance of Dr. Jack Ridge. We used his computer program to count and calibrate the two varve sequences illustrated below in Figure 11.

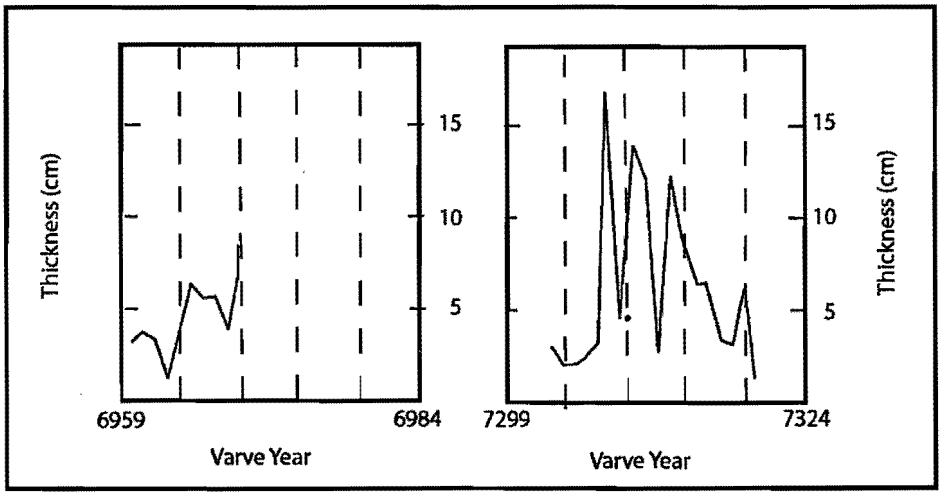

Figure 11. An illustration of the lower 9 varve sequence, on the left, and the upper 17 varve sequence on the right. The preferred match for the lower sequence is shown.

The two varve sequences were matched against the composite record for the upper Connecticut Valley. There were five possible matches for the younger 17-varve (17v) sequence and at least seven for the 9-varve (9v) sequence. Only one match, between varve years 7299 and 7315 is younger than the Bridport Readvance. According to Ridge et al. (1999), the Littleton-Bethlehem/Middlesex Readvance took place between varve years 7200 and 7400; advance no earlier than 7154 and recession no later than 7305. The 9v sequence was deposited between 6717 to 6726 at the earliest and between 6961 to 6970, at the latest. This suggests that a minimum of 230 years, as illustrated, and a maximum of 483 years of varves were removed by the readvance.

THE FIELD TRIP

The field trip will make two stops at the Streetroad delta. Stop #1 will examine the internal sediment and Stop #2 will examine an inversion ridge left by glacial Putnam Creek that delivered sediment to the delta. Then we will descend the Crown Point delta, pointing out the various named lake levels. Stops # 3 and #5 will be brief drive-by stops to point out the localities for Cores #3 and #2, respectively. Stop #4 will be at the Crown Point State Park campground where we will discuss the cores, point out some striae, and have an early lunch. Stop #6 will be a drive-by for the type locality of the Bridport Readvance. There is an alternate Stop #6A, with road log, that visits the East Middlebury delta. Since there is little left to see, we will skip that potential stop. It may be visited later by interested individuals. Stop #7 will be in the Hubbardton River delta for Lake Fort Ann. Stop #8 will be a drive-by on the various surfaces of the Fair Haven delta. Finally, we will traverse Lake Albany, crossing levels of the Glens Falls delta. We will finish at the type locality for the Luzerne Readvance in the Hudson River gorge between Glens Falls and Corinth.

ACKNOWLEDGMENTS

We are especially thankful for the support of The New York State Museum, Research and Collections Division, for Geoprobe coring and hollow stem auger coring in Crown Point, NY and Bridport VT; Lafayette College Committee for Advanced Study and Research, for a 1970 Grant from the Institutional Grant Fund, for the 13.15 and 14.35 ka dates. We thank the Howlett family at Champlainside Farm and the Sears family at St. Pierre Farm, for permission to obtain the cores. We also thank Dr. Jack Ridge, Tufts University, for his assistance in the interpretation of the cores.

REFERENCES CITED

Cadwell D. H., and Dineen, R. J., 1987, Surficial Geologic Map of New York, Hudson-Mohawk Sheet: New York State Museum, Map and Chart Series 40, 1 sheet, 1:250,000.

Cadwell D. H., and Pair, D. L. 1991, Surficial Geologic Map of New York, Adirondack Sheet: New York State Museum, Map and Chart Series 40, 1 sheet, 1:250,000.

Chapman, D. H., 1937, Late glacial and post-glacial history of the Champlain Valley: American Journal of Science, 5th series, v. 34, p. 89-124.

_____, 1942, Late glacial and post-glacial history of the Champlain Valley, Vermont: Vermont State Geologist, Report 23, p. 48-83.

Clark, P. U., Marshall, S. J., Clarke, G. K. C., Hostetler, S. W., Licciardi, J. M., and Teller, J. T., 2001, Freshwater forcing of abrupt climate change during the last glaciation: Science, v. 293, p. 283-287.

Connally, G. G., 1966, Surficial geology of the Mt. Mansfield 15-minute quadrangle, Vermont (unpublished report): Vermont Geological Survey, Burlington, Vermont, 33 p. with map, 1:62,500.

_____, 1968a, The Rosendale Readvance in the lower Wallkill Valley, New York, *In* National Association of Geology Teachers Guidebook, Eastern Section: SUNY College at New Paltz, New York, p. 22-28.

_____, 1968b, Surficial resources of the Champlain Basin, New York (unpublished): Report to New York State Office of Planning Coordination, Albany, New York, 111 p with maps, 1:24,000.

_____, 1970, Surficial geology of the Brandon-Ticonderoga 15-minute quadrangles: Vermont Geological Survey, Studies in Vermont Geology, No. 2, 45 p. with map, 1:62,500.

INFLUENCE OF GEOLOGY ON THE ACIDIFICATION STATUS OF ADIRONDACK LAKES AND STREAMS

Richard April
Department of Geology, Colgate University, Hamilton, NY 13346

Robert Newton
Department of Geology, Smith College, Northampton, MA 01063

INTRODUCTION

The effects of acid deposition on surface water quality in the Adirondack Mountains have been studied intensively since the 1970's. Findings show that the acidification status of streams and lakes is strongly influenced by the geology and hydrology of watersheds. Deposition input quantity and quality, the mineralogy and depth of surficial materials, the hydrological properties of soils, groundwater flow paths, wetland processes, snowmelt, etc., all contribute to the final chemical composition of surface waters. This fieldtrip will explore the processes and conditions that influence the acid-base status of surface waters as we visit lake watersheds in the eastern and central Adirondacks that display a wide range of geochemical, geologic and hydrologic characteristics.

As it turns out, for reasons to be described later, most acidic lakes and streams (pH < 5) are found in the western and southwestern Adirondacks, and also at high elevation and remote areas of the high peaks region. With the 2002 NYSGA/NEIGC meeting and field trips based out of Lake George, it was not feasible to design a one-day trip to encompass all of these areas; they were simply too far away, or too inaccessible. However, the stops selected for this field trip will illustrate how both geology and hydrology play a pivotal role in determining the acid-base status of surface waters contained within watersheds. Lakes and ponds to be visited include Clear Pond, Harris Lake, Arbutus Lake, and Echo and Little Echo Ponds.

THE ADIRONDACK REGION - BACKGROUND

Geology

The Adirondack Park, the largest park in the contiguous United States, comprises about 6 million acres of predominantly forested land dotted with more than 3,000 lakes and ponds (Figure 1). Water drawn from five major drainage basins flows along 1,500 miles of rivers fed by an estimated 30,000 miles of brooks and streams (State of the Park, Adirondack Council). Geologically, the Adirondack region forms the southwestern extension of the Grenville Province of the Canadian Shield with rocks ranging in age from 1.3 to 1.0 billion years old (McLelland and Chiarenzelli, 1990; McLelland, 2001; Figure 2). The major rock units underlying the area can be broadly divided into three types: granitic gneisses, anorthosites, and metasediments. Marble and other calcite-bearing

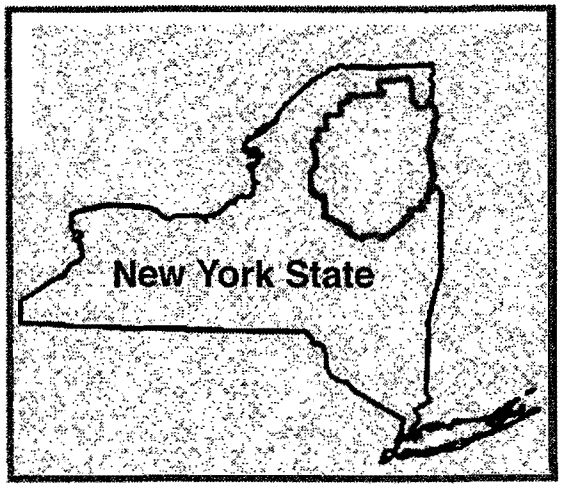

Figure 1. Area encompassed by the Adirondack Park.

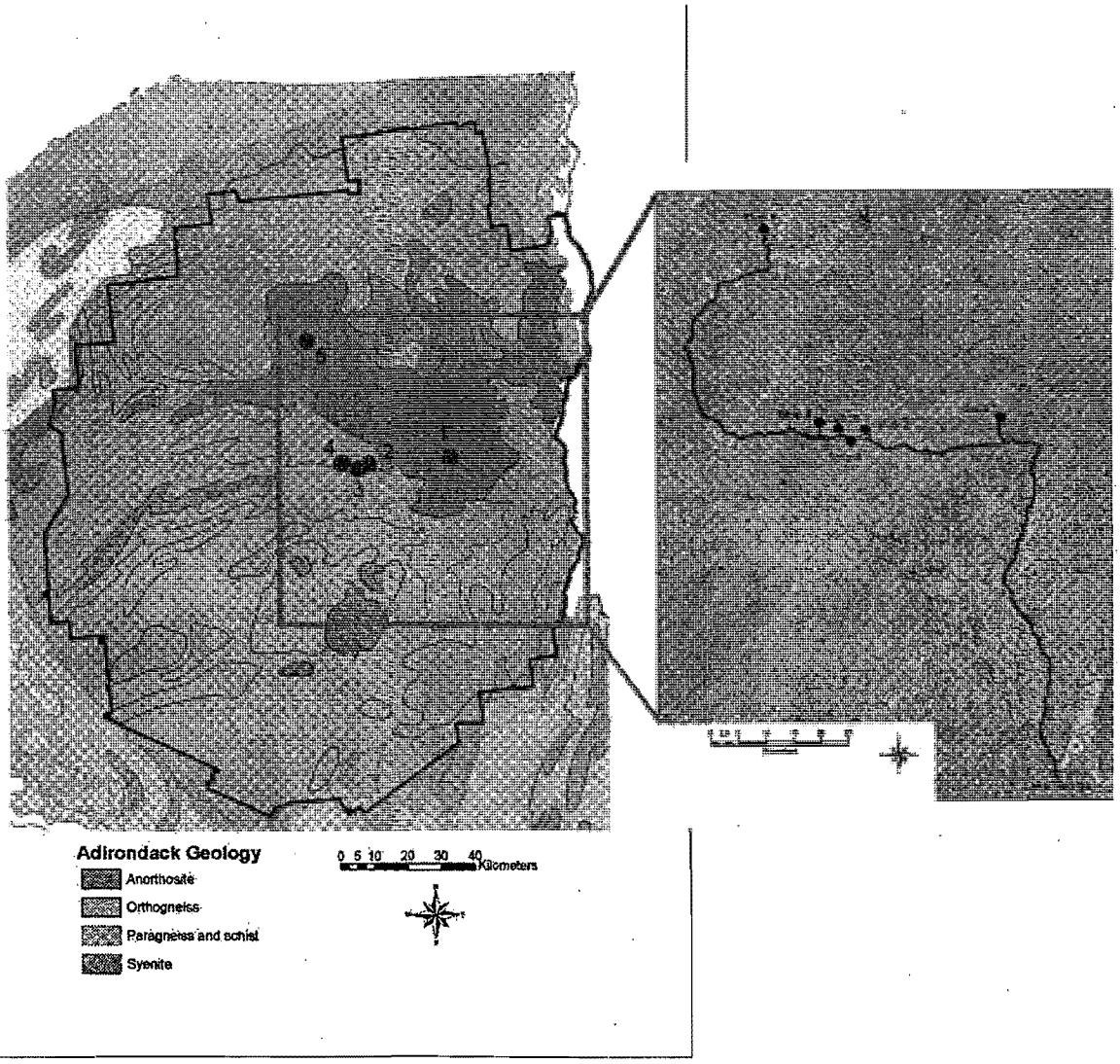

Figure 2. Generalized geologic map of the Adirondacks with field trip stops shown.

Acid Rain

The term 'acid rain' was first coined in 1872 in *Air and Rain: The Beginnings of Chemical Climatology*, a book published by Angus Smith, an English chemist, who was the first to systematically analyze the chemistry of precipitation in industrialized Britain. The effects of acidic deposition on aquatic and terrestrial ecosystems have been studied intensively since the late 1960's and early 1970's, first in Scandinavia, then in Europe, and eventually in the U.S when acid rain emerged as an important ecological issue (Oden, 1968; Likens et al., 1972).

The Adirondack Mountain region of New York State receives elevated inputs of sulfur and nitrogen in the form of 'acid rain.' Prevailing winds from west to east carry pollutants emitted in the Midwest, mainly from coal burning electric utilities, over the northeastern United States and Canada. Acid rain forms when SO_2 and NO_x emissions derived from the combustion of fossil fuels transform in the atmosphere to sulfuric and nitric acids. Long-range transport and deposition of these strong acids over time has resulted in the acidification of surface waters in northeastern North America, and in the Adirondacks in particular. Because components of 'acid rain' may enter terrestrial ecosystems as precipitation (both rain and snow), fog or mist (wet deposition), or as gases or particles (dry deposition), a more appropriate term used for 'acid rain' is acid deposition.

Precipitation in the Adirondacks averages about 100 -150 cm/yr, with about 70% falling as rain and 30% as snow (Johannes, 1985). This large quantity of precipitation results in high amounts of acid being delivered to the region. H^+ deposition averaged about 500 eq/ha/yr over the Adirondacks in the early 1990's. But because precipitation amounts decrease from west to east due to orographic effects, H^+ deposition decreases from west to east, as well, from about 520 eq/ha/yr to 470 eq/ha/yr (Charles, 1991). This is one reason why most acidic lakes and streams are located in the western Adirondacks. Average deposition of H^+ and SO_4^{-2} in the Adirondacks has been declining over the past few decades due to significant decreases in SO_2 emissions following implementation of the Clean Air Act Amendments (CAAA) of 1970 and passage of Title IV of the Acid Deposition Control Program by Congress in 1990. Average annual H^+ deposition fell to about 400 eq/ha/yr over the past decade and average annual pH values have risen from about 4.2 to 4.5 (http://nadp.sws.uiuc.edu/). There has been no significant change in nitrogen deposition, during this same period because CAAA legislation did not specify caps for NO_x emissions (Driscoll et al., 2001).

SURFACE WATER ACIDIFICATION

Most surface water in the Adirondacks is naturally dilute, with low amounts of dissolved solids, low ionic strengths, and low acid neutralizing capacity (ANC). Acid neutralizing capacity is a measure of the ability of water (or soil) to neutralize inputs of strong acid. ANC may be generated by terrestrial processes such as mineral weathering, cation exchange, and adsorption of SO_4^{-2} and N (Charles, 1991), or it may be generated in lakes or marshes by sulfate reduction. The higher the ANC of a water body, the more strong acid it takes to reduce the pH to the equivalence point. Bicarbonate ion, HCO_3^-, is the major acid neutralizing species in most surface waters, but all proton acceptors can contribute to ANC. Stumm and Morgan (1981) define ANC as follows:

$$ANC = [HCO_3^-] + [CO_3^-] + [OH^-] + [\text{other } H^+ \text{ ion acceptors}] - [H^+ \text{ ion donors}]$$

A study conducted by the Adirondack Lakes Survey Corporation (ALSC) in the mid-to late-1980's on 1469 lakes found that lakes with low pH and low ANC are prevalent in the Adirondacks, and that 26% of the waters surveyed had air-equilibrated pH values <5.0 and ANC's <0 (Kretser et al., 1989). Sulfate was identified as the dominant mineral acid anion in the ALSC study, indicating that sulfuric acid is the major source of mineral acidity. Waters with low pH and low ANC were found throughout the region, but were concentrated in the western and southwestern Adirondacks (see Figure 3). This area, which contains large numbers of small, high elevation lakes, also receives the highest levels of precipitation in the region. Another survey (EMAP; Larsen et al., 1994; Stevens 1994) conducted over the period 1991-1994 indicated that 41% of the 1812 Adirondack lakes studied were chronically acid or sensitive to episodic acidification. Of these lakes, 10% had ANC values less than 0 μeq/L, and 31% had ANC values between 0 and 50 μeq/L. Acid sensitive lakes and streams in the northeast U.S. are normally defined as those with ANC values less than 50 μeq/L.

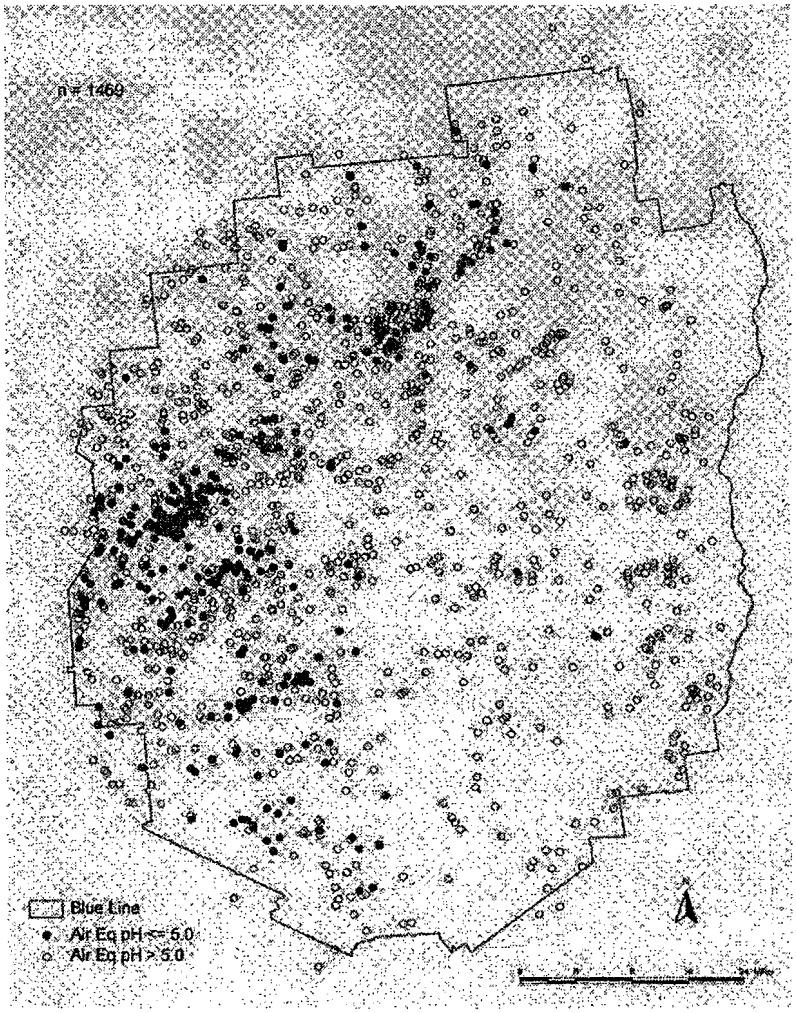

Figure 3. ALSC pH distribution (from Kretser et al., 1989, Adirondack Lakes Study 1984-1987: An Evaluation of Fish Communities and Water Chemistry).

Over the past century, inputs of acid deposition have led to the acidification of surface waters in the Adirondacks. Lakes, ponds, and streams with low ANC were the first affected and continue to be the most severely impacted today. Effects of acid deposition on surface water chemistry may vary with season and with the hydrologic processes prevalent in watersheds. For example, during winter months acidic components of precipitation are stored in the snowpack, which may reach depths of 1-2 m. During spring snowmelt, normally covering about a two-week period in April, large quantities of acid are released and cause surface waters to become more acidic than at other times during the year. This is called an episodic acidification event, and pH and ANC values may drop to less than 5.0 and 0 μeq/L, respectively, for days or weeks at a time. Usually, it is just the upper meter or two of a lake that acidifies during the event, but in streams the entire water column is affected. Episodic acidification of surface water can also occur after a particularly heavy rainfall, for example, from an air mass that might have originated in the Midwest where it encountered high levels of SO_2 and NO_x emissions.

BRIEF SUMMARY OF EFFECTS OF ACID DEPOSITION ON AQUATIC AND TERRESTRIAL ECOSYSTEMS

Introduction

The literature is rich with studies on the effects of acidic deposition on terrestrial and aquatic ecosystems, therefore, for more detail and further reading on this topic we refer you to both the scientific and popular literature that has been produced over the past three decades on this topic. Several excellent summaries worth mentioning here are those written by: Driscoll et al., 2001; Sullivan, 2000; Lawrence and Huntington, 1999; Charles, 1991; and Schindler, 1988.

We also direct your attention to several important and information-rich web sites, including:

http://www.adirondacklakessurvey.org/index.html
http://www.epa.gov/airmarkets/progress/arpreport/index.html
http://www.dec.state.ny.us/website/dar/index.html
http://www.epa.gov/oar/oaq_caa.html
http://nadp.sws.uiuc.edu/

Brief Summary of Effects

Acid deposition results in the mobilization of Al in soil solution, which subsequently enters streams and lakes. Spodosols in the Adirondacks are naturally acidic, but elevated concentrations of inorganic monomeric Al are enhanced by strong mineral acid additions to soils from atmospheric deposition (Cronan and Schofield, 1990). The source of the aluminum in soils is organically bound Al, exchangeable Al, Al-hydroxides and oxides, paracrystalline Al compounds, interlayer Al (in phyllosilicates), and ultimately, primary mineral weathering. Low pH and concomitant elevations of Al in surface waters contribute to the decline of fish, zooplankton and macroinvertebrate species in affected systems (Schindler et al., 1985; Schindler, 1988). Al concentrations in surface waters may reach toxic levels that are sustained throughout the year, or may rise only during episodic acidification events. In the latter case, elevated Al levels may coincide with critical biological events, such as the hatching of fry in the spring. High rates of fish mortality have been linked with acidic water and elevated aluminum concentrations (Baker and Schofield, 1982; Baker et al., 1996).

High levels of Al in soil solution along with the leaching of essential nutrients from soils may lead to reduced tree growth and dieback of forests (Shortle et al., 1997; DeHayes et al., 1999). Adirondack soils naturally have low base saturation and, therefore, any process that accelerates the removal of base cations from exchange sites decreases the ability of the soil to sustain plant growth. Replenishment of exchangeable bases for nutrient uptake depends heavily on primary mineral weathering, but in acid-sensitive soils mineral weathering may be sluggish. In soils that are composed of fairly resistant minerals, such as quartz, K-feldspar and muscovite, base cation supply is low and exchange sites may become occupied by H^+ and Al, rather than Ca^{2+}, Mg^{2+}, and K^+. Minerals such as Ca-plagioclase, biotite, hornblende, diopside, and calcite are much more susceptible to chemical weathering and can provide base cations at rates comparable with depletion rates accelerated by acidic deposition. Important here is consideration of the *quantity* of weatherable minerals present in the soil, the *residence time* of the subsurface water, and the *flowpath* of water through the soil. Calcium depletion seems to be a critical factor in Adirondack and other northeastern forest soils and studies are currently under way to assess the effect of Ca depletion on the dieback of tree species, such as red spruce and sugar maple among others (Driscoll et al., 2001; Lawrence et al., 1999).

Over time, soils receiving acidic deposition will accumulate both S and N, mainly in the form of SO_4^{-2} and NO_3^-. Driscoll et al. (2001) suggest that even though S deposition is declining because of emission controls on SO_2, the slow release of previously accumulated SO_4^{-2} from soils will delay the recovery of surface waters. NO_3^- concentrations are usually low in surface and soil waters because it is generally considered to be a growth-limiting nutrient in forest ecosystems. . However continued nitrate deposition can lead to nitrate saturation of the ecosystem. At this point nitrogen deposition exceeds nutrient uptake and excess nitrate is exported to surface waters. In the Adirondack region there does not seem to be any significant regional change in NO_3^- in surface waters, or in atmospheric deposition

PROCESSES INFLUENCING SURFACE WATER CHEMISTRY

Although much of the Adirondack region is underlain by acid-sensitive bedrock, the chemistry of surface waters varies widely across the region from about neutral to acidic. The extent of neutralization of acidic inputs to surface waters is determined by the interaction of a complex series of factors, including soil, hydrology, vegetation, geology, climate and atmospheric deposition. The relative contribution of these factors in regulating the acid-base status of surface waters is highly variable, even within very small regions. For example, hydrologic factors may dictate drainage water chemistry in one watershed, while an adjoining watershed may be largely influenced by geologic factors (e.g., the presence of carbonate minerals). Base cations are derived primarily from cation exchange and mineral weathering reactions occurring in the soil and in the surficial materials within a watershed (April et al., 1986; Newton et al., 1987). The rate at which these are supplied largely determines the acid-base status of surface water in the watershed.

For most watersheds in the Adirondacks, the routing of water through the soils and geologic materials is the major factor determining the base cation supply rate (Figure 4). The relative routing of water, or flow path, is a function of both the nature of the surficial material within the watershed, as well as the hydrologic retention time, or residence time, within the deposits. Surficial materials in the Adirondacks range from highly acidic upper soil horizons to more base-rich, relatively unweathered till and stratified drift. Rarely do drainage waters in the Adirondacks contact carbonate minerals. However, when carbonate minerals are present in the bedrock, the resulting surface water is enriched in base cations (particularly Ca^{2+} and Mg^{2+}) and ANC.

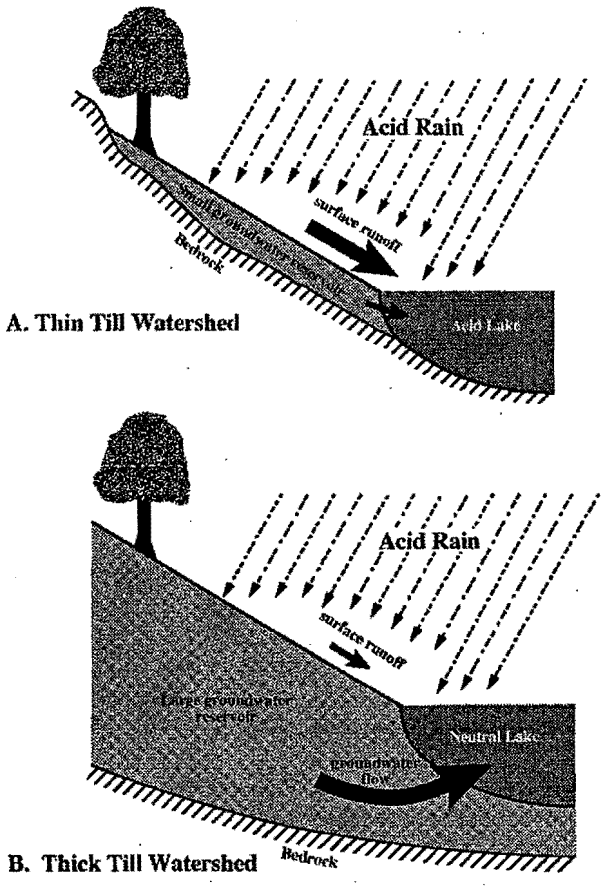

Figure 4. How flow paths of water through unconsolidated glacial sediments influence lake water chemistry.

The flow path of water moving through a watershed can be a function of a number of lake/watershed characteristics including thickness of unconsolidated sediments, hydraulic conductivity, and land slope. However, for most Adirondack watersheds, the dominant flow path is determined by the thickness of the unconsolidated glacial sediments overlying the bedrock (Newton et al., 1987). The thickness is also important, as it defines the size of the potential groundwater reservoir (Figure 4). Watersheds with thick surficial deposits have a large groundwater storage capacity. During precipitation events water infiltrates through soil and moves downward to the groundwater table where it is slowly discharged to streams and lakes. In these basins, deeper flow paths dominate and result in surface waters with higher ANC. In contrast, those watersheds with thin deposits of surficial sediments, or high proportions of bedrock outcrop, have only a small groundwater reservoir, which is rapidly filled during the early part of precipitation and snowmelt events. Subsequent rainfall or snowmelt is forced to move rapidly as shallow interflow through the upper acidic soils horizons, or as overland flow to streams and lakes, resulting in low ANC surface water.

Lakes and watersheds can be classified according to lake type and dominant flowpath. Drainage and seepage lakes represent the two major hydrologic lake types that occur in the Adirondacks. Drainage lakes are defined as lakes having a distinct surface outlet, whereas seepage lakes have none. Approximately 86% of the 1,469 Adirondack lakes surveyed by the ALSC are of the drainage type and 14% are seepage lakes (Figure 5; Kretser et al., 1989). On this trip we will look at three drainage lakes, Clear Pond (thick till), Harris Lake (carbonate and salt impacted), and Arbutus Lake (intermediate), and two seepage lakes, Echo Pond (flow-through) and Little Echo Pond (mounded).

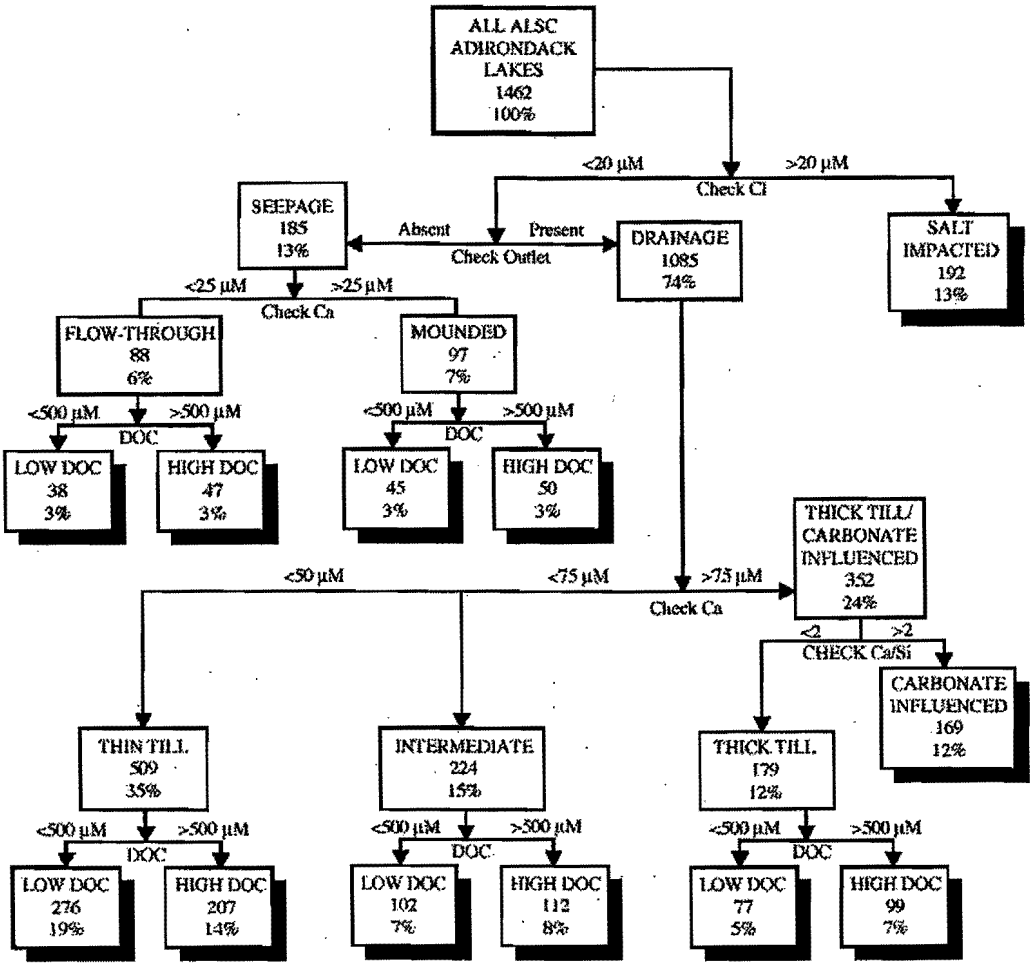

Figure 5. Lake classification diagram for 1,469 Adirondack lakes surveyed by the ALSC (Kretser et al., 1989)

CASE STUDIES OF ADIRONDACK LAKES

Clear Pond – STOP 1.

Clear Pond is a 73 hectare drainage lake occupying a watershed located just a few miles north of the Blueridge Highway (county route 2) (Figure 6). The area of the watershed is 12.06 km^2 and the lake surface elevation is 582 m. A number of fish species are present, including brook trout, cutlips minnow, common shiner, bluntnose minnow, white sucker, pumpkinseed, and banded killfish. The watershed sits at the southern edge of the high peaks region and is underlain by bedrock consisting primarily of metanorthosite with some granitic gneiss. Thin section examination of two bedrock samples (CL 102 and CL-108) revealed the first to be a garnet-biotite-quartz-oligoclase gneiss (metapelitic) with 5% garnet, 5-10% red-brown biotite, 40-50 % quartz and 40-50% oligoclase. The second, CL-108, was a gabbroic anorthosite with 90% plagioclase (~An_{45}) and 10% hypersthene.

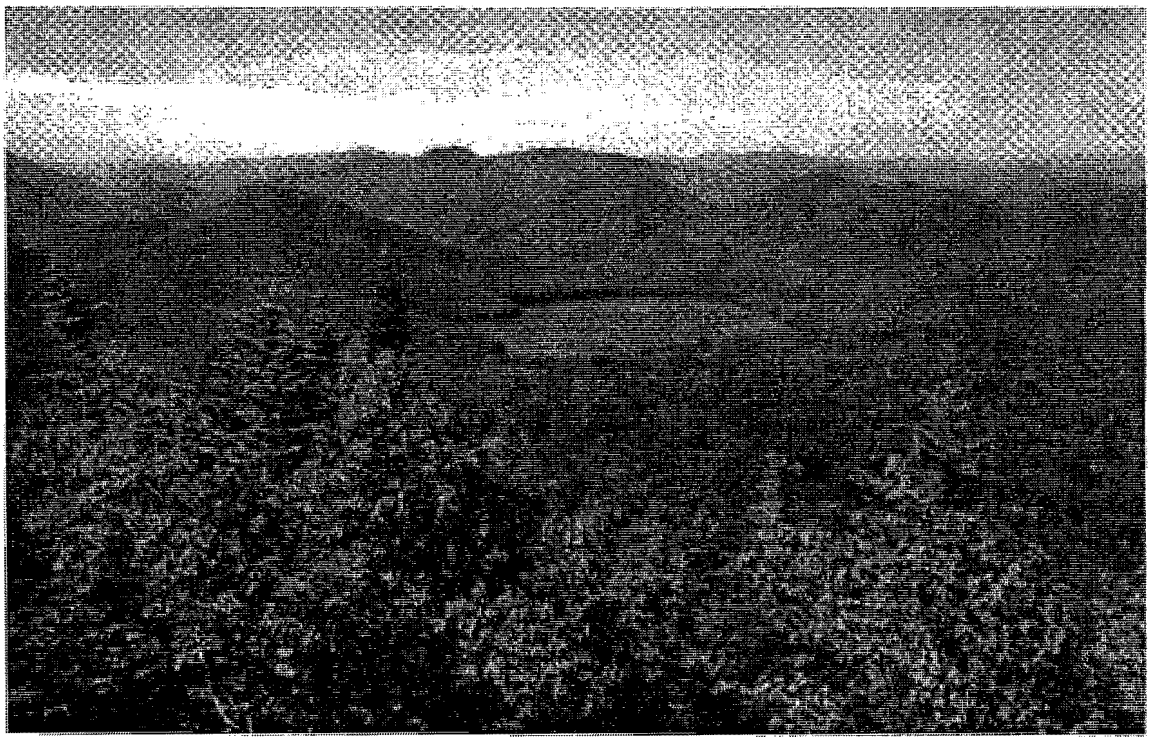

Figure 6. Clear Pond as seen from Sunrise Mountain looking south.

Areas of thick (>3 m) till and stratified drift cover approximately 33% of the watershed, with the remaining area covered by thin (<3 m) glacial deposits and bedrock outcrops (Figure 7). (Some nice till cuts can be seen on the right side of Elk Lake Road as we drive into Clear Pond.) Tills in the watershed contain on average 68% sand, 28% silt, and 4% clay. Quartz and plagioclase are the major minerals present in both the soil and glacial sediments. Vermiculite, mixed layer mica-vermiculite and kaolinite constitute the bulk of the clay mineral fraction. Heavy minerals make up 16.2% of the soil, with major constituents as follows: garnet 36.9%, pyroxene 34.4%, opaques 10.1%, epidote 8.6%, and hornblende 3.8%.

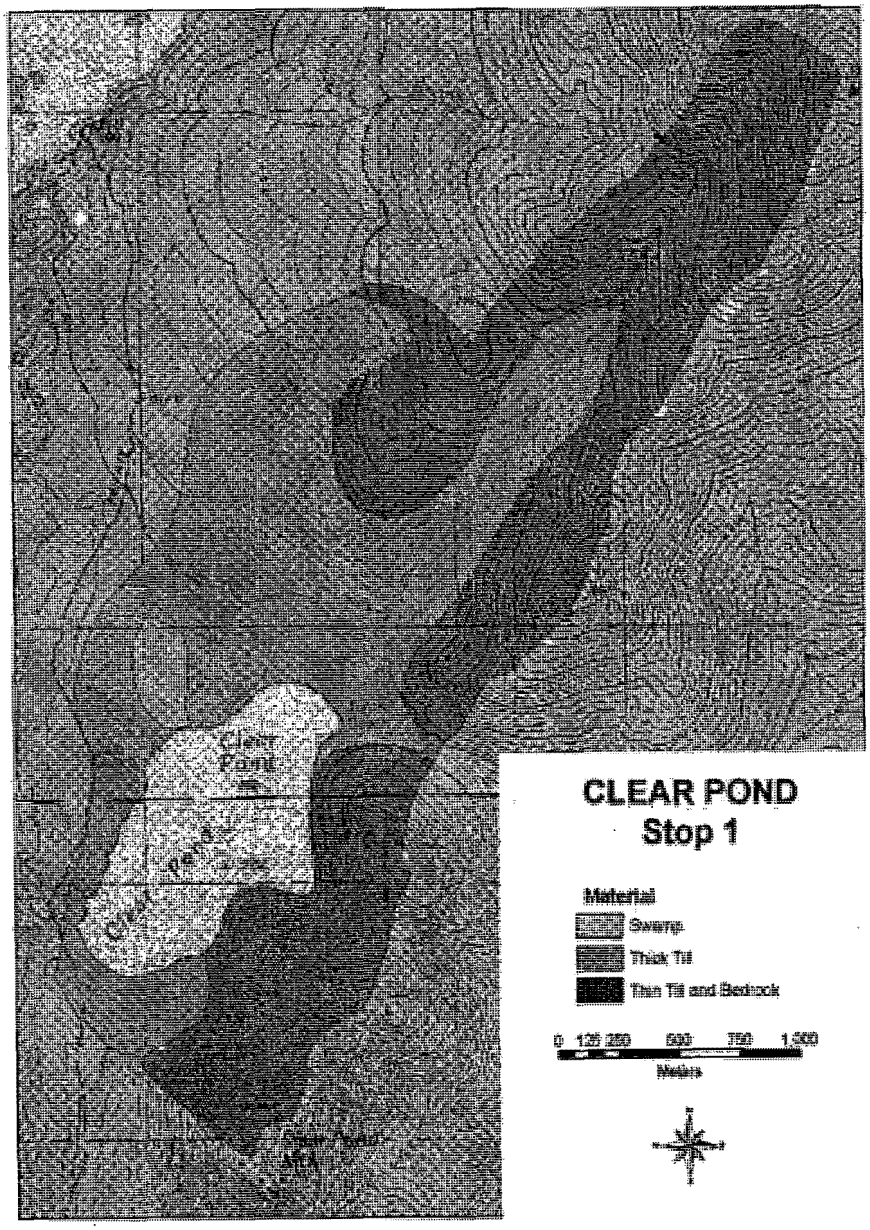

Figure 7. Surficial geology of the Clear Pond watershed.

Comparative values of the chemistry of Clear Pond in 1982-84 and 2002 are shown in Table 1. This is a circum-neutral lake with an ANC of about 100 μeq/L. Compared to other lakes we have studied (Driscoll and Newton, 1985; Table 2), Ca concentrations are relatively high but do not approach values found in some carbonate-influenced lakes. More importantly, the high Ca concentrations are coupled with high SiO_2, suggesting that the Ca is ultimately derived from silicate minerals rather than carbonates. Although there has been a significant decline in SO_4^{-2} (20 μmol/L) over the past 20 years, ANC has remained relatively constant. The nearly one-third drop in SO_4^{-2} suggests that we are seeing the effect of reduced SO_2 emissions over this period of time. The lack of response in

ANC is due to a corresponding decrease in base cations. Ca concentrations have declined by about 10% in twenty years and may reflect decreases in the flux of particulate matter to the watershed

Parameter	Clear Pond (82-84)	Clear Pond 2002
pH	7 (0.2)	7.09
ANC (μeq/L)	100 (19)	101
Ca (μmol/L	79 (11)	63.6
Mg	16 (2)	14.8
Na	37 (4)	38.7
K	4 (.7)	2.6
SO_4	63 (2)	43.7
NO_3	1 (2)	6.5
Cl	7.7 (1.5)	11.6
F	.7 (.3)	1.9
DOC	318 (64)	325
DIC	101 (52)	75.8
H_4SiO_4	70 (5)	209

Table 1. Chemistry of Clear Pond, today and 20 years ago.

Chemical characteristics of Adirondack study lakes[a]

Lake	pH	ANC (μeq/L)	NO_3^- (μeq/L)	SO_4^{2-} (μeq/L)	Ca^{2+} (μeq/L)	Monomeric Al (μmol/L)	DOC (μmol/L)
Arbutus Pond	6.2 ± 0.3	58 ± 21	10 ± 6	141 ± 10	152 ± 11	1.0 ± 0.6	420 ± 65
Barnes Lake[b]	4.7 ± 0.1	-14 ± 10	2 ± 3	65 ± 12	30 ± 4	1.1 ± 0.6	450 ± 136
Big Moose Lake	5.1 ± 0.1	1 ± 10	24 ± 5	140 ± 11	93 ± 10	8.9 ± 2.7	340 ± 78
Black Pond	6.8 ± 0.2	200 ± 21	4 ± 5	130 ± 3	191 ± 11	0.3 ± 0.6	350 ± 65
Bubb Lake	6.1 ± 0.2	41 ± 28	16 ± 7	131 ± 14	108 ± 13	1.8 ± 1.3	280 ± 82
Cascade Lake	6.5 ± 0.3	95 ± 52	29 ± 9	139 ± 10	159 ± 24	2.8 ± 1.9	310 ± 92
Clear Pond	7.0 ± 0.2	100 ± 19	1 ± 2	139 ± 11	157 ± 21	0.8 ± 0.7	320 ± 64
Constable Pond	5.2 ± 0.6	8 ± 22	17 ± 12	149 ± 19	98 ± 10	10.5 ± 4.3	420 ± 80
Darts Lake	5.2 ± 0.2	6 ± 12	24 ± 5	139 ± 7	97 ± 9	7.6 ± 2.7	320 ± 86
Heart Lake	6.4 ± 0.3	43 ± 12	5 ± 6	106 ± 11	119 ± 12	0.6 ± 0.6	310 ± 51
Little Echo Pond[b]	4.3 ± 0.1	-51 ± 17	0 ± 0	78 ± 17	36 ± 6	1.2 ± 0.5	1100 ± 153
Merriam Lake	4.5 ± 0.2	-25 ± 15	21 ± 13	137 ± 11	58 ± 7	19.0 ± 0.6	480 ± 110
Moss Lake	6.4 ± 0.2	66 ± 25	26 ± 6	141 ± 8	146 ± 15	2.2 ± 1.6	310 ± 61
Otter Lake	5.5 ± 0.5	13 ± 16	9 ± 9	138 ± 21	88 ± 11	5.0 ± 3.6	200 ± 54
Lake Rondaxe	5.9 ± 0.5	33 ± 25	23 ± 6	134 ± 7	112 ± 10	4.4 ± 3.0	300 ± 60
Squash Pond	4.6 ± 0.6	-22 ± 39	24 ± 17	131 ± 18	65 ± 28	19.2 ± 7.6	580 ± 127
Townsend Pond	5.2 ± 0.6	18 ± 21	27 ± 15	154 ± 30	95 ± 16	9.9 ± 7.9	260 ± 81
West Pond	5.2 ± 0.5	29 ± 50	10 ± 6	111 ± 13	94 ± 24	6.6 ± 2.1	670 ± 204
Windfall Pond	5.9 ± 0.4	44 ± 30	26 ± 14	141 ± 17	143 ± 19	5.6 ± 2.4	390 ± 92
Woodruff Pond	6.9 ± 0.2	410 ± 140	2 ± 3	147 ± 17	430 ± 120	1.0 ± 1.1	710 ± 161

[a] Arithmetic mean and standard deviations shown for the samples collected
[b] Barnes and Little Echo are seepage lakes; the others are drainage lakes

Table 2. Chemical characteristics of RILWAS Adirondack study lakes (from Driscoll and Newton, 1985).

Questions to consider at this stop are:

1) Is Clear Pond a typical Adirondack drainage lake? Does the preponderance of metanorthosite over granitic gneiss influence the chemistry of the lake water?

2) Is it possible to tie the decline in SO_4^{-2} in Clear Pond over the past 20 years to reductions in SO_2 emissions? Has sulfate (and nitrate) accumulated in soils over time, and if so, how long will sulfate (and nitrate) continue to leach out of soils into stream and lake water?

3) Does the increase in NO_3^- reflect the fact that Knox emissions have remained relatively steady over the past 20 years, whereas SO_4^{-2} has declined? Has the proportion of sulfuric and nitric acid in deposition changed over time?

4) Do lower Ca values reflect a decrease in the influx of Ca from particulate matter, or does it suggest lower weathering rates in the watershed? Ca depletion on exchange sites has been measured in the Adirondacks (and the Catskills, Lawrence et.al., 1999) and it has been suggested that high acid loadings in the Adirondacks have resulted in significant depletion of base cations in the soils. Because ANC values for most Adirondack lakes have not risen over time, is it possible that base cation depletion in soils will delay recovery of Adirondack lakes?

Harris Lake (and Woodruff Pond) – STOP 2

Harris Lake is a 116 hectare drainage lake occupying a watershed located just north of route 28N (Figure 8). The area of the watershed is 183 km^2 and the lake surface elevation is 473 m. Over a dozen fish species inhabit the lake, including northern pike, common shiner, white sucker, brown bullhead, rock bass, smallmouth and largemouth bass, and yellow perch. The watershed straddles a thin belt of metasedimentary rocks comprising calcitic and dolomitic marble, calcsilicate rock, quartzite and interlayered gneisses (Geologic Map of New York, NYS Museum). Harris Lake has not been included in any of our recent studies, so we cannot provide more detailed information concerning the geologic and mineralogic characteristics of the bedrock and glacial deposits within the watershed. However, in walking the southern shoreline one observes outcrops of calcsilicate rocks, containing calcium carbonate (Figure 9). In a class mapping exercise in 1990, Colgate students identified outcrops of calcsilicates on the northeastern shoreline, and also found outcrops of granitic gneiss in the northern areas of the watershed and on the easternmost shore of the lake.

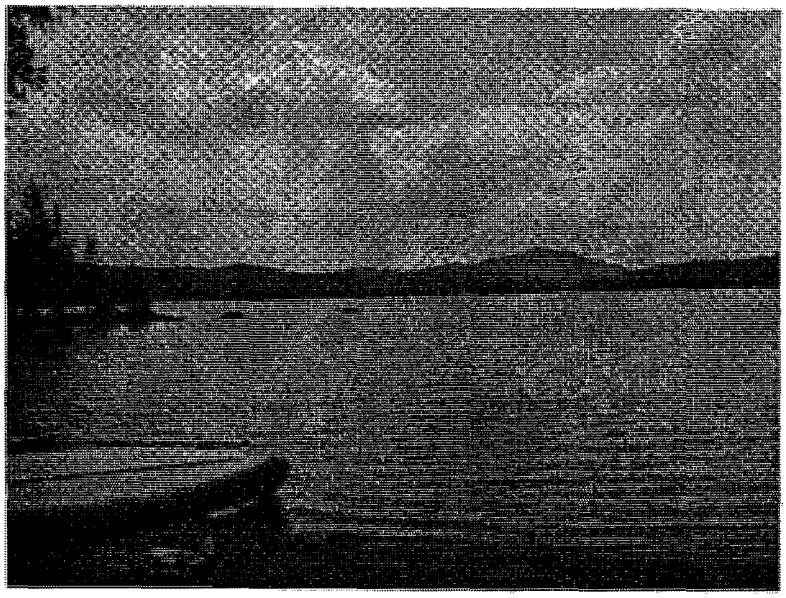

Figure 8. Harris Lake as seen from the NYS campground area.

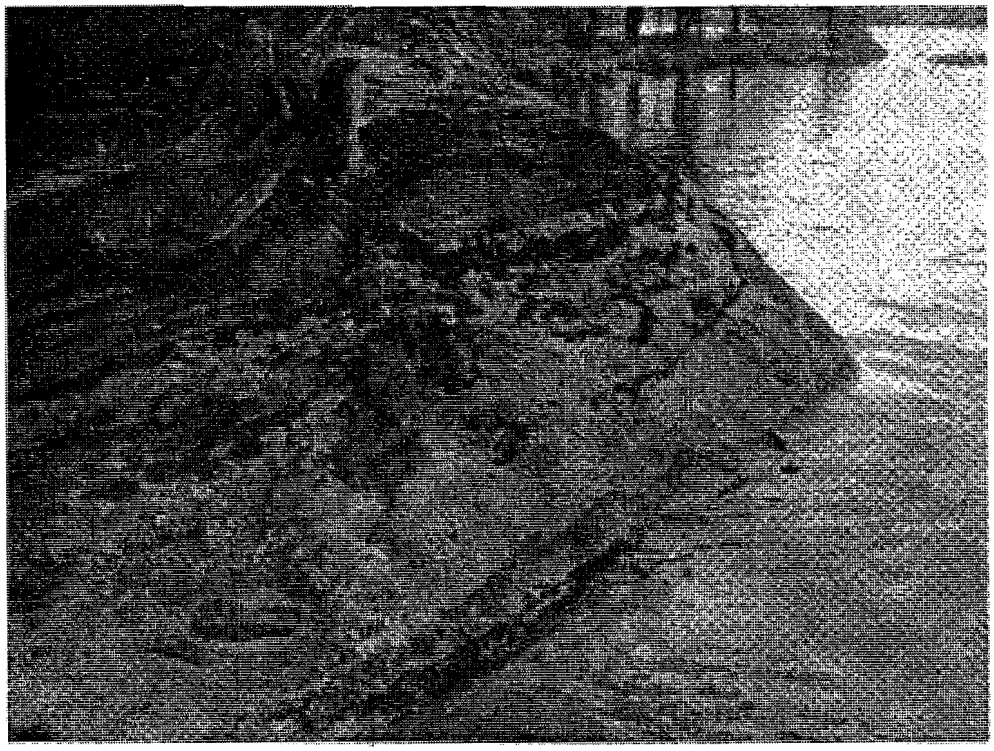

Figure 9. Outcrop of calcsilicate containing calcium carbonate on the southern shore of Harris Lake.

Harris Lake is classified as a salt-impacted lake using the ALSC classification (Figure 5). This reflects the proximity of the highway and other anthropogenic influences within this watershed. Throughout the Adirondacks, developed lakes with cottages and their associated septic systems, roads, etc have relatively high concentrations of Cl^-. We stop at Harris Lake to consider the effect of the presence of carbonate-bearing rock on the chemistry of the lake water. As Table 3 shows, Ca values are high, but compared with other Adirondack lakes (Table 2) the values do not seem so unusually high to suggest that the chemistry of Harris Lake is controlled solely by the dissolution of carbonate minerals. In fact the lake does not have a high enough Ca/Si ratio (2) to qualify as a carbonate controlled lake. Perhaps a better indicator of the impact of carbonate minerals in this watershed is the high ANC of about 200 μeq/L, which is one of the higher values observed in the Adirondack lakes we have studied.

Parameter	Harris Lake 1987 (ALSC data)	Harris Lake 2002
pH	7.17	7.20
ANC (μeq/L)	193.7	232
Ca (μmol/L	119.5	136.5
Mg	35.8	46.9
Na	77.9	134.8
K	8.7	8.2
SO_4	50.0	48.3
NO_3	1.13	16.3
Cl	64.6	117.6
F	3.42	0.95
DOC	558	492

Table 3. Chemistry of Harris Lake, today and 15 years ago.

Only Woodruff Pond, a drainage lake that sits a stone's throw to the south of Harris Lake and whose watershed also sits within the calcsilicate – marble belt, has a higher ANC (and Ca concentration; Table 2). Three bedrock samples from Woodruff Pond were thin sectioned and analyzed with the petrographic microscope. The first was an amphibolite with 40% hornblende, 10% hypersthene, 50% plagioclase and 1-2% biotite. The second was a quartz-diopside calcsilicate with 30-40% quartz, 20-30% diopside, 20% phlogopite, 5-10% calcite and a trace of tremolite. The third was a quartzite with 60% quartz, 20% hornblende, 5% garnet, 5% hypersthene, and 2% calcite. Areas of thin (<3 m) till and stratified drift cover most of Woodruff watershed; calcsilicate boulders are common. Quartz, plagioclase, K-spar, hornblende and pyroxene are the major minerals present in both the soil and glacial sediments. Vermiculite, mixed layer mica-vermiculite, kaolinite and talc constitute the bulk of the clay mineral fraction. Heavy minerals make up 21.1% of the soil, with the major constituents as follows: pyroxene 23.5%, opaques 23.5%, hornblende 20.3%, garnet 11.9%, and epidote 5.8%.

On the basis of the thickness of the surficial deposits one might expect Woodruff Pond to have low ANC. In fact, Woodruff Pond has the highest ANC (410-480 μeq/L) observed of all lakes in the Regional Integrated Lake Watershed Acidification Study (RILWAS; Driscoll and Newton, 1985). The relationship between base flow discharge and sum of the base cations (SBC) for several of the RILWAS lakes is shown in Figure 10. All lakes except Woodruff Pond fall between end members Woods Lake, with a watershed dominated by thin till (average depth 2.3 m), and Panther Lake, with a watershed dominated by thick till (average depth 24.5 m) (April and Newton, 1985). Woodruff Pond has a base flow discharge that is almost as low as Woods Lake, yet it has an ANC of 410 μeq/L and SBC of 600 μeq/L. Woodruff Pond watershed provides a dramatic example of the influence that carbonate minerals have on surface water chemistry. Although the water moves rapidly along shallow flow paths, there is sufficient time for carbonate minerals to react. The dissolution of calcium carbonate is rapid and base cations, in this case Ca, are readily supplied to the drainage water. Hence, flow path is not the major determinant in regulating the acid-base status of Woodruff Pond. Rather, the presence of carbonate in the till, and also in the underlying bedrock, is the chief controlling factor.

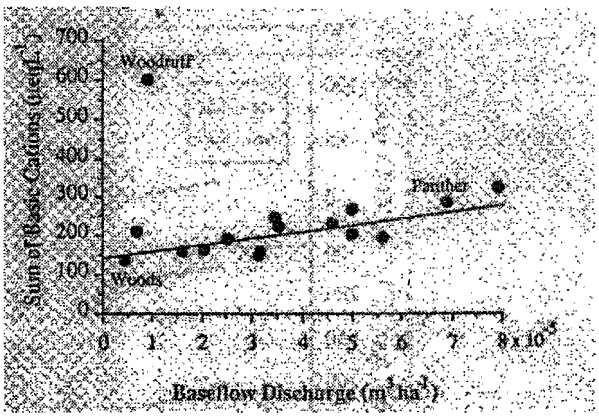

Figure 10. Average ANC as a function of low-flow discharge for the RILWAS and ILWAS watersheds (from Charles, 1991)

Harris Lake watershed probably falls somewhere in between and can be considered a carbonate-influenced (but not controlled) lake. Although carbonate is present in the watershed materials, the entire watershed is not within the calcsilicate-marble belt. Indications are that at least half of the watershed area is underlain by granitic gneiss, and although some of the till in the watershed may contain carbonate minerals, much of the glacial cover is likely 'granitic' in composition and devoid of carbonate minerals. Water in contact with carbonate-bearing outcrops along the shore may contribute to increasing lake water Ca concentrations and ANC. However, the relative contribution of this water to the overall chemistry of Harris Lake, although significant, is probably small. We still have much more to do in Harris Lake watershed, but it serves as a good example of an area where surface water chemistry is influenced, somewhat, by the presence of carbonate minerals.

Questions to consider at this stop are:

1) How do we measure the influence of carbonate minerals on lake water chemistry? Is it the carbonate in the bedrock, or the carbonate in the till, or both, that is most important in raising ANC and pH?

2) Does the Ca to Si ratio in surface water give us an indication of the amount of carbonate mineral weathering taking place? That is, can carbonate influenced water be differentiated from non-carbonate influenced water by calculating the molar ratio of Ca^{2+} to H_4SiO_4?

3) With ANC values of 200 μeq/L or more, are lakes like Harris and Woodruff essentially insensitive to changes caused by acid deposition?

4) Can we artificially create carbonate-influenced lakes by liming techniques? And is it best to lime the lake, or the watershed?

Marble Outcrop – STOP 3

Lunch at Adirondack Visitors Center

Arbutus Lake – Huntington Wildlife Forest – STOP 4.

Arbutus Lake is a 49 hectare drainage lake occupying a watershed located in the Huntington Wildlife Forest (Figure 11). The area of the watershed is 3.75 km^2 and the lake surface elevation is 513 m. The watershed is underlain by granitic gneiss, but small outcrops of amphibolite and biotite-rich gneiss have been identified. The watershed has been gauged at the lake outlet since October 1991 with a V-notch weir. Huntington Forest has also participated in the National Atmospheric Deposition Program (NADP) and the National Trends Network (NTN) since Oct. 31, 1978 (see Figures 12 and 13 for trends in sulfate and pH). In May, installation of an EPA CASTNET dry deposition monitoring system was completed. Time permitting, we will take a short hike to view these instrumentation set-ups.

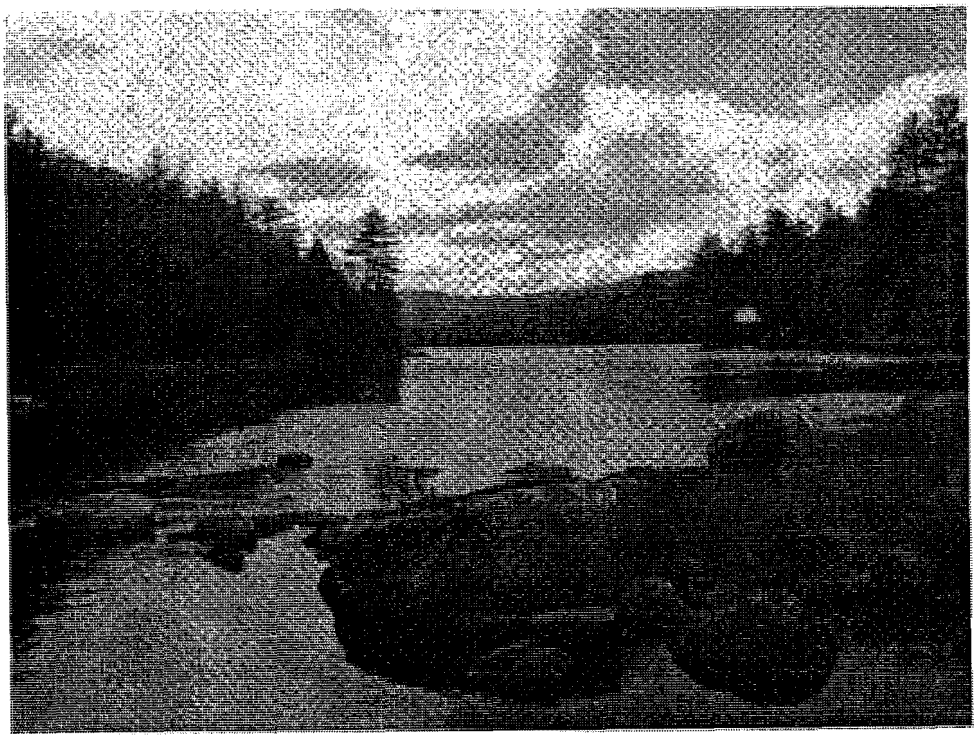

Figure 11. View of Arbutus Lake from the outlet.

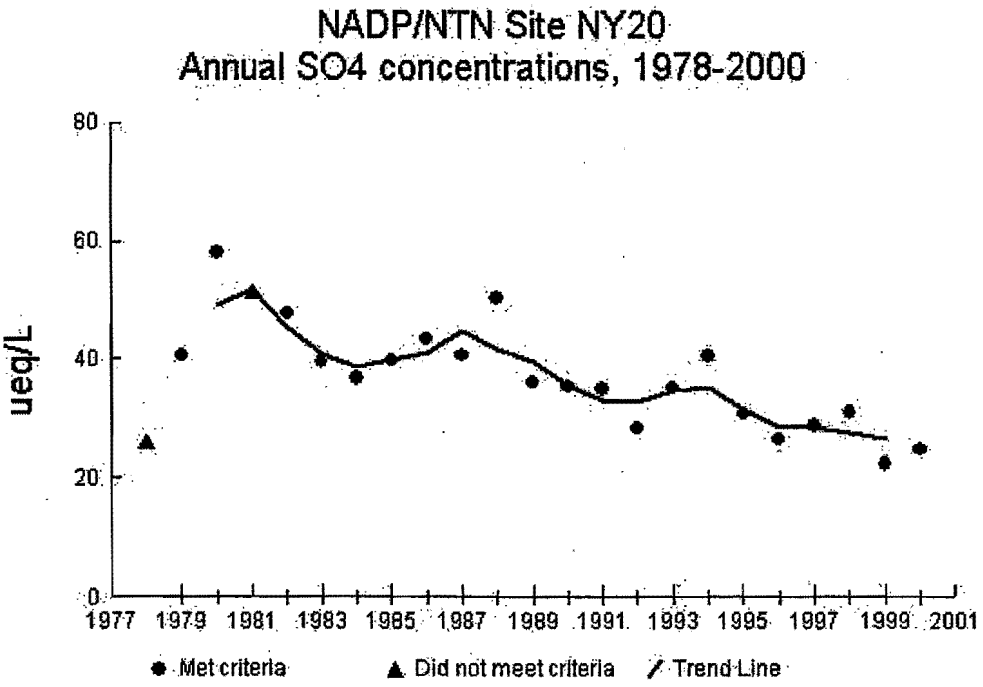

Figure 12. Trends in SO_4^{2-} from the NADP/NTN site at Huntington Forest (from http://nadp.sws.uiuc.edu/nadpdata/siteinfo.asp?id=NY20&net=NADP)

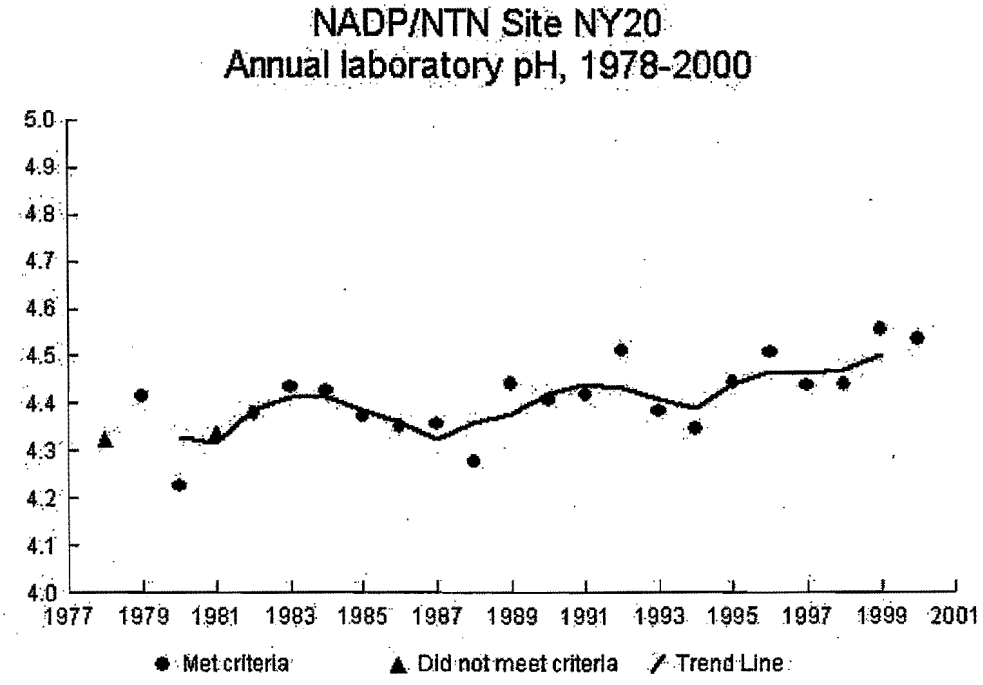

Figure 13. Trends in precipitation pH from the NADP/NTN site at Huntington Forest (from http://nadp.sws.uiuc.edu/nadpdata/siteinfo.asp?id=NY20&net=NADP)

Areas of thin (<3 m) till cover approximately 80-90% of Arbutus Lake watershed; bedrock outcrops are numerous (Figure 14). Tills contain on average 73% sand, 24% silt, and 2% clay. Quartz, K-spar and plagioclase are the major minerals present in both the soil and glacial sediments. Vermiculite, mixed layer mica-vermiculite and kaolinite constitute the bulk of the clay mineral fraction. Heavy minerals make up about 16% of the soil, with major constituents as follows: hornblende 33.6%, opaques (ilmenite and magnetite) 29.5%, pyroxene 20.1%, garnet 7.2%, and apatite 5.4%.

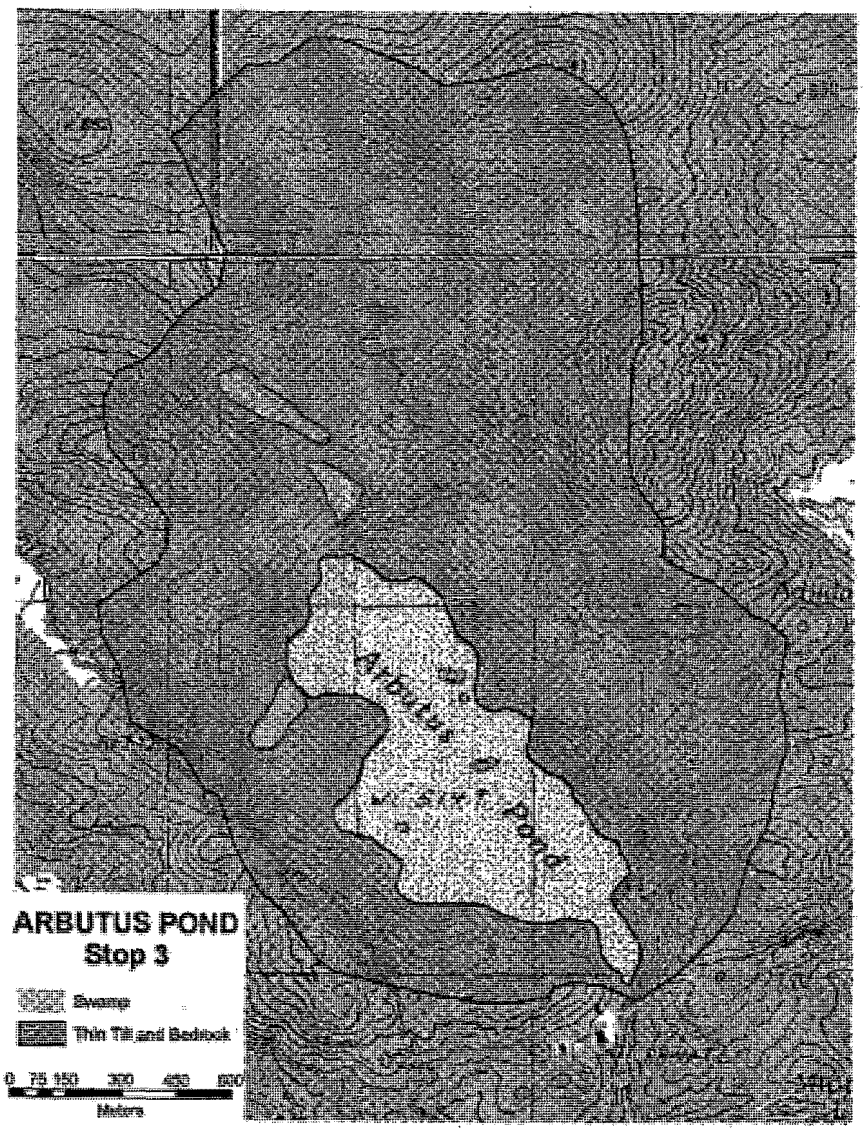

Figure 14. Surficial geology of the Arbutus Lake watershed

Comparative values of the chemistry of Arbutus Lake in 1982-84 and 2002 are shown in Table 4. This is a moderately sensitive water body with an ANC that ranges between 60 - 80 μeq/L. Ca concentrations are relatively high, and may reflect the presence of amphibolitic bedrock, and the presence of carbonate-bearing boulders in the till, especially up in the area around Archer Creek. Unlike Clear Pond, the 20 μmol/L reduction in SO_4^{-2} here has resulted in a concomitant rise of 20 μeq/L in ANC.

Parameter	Arbutus 82-84	Arbutus 2002
pH	6.2 (0.3)	6.6
ANC (μeq/L)	58 (21)	78
Ca (μmol/L	76 (6)	60.1
Mg	22 (3)	17.3
Na	31 (3)	28.7
K	11 (1)	6.1
SO_4	71 (5)	49.4
NO_3	10 (6)	5.8
Cl	10.7 (2.0)	11.9
F	4.5 (.5)	0.8
DOC	422 (65)	441
DIC	112 (20)	48.3
H_4SiO_4	68 (16)	-

Table 4. Chemistry of Arbutus Lake, today and 20 years ago.

Arbutus Lake watershed is a good example of a system in which the combination of thin till, short flow paths, and short residence times, which usually gives rise to surface waters with low ANC and high sensitivity (see Figure 4), is modified by the presence of minerals in the watershed that weather at moderately fast rates (e.g., hornblende, pyroxenes, and garnet) to provide alkalinity to drainage waters. In June of 1989-1991, Colgate students mapping and collecting water samples in Arbutus watershed measured the ANC of all running inlet streams in the watershed. Most streams had ANC values that were in the range of 20-80 μeq/L, but several streams had ANC's that were as high as 160-180 μeq/L. The highest values were measured following a particularly dry spring, and lowest values were measured following a rainy period of several days. During periods of low precipitation, or drought, base flow becomes a proportionately greater fraction of the drainage water reaching the lake and ANC values in Arbutus Lake can rise to their highest levels. Highest ANC values also seemed to be concentrated in the northern part of the watershed, near or within the Archer Creek subcatchment. We are planning to conduct future field studies in this part of the watershed to better characterize the composition of the bedrock, till, and soils.

Questions to consider at this stop are:

1) How does one measure the contribution of mineral weathering to the ANC of surface waters? Can the relative rates of mineral weathering in soils and till be measured, and if so, how do we measure or calculate the relative contribution of *each* mineral to ANC?

2) Why did a reduction in SO_4^{-2} result in an increase in ANC here and not at Clear Pond?

3) Several calcsilicate belts run east-west in the vicinity of the Arbutus watershed. Just a few miles to the east we noted the influence these rocks have on the chemistry of Harris Lake and Woodruff Pond. How much calcsilicate float is incorporated in the till of Arbutus watershed, and to what degree does this float influence the composition of soil and till in Arbutus? One clue, of course, is to look at the heavy mineral content of the till and soil, which includes significant quantities of hornblende and pyroxene.

4) A second possibility is to look at the bulk chemistry of till samples from the watershed. For example, XRF analyses of the < 2 mm (sand) fraction of 13 till samples from the Big Moose watershed, a watershed underlain by granitic gneiss and containing many acid sensitive lakes, has a mean CaO value of 1.64 wt. %. The mean CaO value for till collected from watersheds underlain by metanorthosite or calcsilicates (including samples from Clear Pond and Woodruff Pond) is 4.13 wt. %. Till from Arbutus Lake watershed has a CaO content of 2.54 wt. %, an intermediate value. Does this

indicate that source rocks for the till were both granitic gneiss and calcsilicates, and that the bulk chemistry reflects a mixture of the two? MgO values also suggest the same, as shown below.

Till from watersheds in:	Wt. % CaO	Wt. % MgO
Granitic gneiss	1.64	0.72
Metanorthosite/calcsilicates	4.13	2.02
Arbutus Lake	2.54	1.49

Echo and Little Echo Ponds – STOP 5.

Little Echo Pond is a 0.8 hectare brown water seepage lake surrounded by thick (~8 m)) peat (sphagnum bog) deposits (Figures 15 and 16). Its watershed is estimated to be about 0.11 km^2. Echo Pond, a stone's throw to the NNE, is a slightly larger seepage lake but without peat deposits edging the shoreline (Figure 17). The lake surface elevation of both ponds is 481 m. No fish species are present in Little Echo Pond; no fish population data is available for Echo Pond. The two Ponds sit in an outwash area at the eastern edge of the anorthositic massif, in the Fish Creek Ponds recreational area. Thin section examination of one bedrock sample taken in the vicinity (LE-105) revealed a typical Adirondack gabbroic anorthosite with 85% plagioclase (~An_{45}), 7% magnetite, 3% green clinopyroxene, and 5% garnet.

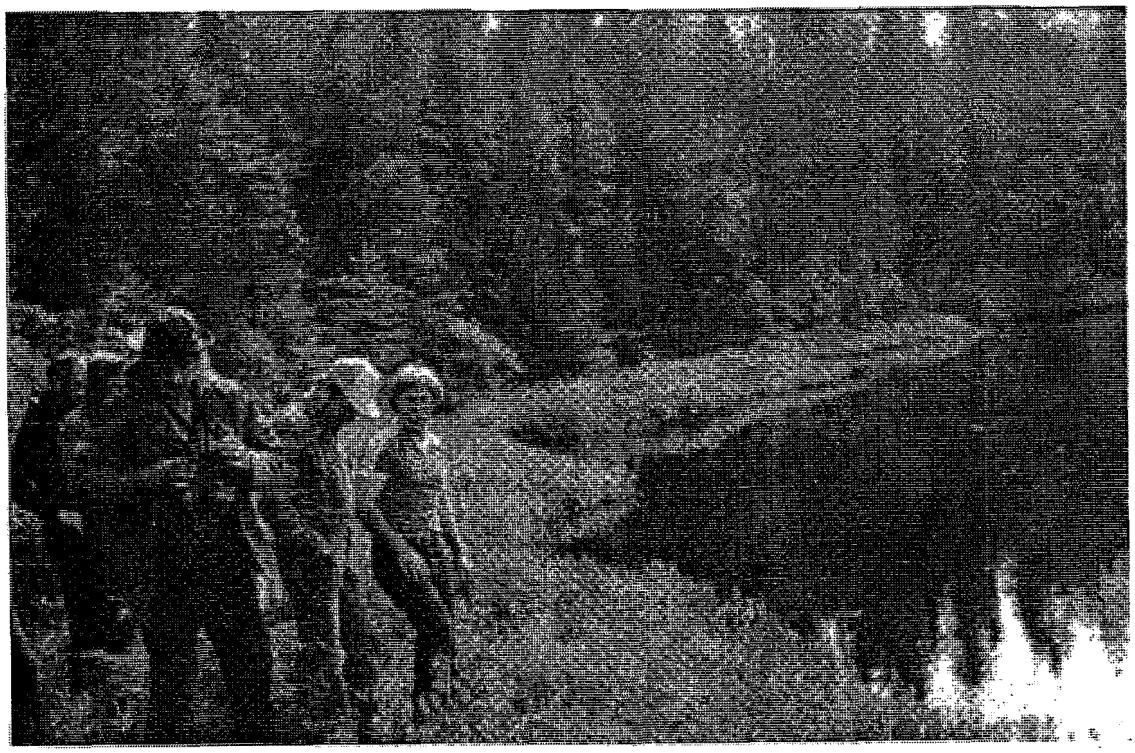

Figure 15. View of Little Echo Pond and the surrounding peat deposits.

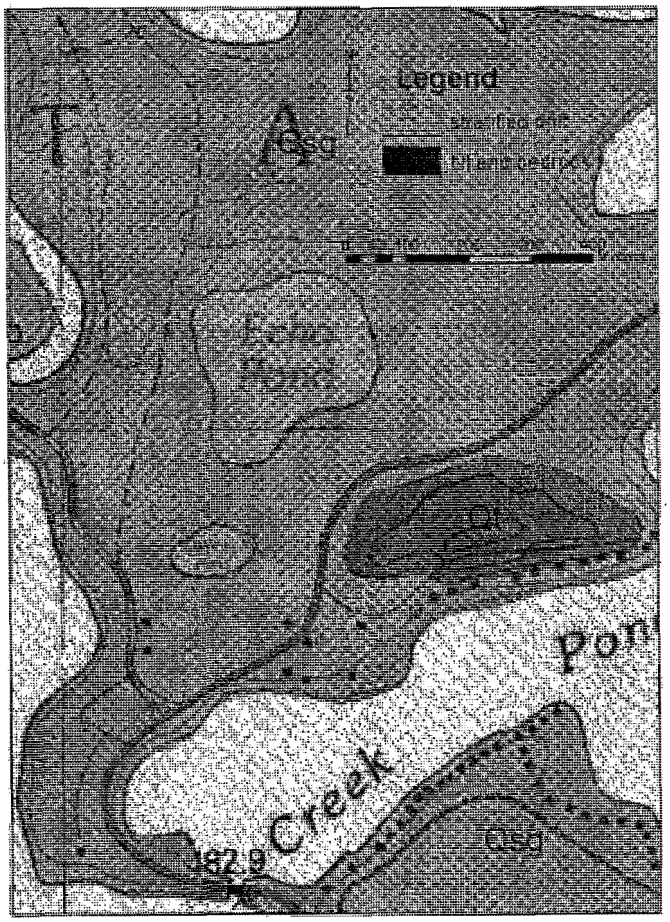

Figure 16. Surficial geology of Little Echo and Echo Ponds.

Figure 17. View of Echo Pond.

Outwash deposits of quartz, K-spar, and plagioclase are composed of 97% sand and 3% silt. Heavy minerals constitute 12.8% of the sand fraction and include 46.3% opaques, 20.1% hornblende, 10.6% pyroxene, 5.6 % garnet, and 2.3% zircon. What little clay is in the soil consists of vermiculite, mixed layer mica-vermiculite, kaolinite, and possibly a trace of talc.

Values of the chemistry of Little Echo Pond in 1982-84 and 2002, and Echo Pond in 2002 are shown in Table 5. What is immediately striking is the difference in water chemistry between these two seepage lakes located not more than 100 m apart. Little Echo is an acidic pond with an ANC that averages about of –50 μeq/L (range from ALSC data is –79.6 to –7.4 μeq/L). The pH is 4.3, the SBC and dissolved Si concentrations are low, and the DOC is high. Concentrations of organic anions are high and are comparable to SO_4^{2-} (on an equivalence basis) (Driscoll and Newton, 1985). The kettle hole that formed Little Echo Pond and the surrounding peatland has almost completely filled in. There is at least one ephemeral channel that drains the lake-peatland system during periods of high water. This lake is virtually isolated from the groundwater in the surrounding outwash aquifer system due to the extremely low hydraulic conductivity of the peat and bottom sediments, both of which form a nearly impermeable barrier around the lake-edge and bottom. Recharge of lake water must depend primarily on direct precipitation, and from runoff through the upper "active" zone of the peat. Although much of the acidity of the pond can be attributed to atmospheric deposition of H_2SO_4, it appears that the peat deposits and the sphagnum mat surrounding the pond release substantial quantities of organic acids that contribute to the overall acidity.

Sulfate concentrations in both the seepage lakes are much lower than in the drainage lakes both in the 1982 and 2002 data (Table 5 and Table 2). This is due to sulfate reduction occurring in the bottom waters of these lakes. The high DOC and long residence time of waters in seepage lakes provide conditions conducive to sulfate reduction. Measured profiles of dissolved oxygen show anoxic conditions in the deeper water of Little Echo Pond. Sulfate reduction is an ANC producing reaction making these lakes less acidic than they would have been had the water column been fully oxygenated.

Silica concentrations are very low in seepage lakes. This is likely due to a combination of a reduced input of groundwater and the removal of silica by the action of diatoms. The long residence time of water in seepage lakes makes it likely that diatoms will remove a substantial amount of silica from the water column.

Parameter	Little Echo 82-84	Little Echo 2002		Echo 2002
pH	4.3 (0.1)	4.3		6.4
ANC (μeq/L)	-51 (17)	-25		40
Ca (μmol/L	18 (3)	8.2		23.7
Mg	7 (1)	14.0		27.2
Na	8 (4)	15.2		9.1
K	4 (1)	13.0		4.9
SO_4	39 (9)	21.7		25.1
NO_3	0 (0)	1.8		3.4
Cl	5.8 (3.1)	19.2		18.9
F	1.3 (0.3)	2.3		1.7
DOC	1038 (153)	1236		450
DIC	113 (31)	0		12
H_4SiO_4	9 (5)	5		8

Table 5. Chemistry of Little Echo Pond and Echo Pond.

Echo Pond is marginally classified as a "flow-through" seepage lake (Figure 18). There is sufficient groundwater contribution in this class of lake to provide enough ANC to neutralize acidic deposition. However,

with a pH of 6.4, an ANC of 40 μeq/L, and relatively low SBC compared with drainage lakes we have studied (Table 2), the chemistry of Echo Pond is still greatly influenced by direct precipitation. Despite the good hydraulic connection between the groundwater and the lake, groundwater inflow is limited. This is likely due to the low hydraulic gradient within the groundwater system. Therefore, the influence of direct precipitation is still relatively high especially during rainy periods and snowmelt. We don't have much time series chemical or hydrologic data from Echo Pond, so, at best, our comments should be taken as suggestions based on work completed at similar seepage lakes.

Questions to consider at this stop are:

1) Why doesn't Echo Pond have a surrounding peat layer?

2) Would Little Echo Pond be acidic if there was no acid rain?

3) How important is sulfate reduction in generating alkalinity?

4) Can we determine the relative proportions of groundwater and precipitation entering Little Echo and Echo Ponds?

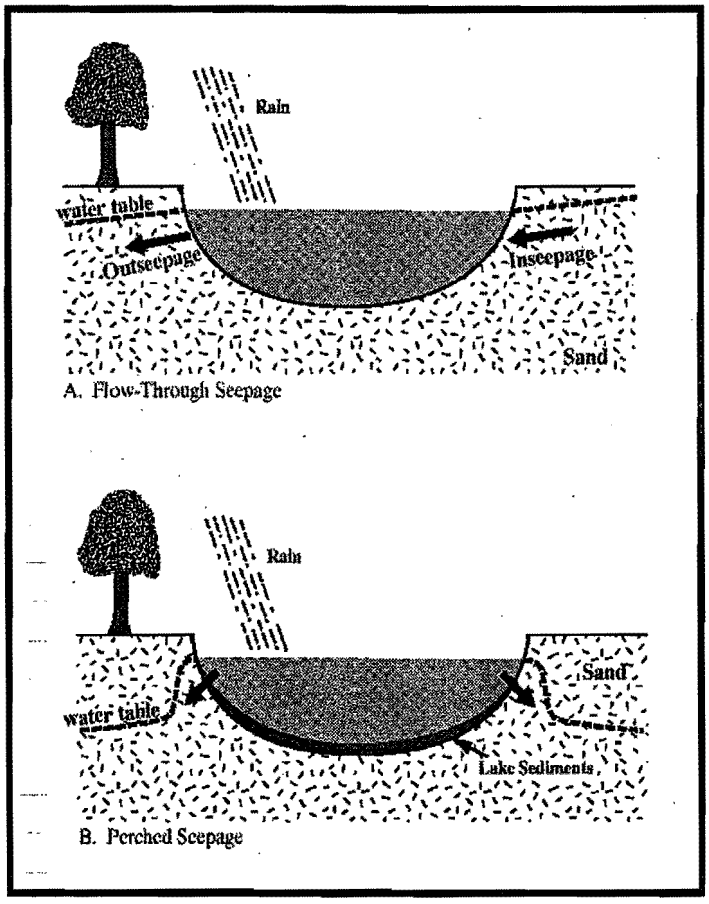

Figure 18. Schematic of the hydrology of flow-through and perched seepage lakes.

REFERENCES

April, R.A. and Newton, R.M., 1985, Influence of geology on lake acidification in the ILWAS watersheds: Water Air Soil Poll., v. 26, p.373-386.

April, R.A., Newton, R.M., and Coles, L.T., 1986, Chemical weathering in two Adirondack watersheds: Past and present-day rates: Geol. Soc. Am. Bull., v. 97, p.1232-1238.

Baker, J.P. and Schofield, C.L., 1982, Aluminum toxicity to fish in acidic waters: Water Air Soil Poll., v. 18, p. 289-309.

Baker, J.P., Van Sickle, C.J., Gagen, C.J., DeWalle, D.R., Sharpe, W.E., Carline, R.F., et al., 1996, Episodic acidification of small streams in the northeastern United States: Effects on fish populations: Ecological Applications, v.6, p. 422-437.

Charles, D.F., ed., 1991, Acidic Deposition and Aquatic Ecosystems: Regional Case Studies: New York, Springer-Verlag.

Cronan, C.S. and Schofield, C.L., 1990, Relationship between aqueous aluminum and acidic deposition in forested watersheds of North America and Northern Europe: Environmental Science & Technology, v. 24, no. 7, p. 1100-1105.

DeHayes, D.H., Schaberg, P.G., Hawley, G.J., and Strimbeck, G.R., 1999, Acid rain impacts calcium nutrition and forest health: BioScience, v. 49, p.789-800.

Driscoll, C.T. and Newton, R.M., 1985, Chemical characteristics of Adirondack lakes: Environmental Science & Technology, v. 19, p.1018-1024.

Driscoll, C.T., Lawrence, G.B., Bulger, A.J., Butler, T.J., Cronan, C.S., Eager, C., Lambert, K.F., Likens, G.E., Stoddard, J.L., and Weathers, K.C., 2001, Acidic deposition in the northeastern United States: Sources and inputs, ecosystem effects, and management strategies: BioScience, v.51, no.3, p.180-198.

Johannes, A.H., Altwicker, E.R., and Clesceri, N.L., 1985, The Integrated Lake-Watershed Acidification Study: Atmospheric inputs: Water Air Soil Poll., v. 26, p.339-353.

Kretser, W.A., Gallagher, J., and Nicolette, J., 1989, Adirondack Lakes Study 1984-1987: An evaluation of fish communities and water chemistry: Adirondack Lakes Survey Corporation, Ray Brook, NY.

Larson, D.P., Thornton, K.W., Urquhart, N.S., and Paulsen, S.G., 1994, The role of sample surveys for monitoring the condition of the nation's lakes: Environmental Monitoring and Assessment, v. 32, p. 101-134.

Lawrence, G.B. and Huntington, T.G., 1999, Soil-calcium depletion linked to acid rain and forest growth in the eastern United States: U.S. Geological Survey WRIR 98-4267.

Lawrence G.B., David, M.B., Lovett, G.M., Murdoch, P.S., Burns, D.A., Baldigo, B.P., Thompson, A.W., Porter, J.H., and Stoddard, J.L., 1999, Soil calcium status and the response of stream chemistry to changing acidic deposition rates in the Catskill Mountains of New York: Ecological Applications, v. 9, p. 1059-1072.

Likens, G.E., Bormann, F.H., and Johnson, N.M., 1972, Acid Rain: Environment, v. 14, no.3, p.33-40.

McLelland, J. and Chiarenzelli, J., 1990, Isotopic constraints on emplacement age of anorthositic rocks of the Marcy massif, Adirondack Mtns., New York: Jour. Geology, v.98, p. 19-41.

McLelland, J., 2001, Rock of Ages: From volcanic islands to Himalayan ranges: the geologic evolution of the Adirondack Mountains: Adirondack Life, July/August, 2001.

Newton, R.M., Weintraub, J. and April, R.A., 1987, The relationship between surface water chemistry and geology in the North Branch of the Moose River: Biogeochemistry, v. 3, p. 21-35.

Oden, S., 1968, The acidification of air precipitation and its consequences in the natural environment: Bull. Ecological Research Communications NFR. Ecology Comm. Bull. no. 1, Stockholm.

Schindler, D.W., Mills, K.H., Malley, D.F., Findlay, S., Shearer, J.A., Davies, I.J., Turner, M.A., Lindsey, G.A., and Cruikshank, D.R., 1985, Long-term ecosystem stress: Effects of years of experimental acidification: Canadian Jour. Fisheries and Aquatic Science, v. 37, p. 342-354.

Schindler, D.W., 1988, Effects of acid rain on freshwater ecosystems: Science, v. 239, p. 149-157.

Shortle, W.C., Smith, K.T., Minocha, R., Lawrence, G.B., and David, M.B., 1997, Acid deposition, cation mobilization, and stress in healthy red spruce trees: Jour. Environmental Quality, v. 26, p. 871-876.

Stevens, D.L., 1994, Implementation of a national monitoring program: Jour. Environmental Management, v. 42, p.1-29.

Stumm, W. and Morgan, J.J., 1981, Aquatic Chemistry: 2nd edition, New York, Wiley-Interscience.

Sullivan, T.J., 2000, Aquatic Effects of Acidic Deposition: Boca Raton, Lewis Publishers/CRC Press LLC.

Websites:

http://www.adirondacklakessurvey.org/index.html

http://www.epa.gov/airmarkets/progress/arpreport/index.html

http://www.dec.state.ny.us/website/dar/index.html

http://www.epa.gov/oar/oaq_caa.html

http://nadp.sws.uiuc.edu/

ACKNOWLEDGEMENTS

Many thanks go to Di Keller in the Department of Geology at Colgate University who assisted in putting together this field guide while getting ready to leave for two weeks in Alaska.

Road Log

Cumulative Mileage	
0.0	Fort William Henry, Lake George, NY
1.0	Turn south onto 9N
1.1	Turn Right onto entrance ramp to I87 northbound
43.2	Exit highway at Exit 29 (Newcomb)
43.4	Turn left at end of ramp onto County Rd #2
47.6	Turn Right onto Elk Lake Road
51.6	**STOP 1** - Park in area on right side of road at the outlet of Clear Pond
51.6	Return to County Rd#2 on Elk Lake Road
55.6	Turn Right on County Rd#2
68.7	Tahawus Rd enters from right
69.6	Bear left
69.8	Turn Right at stop sign onto Rt 28N
73.0	Turn Right onto access road to Harris Lake Campground
73.6	Cross Hudson River on Campground Access Rd
74.4	Entrance to Campground
75.1	**STOP 2** - Camp sites 50 - 52 and Lake boat access
75.1	Return to Rt 28N
77.2	Turn Right onto Rt 28N
77.6	Cross Hudson River on Rt 28N
78.6	**STOP 3** - Marble outcrop on Left side of Rd at Newcomb School
80.3	Marble outcrops along side of Rt 28N
80.5	Turn Right entrance to Adirondack Visitors Center
80.8	**LUNCH STOP** - Parking area
81.1	Return to Rt 28N
83.6	Turn right onto Arbutus Rd - Huntington Wildlife Forest
84.4	Bear right at buildings and cross Arbutus Outlet
84.5	**STOP 4** - Arbutus Pond outlet
85.4	Return to 28N and Turn right (west) on 28N
95.6	Turn right onto Rt 30 in Long Lake
117.9	Turn right at first traffic light in Tupper Lake (east on Rt 3)
118.1	Straight through second traffic light
123.7	Turn Left to continue on Rt 30 north
129.2	Pass entrance to Fish Creek Ponds Camping area on left
	STOP 5 -
	Park in small parking area on right side of road
	Trail to Echo Pond and Little Echo Pond is on the opposite side of the road
129.3	
	Return to Lake George

Contact Info:

Percy Flemming – Elk Lake Lodge 518-332-7616

Harris Lake Campground – 518-582-2503

Adirondack Visitors Center – 518-582-2000

TIMING AND DEPTH OF INTRUSION OF THE MARCY ANORTHOSITE MASSIF: IMPLICATIONS FROM FIELD RELATIONS, GEOCHRONOLOGY, AND GEOCHEMISTRY AT WOOLEN MILL, JAY COVERED BRIDGE, SPLIT ROCK FALLS, AND THE OAK HILL WOLLASTONITE MINE

by

Cory C. Clechenko, Department of Geology and Geophysics, University of Wisconsin, Madison, WI 53706
John W. Valley, Department of Geology and Geophysics, University of Wisconsin, Madison, WI 53706
James McLelland, Geology Department, Colgate University, Hamilton, NY 13346

INTRODUCTION

The depth and timing of intrusion of the Marcy anorthosite massif has critical implications for models of regional Adirondack geological development. Classic localities in the northeastern Adirondacks afford the opportunity to evaluate questions of anorthosite intrusion depth, as well as the timing and relation to granulite facies metamorphism. The first stops, at Split Rock Falls, Woolen Mill, and the Jay covered bridge, allow an examination of anorthositic to gabbroic rocks and magmatic textures and relations. The Split Rock Falls locality exposes a variety of cross cutting and block structures of anorthositic series rocks. At the Woolen Mill locality, clear cross cutting relations of anorthosite and gabbroic lithologies exist. Zircons from these rocks have been recently dated (SHRIMP II). Geochronology indicates intrusion of anorthositic rocks at ca. 1155 Ma. New $\delta^{18}O$ data from zircons provide evidence for the magmatic contamination of the Marcy massif, causing an elevation in $\delta^{18}O$ when compared to "normal" anorthosites worldwide. The data indicate the massif intruded as high $\delta^{18}O$ magmas, and thus fluids did not elevate the $\delta^{18}O$ of the anorthosite during overprinting granulite facies metamorphism. At the Jay covered bridge locality, coarse pyroxene-rich dikes cross cut anorthosite. Recent geochronology yields an age of ca. 1155 Ma for anorthosite here. The final stop, at the Oak Hill wollastonite deposit, exposes field relations of low $\delta^{18}O$ calc-silicate lithologies to presumed marble protoliths and anorthosite. Combined stable isotope, major element chemistry, and trace element chemistry provide significant evidence for formation of the calc silicate lithologies in a complex hydrothermal skarn-forming system adjacent to shallowly intruding anorthosite. Garnet with oscillatory zonation of both major elements and $\delta^{18}O$ from the related, nearby, Willsboro deposit further constrain skarn forming processes.

We plan to show, through field relations, geochemistry, and geochronology that the Marcy anorthosite massif intruded as a high $\delta^{18}O$ crystal mush to depths less than 10 km in the crust at ca. 1155 Ma causing localized contact metamorphism. The anorthosite and contact metamorphic rocks were then subsequently overprinted by the regional metamorphism of the Ottawan orogeny after 1090 Ma.

This field trip guide is written in two parts. The first part includes general background information, including a brief description of anorthositic rocks in the area as well as a more detailed description of the geochemistry and petrogenesis of the Oak Hill and related wollastonite deposits. The second part includes a road log. The first three stops, anorthositic rocks at Split Rock Falls, Woolen Mill, and Jay, include detailed information about the field relations seen there, plus petrologic, geochemical, geochronologic information with interpretations. The last stop, at Oak Hill, includes detailed field descriptions of the rocks analyzed and interpreted in the first part of the guide.

ANORTHOSITIC ROCKS OF THE NORTHEASTERN ADIRONDACKS: GEOCHRONOLOGY, STABLE ISOTOPES, AND FIELD RELATIONS

Rock Types and Field Relations

The anorthosite massif of the Adirondacks is chiefly comprised of a coarse blue gray andesine anorthosite known as the Marcy facies. There is also the Whitface facies, chiefly found at the margins of the massif, and noted

for its smaller grain size and mortar texture (gray phenocrysts surrounded by grain size reduced plagioclase, the presence of garnet, and foliation. A variety of differentiates also may be found, ranging from gabbroic anorthosite to ferrogabbro, ferrodiorite, and oxide apatite gabbronorite.

Outcrops at the stops on this trip provide a great opportunity to examine the magmatic features of the Marcy anorthosite massif and to discuss these features relative to geochronology and geochemistry. We'll see mutual cross cutting relations of different anorthositic rocks and differentiates, the different facies of anorthosite, magmatic features such as foliation, subophitic pyroxenes, and block textures. Block textures contain coarse angular blocks of anorthositic rocks ranging from cm to m scale that are interrupted and surrounded by more magmatic material, generally anorthositic. This suggests the intrusion of the anorthosite as a crystalline mush that was fractured and invaded by later differentiates of the anorthositic parent during such processes as filter pressing. Block textures have been observed in the Northeastern Adirondacks since at least Kemp and Ruedemann (1910). They were named such by Balk (1931). Blocks show magmatic foliation, subophitic textures, and gradations of foliation. The orientation of the foliation in the blocks is variable from block to block.

Geochronology

The temporal relation of Marcy anorthosite intrusion to granulite facies metamorphism in the Adirondacks has long been a source of controversy. Geochronological studies have been conducted to place anorthosite intrusion and regional granulite facies metamorphism into a temporal framework. A general review/synthesis paper summarizing this work is by McLelland et al. (1996). McLelland et al. (1996) outline a time range of 1150-1125 Ma for anorthosite intrusion, a range determined from ages of zircons from granitic and other rocks that mutually cross-cut anorthosite, e.g McLelland and Chiarenzelli (1990) Chiarenzelli and McLelland (1991). Age determinations based on geochronology performed directly on the anorthosite itself are rare, and have given varied results. Silver (1968) obtained zircon from pegmatitic anorthosite in the Westport dome and the Jay dome, and determined ages of 1090 ± 10 and 1070 ± 20, respectively, from bulk zircon separates. Ashwal and Wooden (1983) inferred an anorthosite age as old as 1288 ± 36 based on a 4 pt Sm-Nd isochron. McLelland and Chiarenzelli (1990) obtained and age of 1113 Ma from air abraded cores of zircons from anorthosite, which they considered to be a minimum age of emplacement. Recently, it has been proposed that migmatite formation found just south of the Woolen Mill locality was the result of heat from intruding anorthosite. Zircon geochronology for the migmatite indicated that partial melting event took place at ca. 1040 Ma, and was interpreted to be the time of anorthosite intrusion (Isachsen et al. 2001). New SHRIMP II geochronology on zircons from anorthositic rocks from the Woolen Mill locality provide the first high precision ages for anorthosite intrusion determined directly on anorthositic rocks, and indicate an age of intrusion ca. 1155 Ma (Clechenko et al. 2002). It is important to note that zircon textures as revealed by cathodoluminescence, calculation of Zr saturation, and the uniformity of zircon ages all indicate that the zircons are primary igneous minerals, and are not inherited xenocrysts. Additional new SHRIMP II zircon geochronology on anorthosite and related mafic rocks at many localities in the Adirondacks consistently yields the same result. The dominant events of the Ottawan orogeny have been constrained between 1090-1035 Ma (McLelland et al. 2001), and it would thus seem that the partial melting event dated by Isachsen et al. (2001) is related to regional metamorphism.

Oxygen Isotopes

It has been known since Taylor (1968) that the Marcy anorthosite has high $\delta^{18}O$ values compared to most normal anorthosites worldwide (~9.5‰ vs. 5.8-7.6‰). The Marcy anorthosite is enriched in its $^{18}O/^{16}O$ ratio compared to anorthosite in equilibrium with a normal mantle melt. Taylor (1968) suggested that the enrichment was the result of interaction with high $\delta^{18}O$ metamorphic fluids during regional metamorphism. Valley and O'Neil (1984) and Morrison and Valley (1988) concluded that the enrichment was a magmatic process, and that anorthosite was born of a mantle melt that had assimilated high $\delta^{18}O$ crustal material.

Zircon has been shown in numerous studies to preserve its primary igneous $\delta^{18}O$ through overprinting hydrothermal and metamorphic events. Zircons provide a robust material with which the method of elevation of anorthosite $\delta^{18}O$ values took place. If the elevation of $\delta^{18}O$ was a metamorphic event, zircon should preserve the primary $\delta^{18}O$ in equilibrium with the mantle (5.3‰). Higher zircon $\delta^{18}O$ values would indicate that the elevation of

$\delta^{18}O$ is a magmatic event and that zircon grew in a high $\delta^{18}O$ melt. Valley et al. (1994) report high $\delta^{18}O$ values for zircon from one anorthosite (~8.3). Preliminary results from zircon from anorthosite at Woolen Mill (Clechenko et al. 2002) also show high zircon $\delta^{18}O$ values (8.82 ± 0.02, n=4). These initial results support the hypothesis of that the $\delta^{18}O$ of the Marcy anorthosite was elevated during a magmatic event such as assimilation of higher $\delta^{18}O$ crustal material (Valley and O'Neil 1984, Morrison and Valley 1988).

WOLLASTONITE DEPOSITS OF THE NORTHEASTERN ADIRONDACKS

Introduction

The calc silicate skarns exposed adjacent to anorthosite in the Willsboro-Lewis area of the Northeastern Adirondacks have been an important source of industrial wollastonite for 50 years. The wollastonite ore has the high variance assemblage of Wo + Gt + Cpx with no calcite or quartz, suggesting a metasomatic origin because a protolith with perfect ratios of Cc and Qtz would otherwise be needed to create the observed mineralogy in a closed system. The petrogenesis of the wollastonite deposits has been studied over the same time span, and produced a variety of theories as to the origin of the wollastonite ores. Initial debates centered on an origin involving metasomatism (Buddington and Whitcomb 1941), isochemical metamorphism of original sediments (Broughton and Burnham 1944, Putnam 1958, O'Hara 1976), or combinations of both models (Putnam 1958, DeRudder 1962). As analytical techniques and our understanding of petrologic processes progressed, a metasomatic origin has become accepted. Valley and O'Neil (1982) observed low $\delta^{18}O$ values (as low as ~1.3‰) for wollastonite from the Willsboro deposit, as well as the high variance assemblage, and concluded that meteoric water was involved in skarn formation. The physical relation of the skarn to anorthosite led them to conclude that heat from anorthosite drove meteoric hydrothermal circulation. Valley and O'Neil (1982) concluded that it was unlikely that large volumes of hydrostatically pressured meteoric fluid could penetrate to depths greater than 10 km into the lithostatically pressured ductile regime, and thus anorthosite intrusion must have taken place at shallow crustal levels.

The important conclusions of Valley and O'Neil (1982) served in part to provide strong evidence for a poly-metamorphic model of Adirondack regional geologic development, as summarized by Bohlen et al. (1985), Valley et al. (1990), and McLelland et al. (1996). In this model, anorthosite-mangerite-charnockite-granite (AMCG) intrusion takes place between ca. 1150-1125 Ma (new data mentioned above suggests that it was nearer the older age of 1150 Ma) at shallow (<10km) levels, causing localized contact metamorphism. The intrusion of the AMCG suite was followed by regional, fluid absent, granulite facies metamorphism after ca. 1090 Ma, known as the Ottawan orogeny.

Recent studies have provided further information about the processes that formed the calc silicate skarns. Whitney and Olmstead (1998) used rare earth element (REE) analysis of wollastonite ores and related rocks to develop a two-stage model of wollastonite ore formation. The recent discovery of garnets with oscillatory zoning at Willsboro provides important new insight to the skarn forming processes. A combined oxygen isotope, major element, and trace element study of garnet from wollastonite ores and related rock, along with major element and oxygen isotope analysis of garnet with oscillatory zonation yielded further clues about the skarn petrogenesis (Clechenko 2001). These studies have also provided further evidence of a link between skarn formation and anorthosite intrusion. Any model of Adirondack geologic history that invokes deep intrusion of anorthosite must account for the huge volumes of low $\delta^{18}O$ wollastonite ores and associated skarns, as well as geochemical indications of a link between anorthosite and the skarns. Further, phase equilibria indicates shallow origin for index minerals of contact metamorphism found at Cascade Slide, including wollastonite, monticellite, and akermanite as well as other minerals restricted to low pressure environments: cuspidine and wilkeite. This trip will visit the Oak Hill wollastonite deposit to examine some well-exposed relations of wollastonite ore, related calc-silicate skarn, marble, and igneous lithologies including anorthosite.

Local Geology.

The Oak Hill wollastonite deposit, along with the related deposits at Willsboro, Deerhead, and Lewis, is part of a belt of metasedimentary and metaigneous rocks that is up to ~25km long and 1.5 km wide (FIG 1). The belt overlies, and forms the northern and northeastern border of, the Westport dome of the Marcy anorthosite massif.

Figure 1 After Whitney and Olmstead (1998)

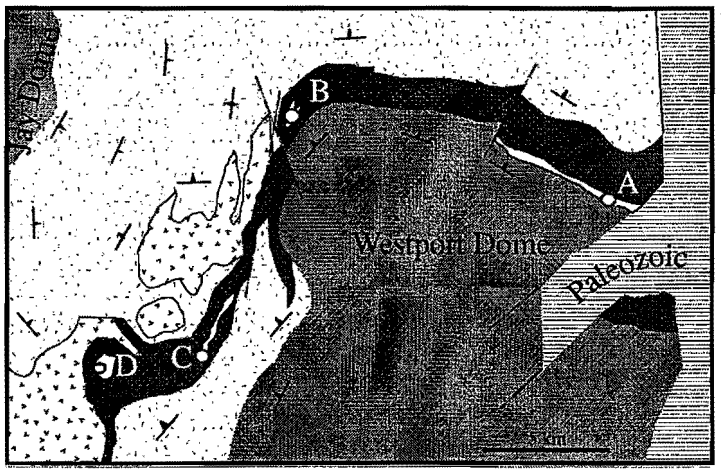

The wollastonite deposits have significant volumes of the wollastonite ore, a granoblastic gneiss consisting of Wo (60%) + Gt + Cpx . The wollastonite ore rocks are foliated, and are compositionally layered with varying ratios of wollastonite: garnet: clinopyroxene. The wollastonite ores are deformed, showing isoclinal fold hinges, foliation, and boudinage.

A variety of other calc silicate skarn lithologies are also found associated with the wollastonite ores, chiefly garnetite and garnet pyroxene skarn. These lithologies are found interlayered with the wollastonite ores and igneous lithologies. Garnetites from Willsboro contain rare euhedral garnets with oscillatory zonation. A representative cross-section from the Oak Hill mine shows the relation of the different lithologies (FIG 2). Nearly all of these lithologies are exposed in outcrop on the surface at the mine.

Garnets with Oscillatory Zonation.

Massive garnetite from the Willsboro mine contains garnets with oscillatory zonation. The zoned garnets are found in clusters and aggregates and appear to be filling void spaces (FIG 3). The remaining space is filled with feldspar (or altered equivalents such as prehnite) and quartz, with occasional titanite, clinopyroxene, and calcite. Similar textures are known from the garnetite at Oak Hill, though no euhedral garnets analyzed from Oak Hill have oscillatory zonation. The growth of the zoned garnets into void spaces, as well as the involvement of meteoric water, is indicative of hydrothermal fluids and shallow depth of formation of these zoned garnets. Centimeter scale open void space could not exist at great depth (Walther and Orville 1982), and hydrostatically pressured meteoric water could not penetrate into ductile rocks.

Suspected zoned garnets were made into polished thick sections, imaged by BSE or X-ray mapping, and quantitatively analyzed for cation concentrations on transects across zonation. Using a thin saw blade, a mm wide strip was then cut out of the thick section along the electron microprobe traverse. The strip was broken up, and the chips were analyzed for oxygen isotope ratio. One such image and the resulting transect are displayed in FIG4. The analyses reveal a correlation between X_{Adr} and $\delta^{18}O$. The magnitude of the fractionation is far greater (at least 10x) than that predicted between the two garnet compositions at elevated T (Kohn and Valley 1998). The garnets record variable inputs of two fluid compositions, one with high $\delta^{18}O$ values and Fe rich (presumably magmatic (anorthositic) in source), and another with lower $\delta^{18}O$ values, with a meteoric source.

Garnet with oscillatory zonation such as this has been reported from numerous Phanerozoic shallow contact metamorphic environments (e.g. Chamberlain and Conrad 1991, Jamtveit and Hervig 1994, Crowe et al. 2001), though the Willsboro garnets are the first known that are preserved in a granulite facies terrane. Such garnets provide a useful comparison to understanding the garnets from Willsboro with oscillatory zonation. It is important to note that the zoned garnets at Willsboro could not have formed at granulite facies conditions as indicated by their

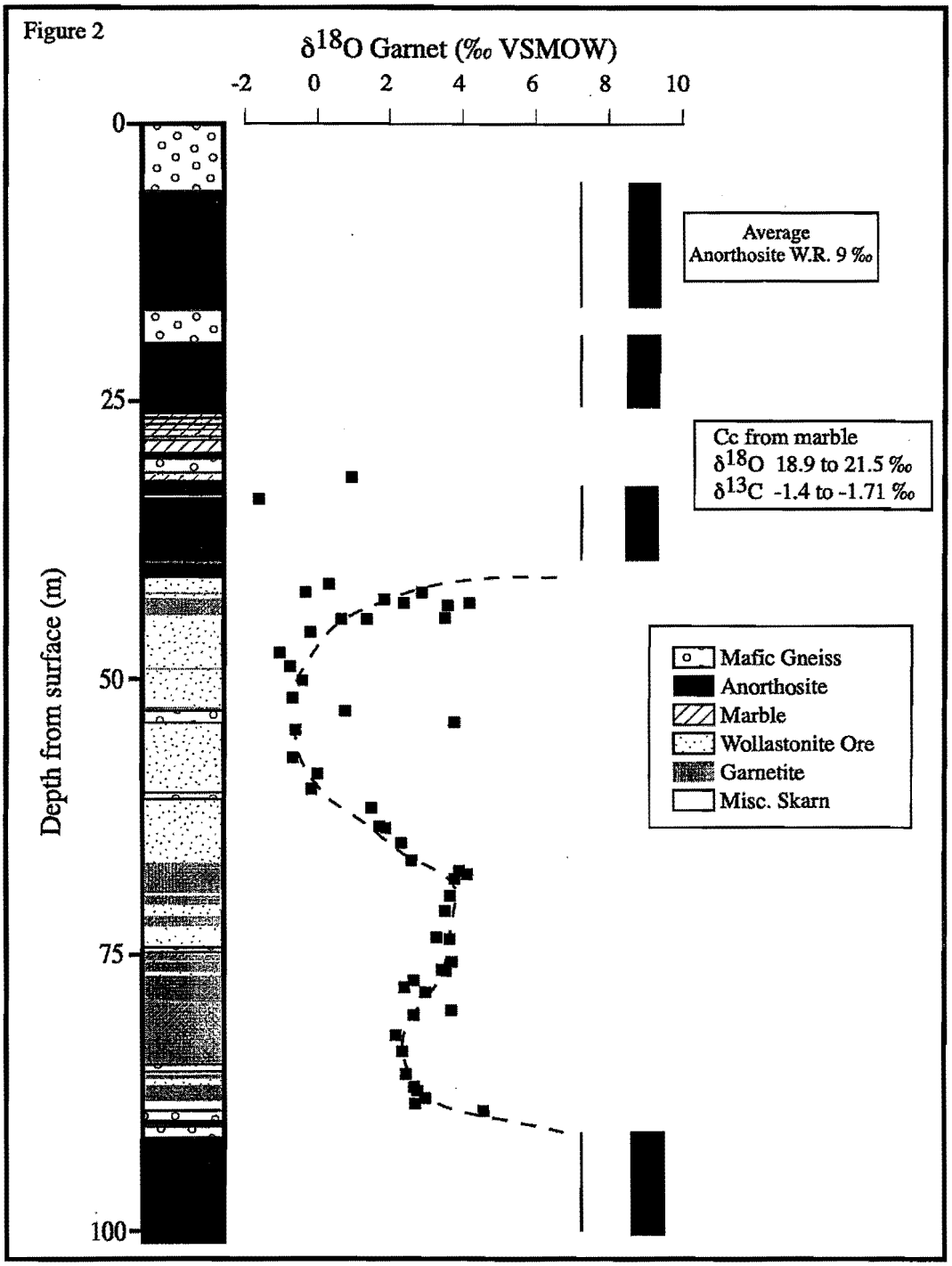

Figure 2. Lithologic and oxygen isotope transect from drill core across the Oak Hill wollastonite deposit. All data from analyses of garnet, summarized in Table 1. Note the generally higher $\delta^{18}O$ values of garnetite compared to wollastonite ores. Calcite $\delta^{18}O$ values suggest heterogeneity of fluid flow during skarn formation, as well as no subsequent cross-contact flow. This geometry suggests tectonic interleaving and deformation subsequent to skarn formation. Thus, the original physical relations of these lithologies during skarn formation is unclear. Black lines left of anorthosite W.R. value are fictive intermediate composition grandite garnets in isotopic equilibrium with intermediate composition plagioclase.

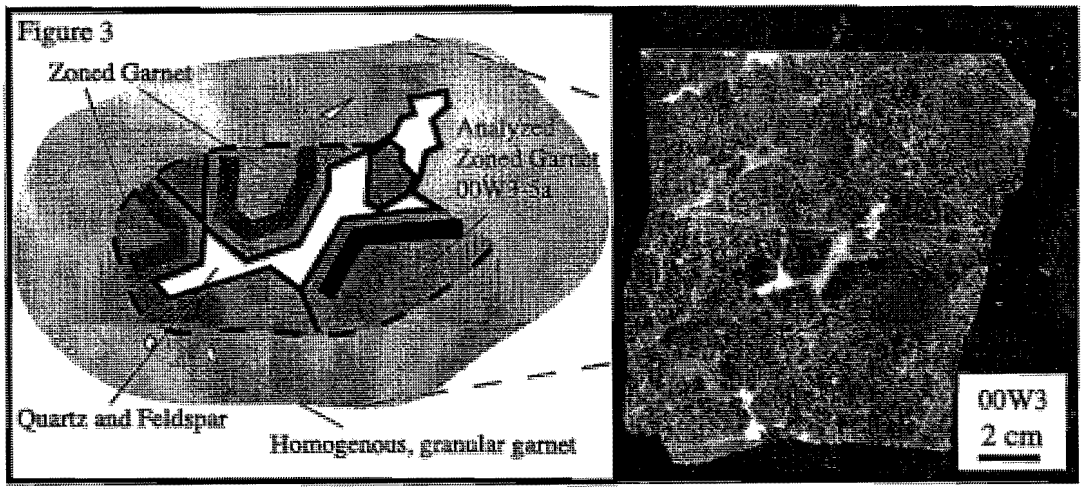

Figure 3. Image of slab of garnetite (00W3) from Willsboro wollastonite mine showing textures associated with zoned garnets. Garnets have grown filling void spaces and are surrounded by a matrix of finer grained, homogenous garnet. Cartoon interpretation included on the left. Limit of zoned garnet occurrence shown by dashed envelope in both images. Garnet zonation patterns shown with lines paralleling garnet crystal faces. The garnet analyzed is reported in Clechenko (2001), and is similar to the zoned garnet shown below in Figure 4.

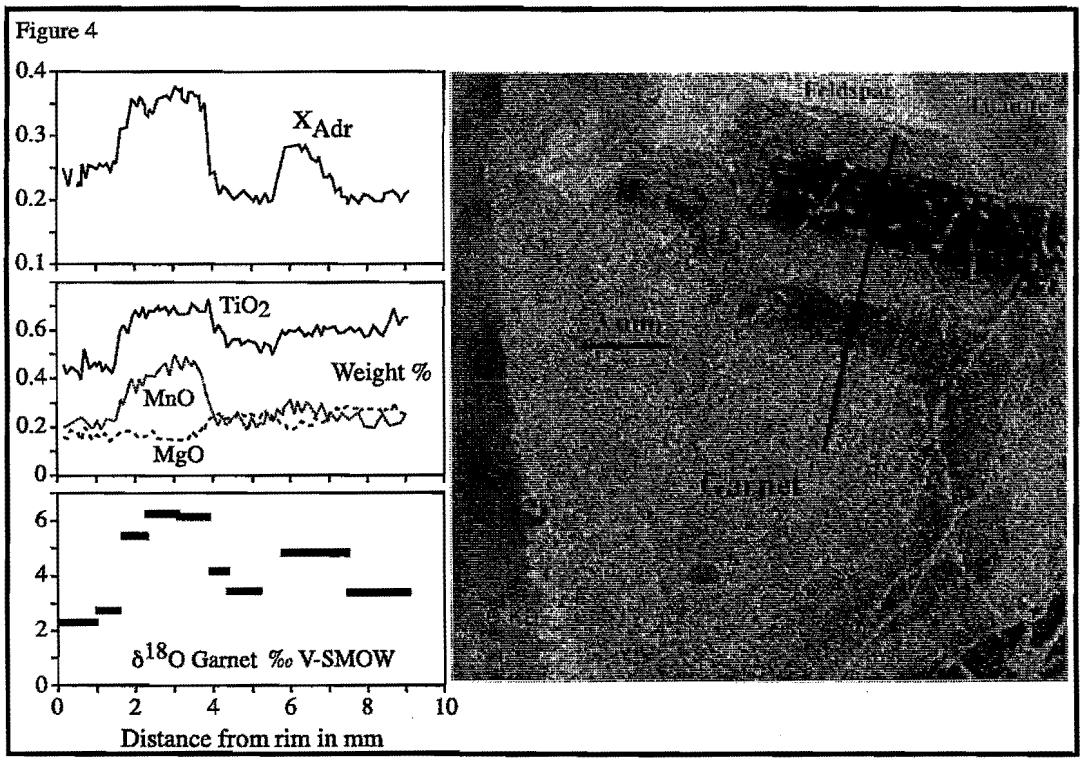

Figure 4. Fe K-α image of zoned garnet 94ADK11. Dark areas are more andraditic, gray areas more grossularitic. Analytical transect across garnet shown by dark line from rim to core on image to right, analytical results shown on left for cations and oxygen isotopes.

growth into void spaces and the involvement of low $\delta^{18}O$ fluids in their growth. Preservation of zoned garnets formed prior to the regional metamorphic overprint is possible due to their large size and the slow diffusion of cations and oxygen in garnet they would be able to survive a granulite facies overprint. Additionally, the garnets survive in massive garnetite and are armored from the effects of deformation and recrystallization as boudins that are surrounded by homogenous, recrystallized garnet.

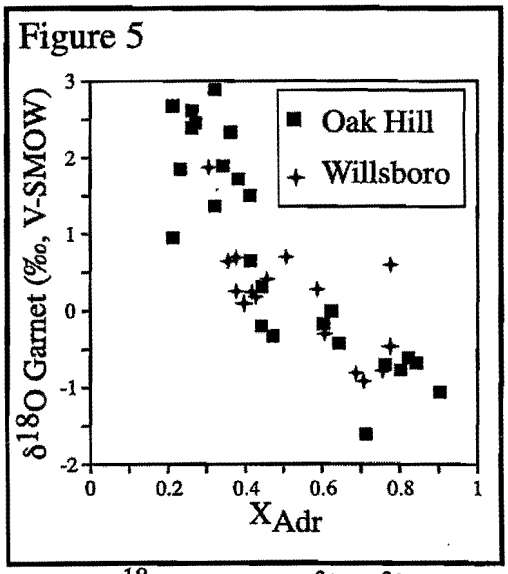

Figure 5. $\delta^{18}O$ vs. X_{Adr} ($Fe^{3+}/(Fe^{3+} + Al)$) of garnet from wollastonite ores from the Oak Hill and Willsboro wollastonite mines, NY.

Chemistry of Garnets from transects across deposits

A general survey of garnet cation chemistry and oxygen isotope values was conducted from drill core and hand samples from the Oak Hill and Willsboro wollastonite mines. The original oxygen isotope transect of Valley and O'Neil (1982) showed low $\delta^{18}O$ values of the wollastonite (to -1.3‰), as well as large variations of $\delta^{18}O$ over short distances of contacts between wollastonite ores and igneous rocks (~8‰ over 4m). The sharp nature of the variation of $\delta^{18}O$ indicates that little cross boundary fluid flow took place during granulite facies metamorphism, assuming that the relative position of the skarn to anorthosite has not changed subsequent to granulite facies metamorphism. A similar, but more detailed, transect of garnet $\delta^{18}O$ values from Oak Hill is shown above (FIG 2). The results are from Clechenko (2001).

Combined garnet $\delta^{18}O$ and cation composition data from the wollastonite ores and other calc silicate assemblages at Willsboro and Oak Hill provide important new clues about the contact metamorphic/hydrothermal processes that formed the skarn. Garnet compositions in ores range from X_{Adr} = 0.2 to 0.9, and garnet $\delta^{18}O$ values are positively correlated with composition, ranging from –1.65 to 2.85‰ (FIG 5). Additionally, correlation of X_{Adr} to rare earth element (REE) patterns in whole rock (Whitney and Olmstead 1998), and a correlation of garnet REE patterns with both X_{Adr} and $\delta^{18}O$, (Clechenko 2001, Clechenko et al. 2001) is observed. These are most readily expressed as a ratio of light REE to heavy REE concentration (Pr/Yb) and the size of the positive Eu anomaly (Eu/Eu*), results are shown in FIG 6. The result is a population of garnet that systematically vary from low X_{Adr}, Eu/Eu*, Pr/Yb and high $\delta^{18}O$ to high X_{Adr}, Eu/Eu*, Pr/Yb, and low $\delta^{18}O$.

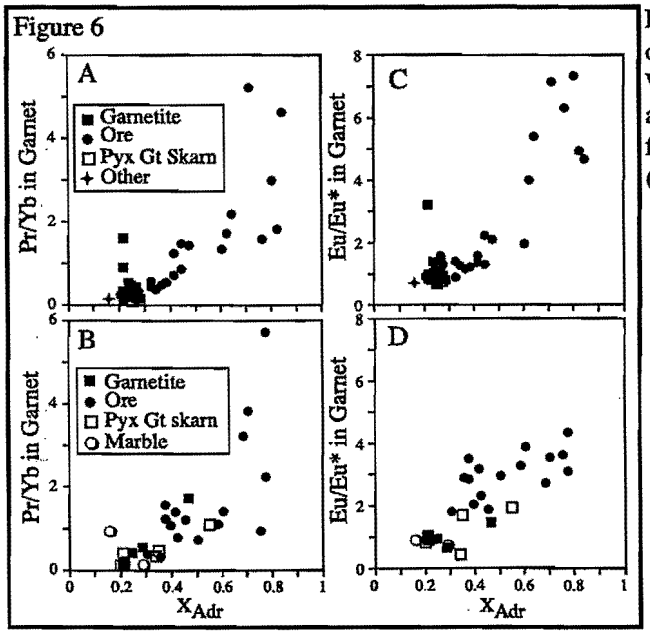

Figure 6. Pr/Yb vs. X_{Adr} ($Fe^{3+}/(Fe^{3+} + Al)$) of garnet from the Oak Hill (A) and Willsboro (B), as well as the size of the Eu anomaly (Eu/Eu*) vs. X_{Adr} for garnet from a variety of lithologies from Oak Hill (C) and Willsboro (D) wollastonite mines.

Formation of the Willsboro-Lewis wollastonite ores

A synthesis of existing knowledge of the origin of the Willsoboro-Lewis wollastonite ores is presented here. Whitney and Olmstead (1998), based on observed whole rock REE patterns, indicated a two-stage model of skarn formation involving contact metamorphism of a carbonate followed by massive metasomatism involving meteoric water. Much additional data from the study of Clechenko (2001) allows an even more detailed understanding of the hydrothermal system that formed the Willsboro-Lewis skarn. We propose that intrusion of anorthosite took place at shallow crustal levels at ca. 1155 Ma causing contact metamorphism of siliceous carbonates to form silicate marbles. Garnet in such a marble would have been relatively high $\delta^{18}O$, HREE enriched, lack an Eu anomaly, and be low X_{Adr}. Magmatic fluids were released periodically by hydrofracturing from the intruding anorthosite as it crystallized, as described by Hanson (1996) for skarns in the Sierra Nevada of California. Late during crystallization, meteoric water started to penetrate the system. The resulting episodic mixing of these fluids in varying amounts gave rise to the localized growth of garnets with oscillatory zonation. The zonation records the relative input of a high $\delta^{18}O$, Fe enriched fluid (magmatic) varying with a low $\delta^{18}O$, relatively Fe poor fluid (meteoric) over the time of garnet growth. Subsequently, after exhaustion of magmatic fluid, the system became dominated by massive amounts of meteoric water heated by the still hot anorthosite. Metamorphic volatiles evolved via contact metamorphism were either channeled away from the system, or diluted by large volumes of the heated meteoric water. Hot, low $\delta^{18}O$ meteoric waters became enriched in Si, Fe, and Eu by interaction with anorthositic rocks, and caused the growth of more silicates (Wo + Gt + Cpx) in the marble, transforming it to skarn. The second stage of wollastonite ore formation just described was postulated by Whitney and Olmstead (1998) based on REE patterns of whole rock. The garnet that precipitated from this fluid was low $\delta^{18}O$, LREE, had large Eu anomalies, and high X_{Adr}. Subsequent fluid-absent granulite facies metamorphism and deformation after 1090 Ma during the Ottawan orogeny caused the homogenization of the skarn minerals (with the exception of the rare large garnets with oscillatory zoning, protected in massive garnetite) and inter-mineral oxygen isotope equilibration. The granulite facies metamorphism inter-mineral equilibration also reset U-Pb and Sm-Nd ages (1035 Ma by both methods, from K. Burton (pers. comm. to JWV) and Basu et al. 1988, respectively). The deformation recrystallized or homogenized many of the original zoned minerals and destroyed much of the original spatial relation of the skarn and fluid flow system.

SUMMARY

The combined geochronologic, field, stable isotope, and petrologic study of the Marcy anorthosite and associated contact metamorphic rocks constrains a detailed geologic understanding of anorthositic magmatism in the Adirondacks. New SHRIMP II zircon geochronology from anorthosites and anorthositic rocks indicates anorthosite intrusion took place at ca. 1155 Ma. The intruding anorthosite was a partially solidified crystal mush that underwent brittle fracture into blocks, magmatic foliation formation, and filter pressing and magmatic evolution. The Marcy anorthosite began as a normal $\delta^{18}O$ mantle melt, the high $\delta^{18}O$ presumably the result of assimilation of crustal material into the mantle melt when it was ponded at the base of the crust. The anorthosite intruded the crust at shallow levels (<10km) as shown by the formation of low $\delta^{18}O$ skarns adjacent to anorthosite. Calc silicate skarn formation was due to a complex hydrothermal system involving multiple stages and fluids from different reservoirs, one of which was meteoric. The Ottawan orogeny, after 1090 Ma, was a mostly fluid absent granulite facies event that largely overprints the anorthosite and the contact metamorphic rocks. The anorthosite behaved as a dry rigid body, and thus was not significantly deformed during regional metamorphism, preserving the igneous features observed in the field. The contact metamorphic rocks had their original geometry destroyed, but much of their chemistry was not significantly altered, allowing a significant understanding of the skarn forming processes.

ACKNOWLEDGEMENTS

The authors wish to thank NYCO Minerals, Inc. for allowing access to the Oak Hill deposit. NYCO graciously allowed access and sampling privileges to CCC and JWV for research that led to CCC's masters thesis. CCC and JWV would especially like to thank Eve Bailey and Marc Buckley of NYCO for all their assistance. Additionally, Mike Hamilton of the Geological Survey of Canada is thanked for all his effort with the SHRIMP II analyses. Lina

Patino of Michigan State University is thanked for providing the opportunity to do, and assistance with, the REE analyses. Mike Spicuzza, John Fournelle, and Brian Hess, all of Univ. of Wisconsin – Madison, are thanked for help with stable isotope analyses, electron probe analyses, and thin and thick section preparation respectively. This work has been supported by NSF grants EAR-9902973 (to JWV) and EAR-0125057 (to JWV, JM, and M.E. Bickford), as well as a DOE grant 93ER14389 (to JWV). CCC gratefully acknowledges a Weeks research assistantship and fieldwork support from the Department of Geology and Geophysics, Univ. of Wisconsin – Madison, as well as a grant for field studies from the Geological Society of America (6863-01).

ROAD LOG

Mileage

From Lake George Village, take I-87 north to Exit 30.

0.0 Exit 30, start odometer at end of off ramp. Take a left onto Rts. 9 and 73.
2.3 Right onto Rt. 9 north toward Elizabethtown.
4.6 After crossing bridge, pull into parking area on right side of road.

STOP 1. SPLIT ROCK FALLS LOCALITY. (OPTIONAL) The roadcut across from the parking area provides evidence for multiple intrusions of anorthositic and gabbroic rock. The dominant rock type is gabbroic anorthosite that encloses altered xenoliths. Subophitic textures are preserved in the more gabbroic xenoliths. Garnetiferous gabbro truncates foliation in some xenoliths and has, itself, a different foliation. Some small xenoliths of anorthosite are elongated and are deformed parallel to the foliation in the gabbroic facies suggesting coeval magmatism. All of the above facies, including the garnetiferous anorthositic gabbro, are disrupted by a more mafic facies similar to Woolen Mill gabbro. Late mafic dikes (Phanerozoic?) with well developed slickensides cut all other lithologies.

The outcrop not only gives good evidence for the composite nature of the Marcy anorthosite massif, but it also demonstrates the manner in which these rocks can acquire foliation during magmatism and without the need for regional strain. Numerous other localities exist in which different members of the anorthosite suite locally develop foliations that are crosscut by other anorthosite facies. The fact that these rocks involved are clearly contemporaneous, and that the fabrics are strictly local, provide compelling evidence that the foliations developed during composite magmatism when semi-consolidated blocks and magmas underwent differential movement.

Turn right out of parking area, continue north on 9N
12.6 Left onto Rt. 9N in Elizabethtown
13.6 Right into turnout on side of road, opposite tall roadcut. Bridge and Lord Rd. on right are just beyond parking area.

STOP 2. WOOLEN MILL LOCALITY. The outcrops exposed in road cuts along Rt. 9N and in the stream at the site of the former Woolen Mill afford an excellent opportunity to examine field relations of cross-cutting anorthosite series rocks. A sketch map is included here as FIG 7. Recent SHRIMP II geochronology has been undertaken on zircons from the different rock types exposed here to constrain the age of emplacement of the Marcy anorthosite massif and related mafic rocks (Clechenko et al. 2002). New oxygen isotope data have provided further evidence for the magmatic enrichment of the anorthosite in $^{18}O/^{16}O$ compared to "normal" magmatic anorthosite, as opposed to enrichment by metamorphic fluids during subsequent metamorphism (Clechenko et al. 2002).

The roadcut on the south side of Rt. 9N shows anorthosite (east end) intruded by a dark, fine-grained rock, first described by Kemp and Ruedemann (1910) as the "Woolen Mill Gabbro". The Woolen Mill Gabbro is a fine to medium grained clinopyroxene-garnet-oligoclase granulite with magnetite-ilmentite, apatite, and minor K-spar and quartz. The gabbro also contains a population of cm scale andesine xenocrysts that have their apparent source from the anorthosite. These may be easily seen as one walks west along the outcrop from the anorthosite contact. The rock is clearly metamorphosed, as indicated by the presence of significant garnet, but lacks significant deformation

features. Zircons obtained from the Woolen Mill Gabbro along the road had cores that exhibited oscillatory zonation, interpreted to be magmatic in origin, and yielded an age of 1154 ± 9 Ma. Thick, structureless, U poor overgrowths imprecisely date a metamorphic zircon growth episode at 1008 ± 32 Ma.

Figure 7

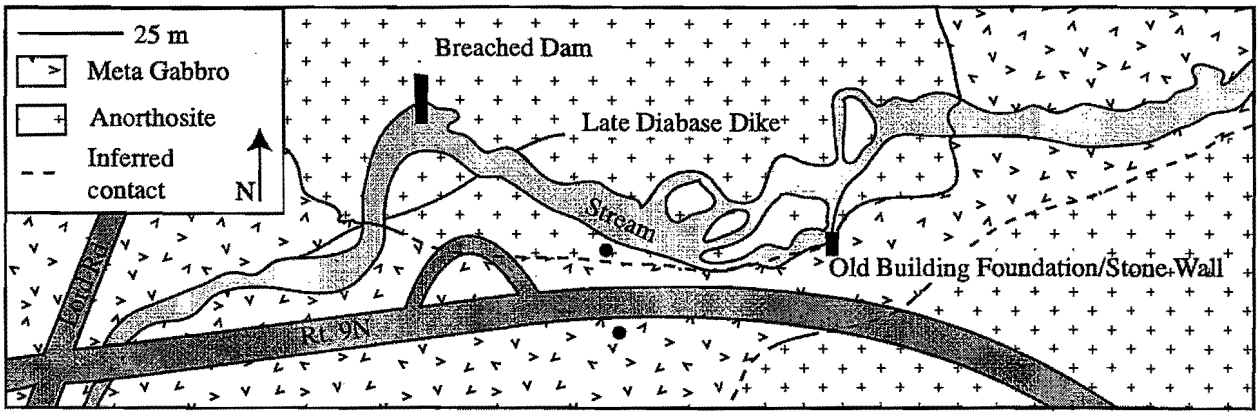

Figure 7. Sketch map of the Woolen Mill area, 1 mile west of Elizabethtown, NY on Rt. 9N. Map is after Kemp and Reudemann (1910). Best exposed cross cutting relations and block texture all found near stream bed within 25 m of turnout off of Rt. 9N and breached dam. Black dots represent approximate location of geochronology samples discussed in text.. Dot on south side of road is location of metagabbro sample, dot under word stream location of pegmatitic anorthosites.

Cross the road to examine the exposures in the streambed. Starting from the west, where the stream flows out from under the Rt. 9N bridge, on the north shore of the stram, more Woolen Mill Gabbro is exposed, and as one walks east (downstream) on the north side of the stream, it may be seen becoming apparently finer grained near the contact. A weak apparent foliation also exists, defined by plagioclase lathes, and is best seen on the weathered surfaces in the streambed. Plagioclase xenocrysts and small anorthosite xenoliths are found in the gabbro in a number of spots near the contact. At the contact, the gabbro is clearly seen cross cutting anorthosite. The contact is irregular, and cuts across a variety of different anorthositic lithologies, including a coarse, pyroxene rich facies. At some points along the contact, anorthosite has broken off and floats in the gabbro. Dikes and veins of the gabbro extend into the anorthosite at a number of areas near the contact, and may also be seen as one moves further downstream away from the contact. Also apparent are a number of light colored, cm scale thick dikes that originate at the contact and extend into the gabbro. These appear anorthositic, as they contain plagioclase that has the blue gray appearance of plagioclase in the anorthosite, but contain significant quartz. These may be mixed lithologies, of the transitional "Keene Gneiss" type of Miller (1919).

Crossing the stream to south bank immediately below the parking turnout and across the stream from the breached dam, the outcrops are of anorthosite. The anorthosite here has a clearly developed "block structure" where several different types of anorthosite have been undergone brittle fracture and been intruded by a variety of mafic (anorthositic to gabbro) and felsic material. The angular blocks vary in size from 10's of cm to meter scale. The blocks are generally of a coarse anorthosite with large plagioclase phenocrysts and megacrysts. One block at the top of the outcrops has "deformed" anorthosite transitional to "undeformed" anorthosite. The occurrence in a block with a preserved transition indicates a magmatic origin of the foliation. Sub-ophitic pyroxene textures of a magmatic origin are also developed in a number of places in the anorthosite.

Some intruding material is equivalent to the Woolen Mill Gabbro, as mentioned above. This material is found as veining throughout the outcrop. In one location at the western edge of the outcrop and near the streambed, intruding Woolen Mill gabbro cuts across a plagioclase megacryst. At another location near the top of the outcrop, just adjacent to the foliated anorthosite block described above, gabbro intrudes the anorthosite in the shape of a reversed "7" when viewed looking to the south. Blocks of the gabbro are broken, forming a series trailing away form the main vein. Much of the intruding material is of an anorthositic gabbro composition. More than one

"generation" of such gabbroic anorthosite material is found, varying in both mafic content and crystal size. Some of the dikes or veins are granitic in nature.

Anorthosite throughout the outcrops contains the characteristic post-metamorphic alteration assemblages of calcite ± chlorite ± sericite that are commonly seen as late-stage, hairline vein fillings or as alteration products of Fe-Mg silicates throughout the Adirondacks (Buddington 1939; Morrison and Valley 1988). Average values of $\delta^{18}O$ and $\delta^{13}C$ for calcite are 12.6 and –2.2 permil, respectively, which suggests that ht ealteration fluids were deep seated in origin and exchanged with igneous as well as metasedimentary rocks. These veins are related to the formation of at least some high density, CO_2-rich fluid inclusions and the temperatures of alteration are estimated at 300-500° C (Valley et al. 1990).

The retrograde fluids that have infiltrated the anorthosite to precipitate calcite have not significantly altered its oxygen isotopic composition. Values of $\Delta_{(Cc-Plg)}$ range from 0.9 to 6.6, indicating that the isotopic composition of the alteration minerals was controlled primarily by the hydrothermal fluid and that the $\delta^{18}O$ of the host rock remaines largely unchanged due to low fluid/rock ratios.

Values of $\delta^{18}O$ (plag) for the blocks and their host anorthosite at this outcrop range from 8.5 to 9.3‰. In general, the metanorthosites in the NE part of the Marcy massif are somewhat more isotopically heterogeneous than those in the northwestern part of the massif, but they show the same roughly 2.5 permil enrichment in the $\delta^{18}O$ relative to normal anorthosites worldwide (Morrison and Valley 1988).

Travelling further downstream, the blocking texture becomes less pronounced. Populations of zircons were obtained from coarse-grained anorthositic pegmatites between the dam and the foundations downstream, as well as from gabbroic anorthosite taken from the outcrop at the dam. Prismatic zircons with sector and oscillatory zoning (interpreted to be igneous) from one of the anorthositic pegmatites yielded an age of 1151 ± 6 Ma. A subordinate population of zircons from the pegmatitic anorthosite have structureless (in CL) rims that give an age of metamorphic growth at 1012 ± 5 Ma. Upon reaching the foundations of the old mill buildings above some falls, more metagabbro is exposed, and below the falls, the rocks in the streambed and on the banks are nearly all Woolen Mill gabbro.

When all relations exposed here are taken in total, they suggest the intrusion of a plagioclase rich cumulate that was fractured and intruded by more mafic differentiates, as well as a small amount of granitic material. This event took place at ca. 1155 Ma, as determined from igneous zircons from both anorthosite and the metagabbro at this locality. These ages are in agreement with new ages determined from zircons separated from Marcy anorthosite at a number of localities across the Adirondacks, and are also in general agreement with ages determined from zircons from granitic rocks that cross cut anorthosite at a number of localities (Chiarenzelli and McLelland 1991). The ages lend no credence to assertions of anorthosite intrusion in this area at ca. 1040 Ma (Isachsen et al. 2001).

Turn right out of parking area, heading westward on 9N (toward Keene).
23.1 Right onto Rts. 9N and 73 toward Keene.
25.0 Right at intersection in Keene, remains Rt 9N, toward Jay
31.2 Remain on Rt. 9N (effectively a right turn) in Upper Jay, still heading toward Jay.
35.0 Right on to Mill Rd. (north edge of the small park) in Jay. Go down hill, bear right over bridge, bear right after bridge.
35.3 Right into turnouts on side of road and park.

STOP 3. COVERED BRIDGE AT JAY (note: covered bridge no longer crosses river, and is set on side of road). Walk a few tens of feet farther south along the paved road from the parking turnouts. At the sharp bend in the road there is a low, polished outcrop that exposes two exceptional examples of rafts of coarse, blue-gray andesine anorthosite of the Marcy facies. The more southerly of these is enveloped in medium grained gabbro similar to a xenolith bearing, gabbroic facies found on Giant Mtn. The gabbro is, in turn, surrounded by a fine grained anorthosite. The northern raft of Marcy anorthosite lacks the rim of gabbro and is directly surrounded by the white, fine-grained anorthosite. The northern raft also contains giant pyroxene whose edges show subophitic relates with plagioclase.

Within the river there occurs a wide area of water-swept exposures of white, fine grained, and highly altered anorthosite containing a few remnant blue-gray andesines as well as a few blocks of subophitic gabbro. The exposures are disrupted by two types of dikes: 1) late unmetamorphosed (Phanerozoic?) diabase paralleling the river, and 2) irregular, pyroxene-rich dikes and veins that trend mainly N-S and E-W but show other orientations and right angle turns, as well. Some of the dikes are 15-20 cm wide but most fall into the 2-5 cm range. Both sharp and gradational contacts exist. Several of the dikes intrude along zones of mafic mylonite that may be of the same composition as the dikes themselves.

Mineralogically, the dikes consist of coarse, emerald green clinopyroxene and Fe, Ti-oxide. Some dikes also contain small quantities of plagioclase, garnet, apatite and titanite. The apatite-free dikes contain very Mg rich clinopyroxene (X_{Mg} ~0.80) while the apatite bearing dikes have less magnesian clinopyroxene (X_{Mg}~0.65). The key to understanding these dikes is to note that some exhibit comb structure defined by pyroxene and plagioclase crystals growing perpendicular to the dike walls. The texture is diagnostic of growth from a fluid and provides compelling evidence that the dikes were intruded as liquid rich magma. Preliminary experimental work by D. Lindsley (pers. comm. to J.M.) indicates that representative dike material reaches its liquidus at 1200°C (max).

It is suggested that the pyroxene-rich, and sometimes apatite bearing, dikes represent immiscible silicate fractions complementary to magnetite-ilmenite deposits. Emplacements may have occurred when jostling about of essentially congealed plagioclase cumulates resulted in fracturing and the development of large blocks whose shifting provided passageways along which pyroxene-oxide magmas could be filter pressed. Depending on the batch of magma tapped, the intruding material would vary from Mg rich to Fe rich with apatite. Some dikes may have been cumulate-rich.

Dikes of the sort exposed in the river at Jay are common throughout the Marcy anorthosite massif, and their presence indicates a substantial, but small, amount of mafic material – and possibly mafic cumulate – in the massif. Invariably these dikes consist of green clinopyroxene and Fe, Ti-oxide, and it is common to find the silicate and oxide phases physically separated within the same vein. It is possible that, where this occurs, it reflects liquid immiscibility operating on late-stage interstitial fractions that are filter-pressed into veins.

Zircons from the clinopyroxene-plagioclase dike contain very low concentrations of uranium and therefor yielded a poorly constrained SHRIMP II age of 1139 ± 89 Ma. Because the zircons show no inherited cores, it is planned to re-date them by single grain TIMS procedures. A pegmatitic gabbroic anorthosite occupying a ductile shear zone in the riverbed yielded abundant zircons that gave a well constrained SHRIMP II age of 1155 ± 13 Ma. This age is consistent with ca. 1155 Ma SHRIMP II ages obtained from six other anorthosite samples from across the Marcy massif, including those described at Woolen Mill. These results make it clear that attempts to argue for a young age of ca. 1040 Ma (Isachsen et al. 2001) for the Marcy anorthosite are without merit and are wrong.

Retrace route to Elizabethtown.

58.0 Jct. of Rts 9 and 9N in Elizabethtown. Left turn (heading north toward Lewis) on Rt. 9.

64.9 Left onto Pulsifer Rd. View of Oak Hill deposit on hillside ahead. Follow around sharp bend to north. Gate to mine located on left side of road at transition from pavement to dirt. Depending on conditions, we will either park here and walk in, or drive up unimproved road to mine.

STOP 4. OAK HILL WOLLASTONITE DEPOSIT. (Private property, seek permission at NYCO offices in Willsboro if coming on your own) The Oak Hill wollastonite deposit provides excellent exposures of interlayered calc silicate skarn and anorthositic lithologies, typical of the low $\delta^{18}O$ wollastonite skarns found between Lewis and Willsboro in a belt of rocks that form the northern and northwestern border of the Westport anorthosite dome. The rocks are exposed on an east-facing hillside of Oak Hill, cleared of trees and overburden within the past few years. The rocks occur in nearly parallel layers, dipping into the hillside, as known from drill core (FIG 2) and outcrop. The lowest units known are anorthositic rocks of varying composition. Overlying this are the calc silicate skarns of the wollastonite ore horizon, and above that, interlayered igneous and marble lithologies. This portion of the trip will entail a short walking transect across lithologies exposed on the hillside and in test pits at Oak Hill. This transect is the surface exposure of the drill core cross section shown previously in this field guide (FIG 2) as well as in Clechenko (2001). A sketch map is included (FIG 8) showing the position of features described in this road log.

Future mining activity at the Oak Hill deposit may alter the appearance of the area, and the features described below and shown on the map may be altered or simply not exist in the future.

Figure 8

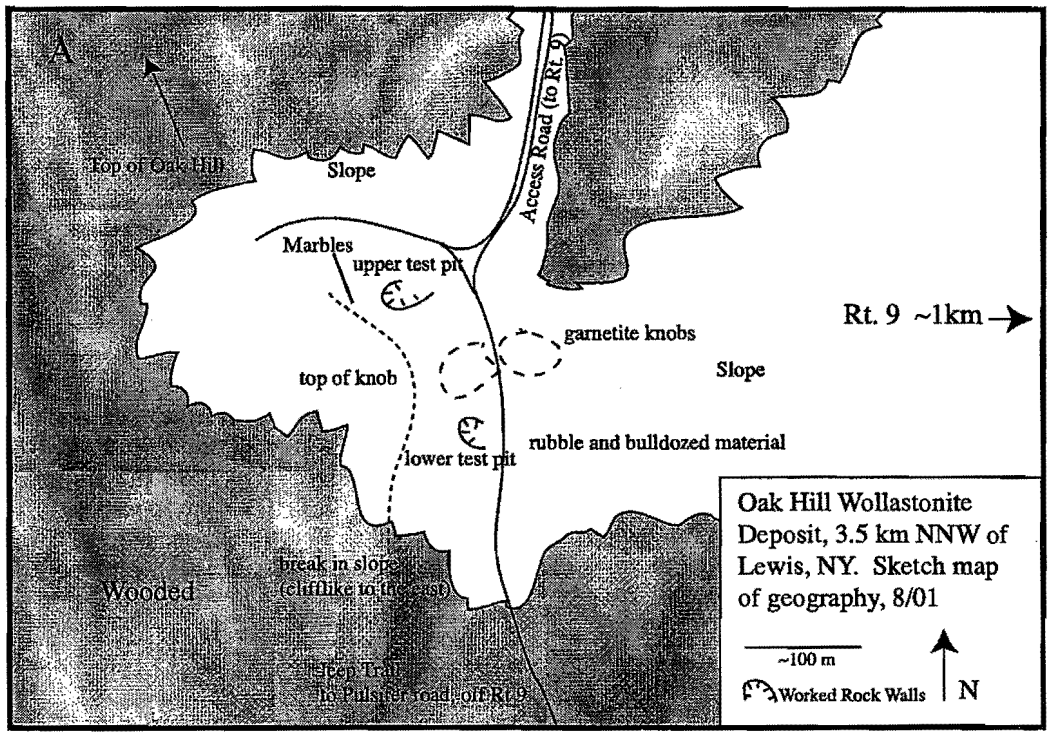

Figure 8. Sketch map of the Oak Hill deposit showing relative location of features described in text.

The footwall of the layered sequence is anorthosite of the Westport dome. These are not seen in outcrop, but are known from drill core. The anorthosite varies in appearance, generally based on the amount of mafic minerals and also quartz, but is typically of the "Whiteface facies" of foliated white anorthosite with crushed and recrystallized plagioclase. Some samples contain noticeable quartz. Minor garnet is found in these anorthosites.

The structurally lowest outcrop exposures in the section are massive garnetites consisting almost entirely of grandite garnet, and are exposed as knobs on either side of one of the southern access road. The garnetites overlie anorthositic rocks at this locality as known from drill core. Garnet from the massive garnetite has a generally restricted compositional range (when compared to garnet from wollastonite ore) that is grossular rich. The garnetite has a range of textures. Some areas are comprised of small, equant sized garnet grains, while other areas are comprised of large (cm scale) euhedral crystals surrounded by feldspar and quartz. This texture is also observed in garnetite from the Willsboro mine (FIG 3), where some of the euhedral garnets have oscillatory zonation. The texture is interpreted to be growth of euhedral garnets into open void spaces. The clusters of large euhedral garnet behaved as rigid boudins during Ottawan metamorphism and deformation, while surrounding garnets could have been recrystallized and chemically homogenized. The low $\delta^{18}O$ nature of the zoned garnet and the demonstrated chemical link between anorthosite and the oscillatory zonation of the garnet indicate that anorthosite intrusion took place at shallow crustal levels. Additional accessory minerals include titanite and clinopyroxene. On the west-side of the western knob, the garnetite is intruded in places by gabbroic anorthosite. Presumably, this represents a late stage anorthositic series magma that intruded the garnetite. The intrusive relation has been armored by garnetite during the major metasomatic wollastonite ore formation event and subsequent deformation.

Stucturally overlying the garnetite, and exposed in two pits (one south of the garnetite, one uphill and west), are the low $\delta^{18}O$ (garnet as low as $-2‰$) wollastonite skarn rocks (Wo + Gt + Cpx), along with related lithologies, including garnetite (Gt ± Qtz ± Fsp) and garnet pyroxene skarn (Gt + Cpx ± Ttn ± Ap). As a general rule, the wollastonite skarn rocks (the wollastonite ore) do not contain primary quartz or calcite, indicating their high

variance and formation in an open system. The wollastonite skarn runs approximately at 50-70% wollastonite, though that is variable on the order of 10's of centimeters. Garnet from wollastonite ores have a range of composition X_{Adr}= 0.1 to 0.9. Color is a general indicator of garnet composition, with darker garnets containing more Fe, and redder garnets more Al. Garnet $\delta^{18}O$ varies with composition, higher X_{Adr} correlates to lower $\delta^{18}O$. The walls of the test pits and numerous blocks lying about afford an excellent opportunity to examine the nature of the wollastonite ores. The ores are a coarse granoblastic combination of wollastonite, grandite garnet, and clinopyroxene. The ore has a weak foliation defined by the tabular wollastonite grains, and a gneissic habit defined by compositional layering of varying modal percentages of wollastonite and the mafic minerals. In the lower test pit (south of the garnetite knobs), typical wollastonite ore may be found, as well as blocks of garnet pyroxene titanite apatite skarn. In the upper test pit (just above the garnetite knob to the west), additional wollastonite ore rocks may be found, as well as a meter thick layer of garnet pyroxene skarn that pinches and swells along the boundary between the wollastonite ores and the overlying anorthosite (Whiteface facies). The anorthosite is typical "Whiteface facies" and is further exposed as one proceeds west above the test pit.

A number of interlayered lithologies, including anorthosite and anorthosite series rocks such as gabbro, marble, and rocks of granitic composition overlie the wollastonite ores. Generally, the interlayering is on the order of 10's of centimeter to meter scale. The anorthositic rocks here are generally similar in appearance to those in the footwall of the deposit that are known from drill core. In places they are more typical Whiteface facies, with occasional plag megacrysts and garnet. Included in one marble layer exposed at the base of the hillside immediately above the upper wollastonite test pit are complexly folded granulite calc-silicate layers. In some places the calc silicates folds and layers are weathering out of the marble, resulting in pieces of rock lying about that give the appearance of dirty dishrags (FIG 9). The complex folding is the result of the contrast in physical properties between the calc silicate layers and the marble. Marbles contain clinopyroxene, titanite, and graphite, and have a measured calcite $\delta^{18}O$ of ~20‰ for three different samples.

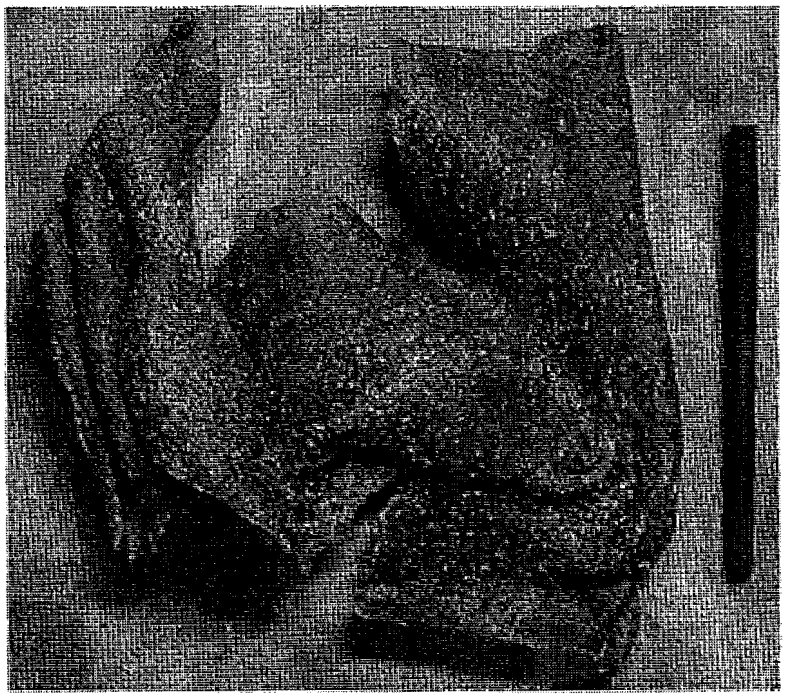

Figure 9. Calc silicate fold ("dishrag") weathered out of marble from Oak Hill wollastonite mine, sample collected from marble layer at base of cliff above wollastonite ore horizon.

The overall given by the exposures and field relations at Oak Hill are as follows. (1) Skarn formation predates the major deformation and recrystallization event. Low $\delta^{18}O$ skarn lithologies are deformed, they exhibit foliation and gneissic layering, and the whole of the deposit is drawn into parallelism with the other lithologies and in accord with the regional grain. These relations are well preserved in the quarry faces at Willsboro. (2) Deformation has

served to obscure the original geometry and spatial relations of the hydrothermal system that formed the skarn. (3) The skarns are intimately related to anorthosite. This is true at Oak Hill and throughout the belt surrounding the Westport dome. (4) The fluid flow system that created the skarns was channelized, as marbles near the skarns have not been affected by infiltration of fluids and turned to calc silicates.

When field relations and textures are combined with geochemical analysis, our understanding of the Willsboro-Lewis skarn belt formation is significantly advanced. All results point to formation at shallow crustal levels adjacent to anorthosite (at ca. 1155 Ma) in a complex hydrothermal system, followed by regional deformation and granulite facies metamorphism at temperatures of ~750° C and pressures of ~7 kb. The metamorphism was fluid-absent, most likely by partitioning of water into small amounts of anatectic melt. Garnet U-Pb ages of ~1035 Ma from skarns indicate closure of U diffusion and end of recrystallization at that time.

End of Day.

REFERENCES

Ashwal, L.D., and Wooden, J.L., 1983. Sr and Nd isotope geochronology, geologic history, and origin of the Adirondack Anorthosite: Geochimica et Cosmochimica Acta, v. 47, p. 1875-1885.

Balk, R., 1931, Structural Geology of the Adirondack Anorthosite: Mineralogische und Petrographische Mitteilungen, Bd. 41. p. 308-434.

Basu, A.R., Faggert, B.E., Jr., and Sharma, M., 1988, Sm-Nd isotopic study of wollastonite skarn and garnet amphibolite metamorphism in the Adirondack Mountains, New York: EOS, v. 69, p. 468.

Bohlen, S.R., Valley, J.W., and Essene, E.J., 1985, Metamorphism in the Adirondacks, Petrology, pressure, and temperature: Journal of Petrology, v. 26, p. 971-992.

Broughton, J.G. and Burham, K.D., 1944, Occurrence and uses of wollastonite from Willsboro, N.Y: American Institute of Mining and Metallurgical Engineers Technical Publication No. 1737, p. 1-8.

Buddington, A.F., 1939, Adirondack Rocks and their Metamorphism: Geological Society of America Memoir 7.

Buddington, A.F., and Whitcomb, L., 1941, Geology of the Willsboro Quadrangle, New York: New York State Museum Bulletin No. 325.

Chamberlain, C.P. and Conrad, M.E., 1991, Oxygen isotope zoning in garnet: Science, v. 254, p. 403-406.

Chiarenzelli, J.R., and McLelland, J.M., 1991, Age and regional relationships of granitoid rocks of the Adirondack highlands: Journal of Geology, v. 99, p. 571-590.

Clechenko, C.C., 2001, Petrogenesis of the Willsboro-Lewis Wollastonite Skarns, Northeastern Adirondack Mountains, New York: unpublished masters thesis, University of Wisconsin – Madison.

Clechenko, C.C., Valley, J.W., and Patino, L., 2001, Petrogenesis of the Willsboro-Lewis wollastonite skarns, Northeast Adirondack Mts., New York: Geological Society of America Abstracts with Programs, v. 33, no. 6, p. A293.

Clechenko, C., Valley, J.W., Hamilton, M.A., McLelland, J., and Bickford, M.E., 2002, Direct U-Pb Dating of the Marcy Anorthosite, Adirondack, NY, USA: Goldschmidt Conference Abstracts, in press.

Crowe, D.E., Riciputti, L.R., Bezenek, S., and Ignatiev, A., 2001, Oxygen isotope and trace element zoning in hydrothermal garnets: Windows into large-scale fluid flow behavior: Geology, v. 29, p. 479-482.

DeRudder, R.D., 1962, Mineralogy, Petrology, and Genesis of the Willsboro Wollastonite Deposit, Willsboro Quadrangle, New York: unpublished PhD thesis, Indiana University.

Hanson, R.B., 1996, Hydrodynamics of magmatic and meteoric fluids in the vicinity of granitic intrusion. In The Third Hutton Symposium on the Origin of Granites and Related Rocks, edited by M. Brown, P.A. Candela, D.L. Peck, W.E. Stephens, R.J. Walker, and E. Zen. Geological Society of America Special Paper 315, p. 249-259.

Isachsen, C., Alcock, J., and Livi, K., 2001, Conditions and timing of emplacement of the Marcy anorthosite, NE Adirondack highlands, inferred from anatectites in its aureole: Part 2, U-Pb geochronology: Geological Society of America Abstracts with Programs, v. 33, no. 6, p. A-292.

Jamtveit, B., and Hervig, R.L., 1994, Constraints on transport and kinetics in hydrothermal systems from zoned garnet crystals. Science, v. 263, p. 505-508.

Kemp, J.F., and Ruedemann, R., 1910, Geology of the Elizabethtown and Port Henry quadrangles: New York State Mueseum Bulletin No. 138.

Kohn, M.J., and Valley, J.W., 1998, effects of cation substitutions in garnet and pyroxene on equilibrium isotope fractionations: Journal of Metamorphic Geology, v. 16, p. 625-639.

McLelland, J., and Chiarenzelli, J., 1990, Isotopic constraints on emplacement age of anorthositic rocks of the Marcy massif, Adirondack Mts., New York: Journal of Geology, v. 98, p. 19-41.

McLelland, J., Daly, J.S., and McLelland, J.M., 1996, The Grenville Orogenic Cycle (ca. 1350-1000 Ma): an Adirondack Perspective: Tectonophysics, v. 265, p. 1-28.

McLelland, J., Hamilton, M., Selleck, b., McLelland, J., Walker, D., and Orrell, S., 2001. Zircon U-Pb geochronology of the ottawan orogeny, Adirondack Highlands, New York: regional and tectonic implications: Precambrian Research, v. 109, p. 39-72.

Miller, W.J., 1919, Geology of the Lake Placid Quadrangle: New York State Museum Bulletin, No. 211.

Morrison, J. and Valley, J.W., 1988, Contamination of the Marcy anorthosite massif, Adirondack Mountains, NY: petrologic and stable isotope evidence: Contributions to Mineralogy and Petrology, v. 98, p. 97-108.

O'Hara, P., 1976. The Economic Geology, Petrology, and the origin of the Willsboro Wollastonite Deposit, New York: unpublished masters thesis, Queens College of the City University of New York.

Putnam, G.V., 1958, Geology of Some Wollastonite Deposits in the Eastern Adirondacks, New York: unpublished masters thesis, Pennsylvania State University.

Silver, L., 1968, A geochronological investigation of the anorthosite complex, Adirondack Mts., New York: In Origin of anorthosites and related rocks, edited by Y. Isachsen, New York State Museum Memoir 18, p. 233-252..

Taylor, H.P., 1968, Oxygen isotope studies of anorthosites, with particular reference to the origin of the bodies in the Adirondack Mountains, New York: in Origin of anorthosites and related rocks, edited by Y. Isachsen, New York State Museum Memoir 18, p. 111-134.

Valley, J.W., Chiarenzelli, J.R., and McLelland, J.M., 1994, Oxygen isotope geochemistry of zircon: Earth and Planetary Science Letters, v. 126, p. 187-206.

Valley, J.W., Bohlen, S.R., Essene, E.J., and Lamb, W., 1990, Metamorphism in the Adirondacks: II. The role of fluids: Journal of Petrology, v. 31, p. 555-596.

Valley, J.W., and O'Neil, J.R., 1982, Oxygen isotope evidence for shallow emplacement of Adirondack anorthosite: Nature, v. 300, p. 497-500.

Valley, J.W., and O'Neil, J.R., 1984, Fluid heterogeneity during granulite facies metamorphism in the Adirondacks; stable isotope evidence: Contributions to Mineralogy and Petrology, v. 85, p. 158-173.

Walther, J.W., and Orville, P.M., 1982, Volatile production and transport in regional metamorphism: Contributions to Mineralogy and Petrology, v. 79, p. 252-257.

Whitney, P.R., and Olmstead, J.F., 1998, Rare earth element metasomatism in hydrothermal systems: the Willsboro-Lewis wollastonite ores, New York, USA: Geochimica et Cosmochimica Acta, v. 62, p. 2965-2977.

PRECAMBRIAN GEOLOGY OF THE WHITEHALL AREA, SOUTHEASTERN ADIRONDACKS

by
Philip R. Whitney, New York State Museum, 3140 CEC, Albany NY 12230
Glenn B. Stracher, Dept. of Geology, East Georgia College, Swainsboro, GA 30401
Timothy Grover, Dept. Of Geology, Castleton State College, Castleton VT 05735

INTRODUCTION

At the easternmost edge of the Adirondack Highlands, between Fort Ann and Whitehall (Fort Ann and Whitehall 7.5' USGS sheets) is a tilted (?) fault block of severely deformed, granulite facies metamorphic rocks of Middle Proterozoic age, called the Pinnacle Range by Hills (1965). The gently sloping eastern side of this block is nearly a dip slope in many locations, and the rocks throughout are not far below the Proterozoic - Paleozoic unconformity, which is exposed at Stop 2. The northern end of the block is a zone of intense ductile shear at least several hundred meters thick that we will refer to as the Whitehall Deformation Zone (WDZ).

Only parts of the area have been mapped in detail. The southern half was mapped by Hills (1965), and the northern third by Stracher (1986, 1989). The map of Fisher (1985), at a scale of 1:48,000 is based on Hills' map and reconaissance mapping by the New York State Geological Survey in 1982 and 1983. A somewhat different picture is presented by the 1:250,000 map of Thompson et al. (1990). Both the Fisher and Thompson maps cover large areas of which the Pinnacle Range is only a small portion; clearly more work is needed to reconcile the differences. Figure 1 shows the general geology of the Pinnacle Range; Figure 2, from Stracher (1992), shows the geology of the northernmost portion, including the WDZ.

The trip will focus on the extraordinary deformational features of the WDZ, as well as on evidence for a retrograde metamorphic event of probable Taconic age. Stop 1 will be a walking traverse in the most strongly deformed part of the WDZ. Stops 2 through 5 will examine road cuts along NY Route 4, from south to north.

LITHOLOGY

Metasedimentary rocks. Metasedimentary rocks in the southeastern Adirondacks consist of large volumes of metapelitic rocks, now metamorphosed to gneisses ranging from migmatitic (sillimanite)-garnet-biotite-quartz-plagioclase ("Kinzigite") to (graphite)-sillimanite-garnet-quartz-K feldspar ("Khondalite"). These are interlayered with calcite marbles (some with late dolomitization) and calcsilicate rocks, and quartzite. This suite of metasedimentary rocks differs from that found farther north and west in the Adirondack Highlands in having a much greater proportion of metapelites relative to carbonates and quartzites.

Metaigneous rocks. Nearly all the varieties of metaigneous rocks found elsewhere in the Highlands are also present here. Olivine metagabbros (Stops 1, 3, and 4) are abundant both as small lenses and in larger plutons. These gabbros, which are lithologically and geochemically similar to those found throughout the Highlands (Stracher, in prep.), are the only rocks that retain primary igneous textures; they appear to have behaved as rigid units in the region-wide ductile deformation. Small amounts of metanorthosite are also present, notably at Battle Hill just north of Fort Ann. Gabbroic anorthosite gneiss is present at Stop 5, as is a mafic gneiss similar to the jotunites commonly associated with anorthosite suites. Charnockite (Stop 5) and megacrystic biotite granite (Stop 4) are the most common felsic lithologies. The anorthosite, jotunite, and charnockites are probably part of the ca 1160-1130 Ma Anorthosite-Mangerite-Charnockite-Granite (AMCG) suite. Metatonalites, found only in the southern and southeastern Highlands, are also present here and in the area north and west of the Pinnacle Range mapped by Berry (1960). They are significant in that they have been dated at 1330-1307 Ma (McLelland and Chiarenzelli, 1990), substantially older than the AMCG suite.

Unmetamorphosed dikes. Diabase dikes, probably latest Proterozoic to early Cambrian, are common throught the eastern Adirondack Highlands (Isachsen et al 1988; Coish and Sinton 1991). The follow the dominant NNE trend of brittle faults that probably originated at the time of the opening of the Iapetus Ocean.

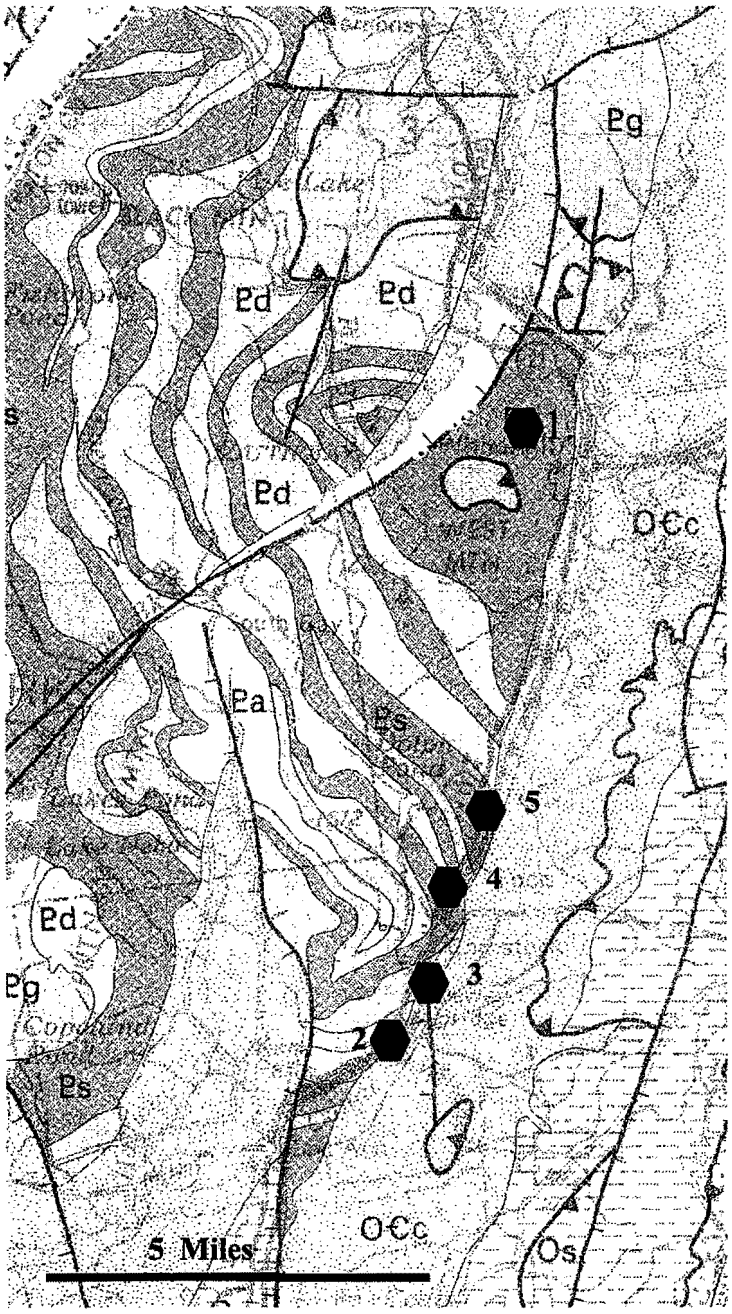

Figure 1. General geology of the pinnacle Range, from Thompson et al. (1990), showing field trip stops. Pa: metanorthosite and related rocks, Pd: Metagabbro and metadiorite; Pg: felsic gneisses; Ps: metasediments. Numbered spots are field trip stops.

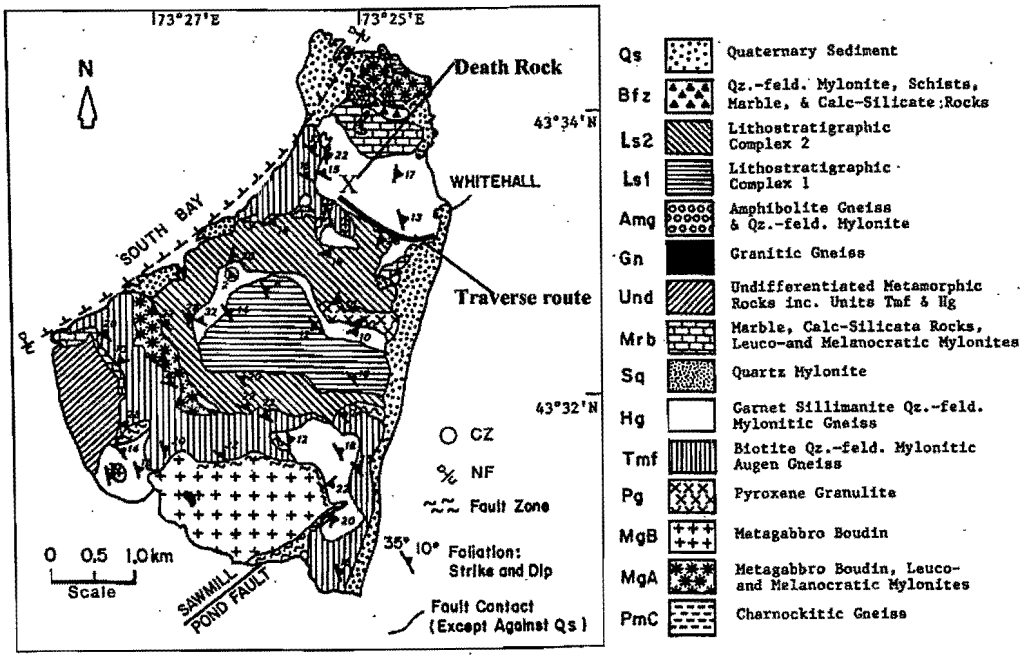

Figure 2. Geologic map of the West Mountain Area, after Stracher (1992), showing route of Stop 1 traverse.

METAMORPHISM

Traces of four separate metamorphic events are present in the Pinnacle Range and in the area immediately to the north and west. The earliest, of probable Elzevirian (pre-1180 Ma) age, has been documented by McLelland et al. (1988) at Dresden Station in the Putnam 7.5' quadrangle, where deformed and metamorphosed metapelites have been intruded and crosscut by olivine metagabbro dated at 1144 +/- 7 Ma (McLelland et al. 1996). The second event is indicated by contact metamorphosed marbles and calcsilicates (Stop 5) adjacent to meta-intrusive rocks that are probably part of the AMCG suite. The third event is the Ottawan granulite facies metamorphism, variously estimated at 1090-1030 Ma (McLelland et al. 1996) and 1050-1000 Ma (Florence et al, 1995). Accompanied by severe deformation, it has overprinted the prior two events and largely obliterated their effects except at scattered locations. The pressure-temperature regime has not been studied in detail; except for two undergraduate theses there is no published data that we are aware of. Zeckhausen (1982), using various geobarometers and geothermometers estimated peak metamorphic conditions of 810 +/- 40 °C and 9 +/- 1 kbar. The pressure estimate was subsequently reduced to 7.5 +/- 0.5 kbar by Glassley (pers. comm., 1985). Clechenko (1999), using different reactions and calibrations, estimated 710 +/- 50 °C and 6.5 +/- 1.5 kbar. The fourth "metamorphism", locally overprinted the granulite facies rocks with low-T (<400 °C) assemblages. It was probably a far-field effect of the Taconic Orogeny (Whitney and Davin , 1987).

STRUCTURE

The rocks seen on this trip are on the upper limb of a large, reclined isoclinal fold that has a southeast-plunging hinge and an east-dipping axial plane (McLelland 1996; Thompson et al. 1990). All show evidence of intense ductile deformation, locally mylonitic, that has produced strongly foliated "straight" gneisses and a pronounced stretching lineation defined variously by quartz blades and ribbons, elongate trains of mafic minerals

including garnet, and oriented sillimanite or hornblende. Only the interiors of olivine metagabbro lenses and large tonalite bodies have escaped the pervasive shearing. The deformation increases in intensity northward, becoming pervasively mylonitic in the WDZ on West Mountain near Whitehall (Stop 1). The WDZ is characterized by pervasive structural discontinuities between internally deformed blocks of granulite facies rocks whose fabrics exhibit high ductile strain and extreme grain-size reduction. The discontinuities form anastomosing arrays resulting from intense stuctural slicing (Stracher, 1992). Kinematic indicators in the sheared rocks throughout the area show a statistical east-over-west sense of shear. Of particular interest in this regard are the large metagabbro lenses at Stop 4, which appear to be large-scale kinematic indicators. Possible Taconic structural effects include slight updip movement along foliation planes marked by low-temperature slickensides (Stop 5) and possible hydrofracturing of rocks near the unconformity surface (Stop 2) followed by filling of the fractures with dolomite-cemented clastic debris (Whitney and Davin, 1987).

REFERENCES

Alling, H.L., 1917, Stratigraphy of the Grenville of the eastern Adirondacks: Geological Society of America Bulletin, v. 38, p. 795-804.

Berry, R.H., 1960, Precambrian geology of the Putnam-Whitehall area, New York: PhD thesis, Yale University.

Clechenko, C.C., 1999, An investigation of the metamorphic and deformation histories of a kinzigite gneiss in the southeastern Adirondack Mountains, New York: BS (honors) thesis, Hobart College, Geneva, NY.

Coish, R.A. and Sinton, C.W., 1991, Geochemistry of mafic dikes in the Adirondack Mountains: implications for late Proterozoic continental rifting: Contributions to Mineralogy and Petrology, v. 110, p.500-514.

Fisher, D.W., 1985, Bedrock Geology of the Glens Falls - Whitehall region, New York: New York State Museum Map and Chart Series 35.

Florence, F.P., Darling, R.S., and Orrell, S.E., 1995, Moderate pressure metamorphism and anatexis due to anorthosite intrusion, western Adirondack Highlands, New York. Contributions to Mineralogy and Petrology, v. 121, p. 424-436.

Hills, F.A., 1965, The Precambrian Geology of The Glens Falls and Fort Ann Quadrangles, southeastern Adirondack Mountains, New York. PhD thesis, Yale University.

Isachsen, Y.W., Kelly, W.M., Sinton, C.W.,. Coish, R.A, and Heizler, M.T., 1988, Dikes of the northeast Adirondack region: Introduction to their distribution, orientation, mineralogy, chronology, magnetism, chemistry, and mystery: New York State Geological Association Field Trip Guide, v. 60, p. 215-243.

McLelland, J. M., and J. Chiarenzelli, 1990, Geochronological studies in the Adirondack Mountains and the implications of a middle Proterozoic tonalitic suite: in Gower, C., Ryan, B., and Rivers, T., eds., Proterozoic geology of the southwestern margin of Laurentia and Baltica, Geological Association of Canada Special Paper 38, p. 175-179.

McLelland, J., Daly, J.S., and McLelland, J.M., 1996, The Grenville orogenic cycle (ca. 1350-1000 Ma): an Adirondack perspective: Tectonophysics, v. 256, p. 1-28.

McLelland, J. M., A. Lochhead, and C. Vyhnal. 1988. Evidence for multiple metamorphic events in the Adirondack Mountains, New York. Journal of Geology, 96:279-298.

McLelland, J. M., and Whitney, P. R., 1990, Anorogenic, bimodal emplacement of anorthositic, charnockitic and related rocks in the Adirondack Mountains, New York: p. 301-316 in Stein, H.J. and Hannah, J.L., eds., Ore-bearing granite systems: petrogenesis and mineralizing processes: Geol. Soc. Amer. Special Paper 246.

Stracher, G.B., 1986, Structure and petrology of Precambrian rocks in zones of high ductile strain - southeast Adirondack Mountains of New York State; MS thesis, University of Nebraska, Lincoln, NE, 77 p.

Stracher, G.B., 1989, Precambrian structural geology, petrology, and geochemistry of a polydeformed Helikian mylonite zone in the southeast Adirondack Mountains of New York State; PhD thesis, University of Nebraska, Lincoln, NE, 222 p.

Stracher, G.B., 1992, Rheology and deformation history of a Precambrian granulite facies SE Adirondack brittle-ductile shear zone: Northeastern Geology, v. 14, p. 113-120.

Thompson, J.B. Jr., McLelland, J.M., and Rankin, D.W., 1990, Simplified geological map of the Glens Falls 1 X 2 degree quadrangle, New York, Vermont, and New Hampshire: USGS Map MF-2073.

Whitney, P.R., 1992, Charnockites and granites of the western Adirondacks, New York, USA: a differentiated A-type suite. Precambrian Research, v. 57, p. 1-19.

Whitney, P.R., and Davin, M.T., 1987, Taconic deformation and metamorphism in Proterozoic rocks of the easternmost Adirondacks: Geology, v. 15, p. 500-503.

Zeckhausen, P.W., 1982, Metamorphic conditions and structural relationships in southeastern Adirondack granulites: BA thesis, Middlebury College, Middlebury, VT.

ROAD LOG

Miles	Increment	
0.0	0.0	Assemble at the parking lot at McDonalds in Whitehall. Carpool if possible; parking is difficult at Stop 1.
0.65	0.65	Traffic signal at intersection of Rtes. 4 and 22; in Whitehall; continue on 22 (Broadway).
0.95	1.2	Turn L on School St.
1.2	0.25	**Stop 1.** Park well off the road wherever space permits. A well-worn trail leaves this dead end road on the R. We will follow this trail W, updip along a dip slope about 0.8 miles to a point just S of Death Rock (Fig. 2). Numerous outcrops in and near the trail are garnet-sillimanite-K feldspar-quartz metapelites, locally containg calcsilicates, quartzites, and graphitic schists, the "Hague Gneiss" of Alling (1917). Elsewhere, these rocks are host to graphite deposits (Alling's "Dixon Schist") that were worked commercially in the nineteenth century. Foliation and lineation are exceptionally well-developed and the rocks exhibit severe grain-size reduction with locally mylonitic textures. The ESE-plunging lineation seen here is typical of much of the southeastern Highlands. Be alert for kinematic indicators. Approaching the height of land S of Death rock, the trail passes outcrops of biotite gneiss with K-feldspar megarcrysts, some of which appear to be rotated porphyroclasts. Well exposed within the biotite gneiss to the N of the trail is a large lens of olivine metagabbro. Foliation in the gneiss wraps around the gabbro lens. Later, at stop 4 we will see more such gabbro lenses that provide (given certain assumptions) clear evidence of shear sense. Further north, at Dresden Station in the Putnam 7.5' Quadrangle, similar metapelites with less extreme deformation are crosscut by 1144 +/- 7 Ma olivine metagabbro, a key piece of evidence for early (Elzevirian?) deformation and metamorphism in the Adirondacks (McLelland et al. 1988, 1996). Our interpretation is that the Whitehall shear zone, of probable Ottawan age, overprints the earlier deformation with resulting loss of the crosscutting relations. After examining the metagabbro and its surroundings, backtrack along the trail to return to the vehicles.

1.5	0.30	Turn R on Broadway from School St.
1.8	0.30	Traffic signal; continue S on Rtes. 4 & 22.
2.45	0.65	Retrieve parked vehicles at the Golden Arches. Coffee and rest stop. We will the proceed to the southernmost stop on Rte. 4 and then work back north.
8.4	5.55	Rtes. 4 & 22 diverge at Comstock; continue S on 4.
10.55	2.15	Turn **L** onto Flat Rock Road; park on R shoulder.

Stop 2. The outcrop on the east side of Route 4 just north of the intersection exposes the unconformity between the Proterozoic gneisses and the Middle to Upper Cambrian Potsdam Sandstone. Missing: roughly 500 million years of the geologic record and 25-30 km of rock. The Potsdam here consists of coarse arkosic sanstones and quartz-pebble conglomerates, locally with carbonate cement. Good exposures of Potsdam are present in railroad cuts a short distance east and downhill. The dip of the unconformity surface is 10-15° east, roughly parallel to the eastern slope of the Pinnacle Range fault block. The unconformity is exposed again at a location 18.6 miles N along Rte. 22 from the intersection of Rtes. 4 and 22 in Whitehall; there, foliation in the gneisses is perpendicular to layering in the potsdam, and pockets of radioactive conglomerate are present at the unconformity surface. If time permits at the end of the trip this can be included as an optional extra stop for those heading N.

A short distance eastward along the S face of the outcrop, the gneisses are complexly fractured and the fractures are filled with a dark, fine-grained clastic rock rich in ferroan dolomite (Fig. 3). In thin section, abundant shreds of fresh biotite and angular grains of feldspar "float" in a matrix of dolomite. What is the origin of this fracture filling? The clastic grains are too fresh to be the result of weathering, and too quartz-poor to be clastic dikes of Potsdam age. Are they simply the host gneiss pervasively shattered by hydrofracturing caused in turn by tectonic overpressures during overriding of the area by Taconic thrust slices? The western edge of the Giddings Brook slice is less than five miles east of here. Ferroan dolomite is ubiquitous as fracture fillings here and at the next three stops, easily visible due to rusty weathering. In the next cuts to the south on the E side of the highway, folded, biotite-rich mafic layers in gneiss contain thin (submillimeter) dolomite veinlets parallel to foliation. In cuts directly across from this stop, crosscutting veins (Fig. 4) contain both dolomite and adularia (low-T K feldspar).

Except for recent weathering of the fracture fillings, there is little evidence for extensive weathering of the unconformity surface, indicating a relatively short interval between erosion of the Proterozoic rocks and deposition of the Potsdam.

Turn around and proceed back N on Rte. 4.

10.8	0.25	Outcrops at the edge of the woods on R are fine-grained white Potsdam ss.
12.1	1.3	Outcrops on L are extensively fractured granitic gneisses close to a N-S fault.
12.2	0.1	Road crosses small pond.
12.3	0.1	Turn **R** on Kelsey Pond Road (dirt track leading to a quarry). Park on R.

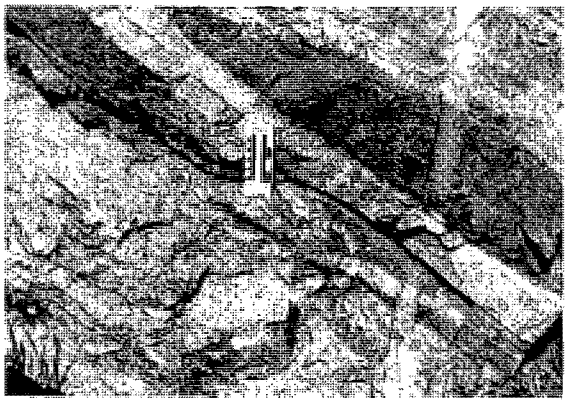

Figure 3. Dolomite-filled fractures in gneiss, Stop 2.

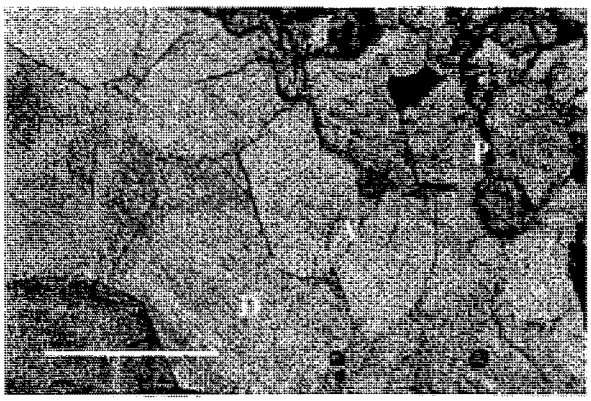

Figure 4. Fracture filling with ferroan dolomite (D), Adularia (A). P = plagioclase in host gneiss. Scale bar = 0.5 mm.

TABLE 1

	FA204.6	FA204.7
SiO_2	31.6	35.15
TiO_2	0.17	0.79
Al_2O_3	17.78	17.35
Fe_2O_3t	9.02	7.5
MnO	0.07	0.05
MgO	23.41	24.32
CaO	4.63	1.85
Na_2O	0.01	0.06
K_2O	0.97	3.55
P_2O_5	0.05	0.1
LOI	12.94	9.43
Total	100.65	100.15
Rb	37	208
Sr	63	120
Ba	37	283
Zr	53	86
Y	31	19
Nb	8	8
Ga	41	33
Cr	21	89
Ni	23	182
V	107	125
Ce	45	284

Table 1 . Chemical analyses of ultramafic lenses, Stop 3.

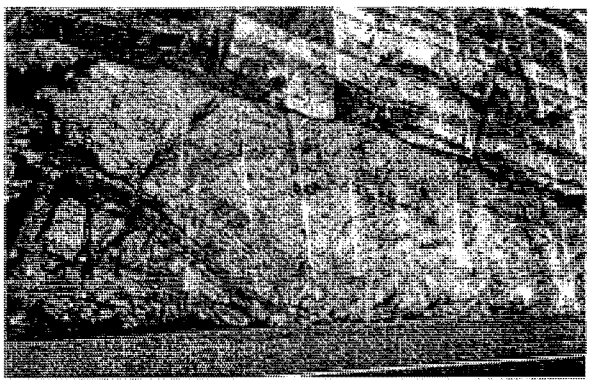

Figure 5. Marble lens in paragneiss, Stop 5. Darker border of lens is dolomite marble; interior is calcite marble.

of movement. Prior to DOT renovation of the roadcut, slight updip offset was visible on a vertical diabase dike that strikes NNE parallel to the road. The orientation of the slickensides is subparallel to the well developed, ca. S50°E granulite facies mineral lineation. This suggests that some foliation surfaces formed during Grenvillian deformation served to localize later, probably Taconic, movement.

END OF TRIP

METAGABBROS OF THE SOUTHEASTERN ADIRONDACKS: EVIDENCE FOR SEPARATE SYN-KINEMATIC, AND POST-KINEMATIC SUITES

Barbara A. Fletcher and W. S. F. Kidd
Department of Earth and Atmospheric Sciences
University at Albany
Albany, NY 12222

INTRODUCTION

This trip will explore some of the metagabbroic intrusions that dot geological maps of the eastern and central Adirondacks and are generally assumed to have been emplaced contemporaneously with the anorthosite massifs of the highlands (Fig.1). However, not only do most metagabbro intrusions in the southeastern Adirondack region lack the penetrative deformation fabric seen in the anorthosites and the host rocks, but many display chilled margins with sharp contacts that cut the foliation of the host gneisses.

Granoblastic texture and the presence of garnet coronas confirm that these rocks experienced granulite facies metamorphism, but without the strong deformation seen in most other rocks of the Adirondacks. Evidence of strain accommodation is limited to small, localized ductile shear zones well within the intrusive bodies. Could these rocks have been emplaced at shallow crustal levels, as is thought for the anorthosites, then buried to the 20-25 km depth necessary for granulite facies metamorphism, and yet somehow have escaped significant deformation? Stops will include several outcrops of undeformed metagabbros with clearly visible host rock contacts and chilled margins, as well as an example of deformed metagabbro with large, stretched garnet porphyroblasts.

GEOLOGIC SETTING

The Adirondack Mountains expose Proterozoic gneisses and calc-silicate rocks that host massif anorthosite, as well as smaller bodies of mangerite, charnockite and granite (known as the AMCG suite) emplaced during the Grenville Orogeny (1-1.3 Ga). Subsequent burial to mid-crustal depths of 20-25 km has been determined on the basis of geo-thermometry and -barometry of minerals in the granulite facies rock. By the Cambrian, the rocks had been exhumed and lay beneath the sea, evidenced by outcrops of Cambrian sandstones overlying Proterozoic gneisses, some of which can be seen in down-dropped blocks in the Lake George graben.

As a result of the convergence tectonics of the Grenville Orogeny, the rocks comprising the Adirondacks were strongly deformed, obliterating almost all original relationships among rock types, sometimes making the determination of even the original rock type difficult. While the pervasive deformation produced some spectacular large-scale fabrics (such as will be seen at Stops 5 and 6 on this trip), field interpretation of these rocks is often quite difficult.

ADIRONDACK METAGABBROS

Because metagabbros are distinctly different in color and texture from the ubiquitous gneisses of the Adirondacks, and because if they are intrusive igneous bodies we can make some assumptions about their pre-deformational structure, they could prove useful as benchmarks. Their identity is usually easily made in the field. They have a mineral assemblage of plagioclase + hornblende + garnet ± pyroxene ± olivine. Garnet coronas are present. And as will be seen from this trip, they fall into two rather clear categories: those that have been severely deformed, and those that have not and retain many relict igneous features. The purpose of this trip is to acquaint participants with the field markers of each category and to present a sampling of the locales at which they can be observed.

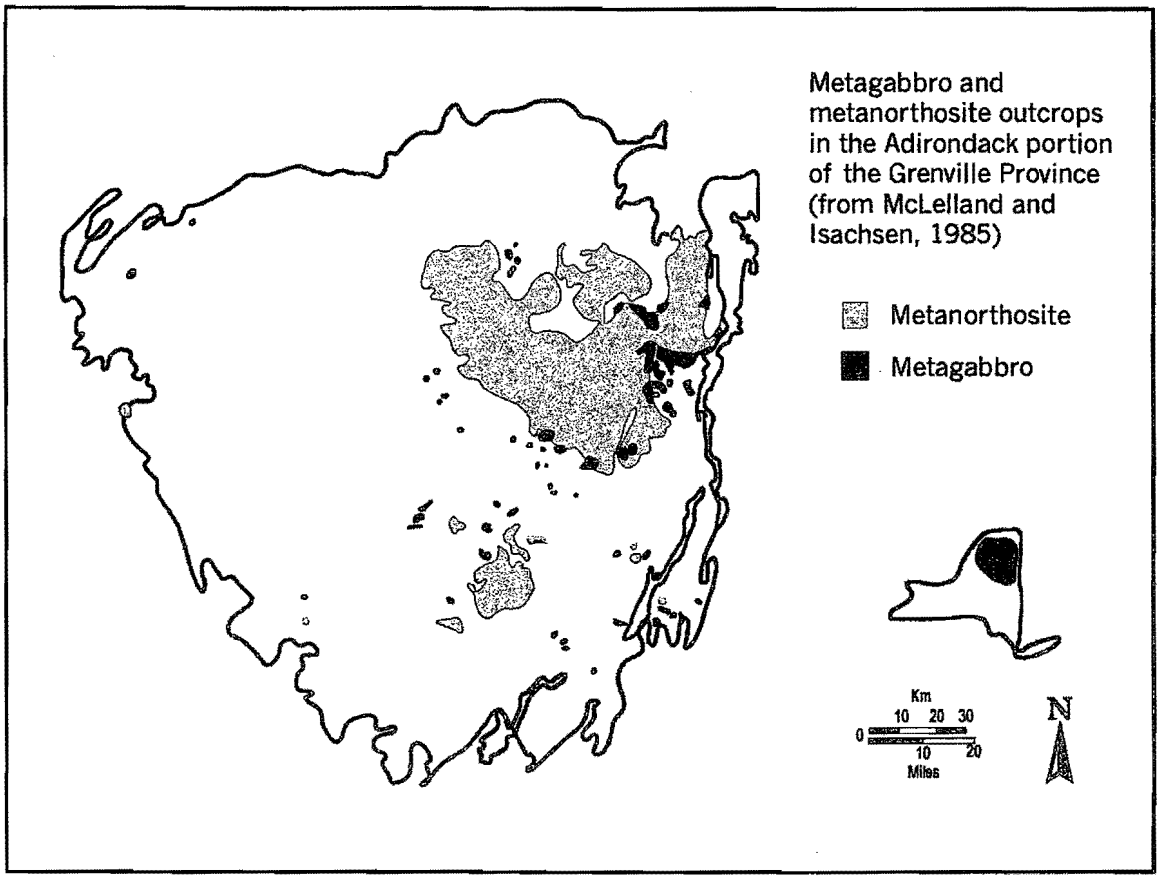

Figure 1. The distribution of metagabbro bodies in the Adirondacks. It should be noted that this map shows only those outcrops large enough to be mappable at this scale.

REFERENCES

Alcock, J. and Muller, P., 1999, The ca. 1144 Ma Dresden Station metagabbro: a re-evaluation: Northeastern Geology and Environmental Sciences, v.21, no. 4, p.275-281.

Fisher, D. W., 1984, Bedrock Geology of the Glens Falls-Whitehall Region, New York, New York State Museum, Map and Chart Series Number 35, 58 pp., map.

McLelland, J., and Isachsen, Y., 1985, Geological evolution of the Adirondack Mountains: a review, *in* Tobi, A., and Touret, J., eds., The Deep Proterozoic Crust of the North Atlantic Provinces: NATO Advanced Studies Inst., v. 158, p.175-217.

McLelland, J., Lochhead, A., and Vyhnal, C., 1988, Evidence for multiple metamorphic events in the Adirondack Mountains, New York: Journal of Geology, v.96, p.279-298.

Valley, J.W. and O'Neil, J.R., 1982, Oxygen isotope evidence for shallow emplacement of Adirondack anorthosite: Nature, v. 300, p.497-500.

ROAD LOG

Most of the outcrops on this trip are roadcuts, but require short walks from where vehicles are parked. PLEASE use utmost CAUTION at roadcuts. Always stay inside guardrails, or well onto shoulders, if there is no guardrail.

One stop requires a short hike (~2 miles round trip) on easy to moderate terrain. Bring a lunch to eat at a pond on the hike. Hiking boots are not a must, but won't hurt either. A hand lens will be useful. No need for hammers.

Prospect Mt. is best accessed by the toll road. The fee is $5.00 per car.

Mile

0.0 Start at parking lot of Fort William Henry Inn, 48 Canada Street, Lake George, NY.

0.1 Turn left onto Canada St.

1.0 At 2nd traffic light, turn right onto Rt. 9N.

1.1 Turn right into Ramada Inn and park behind motel. Walk south, cross Rt. 9N and proceed south on I-87 exit ramp to outcrop on E side of the ramp. STAY OUTSIDE GUARDRAIL AND WATCH FOR TRAFFIC!

STOP 1. INTERCHANGE 21 ROADCUT. Lat 43° 24.125′ N Lon 73° 42.599′ W (30 MINUTES)

At the N end of the outcrop E of the exit ramp,is gray granitoid gneiss with small migmatitic veins and pods, some of which contain 0.5 cm hornblende crystals. ^{40}Ar-^{39}Ar dating of biotite from this outcrop yielded a cooling age in the range of 750-850 Ma (Heizler and Harrison, 1998). Note that the gneissic foliation dips E (280°/40°E), as does most of the regional fabric. Close examination shows small areas of low-grade alteration, a result of contact with fluids during exhumation.

Carefully, climb to the top of the outcrop and proceed S, watching for the contact between gneiss and metagabbro. Partially buried in sand, it is best exposed at the edge of the outcrop where very fine-grained metagabbro sharply truncates the foliation in the gneiss. Just to the left (S) of the contact, a xenolith of gneiss is enclosed in metagabbro. Another gneiss xenolith is seen on the face of the outcrop (Fig. 2).

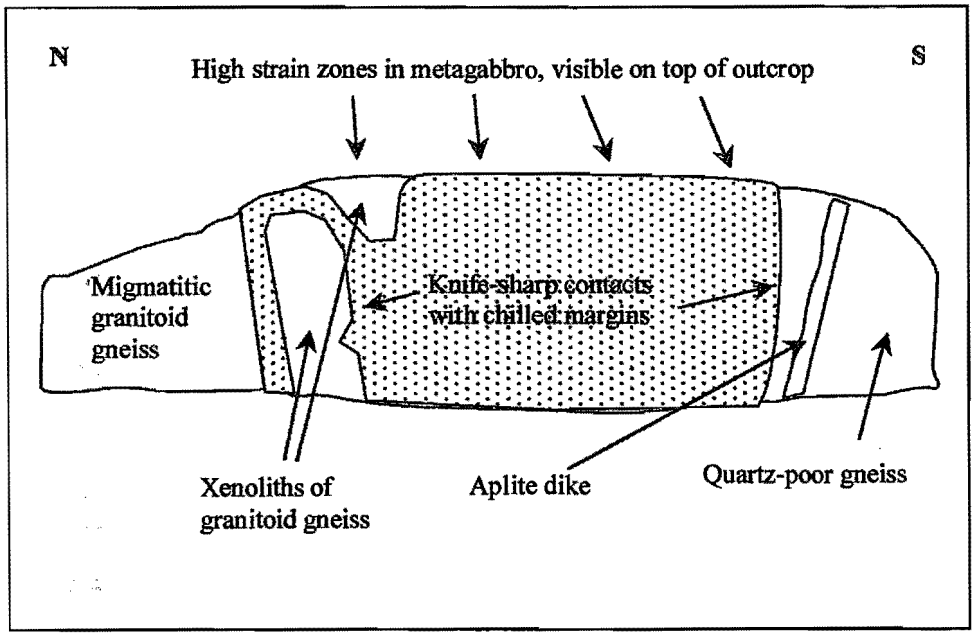

Fig.2 Stop 1. Interchange 21 Roadcut. Diagram of outcrop lithologies and structural features. (not to scale)

Continue to walk S along the top of the outcrop observing the coarsening of grain size in the metagabbro. Over ~2-3 m the grains become large enough to show clearly the relict igneous texture, i.e., ophitic or subophitic,

in which the spaces between the more numerous plagioclase grains are filled by mafic mineral grains. With a hand lens, tiny pale, pink garnets can be seen to "decorate" the plagioclase, evidence that the gabbro was metamorphosed at granulite facies conditions.

Within the coarse-grained metagabbro are several areas that can be seen to have reacted ductilely to localized, intense strain. Determine the sense of shear for each. Are they consistent? Why are they located well within the metagabbro body, rather than nearer the contacts?

Walking S, metagabbro grain size decreases as the contact with a quartz-poor gneiss is approached. Again, the contact is sharp, truncates foliation in the gneiss (although this gneiss is less strained than that at the N end) and the margin was very obviously chilled against the cooler host rock. A meter or so into the gneiss, an aplite dike can be seen. Look carefully at the gneiss for feldspar porphyroclasts.

Returning N, stop in the middle of the metagabbro and look W at the outcrop across the exit ramp. One of the trip leaders always *assumed* that the outcrop was a continuation of the metagabbro, until the other checked it out and found that it is is the same gneiss as that at the N end of the E-side outcrop. When the orientation of the contacts are mapped and projected, it is seen that the contacts are not parallel and their projections intersect in the middle of the ramp. In other words, this intrusion is not a planar structure.

The field evidence from this outcrop can be used to set up a geological scenario for the intrusion of the host rocks by the gabbro. The truncated foliation shows that the host rocks were already deformed when the gabbro intruded. The sharp contacts indicate that the host rocks were cool enough to behave brittlely. The chilled margins in the metagabbro indicate that a temperature difference existed, which is not surprising given that the host rocks were brittle and the gabbro was a melt. So far, this is a typical scenario for magmatic intrusion. The puzzle arises when we attempt to account for the facts that the metagabbro shows granulite facies mineral assemblages, as do the gneisses, but unlike the gneisses, the metagabbro is not pervasively deformed.

1.1 Return to car. Leaving motel parking lot, turn left on Rt. 9N.
1.3 Turn left at light and proceed north on Rt. 9. Stay in left lane.
1.7 At 2nd light, turn left onto Prospect Mt. Highway.
2.5 Toll Booth ($5.00/car).
4.1 Overlook 1.
4.7 Overlook 2.
5.0 Park at Overlook 3 and take a moment to enjoy the view of Lake George, which lies in an Ordovician-aged graben.

STOP 2. METAGABBRO "FINGERS". Lat 43° 25.995′ N Lon 73° 43.869′ W (20 MINUTES)

Carefully cross the road to the outcrop which places you in the vicinity of the two "fingers" labeled 1 and 2 in Fig. 2. You will be able to trace out several faces and contacts of these intrusions, showing that these are more planar in shape than the intrusion at the Stop 1. Notice that they are very fine-grained. This is likely because they chilled uniformly due to their thinness. But like the Stop 1 intrusion, the contacts here are very sharp. Close inspection shows truncated foliation.

Two more fingers occur to the left (SE). The second of these, 4 on Fig. 2, is indicated by a rounded shape with dashed lines because its contacts are vague. Take a look at this one and see what you make of its contacts.

Why do we call these intrusions "fingers"? Because they occur in proximity, the assumption is that they are finger-like protrusions of a larger (hand-like) intrusive body, that worked their way into an array of fractures in brittle-regime host rock.

Contacts and faces of the fingers can be seen on top of the outcrop as well.

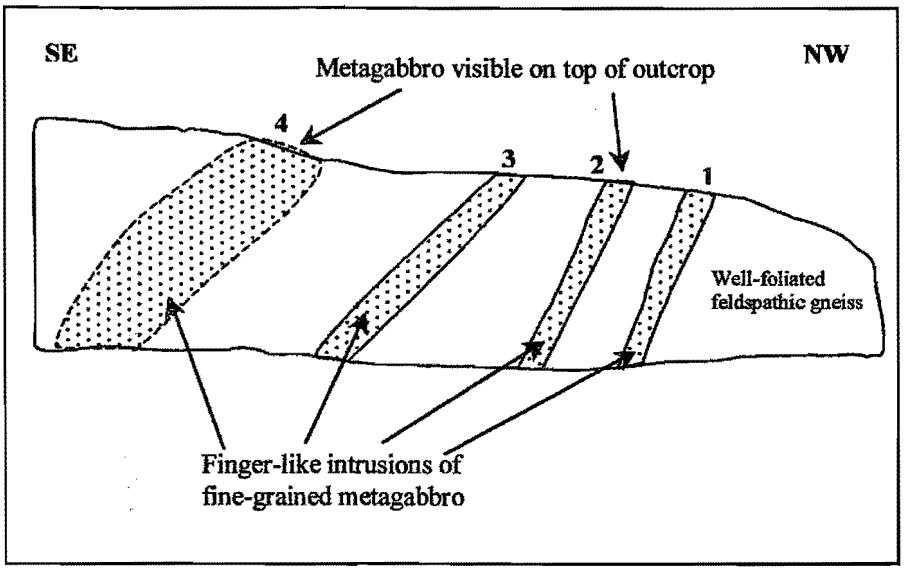

Fig.3. Stop 2. Metagabbro "Fingers" on Prospect Mt. Diagram of location and orientation of metagabbro "fingers" in gneiss host rock (not to scale).

5.0 Leave parking area and bear right, continuing up Prospect Mt. Highway.
7.2 Highway ends in large parking area just below the summit.

STOP 3. SUMMIT OF PROSPECT MT. Lat 43° 25.487′ N Lon 73° 44.789′ W (40 MINUTES)

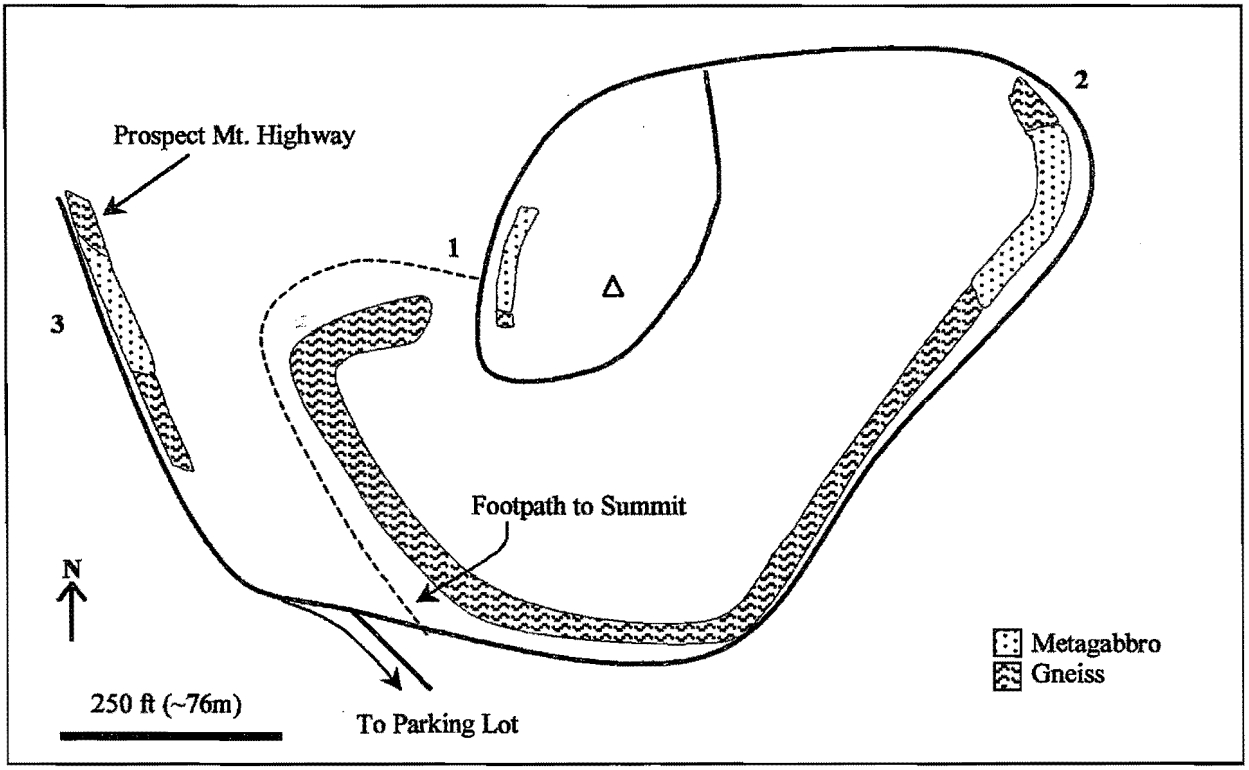

Fig.4. Stop 3. Sketch map of outcrops on top of Prospect Mt.

Walk north and find footpath to summit. The outcrops here are gneiss, largely lichen-covered. A flight of steps near the summit brings the footpath to an end at the summit roadway. (Fig. 4). Cross the road and head for the top. Then backtrack NW to the outcrop next to the roadway (1 on Fig.4). At the S end of the outcrop, reddish-weathered metagabbro is cut by a pegmatite dike. To the right of this, there is a block of metagabbro that looks at first to be detached. A closer look shows that this block is still in place and is underlain by gneiss. The contact strikes 350° and dips 40° N. Like the fingers seen at the previous stop, this exposure of metagabbro appears to be mostly fine-grained. There is no contact visible at the N end of the outcrop.

Continue around the roadway to the NE. Where it begins to loop back toward the SE, there is a large roadcut on the right (W) side of the roadway (2 on sketch map). About 150 ft. (~50 m) into a mass of quartzo-feldspathic gneiss, a contact zone with fine-grained metagabbro is seen. Here there is no sharp contact, but rather a zone in which small blocks of gneiss appear as inclusions in the metagabbro, and vice versa. This intrusion shows coarsening away from the contact. Pegmatite intrusions can be seen with retrograde biotite in the adjacent metagabbro. The S contact of metagabbro and gneiss is a rounded, "bullnose" structure striking 352° with a 50°E dip.

Outcrop 3, on the sketch map (Fig.4), will not be visited on this trip. It consists of a metagabbro intrusion into gneiss with sharp contacts, chilled margins, and localized shear zones within the metagabbro. Although it has not been established in the field, the three outcrops of metagabbro could be connected in the subsurface. Referring to Fig. 4, it can be seen that the intrusions share a similar orientation within the host rock.

Follow the roadway past monotonous walls of gneiss to the parking lot.

7.2 Leave parking area and proceed down Prospect Mt. Highway.
9.9 Overlook 1.
12.5 Jct. Prospect Mt. Highway and Rt.9. Turn right on Rt. 9.
13.0 Turn right at light.
13.1 Turn right onto northbound ramp of I-87.
15.0 Pass Exit 22.
17.5 Pass large pegmatite that intrudes metadiabase. DO NOT STOP.
17.6 Contact of metadiabase and gneiss (covered).
19.2 Bear right for Exit 23.
19.3-19.4 Just past the end of the guardrails on the exit ramp, pull over and park WELL OFF THE SHOULDER. Using EXTREME CAUTION, walk back to the roadcut, walking on the OUTSIDE of the guardrail.

STOP 4. I-87N EXIT 23 ROADCUT. Lat 43° 28.965′ N Lon 73° 45.280′ W (20 MINUTES)

Begin at the N end of this large (~250 m) body of metagabbro. The N contact with the host rock is not exposed. The first 100 ft. (~30 m) shows fine-grained metagabbros enclosed in more coarse-grained rock, suggesting the coarser rock was back-intruded by the finer-grained rock. At about 100 ft. (30 m), the metagabbro is well-foliated for about 30 ft. (10 m). Then a complex zone is seen, in which a 1.5 ft. (0.5 m) -wide pegmatite intruded a 10-ft. (3-m) shear zone in the metagabbro. The zone has also been disrupted by a fault. The shear zone strikes 66°and dips 70° W and has a left lateral shear sense.

Continuing along the outcrop, many pegmatite intrusions of varying sizes are seen. The metagabbro displays subophitic texture and is quite coarse grained. At about 350 ft. (105 m), another shear zone occurs, about 3 ft. (1 m) wide, showing left lateral shear sense. Several more smaller shear zones are seen.

The metagabbro begins fining as the contact with Grenville metasedimentary rocks is approached. The contact is sharp. Look closely at the metasediments. They are strongly foliated, having been isoclinally folded. Metamorphic minerals in these rocks include phlogopite, diopside and garnet.

Return to vehicles, being careful to remain outside of the guardrail.

19.4 Proceed to end of ramp and turn left.

19.7 Turn left (S) onto ramp to I-87 southbound.
25.8 At Exit 21 leave I-87.
26.1 Turn left at end of ramp.
26.5 Turn right at light, proceeding south on Rt 9.
29.0 Turn left (E) at light onto Rt. 149.
32.1 Jct. with Bay Rd. Continue east on Rt. 149.
33.5 Jct. with Rt. 9L. Continue east on Rt. 149.
35.0 Turn right (N) onto Buttermilk Falls Rd.
38.1 Buttermilk Falls Rd. ends; continue north on Sly Pond Rd.
41.4 Parking area on left (guidebooks refer to this as the Lower Hogtown Parking Lot, but there is no sign).

STOP 5. TRAIL TO INMAN POND. Lat 43° 29.339′ N Lon 73° 34.237′ W (60 MINUTES)
Bring your lunch along.

The trail enters the woods from the parking lot and follows a stream on the right (N). Bedrock in the trail is quartzo-feldspathic gneiss, with occasional float (loose) blocks of metagabbro and marble/calc-silicate rock. At a little over a half mile (0.8 km) there is a faint trail on the right (N) that leads to the outcrops. For now, pass that by and continue W toward the pond. At 0.7 mile (1.2 km) a clear trail to the right leads to the north shore of Inman Pond. At 1 mile (1.6 km), there is a stone fire ring in a grove near the water. Lunch!

Return to the first side trail, now on the left (N) and turn onto it. Proceed at a slight angle to the left of the trail and continue right up to the outcrops (1 on Fig.6). The metagabbro here is quite different than what was seen at the previous stops. It has a coarser texture, and is studded with garnet porphyroblasts in the 3-cm range, that have amphibole rims. Look for a block that displays perpendicular faces. The garnet porphyroblasts appear fairly equant on one face of outcrop, but on the perpendicular face they are strongly elongated, with felsic pressure shadows.

A half foot (15 cm) -wide felsic layer is seen within the garnet-bearing metagabbro. It is presumed to have come from the nearby gneiss, perhaps by partial melting of the gneiss during metamorphism. Proceed to the E, noting the change in outcrop to gneiss, and continuing until the faint side trail is encountered. Turn left (N) on the trail. Outcrop 2 (Fig.6) is on the right side of the trail about 100 feet (30 m) ahead, depending on where the trail is picked up.

This outcrop displays a contact zone between metagabbro and gneiss. While there are remnants of the sharp contacts formed when the metagabbro intruded, they are severely disrupted and in some places foliation is continuous across both lithologies. A lens-shaped body of metagabbro is seen, as well as small areas of interfingering between the two rock types. There can be no doubt that this metagabbro was deformed along with the gneiss, and must have been emplaced prior to the peak of dynamic metamorphism.

From Outcrop 2, proceed southeast to outcrop 3, crossing a small ravine and scrambling up a small hill. Continue to the SE edge of the hill, where outcrops will be more numerous. Climb down a bit to find a 10 ft (3 m) -high ledge of interlayered marble, gneiss and strongly foliated metagabbro. The bottom layer is marble with small pods of coarse-grained metagabbro. Above that is a layer of gneiss, with an area of mylonitic fabric near the face of the outcrop. Another layer of gneiss is above that, but this layer has a pronounced oblique fabric that is truncated by yet another layer of horizontally layerd gneiss. This is capped by marble that contains inclusions of folded gneiss.

While a fascinating outcrop in its own right, the relevance to the metagabbro question is that here the metagabbro has been severely dismembered, included in marble and incorporated into a mylonite. Very different from what was seen at the first 4 Stops of this trip.

From here, proceed down the slope to the S and the trail will be encountered in about 300 ft (100 m). Turn left (E) onto the trail and return to the parking lot.

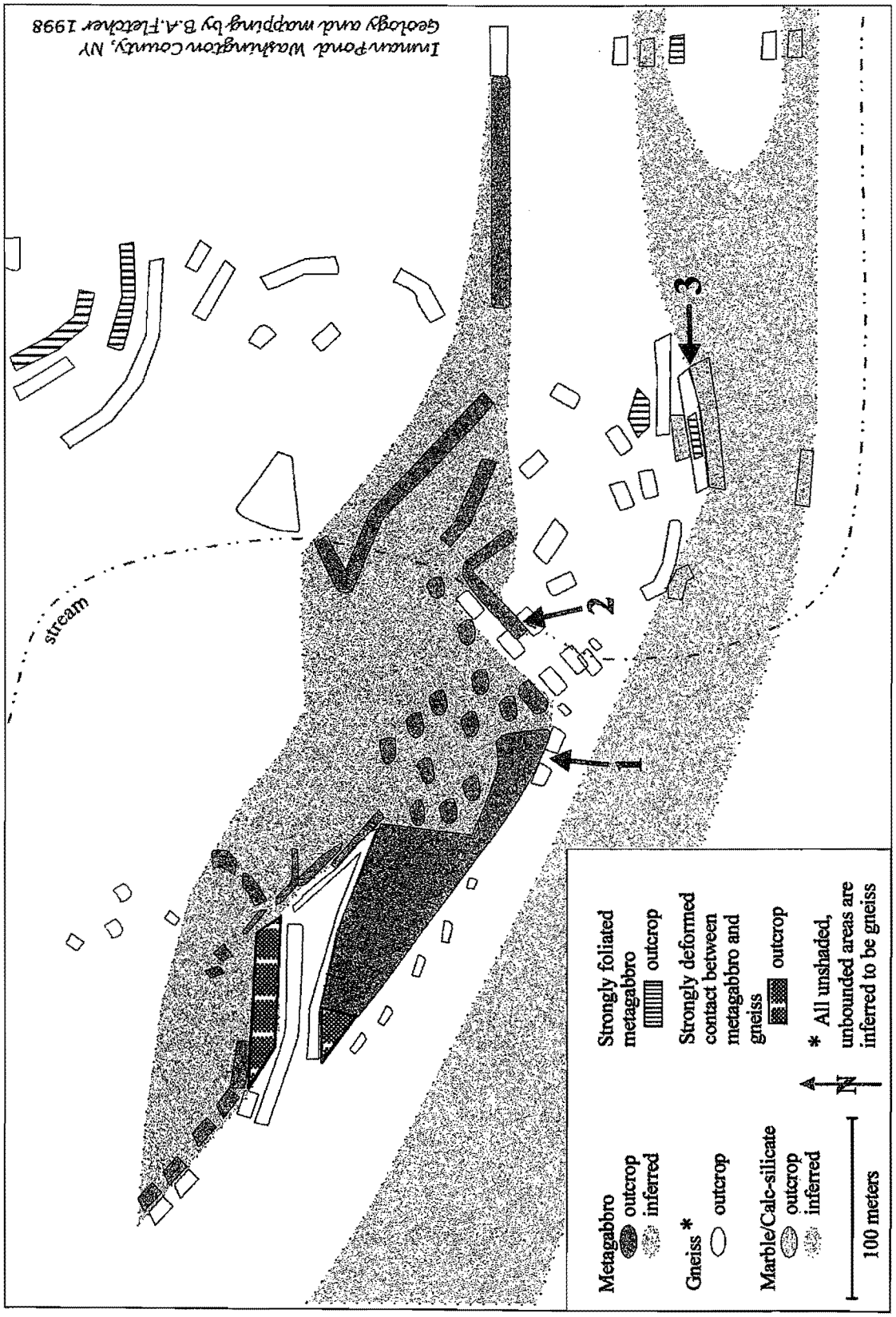

Fig. 6 Stop 5. Outcrops east of Inman Pond. Simplified geologic map showing syn-kinematic intrusion of metagabbro that was strongly deformed along with the host rocks. Numbered arrows refer to outcrops in the text.

41.4 Leaving parking area, turn right (south) on Sly Pond Rd.
44.6 Bear right onto Buttermilk Falls Rd.
47.7 Turn left (east) onto Rt. 149.
53.4 Turn left (north) at light onto Rt. 4 in village of Fort Ann.
57.2 Jct. Rt. 22
57.6-57.7 Roadcut on right. Carefully pull onto shoulder.

STOP 6. METAGABBRO BOUDINS. Lat 43° 27.544′ N Lon 73° 26.670′ W (10 MINUTES)

This spectacular roadcut provides another example of gabbros that were fully involved in the deformation event that produced the Adirondack gneisses, i.e., that were intruded syn-kinematically. On the east side of the road, two large pods of metagabbro are seen. They are continuous with those seen on the left (W) side of the highway. The formation of boudins is the result of competency contrast during deformation, usually folding of a more competent layer surrounded by a less competent layer. The competent layer deforms more brittlely than the less competent layer. However the stretched out tails of the metagabbro layers show that they deformed ductilely as strain continued after boudinage.

57.6-57.7 Return to car. Continue north on Rt. 4.
63.3 Sign for village of Whitehall.
63.9 Jct. Rts. 4 and 22. Proceed north on Rt.22.
66.4 Cross bridge over Lake Champlain.
74.3 Pass road to Dresden Station on right.
74.8 Pass road from Dresden Sta. on right.
75.0 Turn right onto Belden Rd.
75.1 Park on Belden Rd. immediately behind outcrop.

STOP 7. DRESDEN STATION METAGABBRO Lat 43° 40.734′ N Lon 73° 24.655′ W (30 MINUTES)

Walk S on Belden Rd. and turn left (E) onto Rt. 22. BE VERY CAUTIOUS. Traffic moves swiftly and the curves in both directions limit the sight distance. Proceed about 300 ft (100 m) and find a sharp contact between metagabbro and gneiss. Here the gneiss is a khondalite, a name given to aluminous gneisses of sedimentary origin. This one contains purplish garnets, some of which are truncated by the metagabbro. Once again, there are small areas of ductile shear in the metagabbro.

The metagabbro continues across the road, but is harder to trace because the contact between gneiss and metagabbro is subparallel to the face of the roadcut, and the metagabbro is thin or absent in some places. However, on top of the W end of the outcrop the intrusion and its contact are clearly seen.

75.1 Return to car. Turn around and drive back to intersection of Belden Rd. and Rt. 22.
75.2 Turn left (south) on Rt. 22.
83.8 Cross Champlain Bridge.
86.3 Jct. Rts 4 and 22 in Whitehall. Proceed south on Rt. 4.
96.8 Turn right (west) on Rt. 149 in Fort Ann.
111 Jct. of Rts. 149 and 9 in Lake George.

To I-87 North:
Turn right (N) on Rt. 9
Turn left at first light onto Rt. 9L.
Turn right onto ramp for I-87N.

To I-87 South:
Turn left (S) on Rt. 9
After passing through shopping district, turn right at light (Montcalm Restaurant is on corner).
Turn left onto ramp for I-87S.

GEOLOGY OF THE MOUNT INDEPENDENCE STATE HISTORIC SITE, ORWELL, VERMONT

Helen N. Mango, Department of Natural Sciences, Castleton State College, Castleton, VT 05735

INTRODUCTION

History

(The following history is condensed from the Mount Independence information brochure.) Mount Independence is a Revolutionary War site. A fort was built here to guard against British attack from Canada because Fort Ticonderoga, across Lake Champlain, offered a poor view to the north. Lake Champlain narrows considerably between Mount Independence in Vermont and Mount Defiance in New York, and it was assumed that whoever controlled the lake here would have a natural advantage over the opposition.

American troops began clearing land on Mount Independence in June of 1776. By autumn, three brigades (12,000 men) had established camps, and had built two batteries and a picket fort. The combined strength of Mount Independence and Fort Ticonderoga caused the British to retreat quickly to Canada in October, 1776. Many American soldiers went home that winter, reducing the force at Mount Independence to 2,500. Many of those remaining fell ill, and a number froze to death during the winter. Not many replacements reached the camp in the spring, so when British troops staged an attack in July, 1777, the Americans had to evacuate Mount Independence. British and German troops remained there until learning of the British surrender at Saratoga in October, 1777. They retreated back to Canada, burning the structures on Mount Independence as they left.

Mount Independence is a National Historic Landmark, containing the remains of batteries, blockhouses, barracks, a hospital, and other historic features. Archaeological work continues and the trails are being modified and improved to incorporate more of the historical significance and natural beauty of the site. (Note: this trail improvement may mean that, in the future, some stops in this field guide may no longer correspond to described trail markers.)

Geologic Setting

The rock formations found at Mount Independence are typical of Cambrian and Ordovician sedimentary deposition on the passive margin that developed on the east coast of ancient North America (Laurentia). The following description of the geologic history and geologic setting of Mount Independence is taken from various sources, including Fisher, 1984; Rankin, et al., 1989; Thompson, 1990; Selleck, 1997; and Isachsen et al., 2000.

Beginning in the Late Proterozoic, rifting of a supercontinent began, leading to the formation of the Iapetus Ocean (forerunner of the present-day Atlantic Ocean) with Laurentia as the landmass to the west. Approximately 600 m.y. ago, sediment, at first of continental origin, began to accumulate on the eastern margin of Laurentia. As rifting continued, sedimentation on the developing passive margin became of shoreline and shallow marine affinity. The earliest of these sedimentary units occurring in western Vermont (Dalton, Cheshire, Dunham, Monkton, and Winooski Formations) are not found at Mount

Independence; here, the oldest unit is the medial Late Cambrian Potsdam Formation, a quartz sandstone which unconformably overlies the Proterozoic metamorphic rocks of the Adirondack massif just to the west. (An excellent exposure of this unconformity is described in Selleck, 1997). Overlying the Potsdam Formation is the Late Cambrian Ticonderoga Formation, a sandy dolomite which marks the transition from a shoreline to more of a shallow marine environment. Overlying the Ticonderoga Formation is the Late Cambrian/Early Ordovician Whitehall Formation, which is mostly a massive dolomite, and then the cross-bedded sandstone at the base of the Early Ordovician Great Meadows Formation. The Whitehall and Great Meadows Formations belong to the Beekmantown Group. All formations dip gently to the north, at angles of between 4 and 10°, averaging 6 or 7°.

To the east of Mount Independence are numerous exposures of dolomites, limestones and shales of the overlying Chazy, Black River and Trenton Groups. The thick sequence of Cambrian and Early Ordovician clastic and carbonate rocks indicates that water depth throughout this time was quite consistent. Water depth did not increase substantially until the Middle Ordovician, when this deepening water heralded the onset of the Taconic Orogeny.

Mount Independence is offset from rocks immediately to the east by a high-angle normal fault, which brings the Cambrian Ticonderoga Formation in contact with the Early and Middle Ordovician Providence Island and Middlebury Formations. While there is no outcrop for at least a mile to the east of this high-angle fault, there is no doubt that the rocks to the east are indeed younger than the rocks of Mount Independence. The age of this high-angle fault is debatable; pre-Silurian movement is likely, although there may have been re-activation of the faults in the Mesozoic related to rifting that produced the present-day Atlantic Ocean.

STRATIGRAPHY

The rock formations found at Mount Independence have been given a variety of names and descriptions, depending on the focus of the worker. As Rankin et al. (1989) state (in discussion of the sedimentary evolution of the passive margin), "usage of the many local formation names has hindered understanding of regional patterns" (p. 42). The formations of Mount Independence were first described by Brainerd and Seely (1890) for the central Champlain Valley of Vermont; these descriptions have been expanded upon and modified by many other researchers working in the general region, including Cady (1945), Welby (1961), and Fisher (1984).

In 1890, Ezra Brainerd and H. M. Seely of Middlebury College published "The Calciferous Formation in the Champlain Valley" (Brainerd and Seely, 1890). They used the term "Calciferous" to describe the rocks found stratigraphically between the Potsdam Sandstone and the limestones of the Chazy Group. They divided the Calciferous into five "Divisions"; Divisions A and B and the lowermost member of Division C are found on Mount Independence. Their descriptions are as follows (p. 2):

> Division A: Dark iron-grey magnesian limestone, usually in beds one or two feet in thickness, more or less silicious, in some beds even approaching a sandstone. Nodules of white quartz are frequently seen in the upper layers, and near the top large irregular masses of impure black chert, which, when the calcareous matter is dissolved out by long exposure, often appears fibrous or scoriaceous. Thickness.....310 ft.

> Division B: Dove-colored limestone, intermingled with light grey dolomite, in massive beds; sometimes for a thickness of twelve or fifteen feet no planes of stratification are discernible. In the lower beds, and in those just above the middle, the dolomite predominates; the middle and upper beds are nearly pure limestone; other beds show on their weathered surfaces, raised reticulating lines of grey dolomite. Thickness..... ....295 ft.
>
> Division C, unit 1: Grey, thin-bedded, fine-grained, calciferous sandstone, on the edges often weathering in fine lines, forty or fifty to the inch, and resembling close-grained wood. Weathered fragments are frequently riddled with small holes, called *Scolithus minutus* by Mr. Wing.....60 ft.

They describe the geology of Mount Independence as follows (p. 10):

> In the northwest corner of Orwell...is a hill known as Mount Independence. It rises nearly 200 feet above Lake Champlain, and is about a mile in length, the top along the north half being a smooth plane sloping gently to the north....The promontory on which [Fort Ticonderoga] was built is but a continuation of Mount Independence, after an interval of eighty-eight rods of water, and extends for over a mile further northwest.
>
> This whole tract of historic ground consists of Calciferous strata over 1300 feet in thickness, dipping north at an angle of 6°, and overlying 170 feet of Potsdam sandstone....The plateau on the north end of Mount Independence is the top of Division B, the thin-bedded sandstone at the base of Division C having been removed by glacial action, not only here, but farther north, where is now the channel of the lake. The upper layers of B are largely quarried and used for flux in the iron-furnaces....Along the east side of Mount Independence...are marked indications of a downthrow of the strata on the east.

The mapping done by Brainerd and Seely (1890) at Mount Independence is largely correct. The only changes to be made are that (1) Division B is mostly dolomitic (this is an example of the spatial variations seen in many units in the region), (2) there is a fault at the southern end of the peninsula, and (3) the base of Division C *does* occur on Mount Independence.

More recent workers have been more specific, of course, about naming formations for type localities, but this has meant that lateral variations in rock type has meant lateral variations in formation names as well. Because Mount Independence has more in common, geologically speaking, with eastern New York State rather than with the rest of Vermont, the New York stratigraphy will be used here. As a general rule, lithologies found to the west of the Champlain Thrust will be named after their New York counterparts. Comparisons with time-equivalent formations to the east of the Champlain Thrust will be given with individual formation descriptions. Table 1 on the next page gives the correlation between formation names.

The following lithologic descriptions are based on field observations for this study. More complete descriptions of these units in their various other occurrences are found in Cady (1945), Welby (1961), Fisher and Mazzullo (1976), Fisher (1984), Washington and Chisick (1988), and Selleck (1997).

New York – Champlain Valley	Vermont – Middlebury Synclinorium	Brainerd and Seely (1890)
Great Meadows	Cutting	lowest strata of Division C
Whitehall	Shelburne	Division B
Ticonderoga	Clarendon Springs	Division A
Potsdam	Danby	Potsdam

Table 1. New York and Vermont stratigraphic equivalents and corresponding units from Brainerd and Seely (1890).

Several samples of the Ticonderoga and Whitehall Formations were analyzed for their clastic quartz content by determining the insoluble residue remaining after the samples were crushed and dissolved in 3 M HCl. After all reaction had ceased, the residue was filtered, washed and dried. The weight percentage of insoluble residue was then calculated.

Potsdam Formation

The upper portion of the Potsdam Formation occurs at Mount Independence. It is dominantly a pink, tan and gray quartz-cemented quartz sandstone with some thin shaly layers. Sand grains are smooth and rounded and range from fine to coarse size; some show evidence of transport by wind. Fresh surfaces display a vitreous luster. The unit is mostly medium bedded (approximately 0.5 m thick). Some beds contain abundant worm burrows. Layers of pure quartz sandstone weather smooth, while those with variable grain size and bioturbation weather to a rough, moth-eaten texture. Cross-bedding is prominent is some layers, and shows up particularly well on weathered surfaces.

The composition and sedimentary structures suggest that this portion of the Potsdam Formation was deposited in a shoreline environment, where both wind and wave action could take place. The thin shaly layers could represent mudflats. Minor fluctuations in sea level could produce sometimes more sub-aereal, sometimes more sub-aqueous conditions.

The equivalent formation in the Middlebury synclinorium and northwestern Vermont is the Danby Formation, described by Cady (1945) and Mehrtens (1985) as interbedded sandstone and dolomite, representing intertidal to platform edge sedimentation. The Potsdam Formation differs from the Danby Formation in that its depositional environment appears to be limited to intertidal and subtidal zones.

The contact between the Potsdam and Ticonderoga Formations has been described as gradational (e.g. Selleck, 1997), with an increase in carbonate and decrease in quartz marking the transition. At Mount Independence the contact appears to be an erosional surface, with a coarse-grained dolomitic layer lying on top of a wavy surface with truncated cross-beds.

Ticonderoga Formation

The Ticonderoga Formation is a light- to medium-gray, siliceous dolostone. Bedding ranges from medium to fairly massive. It is the thinner beds that are used, in part, to differentiate this unit from the overlying Whitehall Formation. Texture varies from finely to coarsely crystalline, and many layers contain rounded and often frosted quartz sand and more angular quartz silt. Some beds are more correctly

described as dolomitic sandstone, containing over 50% insoluble residue. Terminated quartz crystals in vugs and coarse-grained white calcite knots are characteristic of some layers. On a fresh surface luster is subvitreous, and the quartz sand grains protrude as smooth, rounded and opaque-looking beads. Dark gray and blue-black chert occurs in patches and thin, discontinuous layers. Weathered surfaces are various shades of gray, and sometimes have a pitted appearance; the chert weathers out in high relief.

The likely sedimentary environment of deposition was a shallow ocean bottom with considerable current activity (Welby, 1961). A near-shore environment is required because of the abundance of rounded quartz sand grains. The frosted surface of many quartz grains suggested they were windblown into the shallow ocean.

The equivalent formation farther east, the Clarendon Springs Formation, is described by Cady (1945) as a uniform gray dolomite with "numerous geodes and knots of white quartz" (p. 536), with some sandy beds and patches of chert. Therefore, there is great similarity between the Clarendon Springs and Ticonderoga Formations, but, as suggested by Welby (1961), it is more consistent to use the name Ticonderoga Formation for rocks west of the Champlain Thrust.

The contact between the Ticonderoga Formation and the Whitehall Formation is not easy to find. Welby (1961) suggests a gradational contact between the two, and acknowledges that the contact can be difficult to discern. At Mount Independence, the contact is placed just below the limestone beds that are described in the next section.

Whitehall Formation

At Mount Independence, the lowermost section of the Whitehall Formation contains a small interval of light- to medium-gray limestone or calcic dolostone, which weathers white and contains large, rounded, frosted quartz grains, patches of dark blue-gray chert, rounded chert pebbles, and (especially visible on weathered surfaces), what appear to be stromatolites. The matrix is occasionally earthy-looking. Outcrops are often covered by thick moss. This limestone layer probably corresponds to the Warner Hill Limestone Member as described in Fisher (1984). Welby (1961) also discusses at length the nature of the lowermost unit of this formation. At Mount Independence it appears to be about 3 – 5 m thick.

The rest of the Whitehall Formation at Mount Independence is a thick- to massive-bedded dolostone, the Skene Dolostone Member (as described by Fisher, 1984). It is medium- to dark-gray, sometimes mottled or laminated in light and dark shades, and fine- to medium-grained. It weathers various shades of gray. Black chert occurs as nodules and layers. Rounded quartz sand grains are quite common, and a few layers approach being a dolomitic sandstone. The fine-grained, darker-colored layers have a vitreous luster on a fresh surface, and the fresh break has a slightly fetid odor, perhaps the same as described by Welby (1961) as indicative of certain layers of the Whitehall Formation (although he describes the odor as "strongly fetid" (p. 45)). Within the massive layers, bedding is indicated by laminations, but it is very difficult to get reliable structural measurements of the attitude of bedding.

The percentage of insoluble residue ranges from less than 7% to greater than 55%, with an average of about 10%. Some of this material is rounded quartz sand grains and some is angular quartz silt. Welby (1961) suggests that it is the quartz silt that gives many layers of this formation a vitreous luster.

The equivalent lithology to the east is the Shelburne Marble, which is described by Cady (1945) and is a significantly different rock type. Therefore, the use of the name Whitehall Formation is appropriate, as suggested by Welby (1961).

Great Meadows Formation

Only the basal unit of the Great Meadows Formation is found at Mount Independence. This unit, the Winchell Creek Member, is described by Fisher (1984) as a medium-bedded, cross-bedded, calcareous siltstone. This is the lithology described as resembling "close-grained wood" by Brainerd and Seely (1890). At Mount Independence, even though its exposure is quite limited, the Great Meadows Formation is recognized by a distinctive cross-bedded, fine-grained sandstone with a slightly dolomitic matrix, and also by a sedimentary breccia consisting of fragments of cross-bedded material several centimeters long jumbled about in a dolomitic matrix.

The equivalent unit east of the Champlain Thrust is the Cutting Formation, whose type locality at Cutting Hill in East Shoreham is only about ten miles from Mount Independence. The basal unit is called the C-1 member by Welby (1961) in deference to Brainerd and Seely's (1890) letter designations, and is described by Welby (1961) as follows: "...the most characteristic single feature of the member is the breccia at the base; another striking feature is the cross-bedding associated with the sandstones at the base...." (pp. 53-54). This description is identical to what is found at Mount Independence, but for consistency the name Great Meadows Formation is used here.

ACKNOWLEDGMENTS

This work was funded in part by grants from the Lake Champlain Basin Program and the Vermont Geological Survey. My thanks to Elsa Gilbertson, Regional Historic Site Administrator for the Vermont Division for Historic Preservation, for her support, and to Tim Grover of Castleton State College for his geological expertise and technical know-how.

ROAD LOG

Mount Independence is located in Orwell, Vermont, five miles west of the intersection of Vermont Routes 22A and 73. From that intersection, go west on Rt. 73 (toward Lake Champlain and away from the village of Orwell). In about 0.3 miles, Rt. 73 curves to the right (north); bear left on the road to Mount Independence (there's a sign). Continue to the end of this road. Just after the road turns to dirt, there is a fork in the road. Bear left, up a steep little hairpin turn. The parking lot for the Mount Independence State Historic Site is on the south side of the road (on your left) and the museum is on the north side (it's the building that looks like a boat). Park in the parking lot.

Note: 1.8 miles after the intersection of Rts. 22A and 73, as you head toward Mount Independence, you will go down a short, fairly steep descent. This marks the Champlain Thrust, one of the largest structural features of western Vermont.

Note: Bring a lunch and something to drink. There is nowhere to purchase supplies closer than the village of Orwell, which is six miles away.

This tour is done entirely on foot, and follows the colored and numbered trails of the State Historic Site (make sure you get a trail guide brochure). Therefore, instead of mileage notations, trail numbers and stop location descriptions will be given in this guide. Approximate compass directions will be given for orientation purposes. The trip will take three or four hours, and includes a fairly leisurely 3.5 mile walk and a little scrambling up talus slopes and through the trees.

Warning: Mount Independence is well endowed with poison ivy! Be vigilant!

Warning: Mount Independence is a State Historic Site. To the untrained eye, many of the historically important building remains bear a striking resemblance to scattered outcrops. Please make sure you know what rocks you're looking at before you start examining them too closely!

Start of trip

On the southern side of the parking lot is a signpost. This is where the field trip begins. Field trip stops are shown on Figure 9, which also shows the geology of Mount Independence.

From the signpost, follow the Southern Defense Trail to the east (left). Walk across the grassy area to the stairs. At the base of the stairs is an outcrop of Ticonderoga Formation, showing one of the more massive layers of this unit. We'll see more of the Ticonderoga at a later stop. Continue along the path to a solitary step, about 5 m before a signpost at a junction in the trail.

The flat area around the signpost marks the top of the Potsdam Formation. The rubble upslope is the lowermost Ticonderoga Formation. Continue along the path, and go left at the junction (downhill). From here there is a beautiful view south down the southern end of Lake Champlain. Continue downhill along the path, and go down first a set of three steps, then a set of six steps.

STOP 1. POTSDAM FORMATION. This "stop" begins here and continues down to the water. Typical upper Potsdam sandstone is displayed in the numerous outcrops along this trail. It is in general a pinkish, tan, and gray quartz-cemented quartz sandstone. Fisher (1984) terms this upper arenitic unit the Keeseville Member.

Figure 1 is a photomicrograph of a representative sample, showing the well-sorted, well-rounded nature of the quartz grains. Many of the grains are laced with fluid inclusions; the salinity and temperature of homogenization of the fluid inclusions may help suggest the source rock of the quartz sand.

As the trail descends to the Carillon dock at the water's edge, various features of the Potsdam Formation are visible both in outcrop and in the steps, including grain size differences, shaly layers, worm burrows and cross-bedding. Some of these features cause the rock to weather with a moth-eaten appearance. In other beds, pure quartz-cemented quartz sandstone has the appearance of a quartzite. These various characteristics of the Potsdam Formation suggest an established, mostly intertidal sedimentary

Figure 1. Photomicrograph of Potsdam Formation. Crossed polars. The quartz sand grains are well rounded, and show numerous fluid inclusions. In most cases, the quartz cement is optically continuous.

environment of deposition, with current action producing the cross-bedding, mudflats forming the thin shaly layers, and bioturbation by near-shore/beach-dwelling organisms.

After completing Stop 1, return to the trip starting point, walk down to the road, and then follow the road to the east (in the direction of Orwell) to the hairpin curve. The outcrop in the inside of the curve is the next stop.

STOP 2. TICONDEROGA FORMATION. This outcrop is approximately on strike with the Ticonderoga Formation seen at the base of the first staircase on the Southern Defense Trail. The outcrop displays most of the main features of this formation. It is a light- to medium-gray siliceous dolostone, weathering various shades of gray. It contains rounded quartz grains and scattered knots of white calcite and quartz. Some terminated quartz crystals are also present.

Figure 2 is a photomicrograph of a sample of Ticonderoga Formation taken from one of the lower layers. All features indicate that deposition occurred in a shallow, warm, marine environment, near a quartz sand beach. The rounded, frosted quartz sand grains are windblown from the beach into the water. The peloids (rounded dark masses 75 - 100 μm in diameter) are probably aggregates of carbonate mud (Blatt et al., 1980). The oolith (center of picture) indicates warm, carbonate-saturated water and strong, periodic bottom currents, such as those found in a tidal bar or tidal delta environment (Blatt et al., 1980).

Cross-bedding is also found elsewhere in the Ticonderoga Formation, supporting the notion of strong currents. Figure 3 shows cross-bedding in an upper unit of the Ticonderoga Formation, found on the east side of Mount Independence.

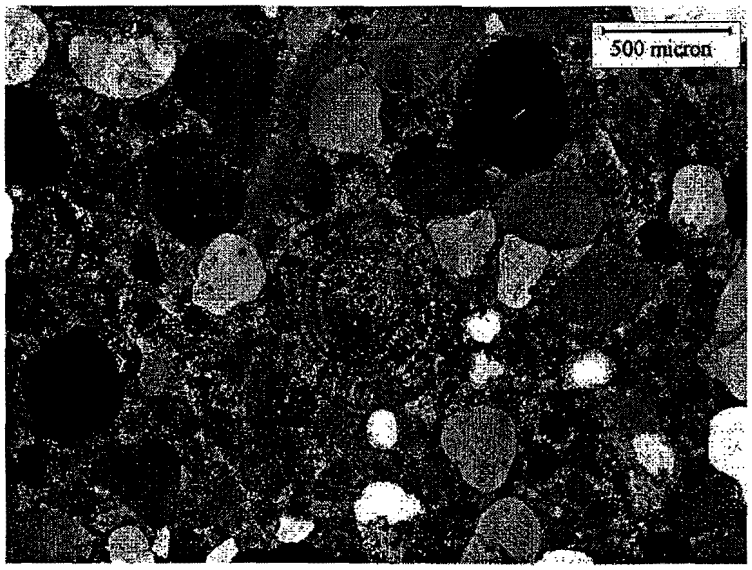

Figure 2. Photomicrograph of Ticonderoga Formation. Crossed polars. Note large, rounded quartz grains, peloids (small, rounded, dark masses), and oolith in center, showing characteristic radial structure around its core.

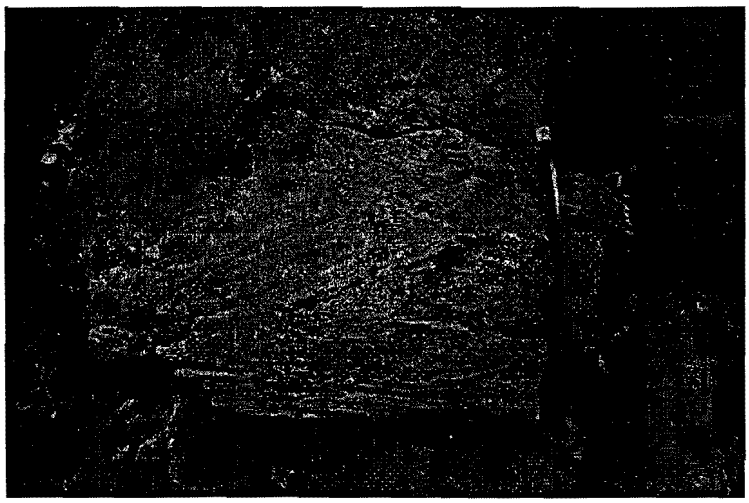

Figure 3. Cross-bedded Ticonderoga Formation, found in upper layer of unit on east side of Mount Independence.

Microscopic examination of the quartz content of the Ticonderoga Formation shows a bimodal distribution, with larger, rounded quartz sand grains and smaller, more angular quartz silt. Figure 4 is a photomicrograph of another sample taken near the one shown in Figure 2. Note the subparallel layering of

the coarser and finer particles. This bimodal size distribution may represent the interplay of wind and fluvial or storm deposition.

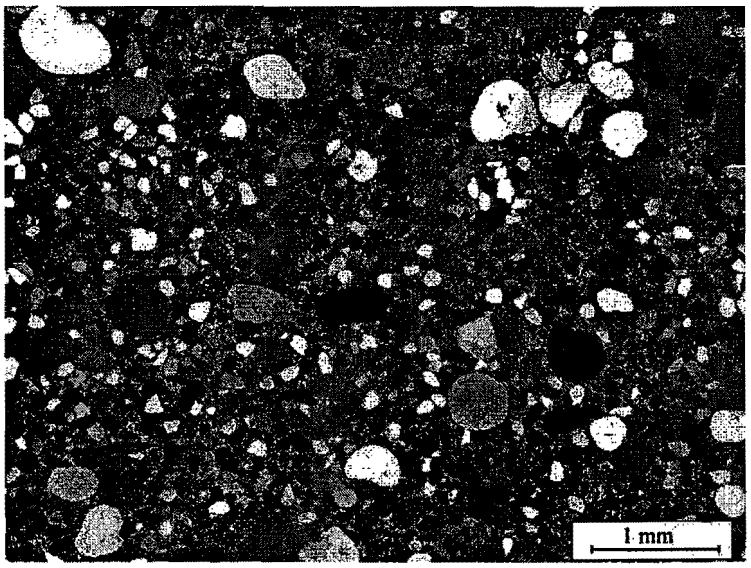

Figure 4. Bimodal distribution of quartz sediment in Ticonderoga Formation, with rounded sand grains and angular silt grains. Note subparallel arrangement of sand and silt layers (angled approximately 30° counterclockwise from horizontal in this particular view). Crossed polars.

Cross road to north and go into the woods at the end of the split rail fence. Be careful of old strands of rusty wire. Go straight uphill and slightly left (west). The outcrop here is of Potsdam Formation with some excellent cross-bedding, structurally higher than the outcrop of Ticonderoga Formation just seen at Stop 2. Therefore, there is a fault between the two outcrops.

This fault continues to the west, just south of the road leading to the marina (see geologic map, Figure 9). All along the fault, Potsdam Formation is on top of Ticonderoga Formation, although the actual fault surface is not visible anywhere. Because the trace of the fault is approximately parallel to contacts, this appears to be a dip-slip fault, either in keeping with the Ordovician "cross-faults" identified by Hayman and Kidd (2002) or the early Mesozoic faults of Stanley (1980) for other sections of the central and northern Champlain Valley of Vermont. As the road approaches the marina to the west of the entrance to the State Historic Site, the land flattens out, forming a terrace-like surface. This flat area is probably underlain by Ticonderoga Formation, although there is no outcrop between an occurrence of this unit at the water's edge and outcrops at the base of the cliff. The coincidence of this rock type (less resistant than the Potsdam Formation below and above) with the approximate level of the surface of the lake suggests that this flat area is indeed a terrace, carved into the softer rock when the lake surface was 5 or 10 m higher than present. Higher lake levels have occurred for much of the last 13,000 years, beginning with the waning of the Wisconsin stage of the last Ice Age (Hunt, 1980).

Walk back up the road to the entrance to the State Historic Site. Go left (west) of the museum and walk up the gravel path, past a low exposure of Potsdam Formation (on strike with what we just saw in the woods).

Note: The Museum and Visitor's Center is excellent and well worth a visit.

Continue up the grassy slope, following the sign to "Trails." The outcrop to the left (west) is also Potsdam Formation. After about 100 m, the trail flattens out briefly. To the right is a small marshy area containing an outcrop.

STOP 3. TICONDEROGA FORMATION. Somewhere in the last 50 m or so just traversed is the contact between the Potsdam and Ticonderoga Formations. This outcrop is therefore near the bottom of the Ticonderoga Formation. The flat surface of the outcrop is approximately equal to bedding, and contains a raised ridge of quartz sandstone. Three possibilities for the origin of this sandstone are:

1. clastic dike
2. sand filling a paleokarst solution cavity
3. sand filling a crack (either a desiccation crack or one tectonically formed)

If either (2) or (3) is correct, this implies a proximal source of sand that could wash into the cavity or crack. While the Ticonderoga Formation does contain quartz sand (as the main rock type of this very outcrop shows upon close examination), it appears to be windblown into the sediment rather than washed in by currents. For scenario (1), the source of the quartz sand would be <u>below</u> the dolomitic sediment. The proximity of the underlying Postdam sands makes this a reasonable prospect, especially if the Ticonderoga sediment was being deposited rapidly on as-yet-unconsolidated Potsdam sand, applying pressure and causing some of the sand to be squeezed upward.

Continue up the path toward the Trail Information Outpost. Approximately halfway between Stop 3 and the Information Outpost, a mown trail heads around a boulder on the right (east) and goes in a southerly direction, at a 30° angle to the trail you just walked up. This is the White Trail, but because we are walking it backwards, the trail markers are only visible if you turn around and look back.

Follow the path downhill through the woods (over ledges of Ticonderoga Formation, showing the medium-bedded nature of this unit), looking back every now and again to see the White Trail markers. The trail goes around a large curve, heading east, and large slabs of rock lie next to and across the trail. About 5 m into this rocky section, a grassy glade is visible downhill and ahead, containing White Trail Stop 3 (Southern Battery). A large, squarish slab of Potsdam formation is on the upslope side of the Trail, and contains some good cross-bedding. Straight ahead along the contour is an outcrop.

STOP 4. POTSDAM/TICONDEROGA CONTACT. This outcrop contains the contact between the Potsdam and Ticonderoga Formations. The contact is taken to be the undulating surface where gray quartz-cemented quartz sandstone (containing truncated cross-bedding) is overlain by pinkish-tan coarse-grained sandy dolostone. This suggests a period of erosion of the Potsdam sands before deposition of the dolomitic sediment; however, if the interpretation of the clastic dike at Stop 3 is correct, the Postdam sediment was not yet lithified when it underwent erosion. Figure 5 is a view of this outcrop, with the contact highlighted.

Continue along the White Trail, past White Trail Stop 2 (Foundation) and uphill over ledges of Ticonderoga Formation. Follow the White Trail to the Information Outpost, and continue west along the Red and Blue Trails. Where these trails diverge, follow the Red Trail (left) all the way to the end (Red

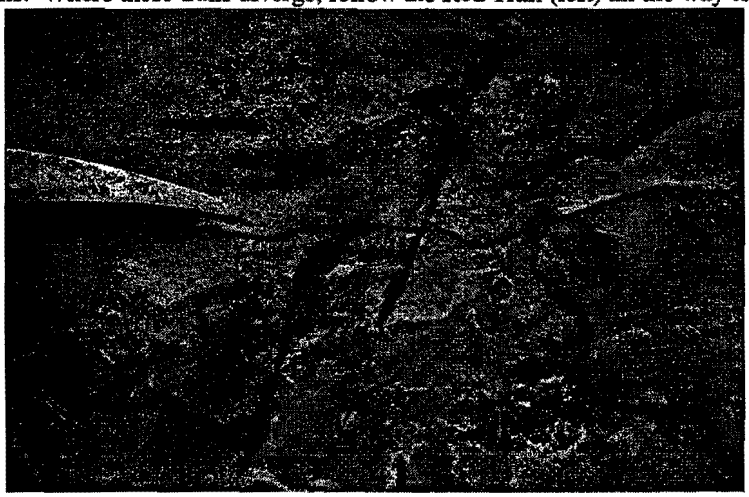

Figure 5. Potsdam/Ticonderoga contact, at level of pick point, highlighted for clarity.

Trail Stop 3). Here there is a lovely view of Mount Defiance west across Lake Champlain, and of Fort Ticonderoga to the north. The large road cuts at the base of Mount Defiance are in Proterozoic metamorphic rocks of the Adirondack massif. Therefore, the high-angle normal fault that bounds the massif on its eastern side lies somewhere under the lake. The boulder of pink granite near the bench is likely from the igneous rock of the massif, transported here by Ice Age ice sheets.

The outcrop just below the overlook is of dolostone containing chert, sandy layers/lenses and laminations. This outcrop is considered to be Whitehall Formation on the basis of the laminations and slightly fetid odor on a freshly broken surface, although the many similarities with the Ticonderoga Formation (dolomitic matrix, sand layers, chert) illustrate the difficulty in placing the contact between the two formations, especially in relatively flat areas where outcrop is discontinuous.

Take the Red Trail back to the junction with the Blue Trail. Go left (north) on the Blue Trail to the first outcrop on the left (west) side in the woods.

STOP 5. WHITEHALL FORMATION – WARNER HILL LIMESTONE MEMBER. This rock is a thick-bedded, light- to medium-gray limestone or calcic dolostone containing large, rounded, frosted quartz sand grains and having an almost conglomeratic appearance. Weathered surfaces are almost white, and contain wavy raised lines that resemble the stromatolites seen in the Warner Hill Limestone Member of the Whitehall Formation in Whitehall, New York. There are patches and pebbles of dark blue/gray chert, and occurrences of coarse calcite crystals stained yellow-orange by iron oxide.

To the east, on the other side of the Blue Trail and in the woods, are numerous discontinuous and moss-covered outcrops of limestone/calcic dolostone with iron oxide staining, occurrences of earthy-looking matrix, patches and stringers of chert, white weathering and variably fetid odor on fresh breaks.

Another feature that is taken to be indicative of the Whitehall Formation is the thick to massive bedding, which makes it very difficult to take structural measurements. (In contrast, the Ticonderoga Formation is mostly medium-bedded, with well-defined bedding planes).

Continue north and downhill along the Blue Trail. Note that the trail is stabilized by black slate that has been brought in from elsewhere. The trail flattens out as the land opens up a bit. About 50 – 100 m past the two-log bridge, there is a Blue Trail marker on a tree on the left (west) side of the trail. Directly across the trail and about 5 m into the woods is a very large boulder of almost pure black chert. Welby (1961) discusses the genesis of the chert in the dolostones, concluding that is was formed penecontemporaneously with the dolostone, and transported by currents as semi-solid masses.

The talus slope to the east at the base of the cliff contains boulders of stromatolitic limestone and "two-tone" mottled and laminated dolostone, all indicating that the cliff is made up of Whitehall Formation.

Where the Blue Trail gets closest to the water (Catfish Bay), there is a Blue Trail marker on the left (west) side of the trail. (This is about 40 m south of Blue Trail Stop 7.) Walk directly east through the trees along a vague trail that climbs up the talus slope to the base of a steep cliff.

STOP 6. WHITEHALL FORMATION – SKENE DOLOSTONE MEMBER. The outcrop is of massive dolostone with layers of chert containing nodules of dolostone, iron oxide staining on groundwater seeps, and a dark shaly layer. The dolostone is mostly medium- to dark-gray and finely crystalline, with a slightly fetid odor on a freshly broken surface. The massive bedding is characteristic of this part of the Whitehall Formation.

Continue north along the Blue Trail. Blue Trail Stop 5 (Spring) has steps made of slabs of laminated Whitehall Formation. Continue along to Blue Trail Stop 4 (Quarry). The rock here is a calcareous dolostone (it reacts weakly without scratching to dilute hydrochloric acid) suggesting it is near the top of the Whitehall Formation, as the reappearance of more calcareous layers is characteristic of the upper portions of the formation.

Continue north along the Blue Trail to its end, at a junction with the Orange Trail. Go left on the Orange Trail, toward the northernmost point of Mount Independence.

STOP 7. LUNCH. The "beach" here is a large outcrop of the fairly featureless, massive gray dolostone that typifies a large part of the Whitehall Formation. Coarse calcite is visible in some cracks. A floating bridge once connected Mount Independence and Fort Ticonderoga at this point. There is also a geological connection, because Fort Ticonderoga is in the direction of dip; the stratigraphy is continuous from this stop, under the water, and onto the other shore, as noted by Brainerd and Seely (1890).

Continue along the Orange Trail (east and south) to Orange Trail Stop 4 (Horseshoe Battery).

STOP 8. GREAT MEADOWS FORMATION – WINCHELL CREEK MEMBER. The basal unit of the Great Meadows Formation, the Winchell Creek Member, occurs all around the Horseshoe Battery in scattered outcrops on the slopes. To the north, along a now-abandoned section of the Orange Trail, are a few small outcrops of the distinct cross-bedding that exemplifies this unit (Figure 7).

Figure 7. Cross-bedding in Winchell Creek Member of Great Meadows Formation. Lens cap for scale.

Bedding orientation is difficult to ascertain, but it appears that this unit is lying conformably above the Whitehall Formation. Other outcrops contain a sedimentary breccia that is also characteristic of the lowermost Great Meadows Formation (it is described for the equivalent Cutting Formation by Welby, 1961). The fragments in the breccia are laminated and cross-laminated. Figure 8 shows an outcrop of this breccia, with two fragments outlined for clarity. The structure of both the cross-bedding and the breccia show up best on weathered surfaces, and are almost invisible on fresh breaks.

Figure 8. Breccia in Winchell Creek Member of Great Meadows Formation. Two cross-laminated fragments are outlined for clarity.

The Winchell Creek Member in its type locality is described by Fisher and Mazzullo (1976) as a cross-bedded quartzofeldspathic siltstone with thin lenses of sandstone, containing ripple marks, desiccation cracks, and trace fossils. Prolonged weathering accentuates the sedimentary structures (giving

the look of "fine grained wood" of Brainerd and Seely, 1890). Fisher and Mazzullo (1976) give a Gasconadian (Early Ordovician) age for this unit, and conclude that the sedimentary environment of deposition was low- to high-energy tidal flats. Therefore, it appears that the sedimentary environment did not vary greatly throughout the deposition of the Ticonderoga, Whitehall and basal Great Meadows Formations. Indeed, Welby (1961) and Fisher and Mazzullo (1976) conclude that this tidal-intertidal environment continued at least until deposition of the limestones of the overlying Fort Cassin Formation (Bascom equivalent).

Continue south along the Orange Trail. Stop 2 of the Orange Trail (Crane) has beautiful views of Mount Defiance and Fort Ticonderoga, as well as outcrop of upper Whitehall Formation. The rock here is a medium- to light-gray, coarsely crystalline dolostone with a slightly fetid odor on a fresh surface.

Continue south along the Orange Trail to where is bends to the east (an unused portion of the trail continues straight). Scattered about the trail are numerous moss-covered boulders and discontinuous outcrops of Winchell Creek breccia, indicating that the contact between the Whitehall and Great Meadows Formations is somewhere between the Crane and this location. Continue along the Orange Trail. At an overlook with a log bench, the outcrop is of fine-grained, vitreous, dark gray dolostone, indicating that the Whitehall/Great Meadows contact has again been crossed.

The Orange Trail continues all the way back to the Trail Information Outpost (about 15 minutes). Continue walking south to get back to the museum and parking lot.

Figure 9 is the geologic map of Mount Independence, on air photo base. The stops of this field trip are also shown in this figure. Figure 10 is a schematic cross section from south to north.

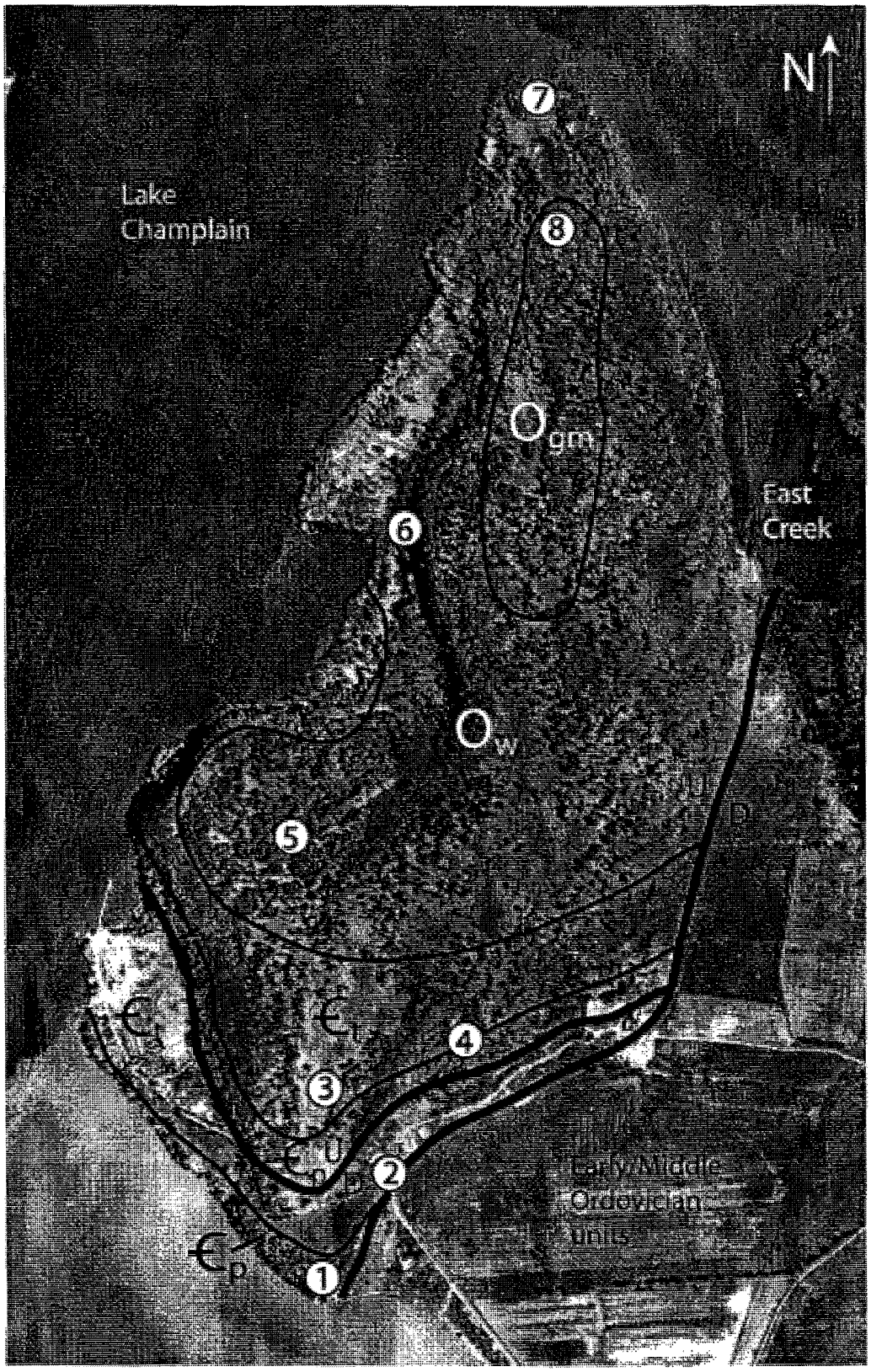

Figure 9. Geologic map of Mount Independence, showing stops of this field guide (numbered circles). Mount Independence is approximately 2 km from north to south and 1 km wide.

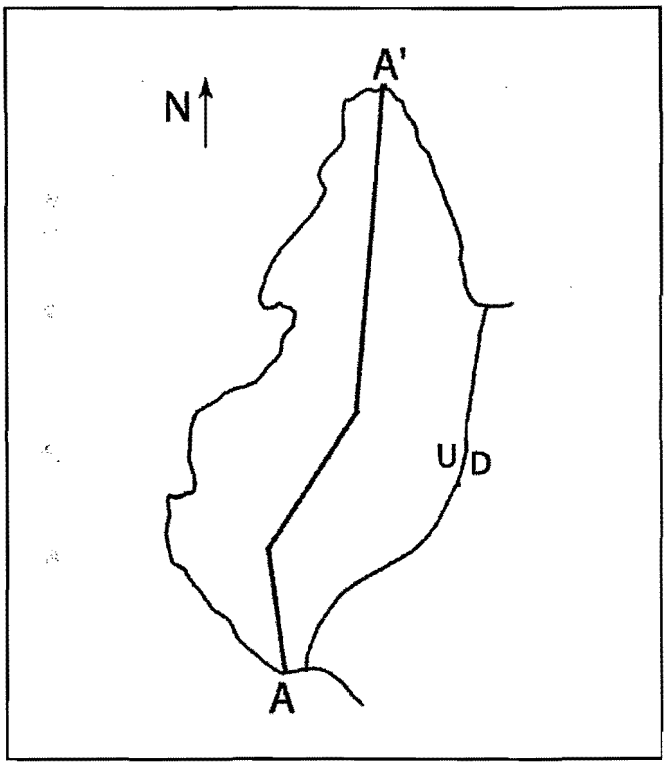

Figure 10 (a). Cross-section line A-A', for geologic cross-section shown in Figure 10 (b).

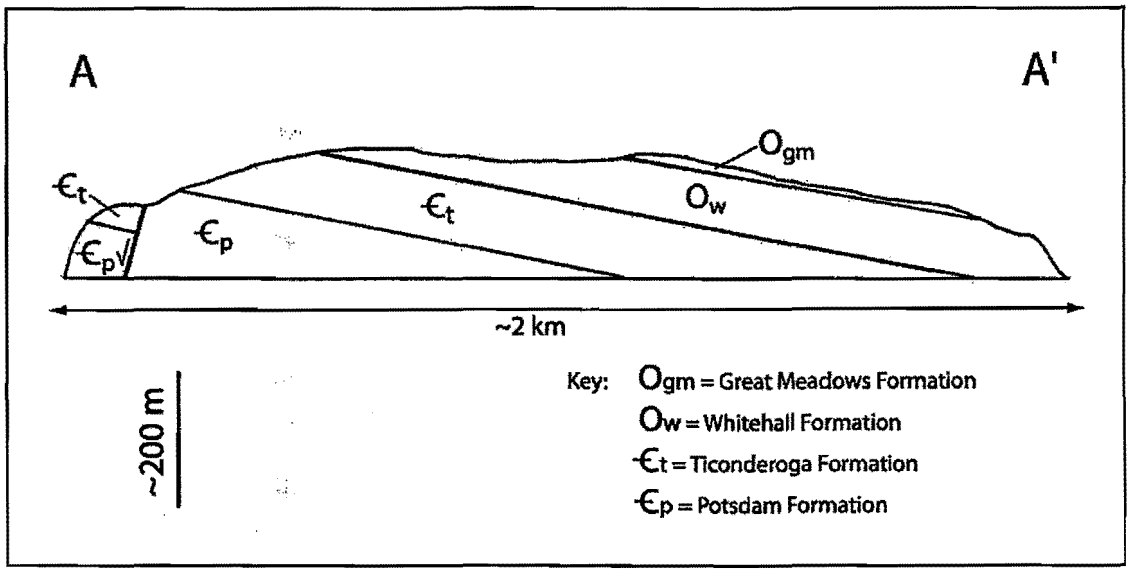

Figure 10 (b). Schematic cross-section of Mount Independence along the line A-A'.

REFERENCES

Blatt, H., Middleton, G. and Murray, R., 1980, Origin of Sedimentary Rocks, 2nd ed.: Prentice-Hall, Englewood Cliffs, 782 p.

Brainerd, E. and Seely, H. M., 1980, The Calciferous Formation in the Champlain Valley: Amer. Mus. Nat. Hist. Bulletin, v. 3, p. 1-23.

Cady, W. M., 1945, Stratigraphy and structure of west-central Vermont: Geol. Soc. Amer. Bulletin, v. 56, p. 515-587.

Fisher, D. W. and Mazzullo, S. J., 1976, Lower Ordovician (Gasconadian) Great Meadows Formation in eastern New York: Geol. Soc. Amer. Bulletin, v. 87, p. 1443-1448.

Fisher, D. W., 1984, Bedrock geology of the Glens Falls-Whitehall region, New York: New York State Museum Map and Chart Series 35. (Note: map is dated 1985, while accompanying text is dated 1984.)

Hayman, N. W. and Kidd, W. S. F., 2002, Reactivation of prethrusting, synconvergence normal faults as ramps within the Ordovician Champlain-Taconic thrust system: Geol. Soc. Amer. Bulletin, v. 114, p. 476-489.

Hunt, A. S., 1980, The stratigraphy of unconsolidated sediments of Lake Champlain: Vermont Geology, v. 1, p. 12-15.

Mehrtens, C. J., 1985, The Cambrian platform in northwestern Vermont: Vermont Geology, v. 4, p. E1-E21.

Rankin, D. W., Drake, A. A., Jr., Glover, L., III, Goldsmith, R., Hall, L. M., Murray, D. P., Ratcliffe, N. M., Read, J. F., Secor, D. T., Jr., and Stanley, R. S., 1989, Pre-orogenic terranes, *in* Hatcher, R. D., Jr., Thomas, W. A., and Viele, G. W., eds., The Appalachian-Ouachita Orogen in the United States: Boulder, Colorado, Geological Society of America, The Geology of North America, v. F-2.

Selleck, B., 1997, Potsdam Sandstone of the southern Champlain Valley – Sedimentary facies, environments and diagenesis, *in* Grover, T. W., Mango, H. N. and Hasenohr, E. J., eds., Guidebook to Field Trips in Vermont and Adjacent New Hampshire and New York, 1997 New England Intercollegiate Geological Conference, p. C3-1–C3-16.

Stanley, R. S., 1980, Mesozoic faults and their environmental significance in western Vermont: Vermont Geology, v. 1, p. 22-32.

Thompson, J. B., Jr., 1990, An introduction to the geology and Paleozoic history of the Glens Falls 1° x 2° quadrangle, New York, Vermont, and New Hampshire, *in* Summary Results of the Glens Falls CUSMAP Project: U. S. Geological Survey Bulletin 1887, Chapter A, p. A1–A13.

Washington, P. A. and Chisick, S. A., 1988, The Beekmantown Group in the central Champlain Valley: Vermont Geology, v. 5, p. F1-F17.

Welby, C. W., 1961, Bedrock geology of the central Champlain Valley of Vermont: Vermont Geological Survey Bulletin, no. 14, 296 p.

ACADIAN EXTENSION AROUND THE CHESTER DOME, VERMONT

by

Paul Karabinos, Department of Geosciences, Williams College, Williamstown, MA 01267

INTRODUCTION

Low-angle normal faults are important both in regions undergoing crustal extension and in mountain belts dominated by crustal shortening. Extension and shortening may be coeval in mountain belts, as has been proposed for the high Himalayas (Hodges et al., 1992) and Tibetan plateau (Molnar and Tapponnier, 1978), or extension may postdate shortening and thickening of continental crust, as has been suggested for the Basin and Range province (Coney, 1979; Sonder et al., 1987). Extension was also an important process in the evolution of ancient mountain chains (e.g. the Alps, Selverstone et al., 1984; Selverstone, 1985).

Although extension appears to be a fundamental process during orogenesis, major Paleozoic normal faults in the Appalachians have not been widely recognized. A notable exception is the Lake Char-Honey Hill fault in southeastern New England, which has been interpreted as an Alleghenian low-angle normal fault (Goldstein,1989; Getty and Gromet, 1992). Before Goldstein's (1989) breakthrough work showed that the sense of displacement was normal on this fault, it was universally regarded as a thrust. Astonishingly little evidence exists for normal faulting during the Acadian orogeny in the New England Appalachians. Castonguay et al. (2001) presented thermochronological evidence for Silurian to Early Devonian exhumation and extension along the St. Joseph fault in Quebec, and Spear (1992) suggested that the Monroe Line along the New Hampshire-Vermont border might be a normal fault based on contrasting styles of metamorphism of rocks across the contact.

Karabinos (1999, 2000) proposed that faults previously interpreted as Taconic thrusts around the Chester dome in southeastern Vermont (Thompson et al., 1990; Ratcliffe et al., 1997) are really Acadian normal faults. This field trip presents evidence for an extensional shear zone around the Chester dome and explores the tectonic implications of Early Devonian crustal extension. If normal faulting occurred in western New England, an entirely new aspect of the Acadian orogeny will have to be taken into account in tectonic reconstructions, the interpretation of geologic maps, and models of ore genesis within the belt.

GEOLOGIC SETTING

Lithotectonic Units

The Berkshire and Green Mountain massifs and the Chester dome are cored by Middle Proterozoic Grenvillian basement (see Karabinos and Aleinikoff (1990), Ratcliffe et al. (1997), and Karabinos et al. (1999) for some geochronological constraints). West of the massifs, the Taconic klippen are composed of Late Proterozoic to Middle Ordovician slate and phyllite originally deposited as shale and siltstone on the continental slope and rise of the passive Laurentian margin (Fig. 1). The klippen structurally overlie a coeval sequence of clastic and carbonate rocks, which formed on the continental shelf of Laurentia. East of the massifs, the Tyson, Hoosac, and Pinney Hollow Formations are equivalent to the basal units found in the Taconic klippen. The Rowe Formation in Massachusetts and the Ottauquechee and Stowe Formations in Vermont form the remnants of an accretionary wedge of oceanic crust and sediments, and the Moretown Formation contains forearc basin deposits (Fig. 1; Rowley and Kidd, 1981; Stanley and Ratcliffe, 1985). The Shelburne Falls arc (Fig. 1) is composed of the Barnard Volcanic Member of the Missisquoi Formation in Vermont and the Hawley Formation in Massachusetts (Karabinos et al., 1998). The Collinsville Formation and the Hallockville Pond Gneiss in Massachusetts are also part of the Shelburne Falls arc, but they form isolated bodies. The Connecticut Valley trough (Fig. 1) contains metasedimentary and metavolcanic rocks of Silurian to Early Devonian age.

Taconic and Acadian Orogenies

During the Ordovician Taconic orogeny (470 to 455 Ma), Laurentia collided with an island arc that formed above an east-dipping subduction zone. The characteristic deformation pattern was westward-directed thrusting of rocks of the continental margin, accretionary wedge, forearc basin, and arc complex (Rowley and Kidd, 1981; Stanley and Ratcliffe, 1985). Until recently the Bronson Hill arc in western New Hampshire and central Massachusetts (Fig. 1) was commonly identified as the arc that collided with Laurentia. However, Tucker and Robinson (1990) pointed out that the 454 to 442 Ma age range of volcanic and plutonic rocks in the Bronson Hill arc is younger than some metamorphic cooling ages from rocks caught in the Taconic collision zone (e.g. Laird et al.,

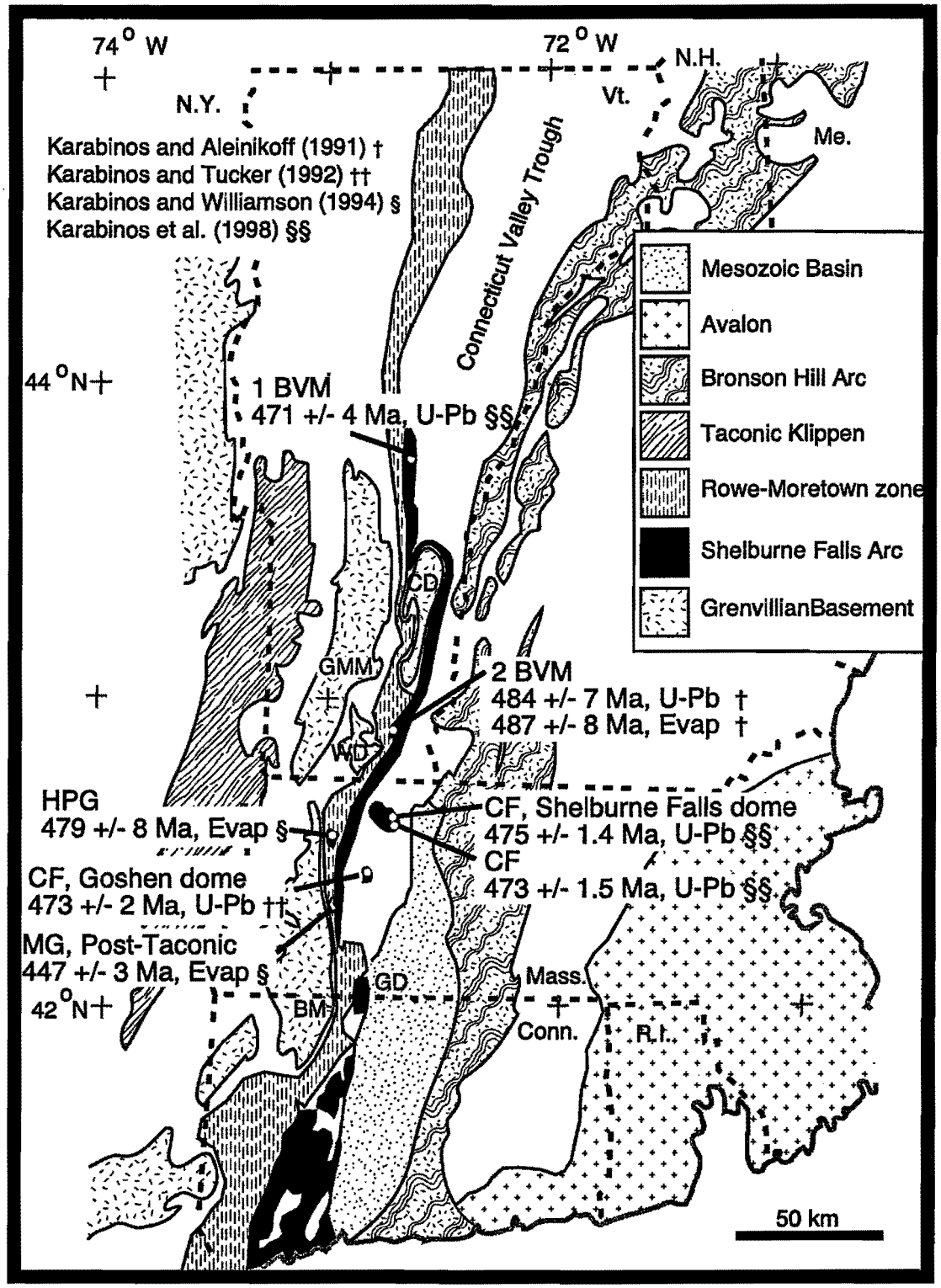

Figure 1. Tectonic map of New England and summary of U-Pb and single-grain evaporation (evap) zircon ages from the Shelburne Falls arc in western New England. Shelburne Falls arc rocks include the Barnard Volcanic Member (BVM), Collinsville Formation (CF), and Hallockville Pond Gneiss (HPG). The post-Taconic Middlefield Granite (MG) indicates that Taconic thrusting ended before ca. 447 +/- 3 Ma. GMM- Green Mountain massif. BM- Berkshire massif. WD- Wilmington dome. GD- Granville dome.CD- Chester dome.

1984). Karabinos et al. (1998) argued that the older Shelburne Falls arc (485 to 470 Ma) in eastern Vermont and western Massachusetts (Fig. 1) collided with Laurentia during the Taconic orogeny, and that the Bronson Hill arc formed above a west-dipping subduction zone after a reversal in subduction polarity. Karabinos et al. (1998) further suggested that this new west-dipping subduction zone accommodated plate convergence, thus bringing the Taconic orogeny to an end and setting the stage for the Acadian orogeny. According to this model, the Laurentian margin was active during the Silurian and the Connecticut Valley trough formed as an extensional back-arc basin above a west-dipping subduction zone (Karabinos et al., 1998; Karabinos, 1998).

The Acadian orogeny began in the Late Silurian and continued into the Middle Devonian; it resulted from the protracted collision of Laurentia and Composite Avalon (Robinson et al., 1998, Bradley et al., 2000, Tucker et al., 2001). Studies using high-precision geochronology have demonstrated that what was formerly regarded as a single 'Acadian' orogeny is, in fact, a complex series of tectonic events spanning tens of millions of years (Robinson et al., 1998; Bradley et al., 2000, Tucker et al., 2001). Bradley (1983) proposed that the collision occurred above two subduction zones, one dipping beneath each continental margin, but other models invoke a single subduction zone under Avalon (e.g. Robinson et al, 1998, Tucker et al., 2001).

In western New Hampshire and eastern Vermont, including the area of the Chester dome, two important phases of the Acadian orogeny have long been central to structural models and were portrayed on the Geologic Map of Vermont (Doll et al., 1961). According to this interpretation, an early nappe stage created kilometer-scale recumbent folds, and a later dome phase refolded the early nappes (e.g., Rosenfeld, 1968; Hepburn et al., 1984; Thompson et al., 1993). Ratcliffe et al. (1997) and Hickey and Bell (2001), however, questioned this long-standing structural interpretation and argued for more complex Acadian folding histories to explain the structures in and around the Chester dome.

In my opinion, the nappe and dome stages of deformation explain much of the structural geometry of the region, although I am not convinced that the nappes involved units structurally below the Silurian and Devonian sequence. However, an important gap in our understanding of the tectonic history of this area is a mechanism for the dramatic thinning of units around the Chester dome and other structures, including the Wilmington dome and the Jamaica anticline. I believe that the evidence points to an intermediate period of extension along a normal-sense shear zone after the nappe stage of deformation but prior to the doming stage.

Timing of Acadian Events

The age of Acadian deformation and metamorphism in southeastern Vermont is reasonably well constrained by a variety of isotopic studies. $^{40}Ar/^{39}Ar$ hornblende cooling ages indicate that Acadian metamorphism was waning by 380 Ma in the vicinity of the Chester dome (Laird et al., 1984; Karabinos and Laird, 1988; Spear and Harrison, 1989). This agrees remarkably well with two studies of the age of garnet growth. Christensen et al. (1989) used the radial variation of $^{87}Sr/^{86}Sr$ to estimate that garnet porphyroblasts from Townsend, Vermont, grew at about 380 Ma over an average interval of approximately ten million years. Vance and Holland (1993) used Sm-Nd and U-Pb measurements and chemical zoning to argue that garnet from Gassetts, Vermont, (Fig. 2A) grew at about 380 Ma during increasing temperature and decompression of 2.5 kbar, corresponding to exhumation of approximately 7 km. Based on U-Pb dating of granitic intrusions and cross-cutting relationships, Ratcliffe et al. (2001) concluded that Acadian deformation in the vicinity of the Chester dome began before 392 Ma and that it persisted with uneven distribution in southeastern Vermont for another thirty million years. To the south, along strike in western Massachusetts, the end of intense Acadian deformation is tightly bracketed by a 376 ± 4 Ma age (U-Pb zircon, TIMS) of a highly deformed tonalitic sill from the Granville dome (Karabinos and Tucker, 1992) and a 373 ± 3 Ma age ($^{207}Pb/^{206}Pb$ zircon, evaporation) for the post-kinematic Williamsburg Granodiorite (Karabinos and Williamson, 1994).

THE CHESTER DOME

Together the Chester (Thompson, 1950) and Athens (Rosenfeld, 1954) domes form an elongated basement-cored structure approximately twelve km wide and thirty km long (Fig. 2). For simplicity, the entire structure is here called the Chester dome. Since the original work by Thompson and Rosenfeld, this classic mantled gneiss dome has been the focus of numerous structural (Rosenfeld, 1968; Nisbet, 1976; Bell and Johnson, 1989; Ratcliffe et al., 1997; Hickey and Bell, 2001) and metamorphic studies (Rosenfeld, 1968; Thompson et al., 1977; Cook and Karabinos, 1988; Christensen et al., 1989; Chamberlain and Conrad, 1993; Vance and Holland, 1993).

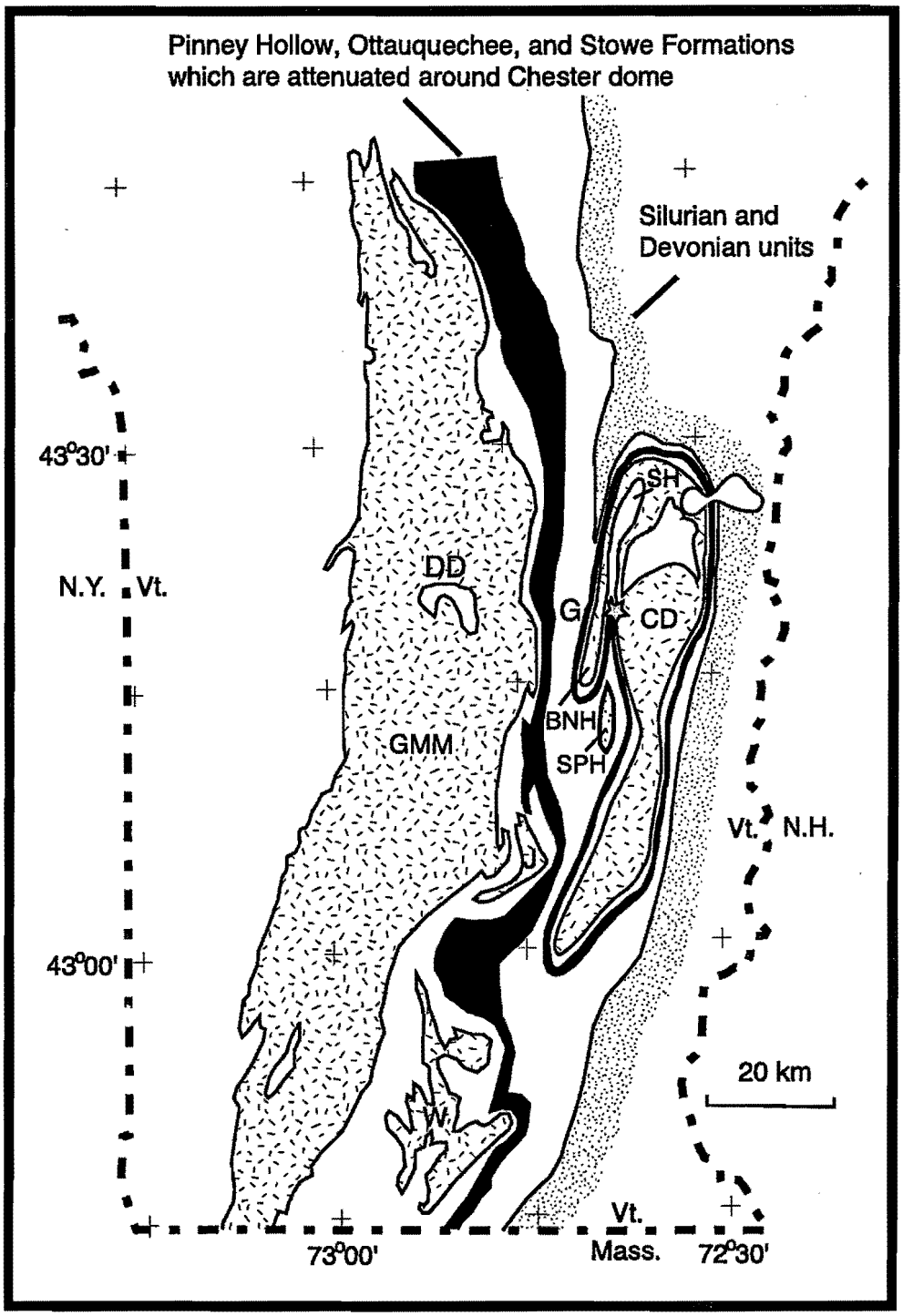

Figure 2A. Simplified map showing the distribution of the Pinney Hollow, Ottauquechee, and Stowe Formations (black), which are extremely thin around the Chester dome (CD). Grenvillian basement- hatchured pattern, Silurian and Devonian units- dotted pattern. DD- Devils Den, G- location of Gassetts road cut (star), GMM- Green Mountain massif, J- Jamaica anticline, W- Wilmington dome. BNH- Butternut Hill fold, SH- Star Hill fold, SPH- Spring Hill fold. Based on Doll et al. (1961).

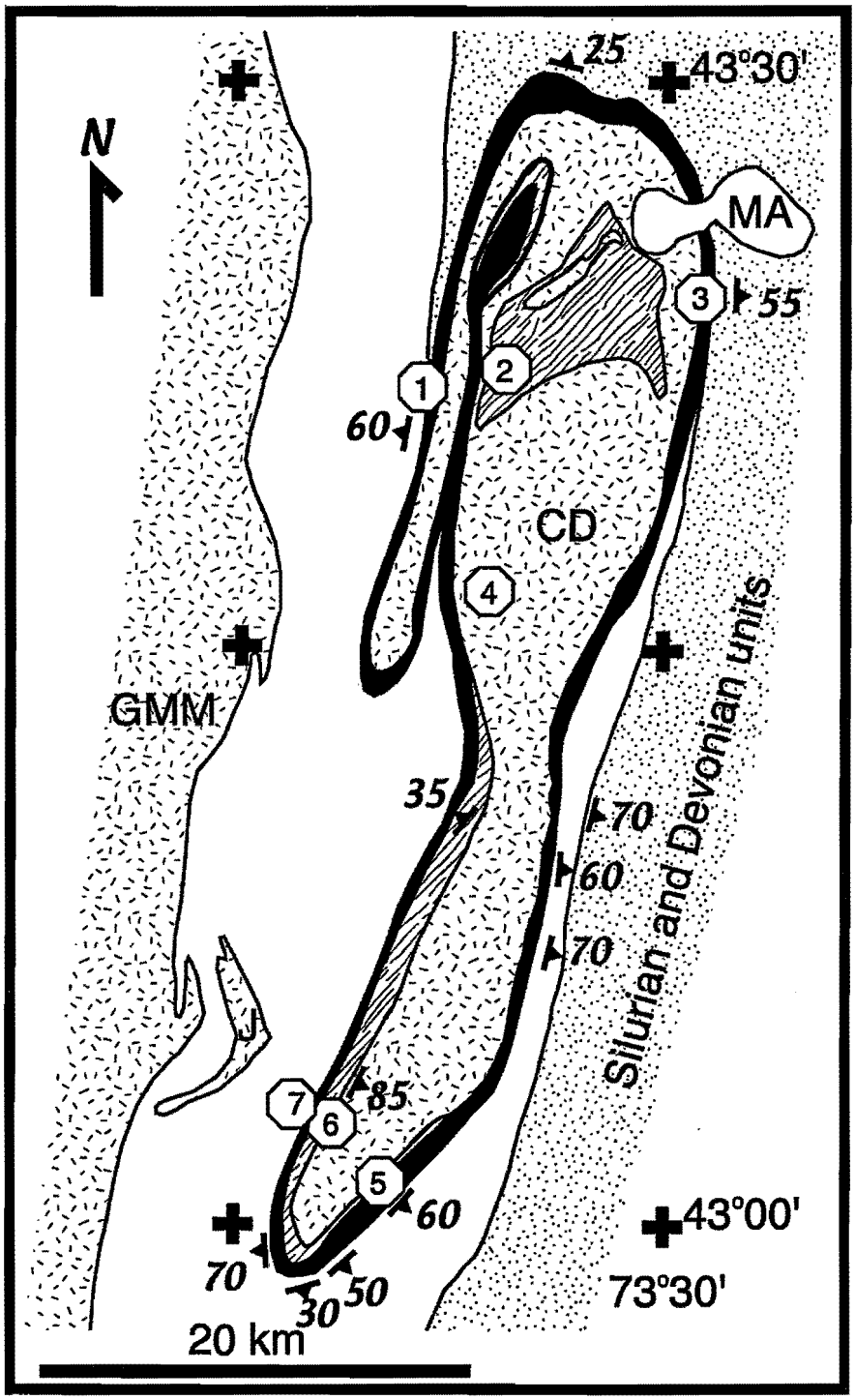

Figure 2B. Map of the Chester dome (CD) showing the distribution of the mylonite zone (black) and the location of field trip stops. Grenvillian basement- hatchured pattern. Hoosac Formation, including Cavendish Formation of Doll et al. (1961)- diagonal wavy lines. GMM- Green Mountain massif. J- Jamaica anticline. MA- Mount Ascutney. Strike and dip symbols show the orientation of the mylonitic fabric.

Most workers informally abandoned the term "Cavendish Formation" because its metasedimentary members were reassigned to other formations and its metaigneous member was reinterpreted as a post-Grenvillian intrusive suite stratigraphically unrelated to the metasedimentary units (Karabinos and Aleinikoff, 1990). However, in a major departure from earlier interpretations, Ratcliffe et al. (1996, 1997) revived the name Cavendish Formation and assigned its metasedimentary units to the Mount Holly Complex. This new interpretation, if correct, would require a dramatic change in structural reconstructions of the Green Mountain massif and Chester dome (e.g., Ratcliffe, 2000a, b).

To test this new age assignment, Karabinos et al. (1999) separated detrital zircons from a quartz-rich bed from Cavendish gorge, the type locality of what Richardson (1929) called the Cavendish Schist. This is also the location where Ratcliffe et al. (1996, 1997) obtained a 1.42 $\pm$ 0.02 Ga age on a tonalite, the Felchville Gneiss, that they interpreted as cutting the Cavendish Formation. It is important to note, however, that the interpretation of an intrusive contact between the Felchville Gneiss and the Cavendish Formation was based on map-scale patterns rather than direct field observations (Ratcliffe et al., 1997). There are no xenoliths of Cavendish Formation in the tonalite, nor are there apophyses of tonalite in the Cavendish Formation. The contact between the 1.42 Ga tonalite and the Cavendish Formation, where best exposed in Cavendish gorge (Stop 2), is highly sheared, hence a more plausible explanation for the truncation of the metasedimentary units is a fault rather than an intrusive contact.

The zircon grains analysed by Karabinos et al. (1999) varied from nearly euhedral to nearly spherical. Virtually all of the grains had pitted surfaces and showed some rounding of edges and terminations. The grains exhibited oscillatory zoning typical of zircons that crystallized from a magma. This is important because it precludes the possibility that metamorphic overgrowths were inadvertently analysed. Karabinos et al. (1999) analyzed ten zircons grains by the Pb evaporation method and fifteen grains by the sensitive high resolution ion microprobe (SHRIMP). All twenty-five grains yielded ages less than 1.42 Ga. Seven of the grains gave ages consistent with derivation from the Bull Hill Gneiss, which postdates the Grenville orogenic cycle. The ages of eight grains fall in the interval of 1.0 to 1.1 Ga and four in the interval of 1.1 to 1.2 Ga; these are very common igneous ages in the Grenville terrane of Canada and the Adirondacks. Three grains yielded ages of approximately 1.3 Ga, consistent with derivation from trondhjemitic gneisses of the Mount Holly complex (Ratcliffe et al., 1991). There is no reason to suspect that this wide range of single grain ages reflects multiple episodes of metamorphic growth of zircon or complicated Pb-loss events, as suggested by Ratcliffe (2000a). On the basis of these zircon ages, the Cavendish Formation should not be assigned to the Mount Holly Complex. In spite of these age constraints, however, Ratcliffe (2000a, b) did include the Cavendish Formation in the basement sequence. Obviously, the correct age assignment of these rocks is crucial for understanding the structural geometry of the northern part of the Chester dome.

Metamorphic Isograds around the Chester Dome

It is important to understand the timing and complex nature of metamorphism around the Chester dome because if extension did occur, there should be a record of contrasting pressure-temperature paths in footwall and hanging-wall rocks. If such a record exists, it would provide strong evidence for extension, constrain the location of the normal shear zone, and help date the extension.

Rosenfeld (1968) was the first to recognize that truncated inclusion trails in garnet porphyroblasts record two separate periods of garnet growth. He suggested that the first growth episode occurred during Taconic metamorphism and that the second episode occurred during Acadian metamorphism. Karabinos (1984) showed that garnets with textural unconformities also preserve reversals in chemical zoning that developed during a period of partial resorption of the garnet cores before the rims grew (Figs. 4A&B). Laird and Lanphere (1981) and Laird et al. (1984) documented polymetamorphic textures, zoning, and isograds in mafic schist from Vermont that are largely consistent with the polymetamorphic history inferred from pelitic rocks. Laird et al. (1984) used $^{40}Ar/^{39}Ar$ cooling ages to show that Taconic metamorphism affected mafic schist in northern Vermont. To date, however, no unequivocal evidence for Taconic metamorphism in the Chester dome has been published, although J. Cheney and F. Spear have unpublished ion-microprobe monazite ages that are consistent with Ordovician metamorphism (J. Cheney, personal communications, 2002).

Cook and Karabinos (1988) used inclusions in garnet porphyroblasts that contain textural unconformities to construct two sets of isograds in southeastern Vermont (Figs. 4C&D). The 'older' set of isograds is based on inclusions found in garnet cores. The 'younger' set is based on inclusions in the garnet rims and the matrix assemblage. The age of the younger metamorphism and garnet rims is clearly Acadian. The garnet cores, however,

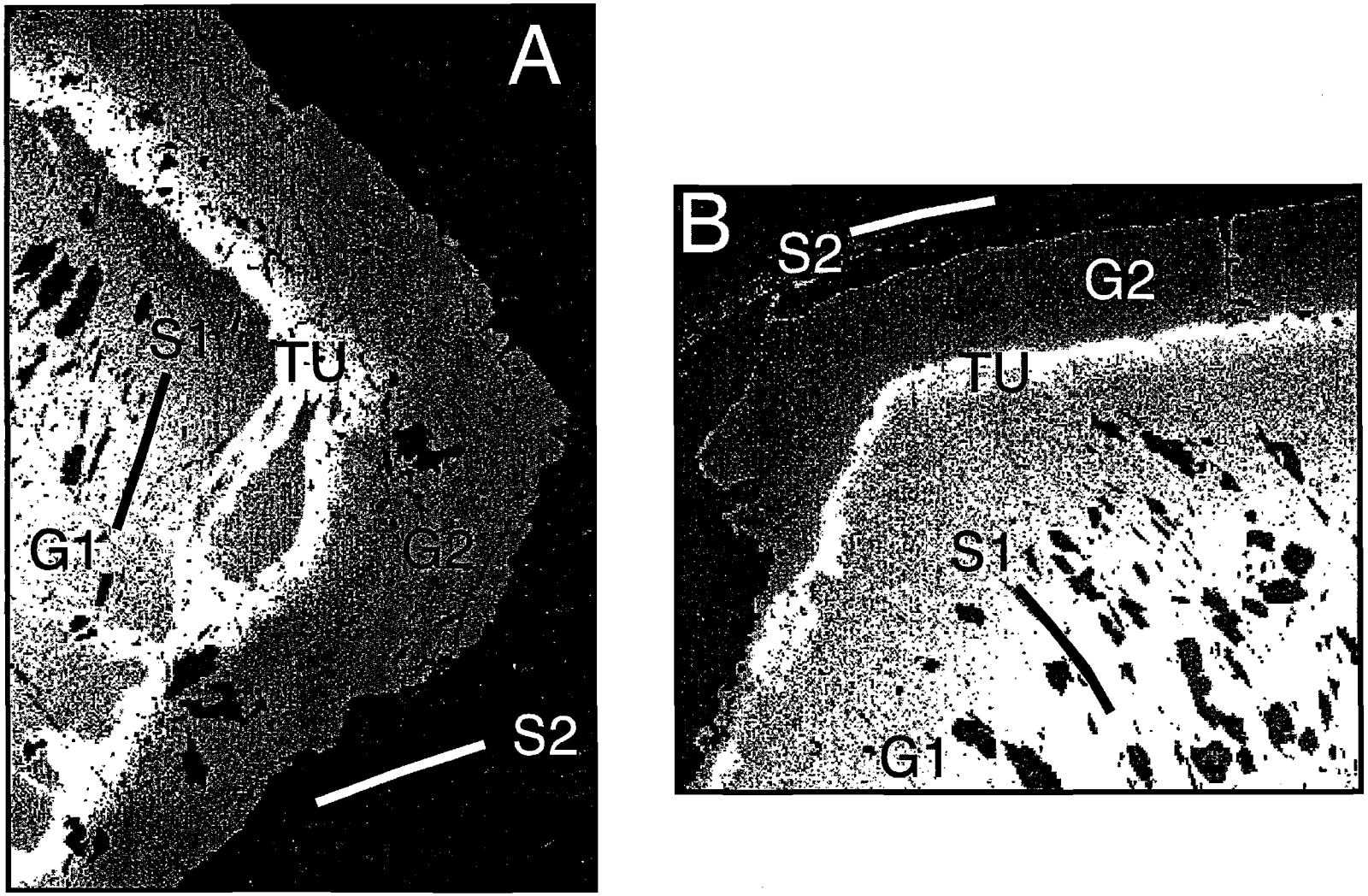

Figure 4. Mn X-ray maps of garnet porphyroblasts. First-stage garnet (G1) overgrew early schistosity (S1) and shows normal growth zoning with decreasing Mn content (light to dark shades of gray). Second-stage garnet (G2) overgrew crenulation cleavage (S2) parallel to matrix fabric (not visible in maps). The bright boundary between the two growth stages corresponds to the high Mn zoning anomaly caused by the partial resoption of first-stage garnet. The textural unconformity (TU) is located along the outer margin of the zoning anomaly. Rutile is abundant as inclusions in first-stage garnet, but absent elsewhere. A. Sample 120D (see Fig. 4C for location). Image is 2.6 by 3.9 mm. B. Sample 2739 (see Fig. 4C for location). Image is 3 by 2.7 mm.

It is important to note that we do not really know the stratigraphic thickness of any of the units in the eastern Vermont sequence because of structural complications. Furthermore, we do not have very good age constraints on these units. A notable exception is a recent 571 ± 5 Ma U-Pb zircon age on a metafelsite from the Pinney Hollow Formation near the north end of the Green Mountain massif (Walsh and Aleinikoff, 1999). This constrains the Tyson, Hoosac, and Pinney Hollow Formations to be Late Proterozoic, if the stratigraphic continuity of these units is accepted. Another age constraint is that the Moretown Member of the Missisquoi Formation must be older than the 479 ± 8 Ma Hallockville Pond Gneiss, which cross-cuts the Moretown in western Massachusetts (Karabinos and Williamson, 1994). Because the units in the eastern Vermont sequence formed in disparate tectonic settings and the boundaries between the units are commonly interpreted as thrust faults (e.g. Rowley and Kidd, 1981; Stanley and Ratcliffe, 1985; Ratcliffe et al., 1997), the relative ages of the units must also be considered uncertain. Despite these limitations, it seems reasonable, as a first-order approximation, to compare the thickness and stacking order of the units on the east flank of the Green Mountain massif with the mantling sequence around the Chester dome.

Figure 5 shows schematically which units are affected by ductile thinning and omission in the mylonite zone around the Chester dome. Unpatterned portions of the "column" represent units that are either extremely thinned in the mylonite zone or absent. The thinning and omission of units is most extreme along the northern and northeastern margin of the dome. The structural section is somewhat less disrupted along the southern and southwestern margin of the dome. These observations are consistent with recent mapping by Ratcliffe (2000a, 2000b), who showed subdivisions of the Moretown Formation directly on the Mount Holly Complex along the northern and eastern margin of the Chester dome, but interpreted the contact as a thrust fault.

In my opinion, extension along a normal-sense shear zone is a more logical explanation for the observations than thrusting. Ductile thinning can occur along thrust faults, but it usually affects rocks on the overturned limbs of thrust nappes. There is no evidence for overturned limbs or structural repetition around the Chester dome. Conceivably, there might be some explanation for the thinning and omission of units that invokes tectonic erosion during Taconic subduction. However, any explanation, whether structural or stratigraphic in nature, must take into account the observation that the zone of attenuated and missing units is spatially correlated with a strongly developed mylonitic fabric and that this fabric must be an Acadian feature.

Kinematic Indicators

Figure 6 shows the sense of shear determined from sparse kinematic indicators found in outcrop, slabbed hand samples, and thin sections. Indicators include c-s fabrics, rotated porphyroclasts, and, most commonly, asymmetric extensional shear bands. The rotation sense inferred from spiral inclusion trails in garnet porphyroblasts is consistent with the kinematic indicators noted above, but this information is not included in the data summarized in Figure 6. To date, I have not found very many unambiguous kinematic indicators in the mylonite zone surrounding the Chester dome. (The numbers next to the large arrows in Figure 6 show how many independent indicators are available at each locality.) One explanation for the scarcity of kinematic indicators is overprinting of the mylonitic fabric during the doming episode of deformation. If the mylonite zone did develop as a normal-sense shear zone, it must have been nearly planar and close to horizontal during extension. Currently it is folded, along with the basement-cover contact, into the elongated Chester dome. The doming event did not produce a strong axial planar fabric but limb rotation and horizontal shortening accompanying doming could have obscured kinematic indicators produced during extension.

Based on the available observations, the hanging-wall rocks above the mylonite zone appear to have been displaced generally westward relative to footwall rocks in the core of the dome. It is not clear, however, from the indicators alone whether the displacement was northwest, west, or southwest. Two observations suggest that the displacement was southwest. First, Rosenfeld (1968) used deformed pebbles and phenocrysts to document strong northeast to southwest Acadian extension. Second, the mantling sequence is most strongly thinned and truncated along the north and northeast margin of the dome and less disrupted along the south and southwest margin, consistent with northeast to southwest displacement (Fig. 5).

Working Model

It seems reasonable to assume that the area of the Chester dome was affected by the Taconic orogeny, but, in my opinion, it is difficult to identify specific features that record Taconic deformation and metamorphism. One candidate is the large exposure of Cavendish Formation in the north-central part of the Chester dome (Doll et al.,

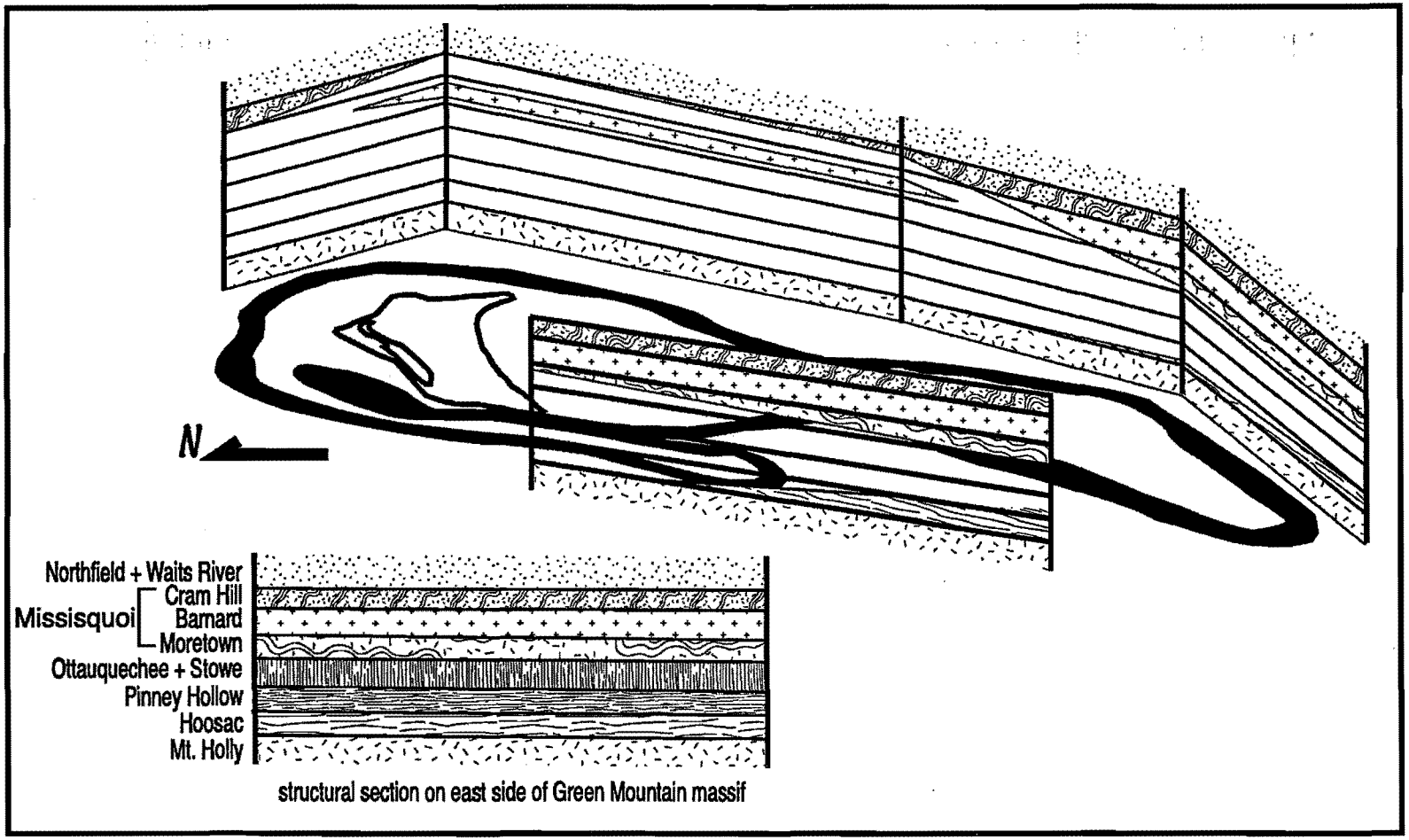

Firgure 5. Schematic fence diagram showing the structural sequence (in foreground) of units on the east side of the Green Mountain massif and the distribution of the same units around the Chester dome. The Chester dome is shown in a perspective view from the west. Blank areas in the fence diagram correspond to units that are missing in traverses around the dome. The locations of the traverses are shown approximately by the bottom of each post in the fence.

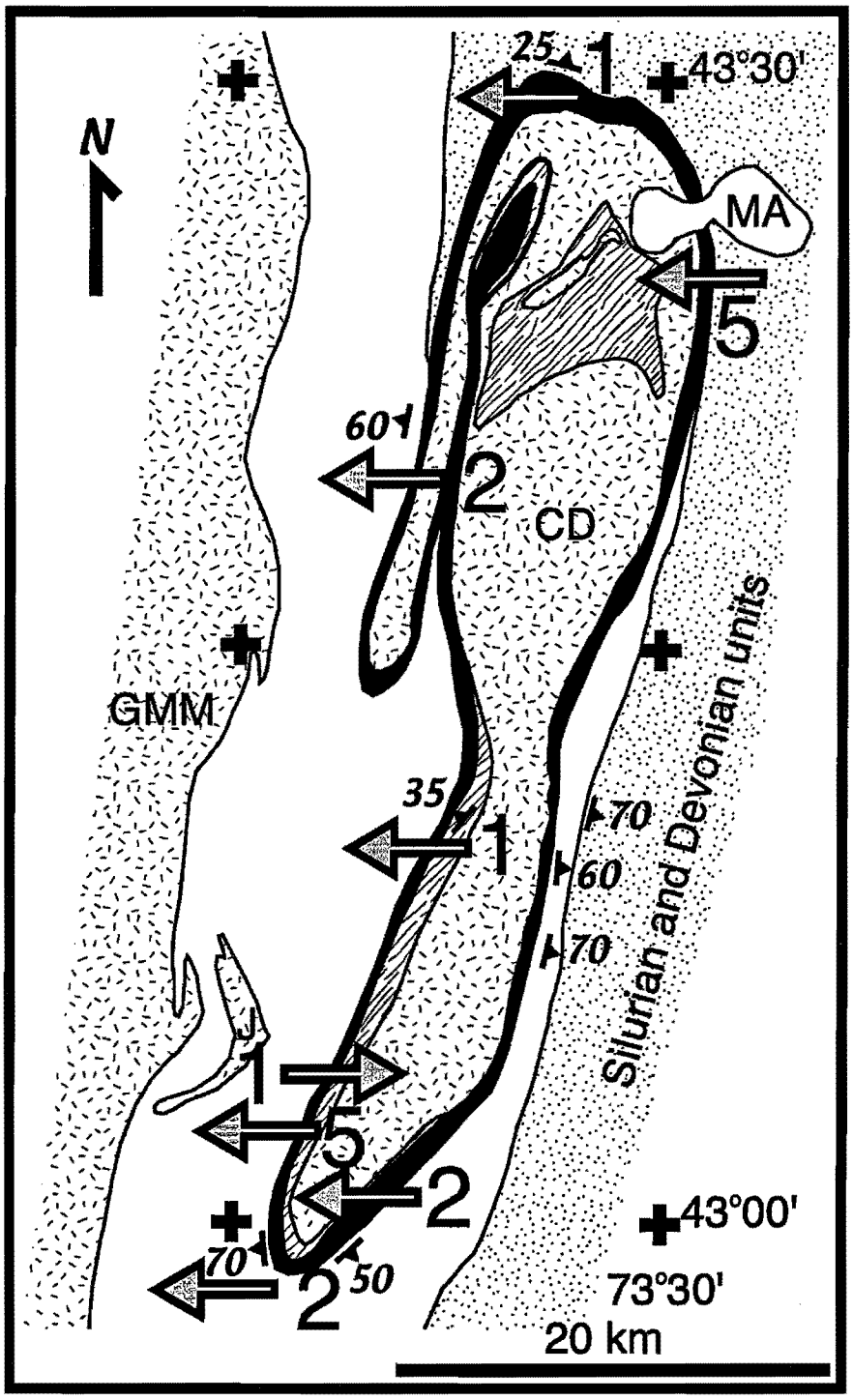

Figure 6. Map of the Chester dome (CD) showing the sense of shear determined from kinematic indicators (arrows) and the number of observations at each locality. The hanging-wall rocks above the mylonite zone (shown in black) appear to have moved west relative to the footwall rocks. The normal-sense shear zone was later folded during the doming episode of deformation.

1961). This exposure of cover rocks appears to be preserved in the footwall of a Taconic thrust beneath Grenvillian basement. Analogous fault geometries are present near the Devils Den, Jamaica anticline, and Wilmington dome (Figs. 2A, 4). The important point is that the dominant fabrics and structures in the Chester dome are Acadian features.

Early Acadian deformation must have involved the development of a thick tectonic cover according to pressure estimates of 8 to 11 kbar during Acadian metamorphism in the Chester dome (Kohn and Spear, 1990; Vance and Holland, 1993; Kohn and Valley, 1994). This tectonic burial logically corresponds to the nappe phase of deformation. The nappes in eastern Vermont involve Silurian and Devonian units deposited in the Connecticut Valley trough. The Connecticut Valley trough probably formed as a back-arc basin between the Shelburne Falls and Bronson Hill arcs (Karabinos et al., 1998). During Acadian deformation the sedimentary rocks in the trough were recumbently folded into west-verging nappes that were transported westward over the area of the Chester dome.

Extension followed the nappe phase of deformation; I infer this from the pressure decrease recorded by the inclusion patterns in garnet porphyroblasts with textural unconformities. Rutile inclusions are ubiquitous in first-stage garnet cores but absent in second-stage garnet rims and matrix, whereas ilmenite is abundant in the second-stage rims and matrix, and this distribution of inclusions is consistent with decreasing pressure (Bohlen et al., 1983). A pressure decrease during garnet growth in the Gassetts schist was also determined by Vance and Holland (1993). Tectonic exhumation of rocks in the core of the Chester dome occurred during ductile thinning and omission of units in the mantling sequence around the Chester dome (Fig. 5). It seems likely that the mylonite zone surrounding the Chester dome formed as a normal-sense shear zone, and that at the time of its formation it was approximately planar and horizontal. If exhumation led to decompression melting within the dome, then the 390 Ma age of Acadian granitic dikes (Ratcliffe et al, 2001) may constrain the time of extension. Extension may reflect gravitational collapse following crustal thickening or transtensional strike-slip faulting parallel to the Acadian orogen. It seems likely that other domes in western New England, such as the Strafford, Pomfret, Guilford, Shelburne Falls, Goshen, and Granville domes, are also related to extension.

The initial doming of the Chester dome may have occurred during extension, perhaps as a core complex, but its present geometry must reflect renewed crustal shortening and folding after development of the mylonitic fabric. The mylonite zone dips moderately to steeply away from the core of the dome, and is slightly overturned along the southwest margin (Fig. 2B). It is difficult to imagine a mechanism that could have formed the mylonitic fabric in it present geometry. Finally, I would interpret the Butternut Hill, Star Hill, and Spring Hill folds (Fig. 2A) on the northwest side of the Chester dome as relatively low-amplitude folds related to the late compression that folded the mylonite zone and created the final dome geometry.

ACKNOWLEDGEMENTS

Twenty-five years ago, Jim Thompson and John Rosenfeld introduced me to the geology of southeastern Vermont. Since then I have benefitted from numerous discussions with them, and their generous advice has been invaluable in my research. Their pioneering and innovative studies set the stage for five decades of fruitful research by many geologists in the region.

Matt Student worked with me in the field during the summer of 2001. David Morris and Elizabeth Mygatt helped me with the road log and, together with Margaret MacEachern, made helpful suggestions for improving the manuscript.

Financial support for this work was provided by the Petroleum Research Fund administered by the American Chemical Society.

ROAD LOG

Mileage

0.0 **MEET AT 8:00 AM IN THE CENTER OF PROCTORSVILLE** at the intersection of Route 131 and Depot St. near the Crows Corner Bakery Café. Drive S on Depot St.

0.5 Intersection of Route 103 and Depot St., turn left, S, on Route 103.

2.0 Park in pullout on right, W, side of road.

STOP 1. BASEMENT-COVER CONTACT, NW MARGIN OF CHESTER DOME. (45 min.) Gneiss on E side of road, opposite pullout, belongs to the Middle Proterozoic Mount Holly Complex (i.e. basement) and is composed of quartz, plagioclase, biotite, epidote, ± muscovite, ± microcline. It contains abundant highly-deformed pegmatites that distinguish it from plagioclase schist and gneiss of the Late Proterozoic Hoosac Formation. Walk N along road. The first outcrop on the W side of the road belongs to the cover sequence. Before looking at it, head into the woods on the E side of the road to see more of the Mount Holly complex. The contact appears to be buried in the small drainage on the E side of the road. The basement gneisses are highly sheared and the mylonitic fabric dips steeply to the W. Outcrops up the hill contain large-scale C-S fabric and rotated boudins that indicate a tops-to-the-west sense of shear.

The first outcrop on the W side of the road is quartz, muscovite, biotite, chlorite, ± plagioclase, ± garnet schist. Many layers contain graphite. Further N are exposures of quartz-rich gneiss with a distinctive pinstripe texture. I think these rocks belong to the Cram Hill and Moretown Members of the Missisquoi Formation of Doll et al. (1961).

Reverse direction and drive N on Route 103.

2.6 Outcrop on E side of road of Barnard Gneiss.

3.5 Turn right, N, on Depot St.

4.0 Turn right, E, on Route 131.

6.1 Turn right on Power Plant Rd.

6.3 Park at gate.

STOP 2. CAVENDISH GORGE, AGE OF THE CAVENDISH FORMATIONS. (30 min.) Walk from gate up the dirt road to the power station. One of the tonalite samples dated by Ratcliffe et al. (1997) was collected from the outcrop next to the power station. Ratcliffe et al. (1997) argued that the 1.4 Ga tonalite intruded the metasedimentary units of the Cavendish Formation here in the gorge, the type locality of the Cavendish Schist of Richardson (1929), making them older than the tonalite and part of the Mount Holly Complex. I think that the contact between the tonalite and the marble, calc-silicate, quartzite, and schist is tectonic in origin. I collected a sample of quartzite from the gorge about 50 m upstream from the power station and separated detrital zircons. Single grain Pb-evaporation and SHRIMP ages of 25 grains are all younger than 1.4 Ga (Karabinos et al., 1999), consistent with a tectonic contact between the tonalite and the metasedimentary rocks, but inconsistent with the intrusive contact interpretation. Furthermore, the plagioclase schist here in the gorge does not contain abundant highly-deformed pegmatite like the gneiss we saw in the basement at Stop 1. I correlate the plagioclase-rich schist with the Hoosac Formation and the marble, calc-silicate, and quartzite with the Tyson Formation.

Turn around and drive back to Route 131.

6.5 Turn right, E, on Route 131.

12.9 Intersection of Rts. 131 and 106. Continue on Route 131.

14.2 Turn right on Gulf Rd.

14.5 Intersection of Gulf Rd and Plains Rd. Continue straight.

15.4 Park in pullout on left side of road.

STOP 3. BASEMENT-COVER CONTACT, NE MARGIN OF CHESTER DOME. (45 min.) Outcrop immediately E of pullout is quartz-rich, biotite, chlorite, ± plagioclase schist with graphite in some layers. Farther E are more outcrops of this lithology and some layers contain highly fractured garnet crystals partially altered to chlorite along the cracks. These rocks are part of the Silurian to Devonian sequence, probably the Northfield or Waits River Formation. As we will see, the intense zone of shearing along the northeastern margin of the Chester dome extends all the way from Middle Proterozoic basement through the pre-Taconic cover sequence and into the Silurian units.

Walk back down the road to the W. Outcrop beneath roots of fallen tree on S side of road is similar to the first outcrop and contains a fine-grained, unmetamorphosed mafic dike, probably related to Mount Ascutney, a Cretaceous intrusion. Outcrop along road is spotty but it is much better in the woods on both sides of the road. Below the schist of the Northfield Formation are highly deformed felsic and mafic gneisses that contain a mylonitic fabric. It is difficut to assign these rocks to a specific unit with certainty, because they are highly deformed and out

of context, but they look more like Barnard Gneiss to me than anything else. This is the only rock type belonging to the Late Proterozoic to Ordovician sequence that I have found along this traverse.

Only 0.3 mile W of the pullout is an outcrop of highly sheared augen gneiss. This rock was mapped as Bull Hill Gneiss by Doll et al. (1961) but not all layers contain microcline, which is typical of Bull Hill Gneiss. In thin section it is clear that the eyes in some layers are composed of plagioclase aggregates. Doll et al. (1961) showed Bull Hill Gneiss directly below Hoosac Formation around much of the Chester dome. It is common to find Bull Hill Gneiss at the basement-cover contact in the southern part of the dome, but other feldspar-rich gneisses belonging to the Mount Holly Complex are more typically found at the contact in the northern part of the dome.

15.6 Intersection of Gulf Rd. and Gravelin Rd. Outcrop on corner contains unmetamorphosed dike. Turn left, N, on Gravelin Rd.

16.0 Turn left, W, on Route 131.

19.4 Turn left, S, on Route 106.

24.1 Turn right, W, on Route 10.

28.4 Turn left, S, on Route 103.

28.9 Park in pulloff on right.

STOP 4. GNEISSES IN MOUNT HOLLY COMPLEX WITH ACADIAN DIKES. (20 min.) The tonalitic gneiss seen here is a common lithology in the Mount Holly Complex of the Chester dome. Also, the deformation fabric in this outcrop is typical of that found in the Mount Holly Complex rocks within the core of the dome, away from the basement-cover contact. Late cross-cutting felsic dikes, like those seen here, are found in many outcrops in the dome below the mylonite zone. Ratcliffe et al. (2001) reported a zircon SHRIMP age from a granitic dike near Gassetts of 392 ± 6 Ma.

Continue S on Route 103.

32.9 Bear right on Route 11 S to connect with Route 35 S.

33.1 Go straight across main highway to take Route 35 S.

40.1 In village of Grafton turn right.

40.3 Turn left, S, on Townshend Rd.

The narrow valley that the road follows S of Grafton parallels the W flank of the dome near the contact between the Hoosac Formation and the Bull Hill Augen Gneiss.

46.8 Bear right. Back on Route 35 S.

50.1 Townshend. Turn left on Route 30 S.

51.7 Turn left on Ellen Ware Rd.

51.8 Park in pullover on left.

STOP 5. BASEMENT-COVER CONTACT, SE MARGIN OF CHESTER DOME. (45 min.) Walk back about 20 m to W to first outcrop; look for signs of blasting dating from construction of the old railway bed parallel to the West River. Rock is quartz, microcline, plagioclase, biotite, epidote gneiss belonging to the Mount Holly Complex. This does not look like typical Bull Hill Gneiss to me, although that is what is shown below the Hoosac Formation by Doll et al. (1961). Walk E along road past pullout. There are some outcrops of plagioclase schist that look like Hoosac Formation. Continue E along road to where the river is just S of the road. River outcrop of mafic schist with some pelitic schist layers. The pelitic schist contains some large garnet crystals that were incompletely altered to chlorite. The extent of retrogression increases significantly to the E along this traverse. This outcrop and others further E contain cleavage surfaces with sprays of biotite after amphibole. There are some outcrops along the road to the E of quartz-rich schist with distinctive pinstripe texture. I would assign the mafic and pelitic schist found in the river outcrops to the Moretown Formation. I see no rocks here that I would assign to the Pinney Hollow, Ottauquechee, or Stowe Formations.

Reverse direction and head back to Route 30.

51.9 Turn right, N, on Route 30.

53.5 Back in the center of Townshend, stay on Route 30.

55.1 Covered bridge on left, outcrop of quartz-rich gneisses on right. These rocks could belong to the lower part of the cover sequence (Rosenfeld, 1988) or to the basement. Approximately 0.3 mi. back to the southeast, near the sharp bend in the road, is sheared Bull Hill augen gneiss on the north side of Route 30. The Bull Hill Gneiss intruded the Mount Holly Complex at approximately 960 Ma (Karabinos and Aleinikoff, 1990), after the Grenville orogeny. Therefore, the deformation fabric in this unit is from the Taconic and Acadian orogenies.

55.2 Park in pullover on left without blocking gate.

STOP 6. TOWNSHEND DAM SPILLWAY, MYLONITE ZONE, SW MARGIN OF CHESTER DOME. (30 min.) Walk around gate and down dirt road past the equipment sheds for Townshend Dam. Just before the road crosses a small and unappealing stream, walk through the reeds to the large outcrop to your right. Here is highly sheared plagioclase schist and gneiss of the Hoosac Formation. Some dark biotite-rich layers are present. Note the extreme isoclinal folds and boudinage in this outcrop.

If it is not too wet, it is possible to walk up the spillway and see rocks on both sides of the cut. Another approach is to walk back to the road, continue across the bridge about 100 m, and head into the pine trees on the right. Look for the end of the chain link fence and then walk around and past it to the N, toward the edge of the spillway using **extreme caution** - there are some steep cliffs with a lot of vertical relief. From the top of the spillway it is possible to look to the other side and appreciate the extreme deformation of these rocks. There are abundant folds, boudinage, and truncated layers. The rocks on this side of the spillway are made up of interlayered mafic and pelitic schist, with sprays of biotite after amphibole, typical of the Moretown Formation. Between the rocks of the Hoosac Formation just seen and the Moretown Formation, there are some layers of garnet-rich pelitic schist that could be part of the Pinney Hollow Formation. They contain quartz, plagioclase, muscovite, biotite, chlorite, and garnet up to 3 cm in diameter. Some of the garnets have quartz inclusion trails that indicate a counter-clockwise sense of rotation when viewed to the N. This is consistent with other kinematic indicators that show tops to the W. An interesting feature of this section is that the degree of retrogressive alteration of garnet to chlorite is highly variable. Furthermore, some layers contain graphite, usually as inclusions in plagioclase and garnet. I believe that the graphite was precipitated from infiltrating fluids during metamorphism and that the variable retrogression reflects irregular fluid flow, probably during the normal-sense shearing that preceded the doming phase of deformation.

This is the location of garnet dated by Christensen et al. (1989) using $^{87}Sr/^{86}Sr$ variations; they found that the garnet grew at approximately 380 Ma over a 10 m.y. interval. Thompson et al. (1993) assigned rocks in the spillway to the Pinney Hollow and Ottauquechee Formations. If this assignment is correct, these units are very thin compared to their outcrop widths on the E flank of the Green Mountain massif.

Continue N on Route 30.

55.5 Turn left in parking area of Townshend Dam.

STOP 7. TOWNSHEND DAM ROADCUT, MORE OF THE MYLONITE ZONE, SW MARGIN OF CHESTER DOME. (30 min.) Please be very careful looking at this roadcut. It is a dangerous curve and cars drive by very fast. Stay off the pavement!

The most prominent feature of this long roadcut is the strong mylonitic fabric parallel to the compositional layering. There are abundant folds, boudinage, and rotated garnets. However, what impresses me is the extent of disrupted layering throughout the outcrop. The pelitic layers contain quartz, plagioclase, muscovite, biotite, chlorite, and garnet. The mafic layers contain quartz, plagioclase, hornblende, muscovite, biotite, garnet, and epidote.

Rosenfeld et al. (1988) called these rocks Ottauquechee Formation. I would prefer to assign them to the Moretown Formation. The rocks on the W side of the roadcut show the distinctive pinstripe texture of the Moretown Formation. Rocks in the middle and eastern end of the roadcut are admittedly more difficult to assign, but look like Moretown Formation to me based on their lithology. Whatever units these intermediate rocks belong to, there is not much distance between rocks belonging to the Hoosac Formation to the E and rocks that are clearly part of the Moretown Formation to the W. Compared with the typical sequence seen on the E flank of the Green Mountain massif, only several kilometers to the W, the section between the Hoosac and Moretown Formations here is highly

attenuated. Outcrops W of here along Route 30 are mapped as Moretown Formation and show the distinctive pinstripe texture. They do not, however, have the strong mylonitic fabric seen in this roadcut.

END OF TRIP.

REFERENCES CITED

Bell, T.H., and Johnson, S.E., 1989, Porphyroblast inclusion trails; the key to orogenesis: Journal of Metamorphic Geology, v. 7, p. 279-310.

Bohlen, S.R., Wall, V.J., and Boettcher, A.L., 1983, Experimental investigations and geological applications of equilibria in the system FeO-TiO_2 -Al_2O_3-SiO_2 -H_2O: American Mineralogist, v. 68, p. 1049-1058.

Bradley, D.C., 1983, Tectonics of the Acadian Orogeny in New England and adjacent Canada: Journal of Geology, v. 91, p. 381-400.

Bradley, D.C., Tucker, R.D., Lux, D.R., Harris, A.G., and McGregor, D.C., 2000, Migration of the Acadian Orogen and foreland basin across the Northern Appalachians of Maine and adjacent areas, U. S. G. S. Professional Paper 1624, 55 p.

Castonguay, S., Ruffet, G., Tremblay, A., and Feraud, G., 2001, Tectonometamorphic evolution of the southern Quebec Appalachians; (super 40) Ar/ (super 39) Ar evidence for Middle Ordovician crustal thickening and Silurian-Early Devonian exhumation of the internal Humber Zone: Geological Society of America Bulletin, v. 113, p. 144-160.

Chamberlain, C. P., and Conrad, M. E., 1993, Oxygen-isotope zoning in garnet; a record of volatile transport: Geochimica et Cosmochimica Acta, v. 57, p. 2613-2629.

Coney, P.J., 1979, Tertiary evolution of Cordilleran metamorphic core complexes, *in* Armentrout, M ; Cole, R ; TerBest, and H, Jr., eds., Cenozoic paleogeography of the western United States, Volume 3: Pacific Coast Paleogeography Symposium: Los Angeles, CA, United States, Pacific Section, Society of Economic Paleontologists and Mineralogists, p. 14-28.

Cook, S.M., and Karabinos, P., 1988, Polymetamorphic isograds from southeastern Vermont: Geological Society of America Abstracts with Programs, v. 20, p. 13.

Christensen, J.N., Rosenfeld, J.L., and DePaolo, D.J., 1989, Rates of tectonometamorphic processes from rubidium and strontium isotopes in garnet: Science, v. 244, p. 1465-1469.

Doll, C.G., Cady, W.M., Thompson, J.B., Jr., and Billings, M.P., 1961, Centennial geologic map of Vermont, Vermont Geological Survey.

Getty, S.R., and Gromet, L.P., 1992, Evidence for extension at the Willimantic Dome, Connecticut; implications for the late Paleozoic tectonic evolution of the New England Appalachians: American Journal of Science, v. 292, p. 398-420.

Goldstein, A.G., 1989, Tectonic significance of multiple motions on terrane-bounding faults in the Northern Appalachians: Geological Society of America Bulletin, v. 101, p. 927-938.

Hepburn, J.C., Trask, N.J., Rosenfeld, J.L., and Thompson, J.B.J., 1984, Bedrock geology of the Brattleboro quadrangle, Vermont-New Hampshire: Vermont Geological Survey Bulletin, v. no. 32, p. 162 p.

Hickey, K.A., and Bell, T.H., 2001, Resolving complexities associated with the timing of macroscopic folds in multiply deformed terrains; the Spring Hill Synform, Vermont: Geological Society of America Bulletin, v. 113, p. 1282-1298.

Hodges, K.V., Parrish, R.R., Housh, T.B., Lux, D.R., Burchfiel, B.C., Royden, L.H., and Chen, Z., 1992, Simultaneous Miocene extension and shortening in the Himalayan Orogen: Science, v. 258, p. 1466-1470.

Karabinos, Paul, 1984, Deformation and metamorphism on the east side of the Green Mountain massif in southern Vermont: Geological Society of America Bulletin, v. 95, p. 584-593.

Karabinos, P, 1998, Tectonic and stratigraphic development of the Connecticut Valley Trough in the New England Appalachians: Geological Society of America Abstracts with Programs, v. 30, p. 191.

Karabinos, P, 1999, Evidence for low-angle normal faulting in the Acadian Orogen: Is the Chester dome a core complex in Vermont?: Geological Society of America, Abstracts with Programs, v. 31, p. A-370.

Karabinos, P, 2000, Tectonic Significance of Textural Unconformities in Garnet from the New England Appalachians: Geological Society of America, Abstracts with Programs, v. 32, p. A-31.

Karabinos, Paul, and Aleinikoff, J. N., 1990, Evidence for a major Middle Proterozoic, post-Grenvillian igneous event in western New England: American Journal of Science, v. 290, p. 959-974.

Karabinos, Paul, and Aleinikoff, J.N., 1991, Zircon U-Pb and Pb-Pb evaporation ages of Paleozoic metavolcanic rocks from eastern Vermont, Geological Society of America, Abstracts with Programs, **23**, p. A310.

Karabinos, Paul, Aleinikoff, J.N., and Fanning, C.M., 1999, Distinguishing Grenvillian basement from pre-Taconian cover rocks in the northern Appalachians, American Journal of Science, **299**, p. 502-515.

Karabinos, P., and Laird, J., 1988, Structure and metamorphism from Jamaica to the Chester Dome, Vermont, in Bothner, W.A., ed., New England Intercollegiate Geologic Conference, Guidebook for Fieldtrips, p. 281-292.

Karabinos, P., Samson, S.D., Hepburn, J.C., and Stoll, H.M., 1998, Taconian Orogeny in the New England Appalachians; collision between Laurentia and the Shelburne Falls Arc: Geology, v. 26, p. 215-218.

Karabinos, P., and Thompson, J.B., Jr., 1997, Basement-cover relationships in southern Vermont, *in* Grover, T.W., Mango, H.N., and Hasenohr, E.J., eds., New England Intercollegiate Geological Conference: Castleton, Vermont, p. B3-1 to B3-20.

Karabinos, Paul, and Tucker, R.D., 1992, The Shelburne Falls arc in western Massachusetts and Connecticut: The lost arc of the Taconian orogeny, Geological Society of America, Abstracts with Programs, **24**, p. A288-289.

Karabinos, Paul, and Williamson, B. F., 1994, Constraints on the timing of Taconian and Acadian deformation in western Massachusetts: Northeastern Geology, v. 16, p. 1-8.

Kohn, M.J., and Spear, F.S., 1990, Two new geobarometers for garnet amphibolites, with applications to southeastern Vermont: American Mineralogist, v. 75, p. 89-96.

Kohn, M.J., and Valley, J.W., 1994, Oxygen isotope constraints on metamorphic fluid flow, Townshend Dam, Vermont, USA: Geochimica et Cosmochimica Acta, v. 58, p. 5551-5566.

Laird, J., and Albee, A.L., 1981, Pressure, temperature, and time indicators in mafic schist; their application to reconstructing the polymetamorphic history of Vermont: American Journal of Science, v. 281, p. 127-175.

Laird, J., Lanphere, M.A., and Albee, A.L., 1984, Distribution of Ordovician and Devonian metamorphism in mafic and pelitic schists from northern Vermont: American Journal of Science, v. 284, p. 376-413.

Menard, T., and Spear, F.S., 1994, Metamorphic P-T paths from calcic pelitic schists from the Strafford Dome, Vermont, USA: Journal of Metamorphic Geology, v. 12, p. 811-826.

Molnar, P., and Tapponnier, P., 1978, Active tectonics of Tibet: Journal of Geophysical Research, v. 83, p. 5361-5375.

Nisbet, B.W., 1976, Structural studies in the northern Chester dome of east-central Vermont: Ph.D. thesis: State University of New York at Albany, Albany, N.Y., 265 p.

Ratcliffe, N.M., 2000a, Bedrock geologic map of the Cavendish Quadrangle, Windsor County, Vermont, U. S. Geological Survey. Reston, VA, Map I-2598, 19 p. 1 sheet 1:24,000.

Ratcliffe, N.M., 2000b, Bedrock geologic map of the Chester Quadrangle, Windsor County, Vt., U. S. Geological Survey. Reston, VA, Map GQ-1773, 16 p, 1 sheet 1:24,000.

Ratcliffe, N.M., Aleinikoff, J.N., Armstrong, T.R., Walsh, G.J., and Hames, W.E., 2001, Intrusive relations and isotopic ages of Devonian granites in southern and central Vermont; evidence for a prolonged Acadian Orogeny and partitioning of compressional strain, *in* Geological Society of America Abstracts with Programs, v. 33 p. 81.

Ratcliffe, N.M., Aleinikoff, J.N., Burton, W.C., and Karabinos, P., 1991, Trondhjemitic, 1.35-1.31 Ga gneisses of the Mount Holly Complex of Vermont: evidence for an Elzevirian event in the Grenville Basement of the United States Appalachians: Canadian Journal of Earth Sciences, v. 28, p. 77-93.

Ratcliffe, N. M., Aleinikoff, J. N., and Hames, W. E., 1996, 1.4 Ga U-Pb zircon ages of metatrondhjemite of the Chester Dome, VT, and probable Middle Proterozoic age of the Cavendish Formation: Geological Society of America Abstracts with Programs, v. 28, p. 93.

Ratcliffe, N.M., Armstrong, T.R., and Aleinikoff, J.N., 1997, Stratigraphy, geochronology, and tectonic evolution of the basement and cover rocks of the Chester and Athens domes, *in* Grover, T.W., Mango, H.N., and Hasenohr, E.J., eds., New England Intercollegiate Geological Conference: Castleton, Vermont, p. B6 1- B6 55.

Richardson, C. H., 1929, The geology and petrography of Reading, Cavendish, Baltimore, and Chester, Vermont: Vermont Geological Survey, Report of the State Geologist for 1928, 16th Annual Report, p. 208-248.

Robinson, P., Tucker, R.D., Bradley, D., Berry, H.N., Osberg, P.H., 1998, Paleozoic orogenies in New England, USA: GFF, v. 120, p. 119-148.

Rosenfeld, J.L., 1954, Geology of the southern part of the Chester dome, Vermont: Ph.D. thesis, Harvard University, Cambridge, Mass., 303 p.

Rosenfeld, J.L., 1968, Garnet rotations due to the major Paleozoic deformations in southeast Vermont, Chap. 14: *in* Studies of Appalachian geology, northern and marine, Zen, E-an, et al., eds., New York, Interscience Publishers, p. 185-202.

Rosenfeld, J.L., Christensen, J.N., and DePaolo, D.J., 1988, Snowball garnets revisited, southeastern Vermont, *in* Bothner, Wallace, ed., New England intercollegiate geological conference 80th annual meeting; Guidebook

for field trips in southwestern New Hampshire, southeastern Vermont, and north-central Massachusetts., p. 223-240.

Rowley, D.B., and Kidd, W.S.F., 1981, Stratigraphic relationships and detrital composition of the Medial Ordovician flysch of western New England: Implications for the tectonic evolution of the Taconic orogeny: Journal of Geology, v. 89, p. 199-218.

Selverstone, J., 1985, Petrologic constraints on imbrication, metamorphism, and uplift in the SW Tauern Window, Eastern Alps: Tectonics, v. 4, p. 687-704.

Selverstone, J., Spear, F.S., Franz, G., and Morteani, G., 1984, High-pressure metamorphism in the SW Tauern Window, Austria; P-T paths from hornblende-kyanite-staurolite schists: Journal of Petrology, v. 25, p. 501-531.

Sonder, L.J., England, P.C., Wernicke, B.P., and Christiansen, R.L., 1987, A physical model for Cenozoic extension of western North America, *in* Coward, P , Dewey, J., and Hancock, F,. eds., Continental extensional tectonics., Volume 28: Geological Society Special Publications: London, United Kingdom, p. 187-201.

Spear, F.S, 1992, Inverted metamorphism, P-T paths and cooling history of west-central New Hampshire; implications for the tectonic evolution of central New England, *in* Robinson, P., and Brady, J., eds., New England Intercollegiate Geological Conference, Guidebook for field trips in the Connecticut Valley region of Massachusetts and adjacent states., p. 446-466.

Spear, F.S., and Harrison, T.M., 1989, Geochronologic studies in central New England; I, Evidence for pre-Acadian metamorphism in eastern Vermont: Geology, v. 17, p. 181-184.

Stanley, R.S., and Ratcliffe, N.M., 1985, Tectonic synthesis of the Taconian orogeny in western New England: Geological Society of America Bulletin, v. 96, p. 1227-1250.

Thompson, A. B., Tracy, R. J., Lyttle, P. T., and Thompson, J. B., Jr., 1977, Prograde reaction histories deduced from compositional zonation and mineral inclusions in garnet from the Gassetts Schist, Vermont: American Journal of Science, v. 277, p. 1152-1167.

Thompson, J.B., Jr., 1950, A gneiss dome in southeastern Vermont: Ph.D. thesis: Massachusetts Institute of Technology, Cambridge, Mass., 149 p.

Thompson, J.B., Jr., McLelland, J.M., and Rankin, D.W., 1990, Simplified geologic map of the Glens Falls 1 degrees X 2 degrees Quadrangle, New York, Vermont, and New Hampshire: Reston, VA, United States, U. S. Geological Survey, 1 sheet p.

Thompson, J.B., Jr., Rosenfeld, J.L., and Chamberlain, C.P., 1993, Sequence and correlation of tectonic and metamorphic events in southeastern Vermont, *in* Cheney, J., T., and Hepburn, J.C., eds., Field trip guidebook for the northeastern United States., Geological Society of America, p. B.1-B.26.

Tucker, R.D., Osberg, P.H., and Berry, H.N.I., 2001, The geology of a part of Acadia and the nature of the Acadian Orogeny across central and eastern Maine: American Journal of Science, v. 301, p. 205-260.

Tucker, R.D., and Robinson, P., 1990, Age and setting of the Bronson Hill magmatic arc: A re-evaluation based on U-Pb zircon ages in southern New England: Geological Society of America Bulletin, v. 102, p. 1404-1419.

Vance, D., and Holland, T., 1993, A detailed isotopic and petrological study of a single garnet from the Gassetts Schist, Vermont: Contributions to Mineralogy and Petrology, v. 114, p. 101-118.

Walsh, G.J., and Aleinikoff, J.N., 1999, U-Pb zircon age of metafelsite from the Pinney Hollow Formation; implications for the development of the Vermont Appalachians: American Journal of Science, v. 299, p. 157-170.

Eurypterids: Central-Eastern New York Fieldtrip
Samuel J. Ciurca, Jr., Joseph LaRussa, Rochester, New York

ROADLOG

START

0.0 Intersection of US20 and NY10, Sharon Springs
Head west on US20.

1.1 Leesville

5.2 Parking Area

5.8 Outcrops on both sides of road. Important sections revealing a number of Early Devonian stratigraphic units including the Kalkberg and included metabentonites.

6.4 EXIT NY 166.

6.5 TURN RIGHT onto NY166.

7.0 **STOP 1 Outcrops of Thacher Formation and overlying units.**
This section exhibits a wonderful stratigraphic sequence of limestones of various characteristics, but is little different from the type Olney Limestone at Split Rock near Syracuse, New York. These units are within the Early Devonian *Erieopterus* Biozone. *Howellella* (occurring in enormous numbers), and *Megambonia* are characteristic here as they are in the type Olney Limestone at Syracuse. In this region (Cherry Valley), *Erieopterus* occurs in beds with these typical marine forms and in ostracodal limestone interbeds. Progressively westward, typical marine forms disappear, especially in the dolomitic units (Chrysler Formation of the Syracuse area, Honeoye Falls Dolostone south of Rochester, and the Clansbrassil Formation of Ontario, Canada.

.

Turn around and head back to US20

7.5 TURN LEFT onto US20 and head west.

11.8 East Springfield

15.1 JCT. NY80

16.2 Petrified Creatures "Museum of Natural History"

17.7 Warren

20.5 Richfield Springs

21.2 JCT. NY167

23.7 Brighton Corners

28.8 East Winfield

29.7 JCT. NY51, TURN RIGHT.

32.8 Cedarville

33.0 TURN LEFT.

33.2 Intersection NY51 North
Continue west (straight) on Cedarville Road.

36.0 Intersection with Jerusalem Hill Road

STOP 2 Litchfield Town Hall Site
While a relatively shallow roadcut, opposite the Litchfield Town Hall, the small exposure of the Phelps Waterlime at the top of the Fiddlers Green Formation here has yielded hundreds of eurypterid specimens. This is not a classic locality as Tollerton (1997) implied. Within Litchfield Township and nearby areas, Clarke & Ruedemann (1912) described that in the 1800s, eurypterids were collected from rock fences and barn foundations. No specimens were obtained from bedrock and the stratigraphy of the eurypterid-bearing beds was poorly known at the time. In the 1960s, the Litchfield Town Hall Site was a glacially polished and striated mass of waterlime that was difficult to examine. A eurypterid carapace appeared on the polished surface and I and some associates began to slowly excavate the upper portions of the Fiddlers Green here. Over the following several years, we extracted hundreds of specimens indicating a fauna identical to that found at the well-known Passage Gulf roadcut. One scorpion has been

recovered from this site as well as cephalopods, ostracods, a phyllocarid and several species of eurypterids—all part of the *Eurypterus remipes* Biozone.

At this stop we will examine the transition from the underlying Victor Member to the overlying Phelps Member of the Fiddlers Green Formation. Various sedimentary structures, including stromatolites and mudcracks, are present and, of course, we will look for eurypterid remains.

TURN AROUND and head back to Cedarville.

38.7 STOP SIGN – TURN LEFT onto NY51 (winding road).

40.5 **STOP 3 Syracuse Formation (Salina Group) on right.**
Small section exhibiting typical Syracuse Formation. The *Waeringopterus* Biozone is found within the lower portions of the Syracuse Formation in this part of the state.

41.0 **STOP 4 Red shale of the Vernon Formation (Salina Group) on left and right.**
Approaching the base of the Salina Group, we see here exposures of the bright red Vernon Formation. In this part of the state, the *Hughmilleria* Biozone occurs within basal beds of the formation. Pterygotids are also well-known, especially those of the Downing Brook Member.

45.7 Village of Illion

47.1 Intersection E. Clark Street TURN RIGHT, head to Mohawk (street changes to E. Main Street).

48.0 Village of Mohawk

48.8 JCT. NY28, continue forward.

49.4 JCT. NY5S, continue to I90, NYS Thruway on right.

49.7 TOLL BOOTH, head west to Canastota exit for next stop.

92.6 Canastota Exit 34, leave Thruway, TURN LEFT on NY13 South.

95.0 Intersection NY5/Oxbow Road, CONTINUE SOUTH.

97.0 Clockville

98.0 REST AREA ON RIGHT, drive in and park.

STOP 5 Roadcut on east side of the highway.
This roadcut reveals one of the most important (eurypterid-bearing) sections in this part of the state. The top of the Fiddlers Green is exposed in a drainage ditch, and upsection, several other Siluro-devonian units are exposed. Eurypterid horizons begin with the top of the Fiddlers Green Formation (Bertie Group)—the Phelps Waterlime, exposed in the ditch, has yielded fragmentary eurypterid remains and salt hoppers. The Cobleskill Formation is also well-exposed on the east side of the road. The formation consists of 3 members: a lower dolostone, middle limestone member, and an upper dolostone. The dolostones are massive, and the upper dolostone is important for the *Eurypterus* fauna it contains. The Silurian-Devonian boundary is placed above this unit. Early Devonian sedimentation is revealed by the waterlime beds (Chrysler Formation) in the sequence above the Cobleskill Formation. *Erieopterus microphthalmus* is characteristic of these waterlimes and also the lower beds of the overlying Thacher Limestone.

TURN AROUND and head back to NY5 (north).

99.0 Clockville

100.0 NY5 TURN LEFT (west).

106.1 Chittenango Falls

106.6 TURN LEFT and follow NY13 (south).

106.8 TURN LEFT towards Cazanovia. Follow NY13 south towards Chittenango Falls State Park.

111.4 REST AREA ON RIGHT, drive in and park.

STOP 6 Roadcut on east side of the highway, Chittenango Falls Roadcut.
This cut begins with the Akron-Cobleskill. While an occasional stromatoporoid has been found in the Akron-Cobleskill here, note the lack of the fossiliferous limestone, observed at Clockville, in the section exposed here. Overlying Chrysler dolostones are known for the fine celestite and calcite specimens obtained here over the years. Large pieces of eurypterid integument have been

observed on some massive chunks of fallen Akron-Cobleskill at this site and at Clockville. Above is a thick sequence of limestones, including the *Erieopterus*-bearing Thacher Limestone.

Turn around and head north on NY13.

115.9 NY5, TURN LEFT (west) Intersection of NY173.
116.0 TURN WEST onto NY173 (west), head towards Manlius and Syracuse.
121.4 Entering Manlius
122.4 JCT. NY92, continue on NY173.
127.4 JCT. NY91 (Jamesville), proceed west on NY173.
130.7 TURN LEFT, follow NY173.
131.5 JCT. US11, continue on NY173 and up the hill.
133.4 JCT. NY175, continue on NY173.
136.7 Onondaga Blvd. (signal light at intersection), TURN LEFT and go to the end of the road (base of Split Rock Quarry).
137.4 Split Rock Quarry – we will walk up the hill to enter this large quarry complex.

Stop 7 Split Rock Quarry

This old abandoned quarry, which we can only hope will be preserved, contains a wonderful section of the Olney Limestone. The Early Devonian *Erieopterus microphthalmus* occurs abundantly in strata just beneath the Olney Limestone, in the lower beds of the Olney, and in several feet of strata near the top. The occurrence is analogous to the famous Bertie Group eurypterid horizons in that the eurypterid remains occur in windrows (current induced accumulations of animal and plant remains). While pterygotid remains are relatively rare here, they been found within the *Erieopterus*-bearing horizons in this quarry.

Turn around and head back to the stoplight. TURN LEFT and head up to NY 5. TURN RIGHT at the light and go to I690 (and the New York State Thruway) and head in the direction you need to go to return home.

LATE CAMBRIAN (SAUK) CARBONATE FACIES IN HUDSON-MOHAWK VALLEY OF EASTERN NEW YORK STATE

Gerald M. Friedman
Department of Geology, Brooklyn College and Graduate Center of the City University of New York, Brooklyn, NY; Northeastern Science Foundation, Inc., affiliated with Brooklyn College, Rensselaer Center of Applied Geology, Troy, NY; For correspondence: Northeastern Science Foundation, 15 Third Street, P.O. Box 746, Troy, NY 12181, USA; gmfriedman@juno.com

GEOLOGIC SETTING

During the Late Cambrian, eastern New York State lay within the tropical zone in the southern hemisphere, in which an enormous tropical carbonate platform was bounded on both north and south (respectively west and east, today) by deep ocean basins. During Cambrian-Ordovician itme, most of the North American continent was a shallow epeiric sea, known as the Great American Bank. At its edge terrigenous and carbonate sediment moved by slides, slumps, turbidity currents, mud flows, and sandfalls down a relatively steep slope to oceanic depths coming to rest at the deep-water basin margin (rise) (Sanders and Friedman 1967; Friedman 1972, 1979; Keith and Friedman 1977, 1978; Friedman and Sanders 1978; Friedman et al. 1982). The paleoslope was probably an active hinge line between the continent to the west and the deep ocean to the east, resembling the Jurassic hinge line of the eastern Mediterranean (Friedman et al. 1971). Such hinge lines in the early history of mountain belts are localized by contemporaneous down-to-basin normal faulting (Rodgers 1968, quoting Truempy, 1960). Later thrusting has lifted the deep-water facies into juxtaposition with the shelf facies along hinge-line faults. This displacement was so great that the Cambrian and Early Ordovician deep-water sediments were shifted far west of their original basin margin.

Figure 1 reconstructs the paleogeomorphic profile across the Late Cambrian passive margin of North America in New York State. Here, the Sauk Sequence is composed predominantly of carbonate rocks and it outcrops in two discrete provinces separated by the "Rickard's line" (R in Fig. 1), across which the Sauk Sequence abruptly thickens toward the east. The absence of Lower to Middle Cambrian rocks in west-central New York in part produces the abrupt change in thickness across Rickard's line. "Rickard's line" corresponds to the "edge of Middle/Lower Cambrian rocks", (plate 3 of Rickard 1973) which has been named by John E. Sanders in Friedman et al. (1993).

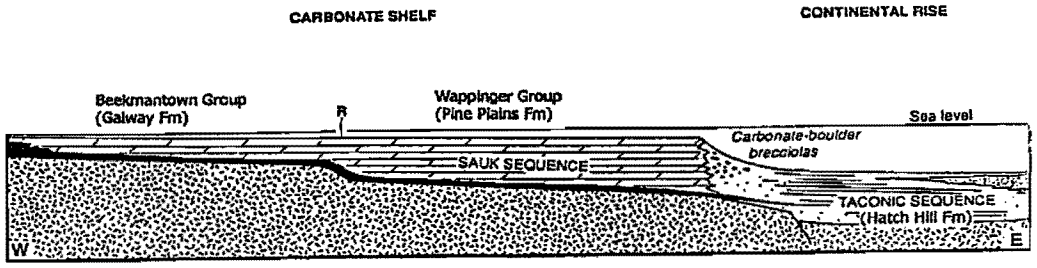

Figure 1

Figure 1. Reconstructed paleogeomorphic profile-section across the Late Cambrian passive margin of North America. This section includes Precambrian basement, basal quartzose sandstone (black), and dolostone-distribution pattern for the Sauk Sequence. The latter includes limestones on the seaward part of the former carbonate shelf (Friedman et al. 1993; Friedman 1995). R="Rickard's line", a feature across which the Sauk Sequence shows an abrupt increase in thickness (see text).

The Sauk Sequence interfingers with the Taconic Sequence. On the shelf the Beekmantown Group includes the Galway Formation and the Wappinger Group includes the Pine Plains Formation (Fig. 1). The Taconic Sequence includes the Hatch Hill Formation (Fig. 1).

Road Log

From Lake George drive to Saratoga then take NY50 to the East Parking Lot of the Saratoga Performing Arts Center (SPAC) (necessitating a left turn). Park near box office of Arts Center.

STOP #1. Saratoga Spa State Park: Modern Nonmarine Limestones (Travertine)

This stop can also be reached through the Main Gate of the State Park on Route 9.

Route of Walk

Walk downhill into a small wood with picnic tables towards a stone building. Bicarbonate- charged, saline waters issue from a faucet at the side of the building and pass through a pipe below dirt road, re-emerging on the bank of Geyser Brook. Calcite precipitates on the steep slope of this bank, forming a terrace of travertine. The water is known as Orenda Spring and the terrace as Orenda Terrace; we will get a better view of this terrace later from below. A walk of a few hundred feet along road leads to the Hayes Well Spring at bridge across Geyser Brook. A taste of this water is "rewarding" for its initial effect. Prolonged drinking is not recommended. From Hayes Well Spring you see the Island Spouter "Geyser" a few hundred feet upstream. The water of this fascinating "geyser" is from a well; the water spouts from a small orifice to a height of about 30 feet. This well was drilled about 80 years ago and the large cone of travertine has formed since.

Follow the path along Geyser Brook upstream. In the bank on the left is an exposure of Middle Ordovician Canajoharie Shale, an outer shelf to slope facies. On occasion, graptolites can be found in this shale. Continue to Orenda terrace to study travertine. Note the rippled surface of the travertine and the brown iron-oxide coloration that occurs in streaks. Up to approximately 4 cm of calcite may precipitate annually at the foot of the terrace. Note "caves" and dripstone at far end of terrace and search for calcite-coated twigs and leaves or impressions of leaves in the travertine (Fig. 2). Pisolites occur in abundance on the walkway between travertine cone and bank of brook, spheroids and oolites are likewise present (Fig. 3) (Friedman 1997a,b; Schreiber et al. 1981).

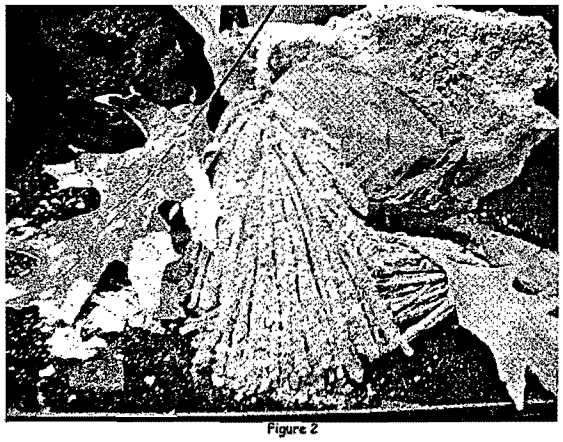

Figure 2. Calcite-coated twigs, leaves, and impressions of leaves in the travertine.

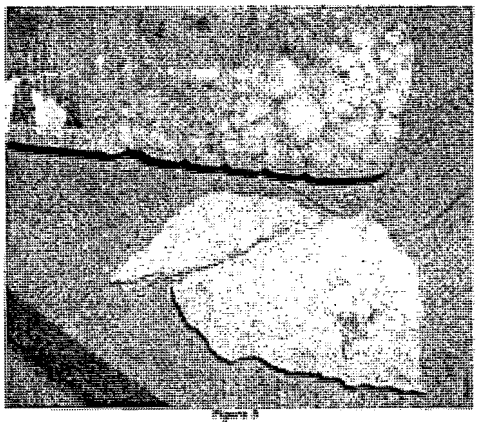

Figure 3. Pisolites from bank between travertine cones and brook.

Discussion

Although in the classical studies on limestones, including the authoritative work of Pia (1933), nonmarine limestones are accorded some measure of importance, the literature on modern carbonates neglects nonmarine carbonates. At this stop you'll see an excellent example of travertine, a rock which, like reef-rock, crystallizes in an initially stony condition.

The term travertine is derived from the Italian word, travertino, a corruption of tiburtino, "the stone of Tibur", which is a former name of the locality now called Tivoli (see Sanders and Friedman, 1967, p. 176), The type locality at Tivoli has been classically described by Lyell (1830, p. 207-210) and Cohn (1864). Some authors make a sharp distinction between the terms travertine, tufa and sinter: others use these terms synonymously (Pia, 1933; Gwinner, 1959, Sanders and Friedman, 1967, p. 176).

Travertine in Saratoga Spa Park gathers around the orifice of wells, on terraces from which water descends, or as a cone around a "geyser". Waters enriched in calcium bicarbonate issue from the subsurface, lose their carbon dioxide and insoluble calcite precipitates:

$$2HCO_3^- + Ca^{++} \leftrightharpoons 2CaCO_3 + H_2O + CO_2 .$$

Twigs and leaves of beech, maple, and oak are preserved as they become coated with calcite or leaves form impressions in the travertine. The calcium bicarbonate-enriched waters originate nearly 1,000 feet below the surface in the underlying Cambrian-Ordovician limestones and dolostones, (Friedman 1997a,b). The waters are confined as in an artesian well beneath a thick cover of impervious Canajoharie Shale from which drilling recovers them. In the early years, the springs issued from natural crevices in the rocks, particularly from the prominent MacGregor fault. Later, pits were dug; the present wells flow through pipes set in bore holes.

The composition of the Saratoga mineral waters is unique among waters that precipitate travertine (Back et al. 1995; New York State Department of Health 1959; Young and Putnam 1979). Most waters that make travertine, especially those of the classical areas in Europe, drain areas of karst, and are of low salinity. By contrast, analyses of Saratoga waters give salinities that geologists classify as "brackish" (approximately 11 %). Inspection of tables of analyses (e.g. Kemp, 1912) indicates the closeness of the composition of these waters to that of formation waters. This is especially true of the high concentration of NaCl. As the waters in the subsurface apparently

dissolve limestones and dolostones, the concentration of the calcium, magnesium, and bicarbonate is higher than that of many formation waters. As in most formation waters, the sulfate content is low. Although the origin of the mineral waters is controversial (Hewitt, McClennan, and Nilsson, 1965), this controversy parallels that of the origin of formation waters. The mineral waters are probably formation waters whose salinity has been lowered as a result of mixing with meteoric water.

Newly precipitated calcite from the Orenda Springs gives a strontium isotopic value of 0.716429 (10) $^{87}Sr/^{86}Sr$ (+/-2S.D)*, a continental crust signature (Fig. 4). If the waters were derived Upper Cambrian formation water, an Upper Cambrian seawater signature would have been obtained (see Fig. 4).

Figure 4. Plot of $^{87}Sr/^{86}Sr$ for Late Cambrian seawater, continental crust, and carbonate samples from passive margin in New York State. Explanation in text.

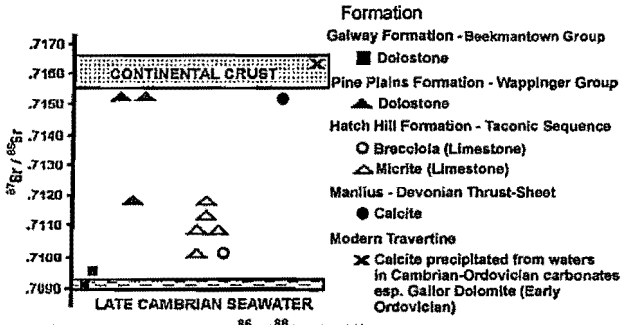

Figure 4

According to Siegel (1996) carbon isotopic analyses likewise hint that the carbon may be expelled from the mantle many kilometers below the fault zone.

The aquifer containing the mineralized water is under carbon-dioxide pore pressures which are estimated to be as high as five atmospheres that spew mineral water and gas several meters high (Siegel 1996). The acidity of the mineral waters depends on how much carbonic acid they contain; pH typically ranges from 5.5 to 6.5. The mineral springs discharge cold water (Sneeringer and Dunn, 1981).

The distribution of the wells, a total of about 200, is controlled by the MacGregor Fault and its subsidiary faults. The mineral waters always occur on the eastern (downthrown side) of the fault.

Puzzling is the observation that the precipitate is calcite rather than aragonite. Travertine in other places is usually calcite, but the composition of the responsible mineral waters shows depletion in magnesium. By contrast the mineral waters of Saratoga are enriched in magnesium and because the magnesium ion inhibits the formation of calcite, aragonite should result, but apparently does not. This question deserves study.

Hollocher (2002) notes that the spring waters are saline and carbonated, and derived from the Beekmantown Group carbonate rock aquifer at depths of 100 m in the Spa State Park. All springs and drilled wells occur just to the east of the Saratoga Springs-McGregor fault, a probable Taconian normal fault.

Comparing the strontium isotopic compositioin of the modern travertine of the Saratoga Spa State Park with the strontium isotopic composition of nearby exposures of Cambrian Beekmantown (Galway) carbonate rock (Fig. 5) shows that the travertine composition overlaps that of continental crust, whereas the Beekmantown Group has the composition of Late Cambrian seawater. The strontium isotopic composition of this travertine reflects extant

* The Sr analyses are normalized to $^{86}Sr/^{88}Sr = 0.11940$. Analyses of NBS 987 averaged 0.710241 (09) (n = 39) during the period of these analyses. Errors on $^{87}Sr/^{86}Sr$ are given as 2 sigma (95%) in the last two digits.

meteoric freshwater that modified the marine Upper Cambrian Beekmantown carbonate and hence yields a continental crust isotopic ratio (Fig. 5).

Leave parking lot of Performing Arts Center and turn north on NY 50.

Cumulative Mileage	Miles From Last Point	Route Description
0.6	0.6	Bear left following sign to NY 29.
1.8	1.2	Drive to traffic light and turn left (west) on NY 29.
3.9	2.1	Turn right (north) on Petrified Sea Gardens Road. Drive past "Petrified Gardens" to Lester Park.
5.1	1.2	Alight at Lester Park.

STOP #2. Lester Park: Domed Cyanobacterial Cabbage-Head Stromatolites: Hoyt Limestone of Late Cambrian Age

This locality is the site of one of the finest domed microbial mats to be seen anywhere preserved in ancient rocks.

It is significant in the history of geology as the area where stromatolites were first described and interpreted (Figs. 5-16). These structures are part of the Hoyt Formation of Late Cambrian (Late Franconian to Early Trempeleauan) age (490-505 Ma).

The stromatolites ("layered stones") were constructed by microscopic cyanobacteria, formerly known as "blue-green algae", on a shallow epeiric sea floor, when New York and the eastern United States lay south of the equator. They represent the activities of organisms that generated the earth's first abundant oxygen. The Hoyt Formation contains trilobites assigned to the Saukia zone of the Late Cambrian (Trempeleauan Stage); it unconformably overlies the Galway or Theresa Formation and underlies the Ordovician Gailor Formation (Fig. 9) (Cushing and Ruedemann 1914; Fisher 1968, 1977, 1980; Flagler 1966; Mazzullo et al. 1978; Landing 1979; Ludvigsen and Westrop 1983; Sternbach and Friedman 1984; Friedman 1985).

The earliest reference to stomatolites was that of Steele (1825) whose first description of North American oolitic limestone also called attention to the presence of what we recognize today as domal stromatolites. "Great quantities of calcareous concretions of a most singular structure; they are mostly hemispherical but many of them are globular and they vary in size from half an inch to that of two feet in diameter"(Steele 1825, p. 17). Hall (1847, 1883) considered these "singular structures" to be the remains of sea plants. In later descriptions Hall (1883) assigned them genus status and proposed the Linnaean binomial, *Cryptozoön proliferum*. Hall recognized several kinds of species to designate "a peculiar form and mode of growth". Early descriptions of these stromatolites include those of Cushing and Ruedemann (1914) and Goldring (1937, 1938). Burne and Moore (1993) termed these structures "the first formally-named stromatolite".

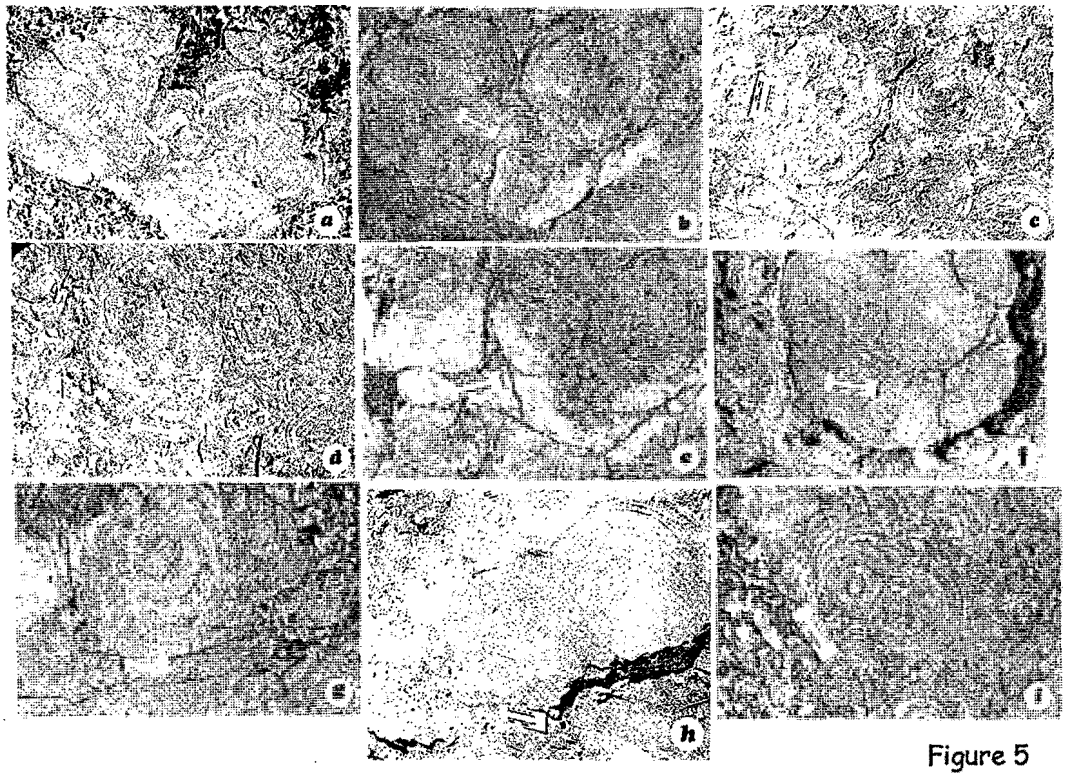

Figure 5

Figure 5a-i. Glaciated surface exposing horizontal section of domal stromatolites at Lester Park showing internal geometry. The composite structures of the stromatolitic hemispherical heads result from concentric growth around centers. Neighboring heads and centers merge and coalesce into one another resulting in complex microbial structures. Lester Park.

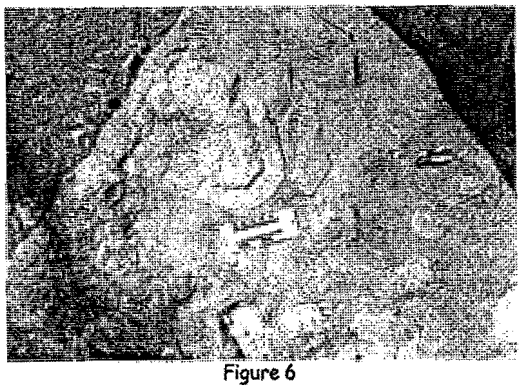

Figure 6

Figure 6. Microbial stromatolite heads distributed through skeletal-oolitic grainstone in which quartz-sand particles are common. Lester Park.

Figure 7

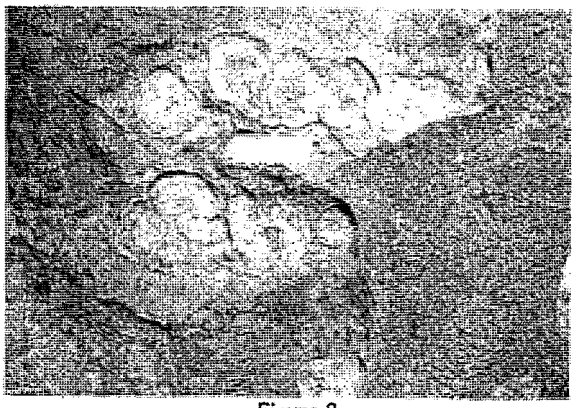

Figure 8

Figures 7-8. Microbial stromatolite heads distributed through skeletal-oolitic grainstone in which quartz-sand particles are common. Lester Park.

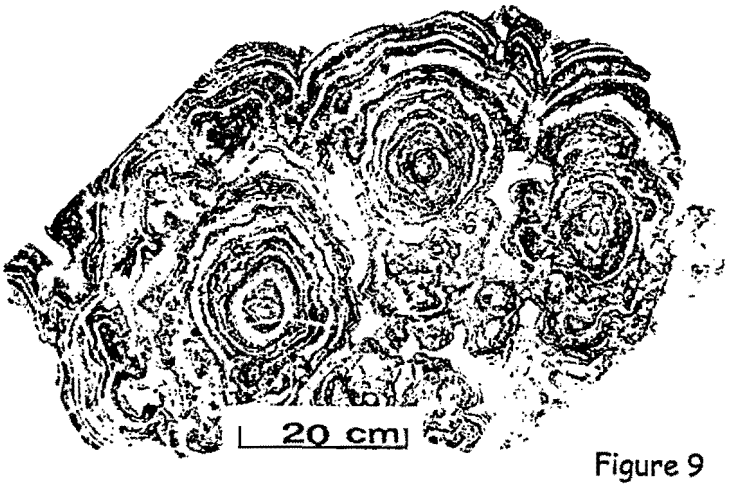

Figure 9

Figure 9. Cross-sectional view of hemispherical stromatolites.

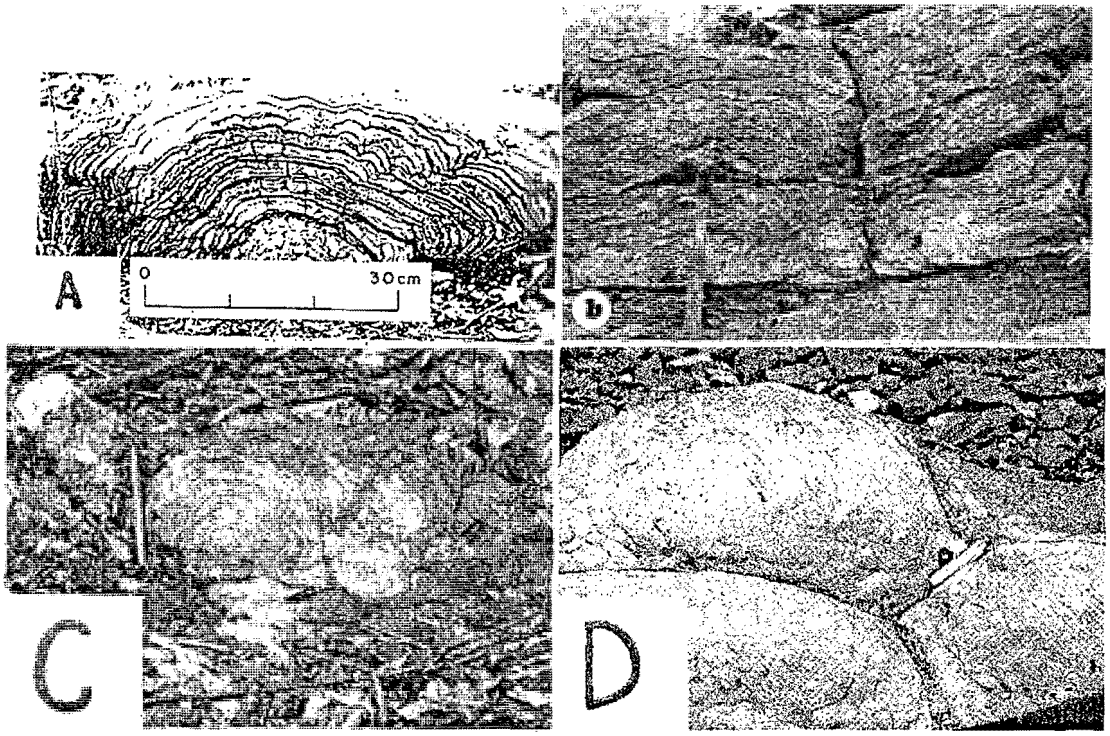

Figure 10

Figure 10 (a-d). Sectional view of microbial stromatolites showing domed laminae known as cabbage-head structures. A) Alternating laminae are composed of recessed calcite laminae and protruding dolomite laminae (Owen and Friedman 1984). B) Laterally-linked domal stromatolites are composed of dolomite. C) Vertical section exposing hemispherical stromatolites. D) Domal stromatolites in correlative rocks near Whitehall, New York, showing three-dimensional configuration.

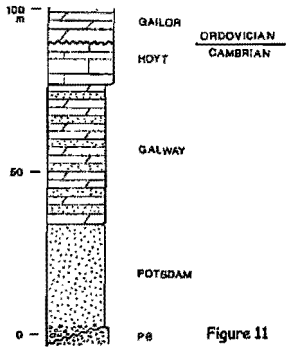

Figure 11

Figure 11. Generalized lithologic column shows upper Cambrian and lowest Ordovician formations exposed in Saratoga County, New York.

Figure 12

Figure 12. Historical marker, Lester Park.

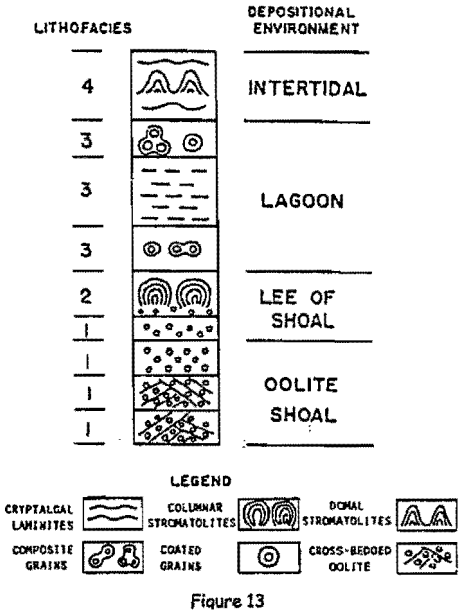

Figure 13

Figure 13. Vertical succession showing continuous progradational sequence. The upward increase in lithofacies number suggests progressively shoreward deposition (Owen and Friedman 1984).

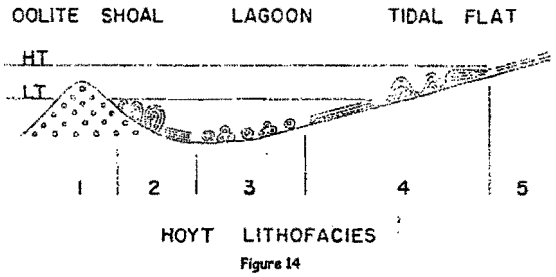

Figure 14

Figure 14. Hypothesized depositional model. The lagoon and intertidal zone are greatly shortened. Total width of Hoyt deposition was probably on the order of 15 to 30 km (Owen and Friedman 1984). Numbers refer to lithofacies shown in figure 11.

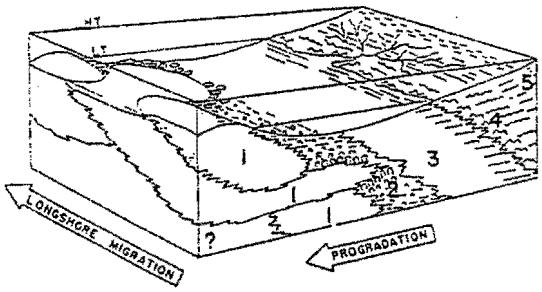

Figure 15

Figure 15. Facies relations resulting from longshore migration of oolite shoals and progradation of carbonate build-up. Block diagram shows generalized facies relations interpreted for dynamic Hoyt depositional model (Owen and Friedman 1984). Numbers refer to lithofacies shown in figure 13.

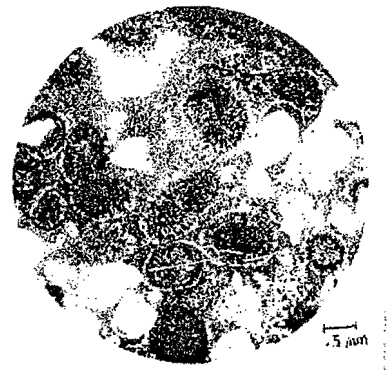

Figure 16

Figure 16. Photomicrograph, x30, of a thin section of Cryptozoön proliferum, showing oölites and quartz grains (clear); Hoyt limestone, Greenfield, New York (Goldring 1938, Fig. 13A, p. 34).

Kalkowsky (1908) coined and defined the term "stromatolith" 83 years after Steele's discovery and 25 years after Hall assigned the term *Cryptozoön*. As Walter (1976, p. 1) notes "the original definition is now of historical interest only". He prefers the definition of stromatolites as "organosedimentary structures produced by sediment trapping, binding, and/or precipitation as a result of the growth and metabolic activity of micro-organisms, principally cyanophytes", an unpublished definition proposed by S.M. Awramik and L. Margulis in 1974. Burne and Moore (1987) proposed the term microbialites for these organosedimentary structures and for deposits of laminated internal structure, such as the cabbage-head microbialites, they employ the term stromatolitic microbialites. Jackson (1997) uses the term microbial laminites.

Interestingly, Grabau and Shimer (1909) placed these domed stromatolites with the stromatoporoids; Rothpletz (1916) concurred with this interpretation. In the interim stromatoporoids which formed large reefs in the Silurian and Devonian were ascribed to coelenterates and sponges (particularly sclerosponges). Hall (1883) noted that these domed structures which we now recognize as stromatolites "have long been known under the name of stromatopora, from their general resemblance in form and structure to that fossil", but objected because "a careful examination of the nature of these bodies proves that while having a concentric structure common to stromatopora they have not the regular succession of tubuli characteristic of species of that genus". Only recently have we returned to Grabau and Shimer and Rothpletz in the idea that Paleozoic stromatoporoids represent fossilized stromatolites (Kazmierczak and Kempe 1990).

Cushing and Ruedemann (1914) assigned the name Hoyt Formation to the stratigraphic interval containing the domed stromatolites referred to by them as *Cryptozoöns*, and Goldring (1938) published an extensive paper on these stromatolites which she considered to be reef builders. The title of her paper speaks for itself: "Algal barrier reefs in the lower Ozarkian of New York with a chapter on the importance of coralline algae as reef builders through the ages". Apparently she considered these microbial structures to be the skeletons of coralline algae. Fisher and Hanson (1951) revised the geology of Saratoga Springs and vicinity, especially the section in which the spectacular stromatolites occur. More recent studies of these domed stromatolites are those by Owen and Friedman (1984) and Friedman (1985, 1987a,b, 1988a,b, 1995, 1997a,b).

Walcott discovered an abundant trilobite fauna and through his publications the Hoyt Limestone became the only fully illustrated and completely described Upper Cambrian trilobite fauna from epeiric carbonates of the eastern United States (Walcott 1879, 1890, 1912). The trilobites are disarticulated but unabraided and transportation appears to have been minimal (Taylor and Halley, 1974). Ludvigsen and Westrop (1983) revised all of the trilobites known to occur in the Hoyt Limestone.

In addition to inarticulate trilobites the fossils present include simple conical conodonts (Landing 1979), and echinoderm debris.

LOCATION AND DISTRIBUTION

Lester Park includes a quarry, named Hoyt Quarry, which serves as geologic reference for the Hoyt Limestone, a rock unit that extends around the southeast side of the adjacent Precambrian Adirondack Mountains. Several Late-Cambrian-age fossils are found only here and farther south along the Hudson River.

Goldring (1938) recognized the presence of three species of stromatolites (which she referred to as calcareous algae): *Cryptozoön proliferum* Hall, *C. ruedemanni* Rothpletz, and *C. undulatum* Bassler. A glaciated surface at Lester Park exposes the spectacular internal geometry of *Cryptozoön proliferum* Hall, noted by her as domal stromatolites (Figs. 5-10).

Across the road (west) from Lester Park Rothplatz (1916) described this same "species", which occurs as a bed of stromatolites resting upon oolitic limestone and oolitic limestone overlies it again. This section of stromatolites is composed of dolomite.

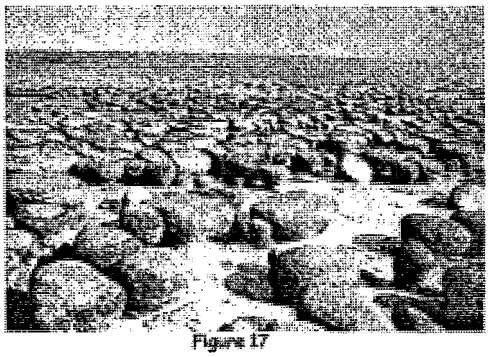

Figure 17. Modern subtidal to intertidal columnar stromatolites at Hamlin Pool, Western Australia. (Shinn 1983). Photo courtesy of R.N. Ginsburg.

GEOLOGIC AND SEDIMENTOLOGICAL SETTING

In places glaciated surfaces expose horizontal sections of domed heads, known as cabbage-head structures (Fig. 5a-i). These cabbage-heads, many of them compound, occur as vertically stacked, hemispherical stromatolites. They are composed of discrete bulbous and domal structures built of hemispheroidal stromatolites expanding upward from a base, although continued expansion may result in the fusion of neighboring colonies (Friedman et al. 1982). The heads, many of them compound, are circular in horizontal sections, and ranging in diameter from a few centimeters to a meter. These structures apparently possessed relief of up to 0.75m above the surrounding substrate. The size of the larger heads suggests that they formed in highly turbulent waters.

The Hoyt Limestone was deposited in a peritidal setting along a prograding shoreline (Owen and Friedman 1984). Oolite shoals and stromatolitic buildups restricted oceanic circulation causing locally increased salinity which contributed to dolomitization.

The lower part of one of the sections (Lester Park) provides the most complete sequence observed in the Hoyt Formation. Five lithofacies have been recognized. A vertical sequence from Lithofacies 1 to Lithofacies 4 is

represented in Figure 13. Lithofacies 1 consists of ooids, some crossbedding, and sparry calcite cement. Lithofacies 2 is composed of partially dolomitized, domal stromatolites containing abundant carbonate particles (skeletal fragments, especially of trilobites, ooids and oncolites) and horizontal burrows. Lithofacies 3 consists of dolomitic micrite to siltstone containing composite particles. These carbonates are dark gray in color and are interpreted as deposits that formed under somewhat reducing conditions. Bioturbation features and lenses of skeletal trilobite debris are present. Channeled indistinct laminae between domal stromatolites have been designated lithofacies 4. Lithofacies 5 consists of stromatolitic laminae with local mudcracks and birdseye textures (not shown in Fig. 13).

Figure 14 shows the depositional environments ranging from the lee of an oolite shoal upward to the lower intertidal zone. The sequence seen here may have resulted from the lowering of sea level (regression) or from the depositional buildup of carbonates (progradation).

Figures 14 and 15 present a cross-section of the interpreted Hoyt depositional model. The following observations support the model: 1) the presence of well-developed ooids in the Hoyt lithologies suggests that the offshore energy barrier was an oolite shoal perhaps similar to that of the western Bahama Bank (Ball 1967) or to that of Abu Dhabi on the Trucial coast (Kendall and Skipwith 1969; Friedman 1995); 2) the presence in the Hoyt of high-relief domal stromatolites immediately overlying cross-bedded oolite, and the dependence of stromatolite morphology on energy (Logan et al. 1964), suggest that the large heads were restricted to high-energy areas; and 3) the presence of coarse calcarenite between the heads. Storm surges may account for mixing of carbonate grains in the different lithofacies.

Figure 15 is a block diagram showing the facies relationships in which a peritidal setting includes oolite shoals, lagoons, and peritidal flats. The evidence for deposition under peritidal conditions for the Hoyt Limestone at Lester Park includes: (1) mud cracks, (2) flat-pebble conglomerate, (3) ripple marks, (4) small channels, (5) cross-beds, (6) birdseye structures, (7) syngenetic dolomite, and (8) the presence of stromatolites (Friedman 1969; Owen and Friedman 1984).

MACRO- AND MICRO-STRUCTURES OF STROMATOLITES

The high-relief domal and bulbous stromatolites contain distinct, generally uniform laminae of dolomite and calcite (Figs. 5-10). The structure of the stromatolites is sharply defined on weathered outcrop surfaces by the differential weathering of the calcite and dolomite. The laminae reflect spurts of the cyanobacterial mats that may correspond to tidal cycles and hence have been designated tidal rythmites. Successive laminae of these structures drape over the ends of previous laminae, many of them curling underneath the heads to form "overturned" laminae.

The alternating calcite and dolomite laminae permit an analogy with modern microbial mats in hypersaline pools of the Red Sea coast (Friedman et al. 1973). In these modern stromatolites aragonite and high-magnesian calcite laminites alternate. In these modern analogs the high-magnesium calcite laminites contain abundant organic matter in which magnesium has been concentrated to form a magnesium-organic complex. Between the magnesium concentration of the high-magnesian calcite and that of the organic matter sufficient magnesium exists in modern microbial laminates to form dolomite (Friedman et al. 1973, 1982). Hence the observation in ancient stromatolites, such as observed in the Hoyt Limestone, that calcite and dolomite in the stromatolites are interlaminated, with calcite probably forming at the expense of aragonite and dolomite forming from high-magnesian calcite. However Burne (1995) pointed out that in modern settings, while some cyanobacteria may provide a substitute for mineralization, no microbiological evidence exists to support the view that cyanobacteria are capable of secreting carbonate minerals. Yet sediment-binding by cementation, i.e. precipitating or secreting carbonate minerals, and/or mat trapping is necessary to preserve stromatolite structure. Whether the morphology of stromatolites is biologically or environmentally controlled is controversial (Duane and Al-Zamel 1999).

Dark centers of the dolomite crystals suggest the concentration of organic material during the early stages of formation of the dolomite. The microcrystalline calcite laminae are commonly compound, i.e. they may consist of two or more micrite laminae without intervening dolomite. The micrite laminae display a wide range of textures, ranging from dense micrite to grumous and pelletoidal textures. Abundant detrital quartz particles are found in the micrite laminae; in contrast, the dolomite laminae only rarely contain detritus. The detrital grains consist almost exclusively of rounded quartz sand or angular quartz silt; carbonate grains are common in the domed stromatolites

and are generally completely dolomitized. Quartz-sand grains obtained from insoluble residues of the microbial heads show strong pitting of surfaces. Between cabbage-head structures, skeletal fragments, especially those of trilobites, brachiopods, and pelecypods are abundant and in places ooids (Fig. 16) and quartz-sand particles are common. Fragments of trilobites are abundant. They belong especially to an assemblage known as *Plethopeltis* (Ludvigsen and Westrop 1983).

MODERN ANALOGUES OF CAMBRIAN SARATOGA SPRINGS STROMATOLITES

Friedman (1987a,b, 1988a,b) compared the petrography of the microbial stromatolites with that of modern cyanobacterial mats in hypersaline pools of the Red Sea coast (Friedman 1985; Friedman et al. 1973). Modern cyanobacteria secrete radial oöids, oncolites, and grapestones which occur in these Cambrian rocks; interlaminated calcite and dolomite which in part compose the stromatolites of the New York Cambrian correspond to alternating aragonite and high-magnesian calcite laminites which modern cyanobacteria secrete. In modern cyanobacteria of sea-marginal ponds of the Red Sea the high-magnesian calcite laminites contain abundant organic matter in which magnesium has been concentrated to form a magnesium-organic complex. Between the magnesian concentration of the high-magnesian calcite and that of the organic matter sufficient magnesium exists in modern microbial mats to form dolomite. Hence the observation in ancient microbialites, such as observed in this classical New York Cambrian locality, that calcite and dolomite are interlaminated, with calcite probably forming at the expense of aragonite and dolomite forming from high-magnesian calcite. The structure of the stromatolites is sharply defined on weathered outcrop surfaces by differential weathering of the calcite and dolomite.

Discovery of the stromatolites at Hamelin Pool in western Australia (Fig. 17) (Logan 1961; Logan et al. 1964) revived interest in the spectacular domed microbial stromatolites of Saratoga Springs, New York, which as *Cryptozoön proliferum* Hall, were the first formally named stromatolites.

Feldspathic Stromatolites

Cumulative Mileage	Miles From Last Point	Route Description
		Turn around and drive back (south)to NY 29.
6.3	1.2	Turn right (west) on NY 29. Pass basal Paleozoic quartz-cobble conglomerate (a possible talus deposit) on weathered Pre-Cambrian gneiss 1/2 mi. east of Cymbal's Corners (NY 147).
25.4	19.1	Turn left (south) on NY 30.
31.7	6.3	City limits of Amsterdam
33.1	1.4	Cross bridge over Mohawk River.
33.3	0.2	Drive straight on Bridge Street (leaving NY 30).
33.4	0.1	Traffic light below Amsterdam Armory; Turn right on Florida Avenue and go west;
33.9	0.5	Turn right on Broadway;
34.7	0.8	Turn right (west) on NY 5;
37.1	2.4	Fort Hunter, turn right (north) on Main Street;
37.3	0.2	Turn right (east) to Queen Ann Street.
38.2	0.9	STOP 3. Fort Hunter Quarry.

STOP #3 FORT HUNTER QUARRY

Alight at slight bend in road and walk to Fort Hunter Quarry which is across a former railroad track (now a bicycle pass) close to Mohawk River. (Fort Hunter Quarry cannot be seen from road; another small quarry visible from road is approximately 0.1 mile farther east, but will not be visited on this trip).

Products of Tidal Environment: Stromatolites

Stromatolites in the Fort Hunter quarry consist almost entirely of dolomite in the form of irregularly bedded, finely-laminated, undulating structures. The rocks in this quarry are part of the Tribes Hill Formation of earliest

Ordocian (Fisher 1954). The lithofacies of the Tribes Hill Formation have been studied in detail by Braun and Friedman (1969) within the stratigraphic framework established by Fisher (1954). Figure 18 is a columnar section showing the relationship of ten lithofacies to four members of the Tribes Hill Formation. At Fort Hunter we will study the lowermost two lithofacies of the Fort Johnson Member (see column at right (east) end of the section, in Fig. 18.

Two lithofacies are observed: (1) lithofacies 1, mottled feldspathic dolomite, and (2) lithofacies 2, laminated feldspathic dolomite. Lithofacies 1 is at the bottom of the quarry, and lithofacies 2 is approximately half way up.

Lithofacies 1

This facies occurs as thin dolostone beds, 2 cm to 25 cm, but locally more than 50 cm thick, with a few thin interbeds of black argillaceous dolostone which are up to 5 cm thick. In the field, the dolomite shows gray-black mottling and in places bird's eye structures. In one sample, the infilling of the bird's eyes shows a black bituminous rim which may be anthraxolite. In the field, trace fossils are abundant, but fossils were not noted. Authigenic alkali feldspar (microcline) is ubiquitous throughout this lithofacies. The insoluble residue makes up 22 to 54% by weight of the sediment in samples studied with most of the residue composed of authigenic feldspar.

Lithofacies 2

This lithofacies is mineralogically identical to the previous facies but differs from it texturally and structurally in being irregularly bedded and in containing abundant undulating stromatolic stuctures ("pseudo-ripples") (Fig. 19) as well as disturbed and discontinuous laminae. In places there are a few thin interbeds of black argillaceous dolostone. The thickness of the laminates of this facies ranges from ½ mm to 2 or 3 mm; on freshly broken surfaces the color of the thinner laminae is black and that of the thicker ones is gray. The insoluble residue, for the most part composed of authigenic feldspar, constitutes between 35 and 67% by weight in samples studied.

These two lithofacies which form the basal unit of the Ordovician, were formed on a broad shallow shelf.

$^{40}Ar/^{39}Ar$ spectrum analysis of the K-feldspar of Sauk-Sequence carbonates of Lithofacies 2, laminated feldspathic dolostone of the Tribes Hill Formation, yielded an age range reflecting the original detrital cores of Sauk age (470 Ma) and an uplift of Pennsylvanian age (320 Ma) (Matt Heizler, analyst) (Friedman 1990). Hearn et al. (1987) using $^{40}Ar/^{39}Ar$ analyses for the authigenic feldspar in Cambro-Ordovician carbonate rocks of the central and southern Appalachians obtained a comparable age for uplift (278-322 Ma). For carbonate rocks in Nova Scotia $^{40}Ar/^{39}Ar$ clocks in feldspar were reset at 300-320 Ma.

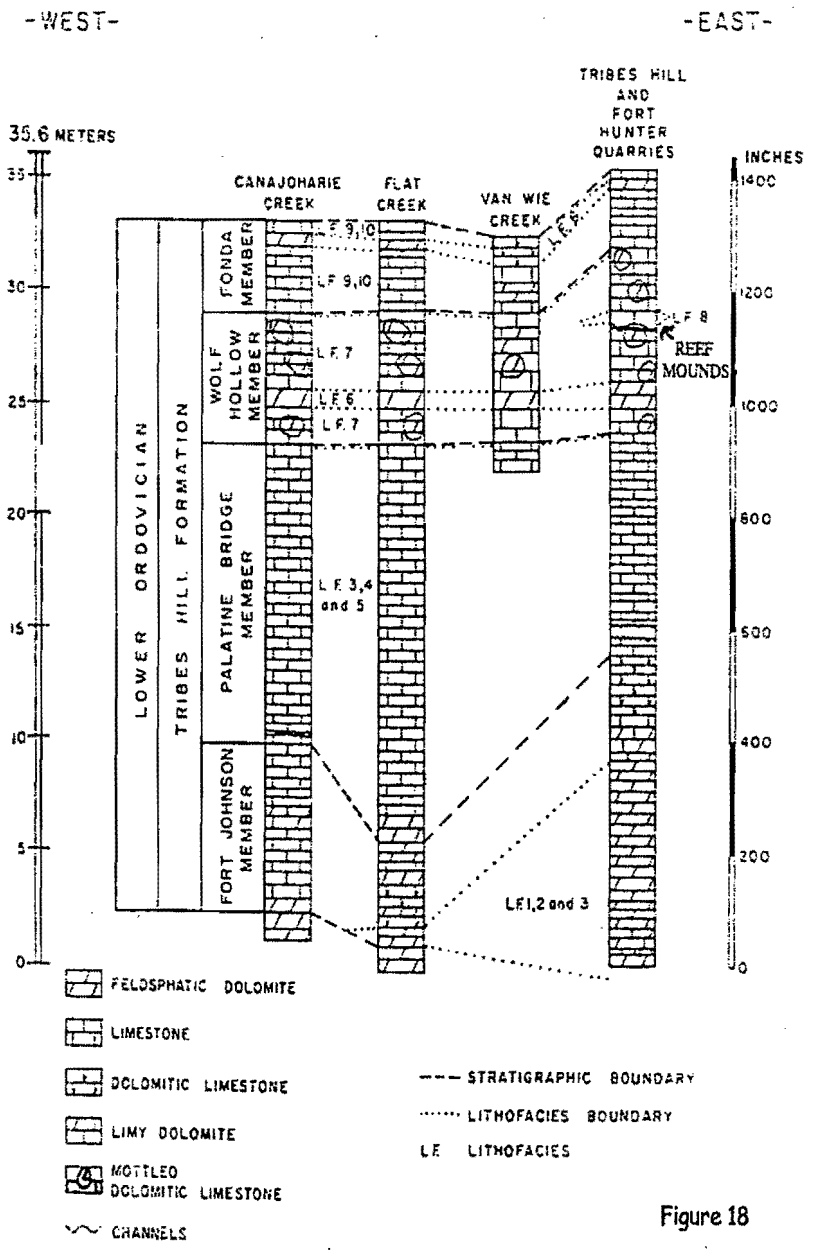

Figure 18

Figure 18. Columnar section showing the relationship of ten lithofacies to four members in Tribes Hill Formation (Lower Ordovician) (after Braun and Friedman 1969).

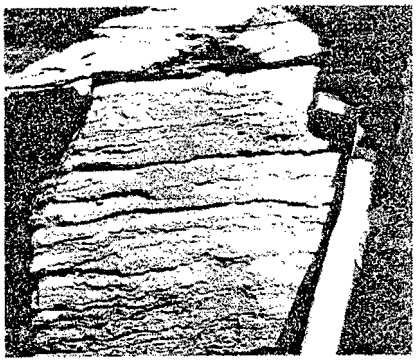

Figure 19

Figure 19. Stromatolite in dolostone rock of lithofacies 2 (laminated feldspathic dolomite), Tribes Hill Formation (Lower Ordovician), Fort Hunter quarry. (Braun and Friedman, 1969, fig. 3, p. 117; Friedman, 1972, fig. 5, p. 21; Friedman et al 1992, fig. 7-41).

Stromatolites, bird's eye structures, scarcity of fossils, bituminous material, syngenetic dolomite, and mottling suggest that these rocks were deposited in a peritidal environment (Friedman et al. 1992). Based on analogy with the carbonate sediments in the modern Bahamas, Braun and Friedman (1969) concluded that these two lithofacies formed under supratidal conditions. However in the Persian Gulf flat microbial mats prefer the uppermost intertidal environment, and along the Red Sea coast they flourish where entirely immersed in seawater, provided hypersaline conditions keep away burrowers and grazers (Friedman et al. 1973). Hence on this field trip we may conclude that the stromatolites indicate peritidal conditions without distinguishing between intertidal and supratidal. For more details on these lithofacies refer to Braun and Friedman (1969).

Data obtained from the analysis of fluid inclusions in calcite-healed fractures of these Lower Ordovician carbonate strata, in which microcline crystals are so prominent, indicate higher paleotemperatures and greater depth of burial than have previously been inferred for the rocks of this region (Urschel and Friedman 1984; Friedman 1987a,b). Average fluid- homogenization temperatures range from 96°C to 159°C. These high paleotemperatures are supported by oxygen-isotope and conodont-alteration data (Harris et al. 1978). A former depth of burial >7 km is implied when a geothermal gradient of 26°C/km (Friedman and Sanders 1982, 1983) is used.

Thus, following subsidence to great depth, Pennsylvanian to Permian epeirogeny uplifted the strata, resulting in deep erosion. This leads to the surprising conclusion that isostatic unroofing following uplift has stripped off thick sections of strata whose presence was previously unsuspected.

Cumulative Mileage	**Miles From Last Point**	**Route Description**
		Turn around and drive back to Main Street, Fort Hunter.
39.1	0.9	Turn right (north) into Main Street, Fort Hunter
39.2	0.1	
		Cross original Erie Canal, built in 1822. Amos Eaton surveyed this route at the request of Stephen Van Rensselaer (1764-1839); after this survey Amos Eaton (1776-1842) and Van Rensselaer decided to found a school for surveying, geological and agricultural training which became Rensselaer Polytechnic Institute.
		Follow Main Street through Fort Hunter.
39.8	0.6	Cross Mohawk River.
40.3	0.5	Turn right (east) on Mohawk Drive (town of Tribes Hill).
40.7	0.4	Turn left (north) on Stoner Trail.
40.9	0.2	Cross Route 5 and continue on Stoner Trail.
43.6	2.7	Turn right on NY 67 (east).
45.1	1.5	Fulton-Montgomery Community College; continue on NY 67.
46.7	1.6	STOP 4. North Tribes Hill Quarry (on left).

STOP #4. North Tribes Hill Quarry

Route of Walk

Take the trail towards old abandoned crusher, but instead of heading towards the quarry move uphill to the first rock exposures. The rocks to be examined are near the edge of steep cliff.

Description and Discussion

At this stop microbial reef mounds are exposed (Friedman, 1996a,b). Ordovician domal thrombolites, termed here microbial reef mounds, occupied the basal part of meter-scale shallowing-upward cycles (Fig. 20). They are part of a high-energy facies that a sharp transgressive surface separates from an underlying low-energy peritidal setting. This erosional surface served as the surface on which one of the reef mounds established itself during initial transgression before further deepening. The others overlie a floor of skeletal grainstone reflecting a high-stand sea-level facies tract. Skeletal grainstone composes the fill between the mounds. A channel and several aggrading hummocks occupy inter-reef mound areas resulting from storm events in a subtidal setting.

Figure 20

Figure 20. Microbial reef mound developed on underlying grainstone (which vegetation obscures). Bench below grainstone is a transgressive marine flooding surface which terminated an underlying shallowing-upward cycle (Friedman 1996a,b).

Reef mounds formed at or near the base of upward-shallowing parasequences. They are part of a high-energy facies which a parasequence surface of emergence or near emergence separates from an underlying parasequence which terminated a low-energy peritidal setting. This erosional surface between the two parasequences is interpreted as a partly lithified hard ground. As elsewhere in the Cambro-Ordovician of North America, microbial reef mounds commonly occur near the bases of upward-shallowing cycles and most rest directly on underlying cycle caps (Osleger and Montañez 1996).

Mound-Foundation Facies

Braun and Friedman (1969) designated the facies underlying the reef mounds as Lithofacies 7: Mottled Dolomitic Micrite and Biomicrite of the Wolf Hollow member (Fig. 18). This lithofacies is made up of a well-bedded, mottled limestone in which the mottles are composed of irregular patches of dolomite. On weathered surfaces, the limestone is whitish and the dolomite buff, but on freshly broken surfaces both limestone and dolomite are very light gray with the limestone somewhat darker and the dolomite of granular appearance. The outlines of large gastropods and cephalopods stand out, in places, on weathered bedding planes. A list of fossils found in this lithofacies was given by Fisher (1954, p. 88-89). Bird's eye structures are present in some beds as are pyrite patches. The limestone contains abundant dolomite-filled burrows, most of which are horizontal (or sub-horizontal) to the bedding plane, but some burrows have oblique to perpendicular orientations with respect to bedding. Many gastropods, especially *Ophileta* and *Ecculiomphalous* are found with the dolomite-filled burrows suggesting that these burrows may have been made by gastropods rather than by worms. However, the morphology of the shells suggests that these gastropods were not burrowers. Hence, worms or other soft-bodied organisms must have been abundant and produced the burrows.

This facies which is part of the Wolf Hollow Member (see Fig. 18), represents a low-energy deposit of micrite of a shallowing-upward cycle terminating in a sharp, planar erosion surface. This erosional parasequence surface is a marine flooding surface and represents a transgressive event for the next high-energy cycle in which the reef mounds formed. Below one of the reef mounds the underlying micrite of mound-foundation facies compacted (Fig. 21).

Figure 21

Figure 21. Undulating bench (on which hammer stands) is the transgressive surface separating the underlying micrite of low-stand sea-level facies tract (Lithofacies 7) from overlying high-stand sea-level facies tract consisting of skeletal grainstone (biosparite) and reef mounds. Note mound on left edge of photograph. Note aggrading hummocks of grainstone (above the trace of drill). Below reef mound on left edge of photograph note grainstone bed which can be traced to lowermost hummock to the right. Below this mound and grainstone bed the underlying micrite of mound- foundation facies compacted resulting in the undulating bench (Friedman 1996b, fig. 6, p. 231).

Differential compaction of this former lime mud, as the solid reef grew, suggests that the lime mud had not yet fully lithified (Friedman 1996a,b). This observation differs somewhat from that of reef mounds in Virginia and Argentina where a solid hard ground served as foundation for the reef mounds (Read and Grover 1977; Cañas and Carrera 1993). However, the original lime mud of the mound-foundation facies of the Tribes Hill mounds was sufficiently lithified to support the growing mounds (Friedman 1996a,b).

Microbial Reef-Mound Facies

Reef mounds are prominent in the Wolf Hollow Member of the Tribes Hill Formation (Figs. 20, 21). They occur as isolated mounds (Friedman 1996a,b). These mounds are approximately one meter in length (measurements vary from 95 cm to 135 cm) and 60 to 70cm in thickness. These measurements are approximate dimensions because the mounds do not stand out freely, and disappear in the enveloping facies. Moreover in the exposure, it is difficult to differentiate between short and long axes of the mounds.

The reef mounds are composed of clotted and peloidal microcrystalline matrix which was microbially precipitated, comparable to that in modern reefs (Friedman et al. 1974). In modern reef settings, peloids display the pattern of calcified coccoid cells which cyanobacteria or chemoorganotrophic bacteria degrading the cyanobacterial organic matter precipitate (Friedman et al. 1985; Krumbein 1983). These textural features are products precipitated by the micro- environment of cyanobacteria (Nadson 1903; Kalkowsky 1908; Pia 1927; Johnson 1954; Endo 1961; Friedman et al. 1973). Peloids have been described as calcified algal filaments (Friedman et al. 1974); such calcification may be the result of precipitation of calcium carbonate on cyano-bacterial filaments in the presence of live bacteria (Chafetz and Buczynski 1992).

Because they are composed of microcrystalline carbonate matrix, the microbial reef mounds have a texture similar to that of the mound-foundation facies lithofacies 7 (see Fig. 18), a micrite. The term matrix has been commonly misapplied as a synonym of micrite, but the mounds are not composed of micrite. Mechanically deposited lime mud, following lithification, is known as micrite (Folk 1959). Identifying even modern reef rock is an experience in

frustration: submarine microcrystalline or cryptocrystalline matrix that is biologically precipitated within millimeters to centimeters of the surfaces of reef rock is identical in appearance to micrite of mechanical origin. Case histories abound in which unwary geologists have misidentified the reef rock for low-energy facies composed of micrite (Friedman 1985, 1994a,b). Since micrite of low-energy origin and microcrystalline or cryptocrystalline matrix of reefs are indistinguishable it is easy to confuse high-energy reef facies for low-energy lime- mud facies (Friedman 1985, 1994a,b). This textural similarity led initially to an interpretation that mounds may be blocks of lithofacies 7 (micrite and biomicrite) that foundered and became lodged in channels (Braun and Friedman 1969). These reef mounds resemble blocks of micrite in tidal channels of the Bahamas that are derived by undercutting of the banks of the channels (Braun and Friedman 1969).

The reef mounds were included with lithofacies 8 of Braun and Friedman (1969) designated intrasparite and biosparite; the lithology is for the most part a skeletal grainstone. This lithofacies was referred to as channel fill, comparable to the Lower Ordovician reef mounds of western Argentina, of which Cañas and Carrera (1993, p. 169) noted "the reef mounds are dissected by conspicuous channels filled with coarse crinoidal grainstone and lithoclastic rudstone" (Fig. 21). This same observation applies in part to the setting of the Tribes Hill Formation. As in western Argentina, the reef mounds of the Tribes Hill Formation formed in part on a previously lithified or partly lithified sediment surface (Cañas and Carrera 1993, p. 169); and as in other places in North America, they occur near the base of an upward-shallowing cycle. The surface on which one of the mounds developed is a sharp transgressive parasequence surface separating the underlying peritidal lithofacies 7 (micrite and biomicrite) from the overlying subtidal reef-mound facies. The other reef mounds nucleated near the transgressive parasequence surface, but on top of underlying skeletal grainstone, during the initial transgression before rapid deepening occurred, a setting which is similar to that of comparable facies in the Great Basin, U.S.A. (Osleger and Montañez 1996).

Inter-Reef Mound Facies

Skeletal grainstone composes the fill between the reef mounds. One channel and several hummocks occupy the inter-reef mound areas (Fig. 22). The top of one of the hummocks rolls into the channel fill. The grainstones form lenses that build on top of one another. The channel displays the typical asymmetric profile of a tidal channel with a steep cut-bank and a low-angle slip-off slope (Fig. 22). However, the channel is entirely within grainstone, hence it is not a normal tidal channel which would be fine-grained on the steep side and coarse-grained on the opposing side. In normal tidal channels, as the channel shifts it leaves behind a layer of coarse debris at the bottom of the channel (Friedman et al. 1992). No such channel-floor lag layer is present in the inter-reef mound facies. Hence the channel must be related to storm deposition of the grainstone since filling is not the result of the shifting of the channel. Truncation by the channel and aggradation of the hummocks occurred at the same time. The channel and hummocks formed as a result of storm events in a subtidal setting. Following transgression, storm tides and currents generated this channel between which reef mounds and inter-reef mound facies accumulated. This channel, which was incised down to 30 cm into the underlying grainstone, is conspicuous and displays sharp margins (Fig. 22).

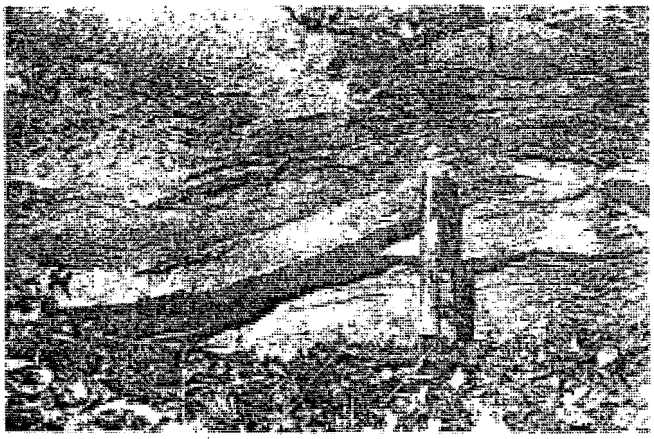

Figure 22

Figure 22. Trucation at base of slip-off slope side of storm tidal channel. Hummock of grainstone underlies truncation surface to right of hammer. Channel is made up of high-energy grainstone of lithofacies 8 (intrasparite and biosparite) and cuts into lithofacies 8 grainstone. Below flat base of the hammer is lithofacies 7 (mottled dolomitic micrite and biomicrite). Lithofacies 7 represents low-energy peritidal flats (Friedman 1996b, fig. 17, p. 236).

Of the various reef mounds one rests directly on the mound-foundation surface; grainstone of inter-reef mound facies makes up the floor of all the others.

The reef mounds formed in shallow-subtidal to possibly low intertidal settings in an agitated environment devoid of lime mud.

Going east on Route 67, after the intersection with Route 147, five roadcuts on either side of Route 67 expose outcrops of the Lower Ordovician Gailor Formation.

STOP #5: Exposures of Gailor Formation

On the north and south sides of the road are exposed a massive dolostone unit overlain by a bedded dolostone unit. Roughly 10' of section are exposed here. The massive unit is dark gray in color while the upper bedded unit is lighter gray and coarser as well. Large clasts in a variety of shapes and sizes, composed of micrite and medium-textured dolostones are scattered all over the outcrop and concentrated in the basal massive unit. Pods and lenses of chert colored black and white are profuse. Calcite mineralization is also a common feature, occurring in patches and veins in orange, white and black. Stromatolites are observed in the section on the north side of the road.

The breccia observed in the section perhaps represents dissolution collapse. The massive unit in the lower part of the section may be a microbial build up. The stromatolites suggest a peritidal origin for these dolostones.

STOP #6.

Farther east on the north and south side of 67 are exposed roughly 27' of section. The following features are observed:

-wavy beds,
-massive units alternating with bedded dolostone units,
-the massive units appear to have a lenticular mound-like form, perhaps representing former microbial build-ups,
-the beds overlying the mounds display dips on flanks of the mounds perhaps indication fore-reef slopes,
-pervasive dolomitization seems to have obliterated original depositional features,
-alternatively the wavy bedding may represent tidal channels or hummocky cross stratification,
-other features observed in these units are fine laminae in the dolostones, burrow mottling, stylolites, presence of pyrite and white calcite mineralization in vugs and fractures.

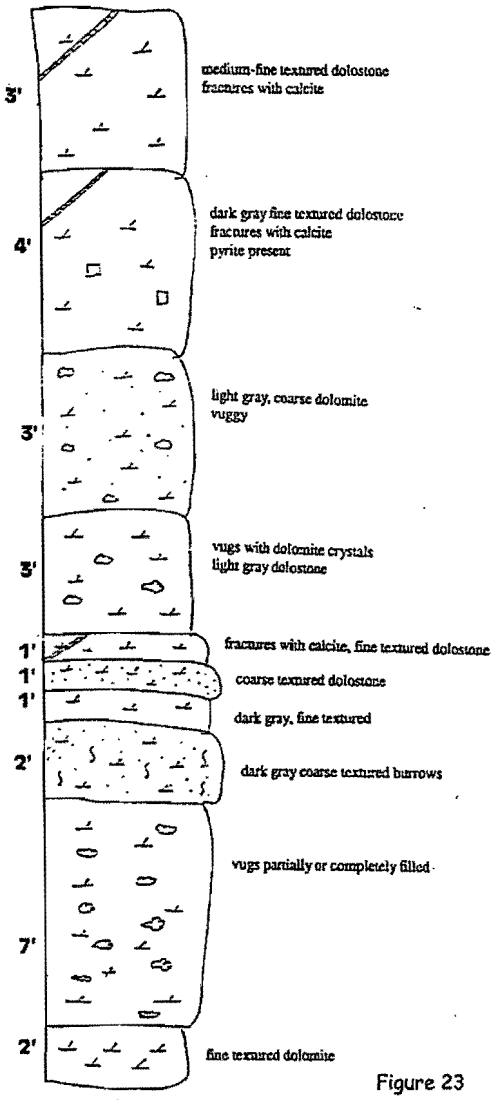

Figure 23

Figure 23 is a sketch of the section exposed at this stop (on Route 67).

STOP #7.

Farther east are exposed roughly 15' of bedded dolostones displaying planar stromatolites, intraclasts, and bird's eye structures indicating peritidal environments of deposition.

STOP #8.

This is a small section on the north side of 67 near Waite Road. The section displays intraclasts and stromatolites.

STOP #9.

Farther east on Route 67 near Manny Corners is a section exposing roughly 26' of bedded dolostones. The following features are observed here:

- planar and domal stromatolites,

- intraclasts ranging in size from 1 to 2 inches,
- vugs and fractures partially or completely filled with black and white calcite,
- bird's eye structures,
-bedded and nodular chert,
-breccia representing dissolution collapse?

The above mentioned features displayed in these fine- to medium-textured dolostones point to a peritidal environment of deposition.

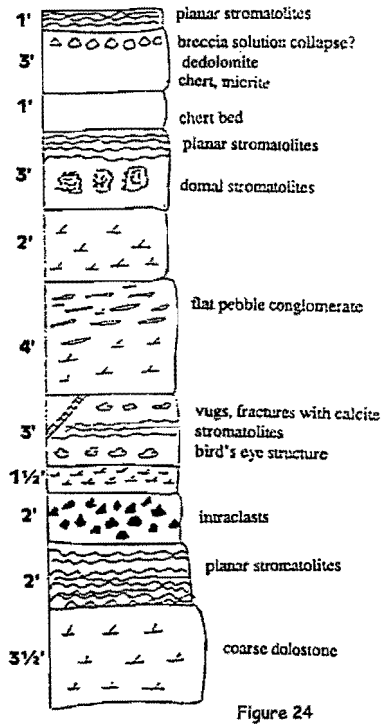

Figure 24

Figure 24 is a sketch of the section exposed at this stop.

REFERENCES

Back, W., Landa, E.R., and Meeks, L., 1995, Bottled water spas, and early years of water chemistry: Ground Water, v. 33, p. 605-614.

Ball, M.M., 1967, Carbonate sand bodies of South Florida and the Bahamas: Journal of Sedimentary Petrology, v. 37, p. 556-591.

Braun, Moshe, and Friedman, G.M., 1969, Carbonate lithofacies and environments of the Tribes Hill Formation (Lower Ordovician) of the Mohawk Valley, New York: Journal of Sedimentary Petrology, v. 39, p.113-135.

Burne, R.V., 1995, Microbial microbiolites of Lake Clifton, Western Australia: Morphological analogues of Cryptozoön proliferum Hall, the first formally-named stromatolite: reply: Facies, v. 32, p. 257.

Burne, R.V., and Moore, L.S., 1987, Microbialites: organosedimentary deposits of benthic microbial communities: Palaios, v. 2, p. 241-254.

Burne, R.V., and Moore, L.S., 1993, Microbial microbiolites of Lake Clifton, Western Australia: Morphological analogues of Cryptozoön proliferum Hall, the first formally-named stromatolite: Facies, v. 29, p. 149-168.

Cañas, Fernando, and Carrera, Marcelo, 1993, Early ordovician microbial-sponge-receptaculitid bioherms of the Precordillera, Western Argentina: Facies, v. 29, p. 169-178.

Chafetz, H.S., and Buczynski, Chris, 1992, Bacterially Induced Lithification of Microbial Mats: Palaios, v. 7, p.

277-293.
Cohn, F., 1864, Ueber die Entstehung, des Travertins in den Wasserfaellen von Tivoli: Neue Jahrbuch fuer Mineralogie, Geologie, und Palaeontologie, v. 32, p. 580-610.
Cushing, H.P., and Ruedemann, R., 1914, Geology of Saratoga Springs and vicinity: New York State Museum Bulletin, No. 169, 177 p.
Duane, M.J., and Al-Zamel, A.Z., 1999, Syngenetic textural evolution of modern sabkha stromatolites (Kuwait): Sedimentary Geology, v. 127, p. 237-249.
Endo, R., 1961, Phylogenetic relationships among the calcareous algae: Saitama University Science Report Ser. B. Endo Commem., p. 1-48.
Fisher, D.W., 1954, Lower Ordovician stratigraphy of the Mohawk Valley, N.Y.: Geological Society of America Bulletin, v. 65, p. 71-96.
Fisher, D.W., 1968, Geology of the Plattsburge and Rouses Point, New York-Vermont, quadrangles, New York State Museum and Science Service Map and Chart Series Number 10. The University of The State of New York/ The State Education Department/Albany.
Fisher, D.W., 1977, Correlation of the Hadrynian, Cambrian, and Ordovician rocks in New York State, New York State Museum and Science Service Map and Chart Series Number 25. The University of the State of New York/ The State Education Department/Albany.
Fisher, D.W., 1980, Bedrock geology of the Central Mohawk Valley, New York State Museum and Science Service Map and Chart Series Number 8. The University of the State of New York/ The State Education Department/Albany.
Fisher, D.W., and Hanson, G.F., 1951, Revisions in the geology of Saratoga Springs and vicinity: American Journal of Science, v. 249, p. 795-814.
Flagler, C.W., 1966, Subsurface Cambrian and Ordovician stratigraphy on the Trenton Group - Precambrian interval in New York State, New York State Museum and Science Service Map and Chart Series Number 8. The University of the State of New York/The State Education Department/Albany.
Folk, R.L., 1959, Practical Petrographic Classification of Limestones: American Association of Petroleum Geologists Bulletin, v. 43, p. 1-38.
Friedman, G.M., 1969, Recognizing tidal environments in carbonate rocks with particular reference to those of the lower Paleozoic in the northern Appalachians (abstract): Geological Society of America, Abstract, Part 1, Northeastern Section, p. 20-21.
Friedman, G.M., 1972, "Sedimentary facies": products of sedimentary environments in Catskill Mountains, Mohawk Valley, and Taconic Sequence, eastern New York State: Guidebook, Society of Economic Paleontologists and Mineralogists Eastern Section, 48 p.
Friedman, G.M., 1979, Sedimentary environments and their products; shelf, slope, and rise of Proto-Atlantic (Iapetus) Ocean, Cambrian and Ordovician periods, eastern New York State: in Joint annual meeting of New York State Geological Association, 51st annual meeting and New England intercollegiate geological conference, 71st annual meeting; guidebook (Friedman, G.M., editor), N.Y. State Geological Association, Annual Meeting, Field Trip Guidebook, No. 51, p. 47-86.
Friedman, G.M., 1985, Cambro-Ordovician shoaling and tidal deposits marginal to Iapetus Ocean and Middle to Upper Devonian peritidal deposits of the Catskill fan-delta complex in Lindemann, R.H., ed., Field Trip Guidebook, New York State Geological Association, 57th Annual Meeting, Skidmore College, p. 5-28.
Friedman, G.M., 1987a, Spectacular domed microbial mats (cabbage heads) and oolitic limestone at Lester Park, near Saratoga, New York (abstract): in Geological Society of America, Northeastern Section, 22nd Annual Meeting, Abstracts with programs -Geological Society of America, v. 19, p. 15.
Friedman, G.M., 1987b, Vertical movements of the crust: case histories from the northern Appalachian Basin: Geology, v. 15, p.1130-1133.
Friedman, G.M., 1988a, Spectacular domed microbial mats (cabbage heads) and oolitic limestone at Lester Park near Saratoga, New York: Northeastern Geology, v. 10, p. 8-12.
Friedman, G.M., 1988b, Cambro-Orrovician Shoaling and Tidal Deposits Marginal to Iapetus Ocean and Middle to Upper Devonian Peritidal Deposits of the Catskill Fan-Deltaic Complex: Field Trip Guidebook, New York State Geological Association, 57th Annual Meeting, September 27-29, 1985, Department of Geology, Skidmore College, p. 5-28.
Friedman, G.M., 1990, Anthracite and concentrations of alkaline feldspar (microcline) in flat-lying undeformed Paleozoic strata; a key to large- scale vertical crustal uplift in Sediments and environmental geochemistry: selected aspects and case historie; D. Heling, et al., eds., Springer Verlag, p. 16-28.

Friedman, G.M., 1994a, Stacking patterns of cyclic parasequences in Cambro-Ordovician carbonates of eastern New York and western Vermont: Northeastern Geology, v. 16, p. 145-157.

Friedman, G.M., 1994b, Upper Cambrian-Lower Ordovician (Sauk) platform carbonates of the northern Appalachian (Gondwana) passive margin: Carbonates and Evaporites, v. 9, p. 143-150.

Friedman, G.M., 1995, Cambro-Lower Ordovician (Sauk) facies and sequences: case histories from eastern North America in P.H. Pausé and M.P. Candelaria, eds., Carbonate Facies and Sequence Stratigraphy: practical applications of carbonate model. Permian basin section-SEPM publication 95-36 and Permian basin graduate center publication 5-95, p. 1-9.

Friedman, G.M., 1996a, Stontium-Isotopic signature reflect an origin of dolomite by fresh-water effluent: the Pine Plains formation (Wappinger Group, Cambrian) of Southeastern New York: Carbonate and Evaporites, v. 11, no. 1, p. 134-140.

Friedman, G.M., 1996b, Early Ordovician Microbial Reef Mounds of the Tribes Hill Formation, Mohawk Valley, New York: Carbonates and Evaporites, v. 11, no. 2, p. 226-240.

Friedman, G.M., 1997a, "Sedimentary facies": products of sedimentary environments in Catskill Mountains, Mohawk Valley, and Taconic Sequence, eastern New York State: Guidebook, Society for Sedimentary Geology, Eastern Section, 57 p.

Friedman, G.M., 1997b, Cambro-Ordovician and modern carbonate facies of the Mohawk-Hudson valleys, New York, p. 63, 65-83 in Rayne, Todd, Bailey, D.G., and Tewksbury, B.J., ed., 1997, Field Trip Guide for the 69th Annual Meeting of the New York State Geological Association, Hamilton College, Clinton, NY, 264 p.

Friedman, G.M., and Sanders, J.E., 1978, Principles of Sedimentology. John Wiley & Sons, New York, 792 p.

Friedman, G.M., and Sanders, J.E., 1982, Time-temperature-burial significance of Devonian anthracite implies former great (~6.5 km) depth of burial of Catskill Mountains, New York: Geology, v.10, p.93-96.

Friedman, G.M., and Sanders, J.E., 1983, Reply on: Time-temperature-burial significance of Devonian anthracite implies former great (~6.5 km) depth of burial of Catskill Mountains, New York: Geology, v. 11, p. 123-124.

Friedman, G.M., Amiel, A.J., and Schneidermann, N., 1974, Submarine Cementation in Reefs: Example From the Red Sea: Journal of Sedimentary Petrology, v. 44, p. 816-825.

Friedman, G.M., Barzel, A., and Derin, B., 1971, Paleoenvironments of the Jurassic in the Coastal Belt of Northern and Central Israel and their significance in the search for petroleum reservoirs: Geological Survey of Israel, Report OD/1/71, 26 p.

Friedman, G.M., Sanders, J.E., and Martini, I.P., 1982, Sedimentary facies: products of sedimentary environments in a cross section of the classic Appalachian Mountains and adjoining Appalachian Basin in New York and Ontario: International Association of Sedimentologists, Eleventh International Congress on Sedimentology, Guidebook, Excursion 17A, variously paginated.

Friedman, G.M., Sanders, J.E., and Kopaska-Merkel, D.C., 1992, Principles of Sedimentary Deposits: Stratigraphy and Sedimentology. MacMillan Publishing Company, New York, 717 p.

Friedman, G.M., Sanders, J.E., and Guo, Baiying, 1993, Predrilling geologic work in connection with proposed Albany basin, New York, deep scientific bore hole to test gas potential of Paleozoic formations: Final report, New York Gas Group, 171 p.

Friedman, G.M., Sneh, A., and Owen, R.W., 1985, The Ras Muhammad Pool: implications for the Gavish Sabkha, p. 218-237 in Friedman, G.M. and Krumbein, W.E., eds., 1985, Hypersaline ecosystems. The Gavish Sabkha. Ecological Studies 53, Berlin, Springer-Verlag, 484 p.

Friedman, G.M., Amiel, A.J., Braun, M., and Miller, D.S., 1973, Generation of carbonate particles and laminites in algal mats - example from sea-marginal pool, Gulf of Aqaba, Red Sea: American Association of Petroleum Geologists Bulletin, v. 57, p. 541-557.

Goldring, Winifred, 1937, On the origin of the Saratoga mineral waters; Cryptozoon, plant nature and distributuion: Science n.s., v. 86, no. 2241, p. 530-531.

Goldring, Winifred, 1938, Algal barrier reefs in the Lower Ozarkian of New York with a Chapter on the importance of coralline algae as reef builders through the ages: New York State Museum Bulletin, no. 315, p. 5-75.

Grabau, A.W., and Shimer, H.W., 1909, North American index fossils; Invertebrates. New York, v. 1, 853 p.

Gwinner, M., 1959, Die Geologie des Blattes Urach (Nr. 7522) 1:25000 (Schwäbische Alb): Arb. a. d. Geol. Palaont. Inst. d. T.H. Stutgart, v.24, Stutgart, no pagination.

Hall, James, 1847, Natural history of New York. Organic remains of the Lower Division of the New York System: Paleontology, v. 1, p. 1-338.

Hall, James, 1883, Cryptozoön proliferum n.sp.: New York State Museum, Annual Report 36, Plate VI and explanation.

Harris, A.G., Harris, L.D., and Epstein, J.B., 1978, Oil and gas data from Paleozoic rocks in the Appalachian basin: Maps for assessing hydrocarbon potential and thermal maturity (conodont color alteration isograds and overburden isopachs): U.S. Geological Survey Miscellaneous Investigations Map I-917-E, scale 1:2,500,000, 4 sheets.

Hewitt, P.C., McClennan, W.E., Jr., and Nilsson, Harold, 1965, Geologic phenomena in the Schenectady area: Guidebook - Field Trips in Schenectady Area, New York State Geological Association, 37th Annual Meeting, p.D1-D13.

Hollocher, Kurt, 2002, Geochemistry and source of the Springs of Saratoga, in Joint meeting of the NEIGC and NYSGA 2002, Williams College, Skidmore, and Colgate University, Sept 27-29, Fort William Henry Resort, Lake George Village, p. 5.

Jackson, J.A., 1997, Glossary of geology. American Geological Institute, Alexander, VA, 769 p.

Johnson, J.H., 1954, An Introduction to the Study of Rock-building Algae and Algal Limestones: Colorado School of Mines, v. Q49, 117 p.

Kalkowsky, E., 1908, Oolith und Stromatolith im Norddeutschen Buntsandstein: Zeitschrift der Deutschen Geologischen Gesellschaft, v. 60, p. 68-125.

Kazmierczak, J., and Kempe, S., 1990, Modern cyanobacterial analogs of Paleozoic stromatoporoids: Science, v. 250, p. 1244-1248.

Keith, B.D., and Friedman, G.M., 1977, A slope-fan-basin-plain model, Taconic sequence, New York and Vermont: Journal of Sedimentary Petrology, v. 47, p. 1220-1241.

Keith, B.D., and Friedman, G.M., 1978, A slope-fan-basin-plain model, Taconic sequence, New York and Vermont, p. 178-199, in Curtis, D.M., ed., Environmental problems in ancient sediments: Society of Economic Paleontologists Mineralogists, Reprint Series 6, 240 p.

Kemp, J.F., 1912, The mineral springs of Saratoga: New York State Museum Bulletin, v. 159, 79 p.

Kendall, C.G.St.C., and Skipwith, Sir P.A.D'E., 1969, Holocene and shallow-water carbonate (sic) and evaporite sediments of Khor al Bazam, Abu Dhabi, southwest Persian Gulf: American Assoication of Petroleum Geologists Bulletin, v. 53, p. 841-869.

Krumbein, W.E., 1983, Stromatolites-challenge of term through space and time: Precambrian Res., v. 20, p. 493-531.

Landing, E., 1979, Conodonts and biostratigraphy of the Hoyt Limestone (Late Cambrian, Trempealeauan) eastern New York: Journal of Paleontology, v. 53, p. 1024-1029.

Logan, B.W., 1961, Cryptozoon and associated stromatolites from the Recent, Shark Bay, Western Australia: Journal of Geology, v. 69, p. 517-533.

Logan, B.W., Rezak, R., and Ginsburg, R.N., 1964, Classification and environmental significance of algal stromatolites: Journal of Geology, v. 721, p. 68-83.

Ludvigsen, Rolf, and Westrop, R.R., 1983, Franconian trilobites of New York State: New York State Museum 23, 45 p.

Lyell, C., 1830, Principles of Geology, v. 1, Murray, London, 511 p.

Mazzullo, S.J., Agostino, P., Seitz, J.N., and Fisher, D.W., 1978, Stratigraphy and depositional environments of the upper Cambrian-lower Ordovician sequence, Saratoga Springs, New York: Journal of Sedimentary Petrology, v. 48, p. 99-116.

Nadson, G., 1903, Die Mikroorganismen als Geologische Faktoren. Petersburger Arb. Komm. Erf. Min Seen, Slavjansk, Peterburg.

New York State Department of Health, 1959, Analysis of springs at Saratoga Springs Spa: Div. Laboratory and Research Environmental Health Center, Report.

Osleger, D.A., and Montañez, I.P., 1996, Cross-platform Architecture of a Sequence Boundary in Mixed Siliciclastic-Carbonate Lithofacies, Middle Cambrian, Southern Great Basin, USA: Sedimentology, v. 43, p. 197-217.

Owen, R.W., and Friedman, G.M., 1984, Late Cambrian algal deposition in the Hoyt Limestone, Eastern New York State: Northeastern Geology, v. 6, p. 222-237.

Pia, J., 1933, Die Rezenten Kalksteine. Akademie Verlag, Leipzig, 420 p.

Pia, J., 1927, Thallophyta. In: Hirmer M. (ed.) Handbuch der Palaeobotanik, Hirmer, Leipzig, v.1, p. 1-136.

Read, J.F., and Grover, G.A., 1977, Scalloped and Planar Erosion Surfaces, Middle Ordovician Limestones, Virginia; Analogues of Holocene Exposed Karst or Tidal Rock Platforms: Journal of Sedimentary

REFERENCES CITED

Bier, J. A, 1964, Landforms of New York (map): Department of Geography, University of Illinois, Geographical Press, Champaign, IL.

Connally, G. G., 1973, Surficial geology of the Glens Falls region, New York: New York State Museum Map and Chart Series No. 23.

Connally, G. G. and Sirkin, L. A., 1969, Deglacial history of the Lake Champlain-Lake George Lowland: in New York State Geological Association. Guidebook to Field Excursions, (ed. S. G. Barnnett), 41st Annual Meeting (SUNY College at Plattsburgh)

Dale, T. N., 1899, The slate belt of eastern New York and western Vermont: U. S. Geological Survey, 19th Annual Report, Part 3, p.159-306.

DeSimone, D. J., 1977, Glacial geology of the Schuylerville Quadrangle: Rensselaer Polytechnic Institute Master's thesis, 77 p.

DeSimone, D. J., 1985, The Late Woodfordian history of southern Washington County, New York: Rensselaer Polytechnic Institute Ph.D. dissertation, 145 p.

DeSimone, D. J. and LaFleur, R. G., 1985, Glacial geology and history of the northern Hudson basin, New York and Vermont: in New York State Geological Association Guidebook, (ed. R. H. Lindemann), 57th Annual Meeting (Skidmore College), p. 82–116.

Dineen, R. J. and Rogers, W. B., 1979, Sedimentary environments in Glacial Lake Albany in the Albany Section of the Hudson-Champlain Lowlands: in Guidebook, Joint Annual Meeting of New York State Geological Association (51st) and New England Intercollegiate Geological Conference (71st), (ed. G. M. Friedman), (Rensselaer Polytechnic Institute, Trip A-3, p. 87-119.

Gates to President of Congress (John Hancock), 15 September 1777, Horatio Gates Papers, ltr.

Heath, R.C., Mack, F. K. and Tannenbaum, J. A., 1963, Ground-water studies in Saratoga County, New York: U. S. Geological Survey, Bulletin GW-49, 128 p.

Johnson, K. G., 1985, Selected landforms of the Saratoga Springs region: a model for relating geomorphology and depositional process in earth science teaching: in New York State Geological Association Special Publication No. 1, Geology of Saratoga, New York: Field Guide for Earth Science Teachers, (ed. R. H. Lindemann), 57th Annual Meeting (Skidmore College), p. 25-34.

Ketchum, R. M., 1997, Saratoga – turning point in America's Revolutionary War: Pimlico, Random House Press, London, 545 p.

La Fleur, R. G., 1965, Glacial lake sequences in the eastern Mohawk – northern Hudson region: New York State Geological Association Guidebook (eds. P.C. Hewitt and L. M. Hall), 37th Annual Meeting (Union College), p. C1 – C23.

La Fleur, R. G., 1979, Deglacial events in the eastern Mohawk – northern Hudson lowland: Guidebook, Joint Annual Meeting of New York State Geological Association (51st) and New England Intercollegiate Conference (71st), (ed., G. M. Friedman), (Rensselaer Polytechnic Institute), Trip B-6, p. 326-350.

Piper, A. S., 1985, Tri-Corn geology: The geology – history-and environmental problems of the upper Hudson Champlain valley: in New York State Geological Association Guidebook, (ed. R. H. Lindemann), 57th Annual Meeting (Skidmore College), p. 224-249.

Pula, J. S., 2000, Engineering American independence:Tadeuscz Kosciuszko's role in the Northern Campaign: Occasional Papers in Polish and Polish American Studies No. 10, Polish Studies Program, Central Connecticut State University, New Britain, CT.

Rodgers, John, 1989, Geology of the Saratoga campaign of 1777: in Field Trip Guidebook T69, (ed., W. M. Jordan), 28th International Geologic Congress, p. 38-39.

Schnitzer, Eric H., 2002, Battling for the Saratoga landscape, 1777: in Cultural Landscape Report for Saratoga Battlefield, Department of the Interior, National Park Service, Olmsted Center for Landscape Preservation, Brookline, MA, 24 p.

Symonds, C. L., 1986, A battlefield atlas of the American Revolution: The Nautical Publishing Company of America, Inc.

Ward, Christopher, 1952, The war of the Revolution: (2 volumes), Macmillan Co., New York, 989 p.

Woodworth, J. B., 1905, Ancient water levels of the Champlain and Hudson valleys: New York State Museum Bulletin 84.

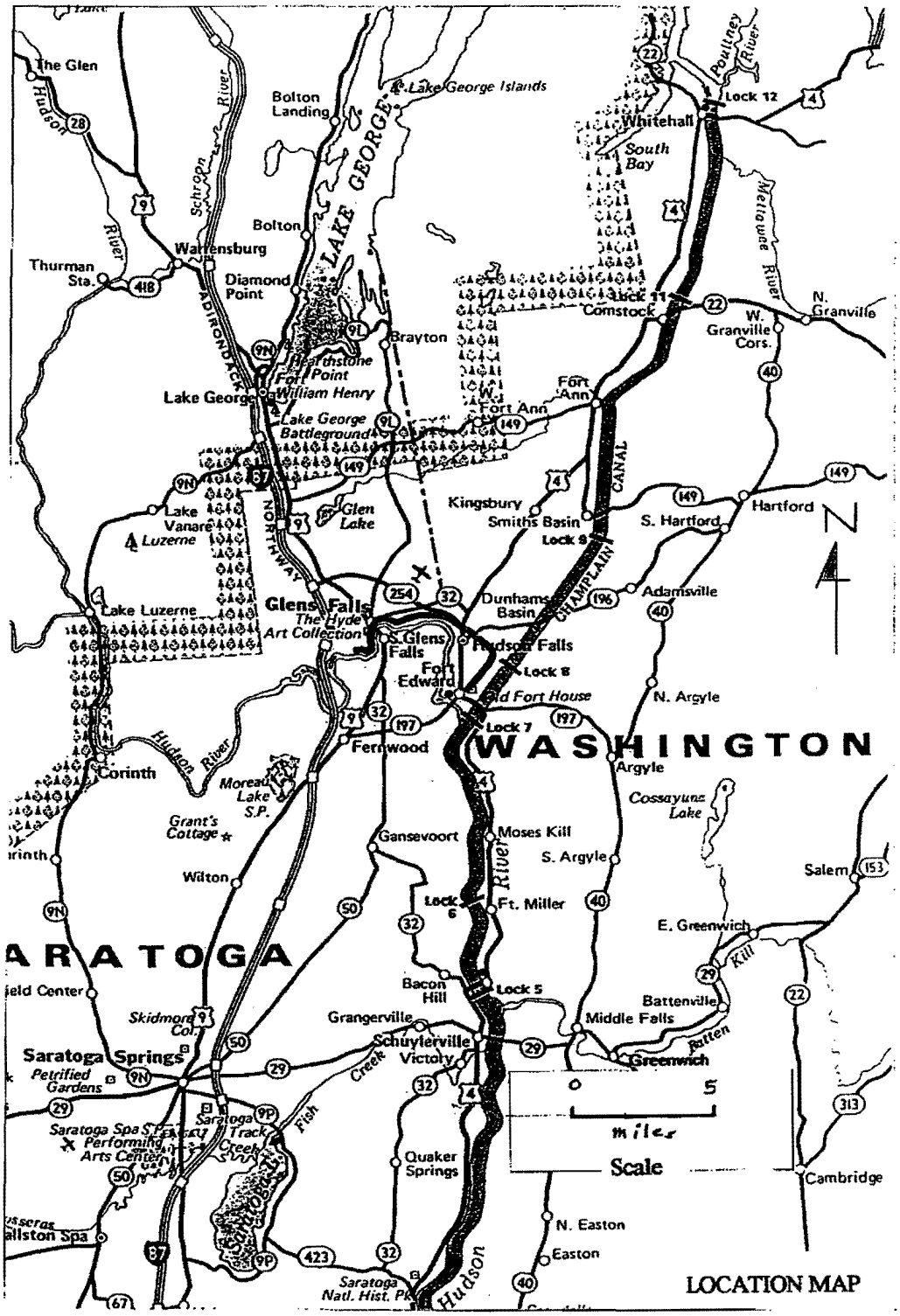
The Glen
Hudson River
Schroon River
Bolton Landing
Lake George Islands
LAKE GEORGE
Poultney River
Whitehall
Lock 12
South Bay
Bolton
Warrensburg
Thurman Sta.
Diamond Point
ADIRONDACK
Lock 11
Comstock
Wetlowne River
N. Granville
W. Granville Cors.
Brayton
Lake George
Battleground
Fort Ann
CANAL
Kingsbury
Smiths Basin
Lock 9
S. Hartford
Hartford
Lake Vanare
Luzerne
Glen Lake
NORTHWAY
Lake Luzerne
Glens Falls
The Hyde Art Collection
Dunhams Basin
CHAMPLAIN
Adamsville
S. Glens Falls
Hudson Falls
Lock 8
Fort Edward
Old Fort House
N. Argyle
Fernwood
Lock 7
WASHINGTON
Argyle
Corinth
Hudson River
Moreau Lake S.P.
Grant's Cottage
Cossayuna Lake
Gansevoort
Moses Kill
S. Argyle
Salem
Wilton
Lock 6
Ft. Miller
E. Greenwich
Kill
Bacon Hill
Lock 5
Battenville
Skidmore Col.
Grangerville
Middle Falls
Saratoga Springs
Schuylerville
Victory
Greenwich
Petrified Gardens
Creek
Saratoga Spa S.P.
Performing Arts Center
Saratoga Track
Fish Creek
Quaker Springs
0 5
miles
Scale
Cambridge
N. Easton
Easton
Saratoga Natl. Hist. Pk.
Hudson
LOCATION MAP

FIGURE 6

Road Log
Field Trip C.9
Geomorphologic Factors in the Failure of General Burgoyne's Northern Campaign of 1777

The first part of this field trip will follow the general path of that portion of Burgoyne's baggage train that was floated south on Lake George from Ticonderoga and then hauled by wagon from Lake George to Fort Edward. Comments on points of interest for this part of the trip are from a paper (1985) by Anson Piper, Professor of Geology Emeritus, Adirondack Community College. The surficial geology of this region has been mapped by Connally (1973).

Cumulative Miles	Miles from Last Point	Route Description
0		In Lake George Village, start at the corner of McGillis St. and Canada St. (Rt. 9) and proceed south on Rt. 9.
2.3	2.3	Bloody Pond, a kettle lake and scene of two French and Indian War skirmishes.
2.6	0.3	On the right (west), an outcrop of Precambrian (Grenville) gneiss. French Mountain, on the left, is a horst on the east side of the Lake George graben. The military road passed below the present road and this was the site of the French ambuscade of the Provincials and Iroquois, known as "The Bloody Morning Scout". Colonel Ephraim Williams, whose estate funded the founding of Williams College, was killed standing on a glacial erratic boulder. The colonials and Mohawks managed to withdraw from "Rocky Gulch" to Lake George, leaving some 100 casualties behind.
4.7	2.1	Kame terrace capped by Lake Albany clays.
5.3	0.6	Immediately north of the Great Escape Amusement Park, on the left, is a low area which is an extension of Glen Lake, an ice block lake. Rt. 9 crosses Five Mile Run, the site of several French and Indian War ambuscades.
5.5	0.2	INTERSECTION – Rt. 9 and Round Pond Rd. – Turn left (east).
6.0	0.5	Round Pond (and Paradise Beach), a kettle lake with an esker on each side at the west end.
6.7	0.7	Round Pond Rd. continues northeast as Blind Rock Rd., which leads down from the kame and esker complex to Bay Road.
7.5	0.8	INTERSECTION – Blind Rock Rd. and Bay Rd. – Turn right (south) on Bay Rd.
7.9	0.4	On left, Adirondack Community College, which is situated on glacio-lacustrine clays overlying Ordovician Beekmantown carbonates.
9.3	1.4	INTERSECTION (at traffic light) – Bay Rd. and Quaker Rd. (at the drainage divide between the Lake Camplain/Lake George basin and the Hudson River basin). – Turn left (east) on Quaker Rd. (Rt.254).

30.4	0.7	CONTINUE down the hill into the southern part of Schuylerville to Rt. 4 and turn right (south).
30.5	0.1	CROSS FISH CREEK, which drains Saratoga Lake about 15 miles to the west. ON THE LEFT, the Schuyler house, manorial home of General Schuyler, which for tactical reasons was burned by Burgoyne during his retreat after the Battles of Saratoga. The house was rebuilt and is now a National Park historical site.
30.0	0.5	On right, an outcrop of Ordovician Normanskill shale. Other outcrops are present along the road farther south.
32.9	1.9	On left, site of Dovegat House, which served as Burgoyne's headquarters.
33.1	0.2	COVEVILLE – The Cove, a Hudson River backwater, is part of a plunge basin formed when the waters of present-day Fish Creek entered glacial Lake Fort Ann at this point. The British used this backwater to anchor some of their transport bateaux just before the Battles at Bemis Heights.
36.0	2.9	Wilbur Road, on right, leads to the Saratoga National Veterans Cemetary.
36.9	0.9	Entering National Park Lands.
37.4	0.5	ENTRANCE to Saratoga National Historical Park. Our manner of entrance and activities there will be determined by the events connected with the 225th Anniversary of the Battles of Saratoga that are taking place on September 29th. STOP #4

SELECTED TILL AND STRATIFIED DRIFT DEPOSITS BETWEEN GLEN'S FALLS AND AMSTERDAM, NEW YORK

by
Donald T. Rodbell, Geology Department, Union College, Schenectady, NY 12308-2311; rodbelld@union.edu

INTRODUCTION

This trip is intended to provide participants with a review of the glacial stratigraphy of the portion of eastern New York State between Glenn's Falls on the northeast and Amsterdam on the southwest (Fig. 1), and to correlate the regional stratigraphy with the better dated sequences of central New York. All of the data presented here were gathered by students in four different classes of *Glacial and Quaternary Geology* (Geo 52) at Union College between 1995 and 2002.

The region covered by this field trip contains a wide variety of glacial deposits—from subglacial till to subaqueous fan deposits to varves to eolian sands. Perhaps what is most interesting about this region is the evidence present for a dynamic history of ice marginal advances and retreats, and the numerous glacial lakes that occupied much of the region during the latter third of marine isotope stage 2 (Martinson *et al.*, 1987). While there has been a plethora of prior work conducted in the area, a near absence of numerical age control coupled with stratigraphic uncertainties generated by a laterally discontinuous and variable lithostratigraphy provides us with considerable room for debate over the details of the glacial history of the region.

BEDROCK GEOLOGY

The bedrock underlying the field trip area comprises diverse lithologies. The Hudson Valley portion of the area is underlain by the Canajoharie shale, and carbonates of the Beekmantown, Trenton, and Black River Formations. The northern third of the Sacandaga Basin is underlain mostly by granitic and syenitic gneiss, with lesser amounts of hornblende-biotite gneiss, and quartzite. The southeastern part of the Sacandaga Basin extending southward to the Mohawk Valley is underlain by calcareous shale of the Dolgeveille Formation, sandstone of the Galway Formation, and oolitic dolomite of the Beekmantown Group. Finally, the eastern Mohawk Valley is underlain by the Canajoharie shale in western portions and sandstone, siltstone and shale of the Shenectady Formation in eastern portions.

PREVIOUS STUDIES ON GLACIAL HISTORY

There have been numerous published works on the Quaternary stratigraphy of this region; here, I summarize some of them. Woodworth (1905) first coined the term *Lake Albany* for the post glacial lake that occupied the portion of the Hudson Valley from Albany south to Kingston, and he was also the first to recognize an avulsed reach of the Mohawk River, which he termed the *Ballston Channel,* located between Schenectady and Ballston Spa. Stoller (1911) focused on the origin of the Ballston channel, the stratigraphic relationship between lacustrine and glacial deposits, and the economic potential of sediment deposited in Glacial Lake Albany. He also noted the presence of widespread eolian deposits, which he attributed to Holocene deflation of Lake Albany shorelines (Stoller, 1911). In later papers, (Stoller, 1918, 1919, 1922) rejected the notion advanced by Fairchild (1918) of a marine strait between the Champlain Sea and the lower Hudson Valley. Cook (1924) asserted that deglaciation of eastern New York did not involve the steady northward retreat of discrete ice margins; instead, he proposed that regional deglaciation generated large regions of dead ice, which he viewed as consistent with the absence of large moraines and the abundance of glacial meltwater features. This is not consistent, however, with observations made by Stoller (1916) of well-defined recessional moraines near Saratoga, NY or with a moraine(s) from a late glacial readvance in the Luzerne region (Connally and Sirkin, 1971). Chadwick (1927) envisaged clear northward-retreating ice margins that enabled the progressive northward development of numerous postglacial lakes in the Hudson Valley. Cook (in Ruedemann, 1930) picked up on observations made by Stoller (1922) and others in focusing on the evolution of the region's surface hydrology. He concluded that there must have been more than one lake level associated with Lake Albany and asserted that Round Lake and Saratoga Lake owe their origin to the existence of local ice blocks.

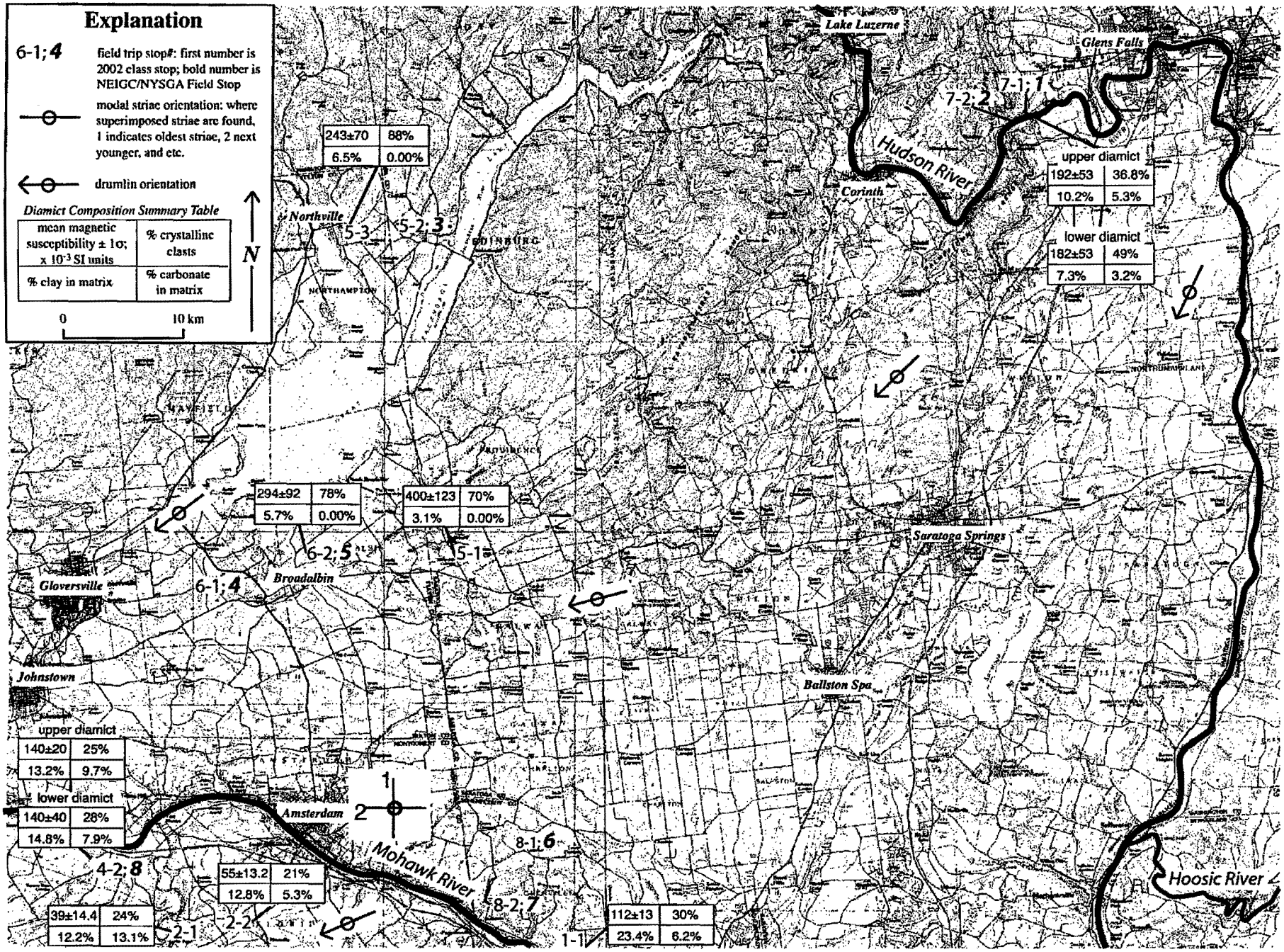

Figure 1. Paleoglacier flow indicators and composition data for diamicts derived from the Adirondack and Hudson-Mohawk lobes of the Laurentide Ice Sheet.

More recent work has focused on the chronology of glacial lakes in the eastern Mohawk and central Hudson Valleys (e.g., LaFleur, 1965; DeSimone, 1985; Wall and LaFleur, 1995 and references therein), and on the age and significance of glacial deposits in the region. Of the latter studies (summarized in Dineen and Hansen, 1995), much emphasis has been placed on determining the history of lobes of the Laurentide Ice Sheet during the last deglacial cycle. The area of this field trip encompasses the border between two principal ice lobes: the *Adirondack Lobe*, which flowed over the Adirondacks, and the *Hudson-Mohawk Lobe*, which flowed down the Hudson Valley and westward up the Mohawk Valley. Deposits from these two lobes can be distinguished according to their texture and composition (Dineen and Hansen, 1995).

Relatively few radiocarbon ages have been reported from diamicts in the study area. One important radiocarbon age constrains the timing of a late glacial readvance in the Hudson Valley near Glens Falls, NY. Connally and Sirkin (1971) reported the glacial stratigraphy exposed along the north side of the Luzerne Gorge of the Hudson River. Here are exposed two diamicts that stratigraphically bound laminated sands and silts. The two tills are similar in composition but yield different fabrics (Hansen *et al.*, 1961). The age of the upper till is constrained by basal radiocarbon dates from Pine Log Camp bog, which is located ~3.2 km north of the village of Lake Luzerne, NY and ~15 km north of the Luzerne Gorge. The basal-most age from this bog of ~13,150 ± 150 ^{14}C years B.P. provides a minimum-limiting age for the upper till, which is attributed to the Luzerne readvance as first recognized by Woodworth (1905). Connally and Sirkin (1971) map the southern limit of the readvance to approximately the latitude of Wilton, NY, ~ 7.25 km south of the Luzerne Gorge.

STOPS FOR THIS FIELD TRIP

There are 8 stops for this field trip. The first two focus on the stratigraphy of the Luzerne Gorge and the possible correlation of stratigraphic units there with the chronology of events in the central Mohawk Valley. Stops 3-5 focus on the Sacandaga basin and evidence there for a large postglacial lake dammed to the south by the Broadalbin Interlobate Moraine (BIM). Finally, Stop 6 and 7 are focused on postglacial lakes in the eastern Mohawk Valley, and Stop 8 provides an excellent exposure of stacked diamicts separated by glacial fluvial deposits.

Table 1.
Summary of Field Trip Stops

STOP #	LOCATION	FEATURES NOTED
1	Luzerene Gorge	diamict typical of till deposited by western side of Hudson Mohawk lobe
2	Luzerne Gorge	varves with drop stones- sandwiched between upper and lower tills
3	Sand and Gravel Pit near Edinburg	climbing ripples, foreset beds with southern paleocurrent directions
4	Herba Gravel Pit	climbing ripples, foreset beds, cut and fill channel
5	Broadalban Town Garage	sand and gravel, cross stratification, climbing ripples, drop stones, diamict stratigraphically on top of section
6	Gravel Pit, North Road West Glenville	foreset beds of kame delta
7	Hoffmans delta	high elevation delta in eastern Mohawk Valley
8	Auriesville Stream Cut	stacked diamicts separated by glacial fluvial gravels

Stop 1

This stop is on the north side of the Luzerne Gorge, in sight of the Hudson River. Exposed along the north side of the Gorge are a thick sequence of diamicts, sand, gravel, and varves (Stop 2). At this stop we will examine the basal till of the Gorge. In addition to a strong NNE-SSW fabric (Fig. 2), this till yields composition indicators that reflect a provenance in the Hudson-Champlain lowlands and from regions underlain by crystalline rocks.

Magnetic susceptibility, carbonate content, texture, and percentage crystalline clasts provide a means to distinguish till deposited from Hudson-Mohawk ice from that deposited by Adirondack ice. Tills deposited by Hudson-Mohawk ice contain >3% carbonate, whereas Adirondack tills are devoid of carbonate (Fig. 1). Similarly, the matrix of tills deposited by Hudson-Mohawk ice contain >10% clay and yield relatively low magnetic susceptibility values (<200 x 10^{-3} SI units). These trends are most obvious when comparing tills in the eastern

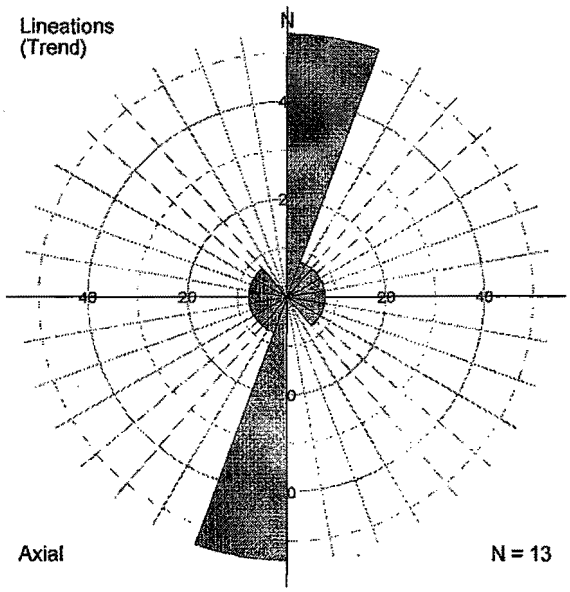

Figure 5. Till fabric from the diamict at the Broadalbin Town Pit (Stop 5).

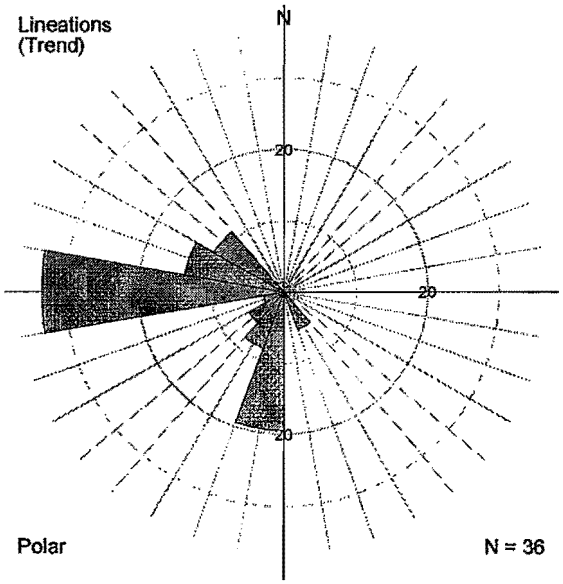

Figure 6. Paleocurrent directions from foreset beds and cross-stratification preserved in the West Glenville gravel pit (Stop 6).

reflect an advance of the Hudson-Mohawk lobe (Yosts Readvance). The presence of rotten shale clasts supports their interpretation, and it is possible that the apparent Adirondack composition reflects Hudson-Mohawk flow lines that overtopped the Kayaderorseras Range ENE of this site. In this case the, it is possible that this till is correlative with the upper till in the Luzerne Gorge (Stop 1), and reflects a Luzerne Readvance that was considerably larger than envisaged by Connally and Sirkin (1971). If so, then the Mt. McGregor moraine of Connally and Sirkin (1971) either represents a younger readvance or a recessional ice position during deglaciation from the Luzerne Readvance.

Stop 6.

This site exposes a kame delta on the northern edge of the Glenville Hills. The deposit is about 20 m thick and contains sand and gravel beds that are inclined at about 20° to the west. This west-southwest flow direction (Fig. 6) likely reflects glacial meltwater off the western side of the Hudson-Mohawk lobe after it had shrunk to open a basin to the west. The elevation of this lake was ~215 m (700') based on the elevation of the top of this kame delta, and on the elevation of numerous sand and gravel pits that demarcate the southern extent of the lake along West Glenville Road to the west of this locality.

Although LaFleur (1965) maps this kame delta at the eastern edge of his "Early Lake Amsterdam", it seems more plausible that this kame was deposited into a much smaller, restricted lake. This smaller lake would have been dammed to the east by the Hudson Mohawk lobe, to the south by the Glenville Hills and to the west and north by bedrock hills within 2 km of this locality. The most likely outlet for this lake was southward down Wolf Creek Hollow and Hoffman's Delta (Stop 7) to the Mohawk River. This is consistent with the elevation of the outlet to Wolf Creek Hollow (~215m), and explains: 1- why Wolf Creek Hollow is devoid of till, and 2- why Hoffman's Delta is so much larger than other deltas in the eastern Mohawk Valley. Proglacial lake drainage down Wolf Creek Hollow would have stripped the valley of drift and induced considerable down cutting. Much of this drift would have been deposited in Hoffman's delta.

Stop 7.

Hoffman's delta is the largest delta in the Mohawk Valley east of Amsterdam. It was deposited at a lake level of ~130 m (~420 '), and according to LaFleur (1965) it was deposited into a late phase of Lake Amsterdam, when the Mohawk Valley was plugged to the east, at approximately Scotia, NY, by the eastward retreating front of the Mohawk lobe.

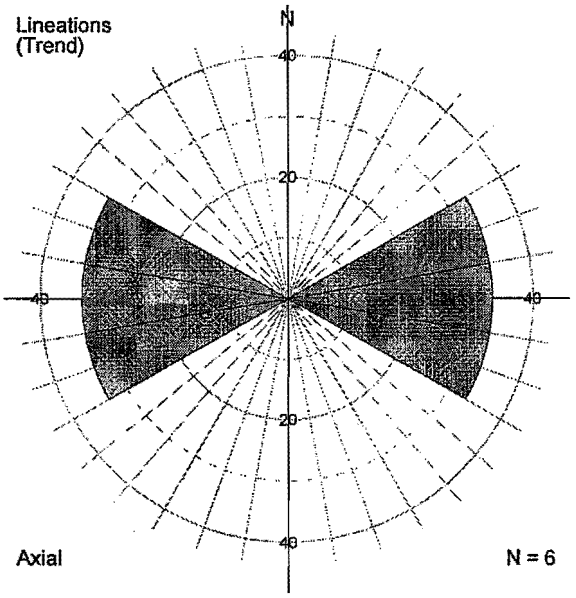

Figure 7. Till fabric from the basal diamict at the Auriesville exposure (Stop 8).

Stop 8.

Here are exposed 40 m of diamicts, gravel and sand. The base of the exposure is marked by a typical lodgement till from the Mohawk lobe that is at least 12 m thick. It contains several lenses of gravel, which may reflect intervals of meltout till. This till is overlain by at least 12 m of sandy colluvium, which appears to be derived from a sand and gravel unit that is at least 4 meters thick. This gravel unit possesses strata that dip northward at ~ 20°. The top of the exposure is marked by a second till, at least 6 meters thick, which is oxidized at its surface, and which is, in turn, overlain by well-sorted fine-medium sand. The sequence appears to reflect multiple ice advances over the site. The two tills are nearly identical in composition, and clearly reflect a Hudson-Mohawk source (Fig. 1). What few fabric data we have from the lower till indicate that it was deposited along an E-W (or W-E) flow path (Fig. 7). . The sand and gravel unit separating the tills appears to be deltaic and indicates the presence of a glacial lake in the Mohawk Valley at an elevation of ~85 m (280').

REFERENCES CITED

Chadwick, G. H., 1928, Ice evacuation stages at Glenns Falls N.Y.: Geological Society of Amercia Bulletin, v. 39, p. 901-922.

Connally, G. C., and Sirkin, L. A., 1971, Luzerne Readvance near Glen's Falls, New York: Geological Society of America, v. 82, p. 989-1008.

Cook, J. H., 1924, Disappearance of last glacial ice-sheet from eastern New York: N. Y. State Museum Bulletin, v. 251.

DeSimone, D. J., 1985, The Late Woodfordian history of Southern Washington County, New York [PhD thesis]: Rensselaer Polytechnic Institute, 145 p.

Dineen, R. J., and Hansen, E., 1995, Glacial Deposits in the Mohawk and Sacandaga Valleys or a Tale of Two Tongues Redux, *in* Garver, J. I., and Smith, J. A., ed., Field Trips for the 67th annual meeting of the New York State Geological Association, Union College: Schenectady, New York, p. 39-55.

Fairchild, H. L., 1918, Pleistocene marine submergence of the Hudson, Champlain, and St. Lawrence Valleys: N. Y. State Museum Bulletin, v. 209-210.

Hansen, E., Porter, S. C., Hall, B. A., and Hills, A., 1961, Decollement structures in glacial-lake sediments: Geological Society of America Bulletin, v. 72, p. 1415-1418.

Harms, J. C., Southard, J. B., and Walker, R. G., 1982, Structures and Sequences in Clastic Rocks, Lecture notes for short course No. 9: Tulsa, Society of Economic Paleontologists and Mineralogists.

LaFleur, R. G., 1965, Glacial Lake sequences in the eastern Mohawk-northern Hudson Region, *in* Hewitt, P. C., and Hall, L. M., ed., New York State Geological Survey 37th Annual Meeting: Union College, Schenectady New York, p. C1-C23.

Martinson, D. G., Pisias, N. G., Hays, J. D., Imbrie, J., Moore, T. C., and Shackleton, N. J., 1987, Age, dating and the orbital theory of the Ice Ages: Development of a high resolution 0 to 300,000-year chronostratigraphy: Quaternary Research, v. v. 27, p. p. 1-29.

Ruedemann, R., 1930, Geology of the Capital District: N. Y. State Museum Bulletin, v. 285.

Stoller, J. H., 1911, Glacial Geology of the Schenectady quadrangle: N. Y. State Museum Bulletin, v. 183.

-, 1916, Glacial geology of the Saratoga quadrangle: N. Y. State Museum Bulletin, v. 183.

-, 1918, Glacial geology of the Cohoes quadrangle: N. Y. State Museum Bulletin, v. 215.

-, 1919, Topographical features of Hudson Valley and question of post-glacial marine waters in Hudson-Champlain: Geological Society of Amercia Bulletin, v. 30, p. 415-422.

-, 1922, Late Pleistocene history of the lower Mohawk and middle Hudson region: Geological Society of Amercia Bulletin, v. 25, p. 515-526.

Wall, G. R., and LaFleur, R. G., 1995, The Paleofluvial record of glacial Lake Iroquois drainage in the eastern Mohawk Valley, New York, *in* Garver, J. I., and Smith, J. A., ed., Field Trips for the 67th annual meeting of the New York State Geological Association: Schenectady, New York, Union College, p. 173-203.

Woodworth, J. B., 1905, Ancient water levels of the Champlain and Hudson Valleys: N. Y. State Museum Bulletin, v. 84, p. 63-265.

ROAD LOG

The starting point is the McDonald's parking lot on the Corinth Road where it crosses I87- The Northway (Exit 18). The parking lot is immediately west of I87, at Exit 18. Reset trip odometers

Total (miles)	Distance from Last (miles)	
0.0	0	Start at McDonald's Parking Lot- Exit 18 of Northway (I87) northwest corner of intersection of I87 with Corinth Road. Proceed west on Corinth Road.
2.4	2.4	Pass West Mountain Road on right; continue straight (west).
3.5	1.1	Park on right side of road; shoulder is narrow; leave 4-way hazard lights blinking.

STOP 1. (Fig. 1- 15 minutes) BASAL TILL OF THE LUZERENE GORGE AND STEEP EXPOSURE OF MULTIPLE DIAMICTS.

3.5	0.0	Continue west on Corinth Road.
4.1	0.6	Park on right side of road; shoulder is narrow; leave 4-way hazard lights blinking; walk up hill along road to out crop on right hand side of road that exposes slumped glacial varves.

STOP 2. (Fig. 1- 15 minutes) VARVES BETWEEN THE UPPER AND LOWER TILLS OF THE LUZERENE GORGE.

4.1	0.0	Continue west on Corinth Road.
9.5	5.4	Turn right on East River Road.
14.3	4.8	Turn left on Bridge Street in the village of Lake Luzerne (this become Rt. 4).
35.4	21.1	Turn right in Edinburg (stay on Rt. 4).
35.8	0.4	Park on right side of road; shoulder is narrow; leave 4-way hazard lights blinking.

STOP 3. (Fig. 1- 30 minutes) DELTA ON NORTH END OF SACANDAGA BASIN.

35.8	0.0	Continue west on Rt. 4 (becomes Fulton County Rt. 113).
37.0	1.2	Route 4 becomes Fulton County Rt. 113.
38.5	1.5	Turn left on Main Street (Northville)
39.8	1.3	Turn left on Bridge Street (Northville)
40.5	0.7	Turn left (south) on Route 30
50.7	10.2	Turn left on Route 30
54.5	3.8	Turn right on Sand Hill Road
55.3	0.8	left into the Herba sand and gravel pit

STOP 4. (Fig. 1- 40 minutes) HERBA SAND AND GRAVEL PIT.

55.3	0.0	Turn right out of the gravel pit onto Sand Hill Road.
56.1	0.8	Turn right onto Route 30.
57.1	1.0	Turn left onto Fulton County Route 155
58.6	1.5	Turn right onto Union Street.
59.7	1.1	Turn left into Broadalbin Town Gravel Pit.

STOP 5. (Fig. 1- 40 minutes) BROADALBIN TOWN GRAVEL PIT.

59.7	0.0 Turn left onto Union Street.
64.0	4.3 Turn right onto Fishhouse Road.
66.7	2.7 Turn left onto Route 29.
68.8	2.1 Turn right onto Route 147.
77.0	8.2 Turn right onto North Road
78.5	1.5 Turn Right into West Glenville Gravel Pit

STOP 6. (Fig. 1- 20 minutes) WEST GLENVILLE GRAVEL PIT.

78.5	0.0 Turn right out of gravel pit onto North Road.
78.8	0.3 Turn right onto West Glenville Road.
79.9	1.1 Turn left onto Wolfe Hollow Road.
80.3	0.4 Stay right here.
81.6	1.3 Park on right side of road; shoulder is narrow; leave 4-way hazard lights blinking.

STOP 7. (Fig. 1- 20 minutes) HOFFMAN'S DELTA.

81.6	0.0 Continue down Wolfe Hollow Road.
82.1	0.5 Turn Right on Route 5.
88.8	6.7 Turn left on Route 30 (follow signs to Route 5S to Auriesville).
89.7	0.9 Turn left onto Route 5S heading west.
96.3	6.6 Turn left onto Ingersoll Road.
96.9	0.6 Park on right side of road; shoulder is narrow; leave 4-way hazard lights blinking.

STOP 8. (Fig. 1- 60 minutes) Auriesville Exposure.

waters. Saratoga Springs mineral and fresh waters were bottled and sold widely to the public, which inevitably brought many of the visitors. Geyser, Hathorn 3, and Coesa mineral springs were bottled from 1935 to 1970, and State Seal spring was also bottled and sold as fresh, non-carbonated water (Saratoga Springs Park Administration brochure, 1999). Both carbonated and non-carbonated versions of Saratoga Springs waters are still bottled and found in stores today. Only one bottling plant and one bath house currently remain in Saratoga Springs.

During the early 1800's most of the natural springs were altered by the drilling of wells as deep as 300 m to increase flow (Kemp, 1912; Siegel, 1996; Davis and Davis, 1997). By 1880, over 200 mineral water wells had been drilled for carbon dioxide gas production alone (Saratoga Springs Park Administration brochure, 1999). Over 150 million gallons (570,000 m^3) of mineral water were removed each year during the period of maximum expansion of the spas and for carbon dioxide production between 1892 and 1904. As a result the aquifer potentiometric surface dropped up to thirty meters (Siegel, 1996). Such severe exploitation of the springs during this time caused many of the springs to cease to flow (Davis and Davis, 1997). Since 1910, the spring waters have been protected by the State of New York as a natural resource; 163 springs and wells on one thousand acres of land were acquired by the State, and by 1912 New York State had closed all but 19 of the mineral water outlets (Davis and Davis, 1997).

THE PROJECT

Since 1996 faculty and students at Union College have been attempting to better characterize the chemical composition of the Saratoga Springs waters, to better understand the origin of the chemical characteristics of the water, and to speculate on the ultimate source of the mineral waters. This work has involved extensive sample collection and analytical programs using modern analytical instrumentation, and extensive geochemical modeling. Chemical analysis of the waters is difficult as chemical components of interest range in concentration from several parts per thousand down into the sub-parts per trillion range. Realistic modeling of the aquifer system is hampered by lack of detailed knowledge of the system and lack of the composition of the most saline mineral water end member. Nonetheless, a plausible conceptual and geochemical model has been developed and so is open to discussion.

GEOLOGY OF THE SARATOGA SPRINGS REGION

Crystalline basement rocks of the Adirondacks are exposed in the northwestern part of the map area (Figure 1). Overlying an early Cambrian unconformity are clastic rocks of the Potsdam and Theresa (Galway) Formations. These are overlain by late Cambrian and Ordovician limestones and dolomites that include the Beekmantown Group, thought to be the principal aquifer rock for the mineral spring waters. These carbonate-rich rocks are overlain by progressively more clastic-dominated rocks of the Chazy Group and Dolgeville Formations. Deepening of the sedimentary basin in the Middle and Late Ordovician (e.g., Hollocher et al., 2002) was caused by the approach of the continental margin to the Taconian volcanic arc subduction zone, with deposition of dark gray Utica (formerly Canajoharie) Shale and Schenectady Formation flysch. The Utica Shale in particular is the cap rock to the mineral water aquifer.

The city of Saratoga Springs lies along part of the Saratoga Springs-McGregor fault system, which runs from the eastern Adirondacks north of Saratoga Springs, south-southwest, sub-parallel to the Taconian deformation front. The Saratoga Springs-McGregor fault, extends from Saratoga Springs, through Ballston Spa, just to the west of Ballston Lake, and through the City of Schenectady. Its fate near the Helderberg Escarpment is unclear. It may die out (as shown in Fisher et al., 1971) or it may continue to the south beneath Silurian and Devonian sediments.

The aquifer rocks that hold the deep, carbonated spring water are the Middle Ordovician Beekmantown Group limestones and dolomites (Figure 2). These rocks crop out along the southeastern margin of the Adirondack foothills (Figure 2) and are between 30 and 200 meters below the surface in Saratoga Springs as indicated by well records, deepening to the south-southwest along the trace Saratoga Springs-McGregor fault. Kemp (1912) states that, on his survey of spring site distribution, nowhere do mineral water springs flow to the surface more than a "few hundred feet from the fault". Cushing and Ruedemann (1914) made it clear that no Saratoga-type mineral springs were found west of the fault. Putman et al. (1978), and Putman and Young (1985) stated that the carbonated spring waters are not known to occur east of Albany or in Paleozoic carbonate rocks elsewhere surrounding the Adirondack Mountains.

A 3-well pump and potentiometric surface test done in the early 1900s suggested that water in the Saratoga Springs-McGregor fault system was flowing to the north (no reference or other details provided; Putman et al., 1978). This observation, combined with the possible southern extent of the Saratoga Springs-McGregor fault system beneath Silurian and Devonian sedimentary cover, suggests a southerly source of the mineral waters.

Figure 1. Geologic map.

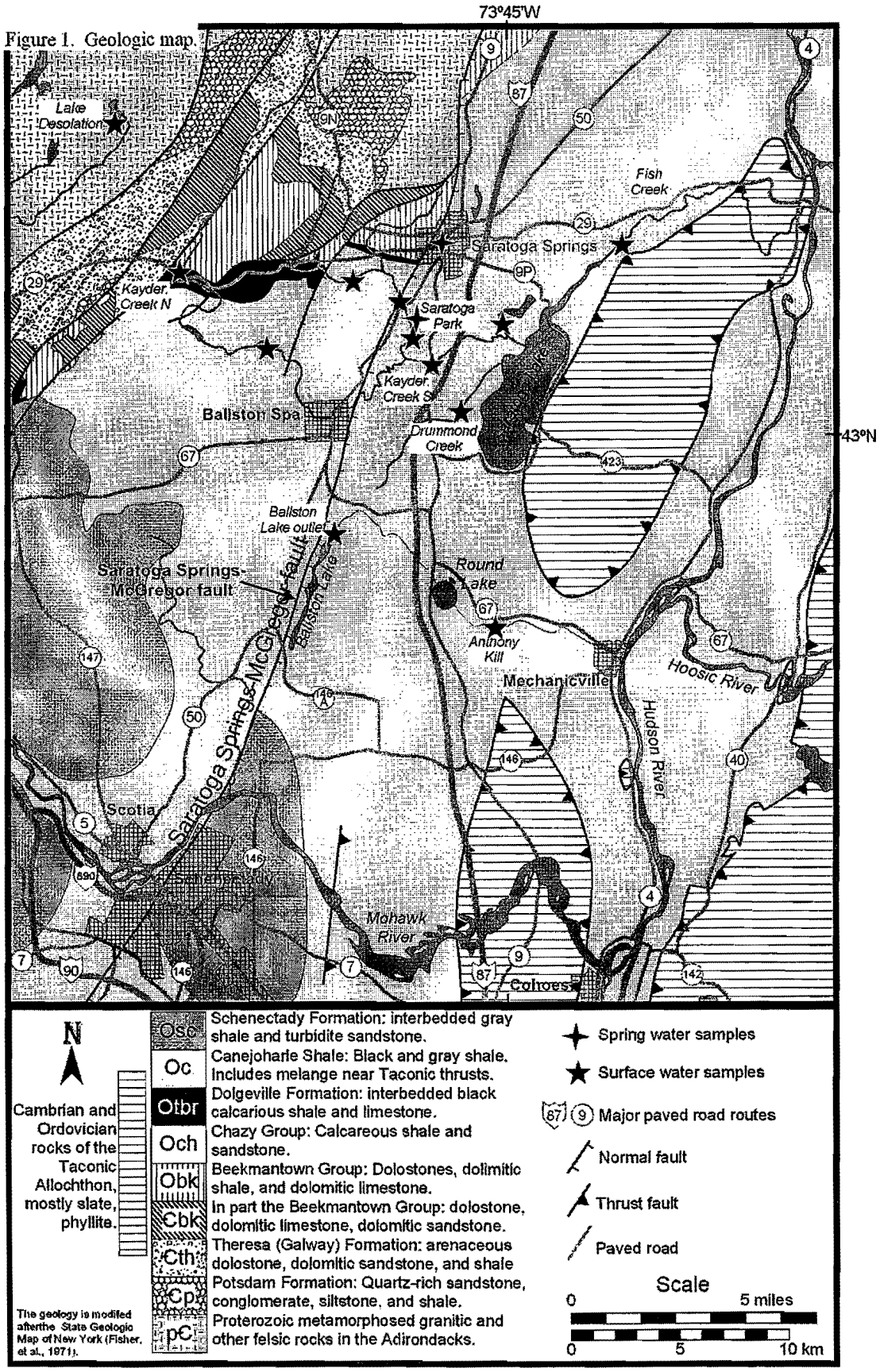

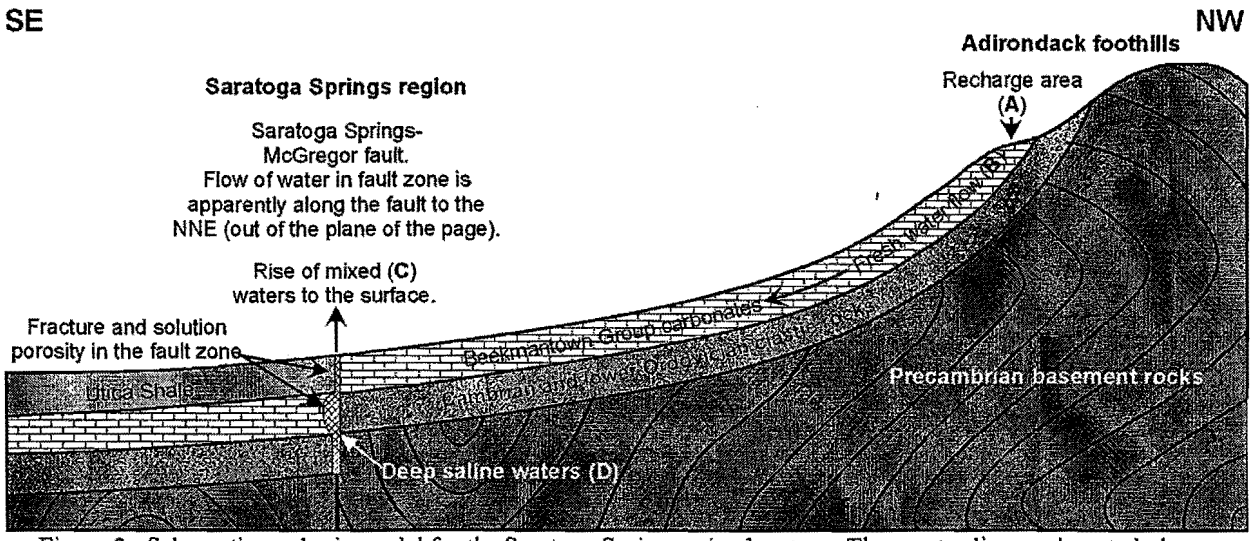

Figure 2. Schematic geologic model for the Saratoga Springs mixed waters. The most saline, carbonated, deep mineral water (model mixing end member **D**). equivalent to or more concentrated than the Hathorn spring, flows northward along solution and fracture porosity in the Saratoga Springs-McGreggor fault zone. Flow is principally in the Beekmantown Group carbonates. Surface precipitation (model mixing end member **A**) enters the aquifer with small quantities of dissolved CO_2 and flows downgradient toward Saratoga Springs. Carbonate rock dissolution and other water-rock interactions yield a hard Ca-, Mg-, and HCO_3^--rich but K-, Na-, and Cl-poor fresh water (composition **B**). The saline and fresh waters mix to yield a density stratified system beneath Saratoga Springs in the fault zone (mixtures **C**). The mixtures are undersaturated with respect to carbonates and therefore dissolve carbonate rock and become more Ca-, Mg-, and HCO_3^--rich. As the deep mineral water flows northward and up dip, it shallows and may start to degas. Rising CO_2 bubbles enter the overlying layer of fresher, CO_2-undersaturated water and go back into solution. This yields a more acidic water that also dissloves adjacent carbonate rock.

Travertine deposits surround various springs, most notably in large mounds surrounding the Island Spouter and Orenda springs. Organic material on these mounds, such as leaves, twigs, and dead insects, can be quickly covered by layers of calcite. Flow of the springs tends to become constricted over time by subsurface deposition of calcite, which can cause the flow path to the surface to be permanently blocked. Periodic re-boring of wells is necessary to maintain flow.

WATER GEOCHEMISTRY

The composition of the average fresh waters sampled in this study, the average composition of three mineral spring waters, including the most saline spring, Hathorn 3, and sea water are given in Table 1. Water chemistry in general is vastly more complex than, say, the chemistry of all igneous rocks, and tables are difficult to comprehend directly. One way to get a grasp of the spring water composition is by normalizing to a familiar geological material such as seawater (Figure 3A). The mineral springs are quite different from seawater, making unlikely the old idea that the mineral springs are diluted, relatively unmodified connate sea water trapped eons ago in local rocks (Kemp, 1912). With the notable exception of Li, there seems to be a pattern of enrichment of large alkali, alkaline earth, and halogen ions compared to small ions in the spring waters compared to sea water. Interestingly, all of the chemical components in Figure 3A, except Ca, Mg, and HCO_3^-, are undersaturated with respect to all phases calculated in modeling. The tremendously high enrichment in Ba in the spring waters over ocean water is permitted by the very low sulfate content of the springs, inhibiting saturation with respect to barite.

Three of the intermediate concentration mineral spring waters have high sulfate, ~27 ppm, in contrast to ~0.2 ppm in the other intermediate springs and in all of the most saline springs (Figure 3B). The strong odor of hydrogen sulfide, the measured presence of NH_4^+, and the relatively high concentrations of Mn^{2+} (0.1 ppm) and Fe^{2+} (~5 ppm) in all of the mineral spring waters indicate that they are all reducing (calculated Eh approximately –200 mV). Note that the mineral waters do not contain a concentrated, fast redox couple, so direct measurement of the water redox potential is difficult. A possible explanation of the three anomalous high sulfate mineral springs is that low sulfate mineral waters mix with sulfate-rich fresh waters soon before reaching the surface, before inorganic or bacteria-mediated reduction of sulfate can occur.

Table 1. Average composition of fresh water and Hathorn 3 spring water. Concentrations in ppm.

	Average fresh water	Old Red	Ferndell	Hathorn 3	Average sea water
pH	7.9	6.4	6.2	6.5	8.0
T°C	16.0	14.0	11.9	10.4	5
Cond. mS	0.37	2.8	5.1	22.7	33.4
O_2	7.4	0.1	0.23*	0.75*	8
HCO_3^-	137	1221	1926	4969	140
Li	0.007	1.0	2.4	14.8	0.17
B	0.03	0.5	1.1	4.3	4.5
NO_2^-	<0.001	<0.001	<0.001	<0.001	~0
NO_3^-	6.3	<0.01	<0.01	<0.01	38
NH_4^+	<0.001	1.4	3.2	27	~0
F	0.13	0.46	0.58	0.23	1.3
Na	22	363	718	4339	10805
Mg	9	61	106	450	1288
Al	0.02	0.02	0.02	0.17	0.0008
SiO_2	8	52	19	14	6.0
PO_4^{3-}	0.01	<0.01	<0.01	<0.01	0.22
SO_4^{2-}	25	0.02	0.28	0.19	2690
Cl	41	454	1188	7178	19499
K	1.3	25	86	374	399
Ca	40	191	334	938	413
V	0.0006	0.002	-	0.001	0.0012
Cr	0.0002	0.0001	-	0.0002	0.0002
Mn	0.04	0.14	0.08	0.09	0.0003
Fe	0.5	5.9	2.9	5.9	0.00006
Co	0.0002	0.0004	0.0006	0.0010	0.000002
Ni	0.001	0.003	-	0.014	0.0005
Cu	0.003	0.001	0.001	0.002	0.0003
Zn	0.007	0.005	0.001	0.004	0.0004
As	0.003	0.003	0.004	0.038	0.002
Se	0.004	0.02	0.04	0.22	0.0001
Br	0.04	4.1	11.6	68	67
Rb	0.0009	0.022	0.08	0.31	0.12
Sr	0.16	3.4	3.4	19.8	7.6
Mo	0.0004	0.00060	0.00002	0.00010	0.011
Cd	0.000009	0.000016	0.000040	0.000370	0.00008
Sn	0.000015	0.000002	-	0.000018	0.0000005
Sb	0.00006	0.00001	-	0.00008	0.00015
Cs	0.000003	0.0008	0.0027	0.0095	0.0003
Ba	0.03	2.9	4.7	28.1	0.014
W	0.000006	0.00002	-	0.00005	0.0001
Tl	0.000003	0.000000	-	0.000004	0.00001
Pb	0.0002	0.00006	0.00004	0.00006	0.000002
U	0.0003	0.000004	0.0028	0.0008	0.0031

*May be contaminated with surface air.

Most previous workers have described the compositional variations among the Saratoga Springs mineral waters as simple mixtures between fresh ground water and a deep saline water end member that may or may not be more saline than that tapped by the Hathorn 3 Spring. In general the mixing concept seems to be correct, but in detail the situation is a little more complicated. Figure 4 shows Ca, K, and Br plotted against the conservative component Cl. Cl is conservative since it is difficult to precipitate, it does not bind readily to mineral surfaces, and it is very low in abundance in most rocks. Cl therefore tends to remain at constant concentration (is conserved) in waters migrating through and reacting with bedrock. The three graphs in Figure 4 illustrate the three principal patterns that different chemical components have among the Saratoga mineral springs.

The Br-type pattern (Figure 4A) is representative of conservative chemical components. Neither Cl nor Br are removed from or added to the waters from the enclosing carbonate rock aquifer in significant amounts because of their low abundance in the rocks and low adsorption affinity. Cl and Br therefore define a straight mixing line.

The Ca-type pattern (Figure 4B) is shared with the components Ca, Mg, and HCO_3^-. The pattern can be approximated with two end members, three distinct linear regression lines, and two line intersections. Rain and snow in precipitation start out as essentially pure water represented by end member **A**. Reaction with surrounding aquifer rock enriches the water in dissolved components. We think the hypothetical fresh groundwater in the deep carbonate aquifer is approximated line intersection point **B**, which is essentially "hard", fresh water. This is consistent with modeled water in contact with carbonate rocks though we have little firm constraint on the hard fresh water P_{CO2}. End member **D** represents the most saline deep water we have available from the Hathorn 3 Spring. The saline and intermediate springs can be approximated by two linear regression line segments that intersect at point **C**. The important point is that **C** is not in fact along a straight mixing line between hard fresh groundwater **B** and saline end member **D**, but rather has a Ca concentration higher that that predicted by a straight mixing line. Since Ca, Mg, and HCO_3^- all follow this same pattern, this suggests that mixed waters can dissolve dolomite and calcite even though ground water **B** and saline end member **D** are probably in equilibrium with these minerals.

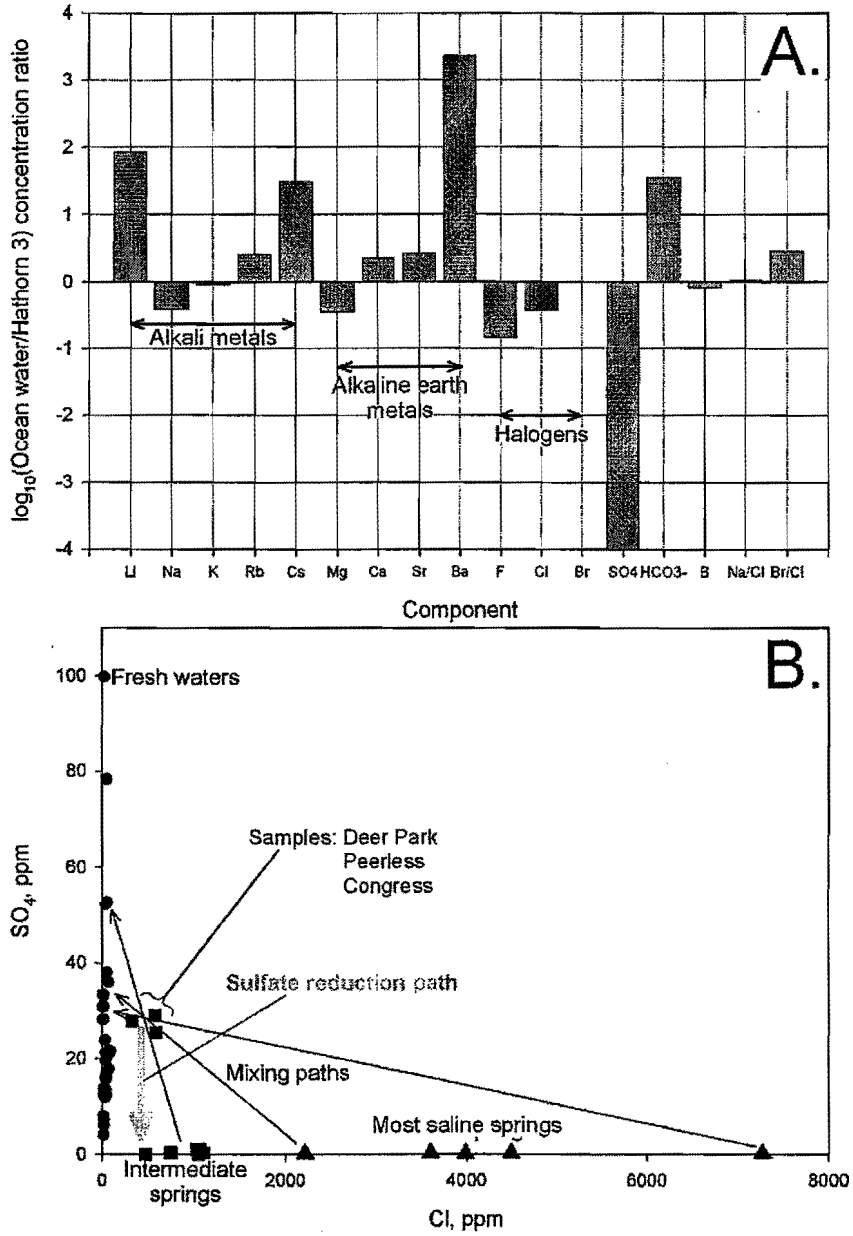

Figure 3.

A. Concentration ratios relative to sea water of several chemical components in the most saline spring, Hathorn 3. High Ba ratio is permitted by very low sulfate ratio, inhibiting barite saturation. In general, larger ions are enriched over smaller ions for the alkali, alkaline earth, and halogen elements. The Li enrichment, however, is exceptional and does not follow this pattern.

B. Surface waters have variable but generally high concentrations of sulfate, derived partially from atmospheric deposition but primarily from the weathering of sulfides in rocks. The mineral spring waters are generally low in sulfate (~0.2 ppm) because of long-term equilibration under reducing conditions (calculated redox potential about -200 mV) that reduce most sulfate to sulfide. Mixing of saline and fresh, sulfate-rich waters soon before the water flows to the surface may permit sulfate-rich mixed waters to reach the surface. Longer term storage of mixed waters in the deep aquifer may allow sulfate reduction to proceed essentially to completion.

Figure 5 shows calculated CO_2 partial pressures for waters having different dissolved solid concentrations, but all with the same dissolved component proportions as the Hathorn 3 Spring. The model calculations were constrained by assuming that the waters were in equilibrium with calcite, dolomite, chalcedony, kaolinite, and pyrite. Calculated P_{CO2} required to maintain this equilibrium varies strongly with concentration. The particular point of interest here is that the P_{CO2} curve for water in equilibrium with these minerals is concave up. All mixtures of more saline and less saline waters therefore become CO_2-enriched over that required to maintain saturation with calcite and dolomite. This means mixed waters are undersaturated with respect these carbonate minerals and can dissolve their host carbonate aquifer rock and so reattain equilibrium by becoming enriched in Ca, Mg, and HCO_3^- relative to a straight mixing line between end member **D** and ground water **B**. It is likely that the intermediate and most saline mineral waters, and mixture **C**, lie along an asymmetric curved line (not shown) rather than along the two regression line segments shown.

The K-type pattern (Figure 4C) is shared with the components Rb, Cs, B, and NH_4^+. Li and Na may also be of this pattern, but for these elements deviation from a straight mixing line is small. The K-type pattern is similar to the Ca-type pattern except that ground water composition **B** is at a lower concentration than a straight **A-C** mixing line might suggest. Hard fresh ground waters in the carbonate aquifer probably do not become strongly enriched in Li, Na, K, Rb, Cs, B, and NH_4^+ because they are not abundant in carbonate rocks, and because, though some are

Figure 4. Graphs of average mineral spring compositions and all fresh water analyses.

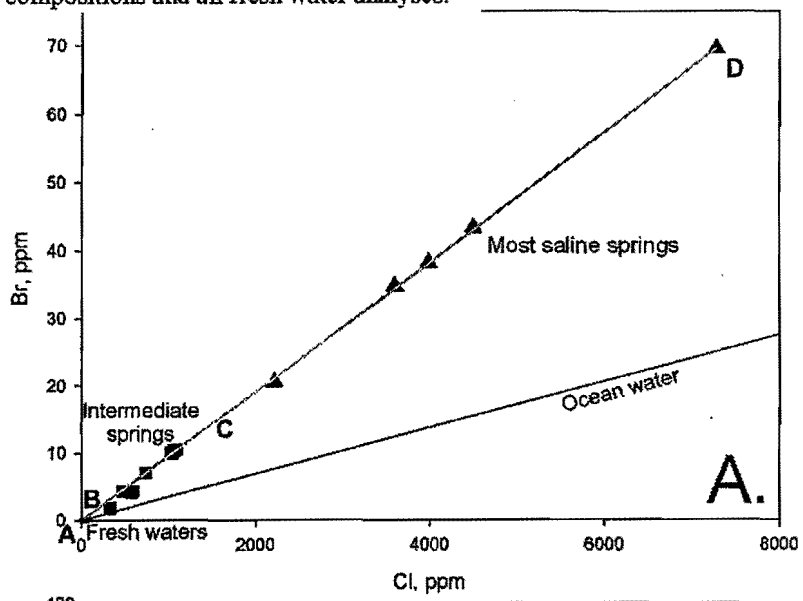

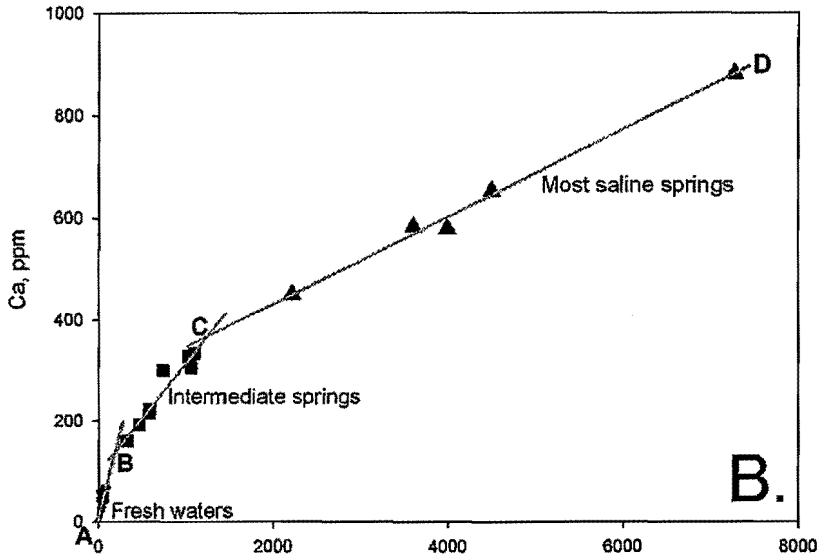

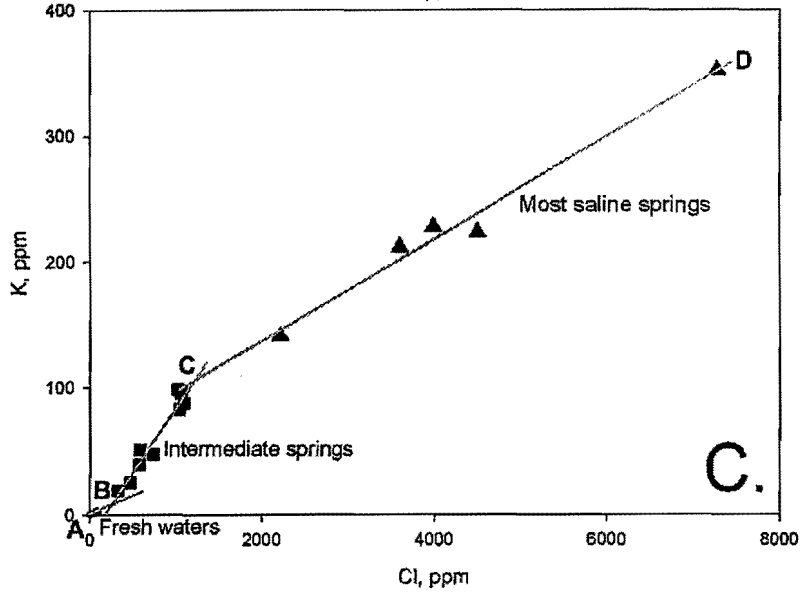

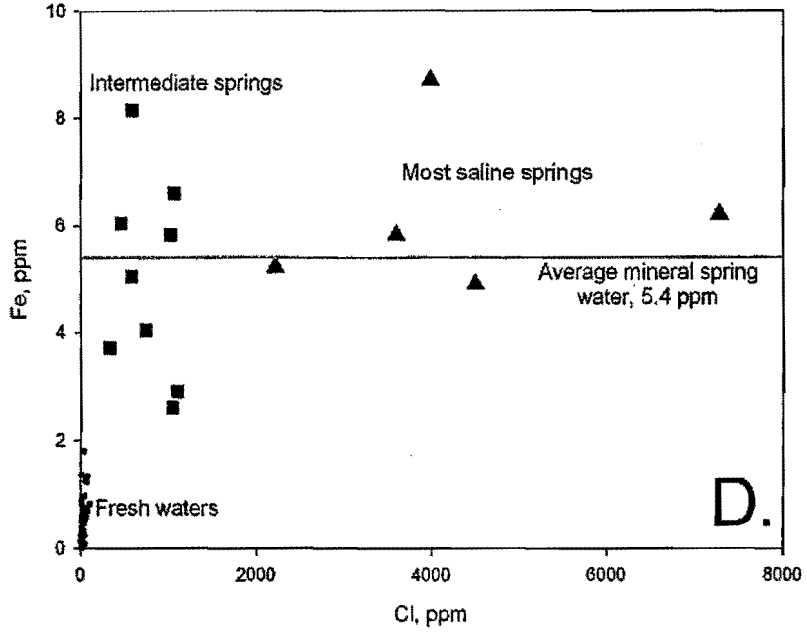

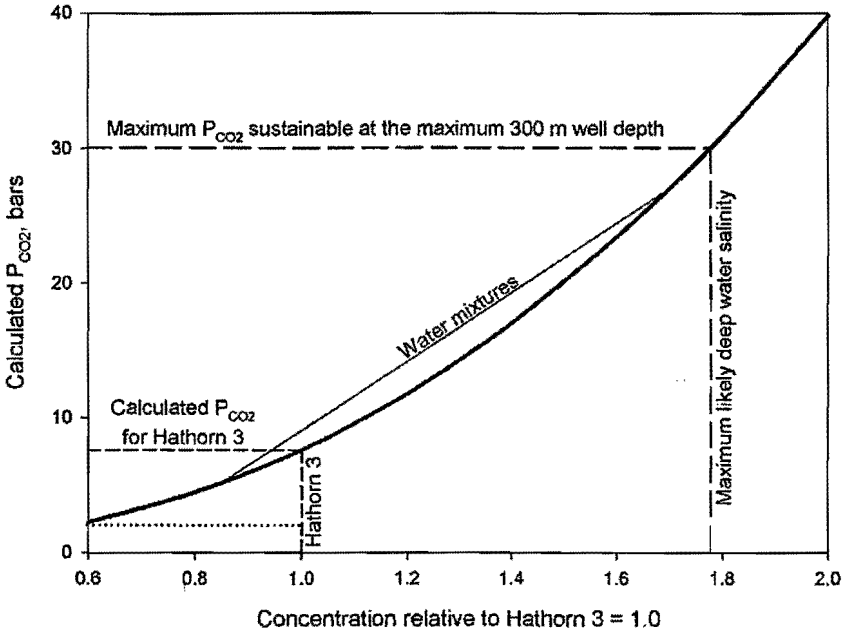

Figure 5. Model P_{CO2} in water spanning a concentration range of 0.6 to 2.0 times that of the Hathorn 3 spring(Table 1). Hathorn 3 water requires a P_{CO2} of ~7.8 bars to maintain calcite and dolomite saturation. Model water at >1.8 times the Hathorn 3 concentration requires >30 bars P_{CO2}, exceeding the hydrostatic head of the overlying 300 m water column of the deepest drilled mineral water well. Mixtures of fresher and more saline water that are at CO_2 saturation become undersaturated with respect to calcite and dolomite and so will dissolve them. Shallowing of CO_2-rich carbonate-saturated waters will allow them to evolve CO_2 gas bubbles.

components of silicates, these are rather insoluble. Intersection point **C** has elevated K concentrations compared to a straight **B-D** mixing line. This may be caused by dissolution of or ion exchange with newly exposed clay and other minerals that are exposed as subsurface mixing promotes dissolution of the enclosing impure carbonate aquifer rock.

Fe (Figure 4D) and Mn (not shown) have essentially flat, though rather scattered concentration patterns having more or less constant 5.4 and 0.1 ppm Fe and Mn, respectively. Fresh waters have much lower and more variable concentrations of Fe and Mn. Calculations indicate that Fe and Mn are almost entirely in the 2+ state, and are undersaturated with respect to various carbonate, hydroxide, and oxide minerals under the low redox potentials in the deep aquifer. However, the Fe and Mn available from carbonate rock dissolution may be relatively constant, resulting in only modest scatter of the data about the average line.

The other chemical components (e.g., Co, As, Mo, Pb, U) either have compositional distributions resembling random scatter, or they follow straight Br-type mixing lines but with a lot of scatter about the line. Though all elements have not been subject to modeling, none of those that have are close to saturation with any model phase. It seems likely that these trace components have variable sources in the rocks undergoing dissolution, and are not buffered.

CONCEPTUAL MODEL AQUIFER SYSTEM

Figure 6 shows our schematic conceptual model for the mineral springs aquifer system. Surface precipitation has a very low content of dissolved solids and represents water component **A**. It picks up CO_2 from the atmosphere and soil and percolates into fractures and solution voids in the Beekmantown Group carbonates in the Adirondack foothills to the north and west of Saratoga Springs (Figures 1 and 2). The residence time of the aquifer water is not known, but water tends to reach equilibrium with carbonate minerals within a matter of days or weeks. The result is a hard fresh water component **B** containing an enhanced dissolved load of carbonate rock components, most notably Ca^{2+}, Mg^{2+}, and HCO_3^-. This water probably has a pH near neutral and a P_{CO2} «1 bar. We assume that at least some of this water remains modestly oxidizing and sulfate-rich.

The composition of the most saline and carbonated deep water is not known. The most saline and carbonated water at the surface is from the Hathorn 3 Spring, and modeling indicates that the deep water at the 300 m depth of the Hathorn 3 well is unlikely to be more than twice as concentrated as the surface Hathorn 3 water. In any case, we use Hathorn 3 as the model saline water end member **D**. As this water flows along the fault zone, from unknown sources to the south, it partially mixes with hard fresh water **B** in the vicinity of Saratoga Springs to create a density stratified aquifer system. Depressurized waters may evolve CO_2 bubbles which may redissolve into CO_2-undersaturated fresher waters above. Mixed saline-fresh waters also form. Mixing and incorporation of CO_2 by fresher water both undersaturate the waters with respect to carbonate minerals, and so will tend to dissolve carbonate rock in the aquifer zone, enlarging the zone to form a cave system. As indicated in Figure 4B, mixed waters are

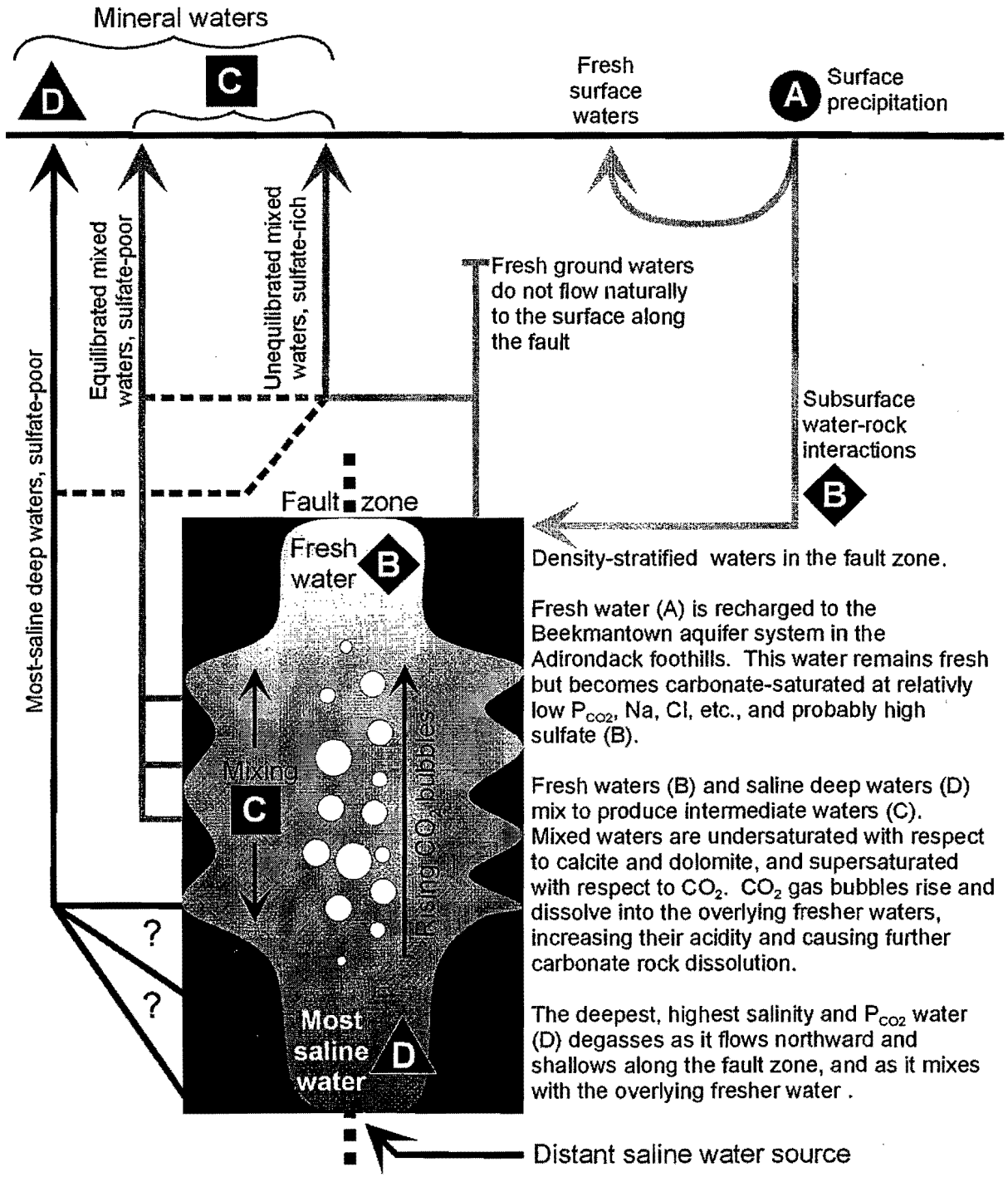

Figure 6. Conceptual model for water mixing, rock dissolution, and tapping of the mineral waters in the aquifer.

indeed enriched in Ca, Mg, and HCO_3^-. The result is mixed waters that have elevated concentrations of various chemical components above those expected from a straight mixing line between water components **B** and **D**.

SOURCE OF THE SALINE WATERS AND CO_2

There is a long history of speculation as to the origin of the Saratoga spring waters, generally divided into the problems of the recharge water source, the CO_2 source, and the source of dissolved minerals. Possible sources for these, culled from the literature, are given in Table 2. The Saratoga mineral waters were compared with a wide

Table 2. Several concepts for the origin of the Saratoga Springs mineral waters, specifically regarding origin of the water proper, the mineral content of the water, and the CO_2 content of the water. Details of citations are too complex to cite specifically here, but are derived from Sylvester (1893), Kemp (1912), Cushing and Ruedemann (1914), Ruedemann (1937), Strock (1941); Putman and Young (1985), Siegel (1996); Quintin (2000); Lesniak and Siegel (2000).

Source	Attempts to explain			Concept	Problems
	Water	CO_2	Minerals		
Magmatic	✓	✓	✓	Crystallization of igneous bodies, and interactions of magmas with surrounding rocks, can release large quantities of mineralized water and CO_2.	The springs are cold and there is no recent magmatic activity or local thermal anomaly. The cited Starks Knob "plug" to the northeast of Saratoga Springs is a Taconian thrust slice of oceanic pillow lavas.
Meteoric	✓			Meteoric water is an abundant and obvious source of spring water.	Does not account for the mineral or CO_2 content of the mineral waters.
Trapped sea water	✓	✓	✓	Sea water was trapped in sediment pores at the time of deposition, providing a source of salty water. CO_2 could be derived from slow decomposition of buried organic material.	Spring waters do not have compositions derivable from sea water by dilution. The organic matter in the shales and other rocks in the area is mostly high-carbon, high molecular weight material not subject to ready bacterial decomposition.
Metamor-phism at depth	✓	✓		Metamorphism releases water and CO_2 from various sedimentary rocks.	No reason to suspect active metamorphism at depth; continental margin has been more or less stable for ~200 Ma.
Mantle degassing		✓		CO_2 released from the mantle via deep fractures.	Deep fractures unlikely to remain open due to ductile flow of rock and precipitation of minerals during fluid cooling and depressurization.
Deep sedimentary basin	✓	✓	✓	Meteoric water percolates downward and mixes with saline deep formation brines and equilibrates with thermally-derived formation gasses (CO_2, CH_4?). Water flows northward along the fault into the Saratoga Springs area. High elevation in the water source are drives hydrostatic flow.	Distant water source, not nearer than beneath the Catskills or Pennsylvania. Requires an enormously long flow conduit. Mechanism of interaction between meteoric water and saline formation waters and gasses unclear.

range of waters from other sources (White et al., 1963; Carpenter, 1969; Campbell et al., 1970; Young and Putman, 1978; Drever, 1982). These indicate that the Saratoga Springs mineral waters are most similar to "oil field brines" and "deep sedimentary basin brines". Though the range of scatter of each water type is tremendous, it seems that it is unlikely that the Saratoga Spring waters are from any type of shallow or hydrothermal source, or that they are from a source closely associated with common gypsum or halite evaporites.

Many seemingly unlikely hypotheses have been proposed for the origin of the unusual Saratoga Spring water components, from clearly outrageous (local magmatic source; Kemp, 1912) to at least superficially implausible (from the north along the Saratoga Springs-McGregor fault, derived from crystalline rocks in the Adirondack highlands; Lesniak and Siegel, 2000). Our concept, which we hope is not worse than superficially implausible, is that the waters and their excess CO_2 is derived from the deep sedimentary basin beneath the Catskills or farther south in Pennsylvania. The higher elevation in these regions causes fresh groundwater to percolate downward, into some region where the meteoric waters can mix with deep basin brines and trapped or dissolved gasses. The hydrostatic head forces the mixed water to flow northward along solution and fracture porosity in the Saratoga Springs-McGregor fault zone, finally mixing in the Saratoga Springs region with local hard, fresh ground waters and finally coming to the surface.

REFERENCES CITED

Campbell, V.K., Miers, J.H., Nichols, B.M., Oliphant, J., Pytlak, S., Race, R.W., Shaw, G.H., and Gresens, R.L., 1970, A survey of thermal springs in Washington State: Northwest Science, v. 44, no. 1, p. 1-11.

Carpenter, A.B., 1969, Geochemistry of saline subsurface water, Saline County (Missouri): Chemical Geology, v. 4, p. 135-167.

Cushing, H.P., and Ruedemann, 1914, Geology of Saratoga Springs and vicinity: New York State Museum, Bulletin 169, 177 p., 2 plates.

Davis S.N., and Davis A.G., 1997, Saratoga Springs and early hydrogeochemistry in the United States: Groundwater, v. 35 , no. 2, p. 347-356.

Drever, J.I., 1982, The Geochemistry of Natural Waters: Prentice Hall, Inc., Englewood Cliffs, NJ, 388 p.

Fish, C.F., 1881, The mineral springs of Saratoga (New York): Popular Science, 1881, p. 24-33.

Fisher, D.W., Isachsen, Y.W., and Rickard, L.V., 1971, Geologic Map of New York: New York State Museum and Science Service, Map and Chart Series, no. 15.

Hollocher, K., Bull, J., and Robinson, P., 2002, Geochemistry of the Metamorphosed Ordovician Taconian Magmatic Arc, Bronson Hill Anticlinorium, western New England: Physics and Chemistry of the Earth, v. 27, p. 5-45.

Kemp, J.F., 1912, The mineral waters of Saratoga: New York State Museum, Bulletin 159, 79 p.

Lesniak, K.A., and Siegel, D.I., 2000, The isotopic geochemistry of the Saratoga "Springs"; implications for the origin of solutes and source of carbon dioxide gas: Geological Society of America Abstracts with Programs, Annual Meeting, v. 32, no. 7, p. 62.

Putman, G.W., and Young, J.R., 1985, The bubbles revisited; the geology and geochemistry of "Saratoga" mineral waters: Northeastern Geology, v. 7, no. 2; p. 53-77.

Putman, G.W., Young, J. R., and Dunn, J. R., 1979, The origin of the mineral waters of Saratoga; possible thermal processes and their bearing on regional neotectonics: Eos, v. 60, no. 18, p. 397.

Quintin, L.L., 2000, Origin of cold, carbonated mineral waters of Saratoga Springs, New York: Undergraduate Senior Thesis, Union College, Geology Department, 71 p.

Ruedemann, R., 1937, Different views held on the origin of the Saratoga mineral springs: Science, v. 86, p. 531-532.

Saratoga Springs Park Administration, 1999, History of the Springs of Saratoga: pamphlets and inserts.

Siegel, D.I., 1996, Natural bubbling brew; the carbonated springs of Saratoga: Geotimes, v. 41, no. 5, p. 20-23.

Young, J.R., and Putman, G.W., 1978, The puzzle of Saratoga - an old solution with a new twist: New York State Geological Survey, Empire State Geogram, v. 14, no. 2, p. 17-31.

White, D.E., Hem, J.D., and Waring, G.A., 1963, Chapter F. Chemical composition of sub-surface waters: in, Mleischer, M., Ed., Data of Geochemistry, 6th edition, USGS Professional Paper 440-F.

ROAD LOG

The starting point is the Wilton Square Mall adjacent to Rt. 50 in Saratoga Springs, just east of the Northway (I-87). To reach the starting point from either direction on I-87 take exit 15 for Rt. 50, Saratoga Springs. At the top of the exit ramp, turn east onto Rt. 50 towards Gansevoort. Cross through the traffic lights at Weibel Ave., stay in the right lane, and turn right at the next set of lights into the Wilton Square Mall (large sign advertising many stores). Take an immediate left into the Price Chopper parking lot adjacent to Rt. 50 and wait there (approximately 43.084°N, 73.741°W). Unfortunately the most recent topographic sheet does not have the new mall, so a more precise location is difficult. Figures 7 and 8 show the trip route and spring locations.

Total miles	From last	
0	0	Start in the Price Chopper parking lot, as described above. Turn right out of the parking lot exit and get in the left lane to turn left onto Rt. 50 toward Saratoga Springs. ***Reset trip odometers to zero at the light.*** Turn left onto Rt. 50.
0.2	0.2	Cross Weibel Ave.
0.6	0.6	Cross over I-87.
1.2	1.2	Turn left at the traffic lights onto Veterans Way (note: the road on the right side of the intersection is Gick Rd., not Veterans Way).
1.4	1.4	Turn right at the stop sign (T intersection) onto Excelsior Ave.
1.6	1.6	Brewery on the right.

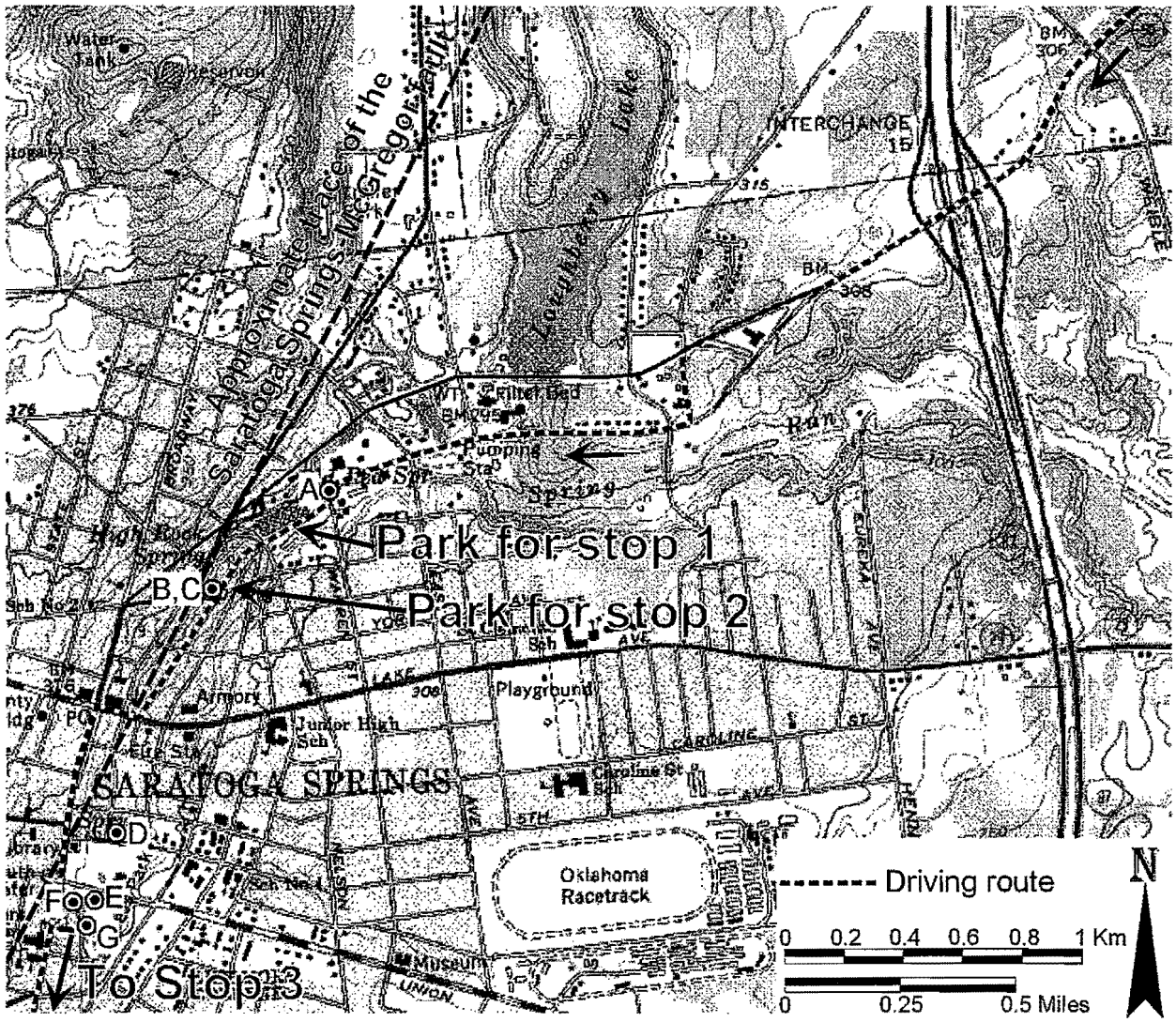

Figure 7. Route from near the start of the trip to Stops 1 and 2, and continuing toward Stop 3 through the Saratoga Springs downtown. Dashed line is the driving route. Springs are labeled A-F: A, Old Red; B, Peerless (the least saline mineral spring has nearly stopped flowing); C, Governor, D, Hathorn 1; E, Congress; F, Columbian (Saratoga Springs municipal drinking water supply); G, Deer Park.

2.1	2.1	Turn left onto Warren St. and then an immediate right onto High Rock Ave. A small pavilion for the Old Red Spring is at this intersection.
2.2	2.2	Park on the right side of the street outside the light yellow building with many columns in front.

STOP 1. OLD RED SPRING. (10 minutes) The Old Red Spring (0.24% TDS, intermediate type, A in Figure 7) is the north-easternmost and one of the lest saline of the existing Saratoga-type mineral springs. Some older literature describes this spring as being highly iron-rich, though chemical analysis shows this water to be unremarkable. It has the second lowest salinity of all of the flowing springs and so is more popular than some of the other saltier and smellier waters.

2.2	0	Continue straight on High Rock Ave.
2.3	0.1	Road curves to the left.
2.4	0.2	Park along the road next to the spring pavilion.

STOP 2. CONGRESS PARK AND ENVIRONS. (1 hour 15 minutes) This is a walking stop at which we will see all of the flowing springs in the Saratoga Springs downtown.

High Rock Spring, originally known as the Big Medicine spring, was the first mineral spring in the area to be introduced to European settlers in 1767 (Siegel, 1996). Though the spring conduit has been cleaned with hand tools repeatedly, the original spring has long since sealed its own conduit by calcite precipitation. Any flowing water in the High Rock Pavilion actually flows by gravity through a pipe from the nearby Governor spring. The cliff to the west of the pavilions is of the Beekmantown Group (Amsterdam Limestone), faulted above the Utica Shale on which the pavilions are built. The fault displacement, calculated at the now vanished Star spring that was located ~100 m northeast of the High Rock Spring, is ~49 m, much less than the total carbonate section here of ~140 m (Cushing and Reudemann, 1914).

Peerless Spring (0.15% TDS, intermediate type, B in Figure 7) is the least saline of the flowing springs. Its salinity has been decreasing over the past decade. Based on the salinity curve over time, we predicted that it would stop flowing in 2001, which in fact it did. However, we found in spring 2002 that it was flowing again if only a trickle. It is called Peerless probably because it is the least saline and so least bad-tasting of the Saratoga Springs.

Governor Spring (0.35% TDS, intermediate type, C in Figure 7) is in the same pavilion as Peerless, though both are piped from the well head across the street.

Hathorn 1 Spring (0.71% TDS, saline type, D in Figure 7) is the first and northernmost of the saline-type springs as defined in Figures 3B and 4. The drilled well is just over 300 m deep and penetrates ~80 m into Cambrian clastic rocks. This spring outlet and pavilion were moved in 1999 from across the street to make room for the parking garage currently at the original spring location.

Congress Spring (0.28% TDS, intermediate type, E in Figure 7) is perhaps the most frequently visited of the springs, its handsome pavilion being a prominent landmark in Congress Park.

Columbian Spring (0.026% TDS, fresh water, F in Figure 7) is actually from the municipal water supply for the City of Saratoga Springs, derived from the Loughberry Lake reservoir. This was once a natural spring or drilled well, converted to municipal water in order to give justification for the pavilion.

Deer Park Spring (0.30% TDS, intermediate type, G in Figure 7) has a miniature pavilion that is unique among the Saratoga Springs. Curious ducks sometimes congregate to watch people collecting samples and making field measurements. Ducks are not, however, big fans of the mineral waters.

2.4	0	Continue straight on High Rock Ave.
2.7	0.3	Turn right (west) onto Lake Ave. (Rt. 29), the first real cross street. Get into the left lane as you climb the hill.
2.8	0.4	Turn left (south) onto Broadway (Rt. 50 and 9), which is the main street in town.
3.3	0.9	Rt. 50 turns off to the right, continue straight on Rt. 9 south.
4.0	1.6	Museum of Dance on the right.
4.1	1.7	Lincoln Baths on the right, the only operating public bath house in Saratoga Springs. This is the location of the Lincoln Spring, for which there is a small monument. The spring has been turned off for many years, presumably to supply mineral water to the baths.
4.2	1.8	Turn right onto the Avenue of Pines, enter Saratoga Spa State Park. This road travels through a remarkable tunnel made of pine trees.
5.0	2.6	Complicated intersection; bear right, following a sign toward Rt. 50.
5.2	2.8	Turn left following the sign to the Hall of Springs Museum. The "Bottling Plant" is on the right (historic; now a car museum).
5.3	2.9	Turn right into the large parking lot after the "Bottling Plant" and park.

STOP 3. SPA PARK SPRINGS AND OTHER WATERS. (2 hours) This is also a walking stop at which we will see all of the flowing springs in the Saratoga Spa Park and much of the park itself including the Saratoga Performing Arts Center (SPAC), the new antique car museum ("Bottling Plant"), and Geyser Brook, the valley for which hosts several of the springs.

State Seal Spring (0.030% TDS, fresh water, A in Figure 8) is by far the most popular spring in the area. There are usually droves of people filling up jugs, canteens, and carboys to bring home for drinking. Little do they realize that this fresh water is completely unrelated to the mineral springs, but in fact is pumped from a nearby shallow well in unconsolidated glacial outwash. The proximity of the well to the surrounding golf course causes this water to have the highest NO_3^- concentration (24 ppm) of any water sampled in this project by a factor of ~50. Doubtless there are organic residues as well, though these were not analyzed by us. The water is tested periodically

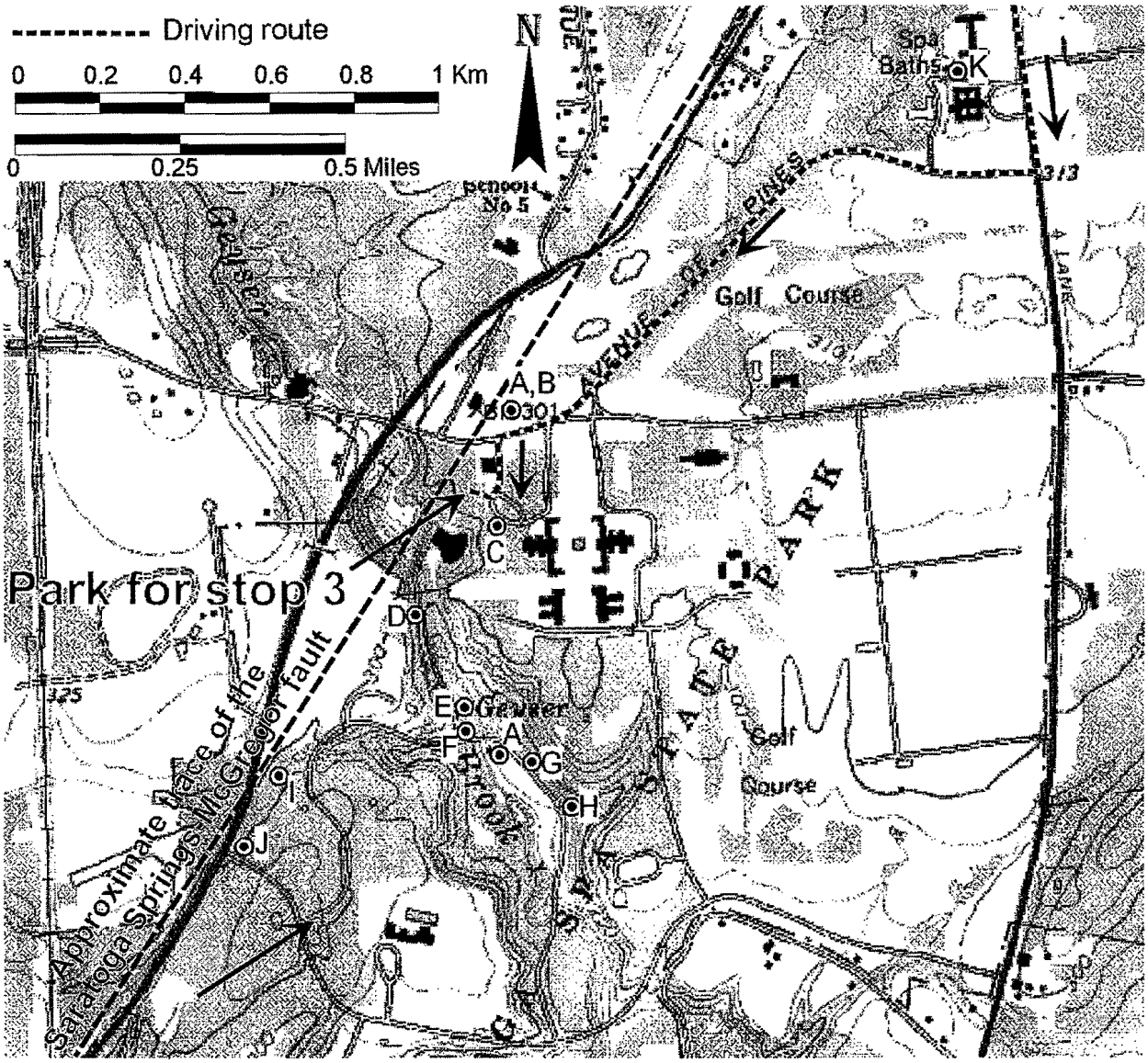

Figure 8. Route from Rt. 9 south from the Saratoga Springs downtown to Stop 3. Dashed line is the driving route. Springs are labeled A-K: A, State Seal (pumped from shallow glacial outwash): B, Geyser; C, Charlie, D, Orenda; E, Island Spouter; F, Hayes; G, Polaris; H, Ferndell; I, Coesa (under a pond); J, Hathorn 3 (the most saline spring); K, Lincoln (dry; diverted to the adjacent Spa Baths).

and is safe for drinking. This water is also piped to a State Seal Spring outlet to the south, that we will see later today.

Geyser Spring (0.51% TDS, intermediate type, B in Figure 8). The original location of this spring was just west of the "Bottling Plant" across the street. As of this writing it is unclear if this water will be piped to the new pavilion at the new location of State Seal Spring. If so, you will see that people are *not* lining up to fill jugs with this real mineral water.

Charlie Spring (0.54% TDS, intermediate type, C in Figure 8) is the only spring water accessible from within the gates of SPAC. When it is flowing, it comes out on both sides of an ornamental wall. Note trace fossils on the stone slabs surrounding this spring.

Orenda Spring. (1.18% TDS, saline type, D in Figure 8) Orenda is the most boisterous of the mineral springs, enthusiastically belching forth CO_2 and traces of H_2S. This is also the most energetic precipitator of travertine, the amount of travertine deposition being estimated at ~2000 kg/year. The travertine mound is mostly along the slope down to Geyser Brook, on the banks of which it forms a fine travertine platform along which a path goes.

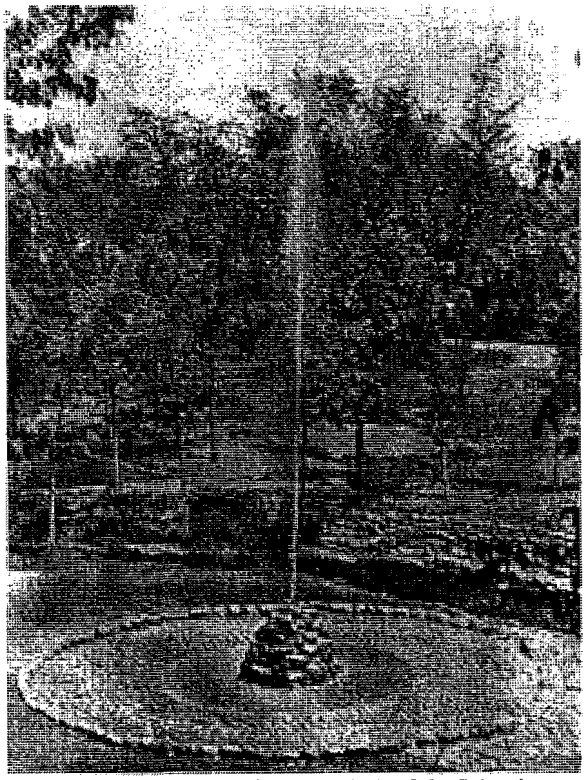

Figure 9. Photograph circa 1930 of the Island Spouter Spring, shown soon after it was ornamented with stonework. Photo source uncertain.

Island Spouter Spring (1.05% TDS, saline type, E in Figure 8) is the most enthusiastic geyser among the flowing springs, spouting these days up to ~7 m high. Originally drilled in the early 1900's for CO_2 production, it was turned into an ornamental island in Geyser Brook in 1930. The ornamentation has either been eroded away or has been buried beneath the nearly 2 m of travertine deposited by the spring in the past 70 years. This spring usually runs through a cycle of varying geyser height that lasts perhaps 30 seconds, terminating in a short period of gas venting without water. Sampling this spring is a wet experience. Figures 9 and 10 show how the appearance of Island Spouter has changed as erosion has taken its course and as nearly 2 m of travertine has been deposited.

Hayes Spring (1.14% TDS, saline type, F in Figure 8) is the third most saline spring after Hathorn 3 and Orenda.

Polaris Spring (0.42% TDS, intermediate type, G in Figure 8) is a gentle continuous geyser typically spouting ~1 m high.

Ferndell Spring (0.44% TDS, intermediate type, H in Figure 8, BEWARE OF POISON IVY) flows to the surface without a notable geyser. It has deposited a broad, low travertine mound that is the third most notable after those of Orenda and Island Spouter.

Coesa Spring (not sampled, presumably saline type, I in Figure 8) bubbles to the surface beneath a small pond. Though it is occasionally seen to be connected to a hose, the pond and fence have so far discouraged sampling.

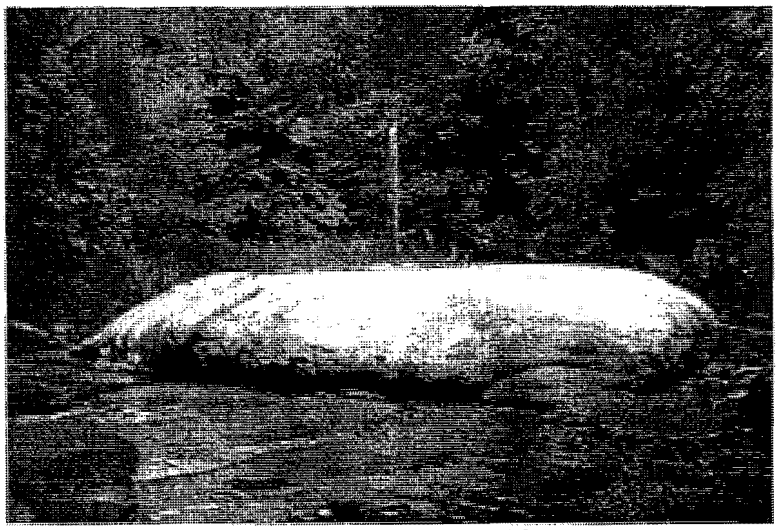

Figure 10. Photograph in 1999 of the Island Spouter Spring, long after the ornamental stonework was eroded away and covered with nearly 2 m of tufa.

Hathorn 3 Spring (1.81% TDS, saline type, J in Figure 8) is the most saline spring currently available. It is an enthusiastic belcher that has deposited a modest travertine sheet on the floor of its pavilion and downstream. Crystalline calcite crusts can commonly be found floating on the surface of quiet pools of the spring water, precipitated as CO_2 degassing raises the pH and supersaturates the water with respect to calcite. This spring, which has a total dissolved solids content ~½ that of sea water, is the worst tasting and smelliest of the currently flowing springs. This spring is used in most of our modeling as being the most saline water end member (**D**), though modeling suggests that more saline waters can exist at depth. In our data set of old spring analyses, the Hathorn 2 spring was probably equivalent to Hathorn 3 in salinity, and the Glacier Spring was slightly more saline. Neither of these two springs are currently flowing and there are no complete analyses of them.